

Repowering public utility grid by integrating hydro, PV and wind into the grid to supply electricity in Palu (Indonesia)

Von der Fakultät für Maschinenbau, Elektro- und Energiesysteme der Brandenburgischen Technischen Universität Cottbus-Senftenberg

zur Erlangung des akademischen Grades eines
Doktors der Ingenieurwissenschaften

genehmigte Dissertation

vorgelegt von

M.Sc. in power engineering

Sari Dewi

geboren am 06. März 1977 in Palu, Indonesien

Vorsitzender: Professor Dr.-Ing. Harald Fien

Gutachter: Professor Dr.-Ing. Harald Schwarz

Gutachter: Professor Zbigniew M. Leonowicz, PhD, DSc

Tag der mündlichen Prüfung: 05.07.2018

Statement of Authentication

I declare that I have prepared this work by myself, unassisted and without using any other resources other than those indicated. All the direct or indirect cited information from other sources (including electronic sources) is duly acknowledged without exceptions. The material, in this or similar form, has not been previously submitted, either in full or in part, for other exams at this or any other academic institution.

Place, Date

Signature

Acknowledgements

At the end of my thesis I would like to thank all those people who made this dissertation possible and an unforgettable experience for me.

First of all, I would like to thank to **Professor Dr.-Ing. Harald Fien** to support my defense as chairman.

I would like to express my deepest sense of gratitude to **Professor Dr.-Ing. Harald Schwarz** and **Professor Zbigniew M. Leonowicz, PhD, DSc** who offered me opportunity to work with them, their continuous advice and encouragement throughout the course of this dissertation. I thank them for the systematic guidance and great effort putting me into training in the scientific field.

I would like to thank to **Professor Dr.-Ing. habil. Sabine Weiß** to allow me to continue my doctoral research in BTU with her great assistance regarding my dissertation.

I am thankful to public utility company branch Palu to provide the data related to the topic of my research work especially grid data, I would like to thank to Meteorology Climatology and Geophysics Council branch Palu that provided me the data of wind speed and solar intensity and also I am very sincere thank to Public Work Ministry branch Palu as a River Center Hall that provided me the data of river flow rate and offered me opportunity to visit the location of the object of their research concern together with the civil engineering consultant.

I thank to Directorate General Higher Education, Ministry of Education and Culture of Republic Indonesia to support me scholarship.

Finally, I thank to my family and colleagues for their support.

Abstract

The use of renewable energy sources either off-grid or on-grid to supply electricity has been done by developed countries since many years ago. Developing countries for example Indonesia especially east part of Indonesia has recently started this way whereas renewable energy potential for example hydro, PV and wind are abundantly available. The lack of research and data is one of the obstacles to precede the use of renewable energy in this area meanwhile this area has electricity shortages problem that occurred quite often.

Combined hydro, PV, wind, coal and diesel generators will solve electricity shortages problem in Palu (Indonesia). Integration of Hydro, PV and wind into PALAPAS utility grid will decrease levelized cost of energy from US\$ 0.145 per kWh to US\$ 0.133 per kWh. Sensitivity analysis against fluctuating fuel cost (from US\$ 0.4 per litre to US\$ 1.6 per litre) will increase levelized cost of energy before integrating renewable energy into the grid from US\$ 0.145 per kWh to US\$ 0.455 per kWh and will increase levelized cost of energy after integrating RE into the grid from US\$ 0.133 per kWh to US\$ 0.403 per kWh.

Repowering grid with integrating hydro, PV and wind will increase power quality especially by using configuration based on homer results. Buses voltage and buses frequency showed better result before, during and after some faults based on Homer simulation results. Voltage spectrum and sinusoidal waveform voltage are showing less distortion after integrating hydro, PV and wind into the grid even with no distortion based on Homer results.

Kurzfassung

Die Nutzung erneuerbarer Energiequellen, die entweder netzunabhängig oder Netz fern Strom liefern, wird seit vielen Jahren von den Industrieländern geleistet. Entwicklungsländer wie Indonesien, insbesondere der östliche Teil, haben vor weniger als 10 Jahren begonnen. Obwohl erneuerbare Energiepotenziale wie beispielsweise Wasserkraft, PV und Wind reichlich verfügbar sind, fehlt der Mangel an Forschung und Daten. Dies ist eines der Hindernisse für den Einsatz von erneuerbaren Energien. In diesem Bereich traten außerdem häufig Probleme mit Stromengpässen.

Kombinierte Wasserkraft-, PV-, Wind-, Kohle- und Dieselgeneratoren werden das Problem der Stromknappheit in Palu (Indonesien) lösen. Durch die Integration von Hydro, PV und Wind in das Versorgungsnetz von PALAPAS werden die gestaffelten Energiekosten von 0,145 US-Dollar pro kWh auf 0,133 US-Dollar pro kWh gesenkt. Sensitivitätsanalysen bei schwankenden Brennstoffkosten (von 0,4 US-Dollar pro Liter auf 1,6 US-Dollar pro Liter) erhöhen die Stromgestehungskosten vor der Integration erneuerbarer Energien von 0,145 US-Dollar pro kWh auf 0,455 US-Dollar pro kWh und erhöhen die Kosten der Energie nach der Integration von RE in das Stromnetz von 0,133 US-Dollar pro kWh auf 0,403 US-Dollar pro kWh.

Das Repowering-Grid mit integrierender Wasser-, PV- und Windenergie wird die Stromqualität erhöhen, insbesondere durch die Konfiguration basierend auf den Homer-Ergebnissen. Die Spannung und Frequenz von Bussen zeigen ein besseres Ergebnis vor, nachdem einige Fehler auf der Basis von Homer-Ergebnissen passierten. Das Spannungsspektrum und die sinusförmige Wellenformspannung zeigen weniger Verzerrung, nachdem Hydro, PV und Wind in das Gitter integriert wurden, selbst wenn keine Verzerrungen aufgrund von Homer-Ergebnissen auftraten.

Contents

STATEMENT OF AUTHENTICATION	I
ACKNOWLEDGEMENTS.....	II
ABSTRACT	III
CONTENTS.....	V
LIST OF TABLES	XXIV
GLOSSARY OF TERMS AND ABBREVIATIONS	XXVIII
1 INTRODUCTION	1
1.1 General Information	1
1.2 Objective of the Thesis.....	2
1.3 Structure of the Thesis	3
2 ELECTRICITY POWER IN STUDY AREA	4
2.1 General Situation of Electricity in Palu and Surrounding Area	5
2.1.1 Electrification Ratio in Central Sulawesi.....	6
2.1.2 Power Balance in Central Sulawesi	7
2.1.3 Installed Capacity in PALAPAS Area	8
2.1.4 Grid Condition in central Sulawesi	9
2.1.5 Shortage Problem in Central Sulawesi.....	11
2.2 Renewable Energy Potential in Palu and Surroundings.....	12
2.2.1 Hydro Potential at Selected Location (Pakava River).....	12
2.2.1.1 Flow Rate of Pakava River.....	13
2.2.1.2 Electrical Potential.....	16
2.2.1.3 Selected Hydro Turbine	17
2.2.1.4 Energy Production From Hydro Source	18
2.2.2 Solar Potential at Selected Location	18
2.2.2.1 Hourly Sun Availability and solar radiation	19
2.2.2.2 Peak Sun Hours.....	19
2.2.2.3 Energy Production from PV.....	20
2.2.3 Wind Potential at Selected Location.....	22
2.2.3.1 Analyzing Wind Speed	22
3 METHODOLOGY OF RESEARCH	24
3.1 HOMER Software.....	24
3.1.1 Load.....	24
3.1.2 Components.....	27
3.1.2.1 Diesel Generator.....	27
3.1.2.2 Photovoltaic	29
3.1.2.3 Wind Turbine.....	30
3.1.2.4 Hydro	33
3.1.2.5 Grid	34
3.1.2.6 Battery.....	39
3.1.2.7 Converter	40
3.1.3 Resources.....	40
3.1.3.1 Solar.....	40

3.1.3.2	Wind.....	41
3.1.3.3	Hydro	41
3.2	Analysis the Real situation	42
3.2.1	Daily Load Profile in Palu	42
3.2.1.1	Different Type of Customer in Indonesia.....	42
3.2.1.2	Weekdays and Weekend Load Profile in Palu	42
3.2.2	Daily Electricity Generation from Hydro, PV and Wind.....	44
3.2.2.1	Daily Electricity Production from PV.....	44
3.2.2.2	Daily Electricity Production from Wind	44
3.2.3	Generation and Load	45
3.2.4	Daily Generation Supplies Base Load.....	46
3.3	Simulation and Modelling	47
3.3.1	Load Input.....	47
3.3.2	Components Used to Model the System.....	49
3.3.2.1	Diesel Generator and Coal.....	49
3.3.2.2	Hydro Turbine	50
3.3.2.3	PV Module	51
3.3.2.4	Converter	51
3.3.2.5	Wind Turbine.....	52
3.3.2.6	Grid	52
3.3.3	Resources.....	53
3.3.3.1	Hydro Resources	53
3.3.3.2	PV Resources	53
3.3.3.3	Wind Resources.....	54
4	TECHNO-ECONOMY OF COMBINED HYDRO, PV AND WIND INTO PALAPAS SYSTEM TO SUPPLY ELECTRICITY IN PALU (INDONESIA)	55
4.1	Diesel Generators Connected into the Grid	56
4.1.1	Electrical Analysis Results of DG Configuration System.....	56
4.1.2	Fuel Summary of DG Configuration System	58
4.1.3	Components Simulation Results on DG Configuration System.....	59
4.1.3.1	DG 1.....	59
4.1.3.2	DG 2.....	61
4.1.3.3	DG 3.....	63
4.1.3.4	DG 4.....	65
4.1.3.5	DG 5.....	67
4.1.4	Emissions of DG Configuration System	69
4.1.5	Grid Analysis of DG Configuration System	70
4.1.6	Cost Summary of DG Configuration System Connected into the Grid	72
4.1.7	Sensitivity Analysis of DG Configuration System Connected into the Grid.....	73
4.2	Off- Grid Diesel Generator Combined with Hydro, PV and Wind	76
4.3	The Comparison of Three Wind Turbines in the Configuration of Diesel Generator Combined with Hydro, PV and Wind Connected into the Grid	77
4.3.1	The Configuration System of Diesel Generator Combined with Hydro, PV and Wind Connected into the Grid	77
4.3.2	Electrical Analysis Result of DG Combined with RE Connected into the Grid.....	79
4.4	DG Combined with RE Connected into the Grid Using Chosen Wind Turbine.....	83

4.4.1	DG 1 on Combined DG and RE	85
4.4.2	DG2 on Combined DG and RE	87
4.4.3	DG 3 on Combined DG and RE	89
4.4.4	DG 4 on Combined DG and RE	91
4.4.5	DG 5 on Combined DG and RE	93
4.4.6	Hydro Power	95
4.4.7	Photovoltaic	96
4.4.8	Wind Power.....	98
4.4.9	Converter System	99
4.4.10	Emissions on Combined DG and RE Connected into the Grid Using Chosen Wind Turbine	100
4.4.11	Grid Analysis of Combined DG and RE Connected into the Grid Using Chosen Wind Turbine	101
4.4.12	Cost Summary of Combined DG and RE Connected into the Grid Using Chosen Wind Turbine	104
4.4.13	Sensitivity Analysis of Combined DG and RE Connected into the Grid Using Chosen Wind Turbine.....	106
5	POWER QUALITY EVALUATION	109
5.1	Integrating Hydro, PV and Wind into the Grid Using ETAP 12.6	109
5.1.1	Hydro	109
5.1.2	PV	110
5.1.3	Wind.....	113
5.2	New Different Configuration of Diesel Generator Using Homer Results	114
5.2.1	Diesel Generator DG1 (30 MW).....	114
5.2.2	Diesel Generator DG2 (20 MW).....	115
5.2.3	Diesel Generator DG3 (10 MW).....	116
5.2.4	Diesel Generator DG4 (15 MW).....	117
5.2.5	Diesel Generator DG5 (55.5 MW).....	118
5.3	Simulation	119
5.3.1	Sag.....	120
5.3.2	Swell	120
5.3.3	Interruption.....	121
5.3.4	Harmonics.....	122
5.4	Simulation Result and Analysis	123
5.4.1	Sag Simulation Results	124
5.4.2	Swell Simulation Results.....	172
5.4.3	Interruption Simulation Results	220
5.4.4	Harmonic Simulation Results	268
6	REFERENCES	321
7	CONCLUSIONS	334
7.1	Conclusion	334
7.2	Future Work	341
8	BIBLIOGRAPHY.....	342
	APPENDIX A.....	350
	APPENDIX B	351

APPENDIX C352

List of Figures

Figure 2-1: Map of Sulawesi Island (Atlas of the World, 2016)	4
Figure 2-2: Upstream of Pakava River	13
Figure 2-3: 7 Years Flow Rate Analysis Results of Pakava River	14
Figure 2-4: 3 Years Flow Rate Analysis Results of Pakava River	15
Figure 2-5: Ten Years Flow Rate of Pakava River	16
Figure 2-6: Different Type of Hydro Turbine Ranges and Application (Boyle, 2003).....	17
Figure 2-7: Average Temperature in Palu in Degree Celcius (World Weather).....	18
Figure 2-8: Electricity Production of PV for 1 Year	21
Figure 2-9: Wind Speed in 2010	22
Figure 2-10: Wind Speed in 2011	22
Figure 3-1: Yearly Load Data Input.....	25
Figure 3-2: Deferrable Load Data (States)	26
Figure 3-3: Thermal Load Setup (States).....	27
Figure 3-4: Window Setup Diesel Generator Data.....	28
Figure 3-5: Real Time Input Rates and Schedule Rates of Annual Purchase Capacity (States)	36
Figure 3-6: Real Time Input Rates and Schedule Rates of Monthly Purchase Capacity (States)	37
Figure 3-7: Load Profile on Weekdays in Palu.....	43
Figure 3-8: Load Profile on Weekend in Palu	43
Figure 3-9: PV Daily Electricity Production on Clear Weather	44
Figure 3-10: Daily Electricity Production from 5 Wind Turbines.....	45
Figure 3-11: Generation and Load on Weekdays	45
Figure 3-12: Generation and Load on Weekend.....	46
Figure 3-13: One Single Day Generation is Supplying Base Load	46
Figure 3-14: Daily Load Profile in Homer Simulation	47
Figure 3-15: Seasonal Load Profile in Homer Simulation	47
Figure 3-16: Yearly Load Profile in Homer Simulation	48
Figure 3-17: Scaled Data Daily Profile in Homer Simulation	48
Figure 3-18: Economic Hydro Turbine Data	50
Figure 3-19: Hydro Turbine Head Data	51

Figure 3-20: Wind Turbine Power Curve from USA Manufacturer52

Figure 3-21: Monthly River Flow Rate53

Figure 3-22: Monthly Solar Radiation54

Figure 3-23: Monthly Wind Speed54

Figure 4-1: DG Configuration Connected into the Grid56

Figure 4-2: Components on DG Configuration System Connected into the Grid56

Figure 4-3: Monthly Electricity Production of All Components57

Figure 4-4: Monthly Fuel Consumption of DG Configuration System58

Figure 4-5: Hourly Fuel Consumption of DG Configuration System59

Figure 4-6: Monthly Fuel Consumption of DG Configuration System59

Figure 4-7: Hourly Output Power of DG 161

Figure 4-8: Hourly Output Power of DG 263

Figure 4-9: Hourly Output Power of DG 365

Figure 4-10: Hourly Output Power of DG 467

Figure 4-11 Hourly Output Power of DG 569

Figure 4-12: Energy Purchased by PALAPAS system from the Grid71

Figure 4-13: Energy sold by PALAPAS System to the Grid71

Figure 4-14: Net Present Cost of DG Configuration System Connected into the
Grid72

Figure 4-15: Monthly Fuel Consumption of DG Combined with RE Connected
into the Grid Using Chosen Wind Turbine84

Figure 4-16: Hourly Fuel Consumption of DG Combined with RE Connected into
the Grid Using Chosen Wind Turbine84

Figure 4-17: Monthly Fuel Consumption Fluctuation of DG Combined with RE
Connected into the Grid Using Chosen Wind Turbine85

Figure 4-18: DG 1 Power Output of Combined DG and RE87

Figure 4-19: DG 2 Power Output of Combined DG and RE89

Figure 4-20: DG 3 Power Output of Combined DG and RE91

Figure 4-21: DG 4 Power Output on Combined DG and RE92

Figure 4-22: DG Power Output of DG 5 on Combined DG and RE95

Figure 4-23: Hydro Power Output96

Figure 4-24: PV Power Output98

Figure 4-25: Wind Power Output98

Figure 4-26: Inverter Output99

Figure 4-27: Rectifier Output	99
Figure 4-28: Combine DG and RE Connected into the Grid Using Chosen Wind Turbine.....	100
Figure 4-29: Energy Purchased by PALAPAS System from the Grid On Combined DG and RE	103
Figure 4-30: Energy Sold by PALAPAS System to the Grid on Combined DG and RE	103
Figure 4-31: Net Present Cost of All Components on Combined DG and RE	104
Figure 5-1: Silae SB4 Bus bar Before Integrating Hydropower.....	110
Figure 5-2: Silae SB4 Bus bar After Integrating Hydropower.....	110
Figure 5-3: Before Integrating PV on Talise SB3 Bus bar Through Bus bar 32	111
Figure 5-4: After Integrating PV on Talise SB3 Bus bar Through Bus bar 32	111
Figure 5-5: Before Integrating PV on PJPP SB1 Bus bar Through Bus bar 40	112
Figure 5-6: After Integrating PV on PJPP SB1 Bus bar Through Bus bar 40	112
Figure 5-7: Before Integrating PVA2 and PVA4 on Parigi SB2 Bus bar	112
Figure 5-8: After Integrating PVA2 and PVA4 on Parigi SB2 Bus bar	113
Figure 5-9: Before Integrating Wind Power into Maesa SB1 Bus bar Through Bus bar 46.....	113
Figure 5-10: After Integrating Wind Power into Maesa SB1 (2) Bus bar.....	113
Figure 5-11: Before Upgrading from DG2 (15 MW) to DG1 (30 MW).....	115
Figure 5-12: After Upgrading DG1	115
Figure 5-13: Before Upgrading Two DG Becoming One DG (DG2)	116
Figure 5-14: After Upgrading Two DG Becoming One DG (DG2)	116
Figure 5-15: Before Downgrading from DG1 (15 MW) to DG3 (10 MW)	117
Figure 5-16: After Downgrading from DG1 (15 MW) to DG3 (10 MW)	117
Figure 5-17: G1 Before Using Homer Results	118
Figure 5-18: G1 After Using Homer Results	118
Figure 5-19: Before Replacing Some DG with one DG (55.5 MW).....	119
Figure 5-20: After Replacing Some DGs with DG5 (55.5 MW).....	119
Figure 5-21: Sag Simulation	120
Figure 5-22: Swell Simulation	121
Figure 5-23: Interruption Simulation	122
Figure 5-24: Harmonic Simulation	123
Figure 5-25: DB1 PJPP Bus Voltage Sag Simulation Results on Situation A.....	124

Figure 5-26: DB1 PJPP Bus Voltage Sag Simulation Results on Situation B	125
Figure 5-27: DB1 PJPP Bis Voltage Sag Simulation Results on Situation C	125
Figure 5-28: Donggala SB1 Bus Voltage Sag Simulatrion Results on Situation A...	126
Figure 5-29: Donggala SB1 Bus Voltage Sag Simulation Results on Situation B....	127
Figure 5-30: Donggala SB1 Bus Voltage Sag Simulation Results on Situation C....	127
Figure 5-31: Maesa SB1 Bus Voltage Sag Simulation Results on Situation A	128
Figure 5-32: Maesa SB1 Bus Voltage Sag Simulation Results on Situation B	129
Figure 5-33: Maesa SB1 Bus Voltage Sag Simulation Results on Situation C	129
Figure 5-34: Parigi DB1 Bus Voltage Sag Simulation Results on Situation A.....	130
Figure 5-35: Parigi DB1 Bus Voltage Sag Simulation Results on Situation B.....	131
Figure 5-36: Parigi DB1 Bus Voltage Sag Simulation Results on Situation C.....	131
Figure 5-37: Parigi SB1 Bus Voltage Sag Simulation Results on Sltuation A.....	132
Figure 5-38: Silae SB1 Bus Voltage Sag Simulation Results on Situation B	133
Figure 5-39: Silae SB1 Bus Voltage Sag Simulation Results on Situation C	133
Figure 5-40: Parigi SB2 Bus Voltage Sag Simulation Results on Situation A.....	134
Figure 5-41: Parigi SB2 Bus Voltage Sag Simulation Results on Situation B.....	135
Figure 5-42: Parigi SB2 Bus Voltage Sag Simulation Results on Situation C.....	135
Figure 5-43: PJPP SB1 Bus Voltage Sag Simulation Results on Situation A	136
Figure 5-44: PJPP SB1 Bus Voltage Sag Simulation Results on Situation B	137
Figure 5-45: PJPP Bus Voltage Sag Simulation Results on Situation C.....	137
Figure 5-46: Silae SB1 Bus Voltage Sag Simulation Results on Situation A	138
Figure 5-47: Silae SB1 Bus Voltage Sag Simulation Results on Situation B	139
Figure 5-48: Silae SB1 Bus Voltage Sag Simulation Results on Situation C	139
Figure 5-49: Silae SB4 Bus Voltage Sag Simulation Results on Situation A	140
Figure 5-50: Silae SB4 Bus Voltage Sag Simulation Results on Situation B	141
Figure 5-51: Silae SB4 Bus Voltage Sag Simulation Results on Situation C	141
Figure 5-52: Talise SB1 Bus Voltage Sag Simulation Results on Situation A	142
Figure 5-53: Talise SB1 Bus Voltage Sag Simulation Results on Situation B	143
Figure 5-54: Talise SB1 Bus Voltage Sag Simulation Results on Situation C	143
Figure 5-55: Talise SB2 Bus Voltage Sag Simulation Results on Situation A	144
Figure 5-56: Talise SB2 Bus Voltage Sag Simulation Results on Situation B	145
Figure 5-57: Talise SB2 Bus Voltage Sag Simulation Results on Situation C	145
Figure 5-58: Talise DB1 Bus Voltage Sag Simulation Results on Situation A	146
Figure 5-59: Talise DB1 Bus Voltage Sag Simulation Results on Situation B	147

Figure 5-60: Talise DB1 Bus Voltage Sag Simulation Results on Situation C 147

Figure 5-61: DB1 PJPP Bus Frequency Sag Simulation Results on Situation A 148

Figure 5-62: DB1 PJPP Bus Frequency Sag Simulation Results on Situation B 149

Figure 5-63: DB1 PJPP Bus Frequency Sag Simulation Results on Situation C 149

Figure 5-64: Donggala SB1 Bus Frequency Sag Simulation Results on Situation
A..... 150

Figure 5-65: Donggala SB1 Bus Frequency Sag Simulation Results on Situation
B..... 151

Figure 5-66: Donggala SB1 Bus Frequency Sag Simulation Results on Situation
C 151

Figure 5-67: Maesa SB1 Bus Frequency Sag simulation Results on Situation A 152

Figure 5-68: Maesa SB1 Bus Frequency Sag Simulation Results on Situation B.... 153

Figure 5-69: Maesa SB1 Bus Frequency Sag Simulation Results on Situation C ... 153

Figure 5-70: Parigi DB1 Bus Frequency Sag Simulation Results on Situation A 154

Figure 5-71: Parigi DB1 Bus Frequency Sag Simulation Results on Situation B 155

Figure 5-72: Parigi DB1 Bus Frequency Sag Simulation Results on Situation C 155

Figure 5-73: Parigi SB1 Bus Frequency Sag Simulation Results on Situation A 156

Figure 5-74: Parigi SB1 Bus Frequency Sag Simulation Results on Situation B 157

Figure 5-75: Parigi SB1 Bus Frequency Sag Simulation Results on Situation C 157

Figure 5-76: Parigi SB2 Bus Frequency Sag Simulation Results on Situation A 158

Figure 5-77: Parigi SB2 Bus Frequency Sag Simulation Results on Situation B 159

Figure 5-78: Parigi SB2 Bus Frequency Sag Simulation Results on Situation C 159

Figure 5-79: PJPP SB1 Bus Frequency Sag Simulation Results on Situation A 160

Figure 5-80: PJPP SB1 Bus Frequency Sag Simulation Results on Situation B 161

Figure 5-81: PJPP SB1 Bus Frequency Sag Simulation Results on Situation C 161

Figure 5-82: Silae SB1 Bus Frequency Sag Simulation Results on Situation A 162

Figure 5-83: Silae SB1 Bus Frequency Sag Simulation Results on Situation B 163

Figure 5-84: Silae SB1 Bus Frequency Sag Simulation Results on Situation C 163

Figure 5-85: Silae SB4 Bus Frequency Sag Simulation Results on Situation A 164

Figure 5-86: Silae SB4 Bus Frequency Sag Simulation Results on Situation B 165

Figure 5-87: Silae SB4 Bus Frequency Sag Simulation Results on Situation C 165

Figure 5-88: Talise SB1 Bus Frequency Sag Simulation Results on Situation A 166

Figure 5-89: Talise SB1 Bus Frequency Sag Simulation Results on Situation B 167

Figure 5-90: Talise SB1 Bus Frequency Sag Simulation Results on Situation C 167

Figure 5-91: Talise SB2 Bus Frequency Sag Simulation Results on Situation A..... 168

Figure 5-92: Talise SB2 Bus Frequency Sag Simulation Results on Situation B..... 169

Figure 5-93: Talise SB2 Bus Frequency Sag Simulation Results on Situation C..... 169

Figure 5-94: Talise DB1 Bus Frequency Sag Simulation Results on Situation A..... 170

Figure 5-95: Talise DB1 Bus Frequency Sag Simulation Results on Situation B..... 171

Figure 5-96: Talise DB1 Bus Frequency Sag Simulation Results on Situation C 171

Figure 5-97: DB1 PJPP Bus Voltage Swell Simulation Results on Situation A..... 172

Figure 5-98: DB1 PJPP Bus Voltage Swell Simulation Results on Situation B..... 173

Figure 5-99: DB1 PJPP Bus Voltage Swell Simulation Results on Situation C..... 173

Figure 5-100: Donggala SB1 Bus Voltage Swell Simulation Results on Situation
 A..... 174

Figure 5-101: Donggala SB1 Bus Voltage Swell Simulation Results on Situation
 B..... 175

Figure 5-102: Donggala SB1 Bus Voltage Swell Simulation Results on Situation
 C 175

Figure 5-103: Maesa SB1 Bus Voltage Swell Simulation Results on Situation C 176

Figure 5-104: Maesa SB1 (2) Bus Voltage Swell Simulation Results on Situation
 B..... 177

Figure 5-105: Maesa SB1 Bus Voltage Swell Simulation Results on Situation C 177

Figure 5-106: Parigi DB1 Bus Voltage Swell Simulation Results on Situation A..... 178

Figure 5-107: Parigi DB1 Bus Voltage Swell Simulation Results on Situation B..... 179

Figure 5-108: Parigi DB1 Bus Voltage Swell Simulation Results on Situation C 179

Figure 5-109: Parigi SB1 Bus Voltage Swell Simulation Results on Situation A..... 180

Figure 5-110: Parigi SB1 Bus Voltage Swell Simulation Results on Situation B..... 181

Figure 5-111: Parigi SB1 Bus Voltage Swell Simulation Results on Situation C..... 181

Figure 5-112: Parigi SB2 Bus Voltage Swell Simulation Results on Situation A..... 182

Figure 5-113: Parigi SB2 Bus Voltage Swell Simulation Results on Situation B..... 183

Figure 5-114: Parigi SB2 Bus Voltage Swell Simulation Results on Situation C..... 183

Figure 5-115: PJPP SB1 Bus Voltage Swell Simulation Results on Situation A..... 184

Figure 5-116: PJPP SB1 Bus Voltage Swell Simulation Results on Situation B..... 185

Figure 5-117: PJPP SB1 Bus Voltage Swell Simulation Results on Situation C..... 185

Figure 5-118: Silae SB1 Bus Voltage Swell Simulation Results on Situation A 186

Figure 5-119: Silae SB1 Bus Voltage Swell Simulation Results on Situation B 187

Figure 5-120: Silae SB1 Bus Voltage Swell Simulation Results on Situation C..... 187

Figure 5-121: Silae SB4 Bus Voltage Swell Simulation Results on Situation A 188

Figure 5-122: Silae SB4 Bus Voltage Swell Simulation Results on Situation B 189

Figure 5-123: Silae SB4 Bus Voltage Swell Simulation Results on Situation C 189

Figure 5-124: Talise SB1 Bus Voltage Swell Simulation Results on Situation A 190

Figure 5-125: Talise SB1 Bus Voltage Swell Simulation Results on Situation B 191

Figure 5-126: Talise SB1 Bus Voltage Swell Simulation Results on Situation C 191

Figure 5-127: Talise SB2 Bus Voltage Swell Simulation Results on Situation A 192

Figure 5-128: Talise SB2 Bus Voltage Swell Simulation Results on Situation B 193

Figure 5-129: Talise SB2 Bus Voltage Swell Simulation Results on Situation C 193

Figure 5-130: Talise DB1 Bus Voltage Swell Simulation Results on Situation A 194

Figure 5-131: Talise DB1 Bus Voltage Swell Simulation Results on Situation B 195

Figure 5-132: Talise DB1 Bus Voltage Swell Simulation Results on Situation C 195

Figure 5-133: DB1 PJPP Bus Frequency Swell Simulation Results on Situation
A..... 196

Figure 5-134: DB1 PJPP Bus Frequency Swell Simulation Results on Situation
B..... 197

Figure 5-135: DB1 PJPP Bus Frequency Swell Simulation Results on Situation
C 197

Figure 5-136: Donggala SB1 Bus Frequency Swell Simulation Results on
Situation A..... 198

Figure 5-137: Donggala SB1 Bus Frequency Swell Simulation Results on
Situation B..... 199

Figure 5-138: Donggala SB1 Bus Frequency Swell Simulation Results on
Situation C 199

Figure 5-139: Maesa SB1 Bus Frequency Swell Simulation Results on Situation
A..... 200

Figure 5-140: Maesa SB1 Bus Frequency Swell Simulation Results on Situation
B..... 201

Figure 5-141: Maesa SB1 Bus Frequency Swell Simulation Results on Situation
C 201

Figure 5-142: Parigi DB1 Bus Frequency Swell Simulation Results on Situation
A..... 202

Figure 5-143: Parigi DB1 Bus Frequency Swell Simulation Results on Situation
B..... 203

Figure 5-144: Parigi DB1 Bus Frequency Swell Simulation Results on Situation C203

Figure 5-145: Parigi SB1 Bus Frequency Swell Simulation Results on Situation A.....204

Figure 5-146: Parigi SB1 Bus Frequency Swell Simulation Results on Situation B.....205

Figure 5-147: Parigi SB1 Bus Frequency Swell Simulation Results on Situation C205

Figure 5-148: Parigi SB2 Bus Frequency Swell Simulation Results on Situation A.....206

Figure 5-149: Parigi SB2 Bus Frequency Swell Simulation Results on Situation B.....207

Figure 5-150: Parigi SB2 Bus Frequency Swell Simulation Results on Situation C207

Figure 5-151: PJPP SB1 Bus Frequency Swell Simulation Results on Situation A.....208

Figure 5-152: PJPP SB1 Bus Frequency Swell Simulation Results on Situation B.....209

Figure 5-153: PJPP SB1 Bus Voltage Swell Simulation Results on Situation C.....209

Figure 5-154: Silae SB1 Bus Frequency Swell Simulation Results on Situation A ..210

Figure 5-155: Silae SB1 Bus Frequency Swell Simulation Results on Situation B ..211

Figure 5-156: Silae SB1 Bus Frequency Swell Simulation Results on Situation C ..211

Figure 5-157: Silae SB4 Bus Frequency Swell Simulation Results on Situation A ..212

Figure 5-158: Silae SB4 Bus Frequency Swell Simulation Results on Situation B ..213

Figure 5-159: Silae SB4 Bus Frequency Swell Simulation Results on Situation C ..213

Figure 5-160: Talise SB1 Bus Frequency Swell Simulation Results on Situation A.....214

Figure 5-161: Talise SB1 Bus Frequency Swell Simulations on Situation B.....215

Figure 5-162: Talise SB1 Bus Frequency Swell Simulation Results on Situation C215

Figure 5-163: Talise SB2 Bus Frequency Swell Simulation Results on Situation A.....216

Figure 5-164: Talise SB2 Bus Frequency Swell Simulation Results on Situation B.....217

Figure 5-165: Talise SB2 Bus Frequency Swell Simulation Results on Situation C217

Figure 5-166: Talise DB1 Bus Frequency Swell Simulation Results on Situation A.....218

Figure 5-167: Talise DB1 Bus Frequency Swell Simulation Results on Situation B.....219

Figure 5-168: Talise DB1 Bus Frequency Swell Simulation Results on Situation C219

Figure 5-169: DB1 PJPP Bus Voltage Interruption Simulation Results on Situation A.....220

Figure 5-170: DB1 PJPP Bus Voltage Interruption Simulation Results on Situation B.....221

Figure 5-171: DB1 PJPP Bus Voltage Swell Simulation Results on Situation C.....221

Figure 5-172: Donggala SB1 Bus Voltage Interruption Simulation Results on Situation A.....222

Figure 5-173: Donggala SB1 Bus Voltage Interruption Simulation Results on Situation B.....223

Figure 5-174: Donggala SB1 Bus Voltage Interruption Simulation Results on Situation C223

Figure 5-175: Maesa SB1 Bus Voltage Interruption Simulation Results on Situation A.....224

Figure 5-176: Maesa SB1 Bus Voltage Interruption Simulation Results on Situation B.....225

Figure 5-177: Maesa SB1 Bus Voltage Interruption Simulation Results on Situation C225

Figure 5-178: Parigi DB1 Bus Voltage Interruption Simulation Results on Situation A.....226

Figure 5-179: Parigi DB1 Bus Voltage Interruption Simulation Results on Situation B.....227

Figure 5-180: Parigi DB1 Bus Voltage Interruption Simulation Results on Situation C227

Figure 5-181: Parigi SB1 Bus Voltage Interruption Simulation Results on Situation A.....228

Figure 5-182: Parigi SB1 Bus Voltage Interruption Simulation Results on Situation B.....229

Figure 5-183: Parigi SB1 Bus Voltage Interruption Simulation Results on Situation C229

Figure 5-184: Parigi SB2 Bus Voltage Interruption Simulation Results on Situation A.....230

Figure 5-185: Parigi SB2 Bus Voltage Interruption Simulation Results on Situation B.....231

Figure 5-186: Parigi SB2 Bus Voltage Interruption Simulation Results on Situation C231

Figure 5-187: PJPP SB1 Bus Voltage Interruption Simulation Results on Situation A.....232

Figure 5-188: PJPP SB1 Bus Voltage Interruption Simulation Results on Situation B.....233

Figure 5-189: PJPP SB1 Bus Voltage Interruption Simulation Results on Situation C233

Figure 5-190: Silae SB1 Bus Voltage Interruption Simulation Results on Situation A.....234

Figure 5-191: Silae SB1 Bus Voltage Interruption Simulation Results on Situation B.....235

Figure 5-192: Silae SB1 Bus Voltage Interruption Simulation Results on Situation C235

Figure 5-193: Silae SB4 Bus Voltage Interruption Simulation Results on Situation A.....236

Figure 5-194: Silae SB4 Bus Voltage Interruption Simulation Results on Situation B.....237

Figure 5-195: Silae SB4 Bus Voltage Interruption Simulation Results on Situation C237

Figure 5-196: Talise SB1 Bus Voltage Interruption Simulation Results on Situation A.....238

Figure 5-197: Talise SB1 Bus Voltage Interruption Simulation Results on Situation B.....239

Figure 5-198: Talise SB1 Bus Voltage Interruption Simulation Results on Situation C239

Figure 5-199: Talise SB2 Bus Voltage Interruption Simulation Results on situation A240

Figure 5-200: Talise SB2 Bus Voltage Interruption Simulation Results on Situation B.....241

Figure 5-201: Talise SB2 Bus Voltage Interruption Simulation Results on Situation C241

Figure 5-202: Talise DB1 Bus Voltage Interruption Simulation Results on Situation A.....242

Figure 5-203: Talise DB1 Bus Voltage Interruption Simulation Results on Situation B.....243

Figure 5-204: Talise DB1 Bus Voltage Interruption Simulation Results on Situation C243

Figure 5-205: DB1 PJPP Bus Frequency Interruption Simulation Results on Situation A.....244

Figure 5-206: DB1 PJPP Bus Frequency Interruption Simulation Results on Situation B.....245

Figure 5-207: DB1 PJPP Bus Frequency Interruption Simulation Results on Situation C245

Figure 5-208: Donggala SB1 Bus Frequency Interruption Simulation Results on Situation A.....246

Figure 5-209: Donggala SB1 Bus Frequency Interruption Simulation Results on Situation B.....247

Figure 5-210: Donggala SB1 Bus Frequency Interruption Simulation Results on Situation C247

Figure 5-211: Maesa SB1 Bus Frequency Interruption Simulation Results on Situation A.....248

Figure 5-212: Maesa SB1 Bus Frequency Interruption Simulation Results on Situation B.....249

Figure 5-213: Maesa SB1 Bus Frequency Interruption Simulation Results on Situation C249

Figure 5-214: Parigi DB1 Bus Frequency Interruption Simulation Results on Situation A.....250

Figure 5-215: Parigi DB1 Bus Frequency Interruption Simulation Results on Situation B.....251

Figure 5-216: Parigi DB1 Bus Frequency Interruption Simulation Results on Situation C251

Figure 5-217: Parigi SB1 Bus Frequency Interruption Simulation Results on Situation A.....252

Figure 5-218: Parigi SB1 Bus Frequency Interruption Simulation Results on Situation B.....253

Figure 5-219: Parigi SB1 Bus Frequency Interruption Simulation Results on Situation C253

Figure 5-220: Parigi SB2 Bus Frequency Interruption Simulation Results on Situation A.....254

Figure 5-221: Parigi SB2 Bus Frequency Interruption Simulation Results on Situation B.....255

Figure 5-222: Parigi SB2 Bus Frequency Interruption Simulation Results on Situation C255

Figure 5-223: PJPP SB1 Bus Frequency Interruption Simulation Results on Situation A.....256

Figure 5-224: PJPP SB1 Bus Frequency Interruption Simulation Results on Situation B.....257

Figure 5-225: PJPP SB1 Bus Frequency Interruption Simulation Results on Situation C257

Figure 5-226: Silae SB1 Bus Frequency Interruption Simulation Results on Situation A.....258

Figure 5-227: Silae SB1 Bus Frequency Interruption Simulation Results on Situation B.....259

Figure 5-228: Silae SB1 Bus Frequency Interruption Simulation Results on Situation C259

Figure 5-229: Silae SB4 Bus Frequency Interruption Simulation Results on Situation A.....260

Figure 5-230: Silae SB4 Bus Frequency Interruption Simulation Results on Situation B.....261

Figure 5-231: Silae SB4 Bus Frequency Interruption Simulation Results on Situation C261

Figure 5-232: Talise SB1 Bus Frequency Interruption Simulation Results on Situation A.....262

Figure 5-233: Talise SB1 Bus Frequency Interruption Simulation Results on Situation B.....263

Figure 5-234: Talise SB1 Bus Frequency Interruption Simulation Results on Situation C263

Figure 5-235: Talise SB2 Bus Frequency Interruption Simulation Results on Situation A.....264

Figure 5-236: Talise SB2 Bus Frequency Interruption Simulation Results on Situation B265

Figure 5-237: Talise SB2 Bus Frequency Interruption Simulation Results on Situation C265

Figure 5-238: Talise DB1 Bus Frequency Interruption Simulation Results on Situation A.....266

Figure 5-239: Talise DB1 Bus Frequency Interruption Simulation Results on Situation B.....267

Figure 5-240: Talise DB1 Bus Frequency Interruption Simulation Results on Situation C267

Figure 5-241: Harmonic Voltages (in %) of DB1 PJPP Bus bar on Situation A268

Figure 5-242: Harmonic Voltages of DB1 PJPP Bus bar on Situation B.....269

Figure 5-243: Harmonic Voltages of DB1 PJPP Bus bar on Situation C269

Figure 5-244: Voltage Waveform of DB1 PJPP Bus bar on Situation A271

Figure 5-245: Voltage Waveform of DB1 PJPP Bus bar on Situation B271

Figure 5-246: Voltage Waveform of DB1 PJPP Bus bar on Situation C272

Figure 5-247: Harmonic Voltage of Donggala SB1 Bus bar on Situation A273

Figure 5-248: Harmonic Voltage of Donggala SB1 Bus bar on Situation B273

Figure 5-249: Harmonic Voltage of Donggala SB1 Bus bar on Situation C274

Figure 5-250: Voltage Waveform of Donggala SB1 Bus bar on Situation A276

Figure 5-251: Voltage Waveform of Donggala SB1 Bus bar on Situation B276

Figure 5-252: Voltage Waveform of Donggala SB1 Bus bar on Situation C276

Figure 5-253: Harmonic Voltage of Maesa SB1 Bus bar on Situation A.....277

Figure 5-254: Harmonic Voltage of Maesa SB1 Bus bar on Situation B.....278

Figure 5-255: Harmonic Voltage of Maesa SB1 Bus bar on Situation C.....278

Figure 5-256: Voltage Waveform of Maesa SB1 Bus bar on Situation A.....280

Figure 5-257: Voltage Waveform of Maesa SB1 Bus bar on Situation B.....280

Figure 5-258: Voltage Waveform of Maesa SB1 Bus bar on Situation C.....281

Figure 5-259: Harmonic Voltage of Parigi DB1 Bus bar on Situation A281

Figure 5-260: Harmonic Voltage of Parigi DB1 Bus bar on Situation B282

Figure 5-261: Harmonic Voltage of Parigi DB1 Bus bar on Situation C282

Figure 5-262: Voltage Waveform of Parigi DB1 Bus bar on Situation A284

Figure 5-263: Voltage Waveform of Parigi DB1 Bus bar on Situation B284

Figure 5-264: Voltage Waveform of Parigi DB1 Bus bar on Situation C285

Figure 5-265: Harmonic Voltage of Parigi SB1 Bus bar on Situation A286

Figure 5-266: Harmonic Voltage of Parigi SB1 Bus bar on Situation B286

Figure 5-267: Harmonic Voltage of Parigi SB1 Bus bar on Situation C287

Figure 5-268: Voltage Waveform of Parigi SB1 Bus bar on Situation A289

Figure 5-269: Voltage Waveform of Parigi SB1 Bus bar on Situation B289

Figure 5-270: Voltage Waveform of Parigi SB1 Bus bar on Situation C289

Figure 5-271: Harmonic Voltage of Parigi SB2 Bus bar on Situation A290

Figure 5-272: Harmonic Voltage of Parigi SB2 Bus bar on Situation B291

Figure 5-273: Harmonic Voltage of Parigi SB2 Bus bar on Situation C291

Figure 5-274: Voltage Waveform of Parigi SB2 Bus bar on Situation A293

Figure 5-275: Voltage Waveform of Parigi SB2 Bus bar on Situation B293

Figure 5-276: Voltage Waveform of Parigi SB2 on Situation C294

Figure 5-277: Harmonic Voltage of PJPP SB1 Bus bar on Situation A.....295

Figure 5-278: Harmonic Voltage of PJPP SB1 Bus bar on Situation B.....295

Figure 5-279: Harmonic Voltage of PJPP SB1 Bus bar on Situation C296

Figure 5-280: Voltage Waveform of PJPP SB1 Bus bar on Situation A.....298

Figure 5-281: Voltage Waveform of PJPP SB1 Bus bar on Situation B.....298

Figure 5-282: Voltage Waveform of PJPP SB1 Bus bar on Situation C298

Figure 5-283: Harmonic Voltage of Silae SB1 Bus bar on Situation A.....299

Figure 5-284: Harmonic Voltage of Silae SB1 Bus bar on Situation B.....300

Figure 5-285: Harmonic Voltage of Silae SB1 Bus bar on Situation C300

Figure 5-286: Voltage Waveform of Silae SB1 Bus bar on Situation A.....302

Figure 5-287: Voltage Waveform of Silae SB1 Bus bar on Situation B.....302

Figure 5-288: Voltage Waveform of Silae SB1 Bus bar on Situation C303

Figure 5-289: Harmonic Voltage of Silae SB4 Bus bar on Situation A.....304

Figure 5-290: Harmonic Voltage of Silae SB4 Bus bar on Situation B.....304

Figure 5-291: Harmonic Voltage of Silae SB4 Bus bar on Situation C305

Figure 5-292: Voltage Waveform of Silae SB4 Bus bar on Situation A.....307

Figure 5-293: Voltage Waveform of silae SB4 Bus bar on Situation B307

Figure 5-294: Voltage Waveform of Silae Sb4 Bus bar on Situation C307

Figure 5-295: Harmonic Voltage of Talise SB1 Bus bar on Situation A308

Figure 5-296: Harmonic Voltage of Talise SB1 Bus bar on Situation B308

Figure 5-297: Harmonic Voltage of Talise SB1 Bus bar on Situation C309

Figure 5-298: Voltage Waveform of Talise SB1 Bus bar on Situation A311

Figure 5-299: Voltage Waveform of Talise SB1 Bus bar on Situation B311

Figure 5-300: Voltage Waveform of Talise SB1 Bus bar on Situation C311

Figure 5-301: Harmonic Voltage of Talise SB2 Bus bar on Situation A312

Figure 5-302: Harmonic Voltage of Talise SB2 Bus bar on Situation B313

Figure 5-303: Harmonic Voltage of Talise SB2 Bus bar on Situation C313

Figure 5-304: Voltage Waveform of Talise SB2 Bus bar on Situation A315

Figure 5-305: Voltage Waveform of Talise SB2 Bus bar on Situation B315

Figure 5-306: Voltage Waveform of Talise SB2 Bus bar on Situation C316

Figure 5-307: Harmonic Voltage of Talise DB1 Bus bar on Situation A316

Figure 5-308: Harmonic Voltage of Talise DB1 Bus bar on Situation B317

Figure 5-309: Harmonic Voltage of Talise DB1 Bus bar on Situation C317

Figure 5-310: Voltage Waveform of Talise DB1 Bus bar on Situation A319

Figure 5-311: Voltage Waveform of Talise DB1 Bus bar on Situation B319

Figure 5-312: Voltage Waveform of Talise DB1 Bus bar on Situation C320

List of Tables

Table 2-1: Regencies and Cities in Central Sulawesi Since 2014 (BPS)	5
Table 2-2: Electrification Ratio in June 2012 (Palu, 2011).....	6
Table 2-3: Power Balance in central Sulawesi (June 2012) (Palu, 2011).....	7
Table 2-4: Total Installed Capacity in PALAPAS Area in 2014 (Palu, 2011)	8
Table 2-5: Grid Data in Central Sulawesi (Palu, 2011).....	11
Table 2-6: Flow Rate of Pakava River for 10 Years (Booklet, 2014).....	14
Table 2-7: Monthly Average Flow Rate of Pakava River	16
Table 2-8: Generated Electricity per Month	17
Table 2-9: Energy Production per Year from Hydro Resource	18
Table 2-10: Monthly Solar Radiation Data in Palu	19
Table 2-11: Peak Sun Hours Results	20
Table 2-12: PV Energy Production	21
Table 2-13: Wind Speed Performance in 2011.....	23
Table 3-1: Zo Description and Value	32
Table 3-2: Diesel Generator Input Data	49
Table 4-1: Electrical Production of All Components.....	57
Table 4-2: Electricity Consumption On DG Configuration System.....	58
Table 4-3: Excess Electricity, Unmeet load and Capacity Shortage on DG Configuration System.....	58
Table 4-4: Generator 1 Electricity Production.....	60
Table 4-5: DG 1 Operation Hours	60
Table 4-6: Fuel Consumption of DG1	61
Table 4-7: DG 2 Electrical Production	62
Table 4-8: DG 2 Operation Hours	62
Table 4-9: Fuel Consumption of DG 2	63
Table 4-10: DG 3 Electrical Production	64
Table 4-11: DG 3 Operation Hours.....	64
Table 4-12: Fuel Consumption of DG 3	65
Table 4-13: DG 4 Electrical Production	66
Table 4-14: DG 4 Operation Hours.....	66
Table 4-15: Fuel Consumption of DG 4	67
Table 4-16: DG 5 Electrical Production	67

Table 4-17: DG 5 Operation Hours	68
Table 4-18: Fuel Consumption of DG 5	68
Table 4-19: Emission of DG Configuration System	70
Table 4-20: Electricity Purchased and Sold by PALAPAS System	70
Table 4-21: NPC of All Components of DG Configuration System Connected into the Grid	72
Table 4-22: Overall Cost of DG Configuration System Connected into the Grid.....	73
Table 4-23: Sensitivity Analysis Result of Fuel Price of DG Configuration System Connected into the Grid	74
Table 4-24: Sensitivity Analysis Result of Fuel Price of DG Configuration System Connected into the Grid	75
Table 4-25: Sensitivity Results of All Costs of DG Configuration Systems Connected into the Grid	76
Table 4-26: Simulation Results of Off-Grid DG Combined with RE Using Battery and Autosized DG	76
Table 4-27: Simulation Results of Off-Grid DG Combined with RE Using Battery without Autosized DG.....	77
Table 4-28: Three Configuration System of DG Combined with RE Connected into the Grid Using three Different Wind Turbines.....	79
Table 4-29: Electricity Production of All Components of DG Combined with RE Connected into the Grid Using Three Wind Turbines.....	80
Table 4-30: Electricity Consumption of DG Combined with RE Connected into the Grid Using Three Different Wind Turbines	81
Table 4-31: Excess Electricity, Unmet Load and Capacity Shortage of DG Combined with RE Connected into the Grid Using THree Different Wind Turbines	81
Table 4-32: Renewable Fraction and Maximum RE Penetration of DG Combined with RE Connected into the Grid Using Three Different Wind Turbines	82
Table 4-33: Costs of DG Combined with RE Connected into the Grid Using Three Different Wind Turbines	82
Table 4-34: Fuel Consumption Summary of DG Combined with RE Connected into the Grid Using Chosen Wind Turbine.....	83
Table 4-35: Electricity Production of DG1 on Combine DG and RE	86

Table 4-36: Operation Hours of DG 1 on Combined DG and RE	86
Table 4-37: Fuel Consumption of DG1 on Combined DG and RE.....	86
Table 4-38: Electricity Production of DG 2 on Combined DG and RE	87
Table 4-39: Operation Hours of DG 2 on Combined DG and RE	88
Table 4-40: Fuel Consumption of DG 2 on Combined DG and RE.....	88
Table 4-41: Electricity Production of DG 3 on Combined DG and RE	89
Table 4-42: Operation Hours of DG 3 on Combined DG and RE	90
Table 4-43: Fuel Consumption of DG3 on Combined DG and RE.....	90
Table 4-44: Electricity Production of DG 4 on Combined DG and RE	91
Table 4-45: Operation Hours of DG 4 on Combined DG and RE	92
Table 4-46: Fuel Consumption of DG 4 on Combined DG and RE.....	92
Table 4-47: Electricity Production of DG 5 on Combined DG and RE	93
Table 4-48: Operation Hours of DG 5 on Combined DG and RE	94
Table 4-49: Fuel Consumption of DG 5 on Combined DG and RE.....	94
Table 4-50: Hydropower Simulation Result by Homer.....	96
Table 4-51: PV Simulation Results by Homer.....	97
Table 4-52: Wind Simulation Results.....	98
Table 4-53: Converter System Simulation Result.....	99
Table 4-54: Emissions of Simulation Results of Combined DG and RE	101
Table 4-55: Purchased and Sold Electricity by Palapas System on Combined DG and RE.....	102
Table 4-56: Costs of All Components on Combined DG and RE Connected into the Grid Using Chosen WInd Turbines.....	105
Table 4-57: Sensitivity Analysis of Fuel Cost Consumed by DG on Combined DG and RE Connected into the Grid Using Chosen Wind Turbine	107
Table 4-58: Sensitivity Results of Electricity Purchased and Sold by PALAPAS System on Combine DG and RE Connected into the Grid Using Chosen Wind Turbine	107
Table 4-59: Sensitivity Anlysis of Costs on Combined DG and RE Connected into the Grid Using Chosen Wind Turbine.....	108
Table 5-1: Voltage Spectrum of DB1 PJPP Bus bar on Situation A, B and C.....	271
Table 5-2: The Reduction of Sinusoidal Waveform of DB1 PJPP Bus bar on Situation A, B and C.....	272
Table 5-3: Voltage Spectrum of Donggala SB1 Bus bar on Situation A, B and C....	275

Table 5-4: The Reduction of Sinusoidal Waveform of Donggala SB1 Bus bar on Situation A, B and C.....277

Table 5-5: Voltage Spectrum of Maesa SB1 Bus bar on Situation A, B and C280

Table 5-6: Voltage Spectrum of Parigi DB1 Bus bar on Situation A, B and C284

Table 5-7: The Reduction of Sinusoidal Waveform of Parigi DB1 Bus bar on Situation A, B and C.....285

Table 5-8: Voltage Spectrum of Parigi SB1 Bus bar on Situation A, B and C.....288

Table 5-9: The Reduction of Sinusoidal Waveform of Parigi SB1 Bus bar on Situation C290

Table 5-10: Voltage Spectrum of Parigi SB2 Bus bar on Situation A, B and C.....293

Table 5-11: : The Reduction of Sinusoidal Waveform of Parigi SB1 (2) Bus bar on Situation A, B and C.....294

Table 5-12: Voltage Spectrum of PJPP SB1 Bus bar on Situation A, B and C.....297

Table 5-13: The Reduction of Sinusoidal Waveform of PJPP SB1 Bus bar on Situation A, B and C.....299

Table 5-14: Voltage Spectrum of Silae SB1 Bus bar on Situation A, B and C302

Table 5-15: The Reduction of Sinusoidal Waveform of Silae SB1 Bus bar on Situation A, B and C.....303

Table 5-16: Voltage Spectrum of Silae SB4 Bus bar on Situation A, B and C306

Table 5-17: Voltage Spectrum of Talise SB1 Bus bar on Situation A, B and C310

Table 5-18: The Reduction of Sinusoidal Waveform of Talise SB1 Bus bar on Situation A, B and C.....312

Table 5-19: Voltage Spectrum of Talise SB2 Bus bar on Situation A, B and C315

Table 5-20: Voltage Spectrum of Talise DB1 Bus bar on Situation A, B and C319

Table 5-21: The Reduction of Sinusoidal Waveform of Talise DB1 Bus bar on Situation A, B and C.....320

Glossary of Terms and Abbreviations

AC	Alternating Current
DB	Bus bar Code
DG	Diesel Generator
ETAP	Electrical Power System Analysis Software
GWh	Giga-Watt-hour
Homer	Hybrid Optimization Model for Multiple Energy Resources
kW	kilo-watt
kWh	kilowatt-hour
kW/m ²	kilowatt per meter square
LCOE	Levelized Cost of Energy
MVAR	Mega Volt Ampere Reactive
MW	Mega-Watt
NPC	Net Present Cost
NASA	National Aeronautics and Space Administration
O&M	Operational and Management
PALAPAS	Palu, Parigi and Sigi
PJPP	Bus bar Code
PLTD	Pembangkit Listrik Tenaga Diesel (Diesel Generator)
PT	Perseroan Terbatas (Limited Liability Company)
PLN	Perusahaan Listrik Negara (Public Utility)
PV	Photovoltaic
RE	Renewable Energy
SB	Bus bar Code
US\$	United States Dollar
VA	Volt-Ampere
WT	Wind Turbine

1 Introduction

Indonesia is the third largest population in the world with the total population of approximately 260 million after China and India. Electrical need continues to increase every year in line with population growth and Gross National Product (GDP). Although public utility installs more capacities every year to meet the demand but the enhancement of installed capacities is not proportional with the demand growth every year.

1.1 General Information

Diesel generator dominates most installed capacity in Indonesia especially in rural area. 72.82 % of installed capacity in Palu are dominated by diesel generators and the rest of 27,17 % is coal. Only few numbers of installed capacities are coming from renewable energy resource but most of them are isolated from the grid. Urban society requires more electricity than rural society to support all their activities. Unfortunately, the availability of installed capacities in urban area is also limited. Power shortage in Palu area is not only caused by the lack of installed capacity but also technical problem with some diesel generators.

Technical problem of diesel generators are caused by the lifetime of diesel generators exceeded more than 20 years. Even some of them are reaching 40 years. Normally the lifetime for the diesel generator to operate for 24 hours was only 10 years or could be maximum for 20 years.

The problem faced by Indonesian government in this case PLN to install more capacity is the funding. The price per kWh of electricity in Indonesia is quite low compared with developed countries. As a result, in addition to the price of electricity can not cover costs PLN also was not able to add new plants. To cover operational costs PLN, the Indonesian government has always subsidized drawbacks.

1.2 Objective of the Thesis

Alternative energies those can be adopted to replace fossil fuel should be a kind of energy that is redundant, clean and sustainable. Renewable energy for example hydro, PV and wind is the right choice to cover base load since they have low operational and maintenance cost. The adoption of renewable energy can contribute and replace some diesel generators to supply base load.

Public utility has to generate electricity as much as demand requires, but renewable energy particularly wind is fluctuating during the time depending on the weather condition. Due to their unpredictable behaviour because of weather condition, it is necessary to analyse wind speed, solar intensity and flow rate river data for some years to acquire an accurate of wind, PV and hydro behaviour potential profile.

Peak time where the system requires more electricity which lasts from 6 pm until 10 pm where there will be no electricity production from PV while at day time there will be more electricity production from PV but the load is low. The best technology of storage system might be adopted to store energy to be used to supply peak load. To be more accurate, the simulation with homer software will be executed to optimize the system. Simulation by using Homer software will determine:

1. To obtain some configurations of hydro, PV, wind and diesel generators that have low net present cost.
2. To obtain the configuration that can satisfy technical and economical side by optimization process to find the configuration that has the lowest net present cost.
3. To obtain the effect of net present cost in dealing with uncertainty of fuel price by sensitivity process to find net present cost of different fuel price of chosen configuration system.
4. To obtain the Levelized Cost of Energy of configuration before and after combining hydro, PV and with into the system.
5. Power quality such as sag, swell, interruption and harmonics is also evaluated in this research by comparing power quality before and after integrating RE into the grid and by implementing Homer results of all main bus bars on public utility

grid (palapas system).

1.3 Structure of the Thesis

The thesis consists of 7 chapters with the following contents:

Chapter 1 contains the introduction explaining the general information, overview of the background of the problem, the objective of the research and the structure of the thesis.

Chapter 2 contains electricity power in study area discussing general situation in Palu and surrounding area, grid condition, shortage problem and renewable energy potential in Palu and surrounding area.

Chapter 3 contains methodology of research discussing about how Homer Pro software simulates the data through the optimizations and sensitivity process to obtain the configuration system of combined hydro, PV, wind, diesel generator and coal-fired with the lowest price and the net present cost of the configuration system by considering different price of fuel.

Chapter 4 contains the result of simulation discussing about some variants configuration systems that meet technical and economical side including the use of different wind turbines from different manufacturer from Asia, Europe and America.

Chapter 5 contains the result of power quality evaluation consisting sag, swell, interruption and harmonics of all main bus bars on public grid (palapas system)

Chapter 6 is the reference containing 100 papers related to this work

Chapter 7 contains the conclusion discussing about the solution for the problem based on the objective of study.

2 Electricity Power in Study Area

Central Sulawesi is a province in Indonesia located at the center of the island of Sulawesi with its capital city of province called Palu. The newest data of the total population in central Sulawesi is not available yet but according to (BPS) the latest census was done in 2010 with the total number of population of 2.6 million and they estimate that the total number of population in 2014 is around 2.8 million.



Figure 2-1: Map of Sulawesi Island (Atlas of the World, 2016)

Central Sulawesi province consists of 13 districts and one city (Palu) and each district area can be seen below.

Table 2-1: Regencies and Cities in Central Sulawesi Since 2014 (BPS)

	Regencies	Area [km²]
1	Banggai Kepulauan	2,488.79
2	Banggai	9,672.70
3	Morowali	3,037.04
4	Poso	7,122.25
5	Donggala	4,275.28
6	Toli-toli	4,079.77
7	Buol	4,043.57
8	Parigi Moutong	5,089.91
9	Tojo Una-una	5,721.15
10	Sigi	5,196.02
11	Banggai Laut	725.67
12	Morowali utara	10,004.28
13	Palu	395.06

2.1 General Situation of Electricity in Palu and Surrounding Area

PLN is the utility owned by Indonesian government that is responsible to produce and supply electricity in Indonesia. Besides PLN, there are several private companies that also acts as a producer of electricity but only PLN is allowed to sell electricity to customers. The Transmission and distribution grid system are also owned by PLN. According to (PLN), there are two branches of PLN those responsible to all cities in Sulawesi province. One PLN branch is responsible for north Sulawesi Province, Gorontalo Province and central Sulawesi province and another one is responsible for South Sulawesi Province, Southeast Sulawesi province and West Sulawesi province. The division of the working area is not for supplying electricity but only to maintain the grid in those areas.

In Central Sulawesi province, there are three branches of PLN that consists of

- PLN of Palu area
- PLN of Toli-toli area
- PLN of Luwuk area

In Palu area, PLN is divided into two working area, they are

- PLN Palapas
- PLN Poso

The working area of PLN Palapas is including Palu, Donggala regency, Parigi regency and Sigi regency while the working area of PLN Poso is including Poso, Tentena, Kolonodale and Bungku. In those areas, PT PLN has branch offices. Palapas area is an interconnected system connecting Palu, Donggala, Parigi and Sigi while PLN Poso was an isolated system. Now Poso is connected to Makassar System (South Sulawesi Province).

2.1.1 Electrification Ratio in Central Sulawesi

According to the data from PT PLN in Palu area, the data of June 2012, electrification ratio in central Sulawesi is dispersed in to the following table below.

Table 2-2: Electrification Ratio in June 2012 (PLN)

	Area	Electrification ratio
1	Palu city, Donggala regency, Parigi regency and Sigi regency (PALAPAS)	56.04 %
2	Poso regency	75.89 %
3	Morowali regency	34.72 %

On Table 2-2, the highest electrification ratio is in Poso regency with electrification ratio of 75.89 %. This is caused by the availability of small scale of hydropower in Sulewana, Tentena located about 50 km from Poso regency. The second highest electrification ratio is Palapas system with electrification ratio of 56.04 %. In Busbar Parigi, there was diesel generator but it does not exist any longer therefore for the electrification ratio in Palapas area is less than 56.04%.

2.1.2 Power Balance in Central Sulawesi

Installed capacity in PALAPAS area consists of diesel generator owned by PLN, diesel generator rented by PLN from private company and coal-fired plant belongs to private company.

According to information obtained from public utility, total installed capacity in central Sulawesi is 193.87 MW. It is including all capacity owned by PLN, rented diesel generator and all capacities belonged to private company. The total rated capacity is 139.78 MW, total peak load is 113.99 MW, and total reserve margin is 8.53 MW. For more details about the location of all installed capacity in central Sulawesi can be seen on table 2-3. The total rated capacity is much lower than the total installed capacity, which has the efficiency only 51.46 %. This is because most of installed capacity (diesel generator) is used much longer than their lifetime.

Table 2-3: Power Balance in central Sulawesi (June 2012) (PLN)

	Area	Installed Capacity [MW]	Rated Capacity [MW]	Peak Load [MW]
1	Toli-toli System	38.37	27.50	25.46
2	Palapas System	125.24	92	92.59
3	Tentena System	6.53	3.13	2.12
4	Poso system	11.32	10.40	7.10
5	Kolonedale system	6.19	4.65	4
6	Bungku System	6.22	2.10	1.97
Sum		193.87	139.78	133.24

2.1.3 Installed Capacity in PALAPAS Area

Since this research has been begun in December 2012 therefore this research is restricted based on the situation before integrating hydro plant Sulewana. The research will be only focused on the area of PALAPAS interconnection system because it is the only interconnected system that exists in Palu while other areas are still an isolated system.

Table 2-4: Total Installed Capacity in PALAPAS Area in 2014 (PLN)

	Machine Model/Type	Starting Operation	Machine Serial Number	Installed Capacity [MW]	Rated Capacity [MW]
1	Mak 8 M 453-AK	1986	26849	2.5	1.8
2	Mak 8 M 453-AK	1986	26850	2.5	1.8
3	Mak 8 M 453-AK	1986	26851	2.5	1.8
4	Mak 8 M 453-AK	1986	26833	2.5	1.8
5	Mak 8 M 453-B	1989	27023	2.5	1.8
6	Mak 8 M 453-B	1989	27025	2.5	1.8
7	New Zulser Diesel 12 ZAV 40 S	1992	740138	7.6	3.5
8	New Zulser Diesel 12 ZAV 40 S	1992	740139	7.6	4.8
9	Hitachi Zulser Diesel 16 ZAV 40S	1999	7354	11	8.5
10	SWD 9 TM 410 RR	1978	3440	4.04	2.2
Total capacity in Silae				45.24	29.8
11	Sewa CPI 1 (Talise)	2010	-	10	7.5
12	Sewa CPI 2 (Silae)	2013	-	5	5
13	Sewa PBE (HSD) (MFO)	2011	-	20	15
14	Sewa KPM 1 (Talise)	2012	-	10	7.5
15	Sewa KPM 2 (Silae)	2013	-	5	2.2
Total Rented Capacity				50	37.2
16	Coal 1	2007	-	15	25
17	Coal 2	2007	-	15	
Total capacity in PALAPAS area				125.24	92

The total installed capacity in PALAPAS area based on the newest data in 2014 that can be seen on the table 3 above. The total installed capacity in PALAPAS area consists of:

1. Some diesel generator owned by PT PLN
2. Rented generators
3. Coal-fired plant owned by Private company

Some diesel generators owned by PT PLN have already reached their lifetime even out of their lifetime between 22 years old – 36 years old but the rest of them are still in the range of their lifetime.

Most of diesel generators owned by PLN are situated in Silae therefore it is named by PLTD Silae. PLTD is the abbreviation of Pembangkit Listrik Tenaga Diesel means diesel power plant. The total installed capacity in this case all diesel generators owned by PLN is 45.24 MW while the total rated capacity is only 29.5 MW. Based on this condition the efficiency of all diesel generators owned by PLN ranging from 46 % to 72.27 %.

Except Sewa CPI I and Sewa KPM I, all rented diesel generator are situated in Silae together with all diesel generator owned by PLN. Sewa CPI 1 and Sewa KPM 1 are situated in Talise substation. The total installed capacity of rented diesel generators is 50 MW while its rated capacity is 37.5 MW. It means their efficiency is around 75 % in average because they are started operating between the year of 2010 -2013.

To run all diesel generators, PLN is using HSD (High Speed Diesel Oil). For economical reason to reduce operational cost, especially for Sewa PBE, PLN uses two types of fuel. When the generator is started up they use HSD but after starting up, they use MFO (Marine Fuel Oil). Marine Fuel Oil is quite cheaper than High Speed Diesel Oil (PLN).

Coal Plant is situated in Mpanau, Tawaeli around 20 km from Palu city. This plant is belonging to private company but the land is belonging to local government in this case Palu government. The total installed capacity of coal plant is 30 MW consisting of 2 x 15 MW generators while the rated power is varied depending on the quality of coal they use. The output power of coal plant is varied between 9 MW – 12 MW.

2.1.4 Grid Condition in central Sulawesi

PALAPAS System is the only interconnection system in central Sulawesi. This system is connecting all area in Palu city and some area around it. Some areas around Palu system connected to PALAPAS system are Sigi, Donggala and Parigi.

Sigi is located about 10 km from Palu city center, Donggala is about 30 km from Palu city center and Parigi is about 100 km from Palu city center. PALAPAS system is connected by 70 kV sub transmission line connecting coal plant located in Tawaeli, Talise substation and Parigi substation. Talise substation will continue the power to the customer in Palu city through some sub-substations (distribution substation), one of them is located in Kamonji. Donggala substation will get electricity from PLTD silae while Tambu will get electricity from Parigi substation. Poso, tentena, Kolonedale, and bungku are some areas, which are out of the city, which are some isolated systems. Table 2-5 is showing the data of sub-transmission line (the length, the number and the voltage), distribution line (the length, the number and the voltage) and sub-distribution line (the length, the number and the voltage).

City (Palu), Kamonji, Tawaeli, Donggala, Tambu and Parigi on table 4 are all the areas connected to PALAPAS interconnection system, which have the total length of 101.1 km, the number of substation of 2 units and the voltage of 70 MVA. Actually there are 3 substation directly connected to the sub-transmission line i.e. Talise substation, Parigi sub-station and coal plant substation. Since coal plant is not own by PLN therefore it is not mentioned on table 4. MVN is the Medium Voltage Network connected sub-transmission line and distribution line has the total length of 2,867 km. LVN is the Low Voltage Network connected distribution substation (sub-substation) and sub-distribution substation with has the total length of 1,951 km and the total voltage of 145,366 MVA.

Table 2-5: Grid Data in Central Sulawesi (PLN)

	Operational Unit	Transmission [Km]	Substation		MVN [Km]	LVN [Km]	Sub-Substation	
			Sum	MVA			Sum	MVA
1	City	101.1	2	70	334.17	553	404	47,800
2	Kamonji				122.75	173	164	17,240
3	Tawaeli				130.50	146	132	13,200
4	Donggala				420.38	372	261	14,230
5	Tambu				253.66	235	129	5,520
6	Parigi				426.35	398	323	18,270
7	Poso	-	-	-	449.47	334	202	13,920
8	Tentena	-	-	-	355.86	164	167	8,031
9	Kolonedale	-	-	-	201.65	153	105	4,405
10	Bungku	-	-	-	172.44	82	65	2,750
	Sum	101	2	70	2,867	2,610	1,951	145,366

2.1.5 Shortage Problem in Central Sulawesi

According to (Lendamanu, 2013), most diesel generators on table above have already reached their lifetime. Some of them even are out of their lifetime about 22 years – 36 years. Because of this reason, some diesel generators, which are out of their lifetime, have technical problem quite often. When one or more diesel generators have technical problem, the system will not have enough capacity to supply demand especially for peak load.

Another reason why the system have shortage problem is because of maintenance schedule. When one or more diesel generators need to have maintenance, the system will not have enough capacity to supply demand. Because of these two reasons (Technical problem and maintenance), the outages for some area have to be executed. In reality outage will be executed not only due to the shortage problem on the supply side but also due to Installation, maintenance and improvement on the grid for example when PLN need to construct pile of distribution or sub distribution system (Lendamanu, 2013).

When some of the diesel generator have technical problem, it usually takes a few days to fix it. When this is occurred, some of load must be disconnected from the system especially during peak time which lasting from 5 pm to 11 pm. The disconnection of the load will be carried out in turns every day while diesel generators are still in the process to be fixed.

Power shortage in PALAPAS system is not only caused by technical problem of diesel generator and maintenance schedule but also caused by the lack of coal generation. The lack of coal generation is caused by the quality of the coal used. When the coal with high quality is used the system can produce 12 MW in each generator but for lower quality coal the system will only produce 9 MW for each generator.

When coal plant cannot produce electricity because of technical problem, large shortage occurs. In this situation the system must disconnect more loads not only on peak time (evening) but also at daytime. Fortunately this situation is rarely found. In this situation Palu, Donggala and Sigi areas are only supplied by the diesel generators situated in Silae and Talise substation. Parigi is supplied by substation Kasimbar but diesel generator in that substation has been shut down. Therefore now Parigi only gets electricity supply from Palu.

2.2 Renewable Energy Potential in Palu and Surroundings

According to (Sutrisna), central Sulawesi has important renewable energy potential especially hydro and geothermal potential. This research will also explore other renewable energy sources for example wind and solar potential.

2.2.1 Hydro Potential at Selected Location (Pakava River)

Pakava River is located in Donggala district around 20 km from the east part of Palu city, which pass through Gimpu Village (sub district of Pinembani) on the upstream and Lalundu village. Pakava river is located on the mountain with the height about 500 m above sea level but to reach the river we have to reach the height of 1200 meter and then go down about 700 meter. The access to reach 1200 m height can be reached by car but to go down for 700 meter only possible by motorbike.

According to (Ayu, 2014), Currently the use of water around Pakava River is relatively low whereas the existence of water from the river is relatively abundant especially in rainy season. The fulfilment of daily water needs of the community around the river are still using the ground water therefore it is necessary to shelter the water from the river to fulfil the lack of water needs by constructing the reservoir.

The ministry of civil work in Palu had conducted the pre-feasibility study to estimate the economic and technical potential of Pakava River. At the moment, they have conducted feasibility study done by civil engineering consultant from Surabaya to calculate economic and technical potential of the river for some utilization. By construction the reservoir hopefully can help to meet electricity need of local community around the river and also can fulfil the need of clean water of local community.



Figure 2-2: Upstream of Pakava River

2.2.1.1 Flow Rate of Pakava River

According to the ministry of civil work in Palu through the research centre of river in Palu, they had measured the flow rate of the river by 2002. The measurement had been conducted every two weeks per month during 10 years on the upstream of the

river. The equipment used to measure the river flow rate is hydrometric and the result of the measurement can be seen on table 2-8 below.

Table 2-6: Flow Rate of Pakava River for 10 Years (Booklet, 2014)

Month	Flow Rate [m ³ /s]										Average Flow rate [m ³ /s]
	2002	2003	2004	2005	2006	2007	2008	2009	2010	2011	
January	3.44	5.92	2.68	4.73	5.15	5.92	7.17	8.62	4.21	7.86	5.57
February	4.98	7.22	3.08	5.51	4.95	6.07	6.66	7.87	4.75	7.48	5.86
March	3.15	7.9	2.79	5.59	3.99	4.97	8.47	5.88	3.81	6.28	5.28
April	2.92	8.06	3.27	6.18	4.9	4.95	11.23	6.35	4.4	5.56	5.78
May	4.82	6.92	4.02	7.49	6.12	4.58	10.2	7.2	5.69	4.15	6.12
June	7.46	7.38	4.26	9.03	7.71	5.36	10.54	6.39	7.46	3.02	6.86
July	6.67	7.41	3.43	7.59	7.06	5.59	10.15	4.33	10	2.23	6.55
August	4.87	7.14	2.86	5.73	5.03	5.42	12.25	3.65	11.58	1.73	6.03
September	4.11	5.66	2.07	4.32	4.74	5.92	12.1	3.27	11.88	2.23	5.63
October	3.15	3.86	1.97	4.16	4.19	5.83	12.15	2.71	10.62	3.48	5.21
November	2.9	2.79	2.71	5.09	3.88	5.9	13.48	3.41	9.75	3.91	5.38
December	4.27	2.28	3.88	5.24	5.15	6.67	11.06	3.93	9.08	3.95	5.5

Table 2-8 shows that the river flow rate varies greatly from month to month throughout the year as long as 10 years depending on the level of rainfall of the river location. Ten years flow rate analysis result is showing that flow rate behaviour of the year 2002, 2004, 2005, 2006, 2007, 2009 and 2010 have the same behaviour closed to 85%. Figure 2-3 is showing 7 years flow rate analysis result of Pakava River.

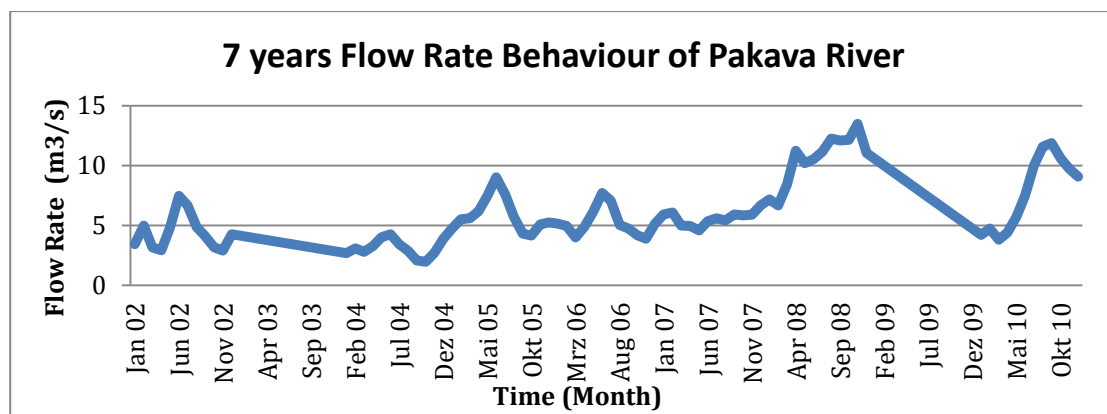


Figure 2-3: 7 Years Flow Rate Analysis Results of Pakava River

The shape of the graph on figure above is showing the same the behaviour but the flow rate is becoming higher from year to year. The minimum flow rate is about 1.75 m³/s and the maximum flow rate is around 14 m³/s.

Flow rates of the last three years are higher than flow rates of 7 years earlier. Their flow rates have the same fluctuation and the value of flow rate from one month to other month is almost the same. A small difference is shown on the peak of last year that shows that there is not fluctuation (no valley). From the Peak, it is going down to 2 m³/s and starting going up again. Flow rate minimum is 2 m³/s but flow rate maximum is 9 m³/s.

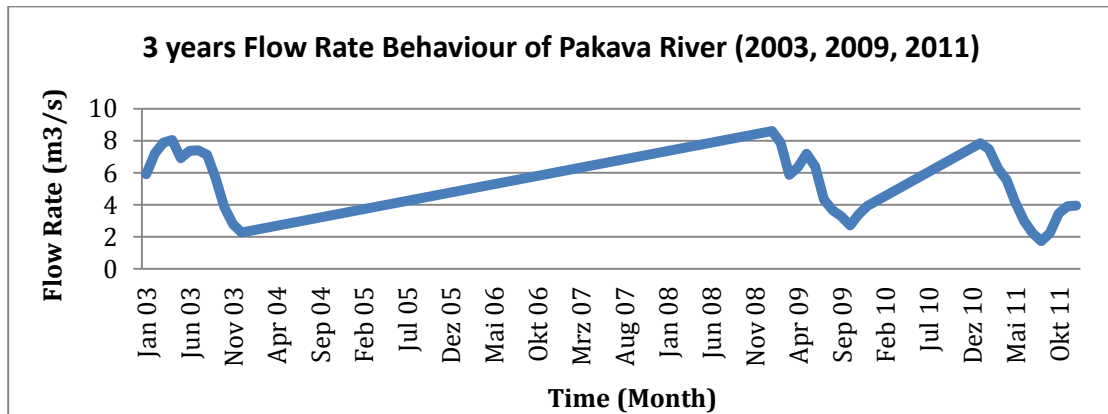


Figure 2-4: 3 Years Flow Rate Analysis Results of Pakava River

To obtain accurate result, it is necessary to analyse long term flow rate fluctuation. Figure 2.5 is showing 10 years' flow rate fluctuation of Pakava River. Electricity production calculation from hydropower is using 10 years flow rate average of the river. Table 2.9 is showing 10 years' flow rate average of Pakava River that shows the highest average flow rate is occurred in June with flow rate of 6.86 m³/s and flow rate minimum is occurred in March with flow rate of 5.28 m³/s. Flow rate average on table 2-9 below is 5.81 m³/s.

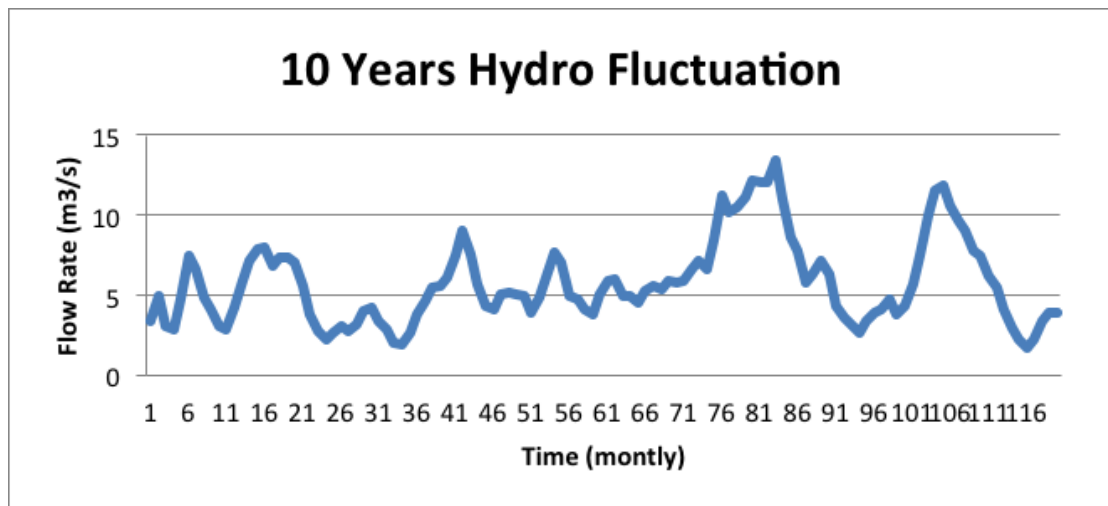


Figure 2-5: Ten Years Flow Rate of Pakava River

Table 2-7: Monthly Average Flow Rate of Pakava River

Month	Average Flow Rate [m ³ /s]
January	5.57
February	5.86
March	5.28
April	5.78
May	6.12
June	6.86
July	6.55
August	6.03
September	5.63
October	5.21
November	5.38
December	5.50
Average	5.81

2.2.1.2 Electrical Potential

According to (Ayu, 2014), the ministry of civil work branch Palu in this case the research centre of river in Palu has decided to build reservoir to accommodate the water before canalizing the water to the turbine through penstock. The head height is not decided yet but it will be around 40 meter to 100 meter.

Before calculating electrical potential of the river, it is necessary to decide the head. In this research it is decided to use 70-meter head.

Table 2-8: Monthly Generated Electricity

Month												
P _{el} [MW]	Jan	Feb	Mar	Apr	May	Jun	Jul	Aug	Sep	Oct	Nov	Dec
	3.12	3.28	2.96	3.23	3.43	3.84	3.67	3.38	3.15	2.92	3.01	3.08
Average	3.26 MW											

Table above shows that the average generated electricity is 3.26 and the highest and the lower are respectively 2.96 MW and 3.84 MW.

2.2.1.3 Selected Hydro Turbine

To select turbine type, the head and the average flow rate need to be considered. In addition to determine the type of hydro turbine, it is necessary to use figure 2-6. The suitable hydro turbine for 70 meters head and average flow rate of 5.81 m³/s is Francis turbine.

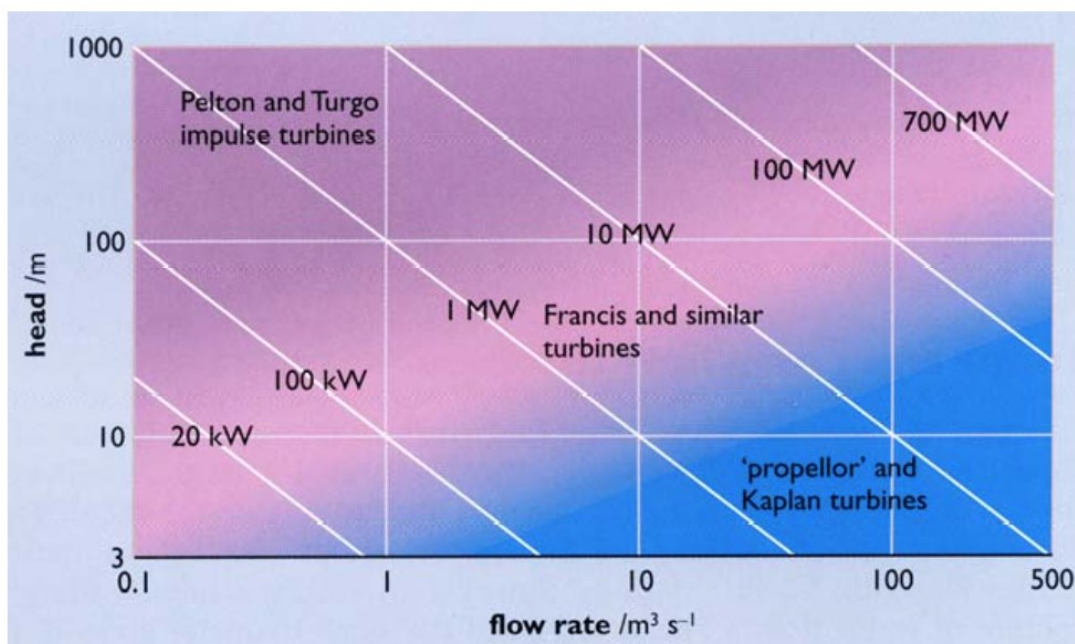


Figure 2-6: Different Type of Hydro Turbine Ranges and Application (Boyle, 2003)

2.2.1.4 Energy Production From Hydro Source

Energy production from hydro source can be calculated by multiplying produced electricity on table 2.10 by the number of hours. Table 2-11 shows the total energy production per year from hydro source is 28.56 GWh. The highest energy production is in January and the lowest energy production is in December.

Table 2-9: Energy Production per Year from Hydro Resource

Month												
Energy [GWh]	Jan	Feb	Mar	Apr	May	Jun	Jul	Aug	Sep	Oct	Nov	Dec
	2.32	2.20	2.20	2.32	2.55	2.76	2.73	2.51	2.27	2.17	2.22	2.29
Total	28.56 GWh(Total Energy Production per Year)											
Average	2.38 GWh											

2.2.2 Solar Potential at Selected Location

Palu is one of cities in Indonesia located on equator with abundant sunshine. According to (World Weather), monthly average temperature in Central Sulawesi varies from 23°C to 34°C that can be seen on figure 2-7. The data for charts above are taken from year of 2000 to 2012.

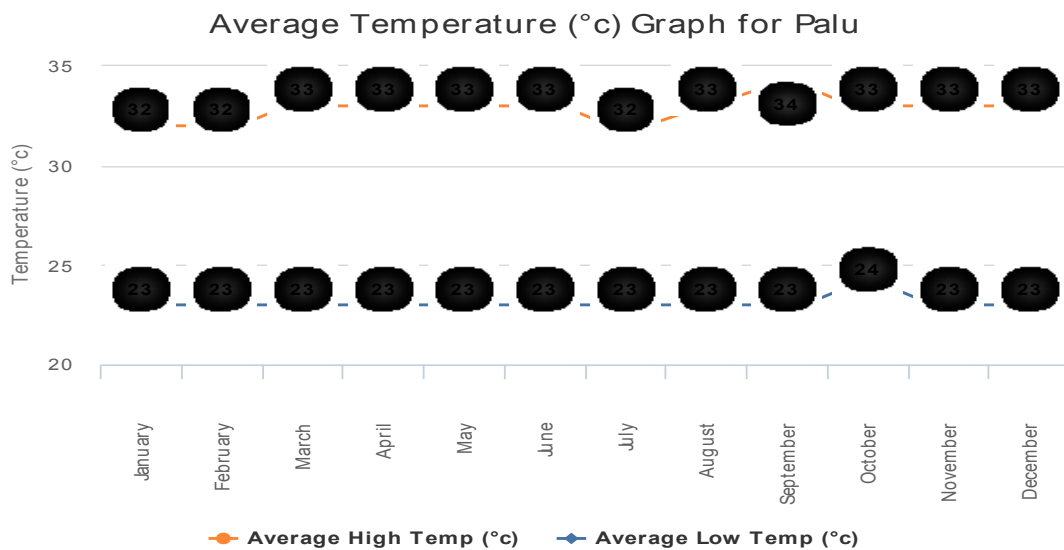


Figure 2-7: Average Temperature in Palu in Degree Celcius (World Weather)

According to (Rumbayan, 2012), “the solar radiation is divided to three classifications, i.e. low (below 4.9 kWh/m²), medium (4.9 - 5.25 kWh/m²) and high (above 5.25 kWh/m²).” Monthly solar insolation data in Palu obtained from (Rumbayan, 2012) can be seen on table below. Based on table 2-12, solar insolation average in Palu for one year is 5.41 h. This means that solar insolation in Palu is categorized as high potential.

Table 2-10: Monthly Solar Radiation Data in Palu (Rumbayan, 2012)

	Jan	Feb	Mar	Apr	May	Jun	Jul	Aug	Sep	Oct	Nov	Dec
Monthly Solar Insolation [Hour]	5.24	5.34	5.43	5.28	5.46	5.2	5.7	5.84	5.6	5.22	4.98	5.67
Average	5.41 h											

2.2.2.1 Hourly Sun Availability and solar radiation

To estimate solar potential in one location it is necessary to get the solar radiation data of that location. The measurement of solar radiation for long period will present accurate solar radiation data of certain location.

Based on interview with the head of data of the Meteorology, Climatology and Geophysics in Palu, they records the sunshine availability using the equipment called Campbell stokes. This equipment consists of a ball made of glass and the tape made from paper with the scale that showing the duration of sunshine. The sunlight will go through the ball and burn the tape. When there is not sun, the tape is not burnt.

2.2.2.2 Peak Sun Hours

According to (International), “peak sun hours are the situation when one location has sunshine that equals to 1,000 w/m², which normally occurred for certain period of time. If the data of solar radiation in one location is not available, peak sun hours data can be used to estimate solar potential in that location.”

The data used for this research is the hourly sun availability data of 2008, 2009, 2013, 2014 and 2015. The data is the percentage of sun availability for one day.

Sorting the data that has sun availability percentage value and converting it to the number of hours and did the calculation of peak sun hours. The result of the calculation of peak sun hours can be seen on.

Table 2-11: Peak Sun Hours Results

Year	Peak Sun Hour
2008	4.84 hours /day
2009	5.12 hours /day
2013	4.64 hours/day
2014	5.70 hours/day
2015	5.50 hours/day
Average	5.16 hours/day

Based on table above, the average peak sun hours are 5.16 hours/day that means it is equal to 5.16 kWh/m². The average of monthly solar insolation on table 2-12 is 5.41 kWh/m² that almost equals to the average peak sun hours on table 2-13 above.

2.2.2.3 Energy Production from PV

Energy production from PV is calculated based on solar insolation converted to solar radiation for 1 year. Solar insolation obtained from weather forecast department in Palu is analysed by taking the average value of solar insolation for 5 years. Figure 2-8 is showing electricity production from PV for 1 year. Energy production from PV is calculated by multiplying solar radiation by sun availability. Energy production from PV can be seen on table below.

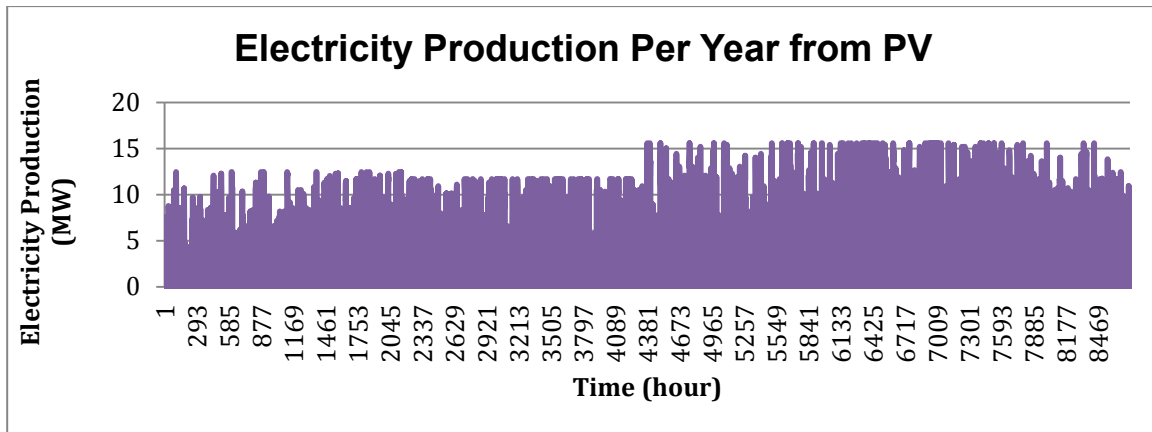


Figure 2-8: Electricity Production of PV for 1 Year

Table 2-12: PV Energy Production

Month	Energy Production [MWh]
January	1458.22
February	1582.80
March	2153.52
April	2017.03
May	2051.45
June	1768.41
July	2274.97
August	2377.93
September	2754.96
October	2968.24
November	2712.50
December	2164.81
Average	2190.40

The highest energy production from PV based on table above occurred in October and the lowest energy production from PV occurred in January. It is caused by high rainfall level in January and low rainfall level in October. The average energy production from PV per month is 2190.40 MWh.

2.2.3 Wind Potential at Selected Location

To obtain wind potential in one location it is necessary to measure wind speed for a long period of time to get brief information about wind behaviour in that location.

2.2.3.1 Analyzing Wind Speed

Compared with other renewable energy sources, wind is more fluctuating. The fluctuation of wind speed in one area depends on the weather condition of the area. Based on its behaviour, wind speed should be accurately analysed. Two years wind speed fluctuation can be seen on figures below.

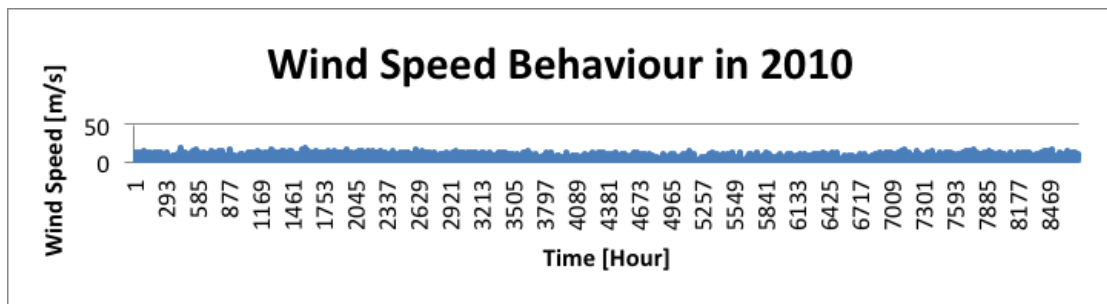


Figure 2-9: Wind Speed in 2010

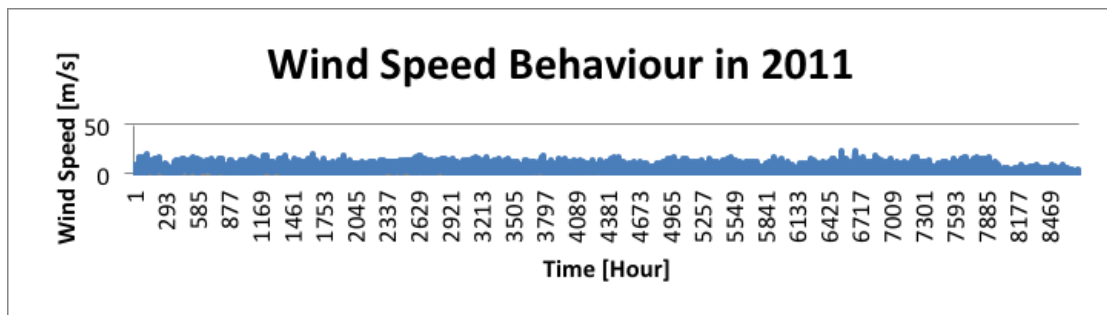


Figure 2-10: Wind Speed in 2011

Figure 2-9 and figure 2-10 above are wind speed fluctuation of 2010 and 2011 obtained from Meteorology Climatology and Geophysics Council in Palu. Wind speed data obtained from that council was in knots and converted to m/s. Wind speed with its relative frequency can be seen on table 2-13 below.

Table 2-13: Wind Speed Performance in 2011

Wind Speed [m/s]	Relative Frequency h_i [%]
0	19.26
1	10
2	14.24
3	10.6
4	9.45
5	7.03
6	6.12
7	5.45
8	4.83
9	4.06
10	3.23
11	2.27
12	1.48
13	0.9
14	0.41
15	0.27
16	0.06
17	0.01

To calculate wind speed distribution for 1 year, the latest wind speed data is used. This research is begun in December 2012. It was decided to have 100 meter hub height and varied wind speed from 0 – 17 m/s.

3 Methodology of research

Homer (Hybrid Renewable and Distributed Generation System) is a simulation and optimization software that can model micro grid and simulate different technology generations based on renewable and non-renewable energy. (States)

3.1 HOMER Software

Homer software aims at micro-grid modelling that considers technical and economical side. Homer software is doing three different tasks; simulation, optimization and sensitivity analysis. Simulation part in Homer will design a configuration system that simulate every hour data over the year to find out the technical behaviour and economical consideration of those configuration systems. Optimization in Homer software is to find out which configuration systems can meet the constraints on technical side and the lowest price. Sensitivity is the process in Homer software to deal with uncertainty for example fuel price that will affect the optimization result especially the net present cost (States)

3.1.1 Load

Homer software provides AC load and DC load. For AC load, Homer provides different type of loads that consists of primary load, thermal load and hydrogen load. Primary load consists of electric load and deferrable load.

In primary load, modeller can specify the type of load for example; commercial load, residential load, industry load or community load. Modeller can input load data manually or import from time series file. The load data used in advanced load is the load for whole year from January to December and modeller also can specify in which month the peak load occurred. Each month there is a single hourly load for 24 hours as an overview of load characteristic in that month as can be seen on figure 3-1 below. Modeller also can separate load data based on weekdays load and weekend load. After inputting load data, modeller can see daily, monthly and yearly load.

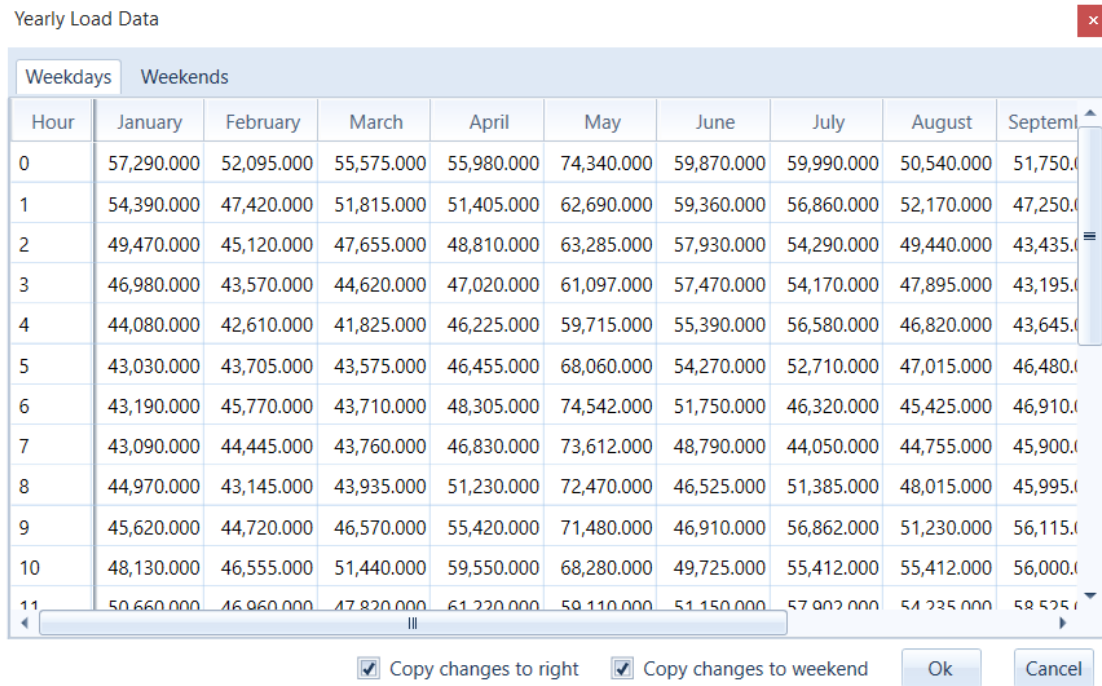


Figure 3-1: Yearly Load Data Input

In primary load, there is a special feature called operating reserves that can be suddenly mobilized if there is an increase of demand and renewable supply is decreased. For grid-connected system it is not necessary to consider the operating reserve since grid will supply if the micro grid system cannot meet its demand. Although the electricity price is quite high to buy from grid but the system will buy electricity from the grid to avoid unmet load that will lead to shortage problem.

If the primary load is a type of load that need to be supplied first, deferrable load is a type of load that can be postponed to supply for example battery bank, water pumps and ice maker. To input the data of deferrable load in Homer software, modeller can input the daily average load in kWh/day for whole year. After input the deferrable load, modeller will obtain the information about the scaled annual average of the load in kWh per day. Modeller can also specify some parameter for example; storage capacity in kWh, peak load in kW and the percentage of minimum load ratio. The schematic of how to input the deferrable load can be seen on figure 3-2 below.

Enter Monthly Averages

Month	Average Load (kWh/d)
January	355,553,738.000
February	23,338,993.000
March	33,388,839.000
April	30,009,377,388.
May	333,999,380.000
June	35,555,499,987.
July	377,735,655,300
August	377,736,663,000
September	3,888,888,839,5
October	388,831,555,630
November	222,992,000,270
December	226,355,477,610

Annual Average (kWh/d): 18,862,956,905,891,380,134,989.42

Figure 3-2: Deferrable Load Data (States)

In Homer software thermal load will be supplied either by boiler or the excess heat production from diesel generator and also from resistive heat by taking from excess electricity. To input thermal load in Homer software, modeller can follow the same way with primary load. Figure 3-2 is showing the window to input deferrable load. Modeller can specify the type of load for example residential, community, industry or commercial. It also provides the feature to input deferrable load data from time series or input manually. Modeller also can specify in which month the peak load occurred.

Create a synthetic load from a profile:

Peak Month: January July None

Profile: Residential

Ok

Import a load from a time series file:

Import and Edit... Import...

Figure 3-3: Thermal Load Setup (States)

To supply load, Homer software is providing AC and DC bus. Sources on AC bus will first supply primary load on AC bus and then supply primary load on DC bus. After that sources on AC bus will supply deferrable load on AC bus and then supply deferrable load on DC bus. After that sources will charge the battery bank and if there is excess electricity, the system will sell it to the grid with certain price.

3.1.2 Components

Homer software provides some components of generation technologies based on renewable energy and non-renewable energy for example; diesel generator, PV, wind turbine, hydro and hydrokinetic. Homer software also provides some products for every component from different manufacturers equipped by their technical data. This can be obtained on the library of Homer software.

3.1.2.1 Diesel Generator

There are different kinds of diesel generator product in Homer software with different power rating from 10 kW to 2000 kW. Besides common diesel generator, Homer also provides auto sized diesel generator functioning as a system backup. The power rating of auto sized diesel generator is adapted to the system configuration modelled in Homer software. Homer also provides prices of all generation technology sources.

To input diesel generator data, modeller can specify different size of diesel generator in search space window. To input the site-specific data of diesel generator, modeller can specify the percentage of the minimum load ratio and heat recovery ratio, minimum run time in minutes and the lifetime of diesel generator in hours.

To input diesel generator price, Homer provides window to input the capital cost, replacement cost and operational/maintenance cost of diesel generator. Operational and maintenance cost is determined based on the fuel price needed to run 1 kW diesel generator per hour. In this case, modeller need to specify the type and the price of fuel used to run the system. Modeller can also consider different fuel price on the sensitivity analysis column on the right side of fuel price.

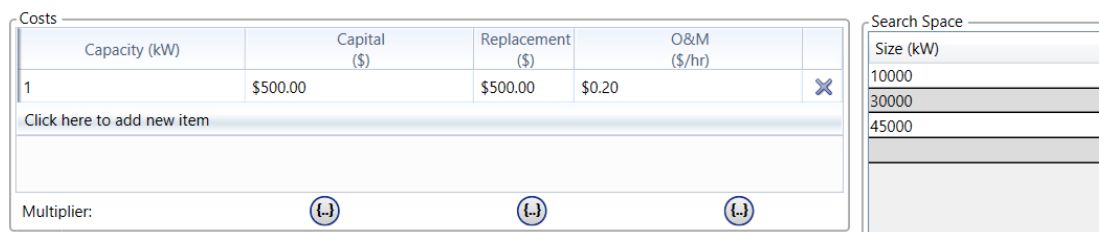


Figure 3-4: Window Setup Diesel Generator Data

Figure 3-4 is showing the window to set up the size and different cost of diesel generator. That window is only to specify one diesel generator. To consider different price of capital, replacement and operational and maintenance cost, modeller can add more than one price of each of them on the space exactly below their specific price. Modeller can add more than one diesel generator including auto size diesel generator. The way to input the data is the same except auto sized diesel generator.

To consider emission produced by each type of diesel generator, Homer also provides its own amount of diesel generator emission by assuming that diesel generator used in the system is new. In this case modeller can also specify own emission production if the diesel generator used in her system is not new. The default setting of emission data provided by Homer for diesel generator using diesel fuel can be seen below (States).

- Carbon Monoxide : 6.5 g/L of fuel
- Unburnt Hydrocarbons : 0.72 g/L of fuel
- Nitrogen Oxides : 58 g/L of fuel
- Proportion of sulphur converted to PM : 2.2 g/L of fuel
- Particulate matter : 0.49 g/L of fuel

To calculate the average electrical efficiency of diesel generator, Homer is using the following equation.

$$\eta_{gen} = \frac{3.6.E_{gen}}{m_{fuel}.LHV_{fuel}} \dots\dots\dots(1) \text{ (States)}$$

where E_{gen} is the total annual electrical production of diesel generator in [kWh/year], m_{fuel} is the total annual fuel consumption of diesel generator in [kg/year], and LHV_{fuel} is fuel lower heating value in [MJ/kg]. The value of 3.6 on the equation set because 1 kWh is equal to 3.6 MJ.

3.1.2.2 Photovoltaic

Homer also provides different product of PV module from selected manufacturers. Two types PV module provided by Homer are generic flat plate module and concentrating module. They are equipped by their own technical data.

Modeller can input the MPPT (Maximum Power Point Tracker) data to match between PV panel and battery bank or grid. Modeller also can include the advanced input consisting of the percentage of ground reflectance and tracking system. To consider the effect of temperature, Homer provides space to input the percentage of temperature effect on power per degree Celsius, nominal operating cell temperature in degree Celsius and the percentage of efficiency of standard test condition.

To input capital cost, replacement cost and operational and maintenance cost is the same like diesel generator. To consider different size of PV Park, modeller can input different size of PV on the search space located on the right side of window space price. The percentage of derating factor of PV and the lifetime in years must be

included on their column spaces. The same like diesel generator, to consider different price of capital cost, replacement cost and operational and maintenance cost, modeller can input different price each of them.

To calculate PV array power output Homer is using the following question.

$$P_w = y_{PV} \cdot f_{PV} \left(\frac{\bar{G}T}{\bar{G}T_{STC}} \right) [1 + \alpha_p (T_c - T_{c,STC})] \dots \dots \dots (2) \text{ (States)}$$

where y_{PV} is PV array rated capacity or power output of PV array under standard test conditions in [kW], f_{PV} is the percentage of derating factor of PV in [%], $\bar{G}T$ is the solar radiation incident on the PV array in the current time step in [kW/m²], $\bar{G}T_{STC}$ is the radiation of incident at standard test conditions in [1kW/m²], α_p is power temperature coefficient in [%/°C], T_c is PV cell temperature in current time step in [°C] and $T_{c,STC}$ is PV cell temperature under standard test condition in [25°C].

According to (States), if modeller does not consider the temperature effect on PV array Homer will presume that temperature coefficient as zero. To do so Homer will use the following equation.

$$PPV = Y_{PV} \cdot f_{PV} \left(\frac{\bar{G}T}{\bar{G}T_{STC}} \right) \dots \dots \dots (3) \text{ (States)}$$

3.1.2.3 Wind Turbine

Homer also provides some product of wind turbines from selected manufacturers with their technical data. The unit on search space of wind turbine window is not in kilowatt but in quantity, which means that modeller should specify the number of wind turbine included on the system.

Site specific input provided by Homer consists of lifetime of wind turbine in years, hub heights in meter and also the consideration of ambient temperature effect. Since

wind turbine is affected by the hub height, modeller also can consider the different hub heights in the sensitivity space.

Homer also provides the input space of power curve data of wind turbine, turbine losses and maintenance schedule. If modeller is using wind turbine, which are not available on Homer library, it needs to input the power curve of chosen wind turbine. Turbine losses provided by Homer software consists of the percentage of availability losses, the percentage of turbine performance losses, the percentage of environmental losses and the percentage of other losses. On maintenance space data, modeller can input the maintenance schedule of wind turbine on interval of operational hour and down time in real time. Modeller also can input the maintenance cost of each schedule.

To input the capital cost, replacement cost and operational and maintenance cost of every number of wind turbine is like diesel generator. To consider about different cost wind turbine, modeller can specify different price of wind turbine on sensitivity space.

To calculate wind resource variation with height Homer is using the following logarithmic:

$$\frac{U_{hub}}{U_{anem}} = \frac{\ln(Z_{hub}/Z_0)}{\ln(Z_{anem}/Z_0)} \dots\dots\dots (4) \text{ (States)}$$

to get the power profile to get the different value of wind speed at different height Homer use the formula as the following :

$$\frac{U_{hub}}{U_{anem}} = \left(\frac{Z_{hub}}{Z_{anem}} \right)^\alpha \dots\dots\dots (5) \text{ (States)}$$

where U_{hub} is wind speed at the certain wind turbine hub height (m/s), U_{anem} is the height of anemometer wind speed (m/s), Z_{hub} is wind turbine hub height (m), Z_{anem} is the height of anemometer (m), Z_0 is the description of the location of wind speed and α is the exponent of power law. The list of Z_0 can be seen on table 3-5 below.

Table 3-1: Zo Description and Value

Terrain Description	Z ₀
Very smooth, ice or mud	0.00001 m
Calm open sea	0.0002 m
Blown sea	0.0005 m
Snow surface	0.003 m
Lawn grass	0.008 m
Rough Pasture	0.010 m
Fallow field	0.03 m
Crops	0.05 m
Few trees	0.10 m
Many trees few buildings	0.25 m
Forest and woodlands	0.5 m
Suburbs	1.5 m
City center, tall buildings	3.0 m

According to (States), to generate synthetic wind data Homer uses some algorithmic steps. Homer is creating auto correlated numbers sequence; one is for every time step of the year by applying first-order autoregressive model.

$$Z_t = a \cdot Z_{t-1} + f(t) \dots \dots \dots (6) \text{ (States)}$$

where Z_t is the value in time step i, Z_{t-1} is the value in time step i-1, a is autoregressive parameter and f(t) is a ‘white noise’ function returning a random number drawn from a normal distribution with mean of zero and a standard deviation of 1. Homer also does the setting that

$$a = r1 \dots \dots \dots (7) \text{ (States)}$$

where r1 is one time step of autocorrelation coefficient. When the time step is not 60 minutes it is necessary to calculate the autocorrelation coefficient of the one-hour autocorrelation factor. Expecting that logarithmic decay of the autocorrelation function by using the equation that set k as a time step of autocorrelation parameter.

$$r_k = r1^k \dots \dots \dots (8) \text{ (States)}$$

where r1 is

$$r1 = exp \left[\frac{\ln(rk)}{k} \right] \dots\dots\dots (9) \text{ (States)}$$

where *rk* is the one-hour autocorrelation factor and *k* is the number of time step fitting for one hour. *k* in this case is

$$k = \frac{60}{t} \dots\dots\dots (10) \text{ (States)}$$

3.1.2.4 Hydro

Hydro component provided by Homer consists of generic hydro and kinetic hydro. Modeller can use generic hydro to model hydropower based on waterfall or river located on the mountain with high head approximately more than 20-meter height. While kinetic hydro can be used to model hydro plant based on river with low head of approximately 10 meter height or less.

To model hydro plant, modeller needs to input hydro turbine data that consists of:

- Available head (m)
- Design flow rate (L/s)
- Minimum flow rate (%)
- Maximum flow rate (%)
- Turbine efficiency (%)

After designer inputs all turbine data above, automatically Homer will determine nominal capacity of hydro plant. Homer also provides the percentage of pipe loss of intake pipe data but designer also can specify this data.

To input capital cost, replacement cost and operational and maintenance cost of hydro turbine, designer can use data provided by Homer. Homer provides the same cost for capital and replacement cost of hydro turbine, without operational and maintenance cost. The lifetime of hydro turbine provided by Homer is 25 years.

As with earlier discussion of some components, designer can consider different data of turbine and different price of hydro turbine cost by inserting in sensitivity column Homer provided. In this simulation designer also can consider her system with or without including hydro plant to compare which configuration has lower cost.

To calculate flow rate available to hydro turbine Homer is applying the equation below.

$$Q_{available} = Q_{stream} - Q_{residual} \dots \dots \dots (11) \text{ (States)}$$

where Q_{stream} is the total stream flow in [m³/s] and $Q_{residual}$ is residual flow in [m³/s].

To calculate electrical power output of the hydro turbine Homer is using the following equation.

$$P_{hydro} = \frac{\eta_{hydro} \cdot \rho_{water} \cdot g \cdot h_{net} \cdot Q_{turbine}}{1000 \text{ W/kW}} \dots \dots \dots (12) \text{ (States)}$$

where P_{hydro} is power output of the hydro turbine in [kW], η_{hydro} is the percentage of hydro turbine efficiency [%], ρ_{water} is water density in [1000 kg/m³], g is acceleration of gravity [9.8 m/s²], h_{net} is head in [m] and $Q_{turbine}$ is the flow rate of hydro turbine in [m³/s].

3.1.2.5 Grid

In addition the use of battery bank to stabilize the micro grid, in Homer simulation designer can connect the system to the grid. Connecting micro grid into the distribution grid will allow micro grid to purchase or to sell electricity. If the micro grid has higher demand than its generation (generation based on renewable energy), the system can decide whether buying electricity from the grid or switching on diesel generator. The decision in this case will be based on comparing the lower price between turning on diesel generator or buying electricity from the grid. Buying

electricity from the grid will contain energy charge and energy demand. Energy charge is built upon the total electricity bought in the term of billing while a demand charge is built upon peak load on the term of billing. If there is excess electricity from the micro grid, the system will automatically sell it to the grid at a particular price.

Connecting micro grid into the grid in Homer simulation will require some additional data. Homer software provides some rates that consist of simple rates, real time rates, schedule rates and grid extension. Designer can specify which rate select for the system.

On simple rates designer only needs to specify two parameters, grid power price in dollar per kilowatt-hour and grid sellback price also in dollar per kilowatt-hour. In this rates designer can decide about net metering whether net purchases calculated monthly or net purchases calculated annually.

On real time series and scheduled rates designer can specify sale capacity in kW and can put different capacities of it on sensitivity column. For purchasing electricity Homer provides two different purchase capacities, annual purchase capacity in kilowatt and monthly purchase capacity in kilowatt. On annual purchased capacity, designer also can put different capacity. On monthly purchase capacity designer can put different capacity of each month over the year.

Figure 3.5 and figure 3.6 are showing real time input rates of annual and monthly purchase capacity. To consider distributed generation cost designer should put interconnection charge cost in dollar and standby charge in dollar per year. On real time series and schedule rates, grid extension cost can be calculated by inserting grid capital cost in dollar per kilometre and the distance in kilometre.

There are two options to optimize the system, simulate system with or without the grid and include the grid in all simulation. Electricity purchase can be restricted by insert maximum net grid purchases in kilowatt-hour per year.

Homer provides some control parameters to restrict selling and purchasing electricity and also the use of the battery. Some parameters are the following:

- Prohibit grid from charging battery above price of (\$/kwh)
- Prohibit any battery charging above price of (\$/kwh)
- Prohibit battery from discharging below price of (\$/kwh)
- Prohibit grid sales for battery below sellback rates of (\$/kwh)
- Prohibit any grid sales below sellback rate (\$/kwh)

On grid extension, designer can specify capital cost in dollar per kilometer, operational and maintenance cost in dollar per year per kilometer, and grid power price in dollar per kilowatt-hour. Designer also can consider different prices of every cost by using sensitivity column.

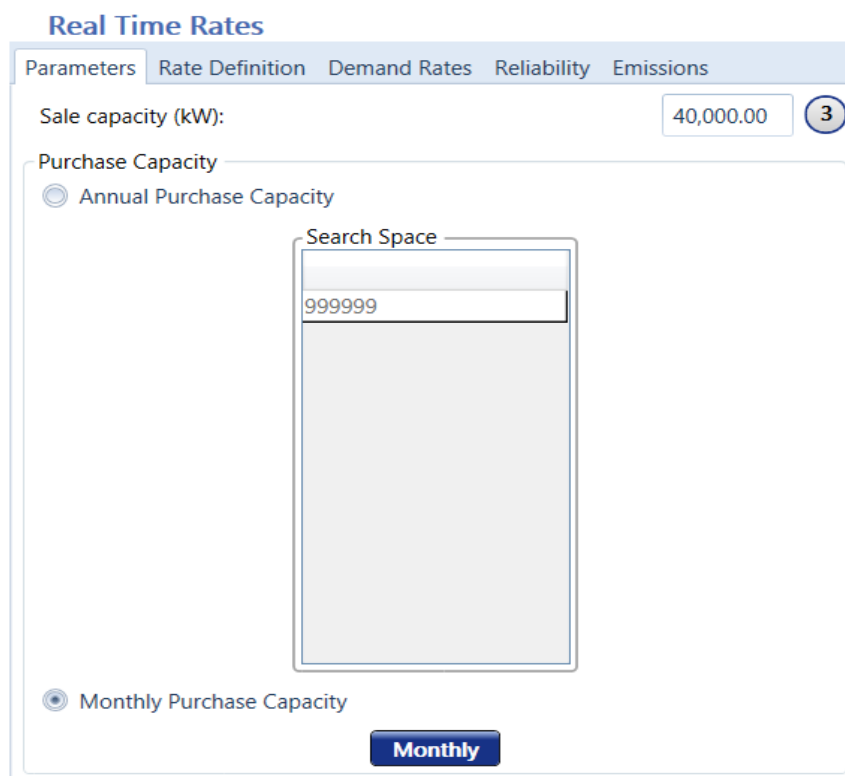


Figure 3-5: Real Time Input Rates and Schedule Rates of Annual Purchase Capacity (States)

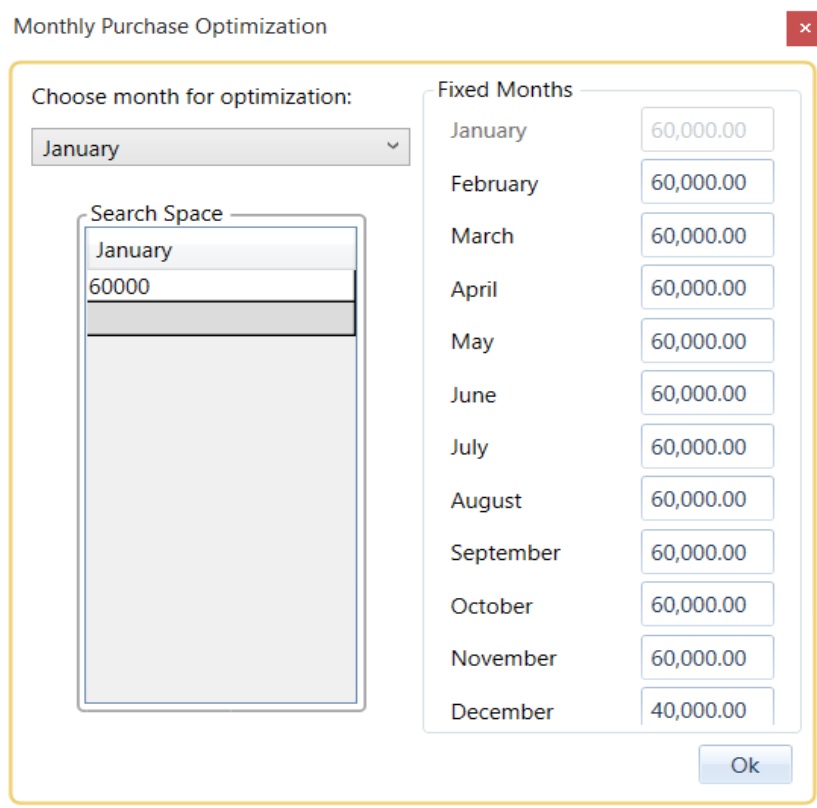


Figure 3-6: Real Time Input Rates and Schedule Rates of Monthly Purchase Capacity (States)

To calculate the total annual energy charge if net metering is not working Homer is using the following equation.

$$G_{grid, energy} = \sum_i^{rates} \sum_j^{12} E_{grid\ purchases, i, j} \cdot C_{power, i} - \sum_i^{rates} \sum_j^{12} E_{grid\ sales, i, j} \cdot C_{sellback, i} \dots \dots \dots (13) \text{ (States)}$$

where $E_{grid\ purchases, i, j}$ is the total energy purchased from the grid in month j during the time that rate i applies in [kWh], $C_{power, i}$ is the grid power price for rate i in [\$/kWh], $E_{grid\ sales, i, j}$ is the total energy sold to the grid in month j during the time that rate i applies in [kWh], $C_{sellback, i}$ is the rate of sellback for rate i in [\$/kWh].

To calculate the total annual energy charge if net metering is working Homer is using the following equation.

$$C_{grid,energy} = \sum_i^{rates} \sum_j^{rates} \left\{ \begin{array}{l} E_{netgridpurchases,i,j} \cdot C_{power,i} \text{ if } E_{netgridpurchases,i,j} \geq 0 \\ E_{netgridpurchases,i,j} \cdot C_{sellback,i} \text{ if } E_{netgridpurchases,i,j} < 0 \end{array} \right\} \dots\dots$$

.....(14) (States)

where $E_{net-grid-purchases}$ is the net energy purchased by the grid in this case energy purchased minus energy sold by the grid in month j during the time that rate I uses in [kWh], $C_{power,i}$ is the price of grid power for rate i in [\$/kWh] and $C_{sellback,i}$ is the rate of sellback for rate i in [\$/kWh].

According to (States), to calculate the total annual energy charged by the grid if net metering is working and the calculation of the generation is annually executed, Homer is using the following equation.

$$C_{grid,energy} = \sum_i^{rates} \left\{ \begin{array}{l} E_{netgridpurchases,i} \cdot C_{power,i} \text{ if } E_{energypurchases,i} \geq 0 \\ E_{netgridpurchases,i} \cdot C_{sellback,i} \text{ if } E_{energypurchases,i} < 0 \end{array} \right\} \dots\dots\dots$$

..... (15) (States)

where $E_{netgridpurchases,i}$ is the total energy purchased annually by the grid after reducing energy sold by the grid in [kWh], $C_{power,i}$ is the price of the grid power for rate i in [\$/kWh] and $C_{sellback,i}$ is the rate of sellback for rate i in [\$/kWh].

According to (States), to calculate the charge of total annual grid demand, Homer is using the following equation.

$$C_{grid,demand} = \sum_i^{rates} \sum_j^{12} P_{grid,peak,i,j} \cdot C_{demand,i} \dots\dots\dots (16) (States)$$

where $P_{grid\ peak, i, j}$ is the peak grid demand per hour in month j during the time that rates i is applied in [kWh] and $C_{demand, i}$ is the rate of grid demand in [\$/kWh/month].

3.1.2.6 Battery

To store the excess electricity designer needs to build battery bank. There are selected products of battery provided in Homer library equipped with their technical specifications. Designer just needs to decide which battery will match to the system.

After deciding the type of battery type, designer needs to specify the number of battery string and the number of battery put on each string. Normally the maximum battery string allowed is three. After specify those matters, automatically designer will get the bus voltage determined by Homer.

Site specific input window need to be filled by designer to determine the percentage of initial state of charge and the percentage of minimum state of charge. Initial state of charge is the parameter to determine maximum capacity the battery will be charged. Normally it could be 100 % or less. Minimum state of charge is the parameter to determine the minimum capacity energy need to be stored in battery. Normally the percentage of minimum state of charge at least 40 % otherwise it will cause permanent damage.

At the end of building battery bank, designer needs to insert minimum lifetime of battery. Depending on how often the system will use the battery. If the battery is used quite rare, it will last normally for 10 years but if the battery is used quite often it will last significantly less than 10 years.

If there is no generation from renewable energy sources, the system has two options to supply load. It depends on the amount of the load that will be supplied. Since the net present cost of diesel generator is getting lower linearly to the load capacity while the net present cost of battery is getting higher linearly to the load therefore the decision to supply the load will be the cross section between two line of battery bank

and diesel generator. Normally if the peak load is higher than base load, it is better to use diesel generator but if the load is lower than base load, it is better to use battery.

3.1.2.7 Converter

Converter is an electronic device to convert AC to DC or vice versa. In Homer software, converter is including inverter and rectifier. To design converter in Homer software, designer needs to specify the capacity of converter on search space window.

Homer separates input data for inverter and rectifier that consists of the percentage of relative capacity, the efficiency and the lifetime in years. To input the capital cost, replacement cost and operational and maintenance cost of converter Homer provides its own price but designer can input own price depending on the type of converter that will be used.

3.1.3 Resources

Homer provides different type of sources based on renewable energy and non-renewable energy. Some of resources provided by Homer are solar, wind, hydro, fuel and biomass.

3.1.3.1 Solar

There are two types of solar provided by Homer, solar global horizontal irradiance resource (GHI) and direct normal irradiance resource (DNI). GHI is used for flat plate PV components while DNI is used for concentrating PV component.

To input the solar radiation data, designer can download it from Internet, insert it manually or import from time series data. If the solar radiation data is downloaded from Internet through NASA website, it will come with monthly clearness index. The solar radiation data used in Homer is the daily solar radiation of every month. After inserting solar radiation data, designer will automatically obtain the annual average of solar radiation data.

3.1.3.2 Wind

Wind speed data needed in Homer is the average wind speed per month. Designer needs to insert average monthly wind speed data in meter per second over the year. After inserting wind speed data over the year, Homer will automatically calculate the annual wind speed data.

Wind speed data of the area can be obtained through NASA website. Designer just needs to type the name of the city and the average monthly wind speed over the year on that area will come. For the wind speed data obtained through NASA website, Homer provides its parameters for the altitude above sea level is zero and anemometer height of 10 meter. Designer can specify own parameters based on the location of wind power.

To consider variation with height, designer can specify surface roughness of wind power location. Normally roughness length depends on the terrain whether it is flat terrain without or with some obstacle for example houses, tree, skyscrapers, etc. The probability of data of wind speed follows Weibull distribution. In this case Homer also provides its own Weibull distribution parameter data that can be used as a general data of any terrains.

3.1.3.3 Hydro

The same like solar and wind, hydro source can be inserted manually, import time series data or download it through NASA website. Normally river flow rate is measured in meter cubic per second but in Homer designer needs to input river flow rate data in litre per second.

The average monthly river flow rate in litre per second has to be inserted over the year to get the annual river flow rate. Designer also can specify the residual of flow in litre per second.

3.2 Analysis the Real situation

Palu is a medium city which most of the population are working as government employees. The rest of population in Palu is working as farmers, fishermen and doing small business. Some small-scale industries exist in Palu but not very significant therefore the load profile over the year in Palu is different compared with any big cities in Indonesia for example Jakarta and Surabaya.

3.2.1 Daily Load Profile in Palu

Daily load profile in Palu will be classified into two different terms, weekday and weekend. Before analysing daily load profile in Palu, it is necessary to discuss about different types of customers in Indonesia.

3.2.1.1 Different Type of Customer in Indonesia

Indonesian government through public utility called PLN classifies four different types of customers; residential, business, government and social. Every type of customer has to pay different electricity price in kilowatt-hour and different base charge. PLN also limit the electricity supply to the customer based on the request of customer. For every type of customer PLN classifies the limitation in some categories based on the request of power request by customers. Some categories are the following:

- Residential : 220 VA – 6600 VA
- Business : 250 VA – 200 kVA
- Industry : 450 VA – 450 kVA
- Government : 250 VA – 200 kVA

3.2.1.2 Weekdays and Weekend Load Profile in Palu

One weekday was taken from load data of 2014 as a representative of weekdays load behaviour in Palu. The differences between weekdays load profile and weekend load profile in Palu is not significant. On weekend load becomes a little bit higher especially in the night but the curve shape of load behaviour is almost the same. It is caused by most people want to spend time in the evening until late night.

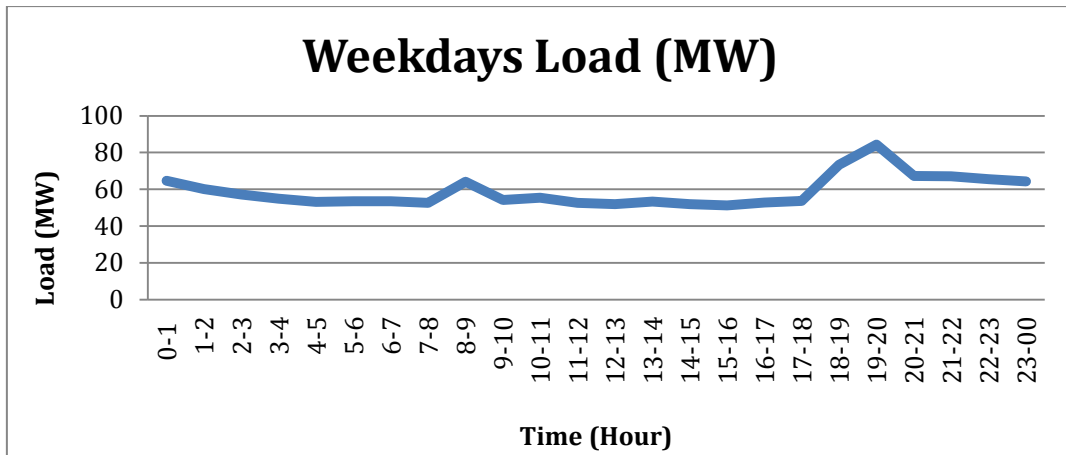


Figure 3-7: Load Profile on Weekdays in Palu

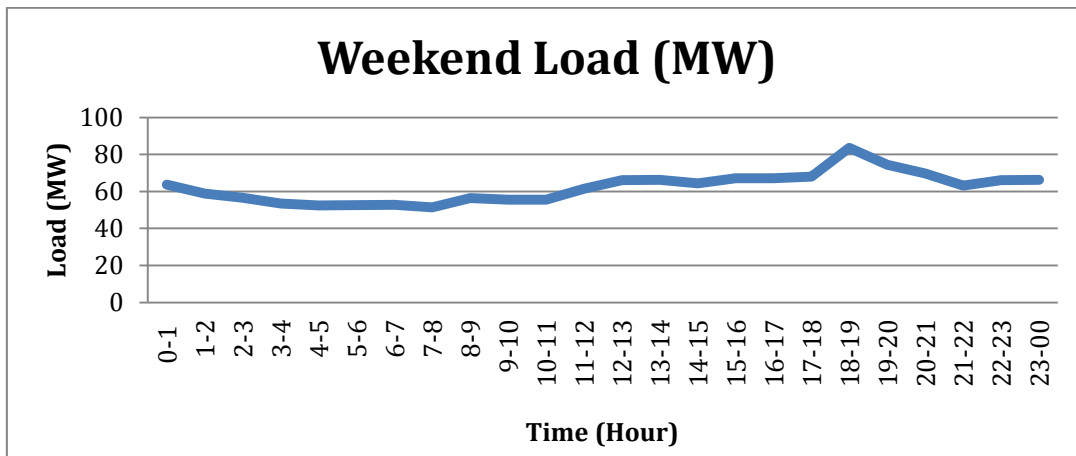


Figure 3-8: Load Profile on Weekend in Palu

Figure 3-7 and 3-8 above are showing load behaviour on weekdays and weekend in Palu. These two daily load profiles are taken from load profile in December 2014 due to the highest peak load. The increase of load in Palu is quite significant from year to year even from January to December in the same year. The increased of demand are caused by the increase of the number of customers and also caused by the increase of demand itself which means existing customers require more electricity. Therefore the load profile from January to December is quite different.

This research has been started since December 2012. There are some changes regarding the data has been done. Due to the lack of data, one-year loads profile data of 2014 is used to represent the existing load profile data in Palu.

3.2.2 Daily Electricity Generation from Hydro, PV and Wind

Daily electricity generation from hydro, PV and wind will not be distinguished into weekdays and weekend generation. In this research, both weekday and weekend electricity production from hydro PV and wind are assumed as a daily electricity production.

3.2.2.1 Daily Electricity Production from PV

When the weather is sunny, solar energy is available from 6 am to 6 pm therefore sun is available for 12 hours. Electricity production in clear weather condition can be seen on figure 3-9. This research will consider a 3 MW PV power plant.

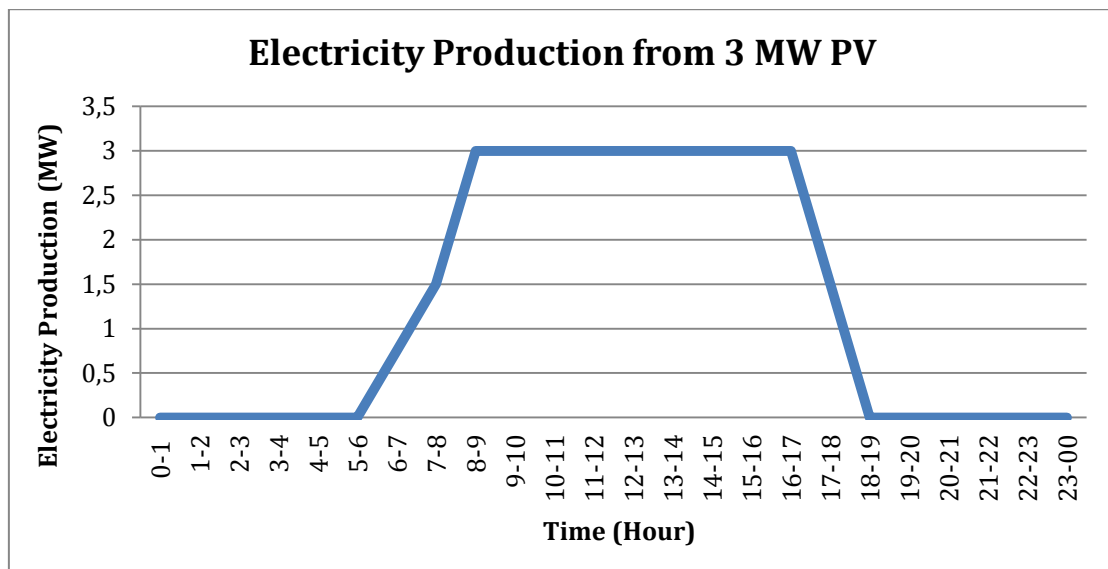


Figure 3-9: PV Daily Electricity Production on Clear Weather

3.2.2.2 Daily Electricity Production from Wind

Daily electricity production from wind is based on single day of hourly wind speed behaviour. One-day wind speed behaviour was taken from January as a representative of daily wind speed capacity. Five wind turbine are used to estimate electricity production from wind. Each turbine is contributing 2.35 MW. Table 3-10 is showing electricity production from wind using 5 wind turbines.

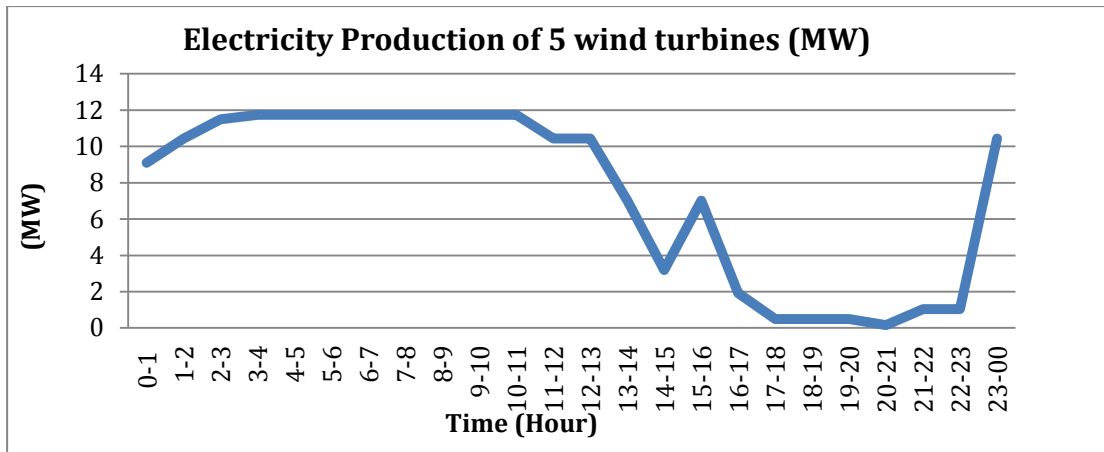


Figure 3-10: Daily Electricity Production from 5 Wind Turbines

3.2.3 Generation and Load

Analysing weekday generation profile of hydro, PV and wind are based on average flow rate of hydro source, solar insolation of one of working days (January 17th 2014), and one of working day of the analysing result of wind speed (January 3th). Load data is taken from one of working days in 2014.

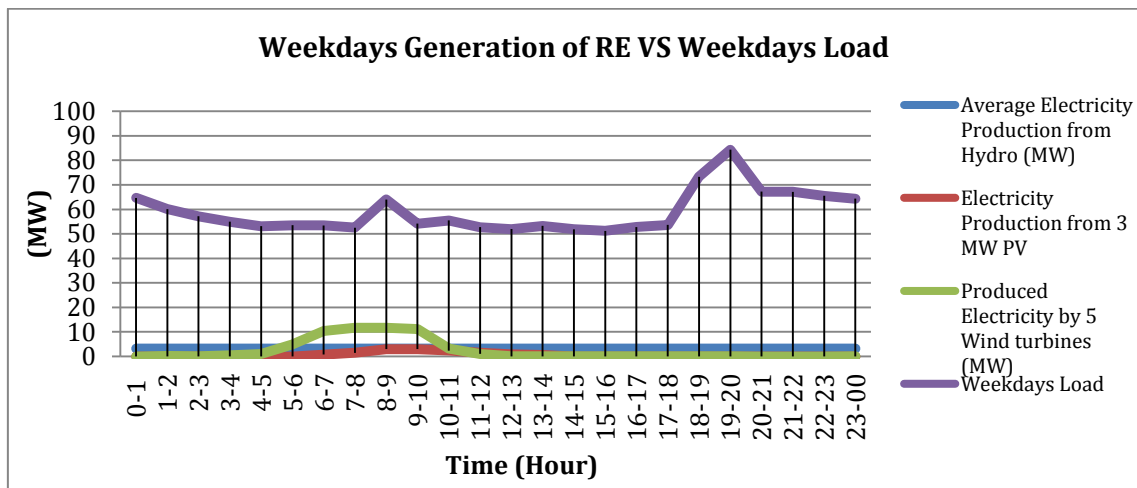


Figure 3-11: Generation and Load on Weekdays

The average electricity production of hydro resource, solar insolation on weekend (January 25th 2009) and the result of wind speed analysis taken from January 3th are used to estimate hydro, PV and wind generation on weekend. Load data is taken from December 24th 2014. Figure 3-12 is explaining about this.

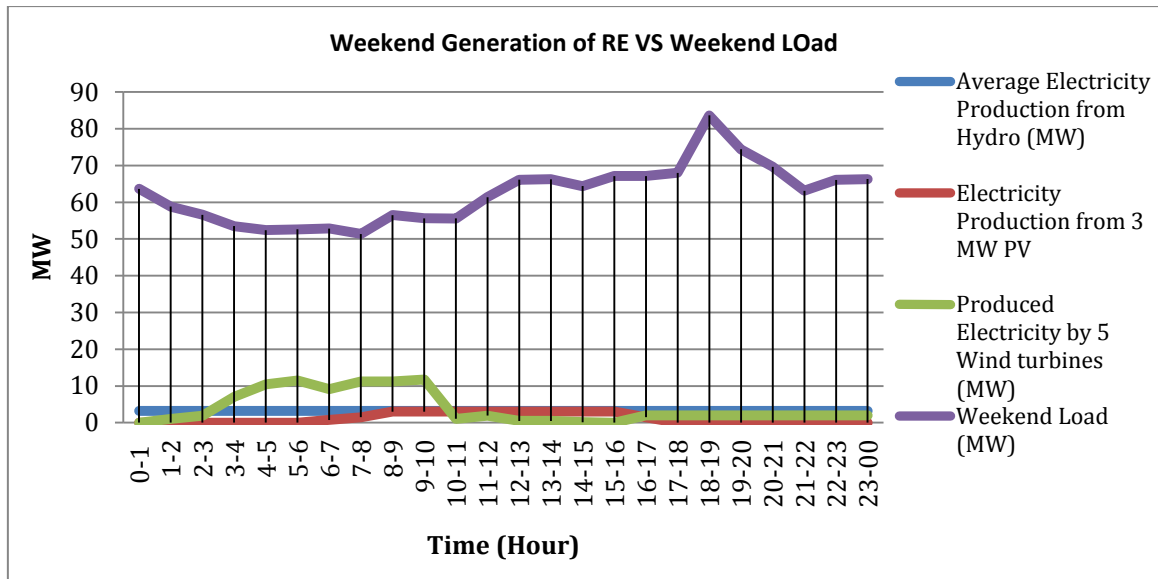


Figure 3-12: Generation and Load on Weekend

3.2.4 Daily Generation Supplies Base Load

The purpose of incorporating hydro, PV and wind into Palapas system is in order to replace some of diesel generator to supply base load.

Figure 3-13 is showing daily electricity production from hydro, PV and wind to supply base load. Based on figure 3-13, the contribution of 3.2 MW hydro, 3.45 MW PV and 5 wind turbines (11.5 MW) is not that significant. However they will give contribution to Palapas system to avoid shortage problem when one or two diesel generators have technical problem.

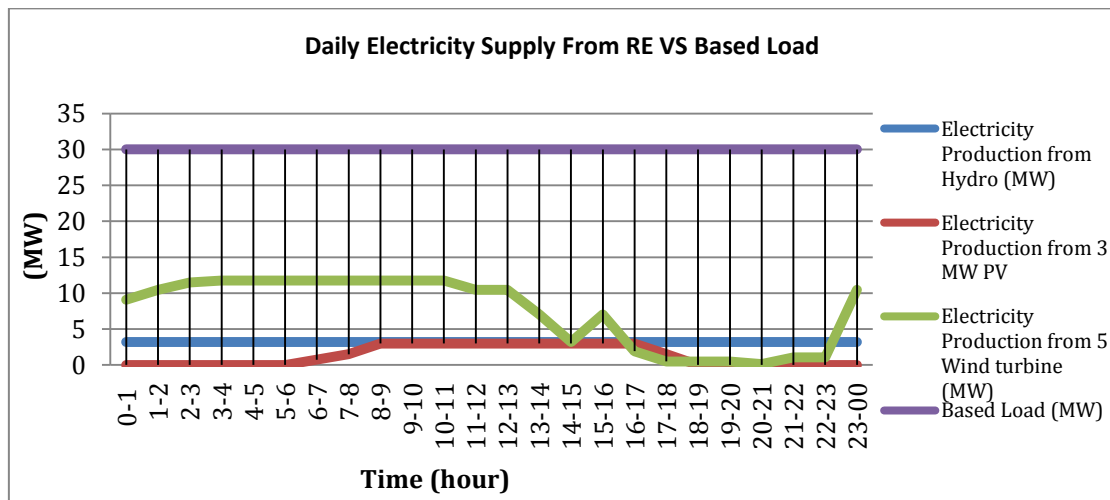


Figure 3-13: One Single Day Generation is Supplying Base Load

3.3 Simulation and Modelling

Palapas system is assumed as a microgrid system. Although in reality Palapas system is a public utility grid that consists of eight substations. Two of eight substations are connecting substations. All lines that connect eight substations are overhead lines with voltage level of 20 kV and 80 kV. Three substations are connected through 70 kV sub-transmission line.

3.3.1 Load Input

In this simulation, one single day load data of the first day of each month was taken. Therefore there are only 12 days load profiles over the year. Figure 3.14 is the daily load profile of Homer version.

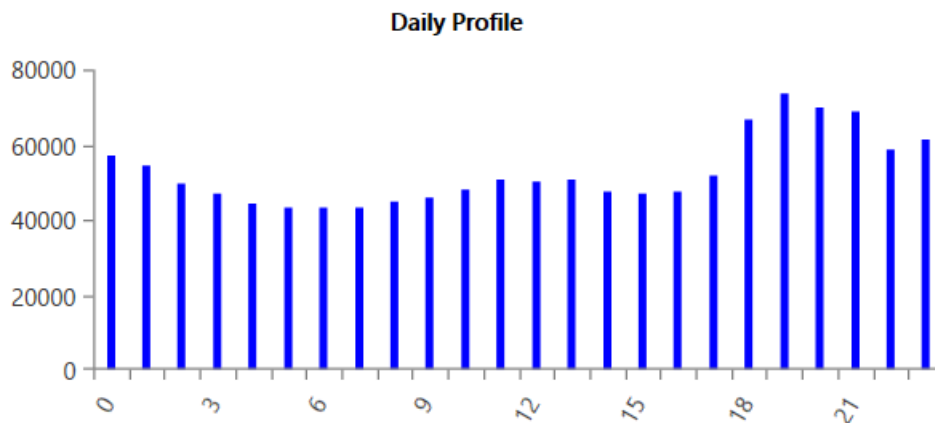


Figure 3-14: Daily Load Profile in Homer Simulation

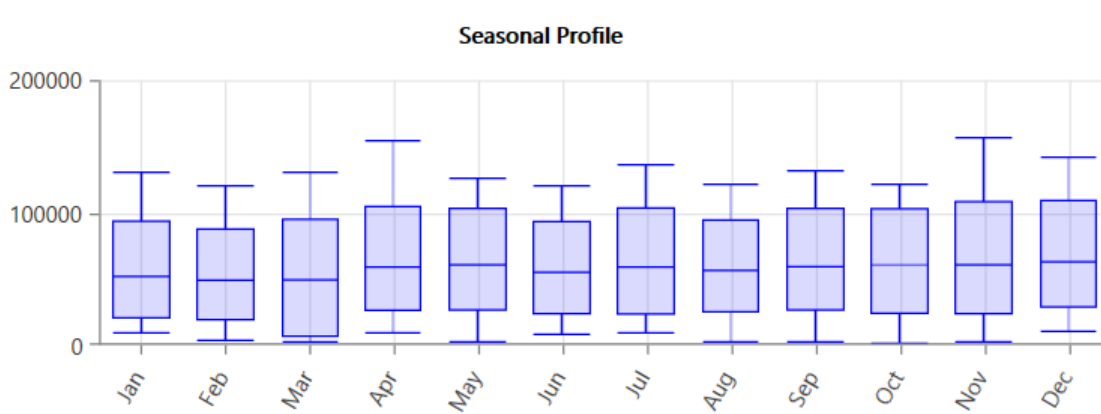


Figure 3-15: Seasonal Load Profile in Homer Simulation

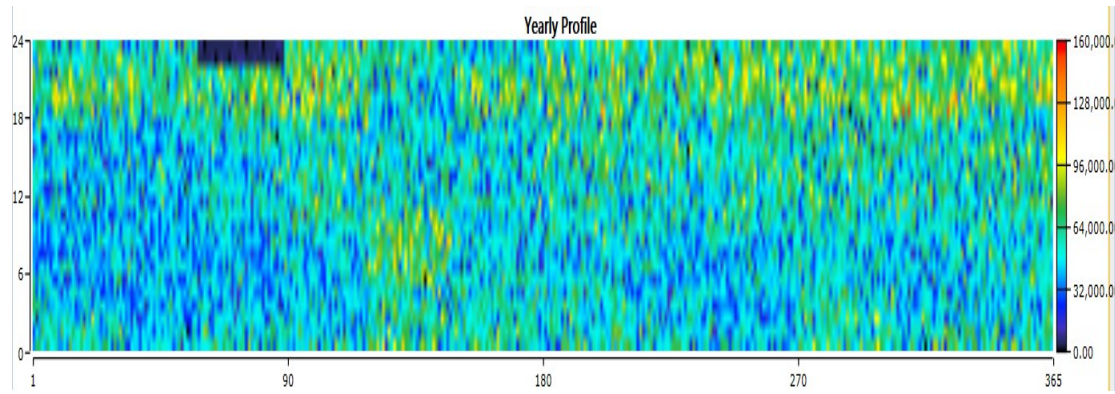


Figure 3-16: Yearly Load Profile in Homer Simulation

Figure 3-15 and figure 3-16 above are seasonal and yearly load profile in Homer simulation. Figure 3.18 is scaled data daily profile of each month over the Year in Homer simulation. Figure 3-17 is showing that each month Palapas system has different load behaviour. The highest load occurred at the end of the year particularly in December. The highest peak load is occurred in December with capacity of 92.50 MW. The peak load is only occurred once in a year.

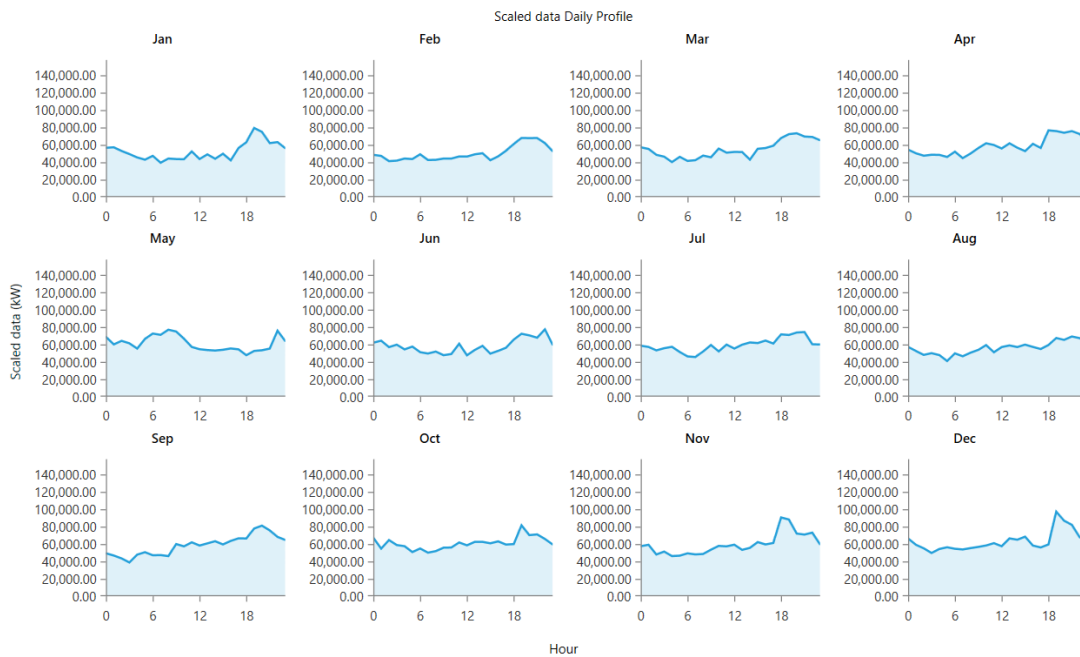


Figure 3-17: Scaled Data Daily Profile in Homer Simulation

3.3.2 Components Used to Model the System

Some of components were not modelled based on the real condition due to the limitation of the software. Although in real condition existing capacities (diesel generator and coal power plant) are not in new condition but in this case they are assumed as new ones.

3.3.2.1 Diesel Generator and Coal

According to real condition the number of diesel generator is more than 10 but in this simulation only 5-diesel generator are used. The capacity of 5 diesel generators is equal to the total capacity of existing diesel generator in real condition. Due to limitation of Homer software, Coal is assumed as DG.

In this simulation 5 diesel generators are used as the representative of all diesel generator and coal in real condition. The input data of 5 diesel generators in this simulation are the following:

Table 3-2: Diesel Generator Input Data

	DG 1	DG 2	DG 3	DG 4	DG 5
Search Space	10,000 kW	10,000 kW	10,000 kW	10,000 kW	10,000 kW
	30,000 kW	20,000 kW	35,000 kW	15,000 kW	15,000 kW
	45,000 kW	30,000 kW	50,000 kW	25,000 kW	25,000 kW
				45,000 kW	35,000 kW
				50,000 kW	45,000 kW
				55,000 kW	55,000 kW
Life Time	175,200 hours	175,200 hours	175,200 hours	175,200 hours	175,200 hours
Capital Cost	US\$ 500/kW	US\$ 500/kW	US\$ 500/kW	US\$ 500/kW	US\$ 500/kW
Replacement Cost	US\$ 500/kW	US\$ 500/kW	US\$ 500/kW	US\$ 500/kW	US\$ 500/kW
O&M	US\$ 0.20/kWh	US\$ 0.20/kWh	US\$ 0.20/kWh	US\$ 0.20/kWh	US\$ 0.20/kWh
Fuel Type	Diesel	Diesel	Diesel	Diesel	Diesel

Table above is showing input data of 5 diesel generators. Designer put varied of 5 diesel generators capacities to allow Homer to find the right capacity for them. Due to the difficulty to get the exact price of diesel generator from manufacturer, designer

assumes capital cost and replacement cost based on the data in Homer. Capital cost and replacement cost of diesel generator is assumed equal.

To run 1 kWh diesel generator, we need 0.27l of diesel fuel and the price of diesel fuel in Indonesia is assumed US\$ 0.60 per litre. Therefore the operational cost of diesel generator is US\$ 0.16 per kWh. To consider maintenance cost, it was assumed US\$ 0.04 per kWh. Therefore the total operational and maintenance cost of diesel generator is US\$ 0.20 per kilowatt-hour.

3.3.2.2 Hydro Turbine

Figure below is showing the input economics data of hydro turbine used in this simulation. The capital cost of hydro turbine is assumed US\$ 3000 – US\$ 5000 per kWh therefore the total cost hydropower with total capacity of 3 MW is around US\$ 16 million. Replacement cost of hydropower is assumed equal to capital cost but O&M cost is assumed zero. The lifetime of hydro turbine is assumed 25 years. Hydro turbine was connected to AC bus on the system configuration and the intake pipe loss is assumed based on availability data in Homer, which is 15 percent.

Economics	
Capital Cost (\$):	16,000,000.0 <input type="button" value="(-)"/>
Replacement Cost (\$):	16,000,000.0 <input type="button" value="(-)"/>
O&M Cost (\$/yr):	0.00 <input type="button" value="(-)"/>
Lifetime (years):	25.00 <input type="button" value="(-)"/>
Electrical Bus	
<input checked="" type="radio"/> AC <input type="radio"/> DC	
Intake Pipe	
Pipe head loss (%):	15.00 <input type="button" value="(-)"/>

Figure 3-18: Economic Hydro Turbine Data

Turbine

Available head (m):	70.00	<input type="button" value="(-)"/>
Design flow rate (L/s):	5,500.00	<input type="button" value="(-)"/>
Minimum flow ratio (%):	50.00	<input type="button" value="(-)"/>
Maximum flow ratio (%):	150.00	<input type="button" value="(-)"/>
Efficiency (%):	90.00	<input type="button" value="(-)"/>

Nominal Capacity: 3,399.165 kW

Systems to consider

- Simulate systems with and without the hydro turbine.
- Include the hydro turbine in all simulated systems.

Figure 3-19: Hydro Turbine Head Data

Figure 3-19 above is showing hydro turbine head data. It was decided to put 70 meter head and designer flow rate 5,500 Litre per second. The percentage of minimum and maximum flow ratios are assumed 50 percent and 150 percent respectively. The efficiency of hydro turbine is assumed 90 percent.

3.3.2.3 PV Module

PV module used in this simulation is generic flat plate with flat plate panel type. Due to high investment cost of PV, it was decided to put only 3 MW PV. The capital and the replacement cost of 3 MW PV are assumed US\$ 3000 per kW with operational and maintenance cost of US\$ 10 per year per kW. The lifetime and the percentage of derating factor are assumed by 25 years and 80% respectively.

3.3.2.4 Converter

The capacity of inverter in this simulation is varied from 2,700 kW to 3,000 kW. On the search space, it was decided to put inverter capacity of 2,700 kW, 2,900 kW and 3,000 kW. The capital and the replacement cost of converter are assumed US\$ 300 per kilowatt. The operational and maintenance cost of inverter is US\$ 50 per year per kilowatt. The efficiency of inverter input is considered by 90 percent while the efficiency of output of rectifier is 85 percent. The relative capacity of rectifier output is 100 percent and the lifetime of converter is assumed by 15 years.

3.3.2.5 Wind Turbine

3 wind turbines from different manufacturers used in this simulation. The use of 3 turbines from 3 different continents (United States, Europe and Asia) is to compare the performance and the net present cost all of them in the configuration system.

Virtually 5-6 wind turbines are used in this simulation therefore the rated capacity of each turbine is multiplied by 5-6 and then the result is divided by rated capacity of wind turbine data provided by homer which is 1,500 kW. Finally the numbers of turbine used in this simulation are 7 (for Asian wind turbine and 8 turbines for European and American wind turbines). According to AWEA (American Wind Energy Association, wind power cost is US\$ 1.3 million per MW. This cost is multiplied by power rating of wind turbines and then multiplied by the number of wind turbines. The operational and maintenance cost of wind turbine is based on the data provided by homer library, which is US\$ 70 per turbine per year.

The hub height of wind turbine is 100 meter and the lifetime is 20 years. After inserting the power output of every wind speed of different turbines, the wind turbine power curve will be obtained. Figure 3-20 is showing the wind turbine power curve.

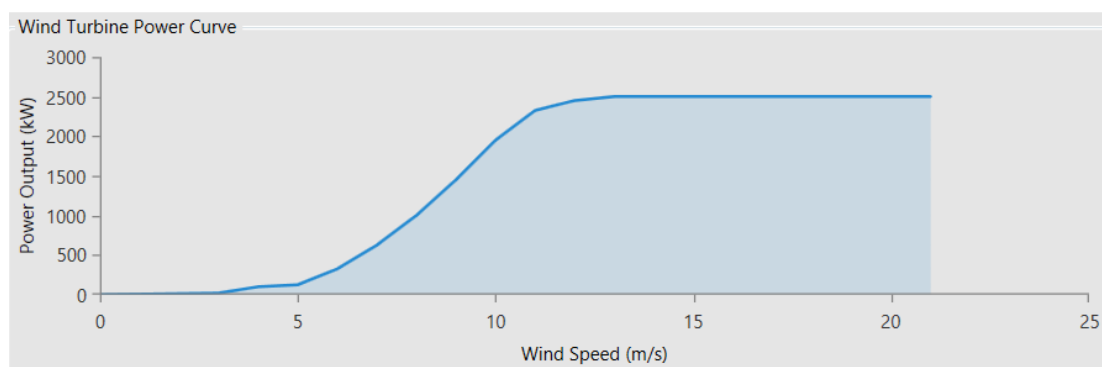


Figure 3-20: Wind Turbine Power Curve from USA Manufacturer

3.3.2.6 Grid

Grid data used in this simulation is based on simple rate therefore the grid data needed is only grid power price in dollar per kilo watt hour and grid sell back is also in

dollar per kilowatt-hour. The price of grid power price put in this simulation is assumed US\$ 3/kWh to avoid buying electricity from the grid. Grid sell price is assumed US\$ 0.09/kWh, which is the average real price of electricity in Indonesia.

3.3.3 Resources

As we discussed earlier that there are 3 different ways to insert the resources based on renewable energy, inserting time series data, inserting manually or download from internet through NASA website.

3.3.3.1 Hydro Resources

Monthly flow rate of the river is in meter cubic per second. After converting into litre per second, the result monthly flow rate of river can be seen on figure 3-21. According to figure 3-21, the average of monthly river flow rate is 5.81 litre per second.

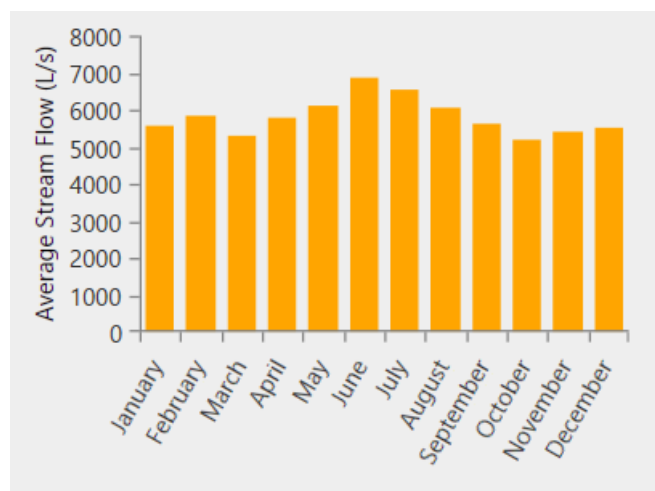


Figure 3-21: Monthly River Flow Rate

3.3.3.2 PV Resources

Daily average solar radiation every month in kilowatt-hour per meter square was obtained from NASA website due to unavailability of solar radiation data in the study area (Palu). Figure 3-22 is showing monthly Solar Radiation over the year with its clearness index. Scaled annual average solar radiation is 5.48 kW/m²/day.

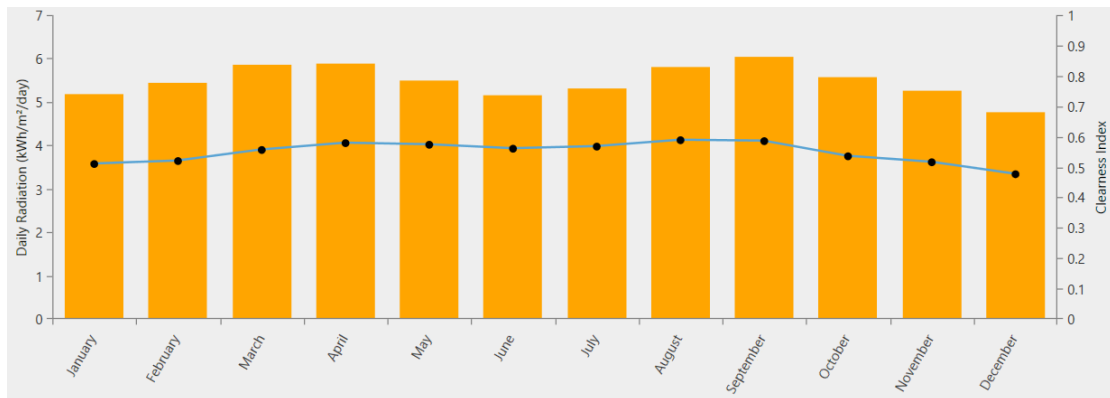


Figure 3-22: Monthly Solar Radiation

3.3.3.3 Wind Resources

Monthly average wind speed is input on wind resource obtained from Meteorology, Climatology and Geophysics Agency. Annual average wind speed based on this data is 3.88 meter per second.

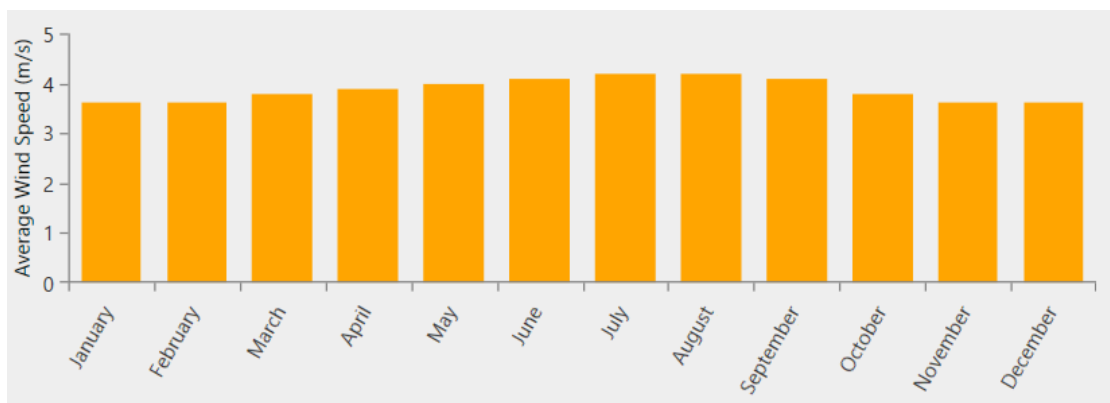


Figure 3-23: Monthly Wind Speed

Meteorology Climatology and Geophysics Council in Palu measures wind speed with anemometer height of 10 meter and altitude above sea level is zero. Roughness used in this simulation is 0.4.

4 Techno-Economy of Combined Hydro, PV and Wind into PALAPAS System to Supply Electricity in Palu (Indonesia)

Public utility PLN collaborated with private sector has been emerging interconnection grid system connecting all cities, districts and sub-districts in Sulawesi Island. In this simulation, Palapas system was assumed as micro-grid system. Therefore in this simulation, whole grid in Sulawesi Island connected to Palapas system is assumed as grid.

The simulation was done before and after incorporating hydro, PV and wind into Palapas system. Due to unavailability of coal plant in Homer software, diesel generator represents coal plant. Due to limited diesel generator available in Homer software, all diesel generators operated in Palapas system were represented by only 4 or 5 diesel generator in Homer simulation with the equal capacity with all diesel generator operated in Palapas system. Each of diesel generators in Homer simulation is presented by different capacities in kilowatt. Homer will decide the total capacity of all diesel generators and the capacity of each diesel generator used in some different configuration systems. All diesel generators used in this simulation are assumed as new ones.

The lifetime of the project is for 25 years with discount rate of 8 % and inflation rate of 2 %. All the lifetime of the components used in this simulation was calculated based on their lifetime specified by the designer. The numbers of the lifetime of components have been specified in hours. Since the aim of this simulation is to avoid shortage problem therefore the percentage capacity shortage specified in this simulation is zero.

Operating reserve in this simulation was set based on the percentage of 10 % load, 15 % solar and 20 % wind. This means the operating reserve is used when there is load increased by 10 %, solar decreased by 15 % and wind decreased by 20 %.

4.1 Diesel Generators Connected into the Grid

The simulation on this section is the representative of the situation before incorporating hydro, PV and wind into Palapas system. Five diesel generators used in this simulation are connected into AC bus bar together with load and grid. The system architecture of the configuration system can be seen on figure 4-1 below.

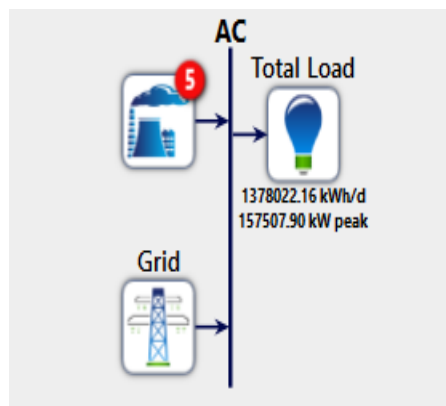


Figure 4-1: DG Configuration Connected into the Grid

The capacity of all components used in the configuration system on figure 4-1 is the following:

Generator 1 (30000 kW)	Generator 2 (20000 kW)	Generator 5 (55500 kW)	Cycle Charging
Generator 3 (10000 kW)	Generator 4 (15000 kW)	Grid (999999 kW)	

Figure 4-2: Components on DG Configuration System Connected into the Grid

4.1.1 Electrical Analysis Results of DG Configuration System

Electricity production of all components used in this configuration system can be seen on table 4-2. According to table 4-2, the total electricity production of this configuration system is 502 GWh per year. Generator 1 produced the highest electricity with the total production of 185 GWh per year and the percentage of 36 %. Generator 5 with total production of 133 GWh per year and the percentage of 26 % produced the second largest electricity production. Generator 2 and generator 4 produce 70 GWh electricity per year with percentage around 14 % of each of them.

The least electricity production comes from generator 3 with electricity production of 37 GWh per year with percentage of only 7 %. Electricity purchased from the grid is only 144 MWh per year with percentage of 0.03 %. This configuration system is using system dispatch of cycle charging by means diesel generator will always produce more electricity than needed whenever diesel generator is switched on. The excess electricity is used as backup to help operating reserve to meet the load.

Table 4-1: Electrical Production of All Components

Production	KWH/year	%
Generator 1	185,053,376	36.84
Generator 3	37,550,380	7.48
Generator 2	75,888,008	15.11
Generator 4	69,864,392	13.91
Generator 5	133,788,536	26.64
Grid Purchases	144,360	0.03
Total	502,289,056	100.00

Monthly average electricity production of all components in this configuration system can be seen figure below.

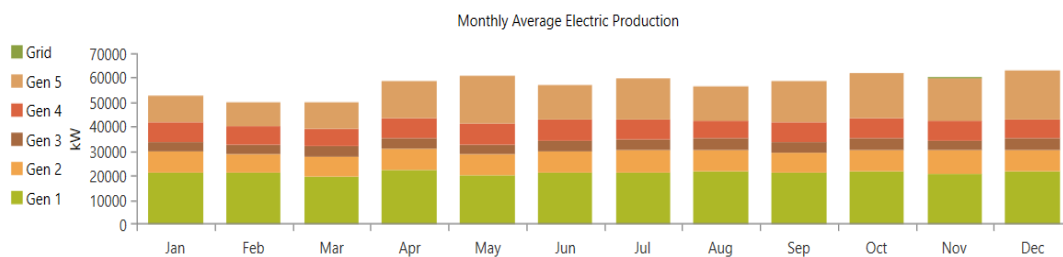


Figure 4-3: Monthly Electricity Production of All Components

Electricity consumption of this configuration system by AC primary load is 502 GWh per year while electricity consumption by DC primary load is zero. This result can be seen on table 4-2 below.

Table 4-2: Electricity Consumption On DG Configuration System

AC Primary Load	KWH/year	%
AC Primary Load	502,289,088	100.00
DC Primary Load	0	0.00
Total	502,289,088	100.00

The simulation result of excess electricity, unmet electric load and capacity shortage in this configuration system are zero, which mean load are fulfilled by the system but in reality it is not. These results can be seen on table 4-3. Since there is no any renewable energy source included in this configuration system therefore renewable fraction and renewable penetration are zero.

Table 4-3: Excess Electricity, Unmeet load and Capacity Shortage on DG Configuration System

Quantity	KWH/Year	%
Excess Electricity	0	0
Unmet Electric Load		
Capacity Shortage		

4.1.2 Fuel Summary of DG Configuration System

Monthly fuel consumption in litre per hour can be seen on figure 4-4. According to figure 4-4, the highest fuel consumption is occurred in November and December while the lowest fuel consumption is in February. The highest fuel consumption in May, November and December is caused by the increased of load.

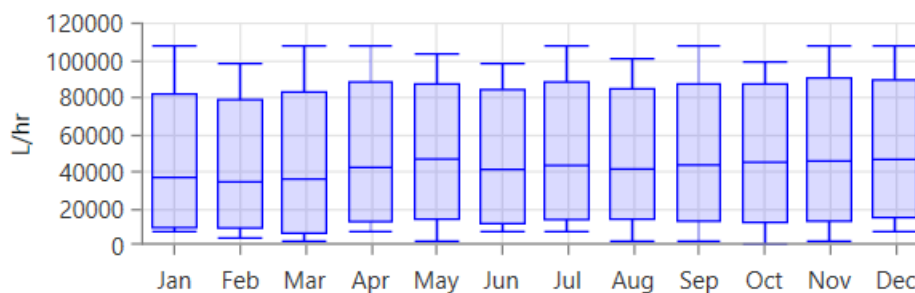


Figure 4-4: Monthly Fuel Consumption of DG Configuration System

Hourly fuel consumption over a year can be seen on figure 4-4. Based on figure 4.4, the highest fuel consumption occurred from 17.00 to 22.00 every day while the lowest fuel consumption is occurred from early morning to afternoon around 12.00. There are some hours when fuel consumption is quite high; possibly it is caused by decreased electricity production from renewable energy source. At the end of the year, there is an increase of fuel consumption in early morning till afternoon compared in the beginning of the year. The dark area around March is caused by electricity production of RE increased therefore the need of fuel is very low.

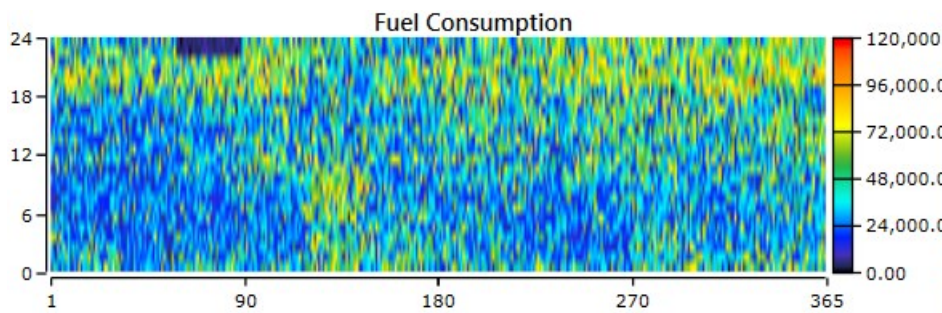


Figure 4-5: Hourly Fuel Consumption of DG Configuration System

The detail of hourly fuel consumption per day can be seen on figure 4-5. Based on figure 4-5, in the beginning of the year, the fluctuation of fuel consumption is thinner than the fluctuation of fuel consumption at the end of the year.

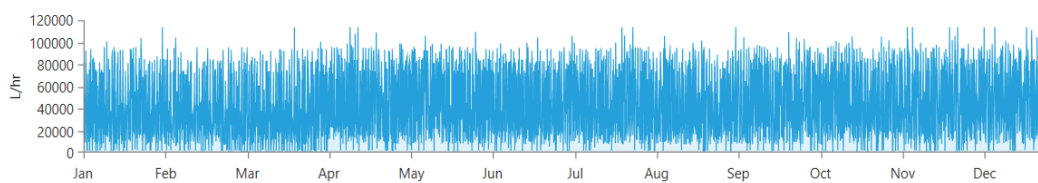


Figure 4-6: Monthly Fuel Consumption of DG Configuration System

4.1.3 Components Simulation Results on DG Configuration System

4.1.3.1 DG 1

Electrical production, mean electrical output, minimum and maximum electrical output of DG 1 can be seen on table 4-4 below.

Table 4-4: Generator 1 Electricity Production

Quantity	Value	Units
Electrical Production	185,053,376.00	kWh/year
Mean Electrical Output	29,925.00	kW
Minimum Electrical Output	25,076.00	kW
Maximum Electrical Output	30,000.00	kW

Operation hours of generator 1 can be seen on table 4-5 below. All diesel generator used in this simulation were set to 20 years lifetime. Based on table 4-5, the total hours of operation of generator 1 is 6,221 hours per year that leads to the increase of it is lifetime by 28.2 years. Based on simulation this result, the number of starts of generator 1 is 1,788 with the average hours of operation by 3.5 hours per start per year.

The capacity factor is the ratio between hours of operation and the maximum of hours of operation of diesel generator. The capacity factor in this configuration system is 70 %. The fixed generation cost needed to produce total electricity per hour in this configuration system is US\$ 1,154. The marginal generation cost needed to produce extra electricity in this configuration system is US\$ 0.146 per kilowatt-hour.

Table 4-5: DG 1 Operation Hours

Quantity	Value	Units
Hours of Operation	6,184	hours/year
Number of Starts	1,810	Starts/year
Operational Life	28.3	year
Capacity Factor	70.4	%
Fixed Generation Cost	1,154	\$/hour
Marginal generation Cost	0.0976	\$/kWh

Fuel consumption of generator 1 can be seen on table 4-6 below. Based on table 4-6, the total fuel consumption of diesel generator 1 in this configuration system is 47 million litre. The specific fuel consumption needed to produce 1-kilowatt hour electricity in this configuration system is 0.26 litre. Fuel energy input produced by fuel in this configuration system is 469 GWh per year. Mean electrical efficiency of diesel generator 1 is 39 %.

Table 4-6: Fuel Consumption of DG1

Quantity	Value	Units
Fuel Consumption	47,750,296.00	L
Specific Fuel Consumption	0.26	L/kWh
Fuel Energy Input	469,862,976.00	kWh/year
Mean Electrical Efficiency	39.39	%

Hourly generator 1 power output over a year can be seen on figure 4-7. Based on figure 4-7, 70 % of colour on this figure is dominated by red which means generator is operated at its maximum capacity. At the beginning of the year, the figure is dominated by orange colour which means generator is operated at around 80 % of its capacity. The end of the year is also rapidly dominated by red colour. As mentioned before, the black area occurred around March is obvious here which means that generator 1 is not operated here.



Figure 4-7: Hourly Output Power of DG 1

4.1.3.2 DG 2

The total electrical production of diesel generator 2 is almost 76 GWh per year while the mean electrical output is almost 19 MW. The minimum electrical output of generator 2 is 15 MW while the maximum electrical output is 20 MW. The detail about electricity production of generator 2 can be seen on table 4-7.

Table 4-7: DG 2 Electrical Production

Quantity	Value	Units
Electrical Production	75,888,008.00	kWh/year
Mean Electrical Output	18,981.00	kW
Minimum electrical Output	15,078.00	kW
Maximum Electrical Output	20,000.00	kW

Operation hours of generator 2 can be seen on table below. Table 4-8 is showing that the total hours of operation of generator 2 is almost 4,000 hours per year. This value is half of the lifetime of diesel generator set by the designer. Therefore it increases the operational life of generator 2, which becomes 43.8 year.

Table 4-8: DG 2 Operation Hours

Quantity	Value	Units
Hours of Operation	3,998	hours/year
Number of Starts	2,136	starts/year
Operational Life	43.8	year
Capacity Factor	43.3	%
Fixed Generation Cost	769	\$/hour
Marginal Generation Cost	0.0976	\$/kWh

The capacity factor of generator 2 in this configuration system is 43 % while the number of starts is 2,136 starts per year. The fixed generation cost and marginal generation cost of generator 2 are respectively US\$ 769 per hour and US\$ 0.09 per kilowatt-hour.

The total fuel consumption of generator 2 to produce electricity in this configuration system is 19 million litre while the specific fuel consumption is 0.26 litre per kilowatt-hour. Fuel energy input of generator 2 is around 193 Giga-Watt hours per year while the mean electrical efficiency is 39.28 %. All these results about fuel consumption of generator 2 can be seen on table 4-9 below.

Table 4-9: Fuel Consumption of DG 2

Quantity	Value	Units
Fuel Consumption	19,636,116.00	L
Specific Fuel Consumption	0.26	L/kWh
Fuel Energy Input	193,219,408.00	kWh/year
Mean Electrical Efficiency	39.28	%

Figure 4-8 is showing the output power of generator 2. Black colour is indicating that generator 2 is not operated while red colour is indicating that generator 2 is operated at its maximum capacity. Red colour is more rapid at the end of the year than at the beginning of the year. Red colour on this figure is only dominating by 40 %.

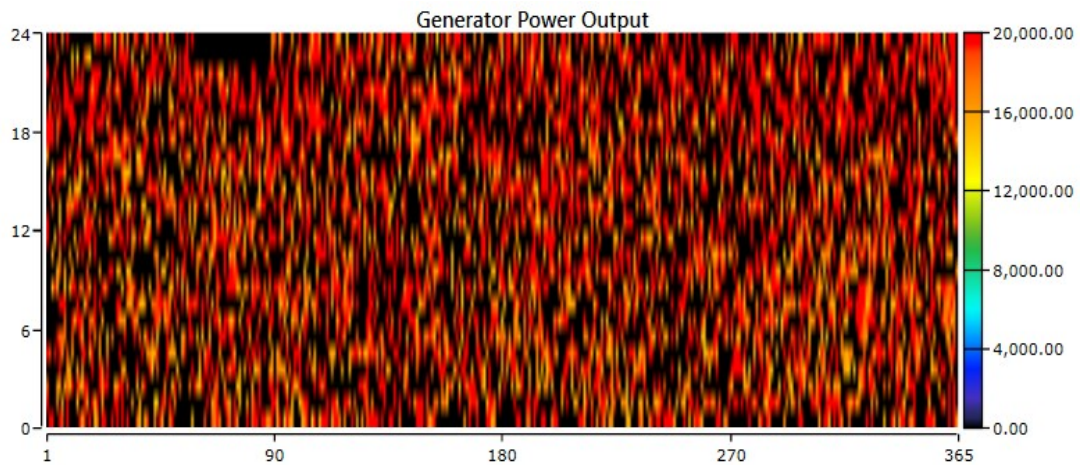


Figure 4-8: Hourly Output Power of DG 2

4.1.3.3 DG 3

The total electricity production of generator 3 in this configuration system is 37 Giga-Watt hours per year therefore and mean electrical output of generator 3 is around 9,600 kW. The maximum electrical output of generator 3 is 10,000 kW and the minimum electrical output of generator 3 is 690 kW. The result of electricity production of generator 3 in this configuration system can be seen on table 4-10 below.

Table 4-10: DG 3 Electrical Production

Quantity	Value	Units
Electrical Production	37,550,380.00	kWh/year
Mean Electrical Output	9,581.60	kW
Minimum Electrical Output	690.43	kW
Maximum Electrical Output	10,000.00	kW

Operation hours of generator 3 can be seen on table 4.11. Based on table 4.11, the total operation hours of generator 3 in this configuration system is 3,900 hours per year. Since the total hour of operation of generator 3 is less than half of its maximum operation hours, it increases its operational life. Therefore the operational life of generator 3 becomes 44 years. The capacity factor of generator 3 is 42.9 % while the fixed generation cost and marginal generation cost are respectively US\$ 385 per hour and US\$ 0.09 per kilo-watt hour.

Table 4-11: DG 3 Operation Hours

Quantity	Value	Units
Hours of Operation	3,919	hours/year
Number of Starts	2,188	starts/year
Operational Life	44.7	year
Capacity Factor	42.9	%
Fixed Generation Cost	385	\$/hour
Marginal Generation Cost	0.0976	\$/kWh

The total fuel consumption of generator 3 in this configuration system is 9.7 million litre and the specific fuel consumption of generator 3 is 0.26 litre per kilowatt-hour. Fuel energy input of generator 3 is 95.5 Giga-watt hours per year and means electrical efficiency of generator 3 is 39.30 %. Fuel consumption of generator 3 can be seen on table 4-12 below.

Table 4-12: Fuel Consumption of DG 3

Quantity	Value	Units
Fuel Consumption	9,710,962.00	L
Specific Fuel Consumption	0.26	L/kWh
Fuel Energy Input	95,555,880.00	kWh/year
Mean Electrical Efficiency	39.30	%

Hourly output power of generator 3 over the year in this configuration system can be seen on figure 4-9. Since the operational hour of generator 3 is almost equal to the operational hour of generator 2 therefore the generator 3-power output figure is also quite similar with the generator 2-power output figure.



Figure 4-9: Hourly Output Power of DG 3

4.1.3.4 DG 4

The capacity of generator 4 in this configuration system is 15,000 kW with the total electricity production of 69.8 Giga-watt hours per year. Mean electrical output of generator 4 is 13,36 kW while the minimum and maximum electrical outputs of generator 3 are respectively 10,000 kW and 15,000 kW. Table 4-13 below is showing the detail about electricity production of generator 4.

Table 4-13: DG 4 Electrical Production

Quantity	Value	Units
Electrical Production	69,864,392.00	kWh/year
Mean Electrical Output	13,358.00	kW
Minimum electrical Output	10,068.00	kW
Maximum Electrical Output	15,000.00	kW

The total operational hours of generator 4 is more than half of its maximum operational hour that leads increasing the operational life of generator 4 by 33.5 years. The operational hour of generator 4 is more than the operational hour of generator 2 and generator 3 but less than operational hour of generator 1. The number of starts of generator 4 is 2,079 starts per year and its capacity factor is 53 %. The fixed and marginal generation costs of diesel generator 4 are respectively US\$ 577 per hour and US\$ 0.09 per kilowatt-hour. Operational hour of generator 4 in this configuration system can be seen on table 4.14 below.

Table 4-14: DG 4 Operation Hours

Quantity	Value	Units
Hours of Operation	5,230	hours/year
Number of Starts	2,079	starts/year
Operational Life	33.5	year
Capacity Factor	53.2	%
Fixed Generation Cost	577	\$/hour
Marginal Generation Cost	0.0976	\$/kWh

The total fuel consumption of generator 4 to produce electricity for 5,149 hours per year is around 18 million litre. The total fuel consumption of generator 4 to produce electricity for 1-kilowatt hour is 0.26 litre. Fuel energy input and the mean electrical efficiency of generator 4 are 178 Giga-watt hours per year and 39 % respectively.

Table 4-15: Fuel Consumption of DG 4

Quantity	Value	Units
Fuel Consumption	18,121,162.00	L
Specific Fuel Consumption	0.26	L/kWh
Fuel energy Input	178,312,256.00	kWh/year
Mean Electrical Efficiency	39.13	%

Although the operational hours of generator 4 is more than operational hour of generator 2 and 3 but generator 4 is generally operated less than its maximum capacity. This reality can be seen on figure 4-10 where yellow and orange colours are dominating the result diagram. Red colour is very rare compared with the result diagram of generator 2 and 3 power output.



Figure 4-10: Hourly Output Power of DG 4

4.1.3.5 DG 5

Generator 5 with capacity of 55,500 kW produces total electricity of 133 Giga-Watt hours per year. Mean electrical output of generator 5 is 53,000 kW while its minimum and maximum electrical output is respectively 45,761 kW and 55,500 kW.

Table 4-16: DG 5 Electrical Production

Quantity	Value	Units
Electrical Production	133,788,536	kWh/year
Mean Electrical Output	53,196.00	kW
Minimum Electrical Output	45,761.00	kW
Maximum Electrical Output	55,500.00	kW

The operational hour of generator 5 is the least one compared with other generator in this configuration system. The operational hour of generator 5 is only around ¼ of its maximum operational hour. The rare use of generator 5 leads increasing its operational life becoming 69.7 years. The frequent of starts of generator 5 is 1,505 starts per year. Capacity factor of generator 5 is only 27.5 % while its fixed and marginal generation cost is respectively US\$ 2,134 per hour and US\$ 0.09 per kilowatt-hour.

Table 4-17: DG 5 Operation Hours

Quantity	Value	Units
Hours of Operation	2,515	hours/year
Number of Starts	1,505	starts/year
Operational Life	69.7	year
Capacity Factor	27.5	%
Fixed Generation Cost	2,134	\$/hour
Marginal Generation Cost	0.0976	\$/kWh

Although generator 5 is only operated for 2,515 hours per year but the total fuel consumption needed to operate such operational hour is 34.5 million litres. The specific fuel consumption of generator 5 to produce electricity of 1-kilowatt hour is 0.26 litre. Fuel energy input of generator 5 is 340 Giga-watt hours per year and the mean electrical efficiency is 39.30 %.

Table 4-18: Fuel Consumption of DG 5

Quantity	Value	Units
Fuel Consumption	34,598,568.00	L
Specific Fuel Consumption	0.26	L/kWh
Fuel Energy Input	340,449,952.00	kWh/year
Mean Electrical Efficiency	39.30	%

The rarely use of generator 5 can be seen on figure below. Based on figure 4-11 below, every time generator 5 is operated, it is only operated at 1/3 of its maximum capacity. Orange colour on this figure is indicating this reality. Around May, generator 5 is operated more often from early morning until afternoon. Generator 5 is quite

often operated in the evening from 15.00 to 23.00 and it is more often used on peak time lasting from 19.00 to 20.00.

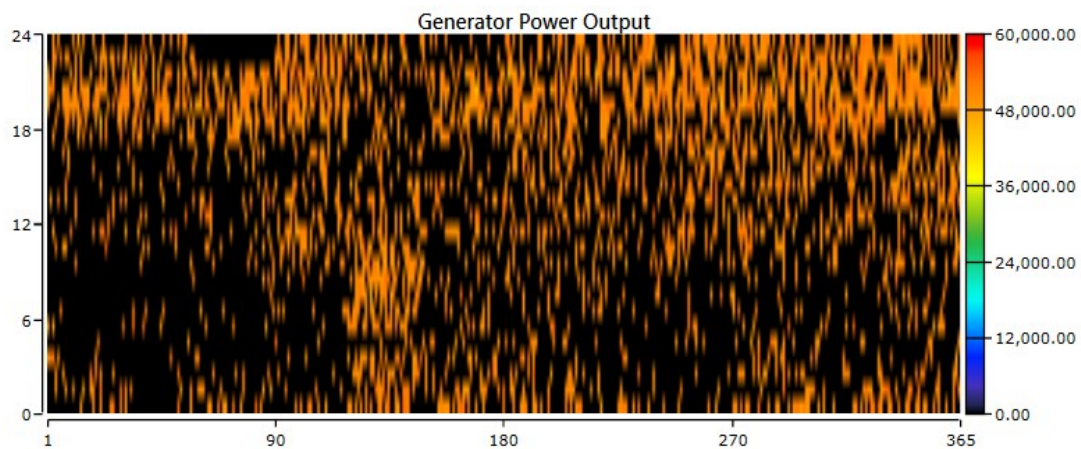


Figure 4-11 Hourly Output Power of DG 5

4.1.4 Emissions of DG Configuration System

Exhaust gases produced by all diesel generators in this configuration system consists of Carbon Dioxide, Carbon Monoxide, unburned hydrocarbons, particulate matter, Sulphur Dioxide and Nitrogen Oxides. The result of exhaust gasses in this simulation was calculated based on the accumulation of exhaust gasses produced by all diesel generators in kilogram per year. The detail of exhaust gasses production by all diesel generators can be seen on table 4-19 below.

Based on table 4-19 below, exhaust gases were dominated by Carbon Dioxide with total amount of 342 million kilogram per year. The second largest amount is occupied by Nitrogen Oxides with total amount of 7 million kilogram per year. The least of all exhaust gasses produced by all diesel generators is particulate matter with total amount of 63 thousands kilogram per year.

Table 4-19: Emission of DG Configuration System

Quantity	Value	Units
Carbon Dioxide	342,005,600.00	kg/year
Carbon Monoxide	843,967.00	
Unburned Hydrocarbons	93,486.00	
Particulate Matter	93,486.00	
Sulfur Dioxide	687,019.00	
Nitrogen Oxides	7,530,978.00	

4.1.5 Grid Analysis of DG Configuration System

Since this configuration system is connected to the grid therefore there might be purchasing and selling electricity between micro-grid (Palapas system) and grid. The detail about price of purchasing and selling of electricity has been discussed on chapter 3. Due to unavailability of components based on renewable energy therefore the system is quite stable by continuous dispatching from diesel generator. The reserve capacity is not urgently required in this configuration system therefore diesel generators only produces electricity equal to the demand. Based on this reality, electricity sold to the grid is zero and electricity purchased from the grid is low. Electricity purchased and sold by Palapas System can be seen on table 4.20 below.

Table 4-20: Electricity Purchased and Sold by PALAPAS System

Month	Energy Purchased [kWh]	Energy Sold [kWh]	Net Energy Purchased [kWh]	Peak Demand [kW]	Energy Charge [US\$]	Demand Charge [US\$]
January	333	0	333	57	998.	0
February	357		357	61	1,070	
March	334		334	55	1,003	
April	30,937		30,937	23,675	92,811	
May	217		217	51	651	
June	352		352	63	1,056	
July	8,218		8,218	5,989	24,653	
August	283		283	54	847	
September	1,500		1,500	1,131	4,501	
October	182		182	54	544	
November	85,806		85,806	27,012	257,419	
December	15,841		15,841	10,723	47,522	
Annual	144,360	144,360	27,012	433,079		

The total annual electricity purchased from the grid is 144 MWh and monthly average electricity purchased from the grid is 12 MWh. The highest electricity purchased from the grid is occurred in November with total purchased electricity of 85 MWh. The lowest electricity purchased is occurred in October with total purchased electricity of 182 kWh. Peak demand provided by the grid is occurred when the micro grid purchased the highest electricity. The higher peak demand the higher electricity purchased by micro grid.

The total annual energy charge is US\$ 433,079. The highest energy charge is occurred in November with total energy charge of US\$ 257,419 and the lowest electricity purchased is occurred in October with total energy charge of US\$ 544. The result diagram of purchasing electricity from the grid and selling electricity to the grid can be seen on figures below.

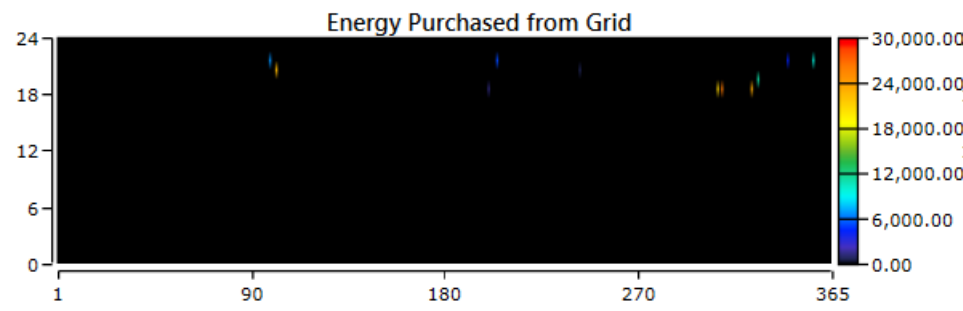


Figure 4-12: Energy Purchased by PALAPAS system from the Grid

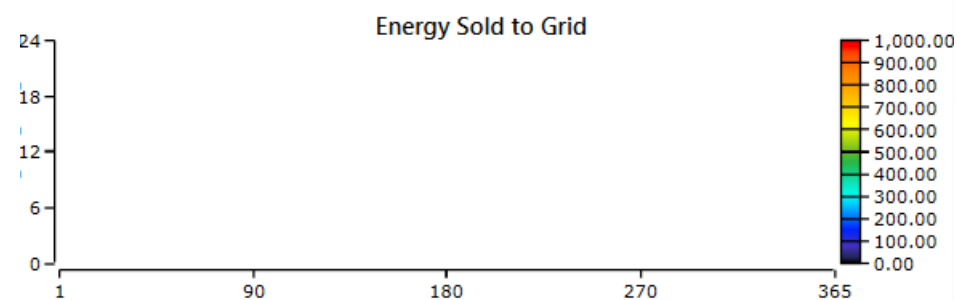


Figure 4-13: Energy sold by PALAPAS System to the Grid

4.1.6 Cost Summary of DG Configuration System Connected into the Grid

Cost of all components used in this simulation has been discussed on chapter 3. Therefore the result of capital cost, replacement cost, operational and maintenance cost and any other costs can be seen on figures 4-14 below.

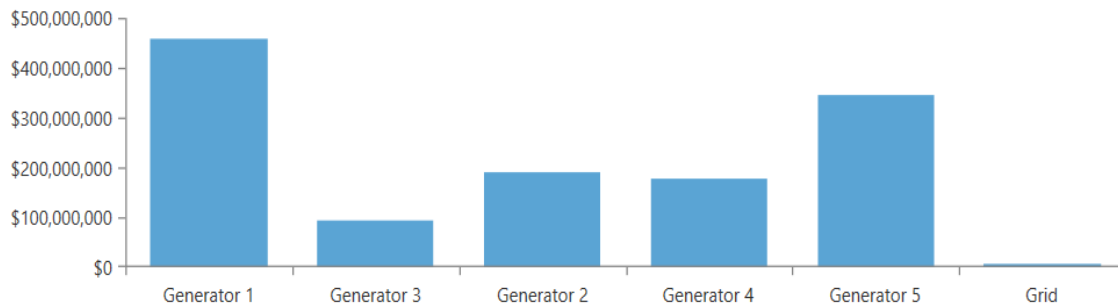


Figure 4-14: Net Present Cost of DG Configuration System Connected into the Grid

Table 4-21: NPC of All Components of DG Configuration System Connected into the Grid

Component	Capital (\$)	Replacement (\$)	O&M (\$)	Fuel (\$)	Salvage (\$)	Total (\$)
Generator 1	15,000,000.00	0	72,251,889.99	247,883,985.47	(409,176.29)	334,726,699.17
Generator 2	10,000,000.00		30,808,857.44	100,918,478.54	(1,037,810.55)	140,689,525.43
Generator 3	5,000,000.00		15,098,046.58	49,868,575.51	(532,407.75)	69,434,214.34
Generator 4	7,500,000.00		30,424,910.20	93,829,117.43	(455,836.75)	131,298,190.88
Generator 5	27,750,000.00		54,133,652.36	178,909,529.59	(4,262,022.32)	256,531,159.63
Grid	0.00		5,598,859.61	0.00	0.00	5,598,859.61
System	62,250,000.00		208,316,216.17	671,409,686.54	6,697,253.66	938,278,649.05

Total NPC is the total of net present cost of the entire system of diesel generators connected into the grid. According to table 4.21 above, total net present cost in this configuration system is US\$ 938 million. LCOE in this case is the total price needed to produce electricity per kilowatt-hour after considering economical and technical sides. Based on table 4-22 below, levelized cost of energy of this configuration system is US\$ 0.1445 per kilowatt-hour.

Table 4-22: Overall Cost of DG Configuration System Connected into the Grid

Total NPC	\$938,277,888.00
Levelized COE	\$0.1445/kWh
Operating Cost	\$67,532,531

Operating cost is the total cost needed to produce electricity for the entire lifetime of the project, which in this case the lifetime of the project is 25 years. The operational cost in the configuration system of diesel generator connected into the grid is dominated by fuel cost.

4.1.7 Sensitivity Analysis of DG Configuration System Connected into the Grid

Although Indonesia is also producing oil but the need of oil in Indonesia is more than the oil Indonesia is producing therefore Indonesia needs to import oil from other countries. Since the oil price is fluctuating it is necessary to consider about the oil price with variability. Ideally considering oil price needs to follow the prediction of oil price in Indonesia for the future but it is difficult to find the accurate information.

In this simulation oil price (fuel price) was considered starting from US\$ 0.4 to US\$ 1.6/l. Based on the result of the simulation, the fluctuation of fuel price will not influence the operational and maintenance cost in this configuration system because Homer separately calculate the fuel cost. The fluctuation of fuel price will significantly influence the total fuel price. The detail about this information can be seen on table 4-23 below.

Table 4-23: Sensitivity Analysis Result of Fuel Price of DG Configuration System Connected into the Grid

Diesel Fuel Price [US\$/liter]	Fuel Cost [US\$]				
	Gen 1	Gen 2	Gen 3	Gen 4	Gen 5
0.4	19,100,118	7,854,446	3,884,385	7,258,066	13,839,427
0.5	24,081,222	9,685,504	4,783,240	9,071,249	17,299,284
0.6	28,806,242	11,692,354	5,772,397	10,872,698	20,760,586
0.7	33,598,744	13,635,697	6,730,850	12,680,153	24,242,410
0.8	33,995,052	17,429,494	8,592,338	14,498,755	27,706,670
0.9	43,354,720	18,522,446	9,148,483	16,304,133	31,174,326
1	48,112,680	19,394,198	9,579,202	18,111,564	34,640,536
1.2	57,198,660	23,573,442	11,652,719	21,738,052	41,641,700
1.4	67,076,980	27,281,444	13,464,806	25,316,370	48,630,456
1.6	76,993,280	30,899,312	15,245,783	28,921,424	55,675,052

Based on table 4-23 above, the higher diesel fuel price the higher full cost will be. Sensitivity analysis is very useful to estimate the fuel cost during the lifetime of the project. According to the result of sensitivity analysis, the increase of fuel price will influence the amount of electricity purchased from the grid. In this simulation Homer software calculated which option is cheaper to produce electricity whether producing electricity by itself or purchasing from the grid. The higher the fuel price, the more electricity purchased from the grid.

The result of sensitivity analysis is also showing that there is no electricity sold to the grid. This phenomenon can be seen on table 4-24 below.

Table 4-24: Sensitivity Analysis Result of Fuel Price of DG Configuration System Connected into the Grid

Fuel Price [US\$/liter]	Grid	
	Energy Purchased [kWh]	Energy Sold [kWh]
0.4	144,360	0
0.5	144,428	
0.6	145,138	
0.7	145,415	
0.8	145,877	
0.9	146,197	
1	146,866	
1.2	147,885	
1.4	149,295	
1.6	150,895	

The increase of fuel price does not significantly take effect to the number of operational hours and the electricity production of all diesel generators operated in this configuration system. Therefore the sensitivity result of these phenomena is not presented here.

Since the increase of fuel price takes effect to the fuel cost and electricity purchase thus it will also influence the operating cost of 25 years of project lifetime, net present cost and levelized cost of energy. Based on table 4-25 below, the increase of fuel price from US\$ 0.4 per litre to US\$ 1.6 per litre will increase operational cost four times, net present cost by three times and levelized cost of energy four times.

Table 4-25: Sensitivity Results of All Costs of DG Configuration Systems Connected into the Grid

Fuel Price [US\$/liter]	Cost		
	Levelized Cost of Energy [US\$/kWh]	Net Present Cost [US\$]	Operational Cost [US\$]
0.4	0.144	938,000,000	67,500,000
0.5	0.170	1,110,000,000	65,300,000
0.6	0.196	1,270,000,000	93,500,000
0.7	0.222	1,440,000,000	106,000,000
0.8	0.248	1,610,000,000	119,000,000
0.9	0.274	1,780,000,000	132,000,000
1	0.300	1,950,000,000	145,000,000
1.2	0.351	2,280,000,000	171,000,000
1.4	0.403	2,620,000,000	197,000,000
1.6	0.455	2,950,000,000	223,000,000

4.2 Off- Grid Diesel Generator Combined with Hydro, PV and Wind

Actually the simulation of off-grid diesel generator combined with hydro, PV and wind was also executed. The configuration system on this simulation was using battery and auto sized diesel generator. The simulation was also executed with using battery but without auto size diesel generator. Due to the unexpected result regarding excess electricity, unmet electric load and capacity shortage, which are not reliable therefore the discussion about this result is ignored. The simulation result of off-grid diesel generator combined with hydro, PV and wind connected into the grid with battery and auto size diesel generator can be seen on table 4-26 below.

Table 4-26: Simulation Results of Off-Grid DG Combined with RE Using Battery and Autosized DG

Quantity	kWh/year	%
Excess Electricity	101,151	0
Unmet Electric Load	3.7	
Capacity Shortage	0.0	

According to table 4-26 above, even though the capacity shortage is zero and unmet electric load is not significantly high but the excess electricity is quite high. Therefore the designer had decided to ignore the discussion about this configuration system.

Table 4-27: Simulation Results of Off-Grid DG Combined with RE Using Battery without Autosized DG

Quantity	kWh/year	%
Excess Electricity	101,157	0
Unmet Electric Load	116,593	
Capacity Shortage	371,447	0.1

Table 4-27 above is showing that the excess electricity in this configuration system is 101 MWh/year, which is quite high, exactly the same with the result with auto sized diesel generator. Unmet electric load is 116 MWh per year and the capacity shortage is 371 MWh per year. These two results are quite high even they are worse than the result of simulation with auto sized diesel generator.

4.3 The Comparison of Three Wind Turbines in the Configuration of Diesel Generator Combined with Hydro, PV and Wind Connected into the Grid

The Simulation of diesel generator combined with hydro, PV and wind connected into the grid consists of three simulations with using 3 different wind turbine type. The aim of this simulation is to find out the best wind turbine type based on technical and economical side. To proceed this simulation, three types of wind turbines from three different continents were input in this simulation. Wind turbine from India is representing wind turbine from Asia, Wind turbine from United States of America is representing wind turbine from America and wind turbine from Germany is representing wind turbine from Europe.

4.3.1 The Configuration System of Diesel Generator Combined with Hydro, PV and Wind Connected into the Grid

According to table 4-28 below, the capacity of all components of Asian and American wind turbine simulation are almost the same except the capacity and the number of

Asian wind turbine. In Asian wind turbine simulation the capacity of wind turbine is 2.1 MW while in American wind turbine simulation the capacity of wind turbine is 2.5 MW. In Asian wind turbine simulation the number of wind turbine is seven while in American wind turbine simulation the number of wind turbine is 8. In European wind turbine simulation, besides the capacity and the number of wind turbine are different, the capacity of some diesel generators are also different compared with Asian and American wind turbine simulation. In European wind turbine simulation the capacity of wind turbine is 2.35 MW and the number of wind turbine is 8. In European wind turbine simulation, homer has decided to put more capacity on diesel generator 3 and less capacity on generator 2. In addition to this simulation on this configuration system, homer has decided to put 25 MW on diesel generator 4 and 15 MW on diesel generator 5.

Table 4-28: Three Configuration System of DG Combined with RE Connected into the Grid Using three Different Wind Turbines

Wind Turbine	Capacity of All Components
Asian Turbine	Hydro (3 MW) PV (3 MW) Wind Turbine 2,1 MW Generator 1 (30 MW) Generator 2 (20 MW) Generator 3 (10 MW) Generator 4 (15 MW) Generator 5 (55.5 MW) Converter (2,7 MW)
European Turbine	Hydro (3 MW) PV (3 MW) Wind Turbine 2,35 MW Generator 1 (30 MW) Generator 2 (20 MW) Generator 3 (50 MW) Generator 4 (25 MW) Generator 5 (15 MW) Converter (2,7 MW)
American Turbine	Hydro (3 MW) PV (3 MW) Wind Turbine 2,5 MW Generator 1 (30 MW) Generator 2 (20 MW) Generator 3 (10 MW) Generator 4 (15 MW) Generator 5 (55.5 MW) Converter (2,7 MW)

4.3.2 Electrical Analysis Result of DG Combined with RE Connected into the Grid

The result of electrical analysis in this configuration system consists of electricity production of all components, electricity consumption, excess electricity, and renewable energy fraction. The brief result of all these analysis can be seen on table 4-29 below.

Based on table 4-29 below, electricity production of hydro and PV in three different wind turbine simulations is exactly the same. Unlike electricity from hydro and PV, electricity from wind turbine in these three simulations is quite different. The number and the nominal capacity of each turbine contribute to the result. The number of Asian wind turbine is 7 and its nominal capacity is the lower than European wind turbine but electricity production produced by it is higher than electricity produced by European wind turbine.

Table 4-29: Electricity Production of All Components of DG Combined with RE Connected into the Grid Using Three Wind Turbines

	Electricity Production of All Components [kWh/year] and the Percentage [%]		
	Asian WT	European WT	American WT
Hydro	26,755,482 (5.29%)	26,755,482 (5.32%)	26,755,482 (5.29%)
PV	4,797,401 (0.95%)	4,797,401 (0.95%)	4,797,401 (0.95%)
Wind	31,537,798 (6.24%)	31,054,322 (6.17%)	36,006,040 (7.12%)
Diesel Generator 1	179,572,656 (35.51%)	98,113,408 (19.51%)	177,182,096 (35.03%)
Diesel Generator 2	75,296,624 (14.89%)	4,717,453 (0.94%)	73,608,664 (14.55%)
Diesel Generator 3	36,437,796 (7.21%)	171,816,432 (34.16%)	36,211,412 (7.16%)
Diesel Generator 4	63,769,080 (12.61%)	105,240,496 (20.92%)	63,611,576 (12.58%)
Diesel Generator 5	87,438,480 (17.29%)	60,284,444 (11.99%)	87,507,288 (17.30%)
Grid Purchases	98,334 (0.02 %)	170,760 (0.03 %)	96,687 (0.02 %)
Total	505,703,616 (100 %)	502,950,176 (100 %)	505,776,672 (100 %)

Electricity production from American wind turbine is the highest one since the nominal capacity is also the highest compare to others. Electricity production from all diesel generators of Asian and American wind turbine simulation are quite similar due to the same nominal capacity and the duration of operation. Unlike Asian and American wind turbine simulation, electricity production of each diesel generator of European wind turbine simulation is different due to the different nominal capacity of diesel generators.

According to table 4-30 below, AC primary load consumption of Asian and American wind turbine are exactly the same compared with AC primary load consumption of European wind turbine. AC primary load consumption of European wind turbine is

lower than Asian and American wind turbine. Since the system is AC therefore DC primary consumption is zero for all of them.

Table 4-30: Electricity Consumption of DG Combined with RE Connected into the Grid Using Three Different Wind Turbines

	Electricity Consumption of Three Different Simulations [kWh/year] and the Percentage [%]		
	Asian WT	European WT	American WT
AC Primary Load	505,125,856 (99.98%)	502,289,088 (99.96%)	505,125,856 (99.97%)
DC Primary Load	0 (0%)	0 (0%)	0 (0%)
Grid Sales	99,137 (0.02%)	181,537 (0.04%)	171,984 (0.03%)
Total	505,224,992 (100%)	502,470,624 (100%)	505,297,824 (100%)

Grid sales of European wind turbine is the highest compared to others with total capacity of 181 MWh per year while grid sale of Asian and American wind turbine are respectively 99 MWh per year and 171 MWh per year. The percentage of grid sale of all wind turbines varies from 0.2 % to 0.04 % in their own configuration system. The total electricity consumption of American and Asian wind turbine simulation are the highest ones while the second is occupied by European wind turbine.

Table 4-31: Excess Electricity, Unmet Load and Capacity Shortage of DG Combined with RE Connected into the Grid Using Three Different Wind Turbines

	Electricity Analysis Result of Three Different Simulations [kWh/year] and the Percentage [%]		
	Asian WT	European WT	American WT
Excess Electricity	0.1 (0%)	0.1 (0%)	0.0 (0%)
Unmet Electric Load	4.3 (0%)	3.9 (0%)	3.9 (0%)
Capacity Shortage	0.0 (0%)	0.0 (0%)	0.0 (0%)

Based on table 4-31 above, in general the excess electricity, unmet electric load and capacity shortage of three different wind turbine simulations are quite the same. American wind turbine result is the best one because it has zero excess electricity and capacity shortage but it has 3.9 kWh per year unmet load. European wind turbine simulation result has excess electricity 0.1 kWh per year and unmet load 3.9

kWh per year. Asian wind turbine simulation result has excess electricity the same amount with European wind turbine but unmet electric load 4.3 kWh per year.

Table 4-32: Renewable Fraction and Maximum RE Penetration of DG Combined with RE Connected into the Grid Using Three Different Wind Turbines

	Electricity Analysis Result of Three Different Simulations		
	in Percentage [%]		
	Asian WT	European WT	American WT
Renewable Fraction	12.4	12.0	13.3
Max. Renew Penetration	102.8	102.8	102.8

According to table 4-32 above, maximum renewable energy penetration of three different wind turbines simulation is exactly the same while renewable energy fraction is a little bit different. Renewable energy fraction of American wind turbines is the highest one compared with Asian and European wind turbine.

Table 4-33 below is showing costs result of three different wind turbines simulation. Asian wind turbine net present cost is the highest compared with others with the total cost of US\$ 876 million. The second highest net present cost is occupied by European wind turbine with total cost of US\$ 873 million. American wind turbine has the lowest net present cost with total cost of US\$ 871 million.

Table 4-33: Costs of DG Combined with RE Connected into the Grid Using Three Different Wind Turbines

	Costs Result of Three Different Simulations [US\$]		
	Asian WT	European WT	American WT
Total Net Present Cost	876,595,000	873,682,800	871,715,100
Levelized Cost of Energy	0.1342 per kWh	0.1345 per kWh	0.1334 per kWh
Operating Cost	59,708,690	59,686,470	59,130,080

Based on table 4-33 above, levelized cost of energy of European wind turbine is the highest compared with Asian and American wind turbines. It is US\$ 0.1345 per kilowatt-hour. The second highest levelized cost of energy is Asian turbine with total cost of US\$ 0.1342 per kilowatt-hour. American wind turbine has the lowest levelized cost of energy with the price of US\$ 0.1334 per kilowatt-hour.

Operating cost of Asian wind turbine is the highest one compared with European and American wind turbines. Operating cost of Asian wind turbine is US\$ 59.708 million. The second highest operating cost is European wind turbine with total cost of US\$ 59.686 million. The lowest operating cost is American wind turbine with total cost of US\$ 59.130 million.

Based on technical and economical considerations, the designer has decided to use American wind turbine on this research to analyze more detail about incorporating hydro PV and wind into the grid.

4.4 DG Combined with RE Connected into the Grid Using Chosen Wind Turbine

Before analyzing more details of every component in this configuration system, it is necessary to analyse detail about fuel consumption of every component. Table 4-34 is showing that total fuel consumption per year is 113 million liter while average fuel consumption per day is 310 thousand litre. The average fuel consumption per hour is 12 thousand litre.

Table 4-34: Fuel Consumption Summary of DG Combined with RE Connected into the Grid Using Chosen Wind Turbine

Quantity	Value	Units
Total Fuel Consumed	113,325,534.00	L
Average Fuel per Day	310,516.36	L/day
Average Fuel per Hour	12,938.18	L/hour

Compared with the configuration before incorporating hydro, PV and wind into the grid, total fuel consumption after incorporating hydro PV and wind is lower by 12.72 %. The difference fuel consumption of these two configurations system is around 16.5 million liter per year. The difference of average fuel consumption of these two configurations system is 45.25 thousands litre per day and the difference of average fuel consumption of them is 1,885 litre per hour.

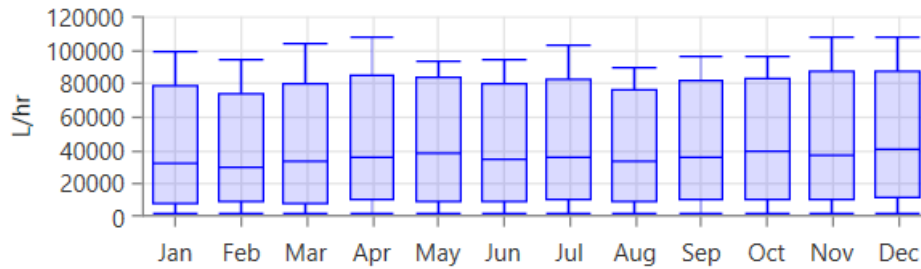


Figure 4-15: Monthly Fuel Consumption of DG Combined with RE Connected into the Grid Using Chosen Wind Turbine

Figure 4-15 above is showing monthly fuel consumption of this configuration system. In general, monthly-daily fuel consumption gets decreased after incorporating hydro, PV and wind into the grid. According to figure 4-15, the need of fuel in May, October and December are higher compared with other months. This phenomenon is also the same before incorporating hydro, PV and wind into the grid but it was higher than 40 thousand liter per hour. While in this configuration system it is 40 thousands litre per day. Except in December, the monthly-daily fuel consumption gets increased after incorporating hydro; PV and wind into the grid. Possibly it is caused by the decreased of renewable energy production.

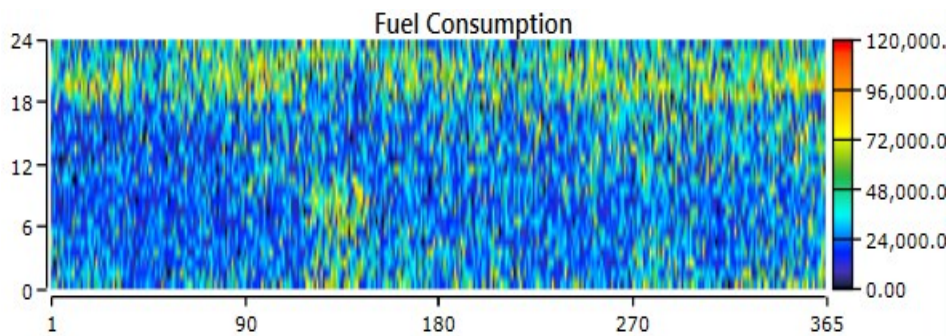


Figure 4-16: Hourly Fuel Consumption of DG Combined with RE Connected into the Grid Using Chosen Wind Turbine

Compared with the situation before integrating RE into the grid, hourly fuel consumption in this configuration system is dominated by blue color, which is dark blue in early year and bright blue at the end of the year. Before integrating RE into the grid, the blue color is less than after integrating RE into the grid. Before Integration RE, it is dominated by bright blue that means that the use of fuel is more than the use of fuel after RE integration. The dark small area before integrating RE

does not exist after integrating RE. It might be caused by the electricity production cost at that time is lower than the electricity sale price to sell to the grid therefore the system has decided to produce electricity to sell it to the grid.

Although the renewable energy fraction is only around 12% - 30% but the use of fuel in this configuration system gets reduced quite significantly. Compared with figure 4-5, the fluctuation of hourly fuel consumption after RE integration is less crowded than before RE integration and the use of fuel from 100,000 litre per day to 120,000 litre per day is rare. In some hours along a year the use of fuel gets decreased significantly. The use of fuel before and after RE integration is more crowded from middle of a year to end of a year but less crowded from early of a year to end of a year.

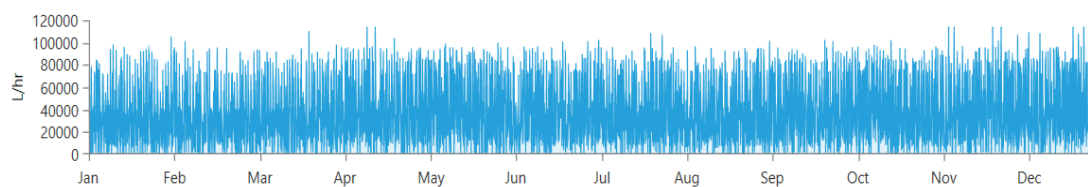


Figure 4-17: Monthly Fuel Consumption Fluctuation of DG Combined with RE Connected into the Grid Using Chosen Wind Turbine

4.4.1 DG 1 on Combined DG and RE

Electricity production by diesel generator 1 in this configuration system is 4.4% lower than the situation before RE integration. Electrical production by diesel generator 1 before incorporating hydro, PV and wind is 185 GWh/year while electricity production of diesel generator 1 after incorporating hydro, PV and wind into the grid is 177 GWh/year. Mean electrical output, minimum and maximum electrical output of diesel generator 1 are the same. This result can be seen on table 4-35 below.

Table 4-35: Electricity Production of DG1 on Combine DG and RE

Quantity	Value	Units
Electrical Production	117,182,096.00	kWh/year
Mean Electrical Output	29,839.00	kW
Minimum Electrical Output	25,075.00	kW
Maximum Electrical Output	30,000	kW

Table 4-36: Operation Hours of DG 1 on Combined DG and RE

Quantity	Value	Units
Hours of Operation	5,938	hours/year
Number of Starts	1,855	starts/year
Operational Life	29.5	year
Capacity Factor	67.4	%
Fixed Generation Cost	1,154	\$/hour
Marginal Generation Cost	0.0976	\$/kWh

Operation hours of generator 1 on table 4-36 above are 5,938 hours/year and operation hours of generator 1 before RE integration are 6,184 hours/year. Number of starts of generator 1 on table 4-36 is 1,855 starts/year while number of starts of generator 1 before RE integration is 1,810 starts/year. This means that generator one is operated longer than previous case. Operational life of generator 1 on table 4-36 is one year longer than operational life of generator 1 before RE integration. Fix and marginal generation cost of generator 1 on both cases are the same because the condition of these two situations is not significantly different.

Table 4-37: Fuel Consumption of DG1 on Combined DG and RE

Quantity	Value	Units
Fuel Consumption	45,726,380.00	L
Specific Fuel Consumption	0.26	L/kWh
Fuel Energy Input	449,947,616.00	kWh/year
Mean Electrical Efficiency	39.38	%

Fuel consumption of generator 1 before RE integration is 47 million liter while fuel consumption of generator 1 after RE integration is 45 million litres. Fuel energy input

of generator 1 before RE integration is 47 GWh/year while fuel energy input of generator 1 after RE integration is 45 GWh/year. Specific fuel consumption of generator 1 on both cases is almost the same.

The difference between hourly generator power output of generator 1 before and after RE integration are not that significant. Black area after RE integration is a little bit more than black area before RE integration. A cluster of black area in early year in the night before RE integration does not exist any longer after RE integration because load at this time is covered by other sources.

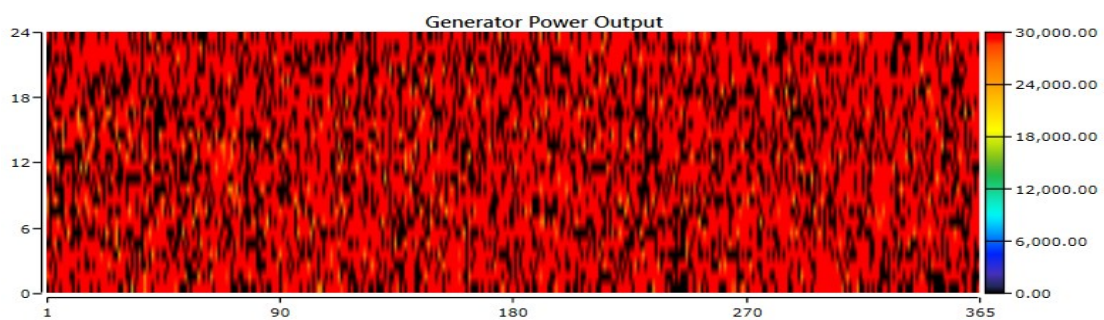


Figure 4-18: DG 1 Power Output of Combined DG and RE

4.4.2 DG2 on Combined DG and RE

Electricity production of generator 2 can be seen on table 4-38 below. Electricity production of generator 2 after RE integration is 73 GWh/year while electricity production of generator 2 before RE integration is 75 GWh/year. Mean electrical output, minimum and maximum electrical output of generator 2 are almost the same.

Table 4-38: Electricity Production of DG 2 on Combined DG and RE

Quantity	Value	Units
Electrical Production	73,608,664.00	kWh/year
Mean Electrical Output	18,831.00	kW
Minimum Electrical Output	15,070.00	kW
Maximum Electrical Output	20,000.00	kW

Operation hours of generator 2 after RE integration are only 89 hours less than hours of operation of generator 2 before RE integration. Number of starts, operational life

and capacity factor of generator 2 on both cases are almost the same. Since most results after and before RE integration are almost the same therefore fixed and marginal generation cost are exactly the same.

Table 4-39: Operation Hours of DG 2 on Combined DG and RE

Quantity	Value	Units
Hours of Operation	3,909	hours/year
Number of Starts	2,170	starts/year
Operational Life	44.8	year
Capacity Factor	42.0	%
Fixed Generation Cost	769	\$/hour
Marginal Generation Cost	0.0976	\$/kWh

Table 4-40: Fuel Consumption of DG 2 on Combined DG and RE

Quantity	Value	Units
Fuel Consumption	19,055,042.00	L
Specific Fuel Consumption	0.26	L/kWh
Fuel Energy Input	187,501,632.00	kWh/year
Mean Electrical Efficiency	39.26	%

Fuel consumption of generator 2 after RE integration is 19.06 million litre while fuel consumption of generator 2 before RE integration is 19.64 million litre. Fuel energy input of generator 2 after RE integration is 187.5 GWh per year but fuel energy input of generator 2 before RE integration is 193 GWh per year. Mean electrical efficiency of generator 2 before and after RE integration is almost the same. Specific fuel consumption of generator 2 on both cases is exactly the same.

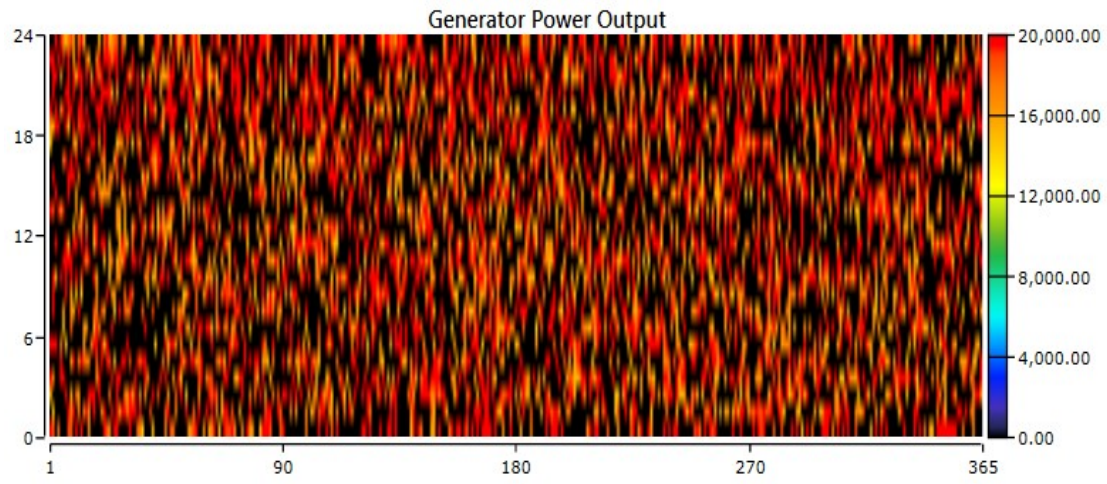


Figure 4-19: DG 2 Power Output of Combined DG and RE

The difference of Hourly generator 2 power output over a year after and before RE integration is not that significant. Only black area before RE integration does not exist longer after RE integration because load at this time is covered by other sources.

4.4.3 DG 3 on Combined DG and RE

Electrical production of generator 3 after RE integration is 36 GWh per year while electrical production before RE integration is 37 GWh per year. Mean electrical output of generator 3 on both cases is similar. Mean electrical output of generator 3 after RE integration is 9.39 MW and before RE integration it is 9.58 MW. Minimum electrical output of generator 3 after RE integration is 177 kW but before RE integration it is 690 kW.

Table 4-41: Electricity Production of DG 3 on Combined DG and RE

Quantity	Value	Units
Electrical Production	36,211,412.00	kWh/year
Mean Electrical Output	9,398.20	kW
Minimum Electrical Output	177.83	kW
Maximum Electrical Output	10,000.00	kW

Hours of operation of generator 3 after RE integration are 3,853 hours per year but before RE integration they are 3,919 hours per day. Number of starts of generator 3 after RE integration is 2,134 starts per year but before RE integration they are 2188

starts per year. Operational life of generator 3 after RE integration is 45.55 years but before RE integration it is 44.7 years. Capacity factor of generator 3 after RE integration is 41.3 % but before RE integration it is 42.9%. Fixed and marginal generation costs of generator 3 after RE integration are US\$ 385 per hour and US\$ 0.097 per kilowatt-hour respectively.

Table 4-42: Operation Hours of DG 3 on Combined DG and RE

Quantity	Value	Units
Hours of Operation	3,853	hours/year
Number of Starts	2,134	starts/year
Operational Life	45.5	year
Capacity Factor	41.3	%
Fixed Generation Cost	385	\$/hour
Marginal Generation Cost	0.0976	\$/kWh

Fuel consumption of generator 3 after RE integration is 9.37 million litres but before RE integration it is 9.71 million litre. Specific fuel consumption of generator 3 on both cases is 0.26 litre per kilowatt-hour. Fuel energy input of generator 3 after RE integration is 92.25 GWh/year but before RE integration it is 95.56 GWh/year. Mean electrical efficiency of generator 3 on both cases is around 39.25%.

Table 4-43: Fuel Consumption of DG3 on Combined DG and RE

Quantity	Value	Units
Fuel Consumption	9,375,009.00	L
Specific Fuel Consumption	0.26	L/kWh
Fuel Energy Input	92,250,096.00	kWh/year
Mean Electrical Efficiency	39.25	%

Black area after RE integration is more than black area before RE integration. This means that generator 3 after RE integration is rarely used than before RE integration. Yellow area in early year in the night before RE integration does not exist after RE integration.

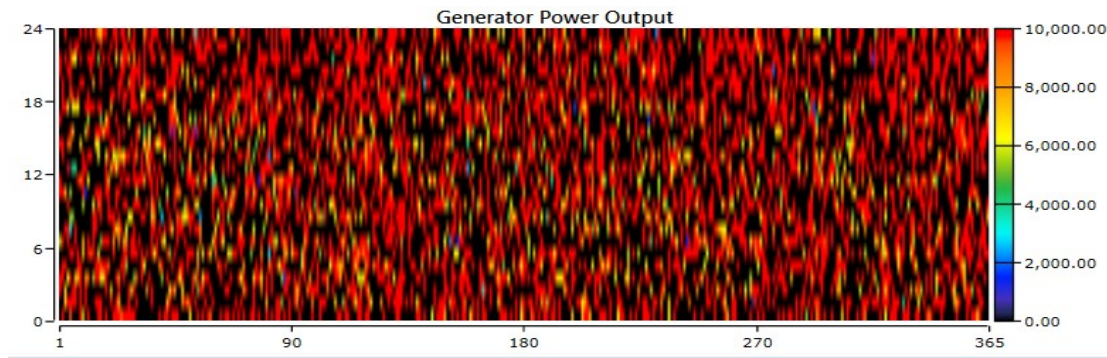


Figure 4-20: DG 3 Power Output of Combined DG and RE

4.4.4 DG 4 on Combined DG and RE

Electricity production of generator 4 after RE integration is 63.61 GWh/year but before RE integration it is 69.86 GWh/year. Mean electrical output of generator 4 after RE integration is 13.11 MW but before RE integration it is 13.36 MW. Minimum and maximum electrical output of generator 4 on both cases are 10.07 MW and 15 MW respectively.

Table 4-44: Electricity Production of DG 4 on Combined DG and RE

Quantity	Value	Units
Electrical Production	63,611,576.00	kWh/year
Mean Electrical Output	13,113.00	kW
Minimum Electrical Output	10,068.00	kW
Maximum Electrical Output	15,000.00	kW

Hours of operation of generator 4 after RE integration is 4,851 hours per year but before RE integration it is 5,230 hours per year that means that generator 4 is rarely used after RE integration. Number of starts of generator 4 after RE integration is 2,129 starts per year but before RE integration they are 2,079 starts per year.

Operational life of generator 4 after RE integration is 36.1 years but before RE integration it is 33.5 years. Capacity factor of generator 4 after RE integration is 48.4 % but before RE integration it is 53.2 %. Fixed and marginal generation costs of generator 4 on both cases are US\$ 577 per hour and US\$ 0.097 per kilowatt-hour respectively.

Table 4-45: Operation Hours of DG 4 on Combined DG and RE

Quantity	Value	Units
Hours of Operation	4,851	hours/year
Number of Starts	2,129	starts/year
Operational Life	36.1	year
Capacity Factor	48.4	%
Fixed Generation Cost	577	US\$/hour
Marginal Generation Cost	0.0976	US\$/kWh

Fuel Consumption of generator 4 after RE integration is 16.53 million litre but before RE integration it is 18.12 million litre. Specific fuel consumption of generator 4 on both cases is 0.26 litre per kilowatt-hour. Fuel energy input of generator 4 after RE integration is 162.75 GWh per year but before RE integration it is 178.31 GWh per year. Mean electrical efficiency of generator 4 on both cases is 39 %.

Table 4-46: Fuel Consumption of DG 4 on Combined DG and RE

Quantity	Value	Units
Fuel Consumption	16,539,937.00	L
Specific Fuel Consumption	0.26	L/kWh
Fuel Energy Input	162,752,992.00	kWh/year
Mean Electrical Efficiency	39.09	%

Black area after RE integration is more than black area before RE integration. This means that generator 4 after RE integration is rarely operated compared with generator 4 before RE integration.

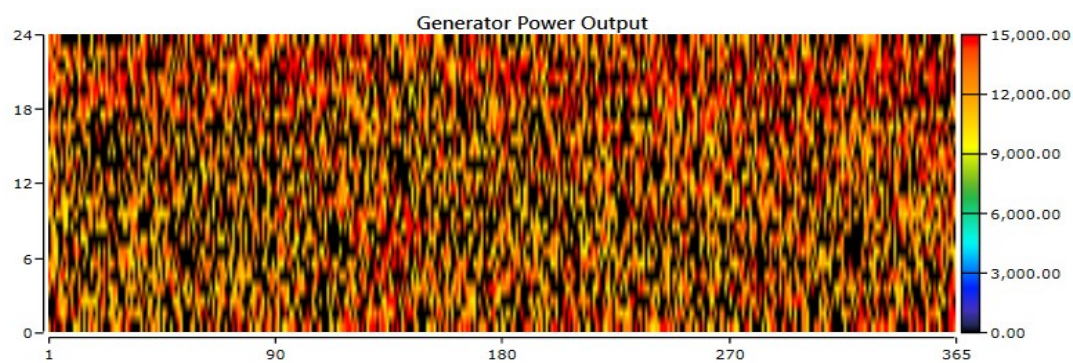


Figure 4-21: DG 4 Power Output on Combined DG and RE

4.4.5 DG 5 on Combined DG and RE

Electricity production of generator 5 on table 4-47 is 87.51 GWh per year but on previous case it is 133.79 GWh per year. The difference of electricity production of both situations is quite significant. Minimum and maximum electrical output of generator 5 on both table 4-47 below and previous case are 46 MW and 55 MW respectively.

Table 4-47: Electricity Production of DG 5 on Combined DG and RE

Quantity	Value	Units
Electrical Production	87,507,288.00	kWh/year
Mean Electrical Output	53,228.00	kW
Minimum Electrical Output	46,425.00	kW
Maximum Electrical Output	55,500.00	kW

Since electricity production of generator 5 after RE integration is quite less than electricity production of generator 5 before RE integration therefore hours of operation of generator 5 after RE integration is also less than before RE integration. Hours of operation of generator 5 after RE integration are 1,644 hours per year but before RE integration they are 2,515 hours per year. Number of starts of generator 5 after RE integration is 1,121 starts per year but before integration they are 1,505 starts per year. Operational life of generator 5 gets increased after RE integration because it is operated less than before RE integration. Operational life of generator 5 after RE integration is 107 years but before RE integration it is 69.7 years. Capacity factor of generator 5 after RE integration is 18% but before RE integration it is 27.5 %. Fixed and marginal generation cost of generator 5 on both cases is US\$ 2.134 per hour and US\$ 0.0976 per kilowatt-hour respectively.

Table 4-48: Operation Hours of DG 5 on Combined DG and RE

Quantity	Value	Units
Hours of Operation	1,644	hours/year
Number of Starts	1,121	starts/year
Operational Life	107	year
Capacity Factor	18.0	%
Fixed Generation Cost	2,134	US\$/hour
Marginal Generation Cost	0.0976	US\$/kWh

Fuel consumption of generator 5 after RE integration is 22.63 million litre but before RE integration it is 34.60 million litre. Fuel energy input of generator 5 after RE integration is 222 GWh per year but before RE integration it is 340 GWh per year. Specific fuel consumption and mean electrical efficiency of generator 5 on both cases are 0.26 liter per kilowatt-hour and 39.30% respectively.

Table 4-49: Fuel Consumption of DG 5 on Combined DG and RE

Quantity	Value	Units
Fuel Consumption	22,629,166.00	L
Specific Fuel Consumption	0.26	L/kWh
Fuel Energy Input	222,671,024.00	kWh/year
Mean Electrical Efficiency	39.30	%

Before incorporating hydro, PV and wind into the grid, the load on black area in early year at night was covered by generator 5. After incorporating hydro, PV and wind into the grid it is covered by other sources either by renewable energy sources or diesel generators. Black area on previous case is more than on previous case, which means that on new case diesel generator 5 is rarely operated.



Figure 4-22: DG Power Output of DG 5 on Combined DG and RE

4.4.6 Hydro Power

Table 4-50 below is showing the simulation result of Hydro Power by Homer. Based on the flow rate of the river, the system decided to put nominal power of hydropower by 3.4 MW with the mean output of 3.05 MW. Capacity factor and hydro penetration of hydropower are 89.85% and 5.30 % respectively.

Total electricity production from hydropower is 26.76 GWh per year with hours of operation of 8760 hours per year. Minimum and maximum hydropower output are 2,737 kW and 3,604 kW respectively. Electricity production cost of hydropower is US\$ 0.05 per kilowatt-hour.

Table 4-50: Hydropower Simulation Result by Homer

Quantity	Value	Units
Nominal Capacity	3,399	kW
Mean Output	3,054	kW
Capacity Factor	89.85	%
Total Production	26,755,482	kWh/year
Minimum Output	2,737	kW
Maximum Output	3,604	kW
Hydro Penetration	5.30	%
Hours of Operation	8760	hours/year
Levelized Cost	0.05	US\$/kWh

Figure 4-23 below is showing the output power of hydropower with nominal capacity of 3.3 MW. According to figure 4-23, hourly output power of hydropower is based on monthly flow rate of the river. The maximum hydropower output is occurred in June while the lowest hydropower outputs are occurred in March and October. In general the highest hydropower output is occurred in the middle of a year.

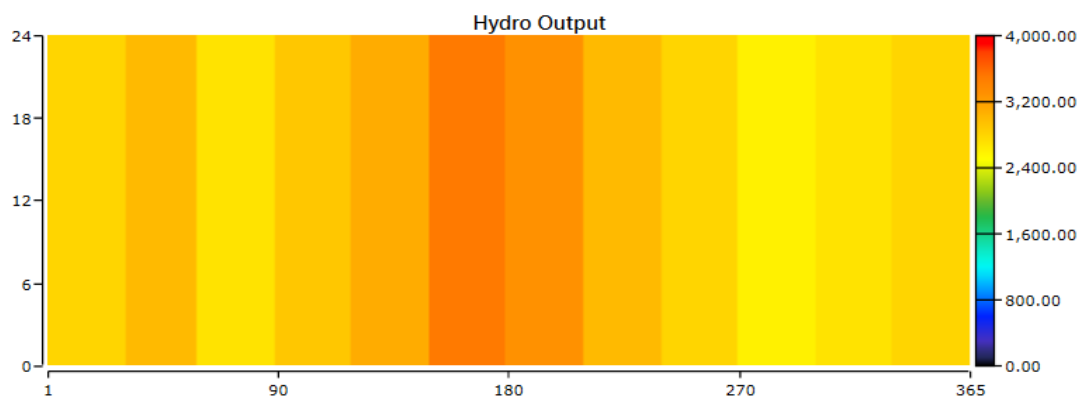


Figure 4-23: Hydro Power Output

4.4.7 Photovoltaic

It was decided to incorporate 3 MW PV connected into the grid. By assuming that solar radiation is the same for whole area in Palu city therefore PV arrays will be connected at any bus bar. In order to reduce the current, 3 MW PV array is separated into 6 groups and they will be connected spreading to some bus bar. According to table 4-51, mean output of PV array is 547 kW and PV rated capacity is

3,000 kW. Total electricity production from PV is 4.79 GWh per year and the mean output of PV is 13 MWh per year.

Minimum and maximum output power of PV are 0 kW and 2.87 MW respectively. Capacity factor of PV is 18.26% while PV penetration is 0.95%. Since the hours of operation of PV depend on the availability of sun therefore in this case it is only 4,380 hours per year. The cost needed to produce electricity 1 kWh from PV is US\$ 0.151.

Table 4-51: PV Simulation Results by Homer

Quantity	Value	Units
Rated Capacity	3,000	kW
Mean Output	547.65	kW
Mean Output	13,144	kWh/day
Capacity Factor	18.26	%
Total Production	4,797,401	kWh/year
Minimum Output	0.00	kW
Maximum Output	2,873	kW
PV Penetration	0.95	%
Hours of Operation	4,380	hours/year
Levelized Cost	0.151	US\$/kWh

Figure 4-24 is showing the output power of PV for whole day for one year. In general, on the clear weather PV power output is available from 6 am to 6 pm. The highest power output from PV is occurred in September from 9 am to 3 pm but the lowest power output is occurred at the end of the year from 5 pm to 6 pm. The dark yellow area indicating the highest PV power output is also occurred in 3 months at early year, some days in middle years and some days at the end of year.

Based on figure 4-24, PV rarely produces electricity at the end of the year. As mentioned on previous chapter that intermittent quite often occurred at the end of the year is caused by rainy season while intermittent rarely occurred in the middle of a year is caused by dry season. However some intermittent PV production is also occurred in the middle of a year.

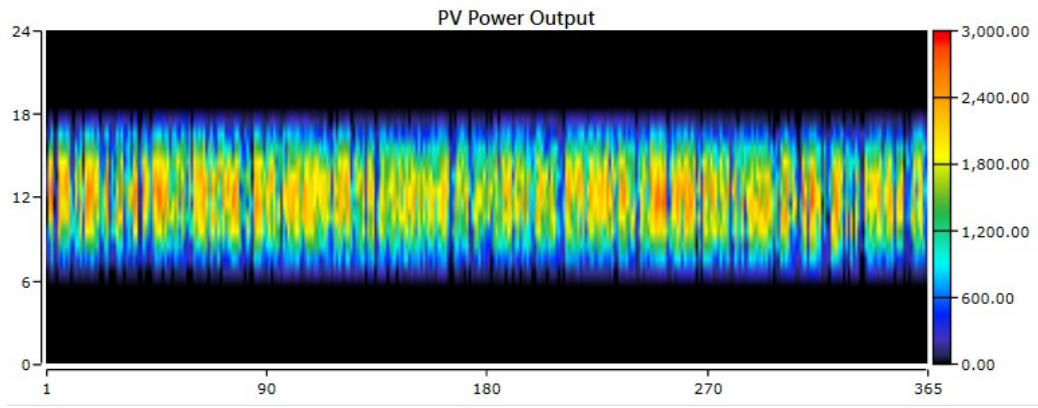


Figure 4-24: PV Power Output

4.4.8 Wind Power

Table 4-52: Wind Simulation Results

Quantity	Value	Units
Total Rated Capacity	12,000	kW
Mean Output	4,110	kW
Capacity Factor	34.25	%
Total Production	36,006,040	kWh/year
Minimum Output	2.79	kW
Maximum Output	20,000	kW
Wind Penetration	7.13	%
Hours of Operation	8760	hours/year
Levelized Cost	0.04	US\$/kWh

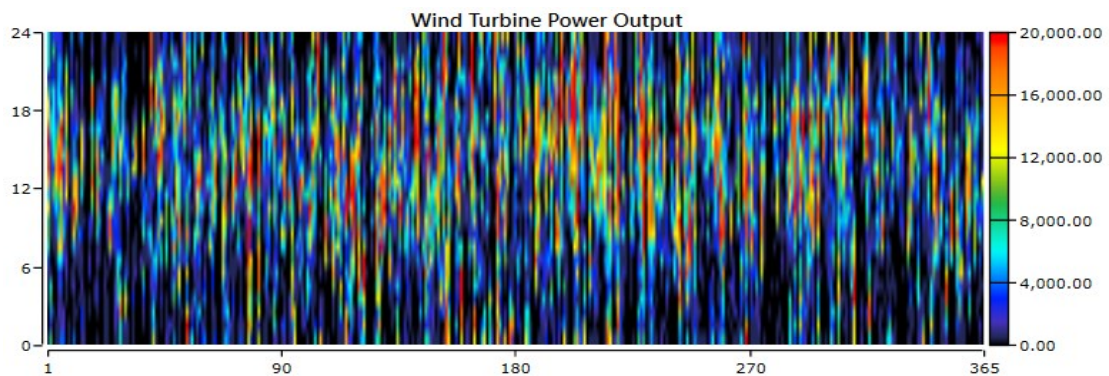


Figure 4-25: Wind Power Output

Based on table 4-52 and figure 4-25 above, total rated capacity of 8 (eight) wind turbines is 12,000 kW, each of them has nominal capacity of 1,500 kW (based on homer default setting). Mean wind power output is 4,110 kW with hours of operation of 8760 hours per year. Total electricity production from wind power is 36 GWh per year. Capacity factor and wind power penetration are 34.25% and 7.13 % respectively. Minimum wind power output is 2.79 kW while the maximum output power is 20,000 kW. Electricity production cost of wind power is US\$ 0.04/kWh.

4.4.9 Converter System

Table 4-53: Converter System Simulation Result

Quantity	Inverter	Rectifier	Units
Capacity	2,700	2,430	kW
Mean Output	492.88	0	kW
Minimum Output	0	0	kW
Maximum Output	2,585	0	kW
Capacity Factor	18.26	0	%
Hours of Operation	4,380	0	hours/year
Energy Out	4,317,672	0	kWh/year
Energy In	4,797,401	0	kWh/year
Losses	479,729	0	kWh/year

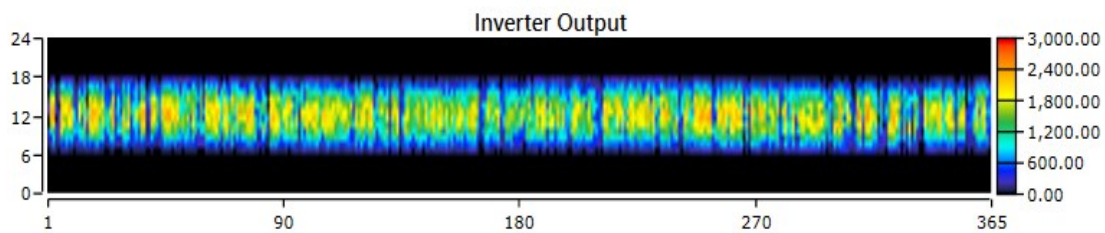


Figure 4-26: Inverter Output

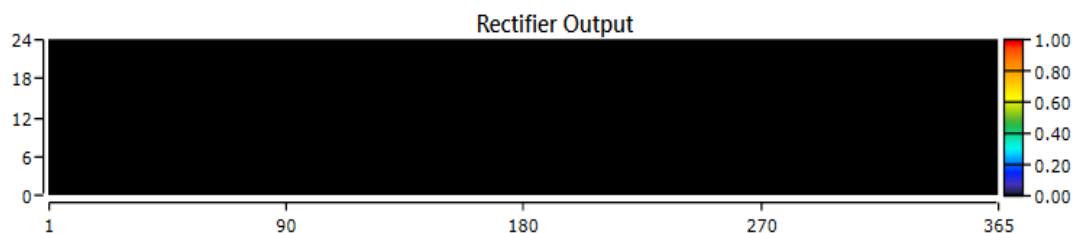


Figure 4-27: Rectifier Output

Since PV is connected into DC bus bar, we need converter that consists of inverter and rectifier to connect DC bus bar into AC bus bar. Figure 4-28 below is showing how all components are connected into AC and DC bus bar. 5 (five) diesel generators that consist of coal and diesel generator itself are connected into AC bus bar simultaneously with hydropower, grid, wind and load.

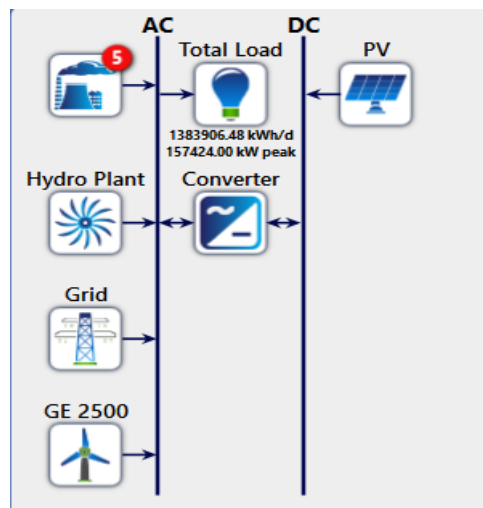


Figure 4-28: Combine DG and RE Connected into the Grid Using Chosen Wind Turbine

Table 4-53, figure 4-26 and figure 4-27 above are simulation result of converter used in this configuration system. The capacity of inverter and rectifier chosen by homer for this configuration system are 2,700 kW and 2,430 kW respectively. Mean output power of inverter is 492 kW while mean output power of rectifier is 0. Minimum output power of inverter and rectifier is zero but the maximum output power is 2,585 kW. Capacity factor of inverter is 18.26 % but capacity factor of rectifier is zero. Hours of operation of inverter are 4,380 hours per year but the hours of operation of rectifier are zero. Input energy of inverter is 4,797,401 kWh per year but inverter output energy is 4,317,672 kWh per year therefore inverter losses are 479,729 kWh per year. The energy input and output of rectifier are zero as well as its losses.

4.4.10 Emissions on Combined DG and RE Connected into the Grid Using Chosen Wind Turbine

Emissions produced by this configuration system can be seen on table 4-54 below. The highest emissions are coming from Carbone Dioxide with total amount of 298

million kilograms per year while on previous case it is 342 million kilogram per year. Compared with the previous case, this value gets decreased by 43 million kilogram per year.

Table 4-54: Emissions of Simulation Results of Combined DG and RE

Quantity	Value	Units
Carbon Dioxide	298,375,840.00	kg/year
Carbon Monoxide	736,616.00	kg/year
Unburned Hydrocarbons	81,594.00	kg/year
Particulate Matter	55,530.00	kg/year
Sulfur Dioxide	599,080.00	kg/year
Nitrogen Oxides	6,572,780.00	kg/year

Carbon Monoxide produced after RE integration is 736 thousand kilogram per year while on previous case it is 843 thousand kilogram per year. Compared with the previous case, this value gets decreased by 107 thousand kilogram per year. Unburned Hydrocarbons produced on this configuration system is 81 thousand kilogram per year but on previous case it is 93 thousand kilogram per year. Particulate matter produced on this configuration system is 55 thousand kilogram per year but on previous case it is 63 thousand kilogram per year. Sulfur dioxides and Nitrogen oxides produced on this configuration system are 599 thousand kilogram per year and 6 million kilogram per year respectively. Compared with the previous case, sulfur dioxides get decreased by 88 thousand kilogram per year and nitrogen oxides gets decreased by 958 thousand kilogram per year.

4.4.11 Grid Analysis of Combined DG and RE Connected into the Grid Using Chosen Wind Turbine

Based on table 4-55 below, the total annual electricity purchased from the grid is 96 MWh but on previous case it is 144 MWh. Monthly average electricity purchased from the grid on this configuration system is 8 MWh but on previous case it is 12 MWh. The highest electricity purchased from the grid is also occurred in November with total purchased electricity of 51 MWh but on previous case it is 85 MWh. The lowest electricity purchased is occurred in February with total purchased electricity of 194

kWh but on previous case it is occurred in October with total purchased electricity of 182 kWh.

Table 4-55: Purchased and Sold Electricity by Palapas System on Combined DG and RE

Month	Energy Purchased [kWh]	Energy Sold [kWh]	Net Energy Purchased [kWh]	Peak Demand [kW]	Energy Charge [US\$]	Demand Charge [US\$]
January	314	29,477	-29,163	61	1,711.30	0
February	194	3,879	-3,685	66	232.82	
March	549	21,565	-21,057	62	294.42	
April	24,659	13,697	10,963	20,357	72,745.00	
May	458	6,706	-6,248	61	770.22	
June	299	15,903	-15,604	62	533.10	
July	401	16,963	-16,562	60	322.53	
August	401	33,527	-33,126	66	1,815.30	
September	302	3,050	-2,748	64	631.75	
October	314	20,278	-19,964	75	882.84	
November	51,782	3,674	48,108	20,356	155,016.00	
December	17,013	3,263	13,750	10,434	50,746	
Annual	96,687	171,984	-75,297	20,357	274,583	

Purchased electricity on table 4-55 is increased in March, August, October and December compared with purchased electricity on previous case. It might be caused by the need to fulfill the operating reserved since in these months the load is high but electricity production from renewable energy is low and electricity production cost by diesel generators on micro grid are higher than purchasing electricity from the grid. Therefore micro grid system decided to buy more electricity from the grid. Based on table 4-55, in April, November and December the purchased electricity by micro grid is higher than electricity sold to the grid therefore the energy charge is much higher compared with other months.

The total annual energy charge on table 4-55 is US\$ 274,583 but on previous case it is US\$ 433,079. The highest energy charge is occurred in November with total energy charge of US\$ 155,016 and the lowest energy charge is occurred in February

with total energy charge of US\$ 232. The result diagram of purchasing electricity from the grid and selling electricity to the grid can be seen on figure 4-29 and figure 4-30 below.

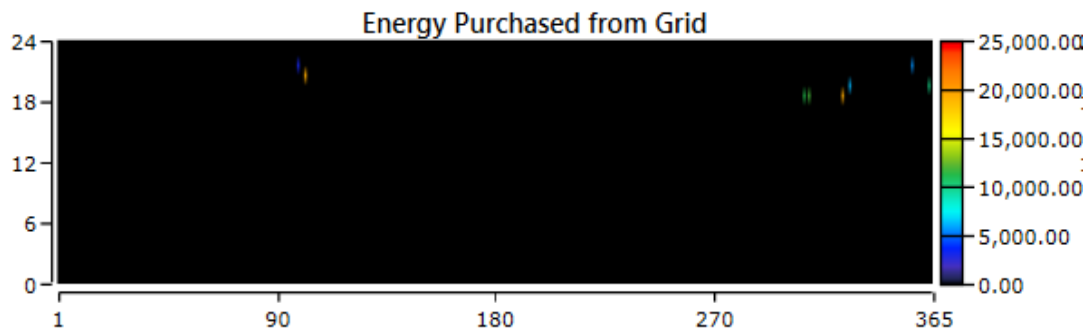


Figure 4-29: Energy Purchased by PALAPAS System from the Grid On Combined DG and RE

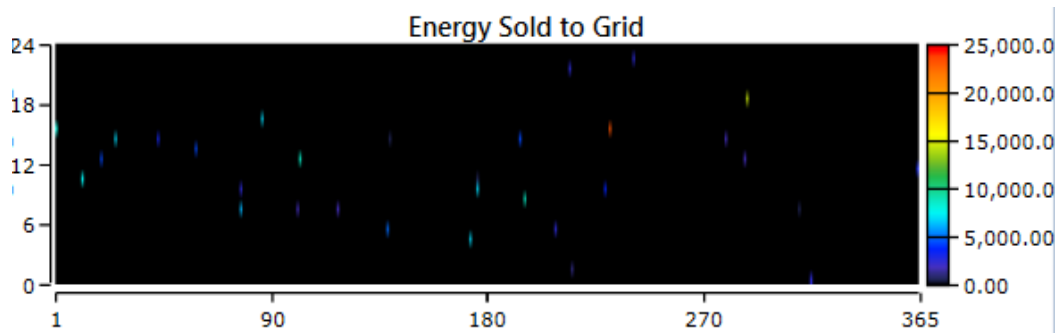


Figure 4-30: Energy Sold by PALAPAS System to the Grid on Combined DG and RE

Figure 4-29 and 4-30 are showing energy purchased from the grid and energy sold to the grid for 24 hours for a year. In this configuration system energy purchased from the grid is lower than energy sold to the grid. Energy purchased from the grid is occurred between 18:00 to 23:00 with frequently occurred at the end of a year and rarely occurred in middle of a year. Energy sold to the grid is mostly occurred between 5:00 to 17:00 and rarely occurred between 18.00 to 12:00.

4.4.12 Cost Summary of Combined DG and RE Connected into the Grid Using Chosen Wind Turbine

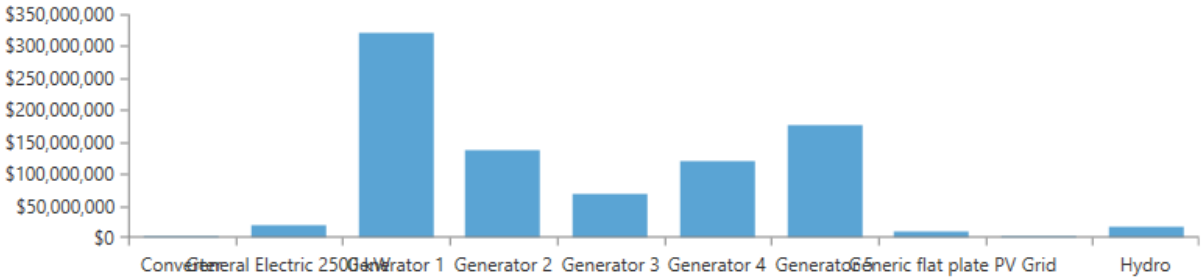


Figure 4-31: Net Present Cost of All Components on Combined DG and RE

Based on figure 4-31 above, after incorporating hydro, PV and wind into the grid, net present cost of non-renewable energy components is decreased compared with the previous case. Net present cost of diesel generator 1 after RE integration is around US\$ 320 million while on previous case it is around US\$ 460 million. Net present cost of diesel generator 5 after RE integration is around US\$ 175 million but on previous case it is around US\$ 346 million. Net present cost of diesel generator 2 after RE integration is US\$ 137 millions but on previous case it is around US\$ 190 million. Net present cost of diesel generator 4 after RE integration is around US\$ 120 million but on previous case it is around US\$ 177 million. Net present cost of diesel generator 3 after RE integration is around US\$ 67 million but on previous case it is around US\$ 94 million.

Net present cost of all non-renewable energy components after incorporating hydro, PV and wind is decreased quite significant. This phenomenon can be seen on diesel generator 1 and 5. In addition of comparing other costs, the detail cost of all components in this configuration system can be seen on table 4-56 below.

Table 4-56: Costs of All Components on Combined DG and RE Connected into the Grid Using Chosen Wind Turbines

Components	Capital [US\$]	Replacement [US\$]	O & M [US\$]	Fuel [US\$]	Salvage [US\$]	Total [US\$]
PV	9,000,000	0	387,825	0	0	18,518,247
Wind	16,250,000	5,180,614	7,240		2,919,611	18,518,246
Hydro	16,000,000	0	0		0	16,000,000
Generator 1	15,000,000		69,250,120	236,967,377	541,466	320,676,031
Generator 2	10,000,000		30,211,606	98,204,754	1,064,131	137,352,229
Generator 3	5,000,000		14,888,620	48,291,494	541,637	67,638,478
Generator 4	7,500,000		28,220,122	85,528,436	553,003	120,695,554
Generator 5	27,750,000		35,385,973	117,015,846	5,088,245	175,063,575
Grid	0		3,550,060	0	0	3,550,060
Converter	810,000	343,662	1,745,214	0	64,680	2,834,195
System	107,310,000	5,524,281	183,646,783	586,007,909	10,772,776	871,716,197

Based on table 4-56 above, total cost of new system is US\$ 871 millions while the total cost of previous case is US\$ 938 million. Therefore the new system can reduce the total cost by US\$ 67 million. Sorted by components, diesel generator 1 occupies the highest total cost. Although the capital cost of diesel generator 1 is lower than other diesel generators but its fuel cost is the highest compared with other components due to frequent use.

Sorted by renewable energy generator, wind occupies the highest total cost, which is US\$ 18.5 million and PV occupies the cheapest total cost with total cost of US\$ 9.4 million. PV and hydropower do not have replacement cost but wind power has replacement cost. Although wind power has replacement cost but it has salvage that can reduce its total cost by US\$ 2.9 million.

Sorted by non-renewable energy generator, all of them do not require replacement cost but they have salvage at the end of the project with total amount of US\$ 7.78 million. Salvage of previous case is US\$ 6.7 million therefore compared with the previous case, new case has salvage that is higher by US\$ 0.1 million than previous case. The total cost of operational and maintenance of all diesel generators of new system is US\$ 183.65 million while on previous case it is US\$ 208.32 million. This means O & M cost of all DG on new system is lower by US\$ 24.67 million than total O & M cost on previous case. Total fuel cost of diesel generators on new system is

US\$ 586 million while on previous case it is US\$ 671 million. This means that total fuel cost on new system is lower by US\$ 85 million than total fuel cost on previous case.

Operational and maintenance cost of grid on new system is around US\$ 3.55 million while on previous case it is US\$ 5.63 million. It means O & M cost of grid on new system is cheaper by US\$ 2.08 million than O & M cost of grid on previous case.

The capital cost of converter on new system is US\$ 810 and its replacement cost is around 1/3 less than its capital cost. Nevertheless at the end of project lifetime it has salvage of US\$ 64 thousand.

4.4.13 Sensitivity Analysis of Combined DG and RE Connected into the Grid Using Chosen Wind Turbine

The total cost of new system is dominated by fuel cost which is US\$ 583 million. Fuel cost is fluctuating therefore it is necessary to consider about fuel cost especially when it is increasing. Fuel cost of diesel generators on new system is lower than fuel cost of diesel generators on previous case. Fuel price of diesel generator 5 significantly decreases from US\$ 268 million to US\$ 117 million and fuel price of diesel generator 1 decreases from US\$ 372 million to US\$ 236 million. Fuel price of diesel generator 2 decreases from US\$ 151 million to US\$ 98 million. Fuel price of diesel generator 3 decreases from US\$ 74 million to US\$ 48 million. Fuel price of diesel generator 4 decreases from US\$ 140 million to US\$ 85 million.

When fuel cost increases from US\$ 0.4 per liter to US\$ 1.6 per litre, fuel cost of diesel generator will also increase. Fuel cost of diesel generator 1 will increase from US\$ 18 million to US\$ 74 million and fuel cost of diesel generator 2 will increase from US\$ 7 million to US\$ 29 million. Fuel cost of diesel generator 3 will increase from US\$ 3 million to US\$ 14 million and fuel cost of diesel generator 4 will increase from US\$ 6 million to US\$ 26 million. Fuel cost of diesel generator 5 will increase from US\$ 9 million to US\$ 31 million.

Table 4-57: Sensitivity Analysis of Fuel Cost Consumed by DG on Combined DG and RE Connected into the Grid Using Chosen Wind Turbine

Diesel Fuel Price [US\$/litre]	Fuel Cost [US\$]				
	Gen 1	Gen 2	Gen 3	Gen 4	Gen 5
0.4	18,290,552	7,622,017	3,750,004	6,615,975	9,051,667
0.5	23,126,201	9,350,725	4,558,776	8,267,301	11,329,505
0.6	27,486,206	11,386,932	5,602,508	9,923,806	13,595,407
0.7	32,242,738	13,171,975	6,469,435	11,576,747	15,861,307
0.8	34,590,924	16,557,448	8,138,746	13,231,530	18,140,584
0.9	41,693,568	16,771,276	8,236,576	14,881,744	20,408,156
1	46,159,928	18,719,668	9,218,830	16,532,212	22,692,442
1.2	54,542,624	23,003,060	11,364,129	19,841,530	27,235,246
1.4	64,486,144	26,285,290	12,974,475	23,122,084	31,781,324
1.6	74,347,704	29,563,354	14,559,349	26,446,802	36,394,072

Table 5-58 below is showing the change of energy purchased from the grid and energy sold to the grid when fuel cost increases. When fuel price increases from US\$ 0.4/litre to US\$ 1.6/litre, it will increase the total annual energy purchased from the grid from 96.69 MWh to 102.43 MWh. This situation will not influence energy sold to the grid.

Table 4-58: Sensitivity Results of Electricity Purchased and Sold by PALAPAS System on Combine DG and RE Connected into the Grid Using Chosen Wind Turbine

Fuel Price [US\$/litre]	Grid	
	Energy Purchased [kWh]	Energy Sold [kWh]
0.4	96,687	171,984
0.5	97,084	
0.6	97,294	
0.7	97,517	
0.8	97,893	
0.9	98,214	
1	98,787	
1.2	99,677	
1.4	100,917	
1.6	102,432	

Table 4-59 below is showing sensitivity analysis of costs when fuel price increases from US\$ 0.4/litre to US\$ 1.6/litre. Levelized cost of energy in this configuration system will increase from US\$ 0.133/kWh to US\$ 0.40/kWh. Net present cost will increase from US\$ 853 million to US\$ 2.61 Billion and operational cost will increase from US\$ 59 Million to US\$ 195 Million.

Table 4-59: Sensitivity Analysis of Costs on Combined DG and RE Connected into the Grid Using Chosen Wind Turbine

Fuel Price [US\$/liter]	Cost [US\$]		
	Levelized Cost of Energy[US\$/kWh]	Net Present Cost [US\$]	Operational Cost [US\$]
0.4	0.133	872 Million	59 Million
0.5	0.156	1.02 Billion	70.5 Million
0.6	0.178	1.16 Billion	81.8 Million
0.7	0.201	1.31 Billion	93.1 Million
0.8	0.223	1.46 Billion	104 Million
0.9	0.246	1.60 Billion	116 Million
1.0	0.268	1.75 Billion	127 Million
1.2	0.313	2.04 Billion	150 Million
1.4	0.358	2.34 Billion	172 Million
1.6	0.403	2.63 Billion	195 Million

On previous case, sensitivity analysis result of all costs on table 4-59 decrease. Levelized cost of energy on new system increases from US\$ 0.133/kWh to US\$ 0.40/kWh but on previous case it increases from US\$ 0.144/kWh to US\$ 0.455/kWh. Net present cost on new system increases from US\$ 853 Million to US\$ 2.61 billion but on previous case it increases from US\$ 938 million to US\$ 2.95 billion. Operational Cost on new case increases from US\$ 59 million to US\$ 195 million but on previous case it increases from US\$ 67.5 million to US\$ 223 million.

5 Power Quality Evaluation

Power Quality evaluation is one of the ways to ensure the reliability of grid power system. Since some different generation technologies will differently react to some disturbances therefore power quality evaluation must be conducted. Sag, swell, interruption and harmonics are created in public utility grid (Palapas System) to analyse how palapas system reacts to some of these disturbances.

5.1 Integrating Hydro, PV and Wind into the Grid Using ETAP 12.6

Before conducting simulation of power quality evaluation it is necessary to integrate hydro, PV and wind into the grid using ETAP 12.6 version. The size and on which bus bar RE sources are connected are explained more details below.

5.1.1 Hydro

All RE sources are connected into the grid through additional bus bar. 3 MW of hydro are connected into Silae SB4 bus bar through additional bus called bus 11. The location of hydro source is more near to Silae bus bar than any other bus bars and Silae SB4 bus bar is the weakest bus bar based on power flow analysis.

On figure 5-1 it is showing that the color of Silae 4 bus bar is red that means critical therefore the function of integrating hydropower in this bus bar is to control MVAR. Since Silae bus bar is only supplied by Silae substation that is connected to far radial system that can result in voltage drop therefore integrating hydropower on this bus bar also can reduce voltage drop on this bus bar. Figure 5-2 is showing the condition after integrating hydropower on Silae 4 bus bar. On figure 5-1 the color of Silae 4 bus bar is changed to pink that means less critical than before.

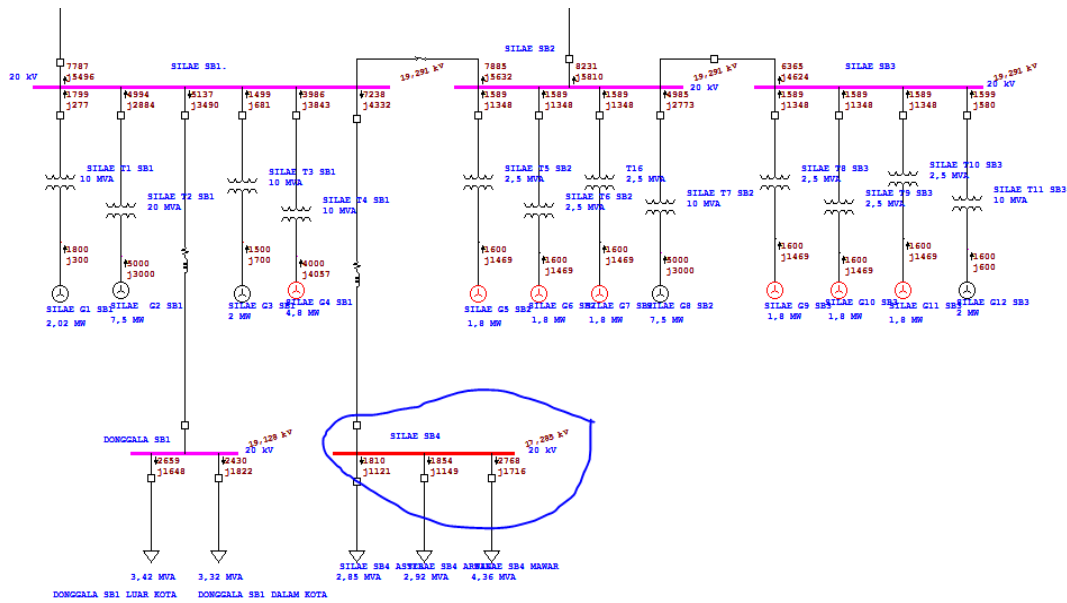


Figure 5-1: Silae SB4 Bus bar Before Integrating Hydropower

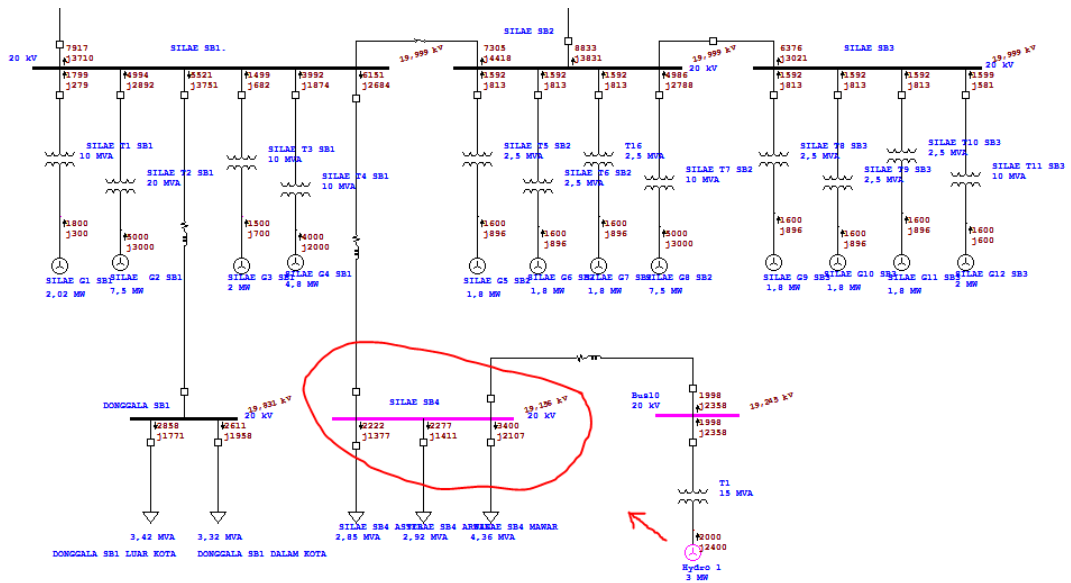


Figure 5-2: Silae SB4 Bus bar After Integrating Hydropower

5.1.2 PV

3 MW PV are distributed in 3 additional bus bar consisting of 5 x 600 kW PV arrays. PV source is injected by 100 % into the grid. PV1 and PV3 are connected to Talise SB3 bus bar through additional bus bar called bus 32. PVA2 and PVA4 are

connected into Parigi SB2 through additional bus bar called bus 36. PVA5 is connected into PJPP SB1 bus bar through additional bus bar called bus 40.

The condition before and after integrating PV into the grid can be seen on figure 5-3, figure 5-4, figure 5-5, figure 5-6, figure 5-7 and figure 5-8 below.

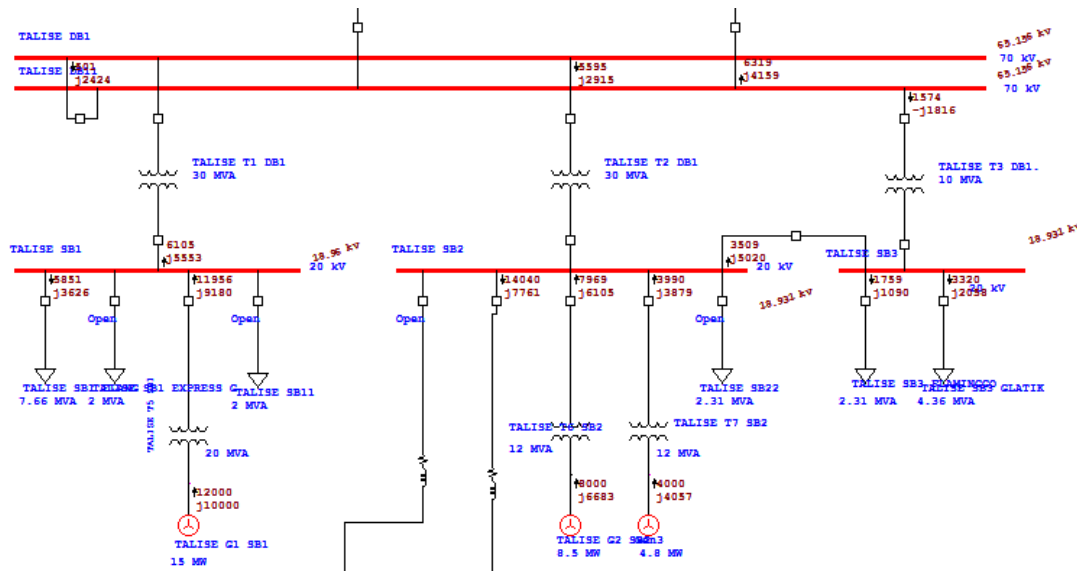


Figure 5-3: Before Integrating PV on Talise SB3 Bus bar Through Bus bar 32

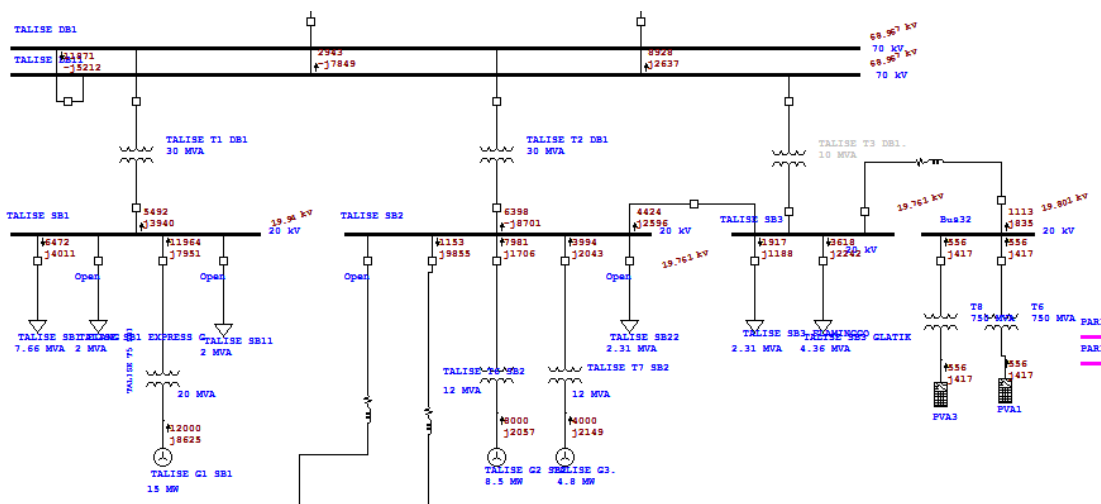


Figure 5-4: After Integrating PV on Talise SB3 Bus bar Through Bus bar 32

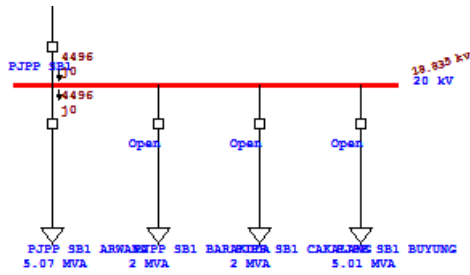


Figure 5-5: Before Integrating PV on PJPP SB1 Bus bar Through Bus bar 40

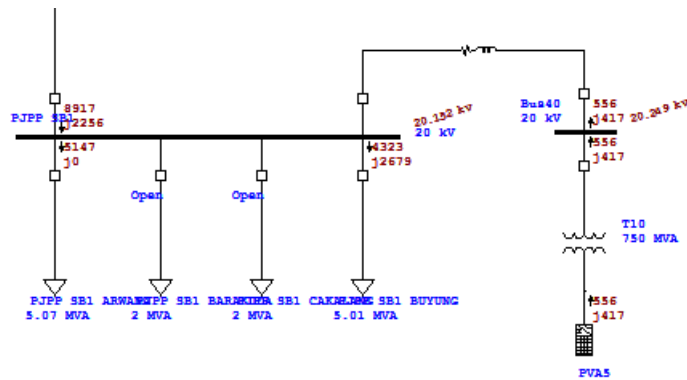


Figure 5-6: After Integrating PV on PJPP SB1 Bus bar Through Bus bar 40

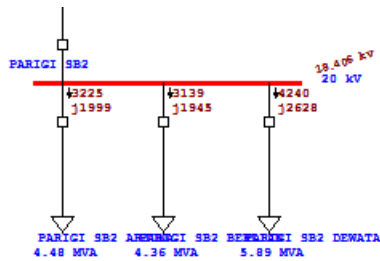


Figure 5-7: Before Integrating PVA2 and PVA4 on Parigi SB2 Bus bar

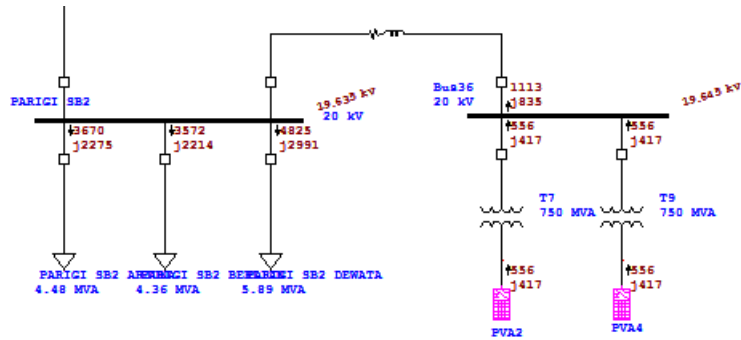


Figure 5-8: After Integrating PVA2 and PVA4 on Parigi SB2 Bus bar

5.1.3 Wind

20 MW wind power consisting 8 wind turbines with each capacity of 2.5 MW is connected into Maesa SB1(2) bus bar through additional bus bar called bus 46. In all simulation wind is injected into the grid by 80%.

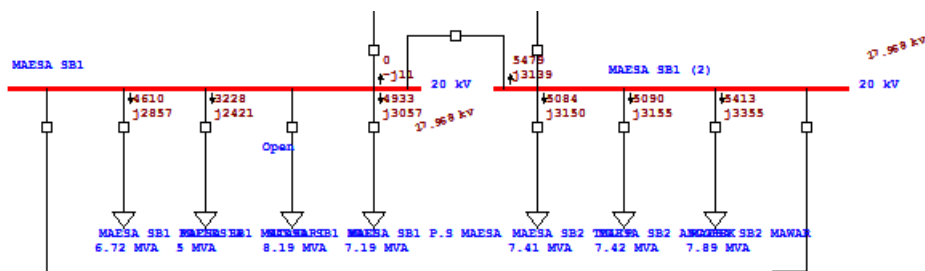


Figure 5-9: Before Integrating Wind Power into Maesa SB1 Bus bar Through Bus bar 46

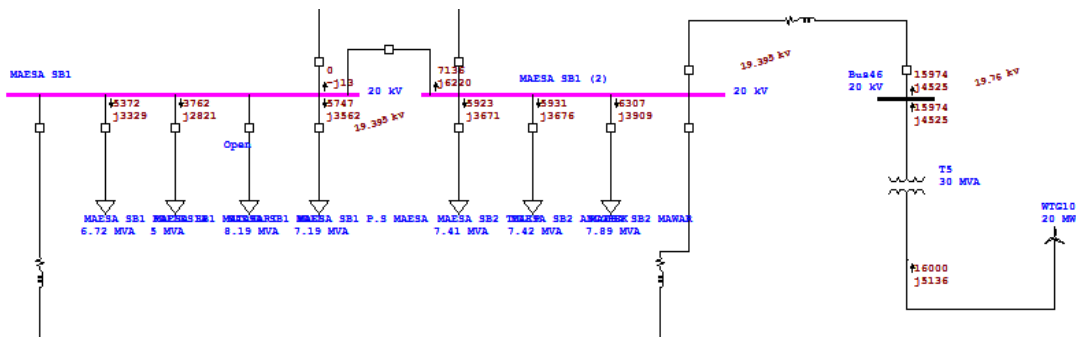


Figure 5-10: After Integrating Wind Power into Maesa SB1 (2) Bus bar

5.2 New Different Configuration of Diesel Generator Using Homer Results

Three simulation consisting before RE integration (Appendix A), after RE integration (Appendix B) and after RE integration based on HOMER simulation results (Appendix C) were executed on this research. Based on HOMER results, only 5 diesel generators installed in Palapas system. Although the number of diesel generator is less than the number of diesel generator in existing situation but the total capacity of diesel generator based on homer result is more than total capacity of diesel generator in existing situation. 5 (five) diesel generators based on homer results are the following:

- DG 1 (30 MW)
- DG 2 (20 MW)
- DG 3 (10 MW)
- DG 4 (15 MW)
- DG 5 (55.5 MW)

All diesel generators are placed on the same bus bar where old diesel generators exist. Only the capacity of diesel generator in existing situation is upgraded but one of them is downgraded. Upgrading old diesel generators based on homer results are the following.

5.2.1 Diesel Generator DG1 (30 MW)

Diesel generator named G2 with capacity of 15 MW connected to double bus bar DB1 PJPP and DB11 PJPP with voltage system of 70 kV is replaced and upgraded with diesel generator DG1 with capacity of 30 MW.

Figure 5.11 is showing the condition before upgrading from G2 (15 MW) to G1 (30 MW). And figure 5.11 is showing the condition after upgrading from G2 (15 MW) to G1 (30 MW).

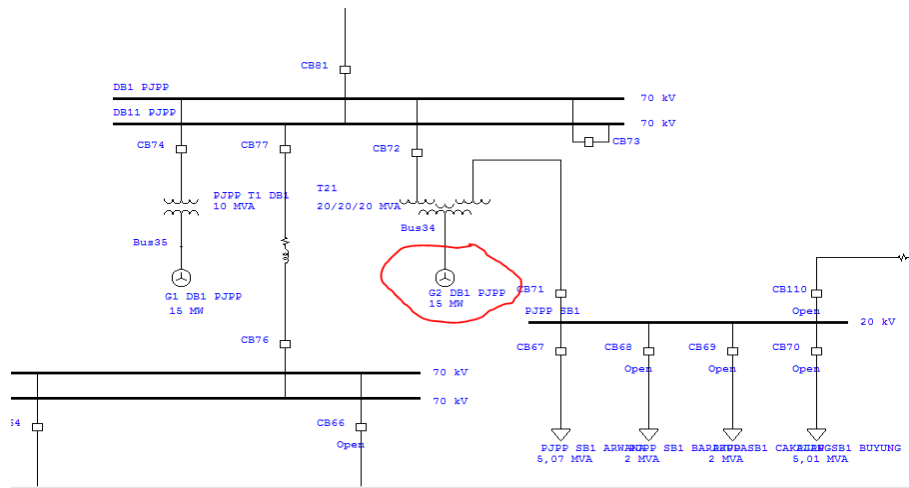


Figure 5-11: Before Upgrading from DG2 (15 MW) to DG1 (30 MW)

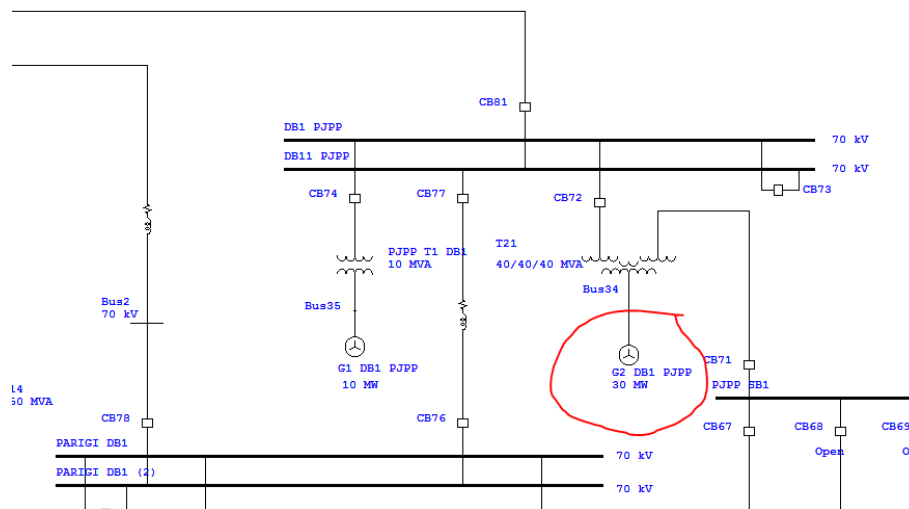


Figure 5-12: After Upgrading DG1

5.2.2 Diesel Generator DG2 (20 MW)

Two diesel generators named G2 (8.5 MW) and G3 (4.8 MW) connected to Talise SB2 bus bar are replaced and upgraded with only one diesel generator named DG2 with capacity of 20 MW. Figure 5.13 and figure 5.14 are showing the condition before and after upgrading from two diesel generators mentioned above with one diesel generator based on homer results.

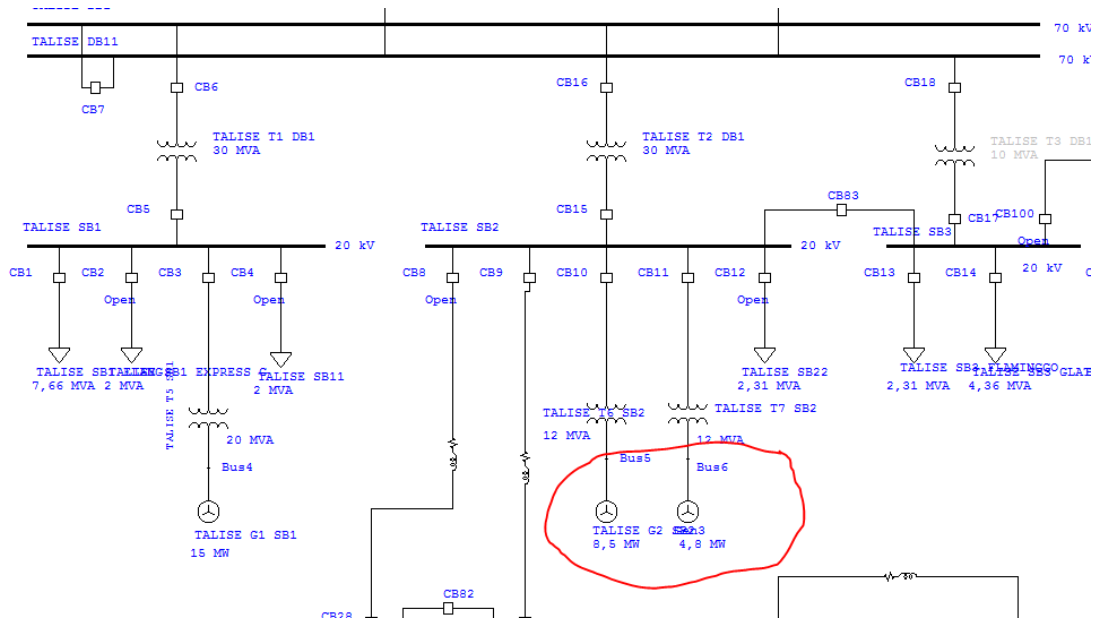


Figure 5-13: Before Upgrading Two DG Becoming One DG (DG2)

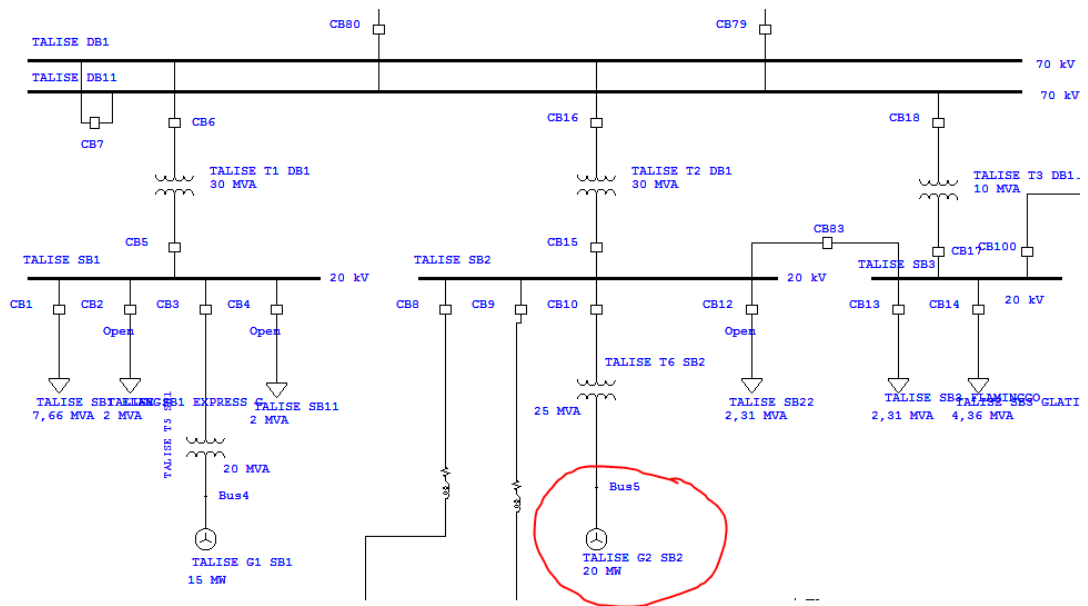


Figure 5-14: After Upgrading Two DG Becoming One DG (DG2)

5.2.3 Diesel Generator DG3 (10 MW)

One diesel generator named G1 with capacity of 15 MW connected to double bus bar DB1 PJPP and DB11 PJPP is replaced and downgraded to G1 with capacity of 10 MW. Figure 5-15 and figure 5-16 are showing the condition before and after downgrading from existing capacity to the situation based on homer results.

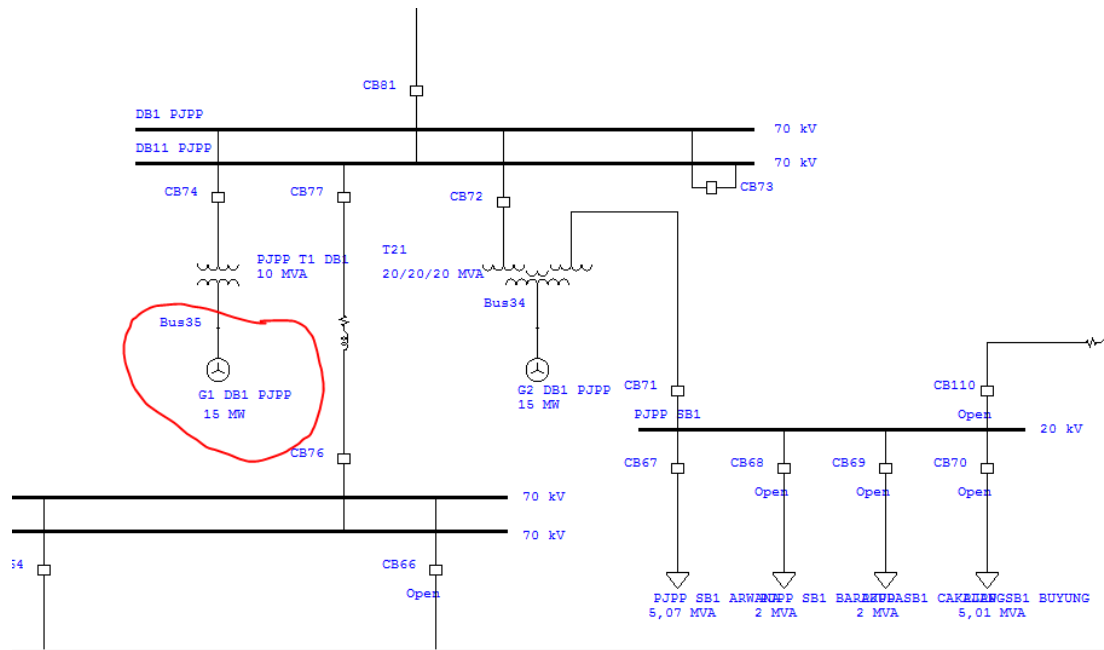


Figure 5-15: Before Downgrading from DG1 (15 MW) to DG3 (10 MW)

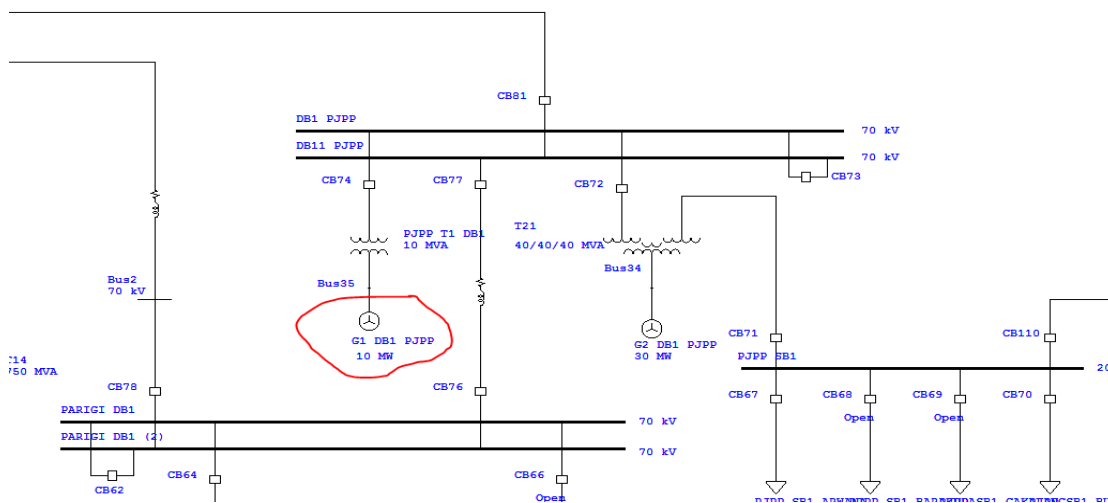


Figure 5-16: After Downgrading from DG1 (15 MW) to DG3 (10 MW)

5.2.4 Diesel Generator DG4 (15 MW)

Diesel generator G1 with the same capacity based on homer results replaces Diesel generator G1 with capacity of 15 MW connected to Talise SB1 bus bar in existing capacity. Figure 5-17 and figure 5-18 are showing the condition before and after using homer result, which is same.

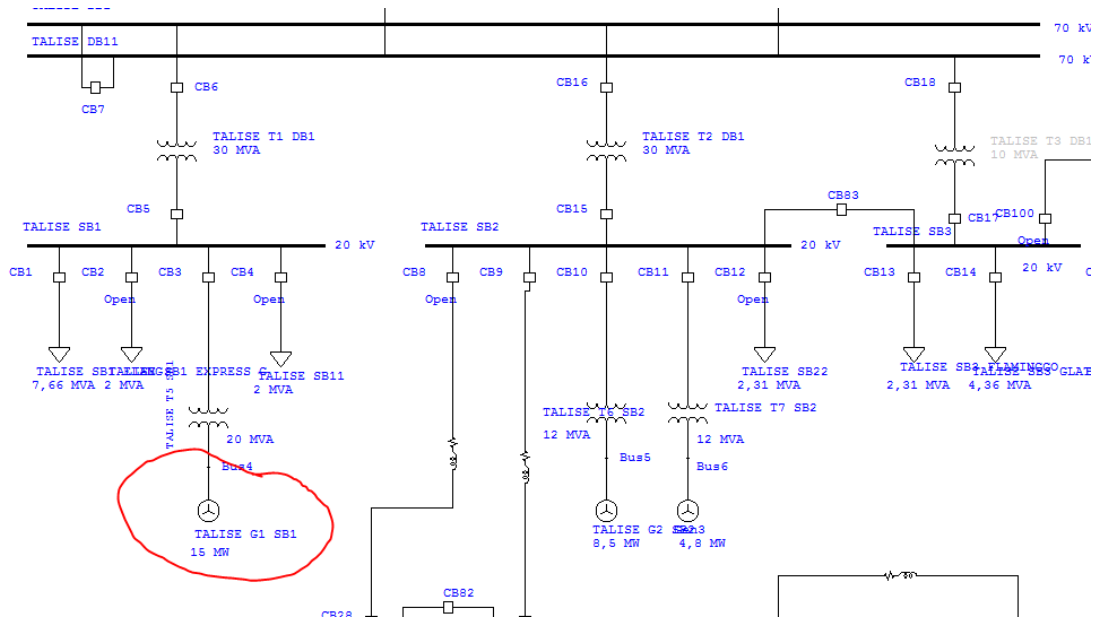


Figure 5-17: G1 Before Using Homer Results

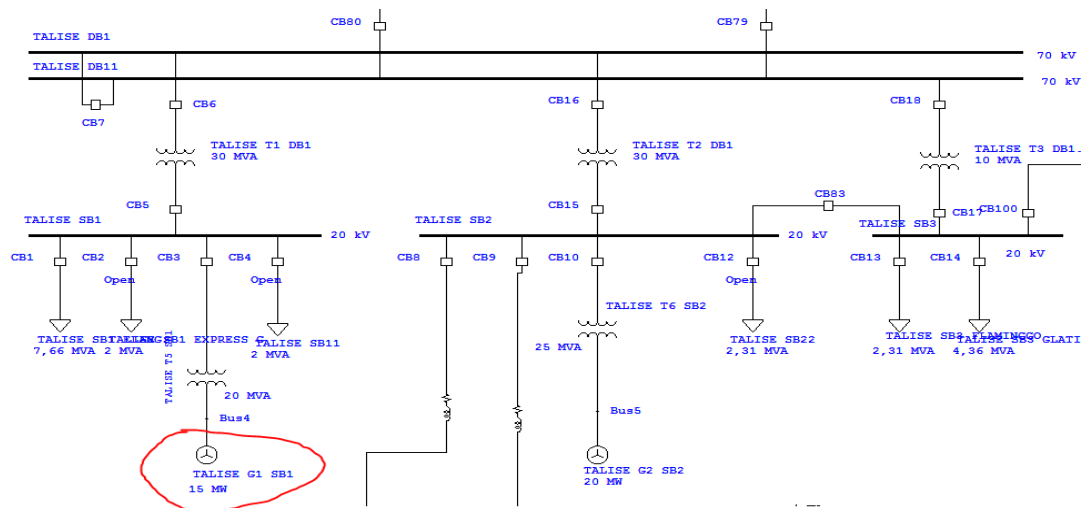


Figure 5-18: G1 After Using Homer Results

5.2.5 Diesel Generator DG5 (55.5 MW)

One diesel generator with capacity of 55.5 MW is replacing twelve diesel generators with total capacity of 36.62 MW connected to Silae SB1 bus bar, Silae SB2 bus bar and Silae SB3 bus bar. The new bus bar based on homer results is placed on Silae SB2 bus bar. This situation can be seen on figure 5-19 and figure 5-20 below.

After upgrading, Silae SB1 bus bar is functioned as load bus and Silae SB3 bus bar is removed due to previous function of this bus only as generator bus bar.

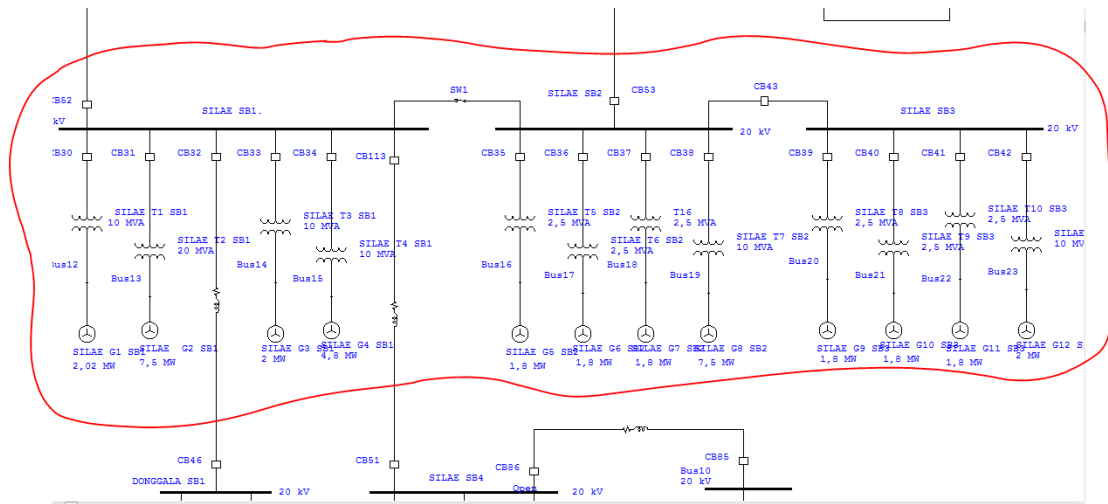


Figure 5-19: Before Replacing Some DG with one DG (55.5 MW)

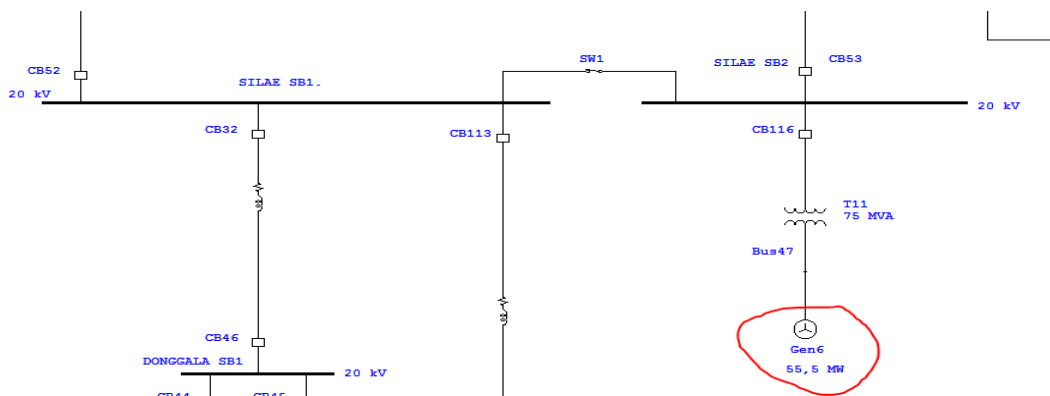


Figure 5-20: After Replacing Some DGs with DG5 (55.5 MW)

5.3 Simulation

These simulations consist of 3 different cases; before integrating RE into the grid, after integrating into the grid and after integrating RE into the grid using optimized homer results. Power quality events created in this simulation are a short duration events consisting of sag, swell, interruption and harmonics. Therefore there are 12 simulations in which every simulation will evaluate 19 main bus bars in public utility (palapas system).

5.3.1 Sag

Three-phase fault was created on bus maesa SB1 to run simulation of sag event. The fault duration lasts for 1 second started from 0.5 second to 1.5 second. The total simulation is run for 1.5 seconds with simulation time step of 0.001 dt and plot time step of 20 x dt. The sag event can be seen on figure 5-21 below.

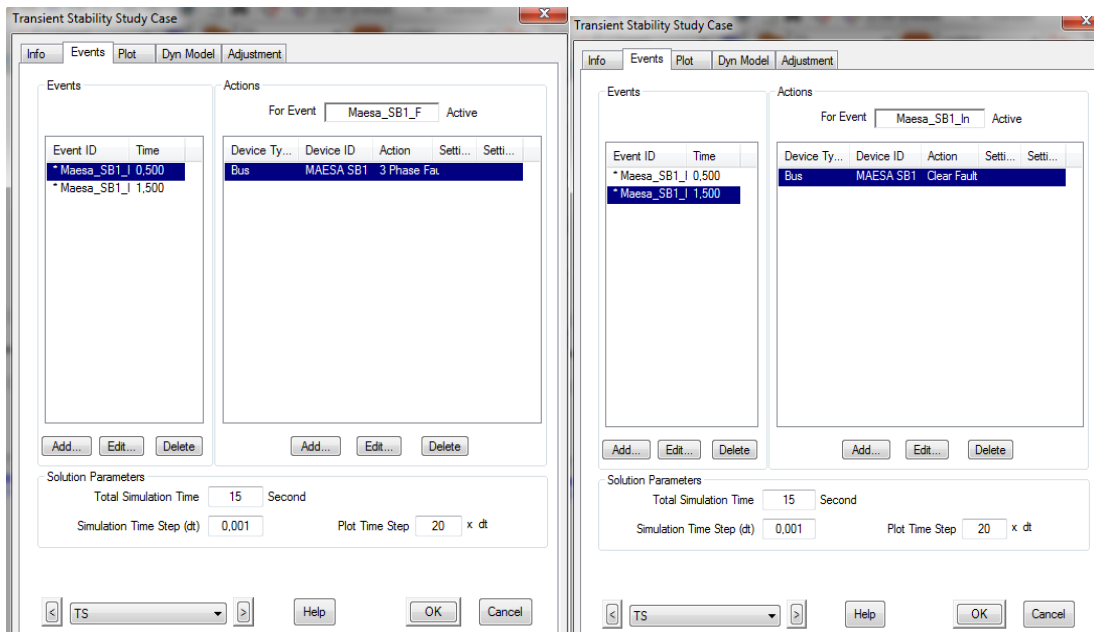


Figure 5-21: Sag Simulation

5.3.2 Swell

Swell event in this simulation is created by opening CB 20, CB 21, CB 23, CB 24 and CB 25 to disconnect some loads on maesa bus bar. The swell event is started from 0.5 second to 1.5 seconds. The total simulation is run for 1,5 seconds with time step of 0.001 dt and plot time step 20 x dt. The swell event in this simulation can be seen on figure 5-22 below.

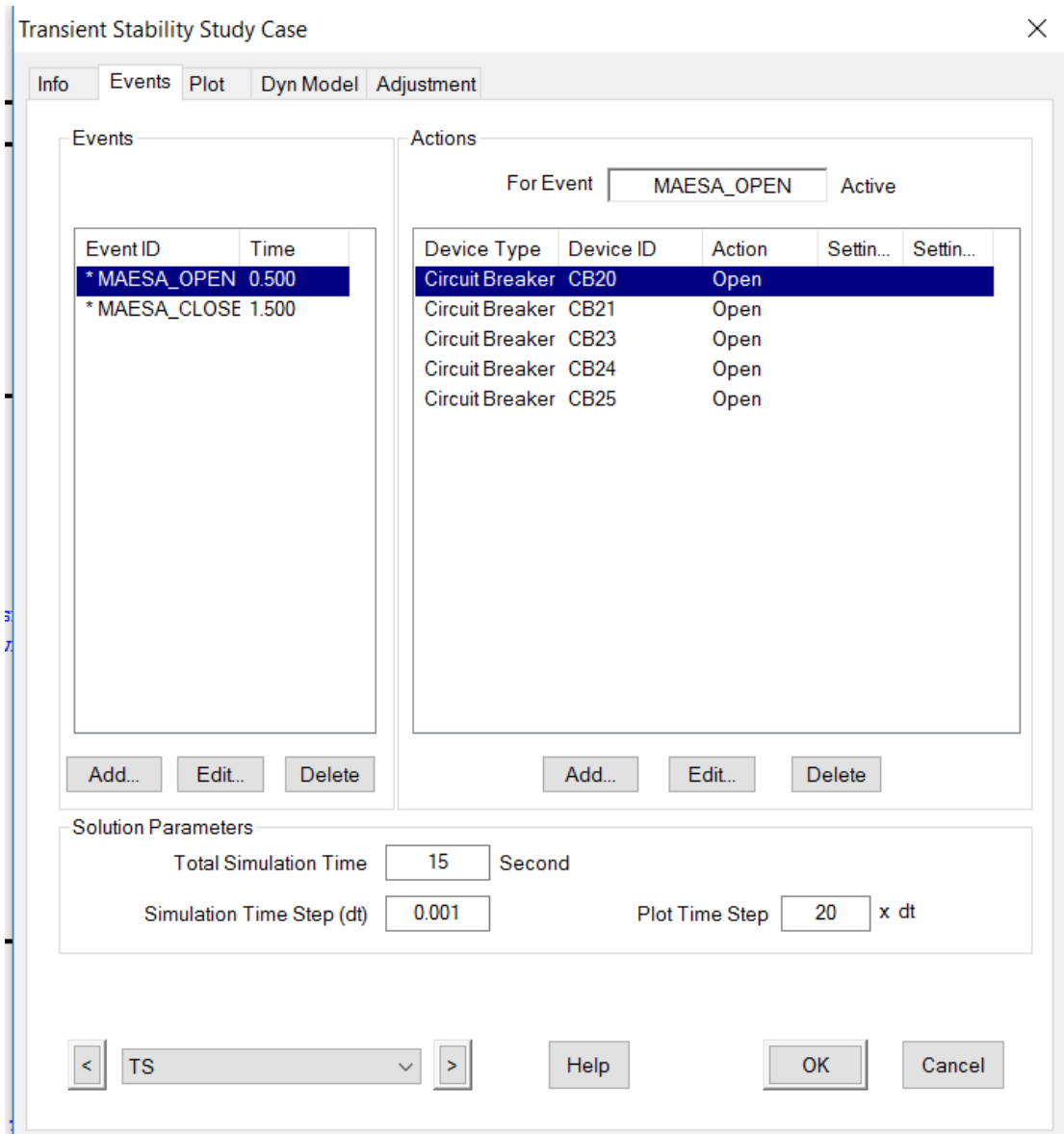


Figure 5-22: Swell Simulation

5.3.3 Interruption

All generators including generator based on RE technology (hydro, pv and wind) are disconnected to create interruption event in this simulation. CB 10, CB 11, CB 30, CB 31, CB 33, CB 34, CB 35, CB 36, CB 37, CB 38, CB 39, CB 40, CB 41, CB 42, CB 3, CB 74, CB 71 and CB 72 are opened to disconnect all generators (non-renewable energy and renewable energy) from the grid. This event is created to observe how all generators from different technologies synchronize each other and starting working after disconnecting them from the grid. They are disconnected started from 0.5

second to 1.5 second therefore the total simulation lasts for 1.5 second. Figure 5-23 is showing how this event was created.

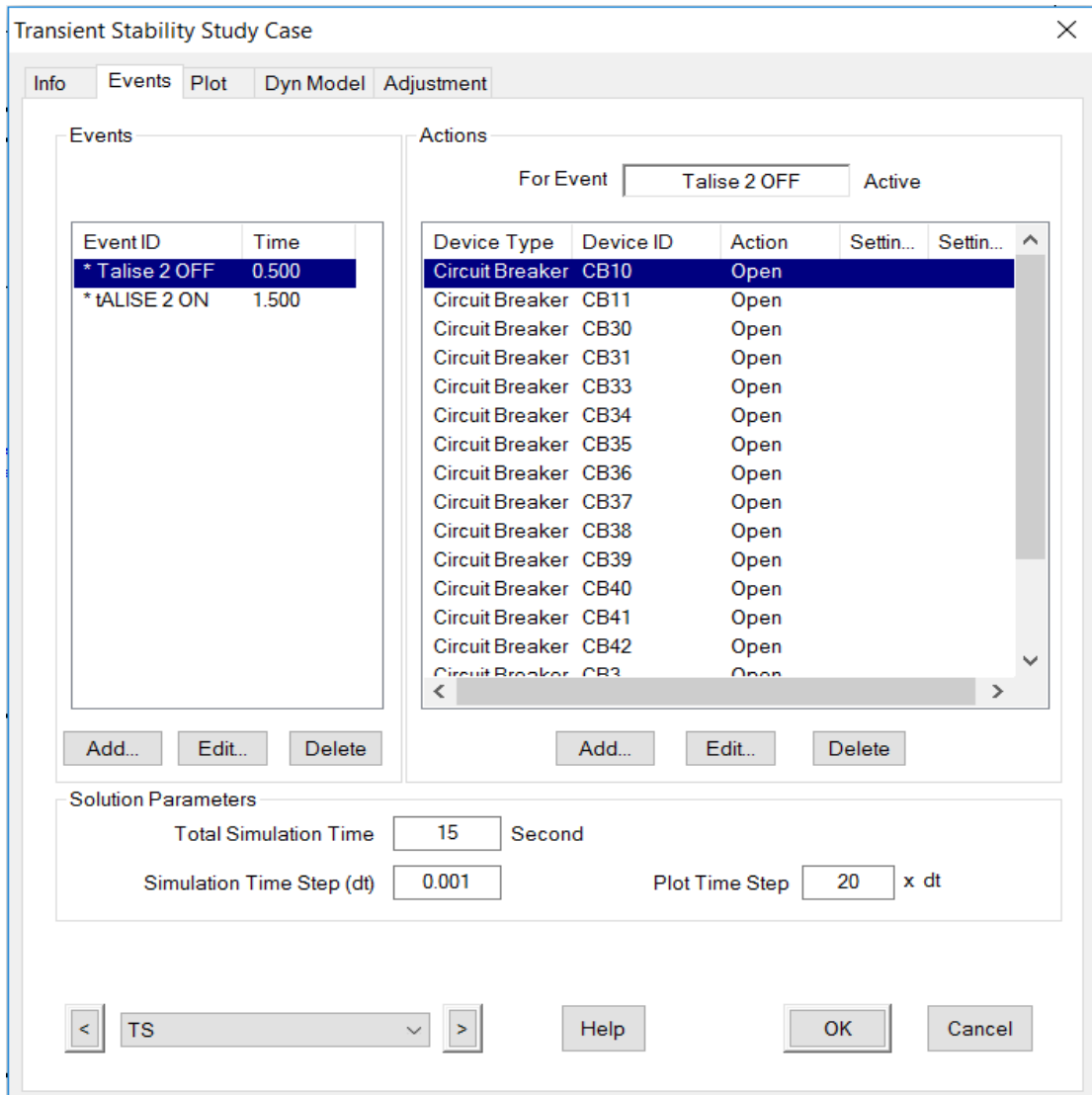


Figure 5-23: Interruption Simulation

5.3.4 Harmonics

To create harmonics event in this simulation, it is assumed that load on bus Maesa SB1 is contributing harmonics. Load Maesa SB1 Bus bar is assumed an equipment of certain model from one manufacturer contributing harmonics from current source. Figure 24 is showing how harmonics event is created in this simulation.

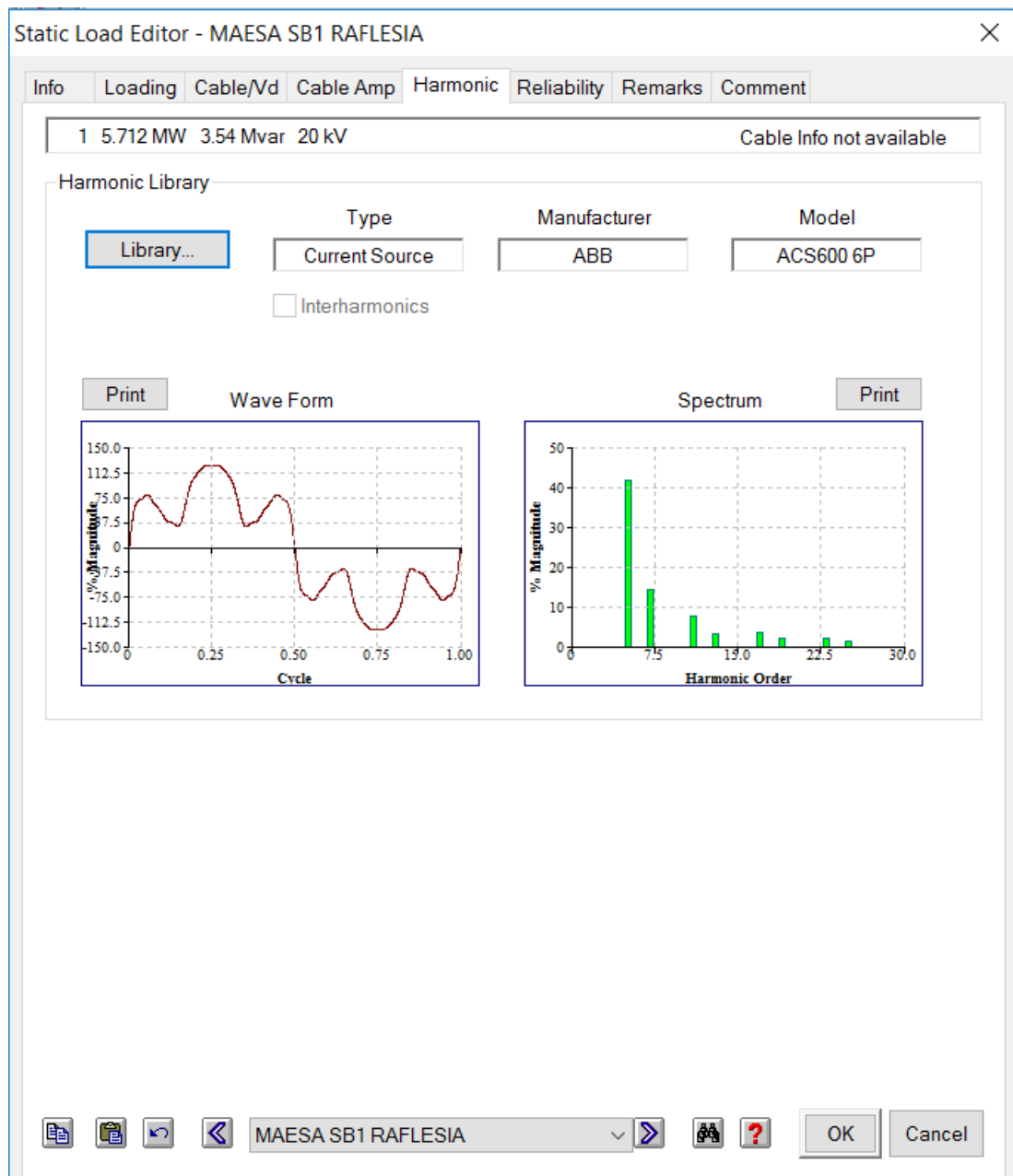


Figure 5-24: Harmonic Simulation

5.4 Simulation Result and Analysis

Simulation consists of sag, swell, interruption and harmonics. This research will analyse 3 (three) parameters of 19 main bus bars consisting of percentage of bus nominal in % kV and bus frequency in %.

5.4.1 Sag Simulation Results

Bus voltage of sag simulation results of bus bar DB1 PJPP before RE integration, after RE integration and after RE integration using homer results.

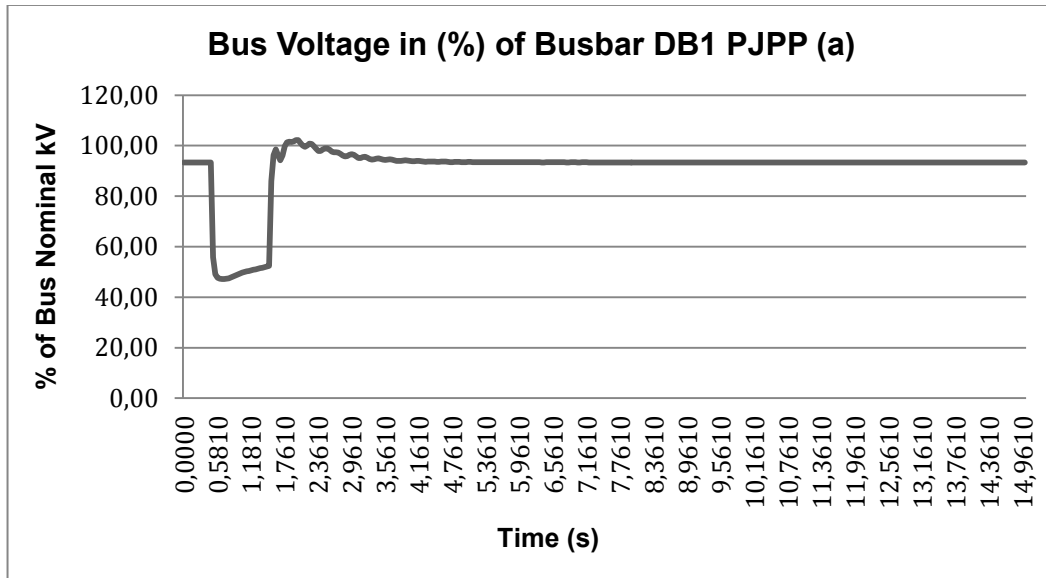


Figure 5-25: DB1 PJPP Bus Voltage Sag Simulation Results on Situation A

Based on figure 5-25 above, before sag percentage of bus voltage was at 91.7 % kV. When sag was occurred (from 0.5 s – 1.5 s), it was going down to 43.6 % kV and then it had been going up to 51 % kV for 1 second during sag. After sag, percentage of bus voltage was going up to 97 % and then it had been going down to 92 % kV in 0.1 second. It had been going up to 101.2 % kV in 0.3 seconds and then it was getting stable at 91.7 % kV at 5.1st second.

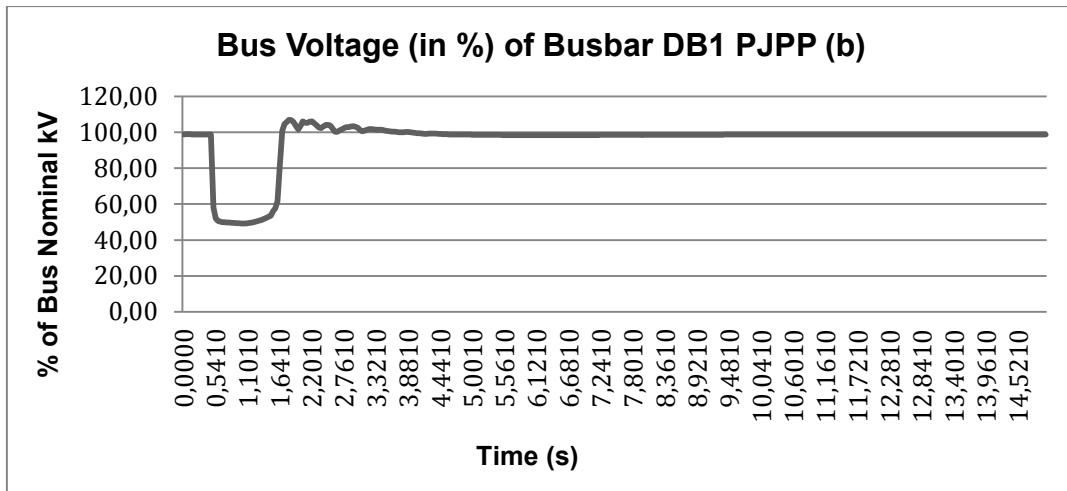


Figure 5-26: DB1 PJPP Bus Voltage Sag Simulation Results on Situation B

Based on figure 5-26, before sag percentage of bus voltage was at 99 % kV. When sag was occurred (from 0.5 s – 1.5 s), it had been going down to 52 % kV in 0.5 seconds and then it had been going up to 54.5 % kV in 0.5 second. After sag, percentage of bus voltage had been going up to 106 % kV in 0.1 second and then it was getting stable at 99 % kV at 9.2nd second.

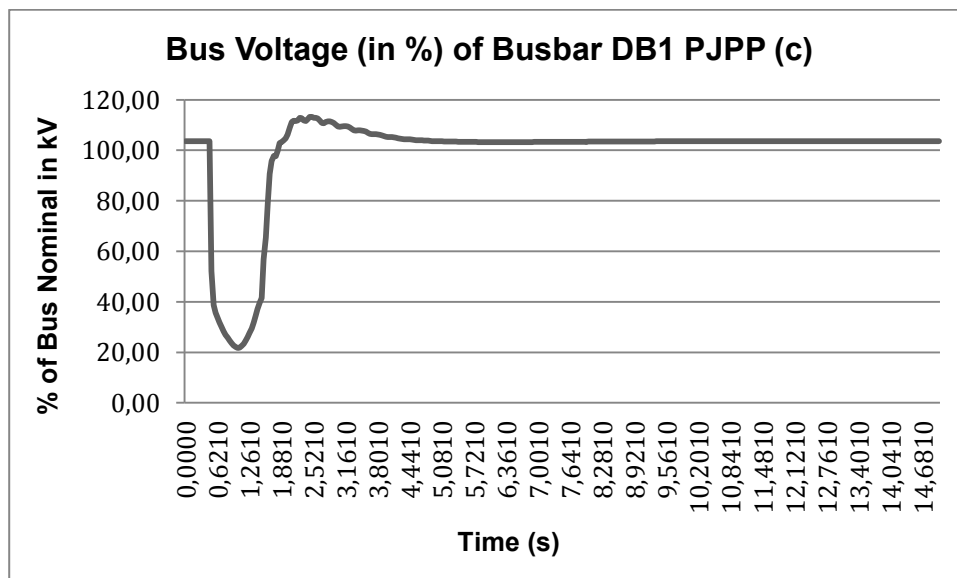


Figure 5-27: DB1 PJPP Bis Voltage Sag Simulation Results on Situation C

Before sag, bus voltage was at 102.2 % kV. When sag was occurred (from 0.5 s – 1.5 s), percentage of bus voltage had been going down to 36 % kV in 0.3 seconds and then it had been going up to 44 % kV in 0.7 seconds. After sag, bus voltage was

going up to 102 % kV and then it had been going down to 96 % kV in 0.1 second. It had been going up to 99 % kV in 0.2 seconds and then it was getting stable at 102.2 % kV at 11.5th second.

Bus voltage of sag simulation results of DB11 PJPP bus bar before, after integrating RE into the grid and using homer results is equal to bus voltage sag simulation results of DB1 PJPP bus bar in all situations.

Bus voltage of sag simulation results of bus bar Donggala SB1 before, after integrating RE into the grid and using homer results can be seen below.

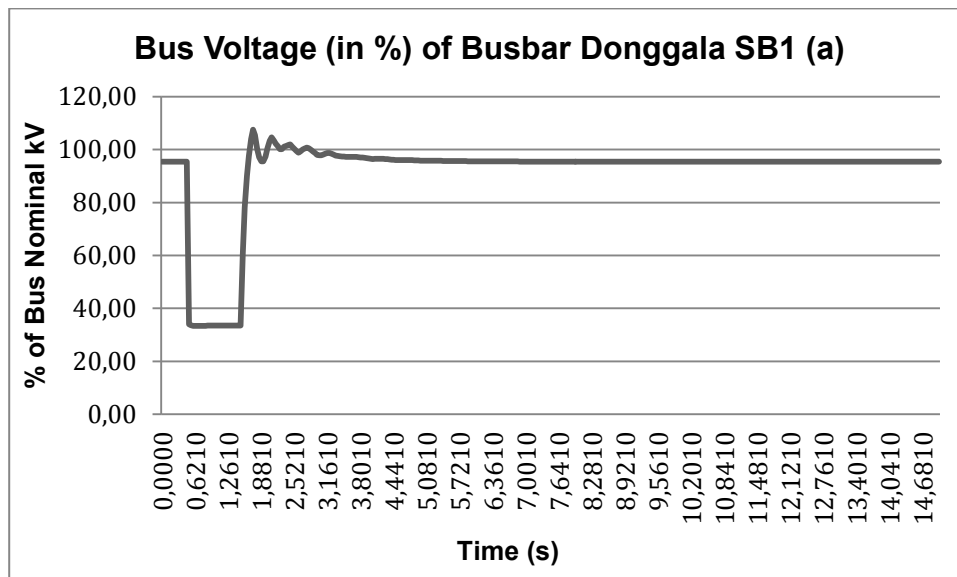


Figure 5-28: Donggala SB1 Bus Voltage Sag Simulatrion Results on Situation A

Based on figure 5-28 above, before sag, percentage of bus voltage was at 96 % kV. When the sag was occurred (from 0.5 s – 1.5 s), it was going down to 34 % kV and it had been staying there for 1 second during sag. It dropped to 26 % kV. After sag, bus voltage was going up to 105 %kV and it had been going down to 93 % kV. It was getting stable at 96 % kV at 6.5th second.

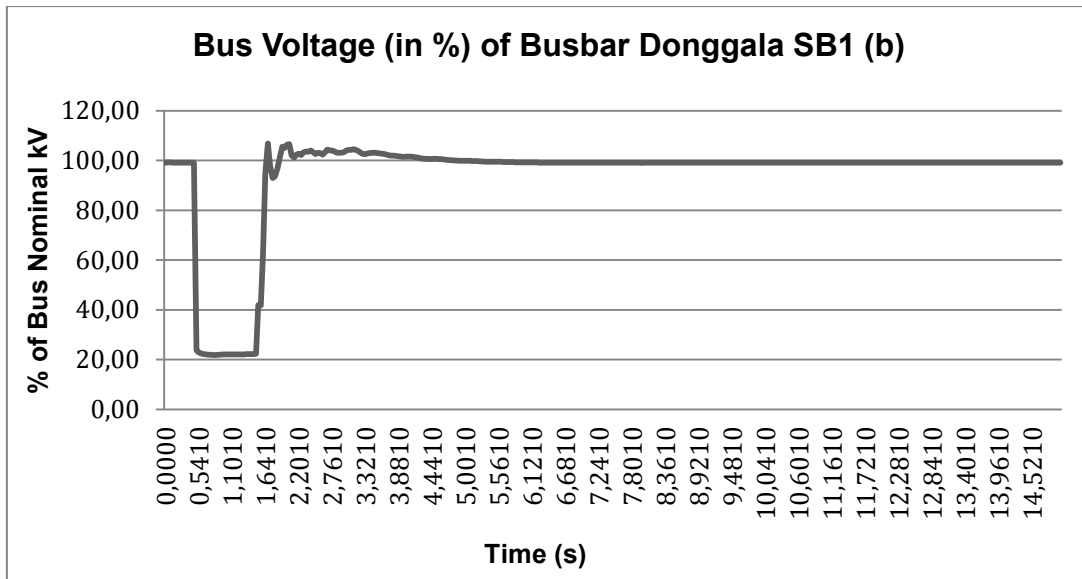


Figure 5-29: Donggala SB1 Bus Voltage Sag Simulation Results on Situation B

Based on figure 5-29 above, before sag, percentage of bus voltage was at 97 % kV. When sag was occurred (from 0.5 s – 1.5 s), it was going down to 22 % kV and it had been staying there for 1 second during sag. After sag, percentage of bus voltage was going up to 103 % kV and it had been going down to 93 % kV in 0.1 second. It was getting stable at 97 % kV at 5.2nd second.

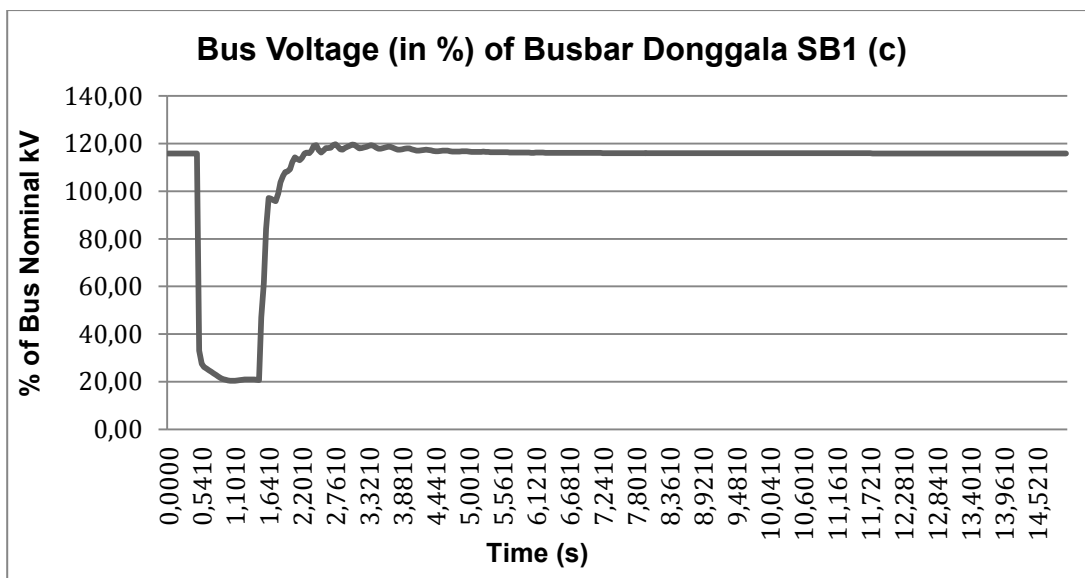


Figure 5-30: Donggala SB1 Bus Voltage Sag Simulation Results on Situation C

Based on figure 5-30, before sag, percentage of bus voltage was at 106.5 % kV. When sag was occurred (from 0.5 s – 1.5 s), it had been going down to 22 % kV in 0.5 seconds and then it had been going down again to 20 % kV in 0.5 seconds. After sag, percentage of bus voltage was going up to 104 % kV and it had been going down to 103 % kV in 0.3 seconds. It was getting stable at 106.5 % kV at 7.4th second.

Bus voltage of sag simulation results of bus bar Maesa SB1 before, after integrating RE into the grid and using homer results can be seen below.

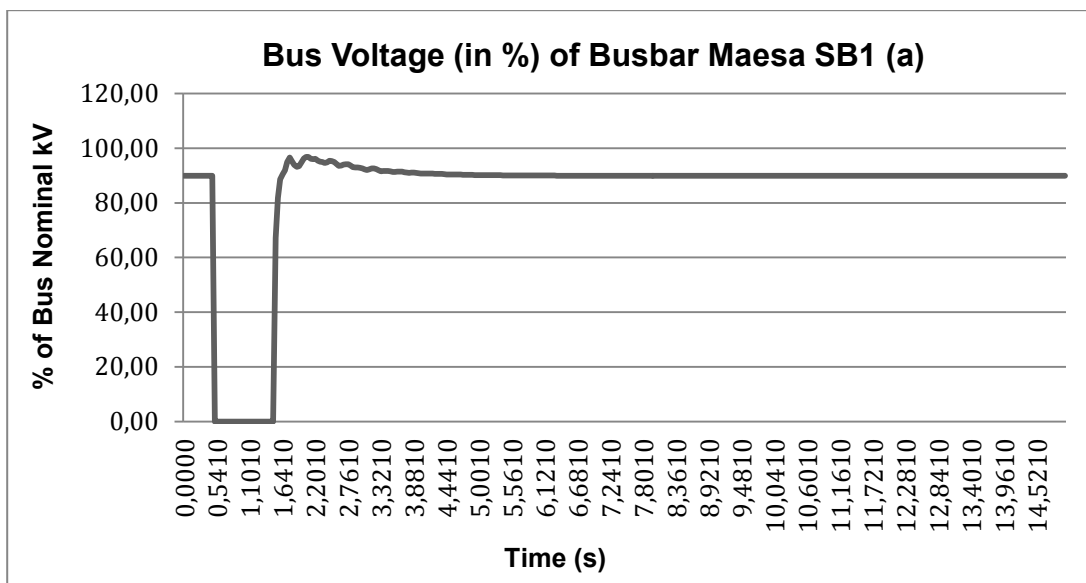


Figure 5-31: Maesa SB1 Bus Voltage Sag Simulation Results on Situation A

According to figure 5-31, before sag, percentage of bus voltage was at 97 % kV. When the sag was occurred (from 0.5 s – 1.5 s), it had been dropped to zero for 1 second during sag. After sag, percentage of bus voltage was going up to 99 %kV and it had been going down to 93 % kV in 0.1 second. It was getting stable at 97 % kV at 5.5th second.

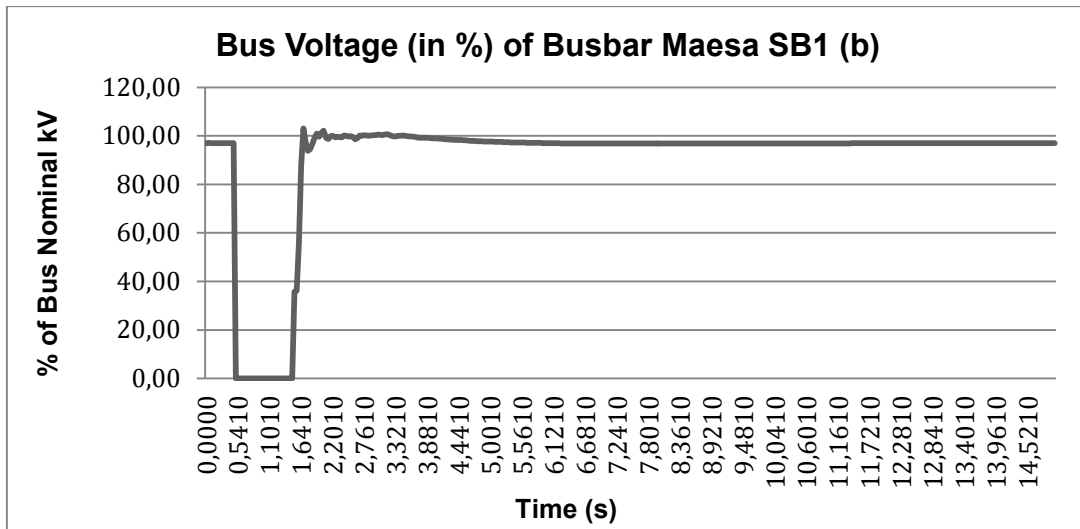


Figure 5-32: Maesa SB1 Bus Voltage Sag Simulation Results on Situation B

Based on figure 5-32, before sag, percentage of bus voltage was at 97 % kV. When sag was occurred (from 0.5 s – 1.5 s), it had been dropped to zero for 1 second during sag. After sag, percentage of bus voltage was going up to 99 % kV and it had been going down to 92 % kV in 0.1 second. It was getting stable at 97 % kV at 5.5th second.

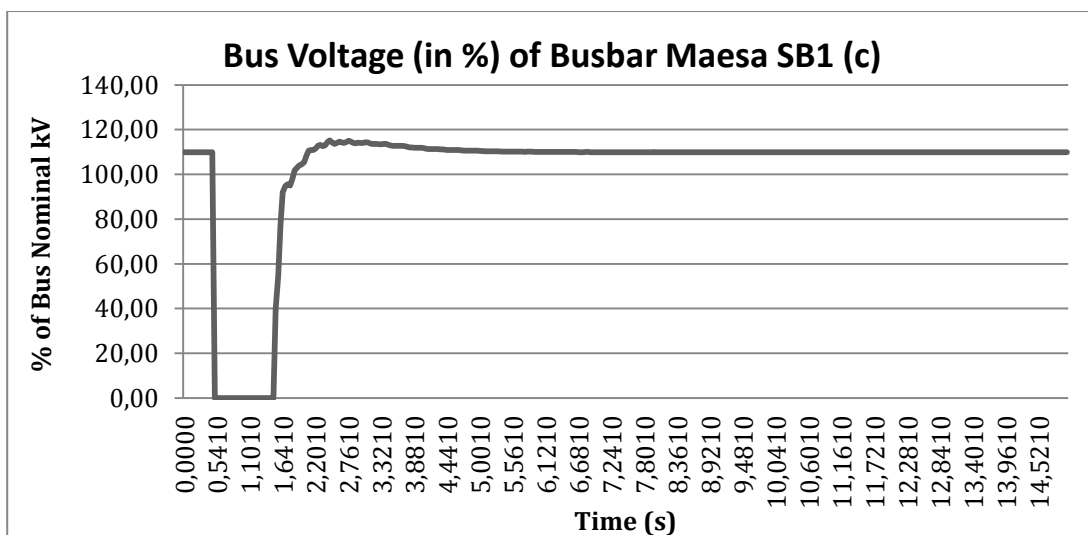


Figure 5-33: Maesa SB1 Bus Voltage Sag Simulation Results on Situation C

Based on figure 5-33, before sag, percentage of bus voltage was at 107 % kV. When the sag was occurred (from 0.5 s – 1.5 s), it had been dropped to zero for 1 second

during sag. After sag, bus voltage had been going up to 109 % kV in 1.5 seconds and it was getting stable at 107 % kV at 7.2nd second

Bus voltage of sag simulation results of Maesa SB1 (2) bus bar before, after integrating RE into the grid and using homer results is equal to bus voltage of sag simulation results of Maesa SB1 bus bar in all situations.

Bus voltage of sag simulation results of bus bar Parigi DB1 before, after integrating RE into the grid and using homer results can be seen below.

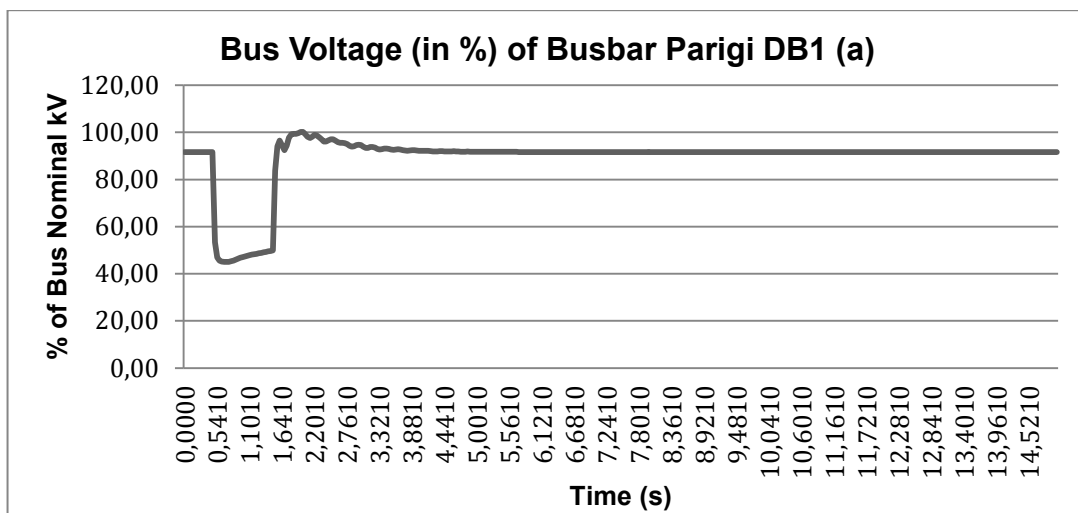


Figure 5-34: Parigi DB1 Bus Voltage Sag Simulation Results on Situation A

Based on figure 5-34, before sag, percentage of bus voltage was at 92 % kV. When the sag was occurred (from 0.5 s – 1.5 s), it had been going down to 46 % kV for 0.2 seconds. It had been going up to 52 % kV in 0.8 seconds. After sag, it was going up to 98 %kV and then it had been going down to 89 % kV in 0.1 second. It was getting stable at 90 % kV at 4.2nd second.

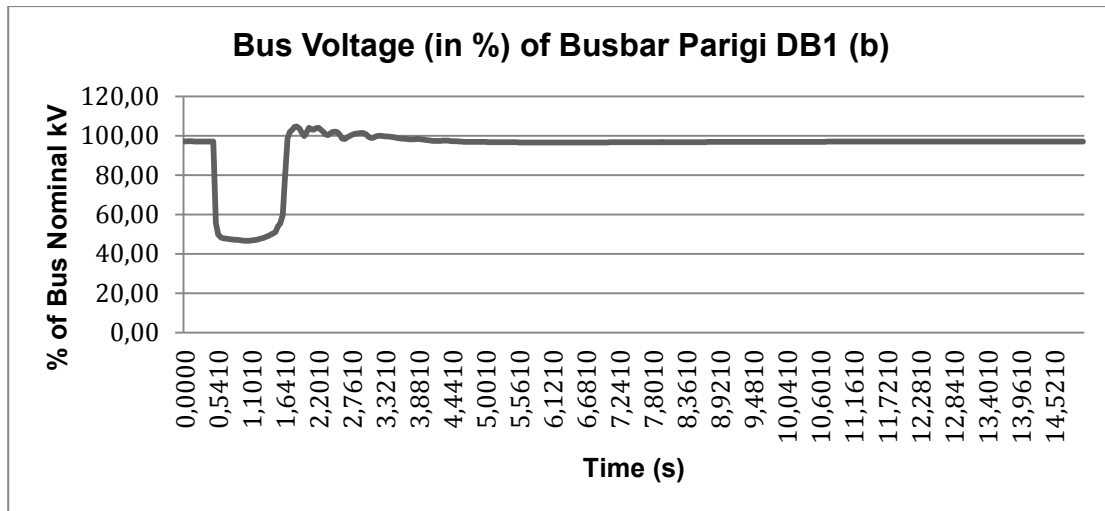


Figure 5-35: Parigi DB1 Bus Voltage Sag Simulation Results on Situation B

Based on figure 5-35, before sag, percentage of bus voltage was at 97 % kV. When the sag was occurred (from 0.5 s – 1.5 s), it had been going down to 49 % kV in 0.5 seconds and then it had been going up to 52 % kV in 0.5 seconds. After sag, it was going up to 103 % kV and then it had been going down to 100 % kV in 0.4 seconds. It was getting stable at 97 % kV at 5th second.

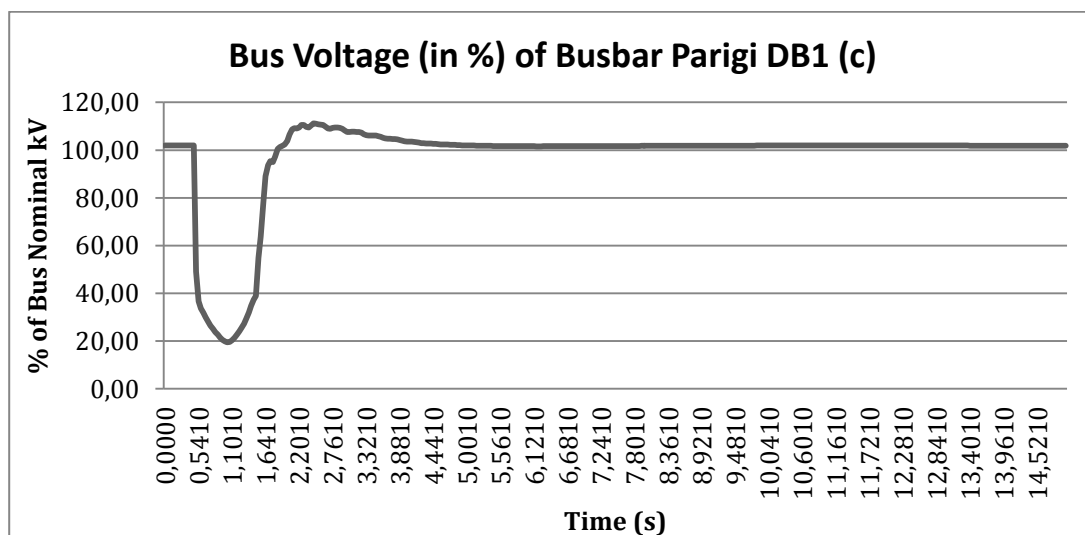


Figure 5-36: Parigi DB1 Bus Voltage Sag Simulation Results on Situation C

Based on figure 5-36, before sag, percentage of bus voltage was at 101 % kV. When the sag was occurred (from 0.5 s – 1.5 s), it had been going down to 30 % kV in 0.4 seconds and then it had been going up to 36 % kV in 0.6 seconds. After sag, it was

going up to 96 % kV and it had been going down to 93 % kV in 0.1 second. It had been going up again to 108 % kV in 0.8 second and then it was getting stable at 101 % kV at 5th second.

Bus voltage of sag simulation results of Parigi DB1 (2) bus bar before, after integrating RE into the grid and using homer results is equal to bus voltage of sag simulation results of Parigi DB1 bus bar in all situations.

Bus voltage of sag simulation results of bus bar Parigi SB1 before, after integrating RE into the grid and using homer results can be seen below.

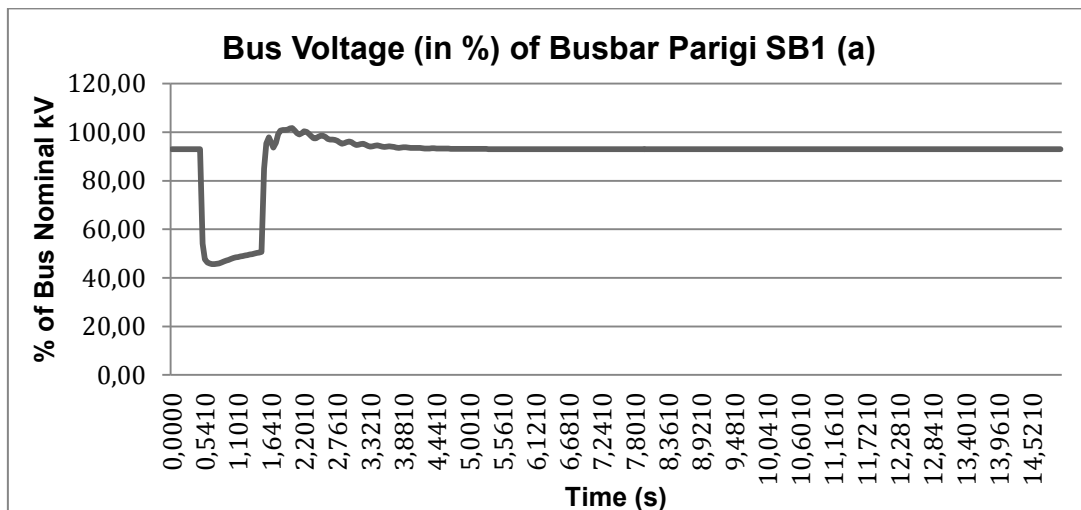


Figure 5-37: Parigi SB1 Bus Voltage Sag Simulation Results on Situation A

Based on figure 5-37, before sag, percentage of bus voltage was at 93 % kV. When the sag was occurred (from 0.5 s – 1.5 s), it had been going down to 47 % kV for 0.2 seconds. It had been going up to 52 % kV in 0.8 seconds. After sag, it was going up to 99 %kV and then it had been going down to 91 % kV in 0.1 second. It was getting stable at 93 % kV at 4.6th second.

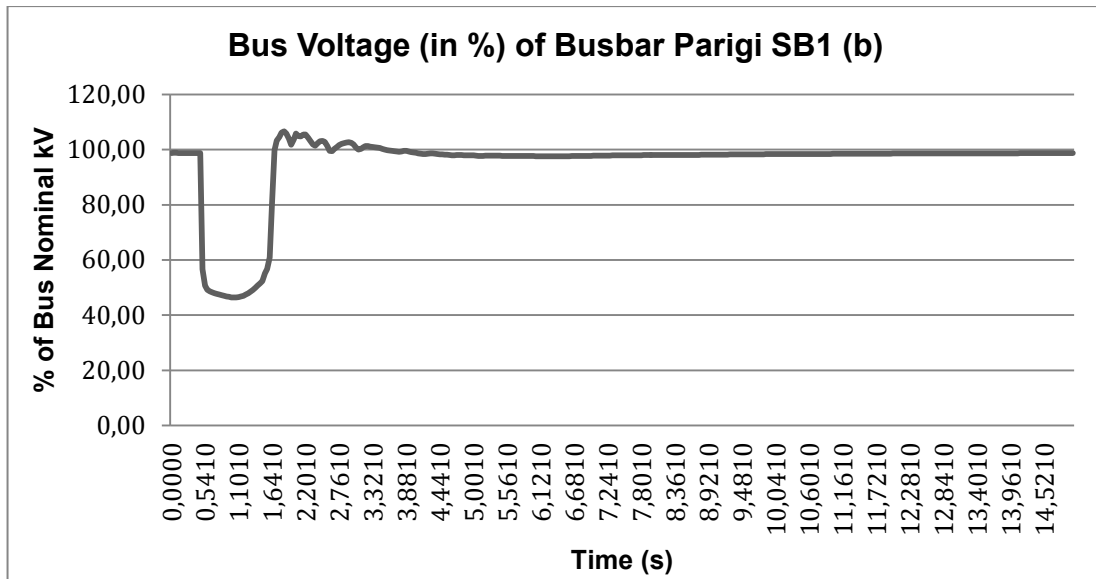


Figure 5-38: Silae SB1 Bus Voltage Sag Simulation Results on Situation B

Based on figure 5-38 above, before sag, bus voltage is at 99 % kV. When the sag was occurred (from 0.5 s – 1.5 s), it had been going down to 49 % kV in 0.5 seconds and then it had been going up to 53 % kV in 0.5 seconds. It was going up to 104 % kV and it had been going down to 102 % kV in 0.3 seconds. It was getting stable at 99 % kV at 4.5th second.

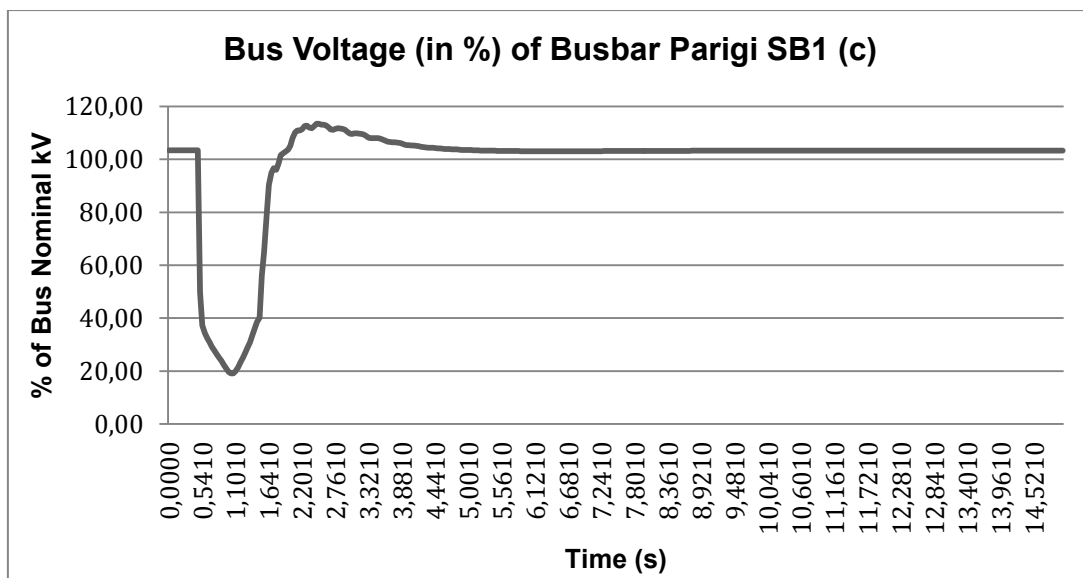


Figure 5-39: Silae SB1 Bus Voltage Sag Simulation Results on Situation C

Based on figure 5-39, before sag, percentage of bus voltage was at 102.5 % kV. When the sag was occurred (from 0.5 s – 1.5 s), it had been going down to 31 % kV in 0.5 seconds and then it had been going up to 36 % kV in 0.5 seconds. After sag, it was going up to 96 % kV and it had been going down to 94 % kV in 0.1 second. It had been going up again to 110 % kV in 0.8 second and then it was getting stable at 102.5 % kV at 5th second.

Bus voltage of sag simulation results of bus bar Parigi SB2 before, after integrating RE into the grid and using homer results can be seen below.

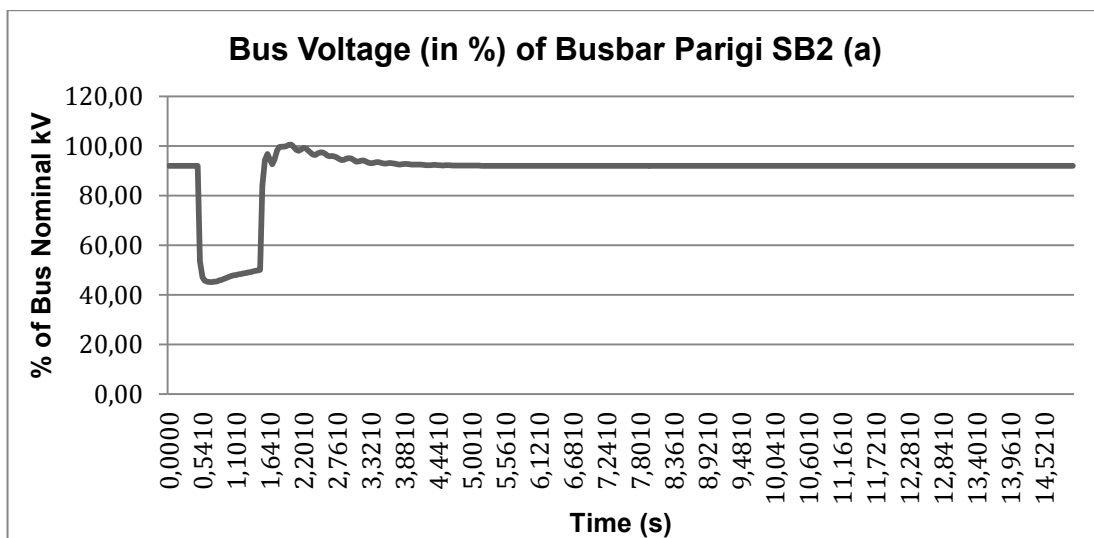


Figure 5-40: Parigi SB2 Bus Voltage Sag Simulation Results on Situation A

Based on figure 5-40 above, before sag, percentage of bus voltage was at 92 % kV. When sag was occurred (from 0.5 s – 1.5 s), it had been going down to 46.5 % kV for 0.3 seconds. It had been going up to 52 % kV in 0.7 seconds. After sag, it was going up to 98 %kV and it had been going down to 90 % kV in 0.1 second. It reached stable at 92 % kV at 4.2nd second.

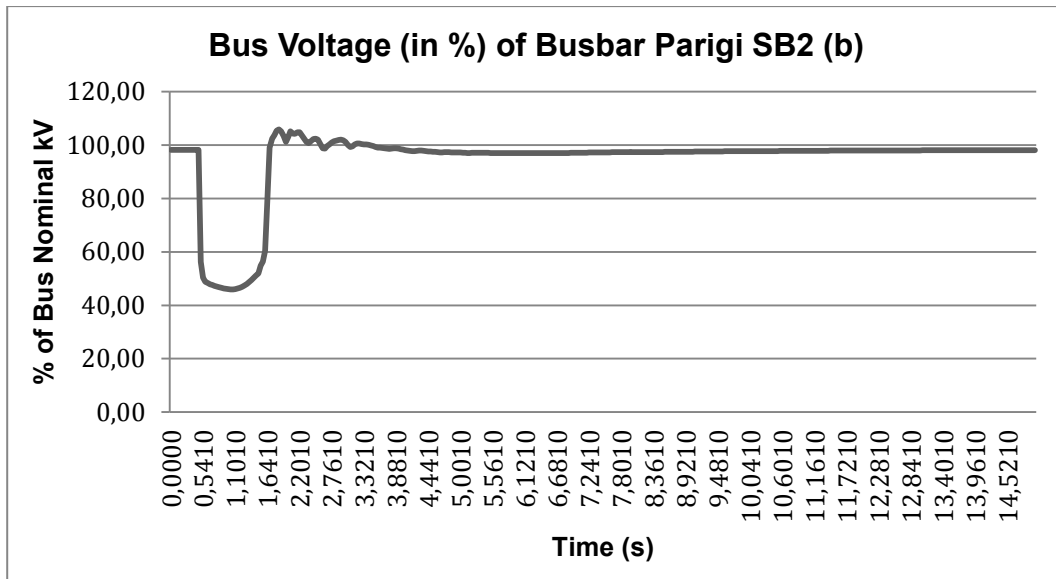


Figure 5-41: Parigi SB2 Bus Voltage Sag Simulation Results on Situation B

Based on figure 5-41, before sag, percentage of bus voltage was at 98 % kV. When the sag was occurred (from 0.5 s – 1.5 s), it had been going down to 49 % kV in 0.6 seconds and then it had been going up to 52 % kV in 0.4 seconds. After sag, it was going up to 104 % kV and it had been going down to 102 % kV in 0.3 seconds. It reached stable at 98 % kV at 5th second.

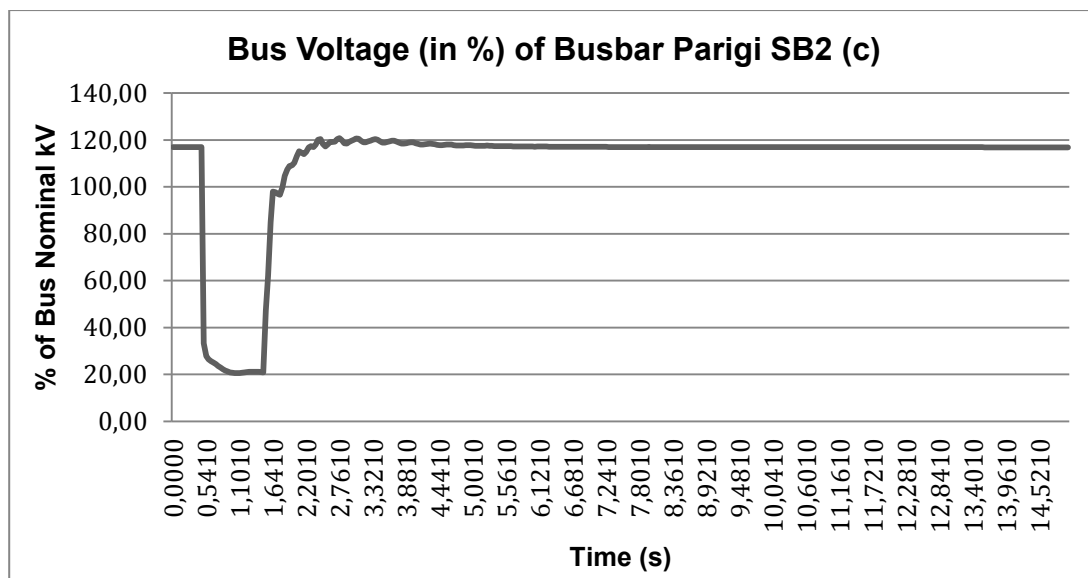


Figure 5-42: Parigi SB2 Bus Voltage Sag Simulation Results on Situation C

Based on figure 5-42, before sag, percentage of bus voltage was at 102 % kV. When the sag was occurred (from 0.5 s – 1.5 s), it had been going down to 30 % kV in 0.5 seconds and then it had been going up to 36 % kV in 0.5 seconds. After sag, it was going up to 96 % kV and then it had been going down to 93 % kV in 0.1 second. It had been going up again to 110 % kV in 0.8 second and then it was getting stable at 102 % kV at 4.8th second.

Bus voltage of sag simulation results of bus bar PJPP SB1 before, after integrating RE into the grid and using homer results can be seen below.

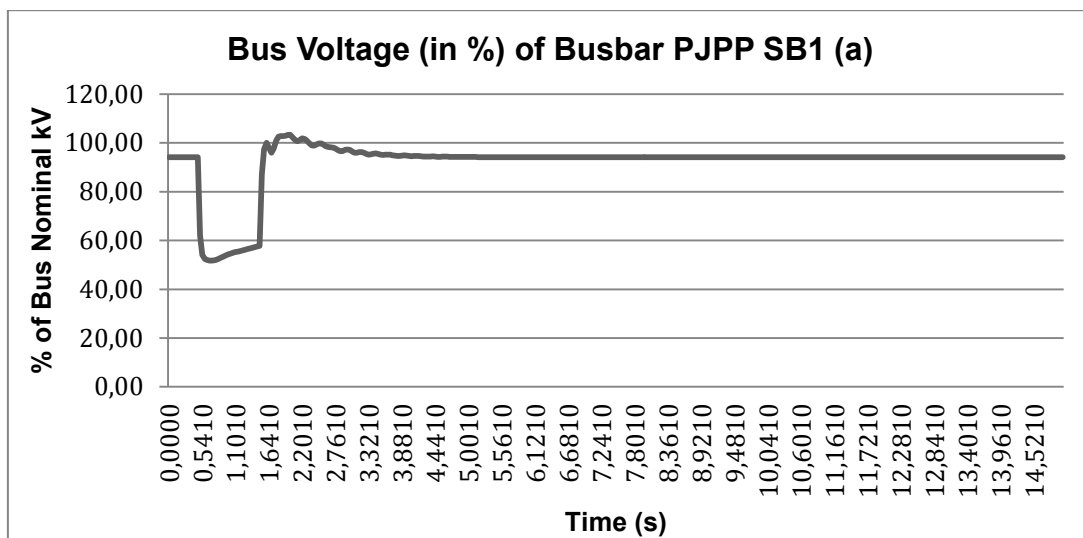


Figure 5-43: PJPP SB1 Bus Voltage Sag Simulation Results on Situation A

Based on figure 5-43, before sag, percentage of bus voltage was at 94 % kV. When the sag was occurred (from 0.5 s – 1.5 s), it had been going down to 53 % kV for 0.3 seconds. It had been going up to 60 % kV in 0.7 seconds. After sag, it was going up to 101 %kV and then it had been going down to 93 % kV in 0.1 second. It was getting stable at 94 % kV at 3.8th second.

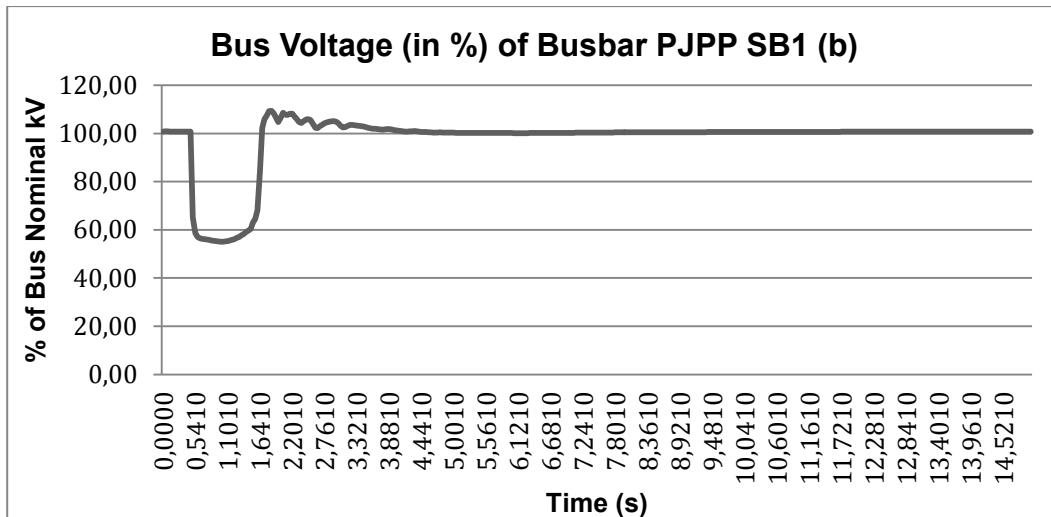


Figure 5-44: PJPP SB1 Bus Voltage Sag Simulation Results on Situation B

Based on figure 5-45, before sag, percentage of bus voltage was at 100.5 % kV. When the sag was occurred (from 0.5 s – 1.5 s), it had been going down to 58 % kV in 0.5 seconds and then it had been going up to 61 % kV in 0.5 seconds. After sag, it was going up to 108 % kV and it had been going down to 105 % kV in 0.3 seconds. It reached stable at 100.5 % kV at 4.5th second.

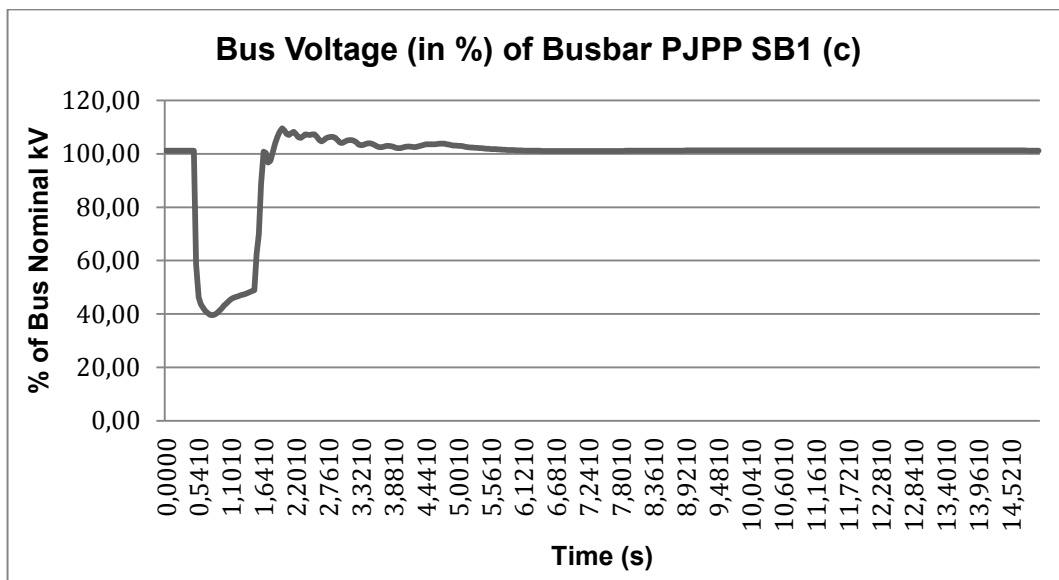


Figure 5-45: PJPP Bus Voltage Sag Simulation Results on Situation C

Based on figure 5-45, before sag, percentage of bus voltage was at 101 % kV. When the sag was occurred (from 0.5 s – 1.5 s), it had been going down to 35 % kV in 0.4

seconds and then it had been going up to 44 % kV in 0.6 seconds. After sag, it was going up to 98 % kV and then it had been going down to 95 % kV in 0.1 second. It had been going up again to 110 % kV in 0.8 second. It reached stable at 101 % kV at 6th second.

Bus voltage of sag simulation results of bus bar Silae SB1 before, after integrating RE into the grid and using homer results can be seen below.

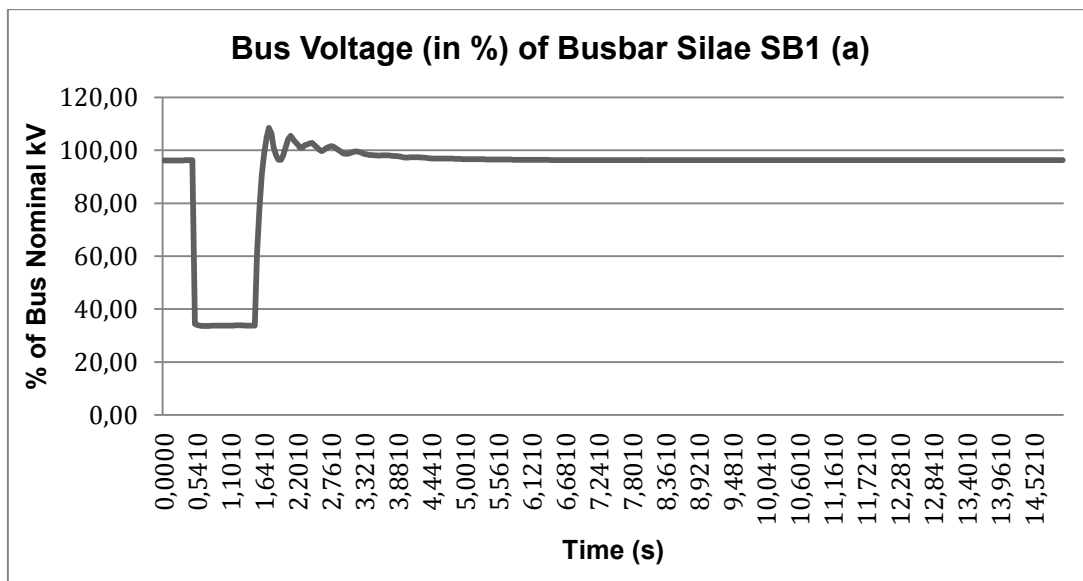


Figure 5-46: Silae SB1 Bus Voltage Sag Simulation Results on Situation A

Based on figure 5-46, before sag, percentage of bus voltage was at 97 % kV. When the sag was occurred (from 0.5 s – 1.5 s), it had been going down to 34 % kV for 1 second during sag. It dropped to 26 % kV. After sag, it was going up to 106 %kV and then it had been going down to 94 % kV in 0.3 seconds. It reached stable at 97 % kV at 5th second.

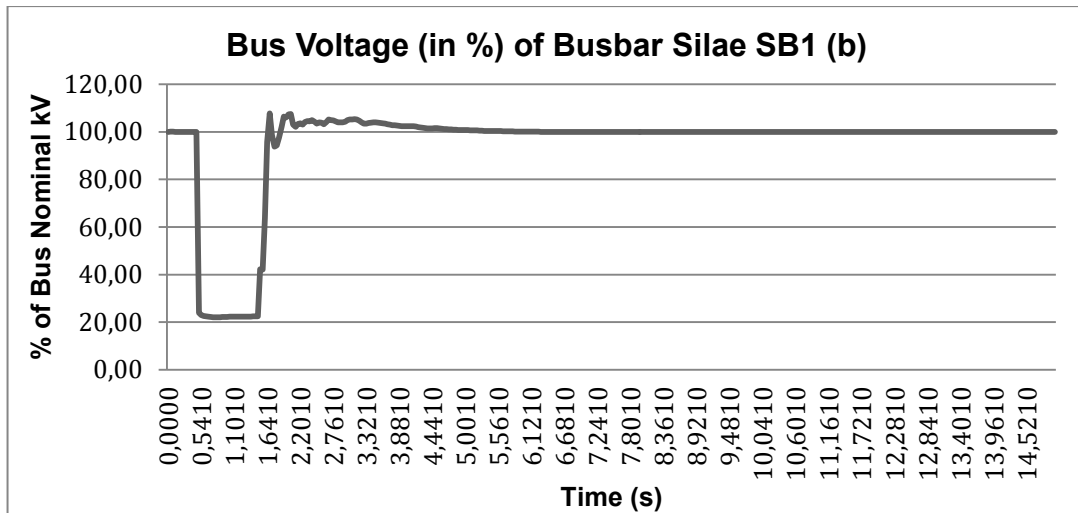


Figure 5-47: Silae SB1 Bus Voltage Sag Simulation Results on Situation B

Based on figure 5-48, before sag, percentage of bus voltage was at 100 % kV. When the sag was occurred (from 0.5 s – 1.5 s), it had been going down to 23 % kV for 1 second during sag. After sag, bus it was going up to 104 % kV and then it had been going down to 94 % kV in 0.1 seconds. It reached stable at 100 % kV at 6.2nd second.

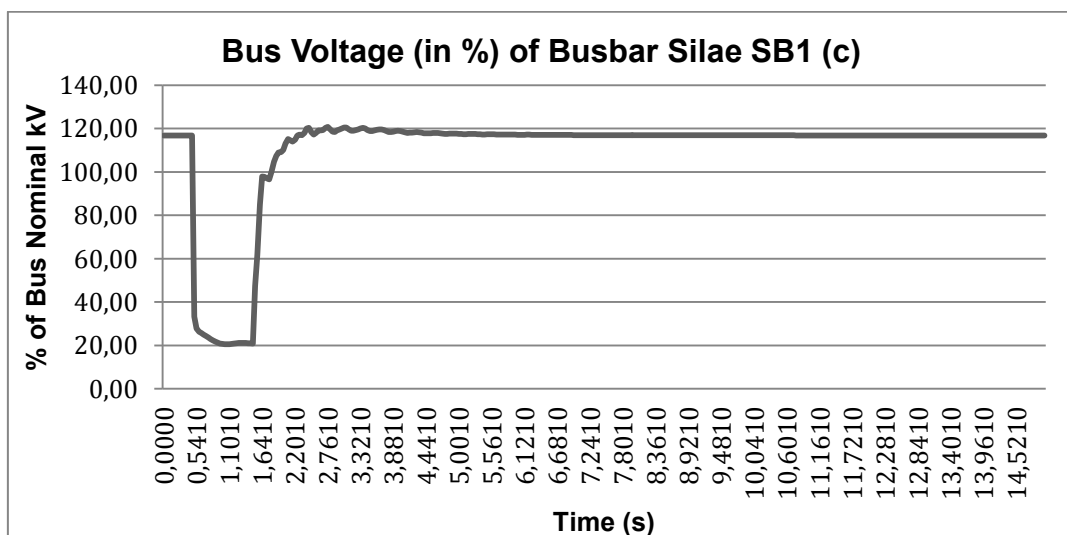


Figure 5-48: Silae SB1 Bus Voltage Sag Simulation Results on Situation C

Based on figure 5-48, before sag, percentage of bus voltage was at 107.5 % kV. When the sag was occurred (from 0.5 s – 1.5 s), it had been going down to 20 % kV for 1 second during sag. After sag, it was going up to 104 % kV and then it had been

going down to 103 % kV in 0.3 second. It had been going up again to 108 % kV in 1.5 seconds. It reached stable at 107.5 % kV at 5.6th second.

Bus voltage of sag simulation results of Silae SB2 and Silae SB3 bus bar before, after integrating RE into the grid and using homer results is equal to bus voltage of sag simulation results of Silae SB1 bus bar on all situations.

Bus voltage of sag simulation results of bus bar Silae SB4 before, after integrating RE into the grid and using homer results can be seen below.

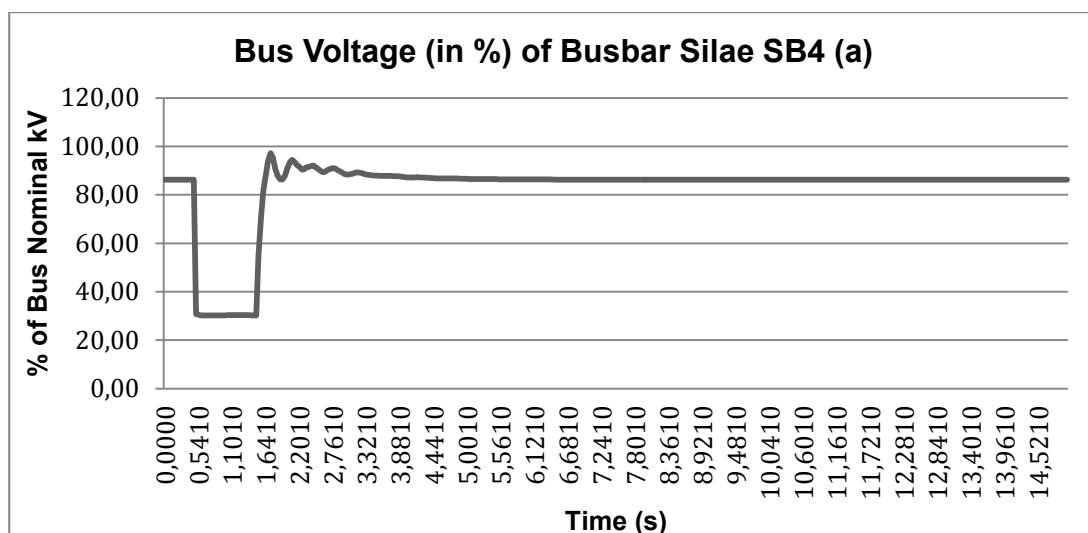


Figure 5-49: Silae SB4 Bus Voltage Sag Simulation Results on Situation A

Based on figure 5-49, before sag, percentage of bus voltage was at 86 % kV. When the sag was occurred (from 0.5 s – 1.5 s), it had been going down to 30 % kV for 1 second during sag. It dropped to 24 % kV. After sag, it was going up to 95.5 %kV and it had been going down to 84.3 % kV in 0.3 seconds. It reached stable at 86 % kV at 4.8th second.

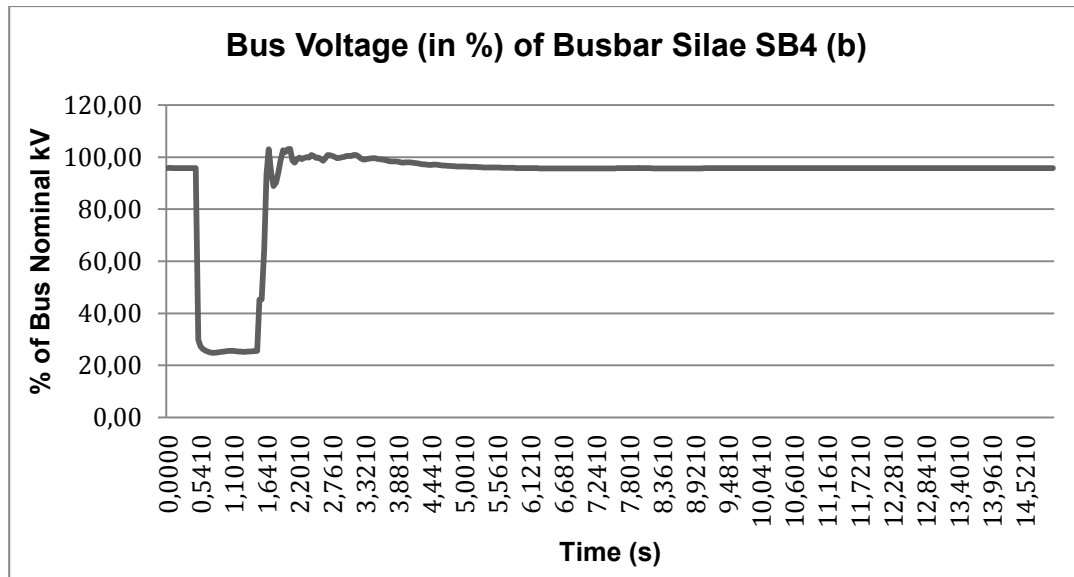


Figure 5-50: Silae SB4 Bus Voltage Sag Simulation Results on Situation B

Based on figure 5-50, before sag, percentage of bus voltage was at 96 % kV. When the sag was occurred (from 0.5 s – 1.5 s), it had been going down to 25 % kV in 0.3 seconds and then it had been going up to 26 % kV in 0.7 seconds. After sag, it was going up to 101 % kV and it had been going down to 89 % kV in 0.1 seconds. It reached stable at 96 % kV at 6.2th second.

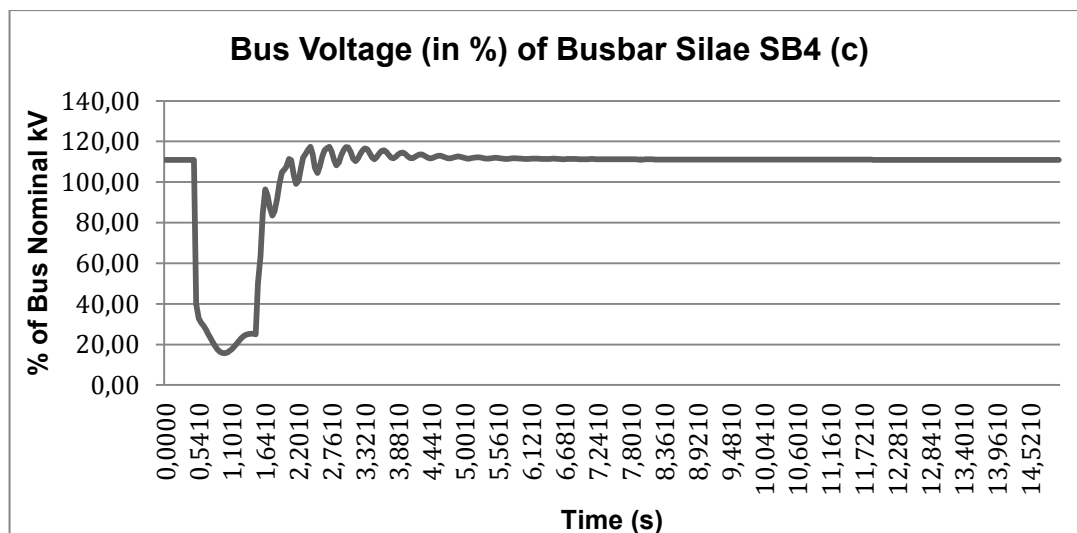


Figure 5-51: Silae SB4 Bus Voltage Sag Simulation Results on Situation C

Based on figure 5-51, before sag, percentage of bus voltage was at 109 % kV. When the sag was occurred (from 0.5 s – 1.5 s), it had been going down to 16 % kV in 0.4

seconds and then it had been going up to 26 % kV in 0.5 seconds. It had been dropped to 6 % kV in 0.1 second. It was going up to 104 % kV and then it had been fluctuating for 1.7 seconds. It reached stable at 109 % kV at 6.6th second.

Bus voltage of sag simulation results of bus bar Talise SB1 before, after integrating RE into the grid and using homer results can be seen below.

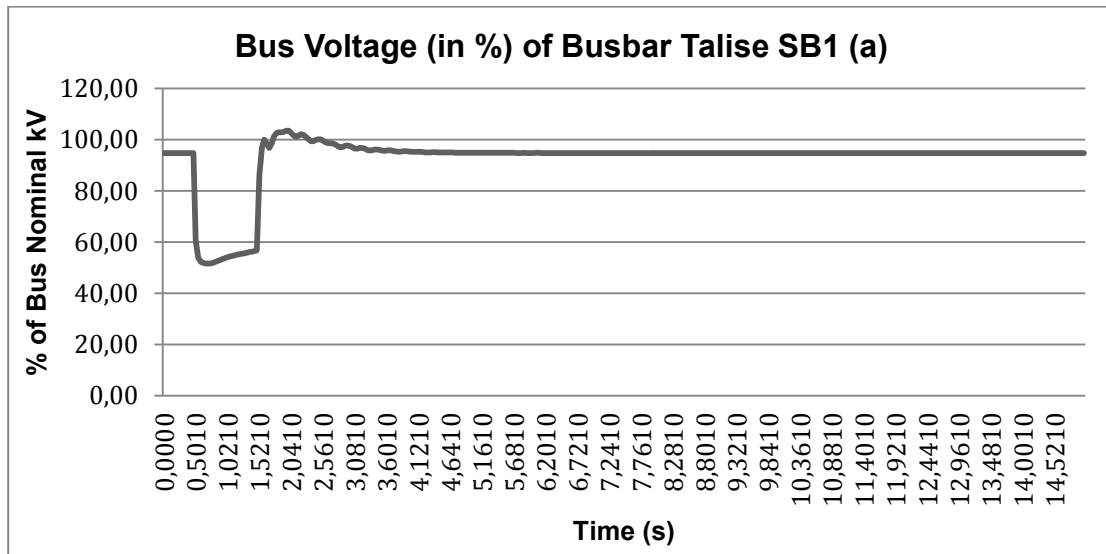


Figure 5-52: Talise SB1 Bus Voltage Sag Simulation Results on Situation A

Based on figure 5-52, before sag, percentage of bus voltage was at 95 % kV. When the sag was occurred (from 0.5 s – 1.5 s), it had been going down to 53 % kV in 0.2 seconds and then it was going up to 59 % kV in 0.8 % kV. After sag, it was going up to 101 %kV and it had been going down to 94 % kV in 0.2 seconds. It reached stable at 95 % kV at 5.6th second.

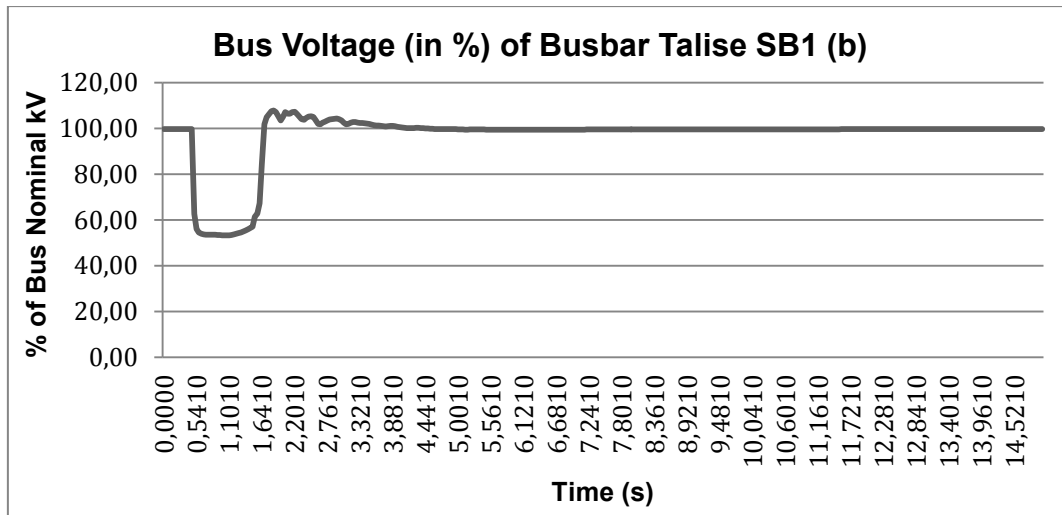


Figure 5-53: Talise SB1 Bus Voltage Sag Simulation Results on Situation B

Based on figure 5-53, before sag, percentage of bus voltage was at 99 % kV. When the sag was occurred (from 0.5 s – 1.5 s), it was going down to 56 % kV and staying there for 0.6 seconds. It had been going up to 58 % kV in 0.4 seconds. After sag, percentage of bus voltage was going up to 107 % kV and it had been going down to 104 % kV in 0.3 seconds. It reached stable at 99 % kV at 7th second.

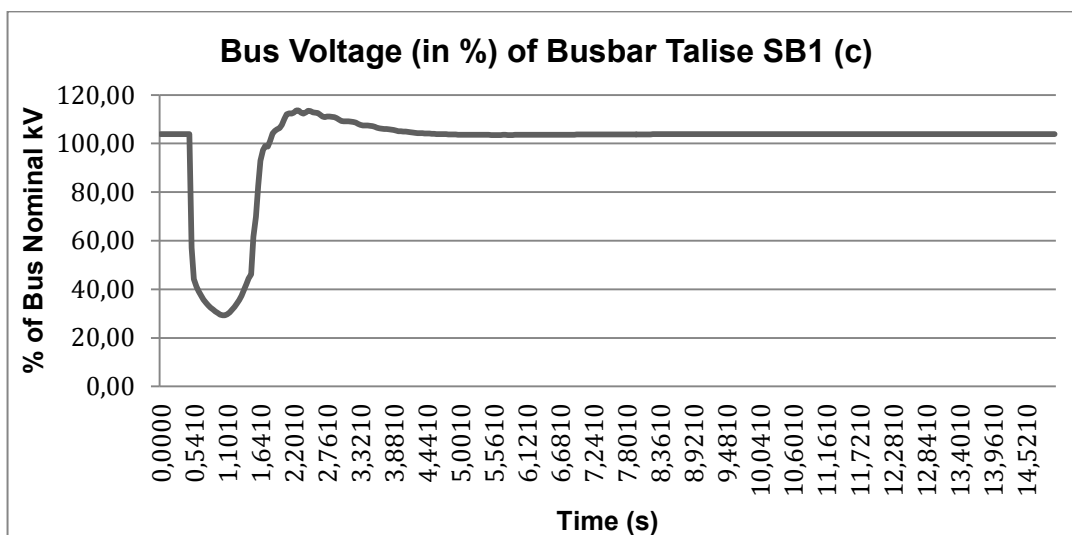


Figure 5-54: Talise SB1 Bus Voltage Sag Simulation Results on Situation C

Based on figure 5-54, before sag, percentage of bus voltage was at 103 % kV. When the sag was occurred (from 0.5 s – 1.5 s), it had been going down to 38 % kV in 0.2 seconds and it had been staying there for 0.1 second. It was going up to 44 % kV in

0.7 seconds. After sag, percentage of bus voltage was going up to 100 % kV. It reached stable at 98 % kV in 4.6th seconds.

Bus voltage of sag simulation results of bus bar Talise SB2 before, after integrating RE into the grid and using homer results can be seen below.

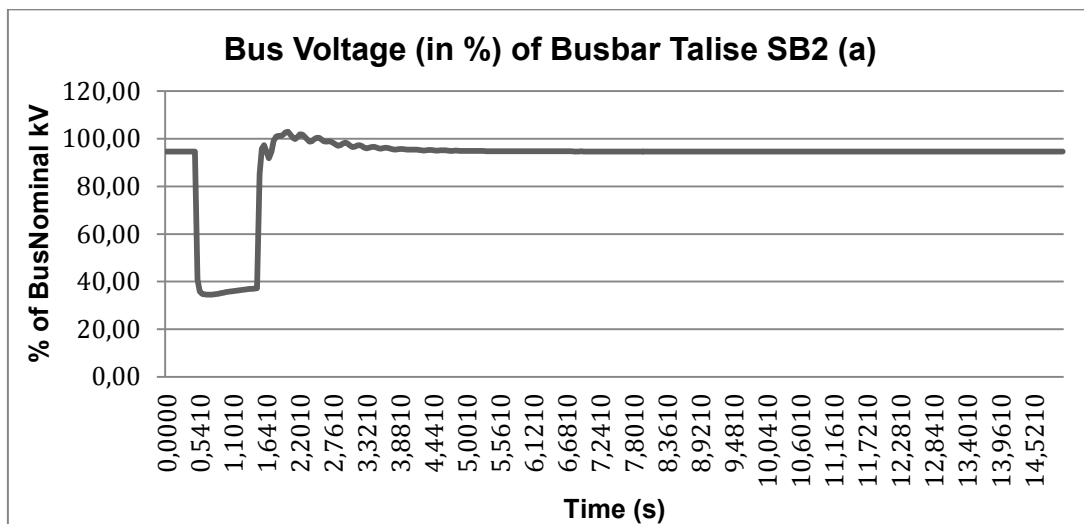


Figure 5-55: Talise SB2 Bus Voltage Sag Simulation Results on Situation A

Based on figure 5-55, before sag, percentage of bus voltage was at 95 % kV. When the sag was occurred (from 0.5 s – 1.5 s), it had been going down to 34 % kV in 0.2 seconds and then it had been going up to 36 % kV in 0.8 % kV. After sag, it was going up to 99 %kV and it had been going down to 87 % kV in 0.2 seconds. It reached stable at 95 % kV at 4.8th second.

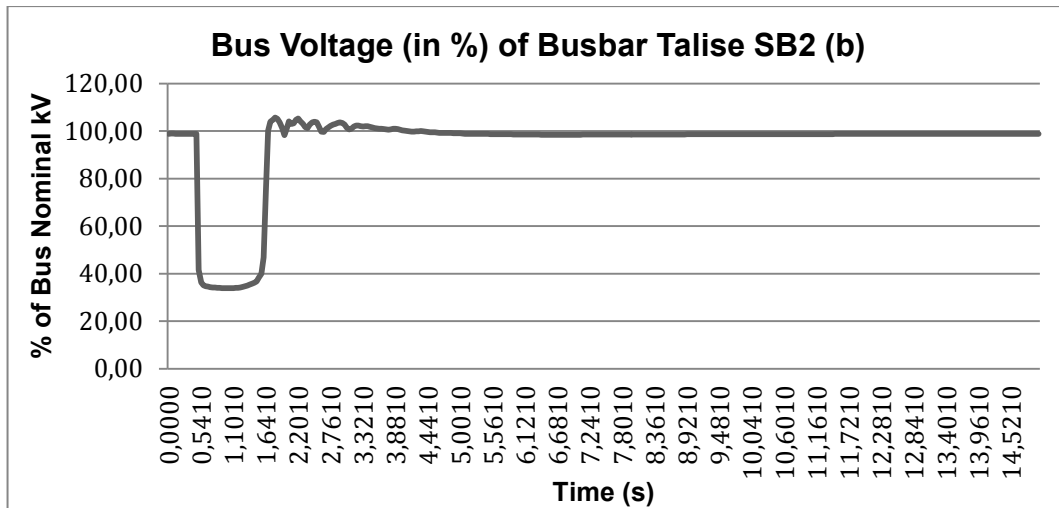


Figure 5-56: Talise SB2 Bus Voltage Sag Simulation Results on Situation B

Based on figure 5-56, before sag, percentage of bus voltage was at 99 % kV. When the sag is occurred (from 0.5 s – 1.5 s), it had been going down to 33 % kV in 0.5 seconds and then it had been going up to 34 % kV in 0.5 seconds. After sag, percentage of bus voltage was going up to 104 % kV and it had been going down to 98 % kV in 0.4 seconds. It reached stable at 99 % kV at 5.7th second.

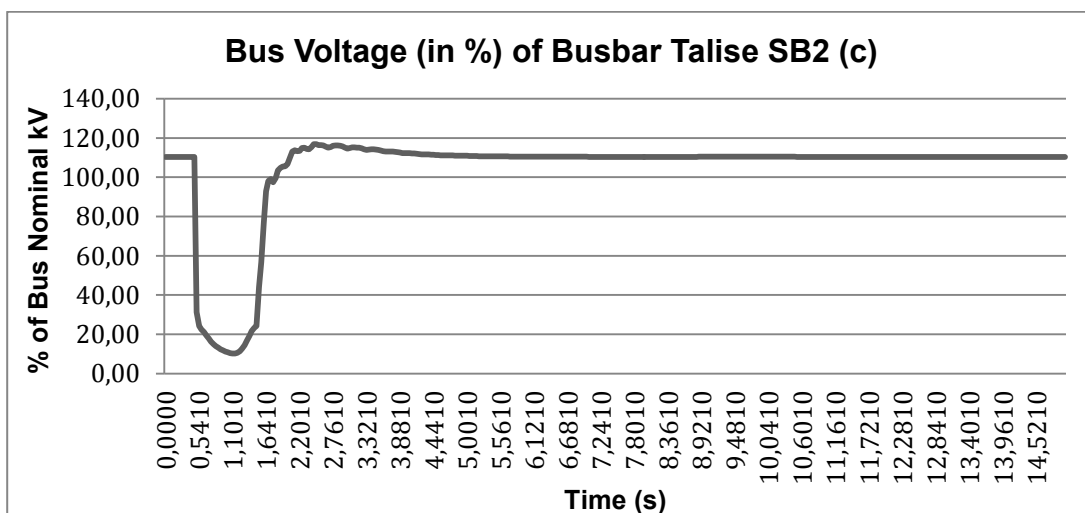


Figure 5-57: Talise SB2 Bus Voltage Sag Simulation Results on Situation C

Based on figure 5-57, before sag, percentage of bus voltage was at 104 % kV. When the sag was occurred (from 0.5 s – 1.5 s), it had been going down to 19 % kV in 0.2 seconds and it had been staying there for 0.1 second. It was going up to 21 % kV in 0.7 seconds. After sag, percentage of bus voltage was going up to 100 % kV and it

had been going down to 98.5 % kV in 0.1 seconds. It had been going up again to 106 % kV in 0.9 seconds. It reached stable at 104 % kV at 6th second.

Bus voltage of sag simulation results of Talise SB3 bus bar before, after integrating RE into the grid and using homer results is equal to bus voltage of sag simulation results of Talise SB2 bus bar on all situations.

Bus voltage of sag simulation results of bus bar Talise DB1 before, after integrating RE into the grid and using homer results can be seen below.

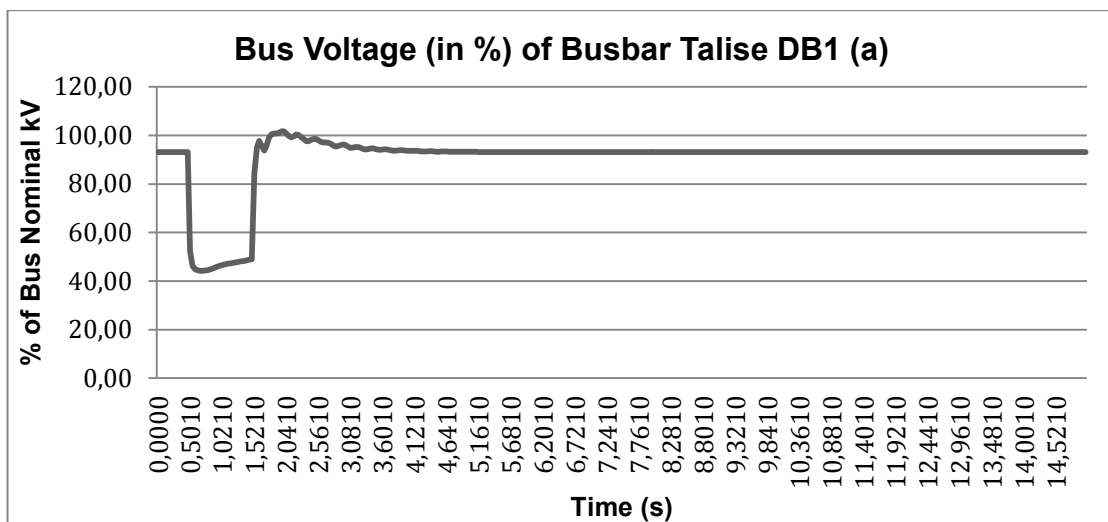


Figure 5-58: Talise DB1 Bus Voltage Sag Simulation Results on Situation A

Based on figure 5-58, before sag, percentage of bus voltage was at 93 % kV. When the sag was occurred (from 0.5 s – 1.5 s), it had been going down to 46 % kV in 0.3 seconds and then it was going up to 51 % kV in 0.7 % kV. After sag, percentage of bus voltage was going up to 99 %kV and it had been going down to 91 % kV in 0.2 seconds. It reached stable at 95 % kV at 4.8th second.

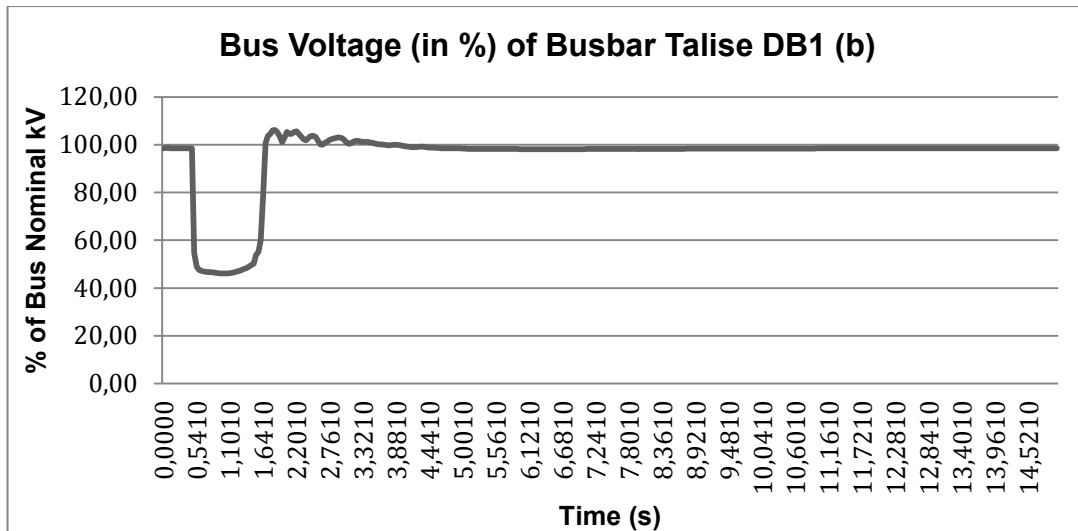


Figure 5-59: Talise DB1 Bus Voltage Sag Simulation Results on Situation B

Based on figure 5-59, before sag, percentage of bus voltage was at 98.5 % kV. When the sag is occurred (from 0.5 s – 1.5 s), it had been going down to 49 % kV in 0.5 seconds and then it had been going up to 51 % kV in 0.5 seconds. After sag, percentage of bus voltage was going up to 105 % kV and it had been going down to 102 % kV in 0.4 seconds. It reached stable at 98.5 % kV at 5.3rd second.

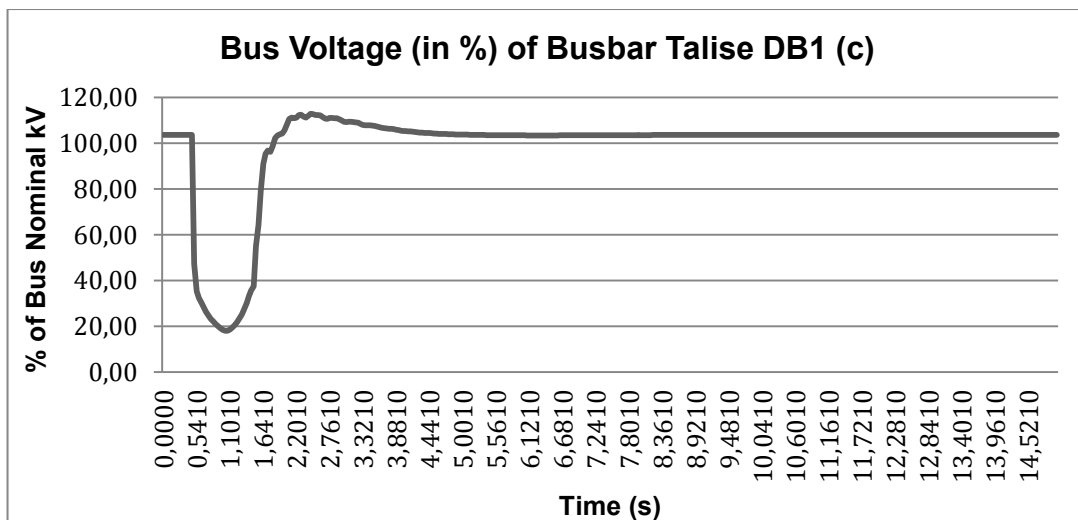


Figure 5-60: Talise DB1 Bus Voltage Sag Simulation Results on Situation C

Based on figure 5-60, before sag, percentage of bus voltage was at 103 % kV. When the sag was occurred (from 0.5 s – 1.5 s), it had been going down to 28 % kV in 0.4 seconds. It had been going up to 35 % kV in 0.6 seconds. After sag, it was going up

to 98 % kV and it had been going down to 96 % kV in 0.1 seconds. It had been going up again to 110 % kV in 0.8 seconds. It reached stable at 103 % kV at 5.5th second.

Bus voltage of sag simulation results of Talise DB11 bus bar before, after integrating RE into the grid and using homer results is equal to bus voltage of sag simulation results of Talise DB1 bus bar on all situations.

Bus frequency of sag simulation results of bus bar DB1 PJPP before, after integrating RE into the grid and using homer results can be seen below.

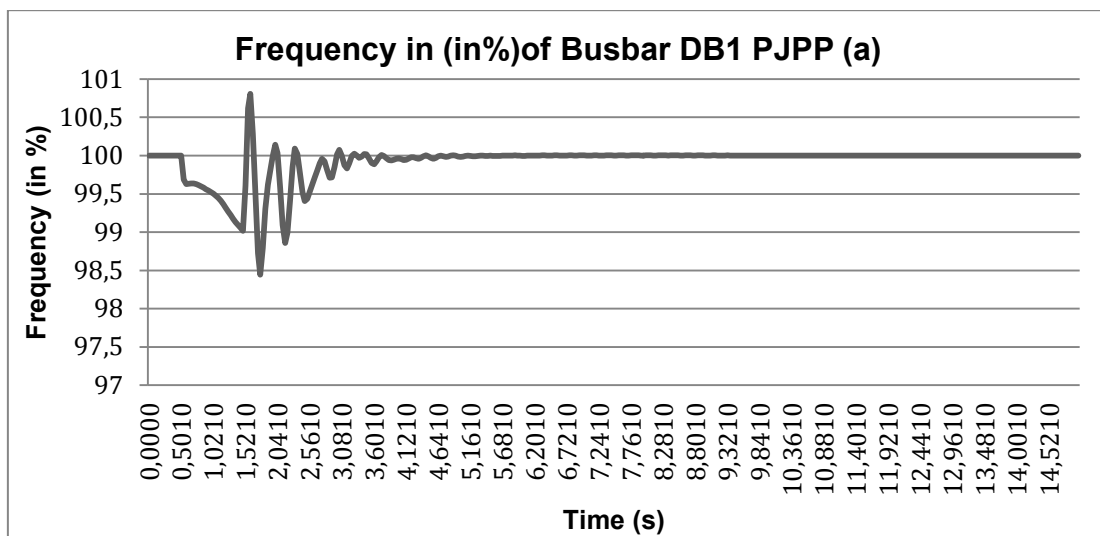


Figure 5-61: DB1 PJPP Bus Frequency Sag Simulation Results on Situation A

Based on figure 5-61, before sag, percentage of bus frequency was at 100 %. When the sag was occurred (from 0.5 s – 1.5 s), it was going down to 99.8 % and then it had been going down to 99.2 % for 1 second during sag. After sag, it was going up to 101 % and it was gradually getting stable at 100 % at 5.4th second.

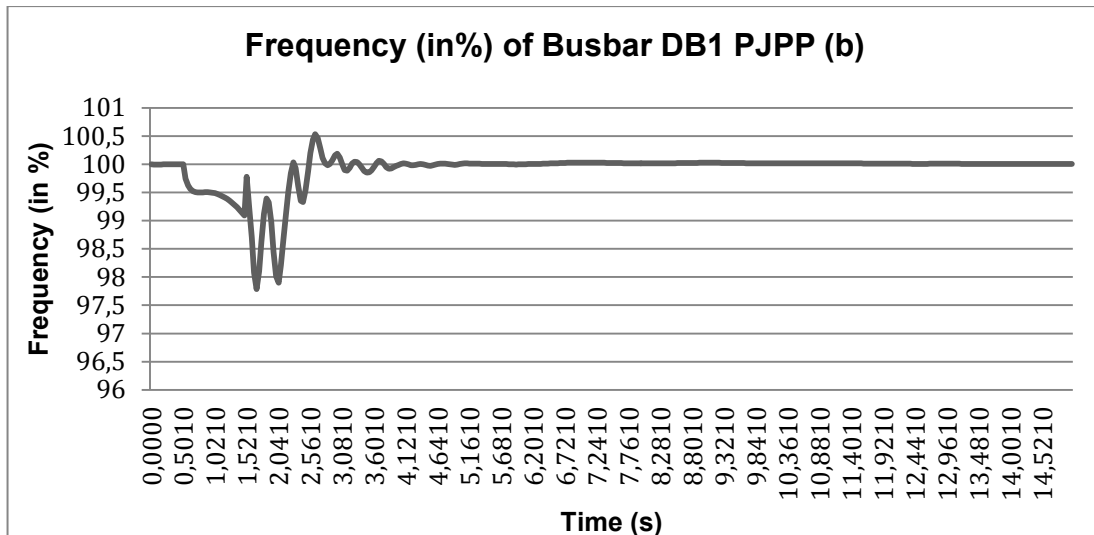


Figure 5-62: DB1 PJPP Bus Frequency Sag Simulation Results on Situation B

Based on figure 5-62, before sag, percentage of bus frequency was at 100 %. When the sag was occurred (from 0.5 s – 1.5 s), it had been going down to 99.4 % for 1 second during sag and then it was going up to 100 %. After sag, percentage of bus frequency has been fluctuating between 99.6 % and 97.7 % for 1 second. It had been going up to 100.6 % in 0.3 seconds. It reached stable at 100 % at 6.5th second.

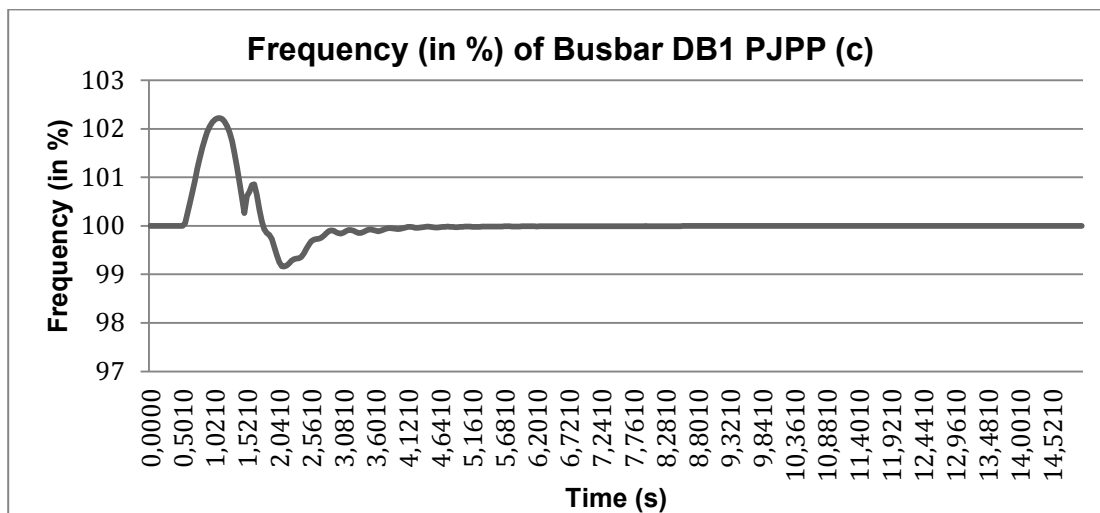


Figure 5-63: DB1 PJPP Bus Frequency Sag Simulation Results on Situation C

Based on figure 5-63, before sag, percentage of bus frequency was at 100 %. When the sag was occurred (from 0.5 s – 1.5 s), it had been going up to 101.2 % for 0.5 seconds and then it had been going down to 100.2 % for 0.5 seconds. After sag,

percentage of bus frequency had been going down to 99.02 % for 0.5 seconds and then it was going up to 100 % in 0.5 seconds. It reached stable at 100 % at 5.2nd second.

Bus frequency of sag simulation results of bus bar DB11 PJPP before, after integrating RE into the grid and using homer results is equal to bus frequency of sag simulation results of DB1 PJPP bus bar on all situations.

Bus frequency of sag simulation results of bus bar Donggala SB1 before, after integrating RE into the grid and using homer results can be seen below.

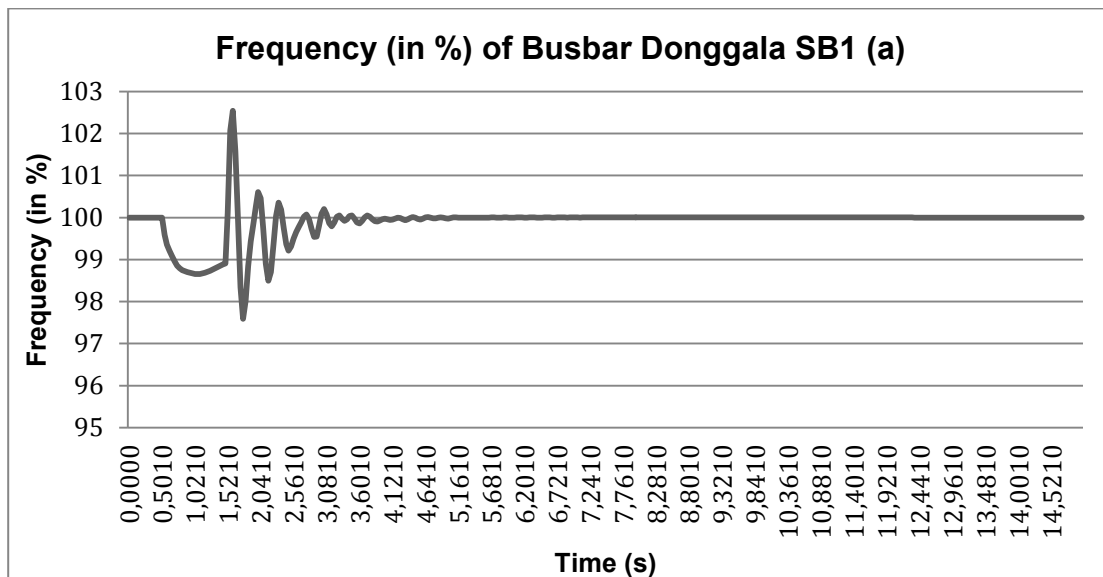


Figure 5-64: Donggala SB1 Bus Frequency Sag Simulation Results on Situation A

Based on figure 5-64, before sag, percentage of bus frequency was at 100 %. When the sag was occurred (from 0.5 s – 1.5 s), it had been going down to 98.7 % for 0.5 seconds and then it had been going up to 99 % for 0.5 seconds. After sag, it was going up to 103.5 %. It reached stable at 100 % at 5.2nd second.

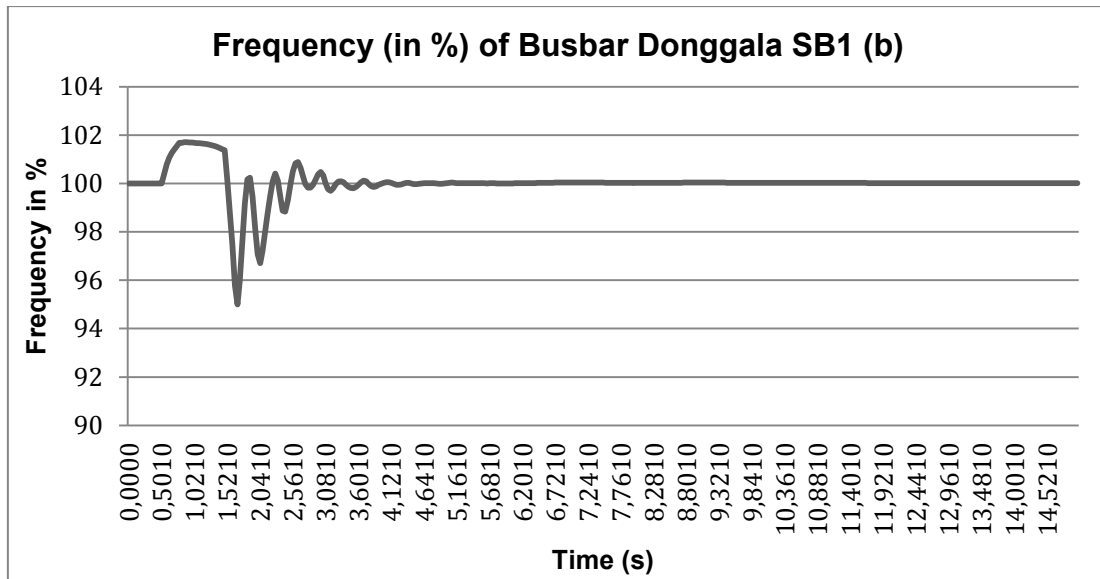


Figure 5-65: Donggala SB1 Bus Frequency Sag Simulation Results on Situation B

Based on figure-65, before sag, percentage of bus Frequency was at 100 %. When the sag was occurred (from 0.5 s – 1.5 s), it had been going up to 101.9 % in 0.3 seconds and then it had been going down to 101.5 in 0.7 seconds. After sag, it was going down to 96.1 % and then it had been fluctuating between 100 % and 96.1 % for 0.9 seconds. It had been going up to 101 % in 0.3 seconds. It reached stable at 100 % at 11.4th second.

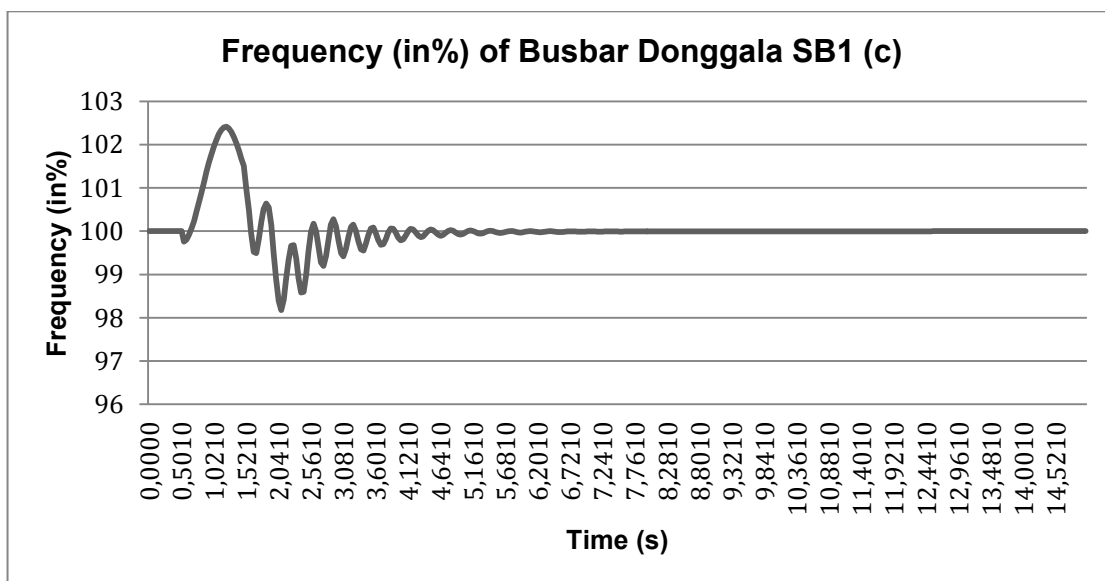


Figure 5-66: Donggala SB1 Bus Frequency Sag Simulation Results on Situation C

Based on figure 5-66, before sag, percentage of bus frequency was at 100 %. When the sag was occurred (from 0.5 s – 1.5 s), it had been going down to 99.2 % in 0.2 seconds and then it had been going up to 101.6 % for 0.3 seconds and then it had been fluctuating between 101.6 % and 100.6 % in 0.5 seconds. After sag, percentage of bus frequency was going up to 102 % and then it had been going down to 98.1 % in 0.3 seconds and then it had been fluctuating between 99.6 % and 98.2 % for 0.5 seconds. It had been going up to 100 % in 0.5 seconds. It reached stable at 100 % at 9.8th second.

Bus frequency of sag simulation results of bus bar Maesa SB1 before, after integrating RE into the grid and using homer results can be seen below.

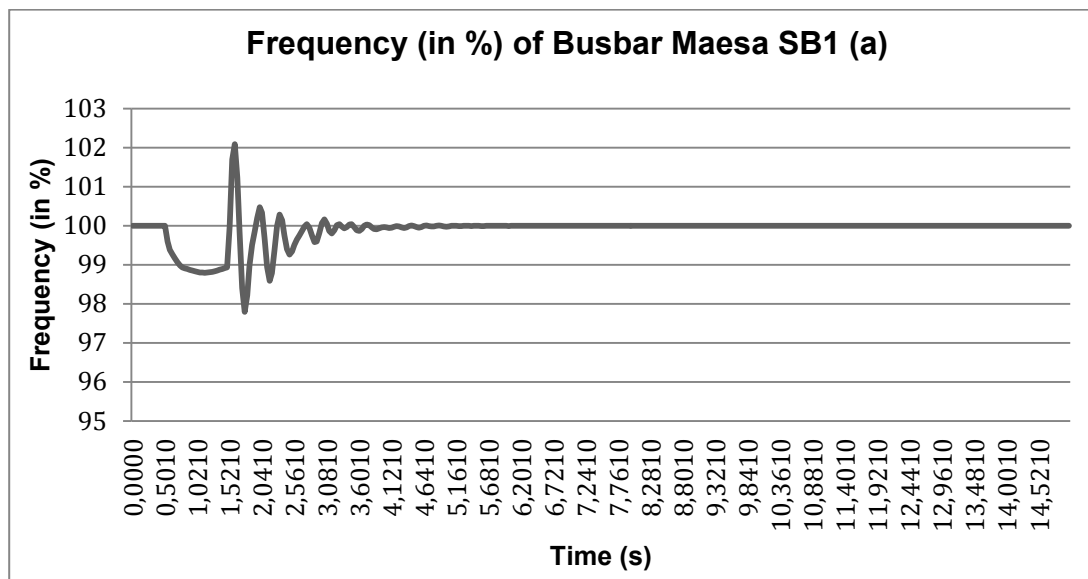


Figure 5-67: Maesa SB1 Bus Frequency Sag simulation Results on Situation A

Based on figure 5-67, before sag, percentage of bus frequency was at 100 %. When the sag was occurred (from 0.5 s – 1.5 s), it had been going down to 98.9 % for 0.5 seconds and then it had been going up to 99 % for 0.5 seconds. After sag, it was going up to 102.8. It was gradually getting stable at 100 % at 5.1st second.

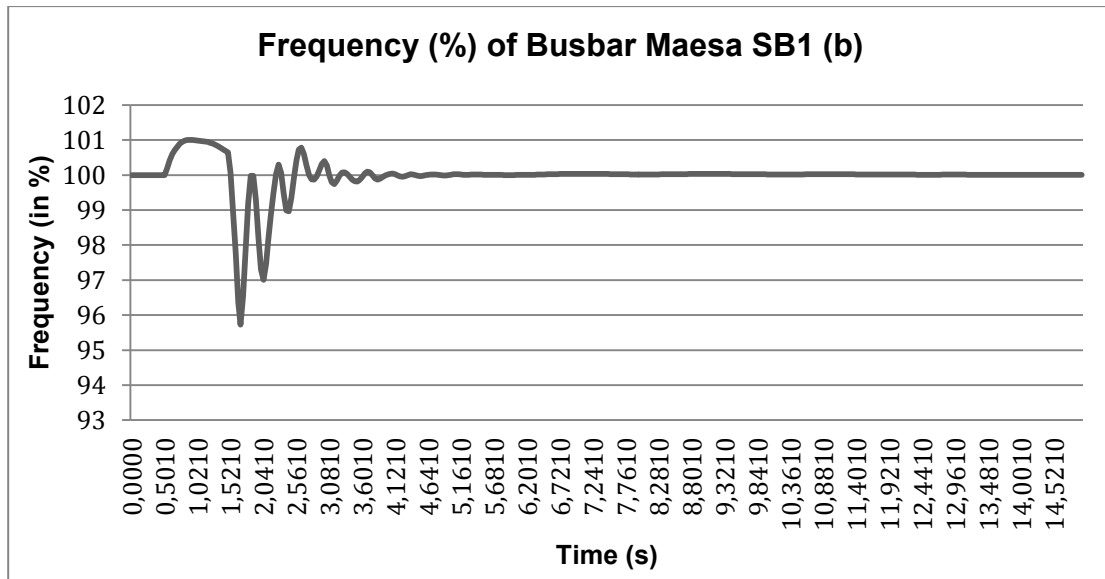


Figure 5-68: Maesa SB1 Bus Frequency Sag Simulation Results on Situation B

Based on figure 5-68, before sag, percentage of bus frequency was at 100 %. When the sag was occurred (from 0.5 s – 1.5 s), it had been going up to 101.1 % in 0.3 seconds and then going down to 100.8 in 0.7 seconds. After sag, percentage of bus frequency was going down to 96.7 % and then it had been fluctuating between 100 % and 96.8 % for 0.9 seconds. It had been going up to 100.8 % in 0.3 second. It reached stable at 100 % at 6.4th second.

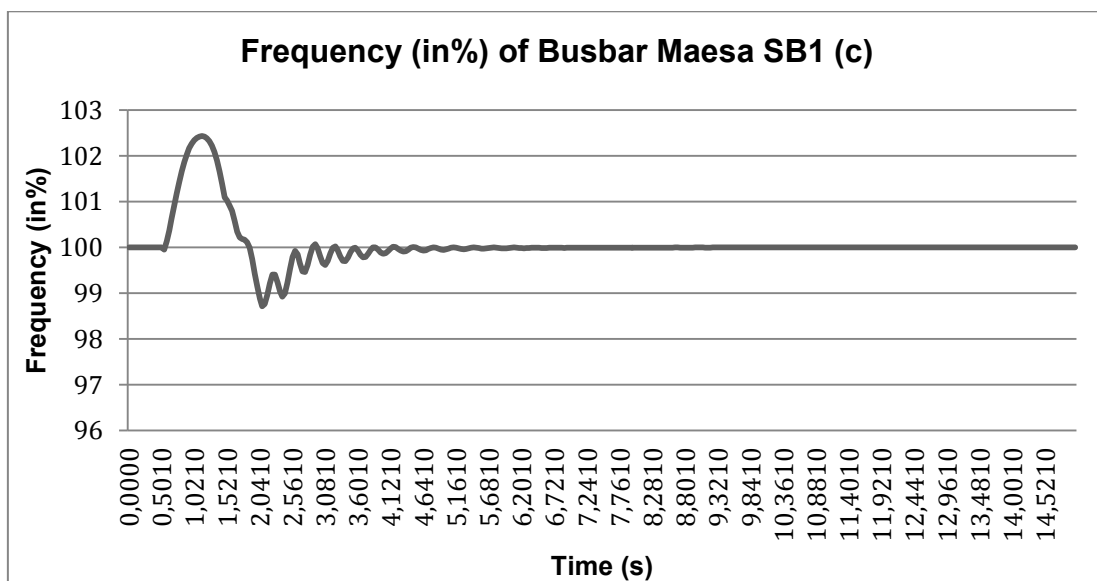


Figure 5-69: Maesa SB1 Bus Frequency Sag Simulation Results on Situation C

Based on figure 5-69, before sag, percentage of bus frequency was at 100 %. When the sag was occurred (from 0.5 s – 1.5 s), it had been going down to 99.8 % in 0.1 seconds and then it had been going up to 101.2 % for 0.3 seconds and then it had been going down to 100.4 % in 0.7 seconds. After sag, percentage bus frequency was going up to 101 % and then it had been going down to 98.8 % in 0.3 seconds and then it had been fluctuating between 99.5 % and 98.8 % for 0.7 seconds. It had been going up to 100.1 % in 0.7 seconds and it was getting stable at 100 % at 6th second.

Bus frequency of sag simulation results of Maesa SB1 (2) bus bar before, after integrating RE into the grid and using homer results is equal to bus frequency of sag simulation results of Maesa SB1 bus bar on all situations.

Bus frequency of sag simulation results of bus bar Parigi DB1 before, after integrating RE into the grid and using homer results can be seen below.

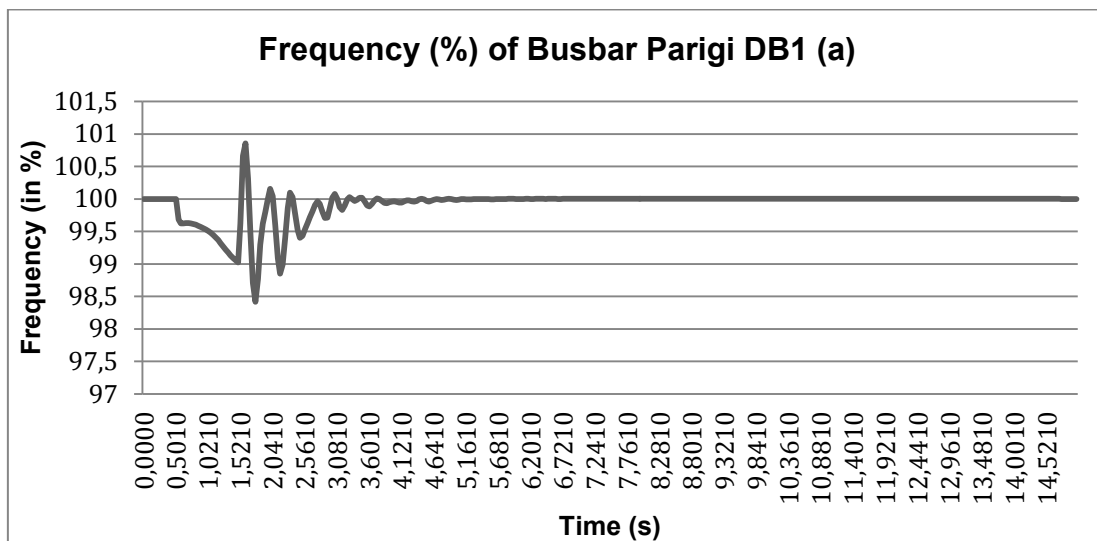


Figure 5-70: Parigi DB1 Bus Frequency Sag Simulation Results on Situation A

Based on figure 5-70, before sag, percentage of bus frequency was at 100 %. When the sag was occurred (from 0.5 s – 1.5 s), it had been going down to 99.1 % for 1 second. After sag, it was going up to 101 % and it was gradually getting stable at 100 % at 5.3rd second.

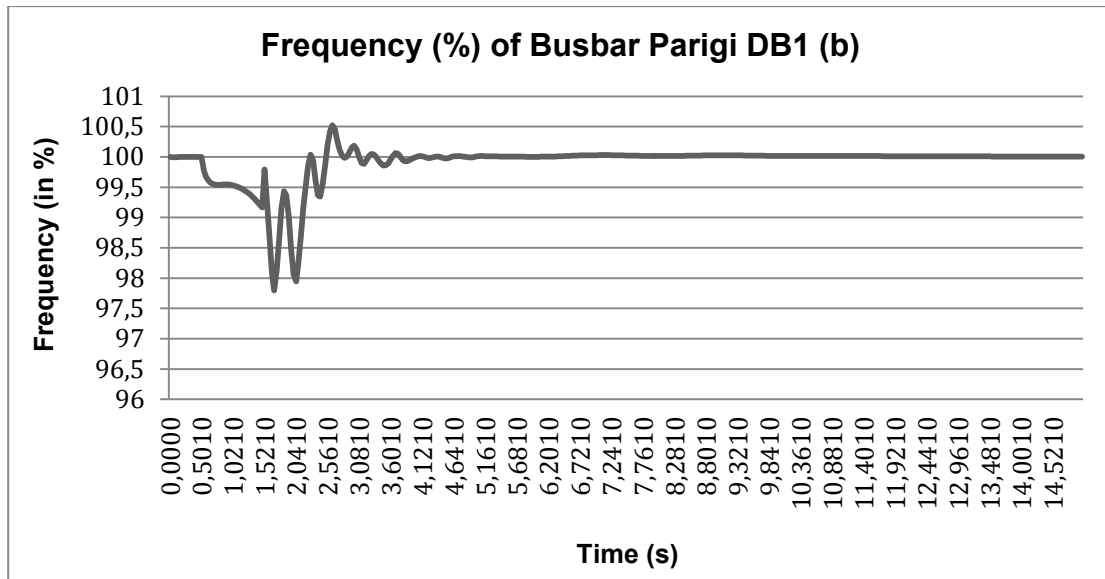


Figure 5-71: Parigi DB1 Bus Frequency Sag Simulation Results on Situation B

Based on figure 5-71, before sag, percentage of percentage of bus frequency was at 100 %. When the sag was occurred (from 0.5 s – 1.5 s), it had been going down to 99.3 % in 1 second. After sag, it was going up to 100.2 % and then it had been fluctuating between 99.4 % and 97.8 % for 0.9 seconds. It had been going up to 100.6 % in 0.3 seconds and it was getting stable at 100 % at 6.6th second.

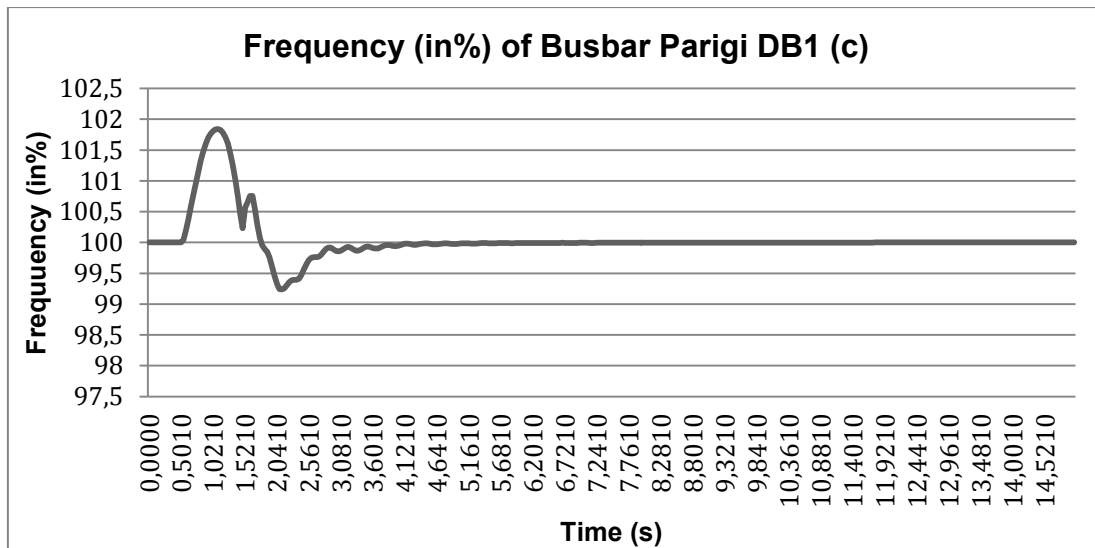


Figure 5-72: Parigi DB1 Bus Frequency Sag Simulation Results on Situation C

Based on figure 5-72, before sag, percentage of bus frequency was at 100 %. When the sag was occurred (from 0.5 s – 1.5 s), it had been going up to 101 % in 0.5

seconds and then it had been going down to 100.2 % in 0.5 seconds. After sag, percentage of bus frequency had been going down to 99.2 % in 0.5 seconds and then it had been going up to 100 % in 0.7 seconds. It was getting stable at 100 % at 5.1th second.

Bus frequency of sag simulation results of Parigi DB1 (2) bus bar before, after integrating RE into the grid and using homer results is equal to bus frequency of sag simulation results of Parigi DB1 bus bar on all situations.

Bus frequency of sag simulation results of bus bar Parigi SB1 before, after integrating RE into the grid and using homer results can be seen below.

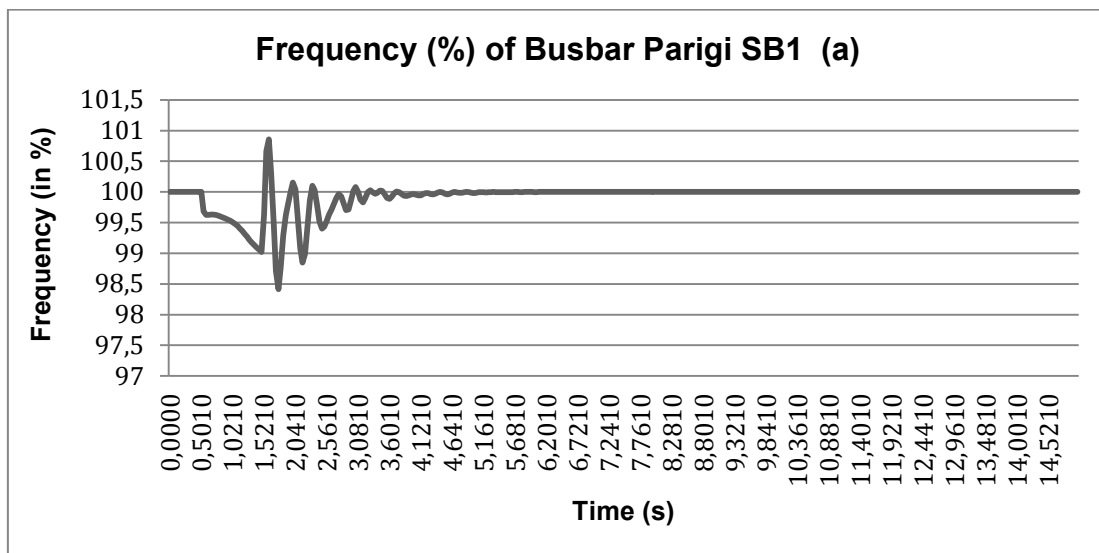


Figure 5-73: Parigi SB1 Bus Frequency Sag Simulation Results on Situation A

Based on figure 5-73, before sag, percentage of bus frequency was at 100 %. When the sag was occurred (from 0.5 s – 1.5 s), it had been going down to 99 % for 1 second. After sag, percentage of bus frequency was going up to 101 % and it was gradually getting stable at 100 % at 5th second.

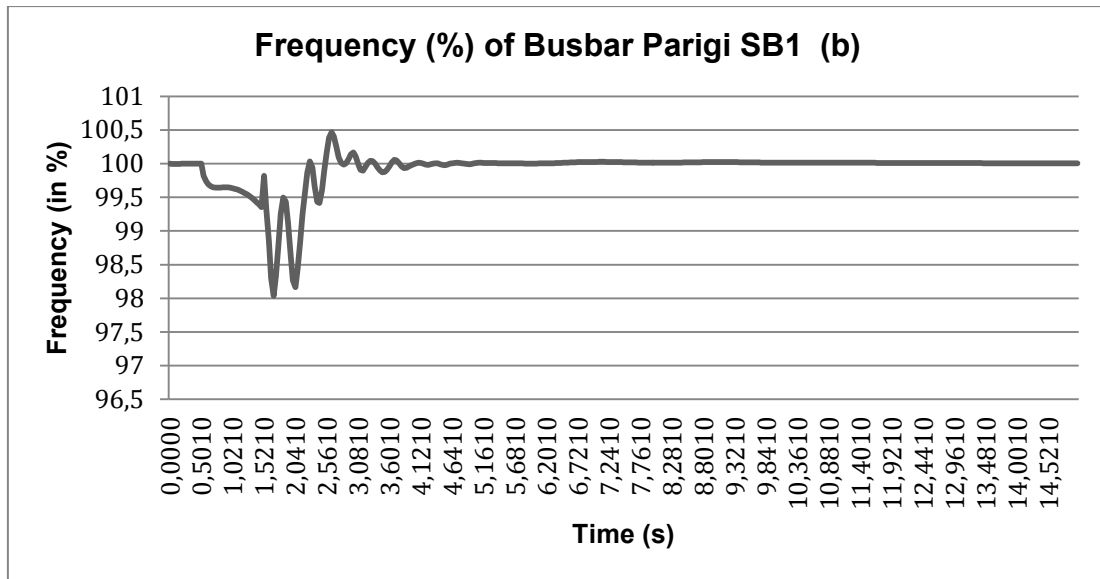


Figure 5-74: Parigi SB1 Bus Frequency Sag Simulation Results on Situation B

Based on figure 5-74, before sag, percentage of bus frequency was at 100 %. When the sag was occurred (from 0.5 s – 1.5 s), it had been going down to 99.4 % in 1 second. After sag, percentage of bus frequency was going up to 100.1 % and then it had been fluctuating between 99.6 % and 98 % for 0.9 seconds. It had been going up to 100.5 % in 0.3 seconds and it was getting stable at 100 % at 7.5th second.

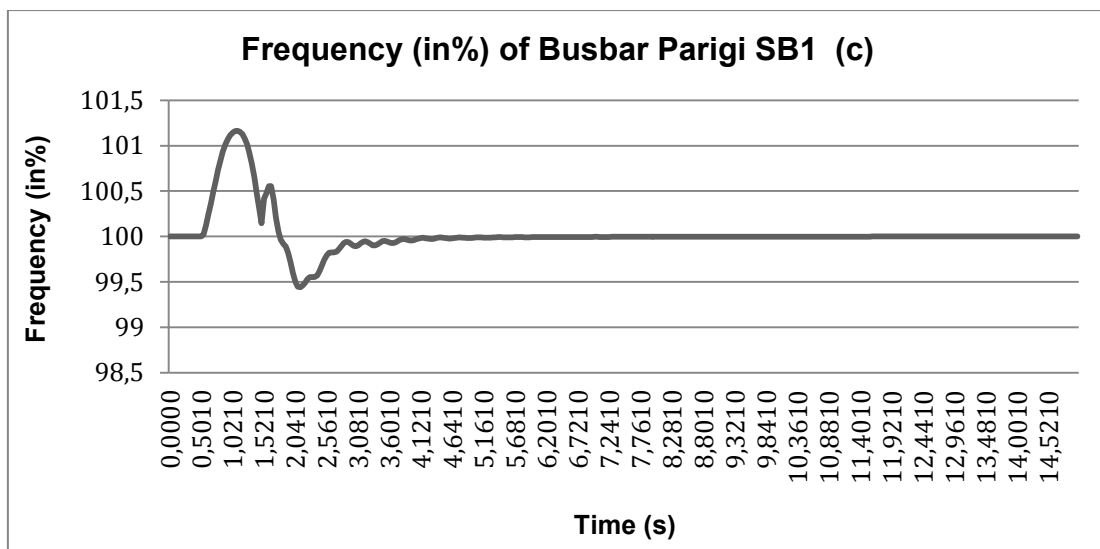


Figure 5-75: Parigi SB1 Bus Frequency Sag Simulation Results on Situation C

Based on figure 5-75, before sag, percentage bus frequency was at 100 %. When the sag was occurred (from 0.5 s – 1.5 s), it had been going up to 100.7 % in 0.5

seconds and then it had been going down to 100.1 % in 0.5 seconds. After sag, it had been going down to 99.4 % in 0.5 seconds and then it had been going up to 100 % in 0.5 seconds. It was getting stable at 100 % at 14th second.

Bus frequency of sag simulation results of bus bar Parigi SB2 before, after integrating RE into the grid and using homer results can be seen below.

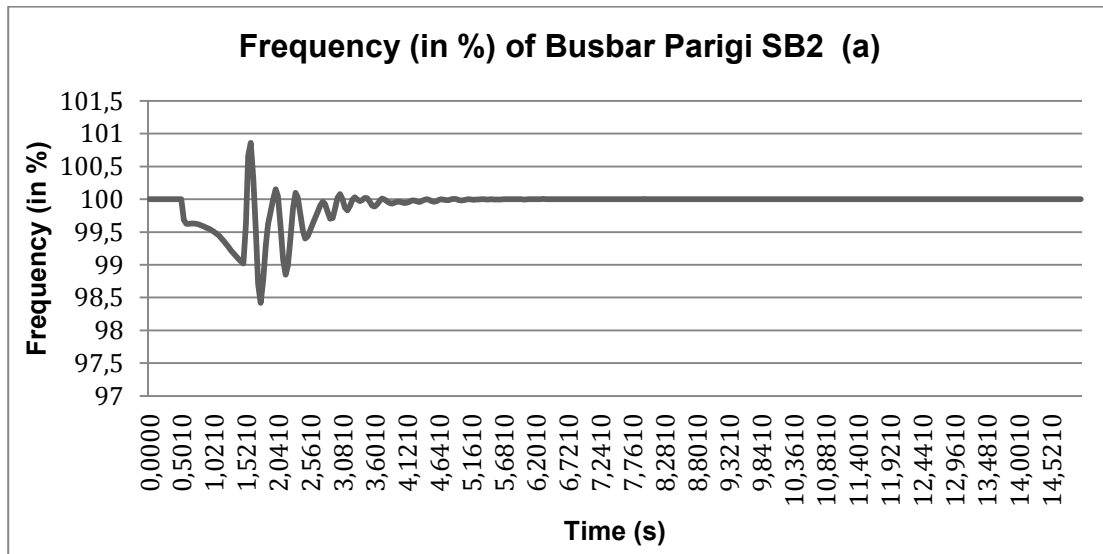


Figure 5-76: Parigi SB2 Bus Frequency Sag Simulation Results on Situation A

Based on figure 5-76, before sag, percentage of bus frequency was at 100 %. When the sag was occurred (from 0.5 s – 1.5 s), it had been going down to 98.8 % for 1 second. After sag, it was going up to 101.2 % and it was gradually getting stable at 100 % at 9.8th second.

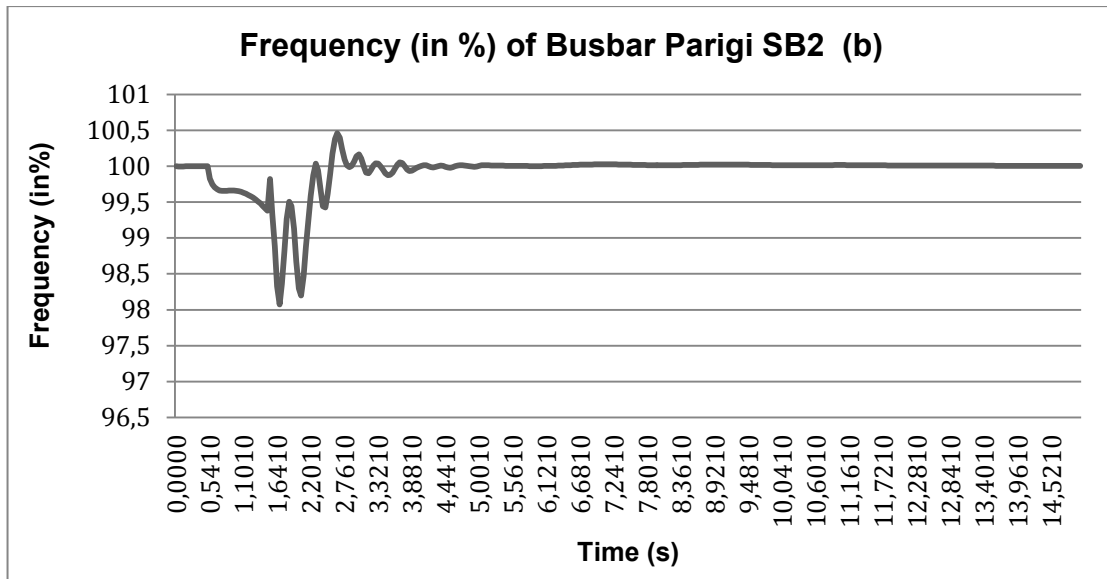


Figure 5-77: Parigi SB2 Bus Frequency Sag Simulation Results on Situation B

Based on figure 5-77, before sag, percentage of bus frequency was at 100 %. When the sag was occurred (from 0.5 s – 1.5 s), it had been going down to 99.6 % in 1 second. After sag, it was going up to 100.2 % and then it had been fluctuating between 99.5 % and 98.1 % for 0.9 seconds. It had been going up to 100.5 % in 0.3 seconds and getting stable at 100 % at 6.5th second.

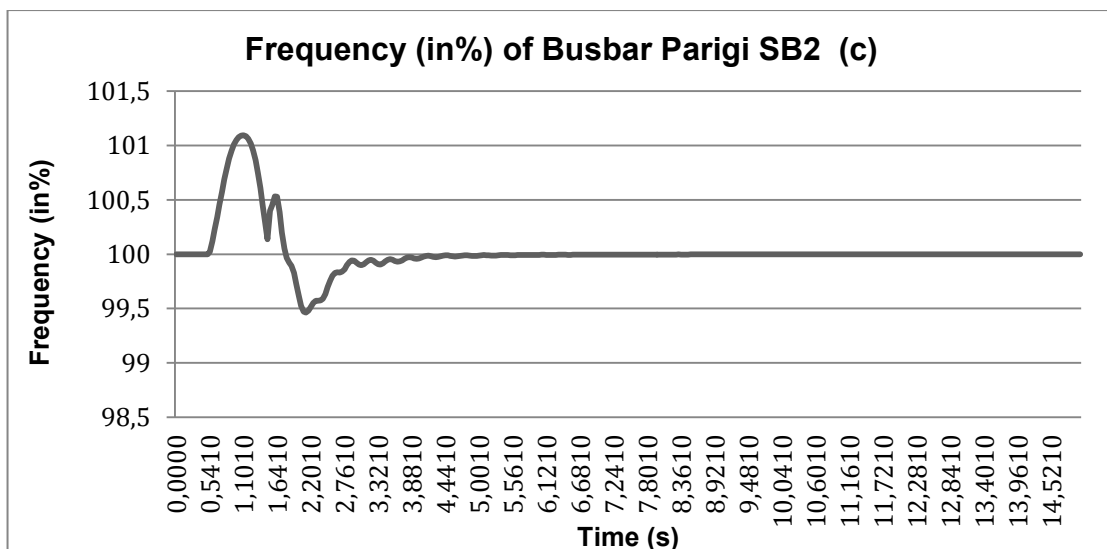


Figure 5-78: Parigi SB2 Bus Frequency Sag Simulation Results on Situation C

Based on figure 5-78, before sag, percentage of bus frequency was at 100 %. When the sag was occurred (from 0.5 s – 1.5 s), it had been going up to 100.7 % in 0.5

seconds and then it had been going down to 100.1 % in 0.5 seconds. After sag, it had been going down to 99.4 % in 0.5 seconds and then it had been going up to 100 % in 0.5 seconds. It was getting stable at 100 % at 5.3rd second.

Bus frequency of sag simulation results of bus bar PJPP SB1 before, after integrating RE into the grid and using homer results can be seen below.

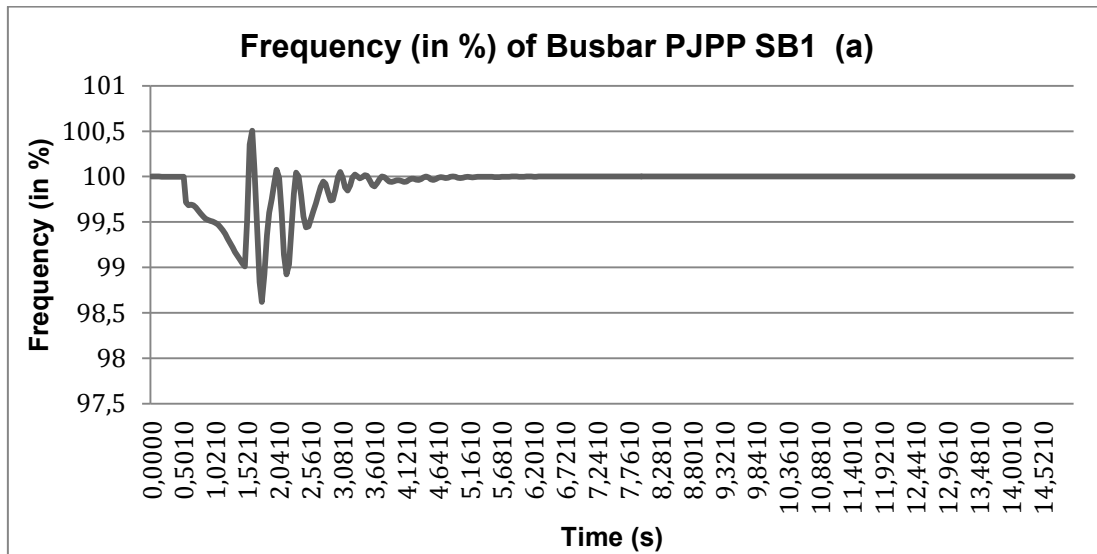


Figure 5-79: PJPP SB1 Bus Frequency Sag Simulation Results on Situation A

Based on figure 5-79, before sag, percentage of bus frequency was at 100 %. When the sag was occurred (from 0.5 s – 1.5 s), it had been going down to 99.2 % for 1 second. After sag, percentage of bus frequency was going up to 100.7 % and it was gradually getting stable at 100 % at 5.2nd second.

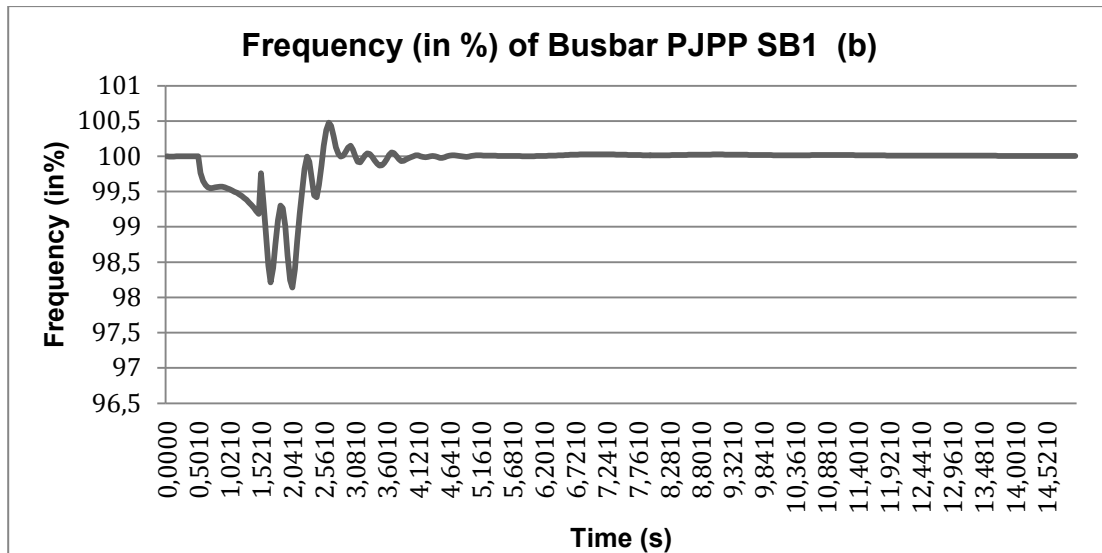


Figure 5-80: PJPP SB1 Bus Frequency Sag Simulation Results on Situation B

Based on figure 5-80, before sag, percentage of bus frequency was at 100 %. When the sag was occurred (from 0.5 s – 1.5 s), bus it had been going down to 99.4 % in 1 second. After sag, percentage of bus frequency was going up to 100 % and then it had been fluctuating between 99.2 % and 98 % for 0.9 seconds. It had been going up to 100.5 % in 0.3 seconds and it was getting stable at 100 % at 11.4th second.

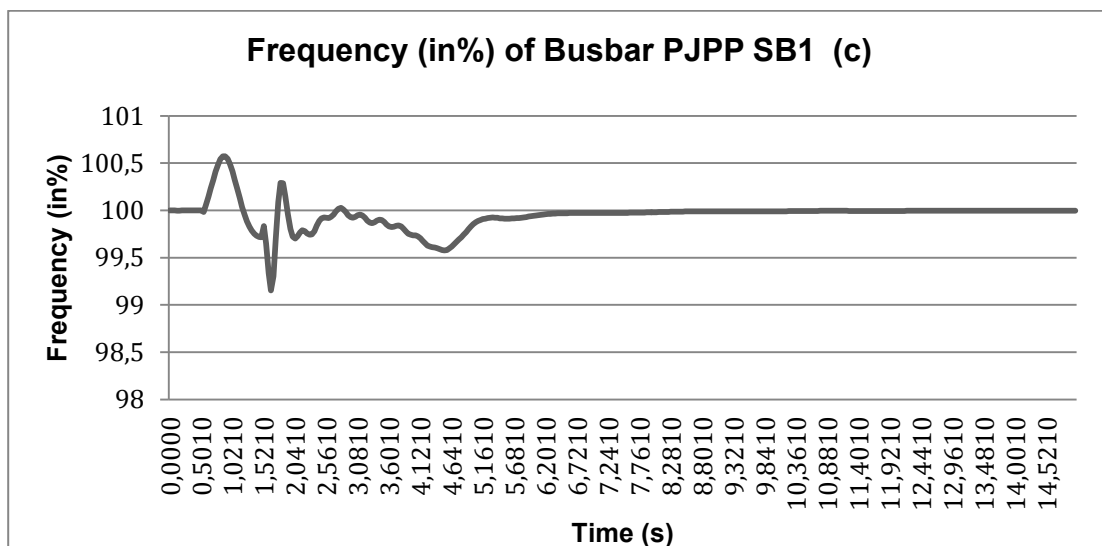


Figure 5-81: PJPP SB1 Bus Frequency Sag Simulation Results on Situation C

Based on figure 5-81, before sag, percentage of bus frequency was at 100 %. When the sag was occurred (from 0.5 s – 1.5 s), it had been going up to 101.1 % in 0.5

seconds and then it had been going down to 100 % in 0.5 seconds. After sag, percentage of bus frequency had been going down to 99.6 % in 0.1 second and then it had been staying there for 0.2 seconds. It had been going down to 99.1 % in 0.7 seconds. It was getting stable at 100 % at 8.5th second.

Bus frequency of sag simulation results of bus bar Silae SB1 before, after integrating RE into the grid and using homer results can be seen below.

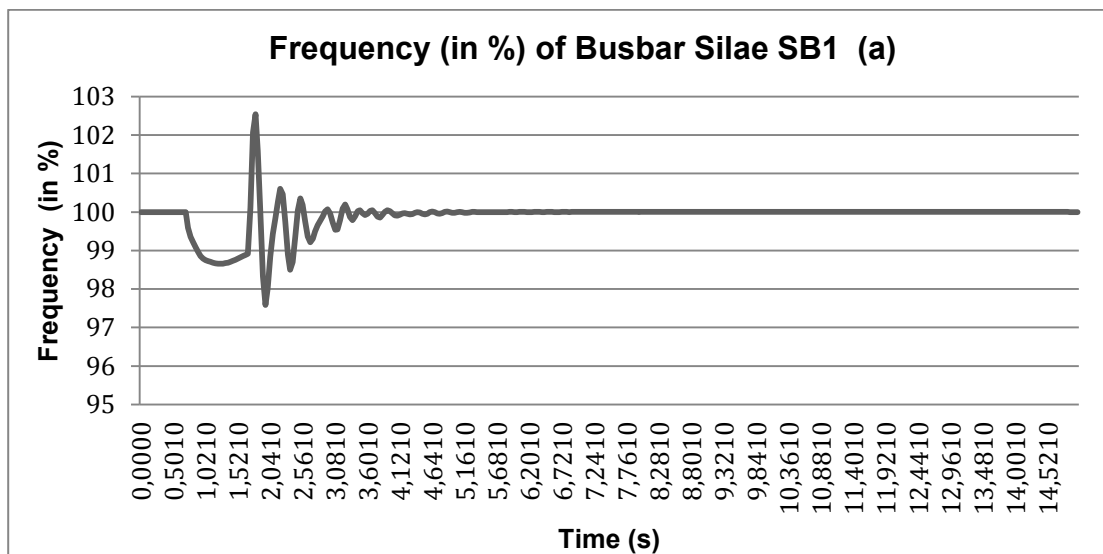


Figure 5-82: Silae SB1 Bus Frequency Sag Simulation Results on Situation A

Based on figure 5-82, before sag, percentage of bus frequency was at 100 %. When the sag was occurred (from 0.5 s – 1.5 s), it had been going down to 98.8 % in 0.5 seconds and then it had been going up to 99 in 0.5 seconds. After sag, bus voltage frequency was going up to 103.3 % and it was gradually getting stable at 100 % at 6.6th second.

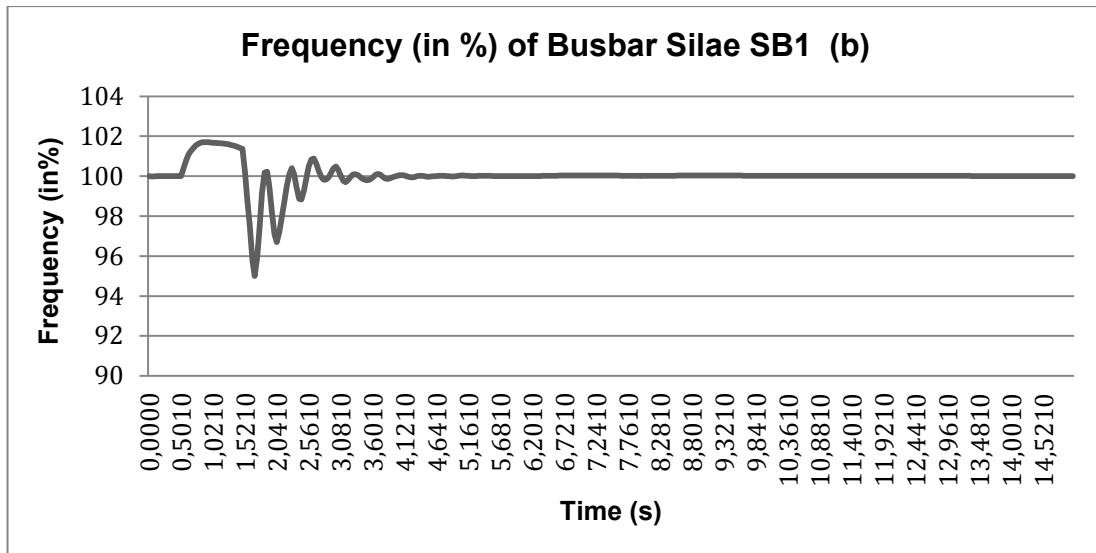


Figure 5-83: Silae SB1 Bus Frequency Sag Simulation Results on Situation B

Based on figure 5-83, before sag, percentage of bus frequency was at 100 %. When the sag is occurred (from 0.5 s – 1.5 s), it had been going up to 101.7 % in 0.3 seconds and then it had been going down to 101.5 in 0.7 seconds. After sag, percentage of bus frequency had been going down to 96.1 % in 0.1 second and then it had been fluctuating between 100 % and 96.5 % for 0.9 seconds. It had been going up to 100.9 % in 0.3 seconds and it was getting stable at 100 % at 6.5th second.

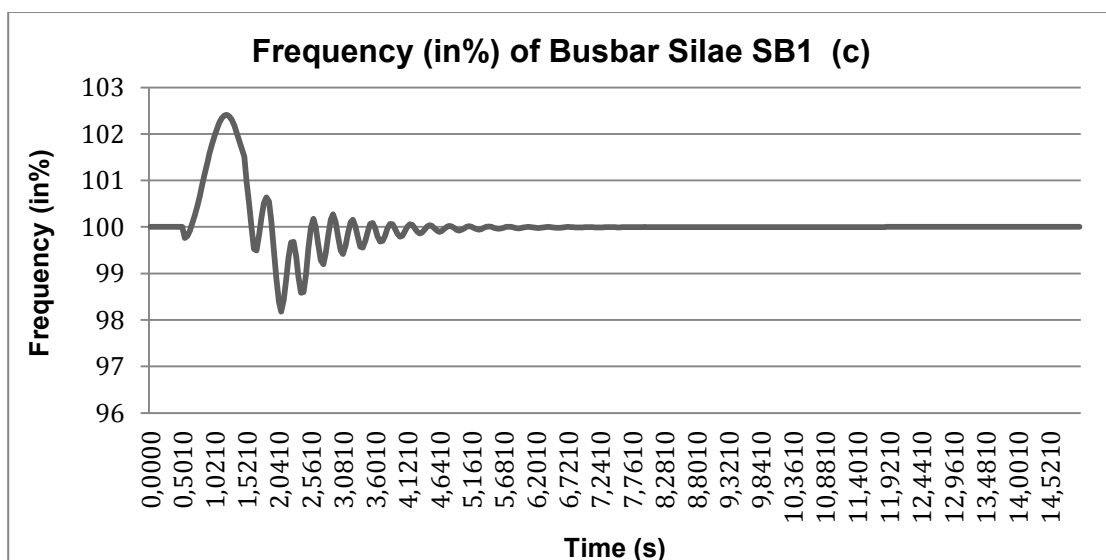


Figure 5-84: Silae SB1 Bus Frequency Sag Simulation Results on Situation C

Based on figure 5-84, before sag, percentage of bus frequency was at 100 %. When the sag was occurred (from 0.5 s – 1.5 s), it had been going down to 102.5 % during 1 second. After sag, percentage of bus frequency was fluctuating between 100.5 % and 98 % for 2.5 seconds. It was getting stable at 100 % at 9.3rd second.

Bus frequency of sag simulation results of Silae SB2 and Silae SB3 bus bar before, after integrating RE into the grid and using homer results is equal to bus frequency of sag simulation results of Silae SB1 bus bar on all situations.

Bus frequency of sag simulation results of bus bar Silae SB4 before, after integrating RE into the grid and using homer results can be seen below.

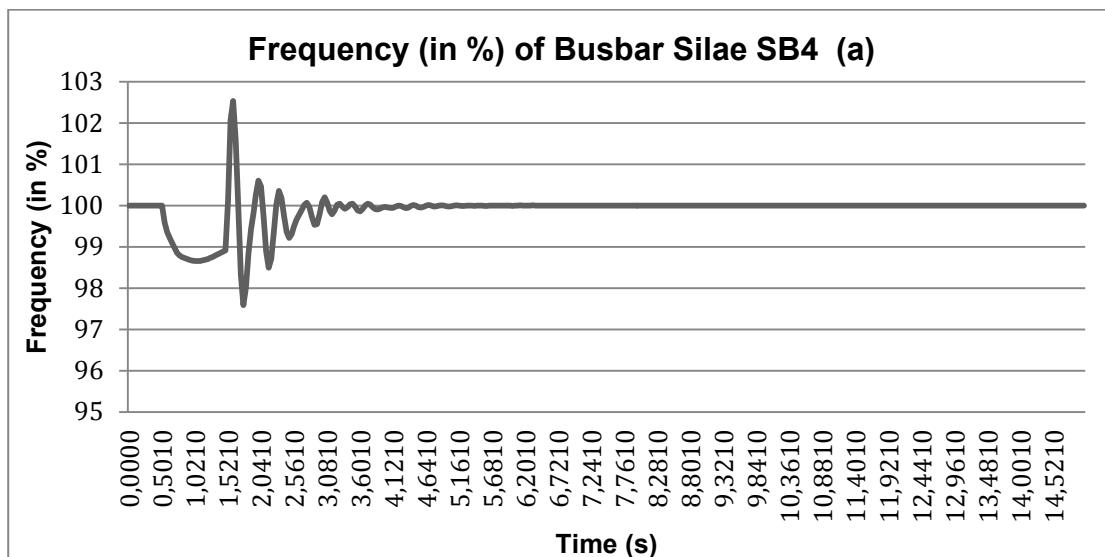


Figure 5-85: Silae SB4 Bus Frequency Sag Simulation Results on Situation A

Based on figure 5-185, before sag, percentage of bus frequency was at 100 %. When the sag was occurred (from 0.5 s – 1.5 s), it had been going down to 98.8 % in 0.6 seconds and then it had been going up to 99 in 0.4 seconds. After sag, percentage of bus frequency was going up to 103.5 % and it was gradually getting stable at 100 % at 5.1st second.

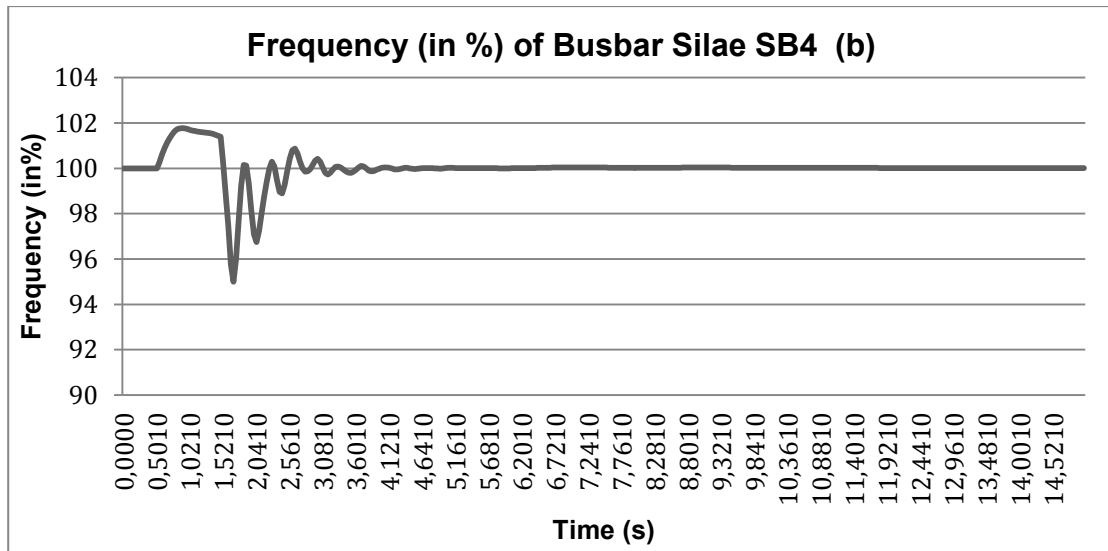


Figure 5-86: Silae SB4 Bus Frequency Sag Simulation Results on Situation B

Based on figure 5-86, before sag, percentage of bus frequency was at 100 %. When the sag was occurred, (from 0.5 s – 1.5 s), it had been going up to 101.9 % in 0.3 seconds and then it had been going down to 101.5 in 0.7 seconds. After sag, percentage of bus frequency had been going down to 96.1 % in 0.1 second and then it had been fluctuating between 100 % and 96.8 % for 1 second. It had been going up to 100.9 % in 0.3 seconds and it was getting stable at 100 % at 8.5th second.

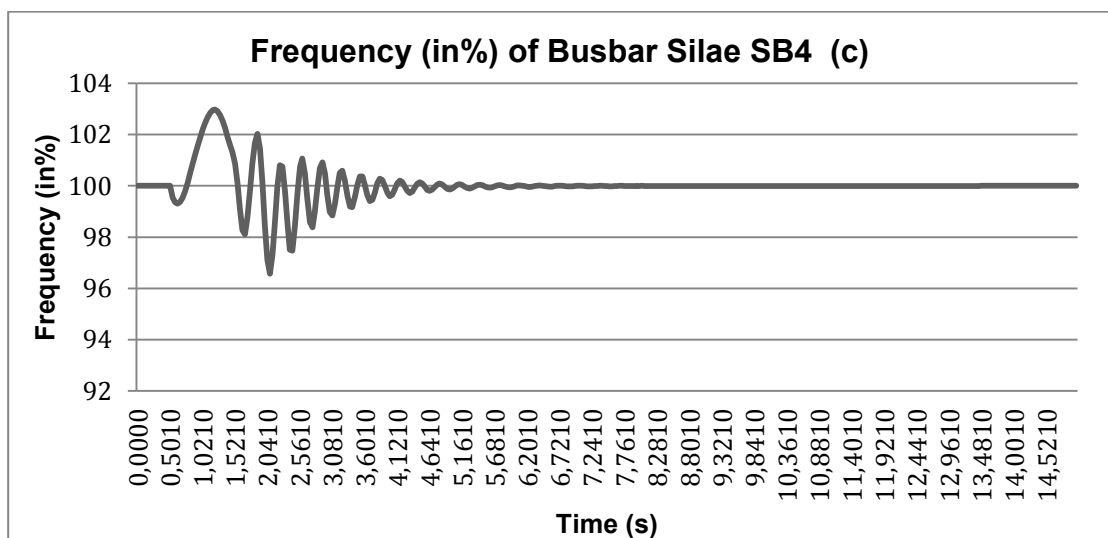


Figure 5-87: Silae SB4 Bus Frequency Sag Simulation Results on Situation C

Based on figure 5-87, before sag, percentage of bus frequency was at 100 %. When the sag was occurred (from 0.5 s – 1.5 s), it had been going down to 98.5 % in 0.1 seconds and then it had been going up to 103 % for 0.9 seconds. After sag, percentage of bus frequency was going down to 98 % and then it had been fluctuating between 102 % and 96.5 %. It was getting stable at 100 % at 6.7th second.

Bus frequency of sag simulation results of bus bar Talise SB1 before, after integrating RE into the grid and using homer results can be seen below.

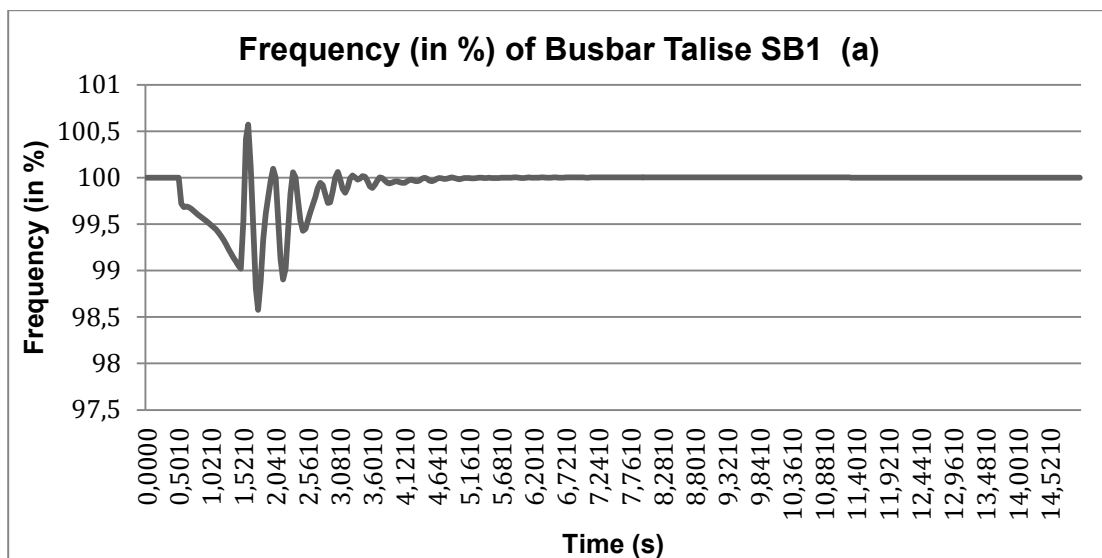


Figure 5-88: Talise SB1 Bus Frequency Sag Simulation Results on Situation A

Based on figure 5-88, before sag, percentage of bus frequency was at 100 %. When the sag was occurred (from 0.5 s – 1.5 s), it had been going down to 99.2 % for 1 second during sag. After sag, percentage of bus frequency was going up to 100.4 % and it was gradually getting stable at 100 % at 5.1st second.

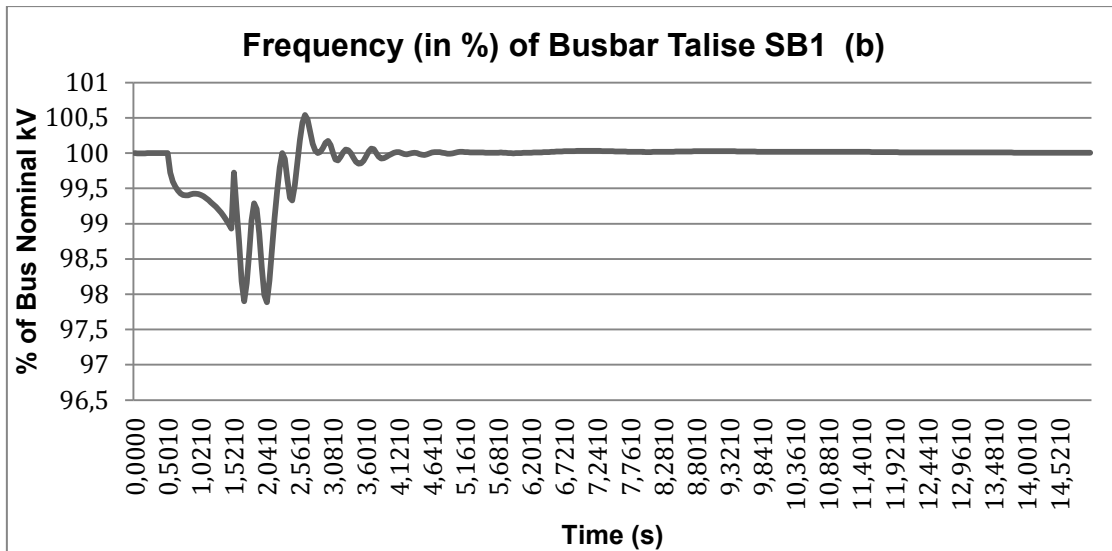


Figure 5-89: Talise SB1 Bus Frequency Sag Simulation Results on Situation B

Based on figure 5-89, before sag, percentage of bus frequency was at 100 %. When the sag was occurred (from 0.5 s – 1.5 s), it had been going down to 99.2 % for 1 second during sag. After sag, percentage of bus frequency was going up to 100.2 % and then it had been going down to 98.1 % in 0.1 second. It had been fluctuating between 99.4 % and 97.7 % for 0.9 seconds. It had been going up to 100.5 % in 0.2 seconds. It reached stable at 100 % at 10.6th second.

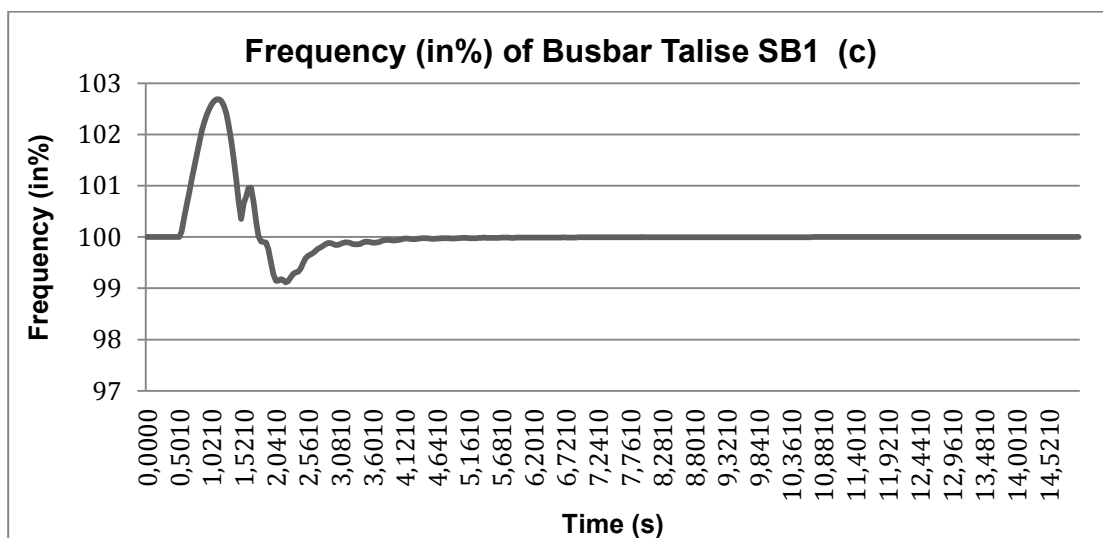


Figure 5-90: Talise SB1 Bus Frequency Sag Simulation Results on Situation C

Based on figure 5-90, before sag, percentage of bus frequency was at 100 %. When the sag was occurred (from 0.5 s – 1.5 s), bus it had been going up to 102.8 % for 1 second. After sag, percentage of bus frequency had been going down to 100.5 % in 0.8 seconds and then it had been going up to 101 % in 0.3 seconds. It reached stable at 100 % at 4.6th second.

Bus frequency of sag simulation results of bus bar Talise SB2 before, after integrating RE into the grid and using homer results can be seen below.

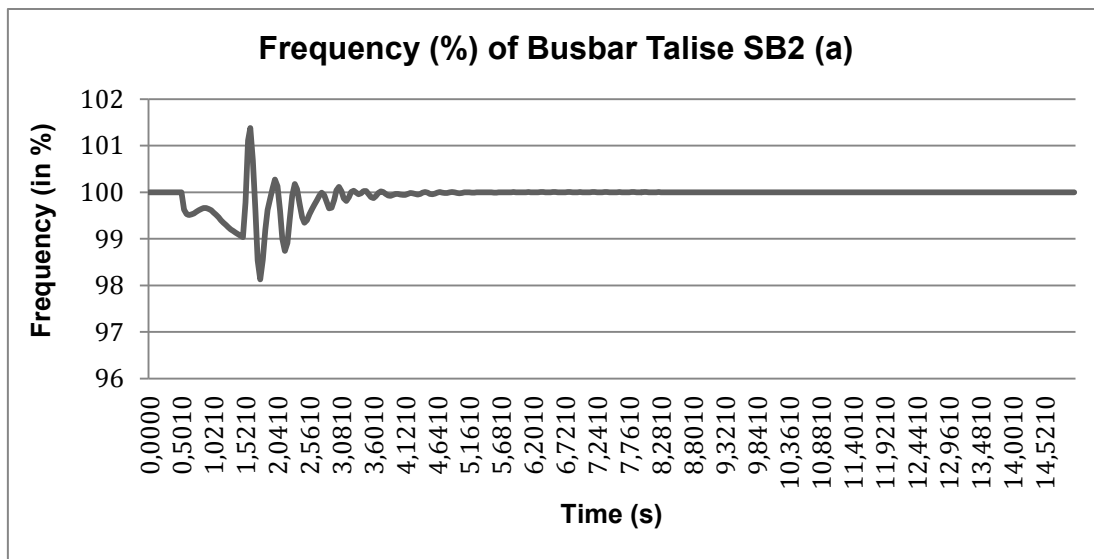


Figure 5-91: Talise SB2 Bus Frequency Sag Simulation Results on Situation A

Based on figure 5-91, before sag, percentage of bus frequency was at 100 %. When the sag was occurred (from 0.5 s – 1.5 s), it had been going down to 99.7 % in 0.2 seconds and then it had been going up to 100 % in 0.3 seconds. It had been going down to 99.2 % in 0.5 seconds. After sag, it was going up to 102 % and then it was getting stable at 100 % at 5.1st second.

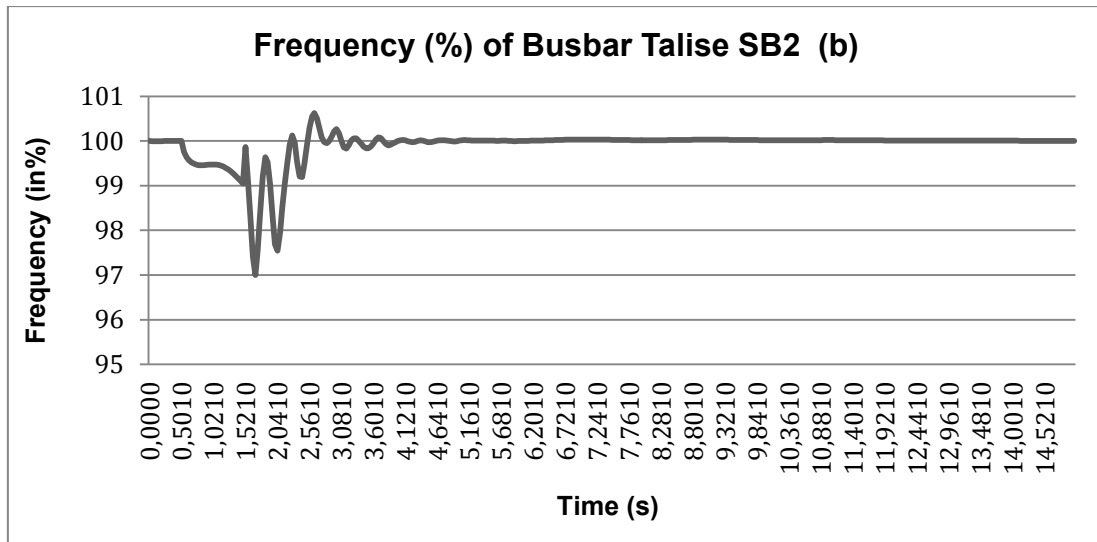


Figure 5-92: Talise SB2 Bus Frequency Sag Simulation Results on Situation B

Based on figure 5-92, before sag, percentage of bus frequency was at 100 %. When the sag was occurred (from 0.5 s – 1.5 s), it had been going down to 99.2 % for 1 second during sag. After sag, percentage of bus frequency was going up to 100.4 % and then it had been going down to 97.6 % in 0.1 second. It had been fluctuating between 99.6 % and 97.3 % for 0.9 seconds. It had been going up to 100.6 % in 0.2 seconds and it was getting stable at 100 % at 6.2nd second.

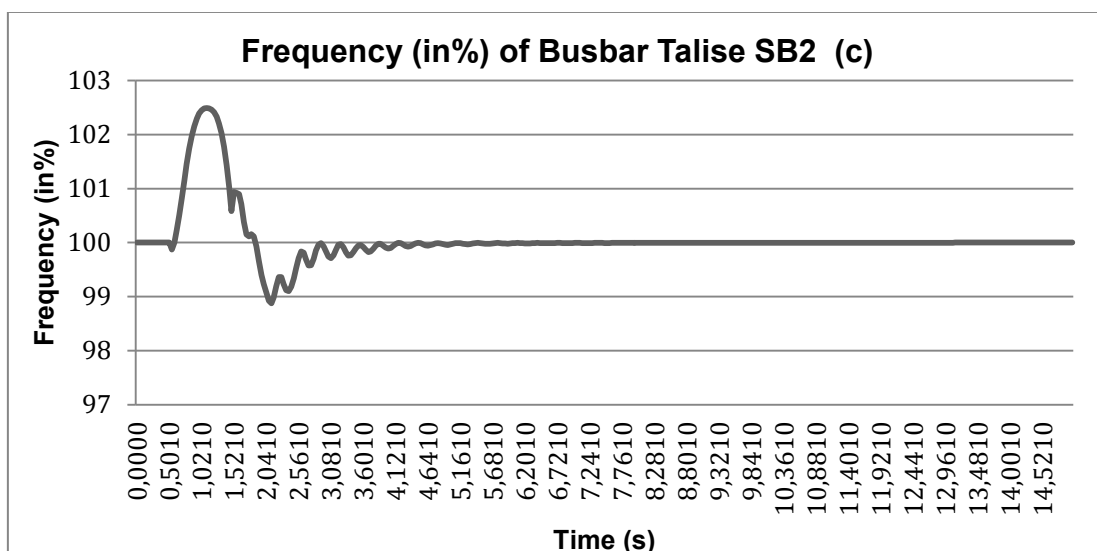


Figure 5-93: Talise SB2 Bus Frequency Sag Simulation Results on Situation C

Based on figure 5-93, before sag, percentage of bus frequency was at 100 %. When the sag was occurred (from 0.5 s – 1.5 s), it had been it had been going up to 101 % in 0.5 seconds and then it had been going down to 100.1 % in 0.5 seconds. After sag, percentage of bus frequency was going down to 98.8 % and then it was fluctuating below 100 %. It reached stable at 100 % at 5.5th second.

Bus frequency of sag simulation results of Talise SB3 bus bar before, after integrating RE into the grid and using homer results is equal to bus frequency of sag simulation results of Talise SB2 bus bar on all situations.

Bus frequency of sag simulation results of bus bar Talise DB1 before, after integrating RE into the grid and using homer results can be seen below.

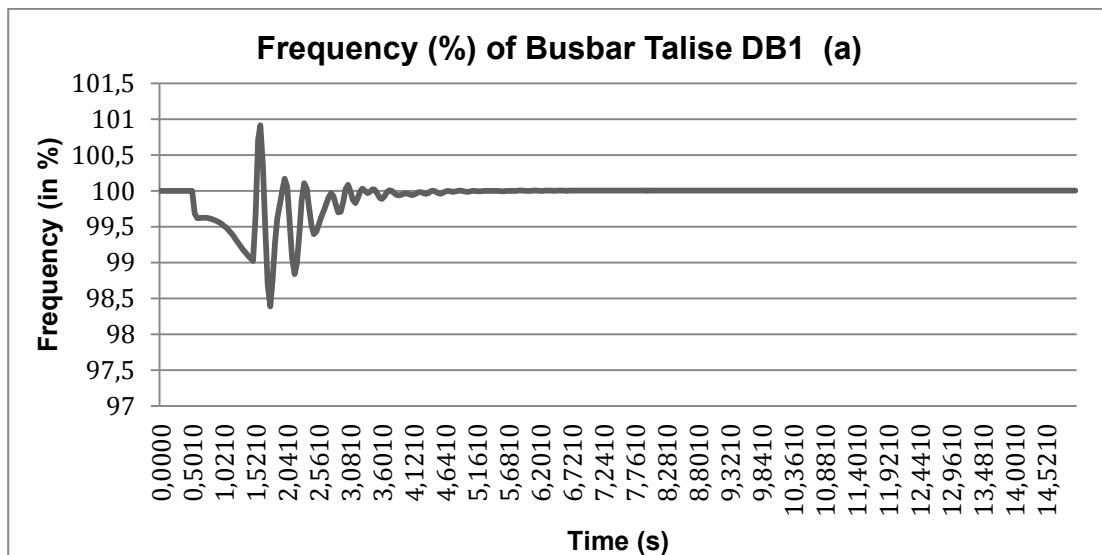


Figure 5-94: Talise DB1 Bus Frequency Sag Simulation Results on Situation A

Based on figure 5-94, before sag, percentage of bus frequency was at 100 %. When the sag was occurred (from 0.5 s – 1.5 s), it had been going down to 99.2 % for 1 second during sag. After sag, percentage of bus frequency was going up to 101.2 % and then it was getting stable at 100 % at 6.1st second.

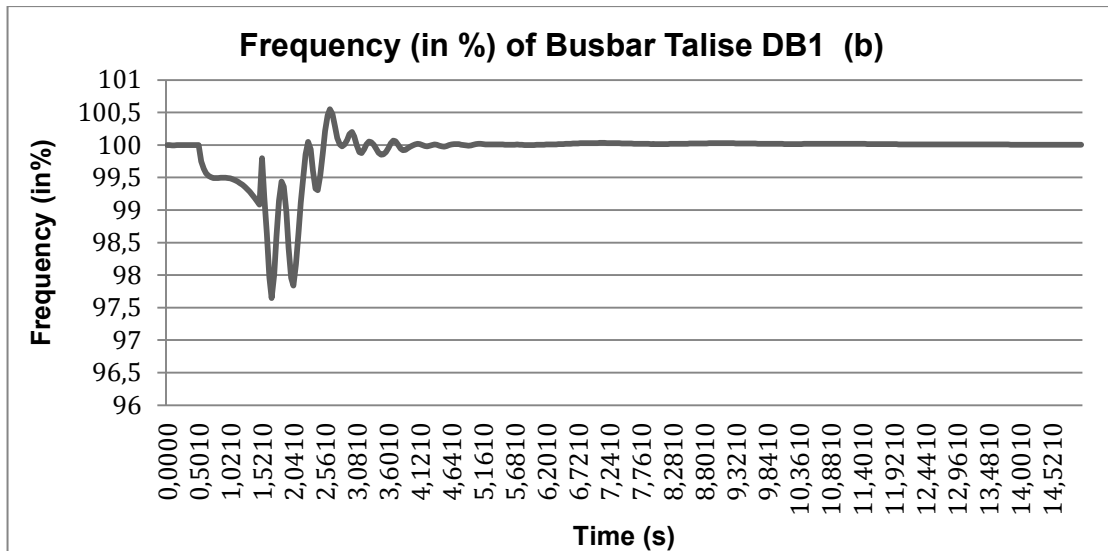


Figure 5-95: Talise DB1 Bus Frequency Sag Simulation Results on Situation B

Based on figure 5-95, before sag, percentage of bus frequency was at 100 %. When the sag was occurred (from 0.5 s – 1.5 s), it had been going down to 99.5 % for 1 second during sag. After sag, percentage of bus frequency was going up to 100.2 % and then it had been going down to 98.3 % in 0.1 second. It had been fluctuating between 99.4 % and 97.7 % in 0.8 seconds and then it had been going up to 100.6 % in 0.2 seconds. It was getting stable at 100 % at 7.7th second.

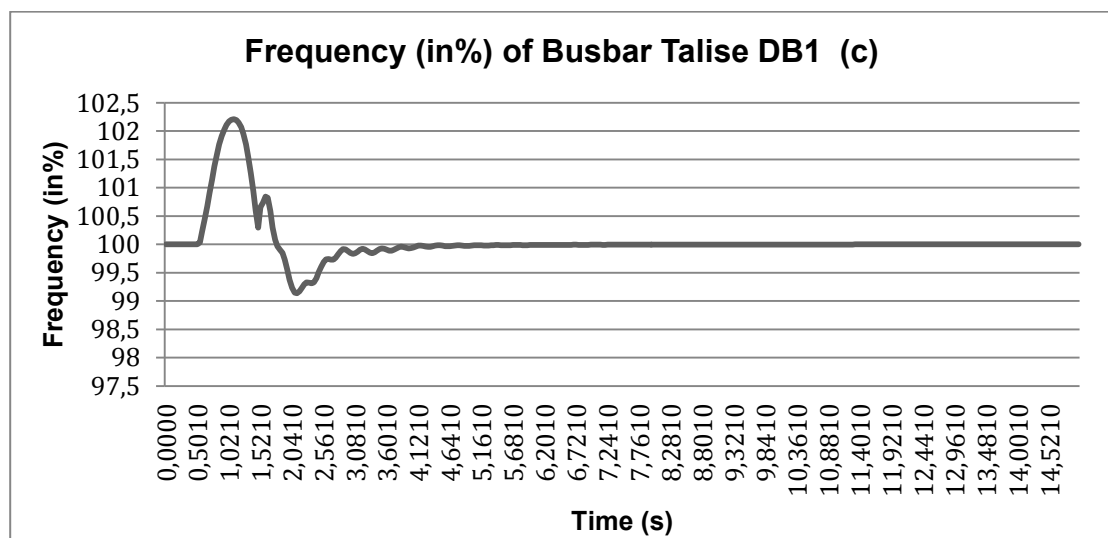


Figure 5-96: Talise DB1 Bus Frequency Sag Simulation Results on Situation C

Based on figure 5-96, before sag, percentage of bus frequency was at 100 %. When the sag was occurred (from 0.5 s – 1.5 s), it had been going up to 102.3 % in 0.5 seconds and then it had been going down to 100.2 % in 0.5 seconds. After sag, percentage of bus frequency had been going down to 99.1 % in 0.6 second and then it had been going up to 100 % in 0.5 seconds. It was getting stable at 100 % at 5.1st second.

Bus frequency of sag simulation results of Talise DB11 bus bar before, after integrating RE into the grid and using homer results is equal to bus frequency of sag simulation results of Talise DB1 bus bar on all situations.

5.4.2 Swell Simulation Results

Bus voltage of swell simulation results of bus bar DB1 PJPP before RE integration, after RE integration and after RE integration using homer results can be seen below.

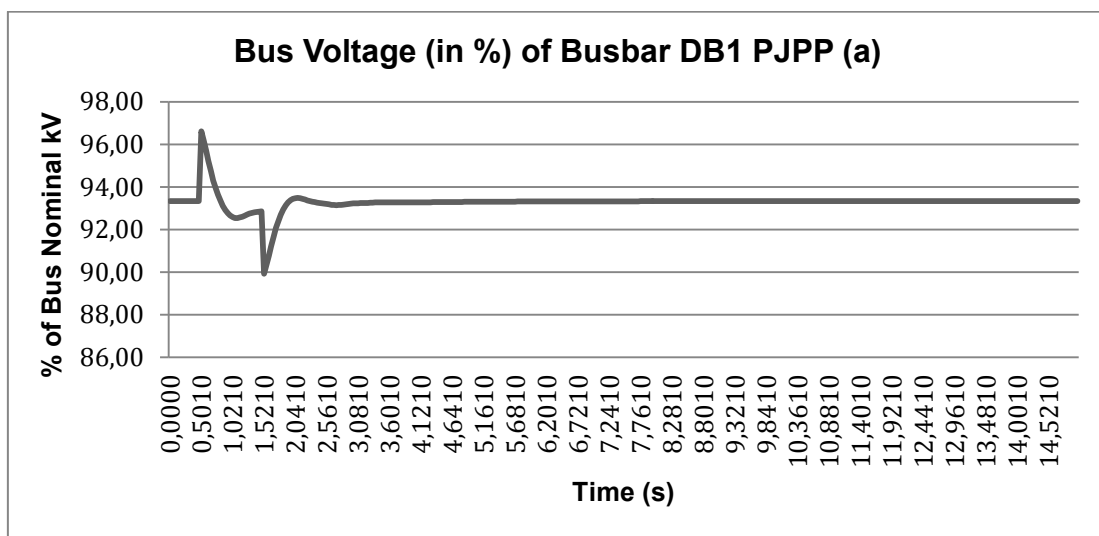


Figure 5-97: DB1 PJPP Bus Voltage Swell Simulation Results on Situation A

Based on figure 5-97, before swell, percentage of bus voltage was at 93.3 % kV. When the swell was occurred (from 0.5 s – 1.5 s), it was going up to 96.7 % kV and then it had been going down to 94 %kV in 1 second. After swell, percentage of bus voltage dropped to 91 % kV. It was getting stable at 93.3 %kV at 5.5th second.

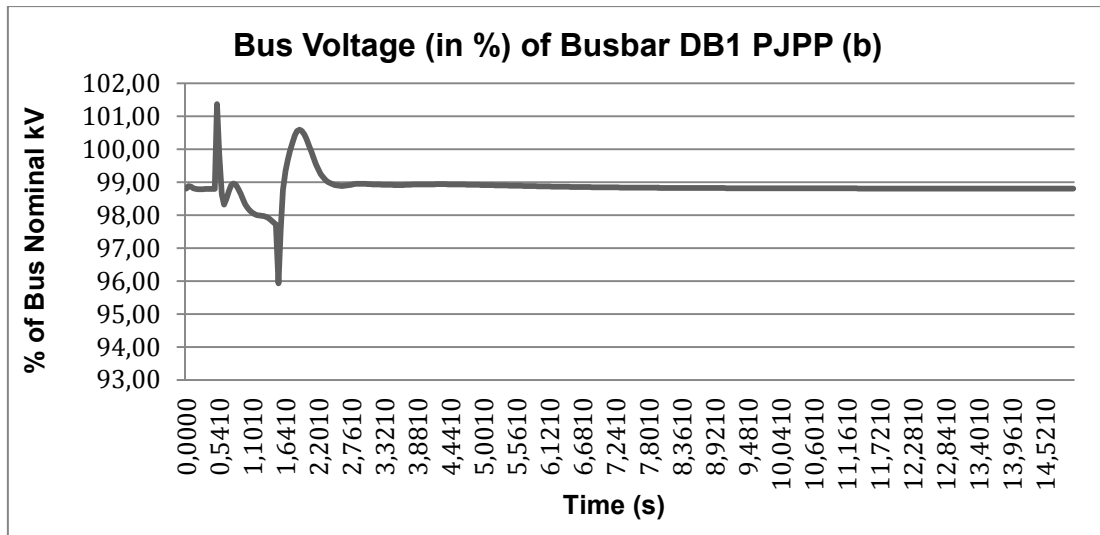


Figure 5-98: DB1 PJPP Bus Voltage Swell Simulation Results on Situation B

Based on figure 5-98, before swell, percentage of bus voltage was at 99 %kV. When the swell was occurred (from 0.5 s – 1.5 s), it had been going up to 102 %kV for 1 second and then it had been going up to 100 %kV in 0.3 seconds. It had been going down to 97 %kV in 0.6 seconds. After swell, percentage of bus voltage dropped to 94 %kV and then it had been going up again to 97.3 %kV in 0.1 second. It had been going up to 100.2 %kV in 0.7 seconds. It was getting stable at 99 %kV at 7th second.

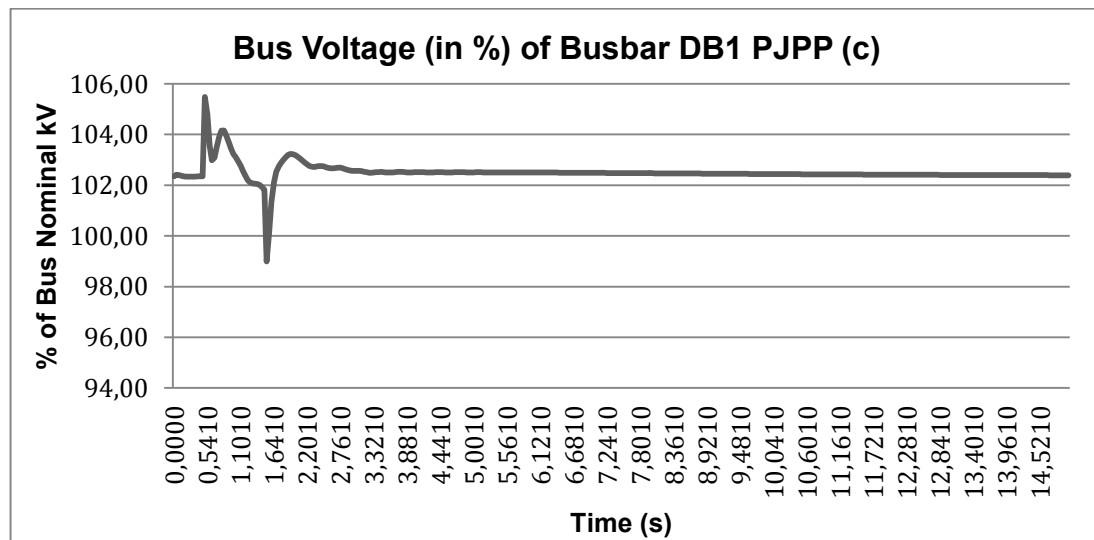


Figure 5-99: DB1 PJPP Bus Voltage Swell Simulation Results on Situation C

Based on figure 5-99, before swell, percentage of bus voltage was at 102.5 %kV. When the swell was occurred (from 0.5 s – 1.5 s), it was going up to 104.5 %kV and

then it had been going down to 103.3 %kV in 0.1 seconds. It had been going up to 104.6 %kV in 0.3 second and then it had been going down again to 103.3 %kV in 0.6 seconds. After swell, percentage of bus voltage dropped to 101.4 %kV and then it had been going up again to 103.9 %kV in 0.2 seconds. It was getting stable at 102.5 %kV at 13.5th second.

Bus voltage of swell simulation results of DB11 PJPP bus bar before, after integrating RE into the grid and using homer results is equal to bus voltage of swell simulation results of DB1 PJPP bus bar on all situations.

Bus voltage of swell simulation results of bus bar Donggala SB1 before, after integrating RE into the grid and using homer results can be seen below.

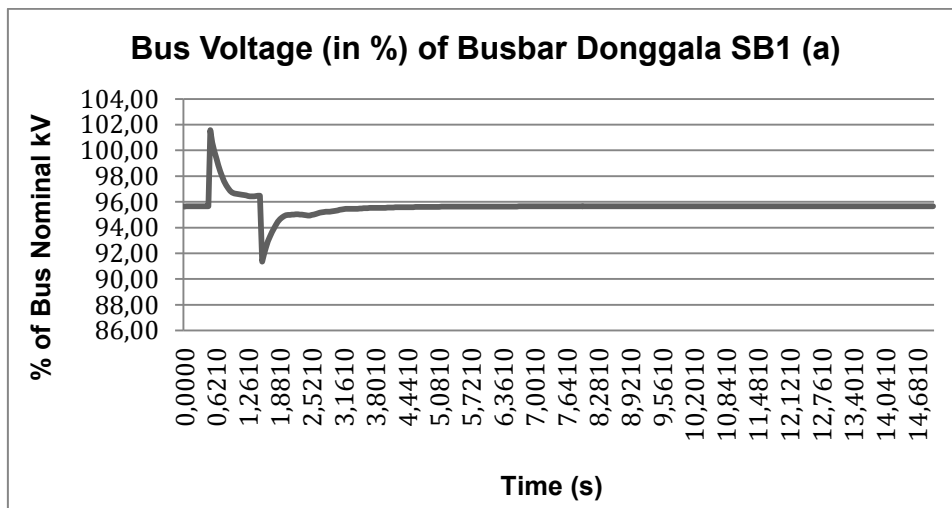


Figure 5-100: Donggala SB1 Bus Voltage Swell Simulation Results on Situation A

Based on figure 5-100, before sag, percentage of bus voltage was at 93.3 % kV. When the swell was occurred (from 0.5 s – 1.5 s), it was going up to 101.7 % kV and then it had been going down to 97.8 %kV in 1 second. After swell, percentage of bus voltage dropped to 92 % kV and then it was getting stable at 93.3 %kV 4.5th second.

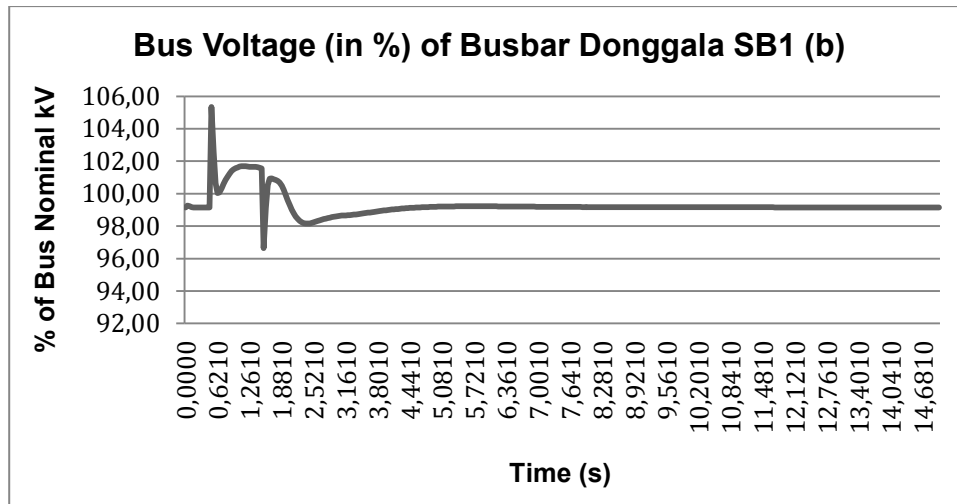


Figure 5-101: Donggala SB1 Bus Voltage Swell Simulation Results on Situation B

Based on figure 5-101, before swell, percentage of bus voltage was at 99.2 %kV. When the swell was occurred (from 0.5 s – 1.5 s), it was going up to 101.5 %kV and then it had been going down to 101 %kV in 0.1 seconds. It had been going up to 102.7 %kV in 0.3 seconds and then it had been going down to 102 %kV in 0.6 seconds. After swell, percentage of bus voltage dropped to 95.6 %kV and then it had been going up again to 100 %kV in 0.1 second. It had been going up down to 98.2 %kV in 0.8 seconds. It was getting stable at 98.9 %kV at 6.9th second.

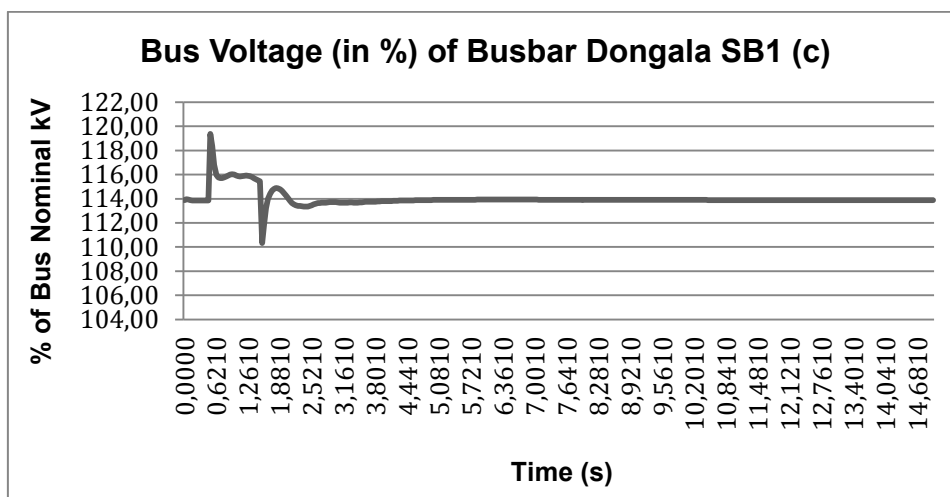


Figure 5-102: Donggala SB1 Bus Voltage Swell Simulation Results on Situation C

Based on figure 5-102, before swell, percentage of bus voltage was at 114 %kV. When the swell was occurred (from 0.5 s – 1.5 s), it was at going up to 119.7 %kV

and then it had been going down to 116.8 %kV in 0.1 seconds. It had been going up to 117 %kV in 0.3 second and then it had been going down again to 115.7 %kV in 0.6 seconds. After swell, percentage of bus voltage dropped to 110.3 %kV and then it had been going up again to 114 %kV in 0.2 seconds. It was getting stable at 114 %kV at 7.5st second.

Bus voltage of swell simulation results of bus bar Maesa SB1 before RE integration, after RE integration and after RE integration using homer results can be seen below.

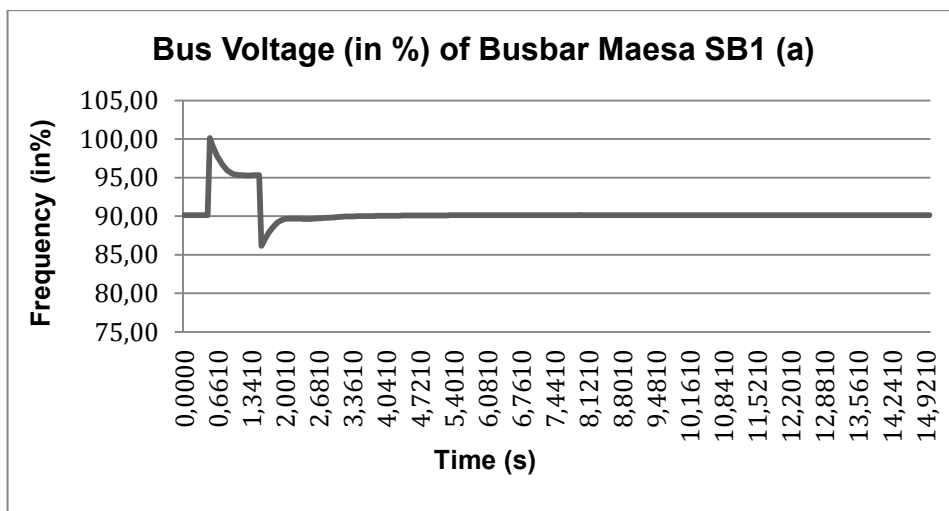


Figure 5-103: Maesa SB1 Bus Voltage Swell Simulation Results on Situation C

Based on figure 5-103, before swell, percentage of bus voltage was at 90 %kV. When the swell was occurred (from 0.5 s – 1.5 s), it was going up to 100 % kV and then it had been going down to 96.8 %kV in 1 second. After swell, percentage of bus voltage dropped to 87 % kV and then it was getting stable at 90 %kV 4.1st second.

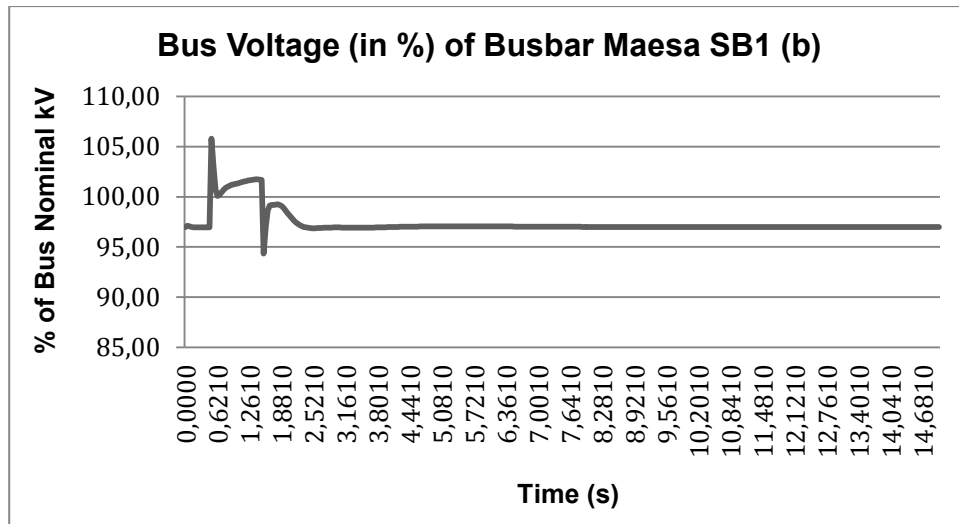


Figure 5-104: Maesa SB1 (2) Bus Voltage Swell Simulation Results on Situation B

Based on figure 5-104, before swell, percentage of bus voltage was at 97 %kV. When the swell was occurred (from 0.5 s – 1.5 s), it was going up to 108 %kV and then it had been going down to 102 %kV in 0.1 seconds. It had been going up to 103.4 %kV in 0.3 seconds and then it had been going down to 102.7 %kV in 0.6 seconds. After swell, percentage of bus voltage dropped to 92 %kV and then it was going up again to 97.7 %kV in 0.1 second. It had been going up to 98 %kV in 0.6 seconds and it was getting stable at 97 %kV at 4.2nd second.

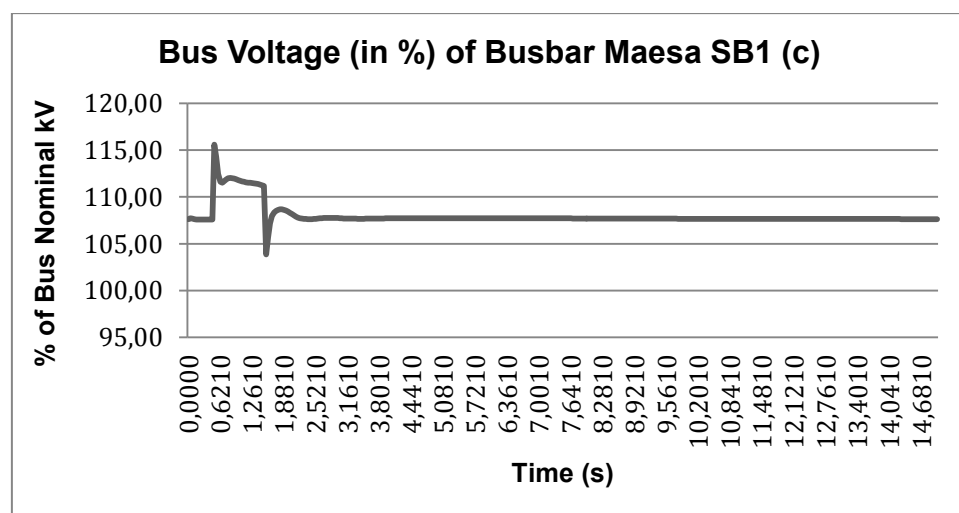


Figure 5-105: Maesa SB1 Bus Voltage Swell Simulation Results on Situation C

Based on figure 5-105, before swell, percentage of bus voltage was at 107.6 %kV. When the swell was occurred (from 0.5 s – 1.5 s), it was going up to 111.9 %kV and then it had been going down to 110.2 %kV in 0.1 second. It had been going up to 110.9 %kV in 0.3 second and then it had been going down again to 110.4 %kV in 0.6 seconds. After swell, percentage of bus voltage dropped to 106 %kV and then it had been going up again to 107.9 %kV in 0.2 seconds. It was getting stable at 107.6 %kV at 4.2nd second.

Bus voltage of swell simulation results of Maesa SB1 (2) bus bar before RE integration, after RE integration and after RE integration using homer results is equal to bus voltage of swell simulation results of Maesa SB1 bus bar on all situations.

Bus voltage of swell simulation results of bus bar Parigi DB1 before RE integration, after RE integration and after RE integration using homer results can be seen below.

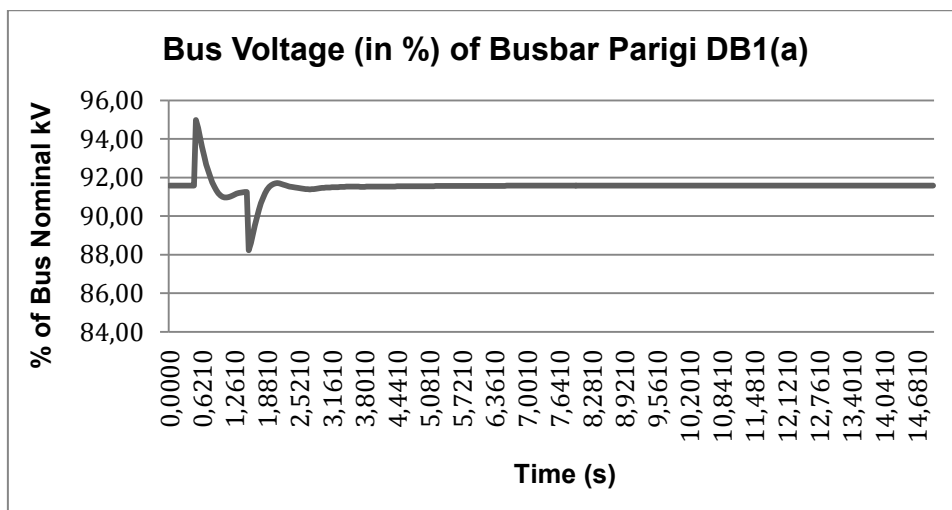


Figure 5-106: Parigi DB1 Bus Voltage Swell Simulation Results on Situation A

Based on figure 5-106, before swell, percentage of bus voltage was at 91.6 %kV. When the swell was occurred (from 0.5 s – 1.5 s), it was going up to 95 % kV and then it had been going down to 89.3 %kV in 1 second. After swell, percentage of bus voltage dropped to 89.3 % kV and it was getting stable at 91.6 %kV 9.2nd second.

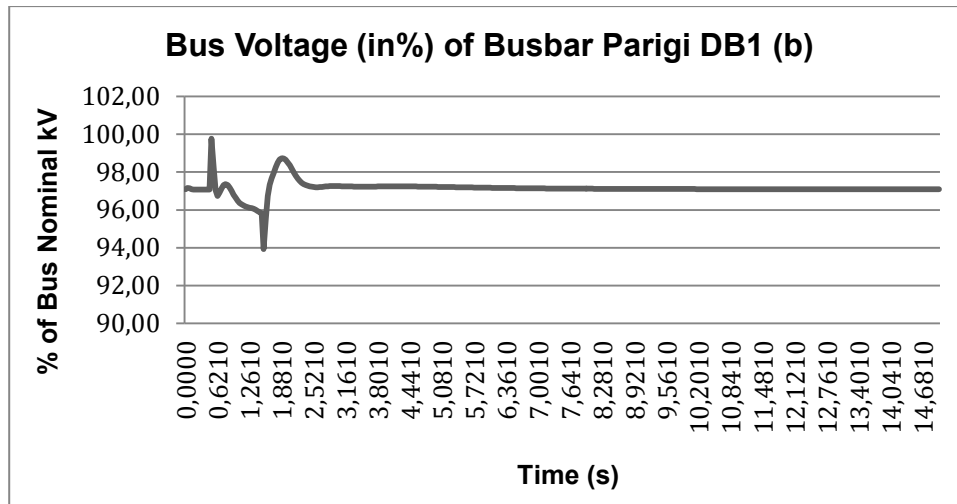


Figure 5-107: Parigi DB1 Bus Voltage Swell Simulation Results on Situation B

Based on figure 5-107, before swell, percentage of bus voltage was at 97 %kV. When the swell was occurred (from 0.5 s – 1.5 s), it was going up to 100.5 %kV and then it had been going down to 97.5 %kV in 0.1 seconds. It had been going up to 98.5 %kV in 0.3 second and then it had been going down to 95 %kV in 0.6 seconds. After swell, percentage of bus voltage dropped to 92 %kV and then it had been going up again to 95.1 %kV in 0.1 second. It had been going up to 98.3 %kV in 0.7 seconds and it was getting stable at 97 %kV at 9.9th second.

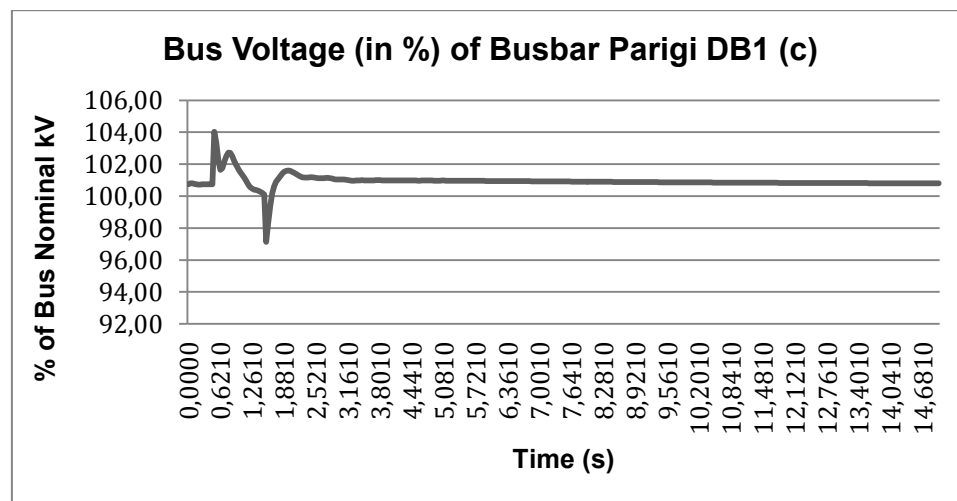


Figure 5-108: Parigi DB1 Bus Voltage Swell Simulation Results on Situation C

Based on figure 5-108, before swell, percentage of bus voltage was at 100.8 %kV. When the swell was occurred (from 0.5 s – 1.5 s), it was going up to 102.8 %kV and

then it had been going down to 101.8 %kV in 0.1 second. It had been going up to 102.9 %kV in 0.3 second and then it had been going down again to 101.8 %kV in 0.6 seconds. After swell, percentage of bus voltage dropped to 100 %kV and then it had been going up again to 101.3 %kV in 0.2 seconds. It was getting stable at 100.8 %kV at 10.8th second.

Bus voltage of swell simulation results of Parigi DB1 (2) bus bar before RE integration, after RE integration and after RE integration using homer results is equal to bus voltage of swell simulation results of Parigi DB1 bus bar on all situations.

Bus voltage of swell simulation results of bus bar Parigi SB1 before RE integration, after RE integration and after RE integration using homer results can be seen below.

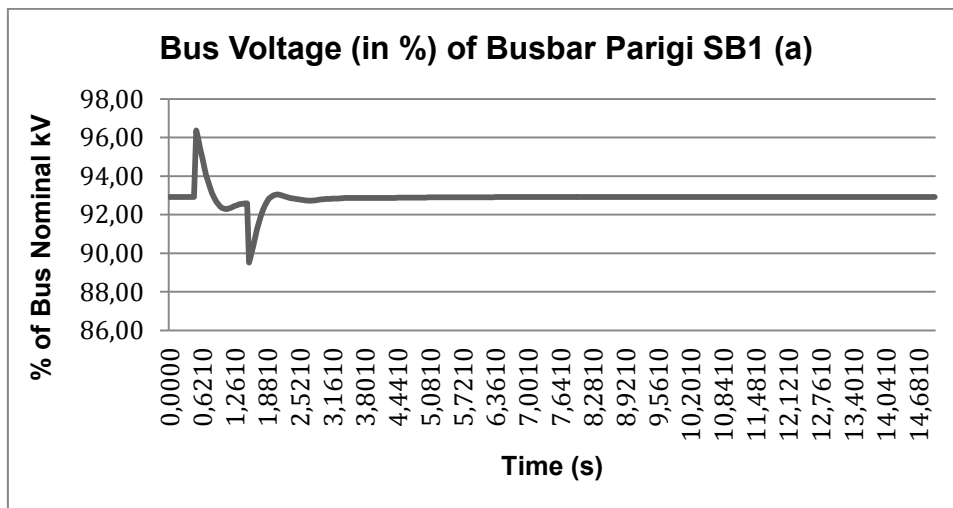


Figure 5-109: Parigi SB1 Bus Voltage Swell Simulation Results on Situation A

Based on figure 5-109, before swell, percentage of bus voltage was at 93 %kV. When the swell was occurred (from 0.5 s – 1.5 s), it was going up to 95 % kV and then it had been going down to 92.5 %kV in 1 second. After swell, percentage of bus voltage dropped to 90.5 % kV and it was getting stable at 91.6 %kV 4.5th second.

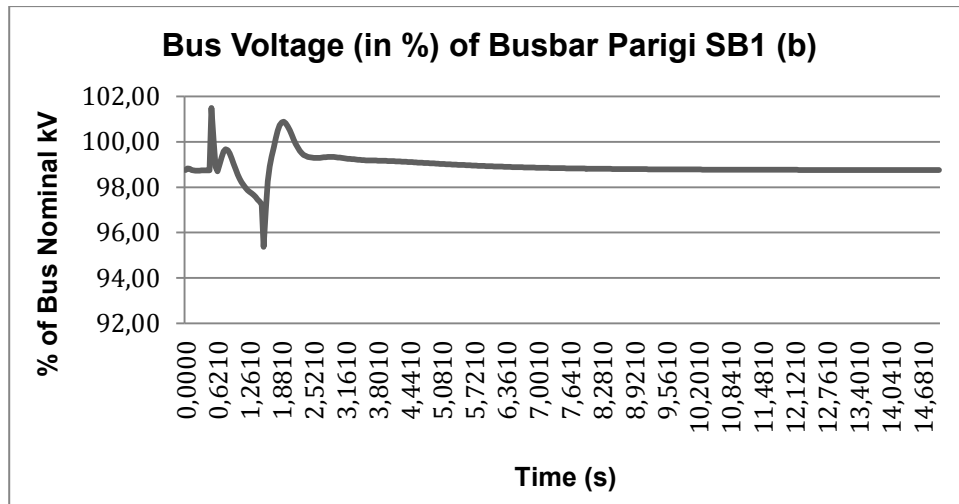


Figure 5-110: Parigi SB1 Bus Voltage Swell Simulation Results on Situation B

Based on figure 5-110, before swell, percentage of bus voltage was at 99 %kV. When the swell was occurred (from 0.5 s – 1.5 s), it was going up to 101.5 %kV and then it had been going down to 99 %kV in 0.1 seconds. It had been going up to 99.8 %kV in 0.3 seconds and then it had been going down to 95.6 %kV in 0.6 seconds. After swell, percentage of bus voltage dropped to 96.6 %kV and then it had been going up again to 100.8 %kV in 0.1 second and it was getting stable at 99 %kV at 9.4th second.

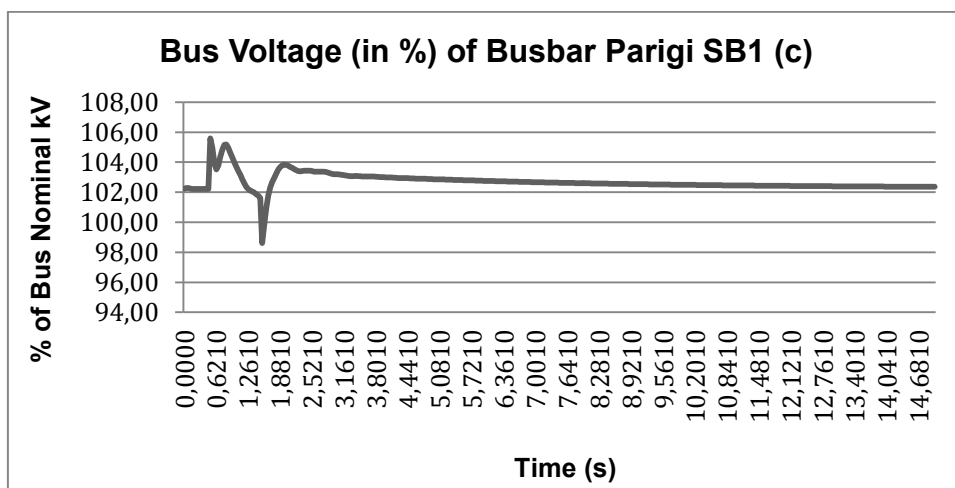


Figure 5-111: Parigi SB1 Bus Voltage Swell Simulation Results on Situation C

Based on figure 5-111, before swell, percentage of bus voltage was at 102.4 %kV. When the swell was occurred (from 0.5 s – 1.5 s), it was going up to 105.6 %kV and

then it had been going down to 103.7 %kV in 0.1 seconds. It had been going up to 105.4 %kV in 0.3 second and then it had been going down again to 102 %kV in 0.6 seconds. After swell, percentage of bus voltage dropped to 98.8 %kV and then it had been going up again to 103.9 %kV in 0.2 seconds. It was getting stable at 102 %kV at 13.6th second.

Bus voltage of swell simulation results of bus bar Parigi SB1 before RE integration, after RE integration and after RE integration using homer results can be seen below.

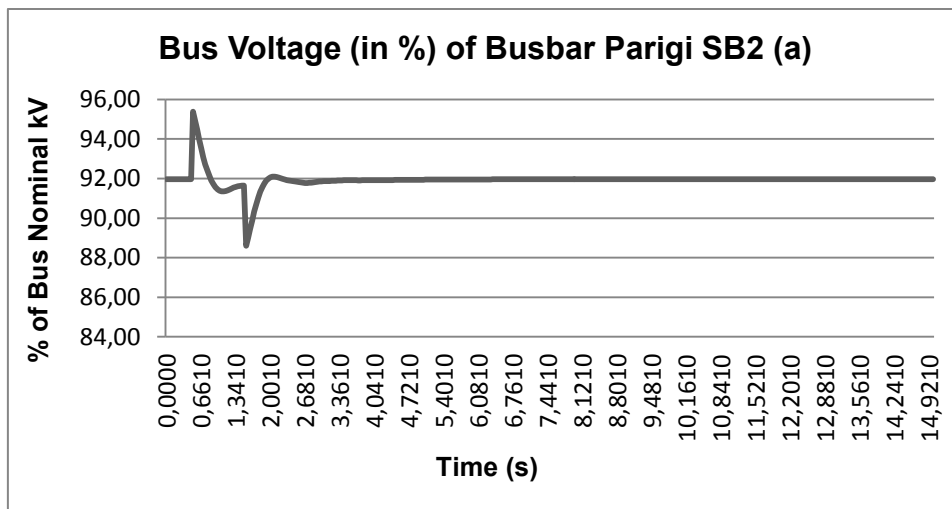


Figure 5-112: Parigi SB2 Bus Voltage Swell Simulation Results on Situation A

Based on figure 5-112, before swell, percentage of bus voltage was at 92 %kV. When the swell was occurred (from 0.5 s – 1.5 s), it had been going up to 95.4 % kV in 0.4 second and then it had been going down to 91.8 %kV in 0.6 second. After swell, percentage of bus voltage dropped to 89.6 % kV and it was getting stable at 92 %kV 5th second.

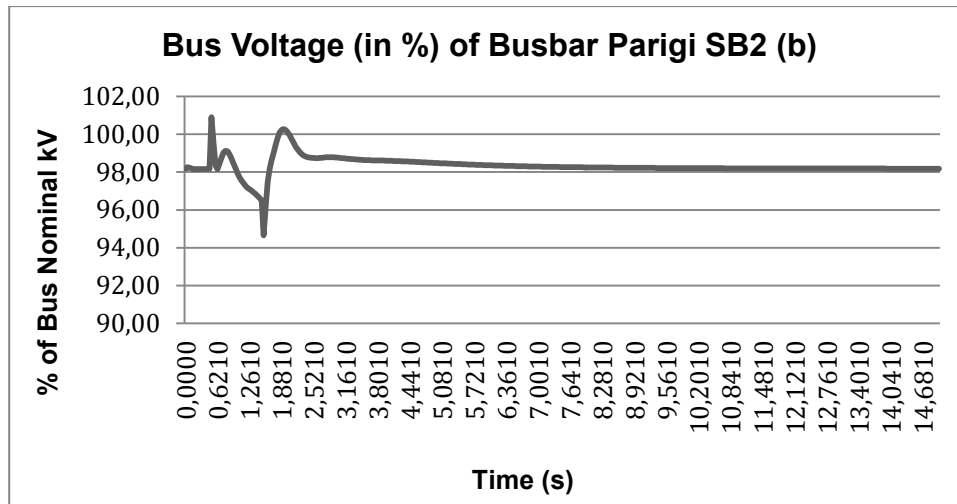


Figure 5-113: Parigi SB2 Bus Voltage Swell Simulation Results on Situation B

Based on figure 5-113, before swell, percentage of bus voltage was at 98.2 %kV. When the swell was occurred (from 0.5 s – 1.5 s), it was going up to 101.7 %kV and then it had been going down to 98.7 %kV in 0.1 seconds. It had been going up to 99.9 %kV in 0.3 seconds and then it had been going down to 94.3 %kV in 0.6 seconds. After swell, percentage of bus voltage dropped to 91.9 %kV and then it had been going up again to 95 %kV in 0.1 second. It had been going up to 100 %kV in 0.7 seconds and getting stable at 98.2 %kV at 9th second.

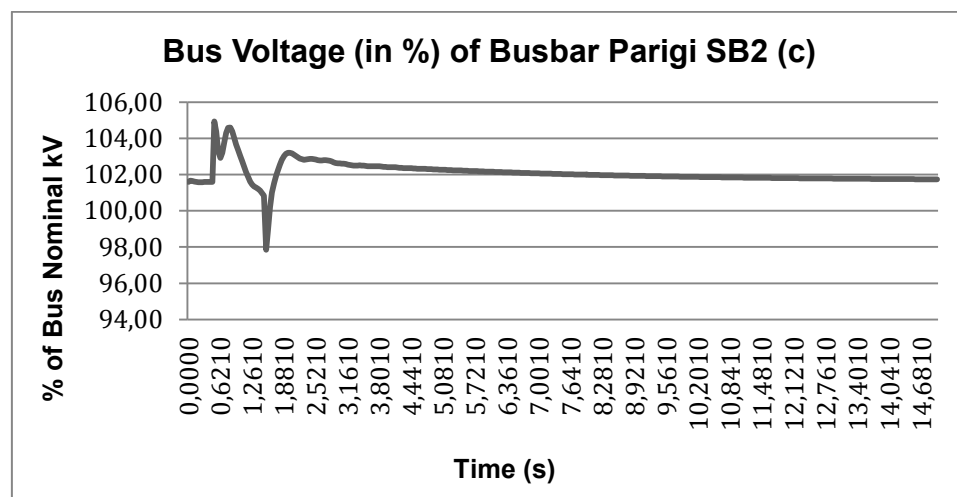


Figure 5-114: Parigi SB2 Bus Voltage Swell Simulation Results on Situation C

Based on figure 5-114, before swell, percentage of bus voltage was at 101.7 %kV. When the swell was occurred (from 0.5 s – 1.5 s), it was going up to 105 %kV and

then it had been going down to 102.8 %kV in 0.1 seconds. It had been going up to 104.4 %kV in 0.3 second and then it had been going down again to 103.4 %kV in 0.6 seconds. After swell, percentage of bus voltage dropped to 98 %kV and then it had been going up again to 102.9 %kV in 0.2 seconds. It was getting stable at 101.7 %kV at 14th second.

Bus voltage of swell simulation results of bus bar PJPP SB1 before RE integration, after RE integration and after RE integration using homer results can be seen below.

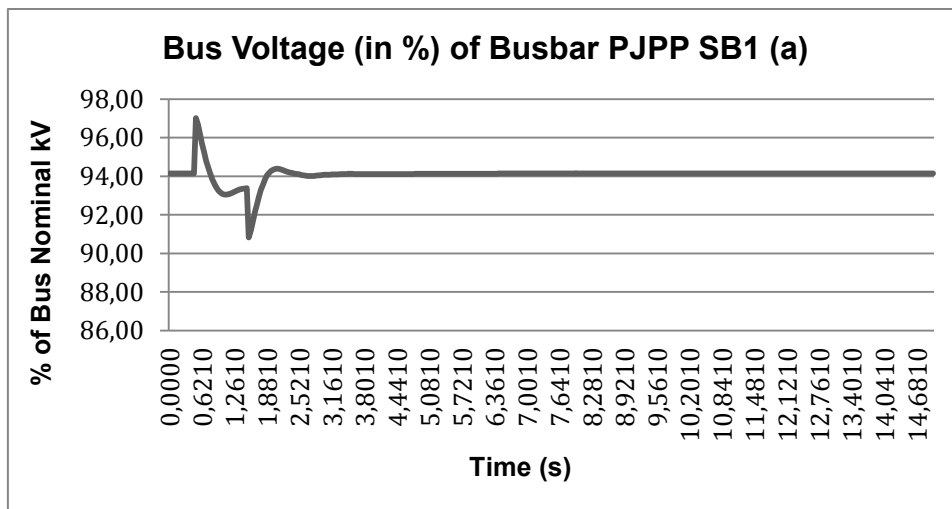


Figure 5-115: PJPP SB1 Bus Voltage Swell Simulation Results on Situation A

Based on figure 5-115, before swell, percentage of bus voltage was at 94.2 %kV. When the swell was occurred (from 0.5 s – 1.5 s), it was going up to 97.2 % kV and then it had been going down to 94.7 %kV in 1 second. After swell, percentage bus voltage dropped to 90.8 % kV and it was getting stable at 94.2 %kV 7th second.

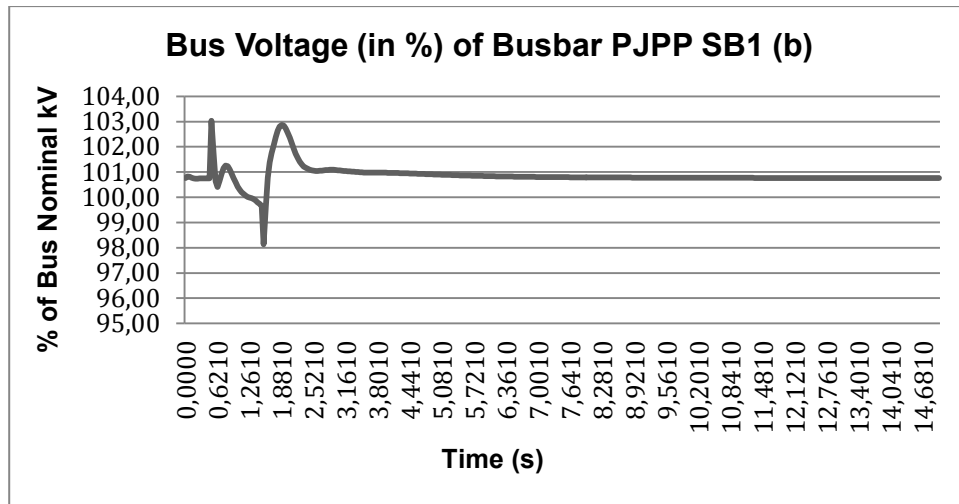


Figure 5-116: PJPP SB1 Bus Voltage Swell Simulation Results on Situation B

Based on figure 5-116, before swell, percentage of bus voltage was at 100.9 %kV. When the swell was occurred (from 0.5 s – 1.5 s), it was going up to 103.5 %kV and then it had been going down to 100.5 %kV in 0.1 seconds. It had been going up to 101.4 %kV in 0.3 seconds and then it had been going down to 98.5 %kV in 0.6 seconds. After swell, percentage of bus voltage dropped to 98.2 %kV and then it had been going up again to 98.9 %kV in 0.2 seconds. It was going up again to 102.6 %kV and then it was getting stable at 100.9 %kV at 8.5th second.

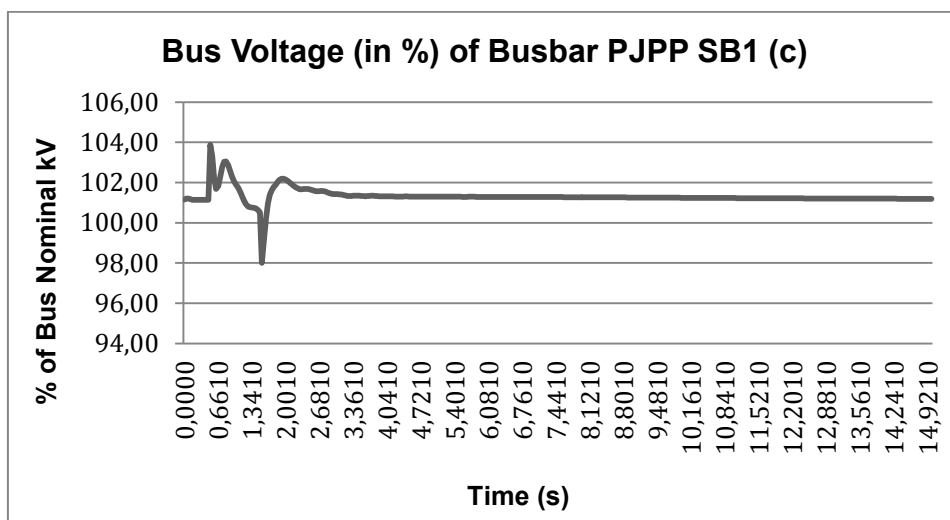


Figure 5-117: PJPP SB1 Bus Voltage Swell Simulation Results on Situation C

Based on figure 5-117, before swell, percentage of bus voltage was at 101.2 %kV. When the swell was occurred (from 0.5 s – 1.5 s), it was going up to 104 %kV and

then it had been going down to 98 %kV in 0.1 seconds. It had been going up to 103.2 %kV in 0.3 second and then it had been going down again to 102.1 %kV in 0.6 seconds. After swell, percentage of bus voltage dropped to 98 %kV and then it had been going up again to 102.2 %kV in 0.2 seconds. It was getting stable at 101.2 %kV at 12.9th second.

Bus voltage of swell simulation results of bus bar Silae SB1 before RE integration, after RE integration and after RE integration using homer results can be seen below.

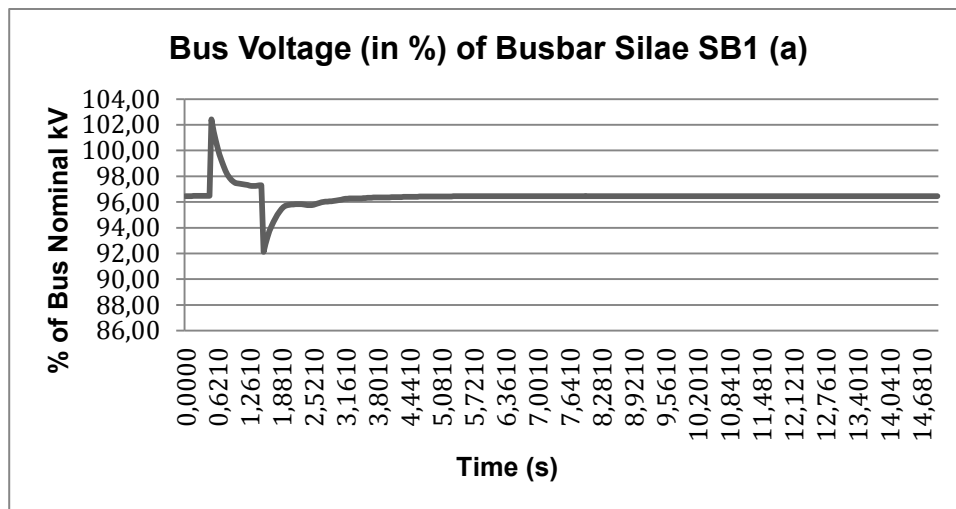


Figure 5-118: Silae SB1 Bus Voltage Swell Simulation Results on Situation A

Based on figure 5-118, before swell, percentage of bus voltage was at 96.5 %kV. When the swell was occurred (from 0.5 s – 1.5 s), it was going up to 102.5 % kV and then it had been going down to 97.5 %kV in 1 second. After swell, percentage of bus voltage dropped to 92 % kV and it was getting stable at 96.5 %kV 4.5th second.

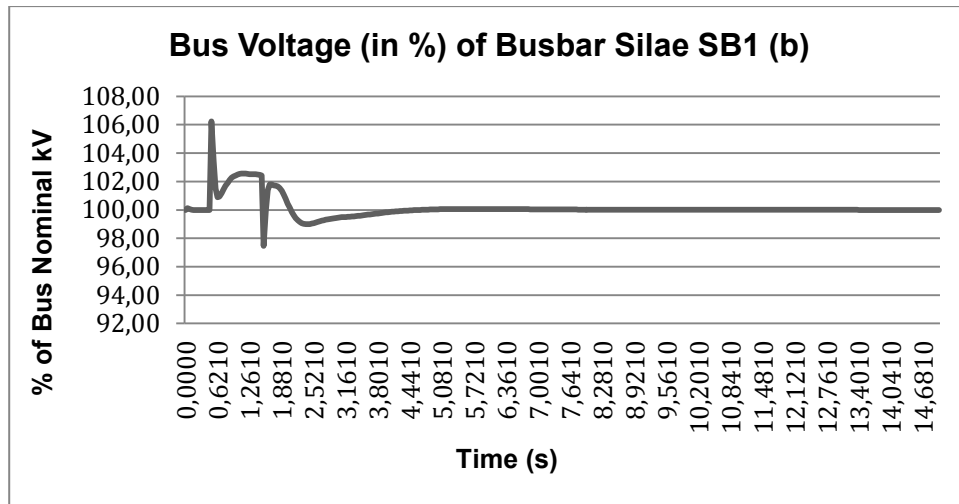


Figure 5-119: Silae SB1 Bus Voltage Swell Simulation Results on Situation B

Based on figure 5-119, before swell, percentage of bus voltage was at 100 %kV. When the swell was occurred (from 0.5 s – 1.5 s), it was going up to 106.3 %kV and then going down to 101.8 %kV in 0.1 seconds. It had been going up to 102.4 %kV in 0.9 seconds. After swell, percentage of bus voltage dropped to 97.5 %kV and then it had been going up again to 101.8 %kV in 0.2 seconds. It had been going down to 99.2 %kV in 0.1 second and then it was going up to 100.7 %kV. It had been going down to 99.1 %kV in 0.4 seconds and it was getting stable at 100 %kV at 7.6th second.

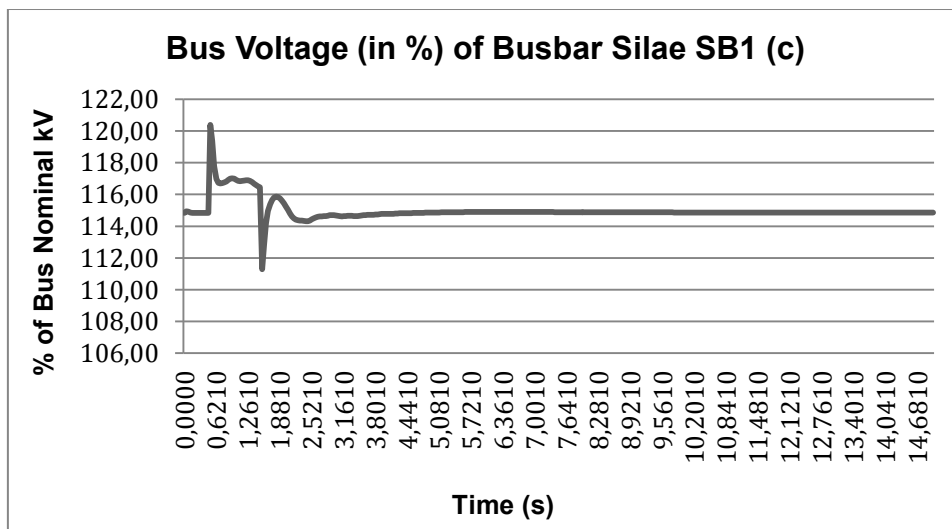


Figure 5-120: Silae SB1 Bus Voltage Swell Simulation Results on Situation C

Based on figure 5-120, before swell, percentage of bus voltage was at 114.7 %kV. When the swell was occurred (from 0.5 s – 1.5 s), it was going up to 120.5 %kV and then it had been going down to 117 %kV in 0.2 seconds. It had been going up to 116.8 %kV in 0.3 second and then it had been going down again to 116.2 %kV in 0.5 seconds. After swell, percentage of bus voltage dropped to 111.2 %kV and then it had been going up again to 115.7 %kV in 0.2 seconds. It was getting stable at 114.7 %kV at 6.5th second.

Bus voltage of swell simulation results of Silae SB2 and Sila SB3 bus bar before RE integration, after RE integration and after RE integration using homer results is equal to bus voltage of swell simulation results of Silae SB1 bus bar on all situations.

Bus voltage of swell simulation results of bus bar Silae SB4 before RE integration, after RE integration and after RE integration using homer results can be seen below.

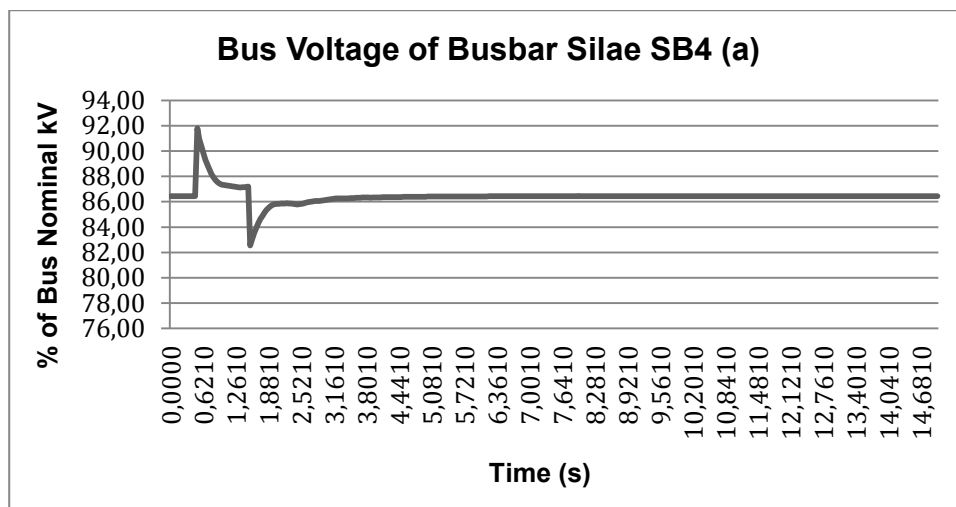


Figure 5-121: Silae SB4 Bus Voltage Swell Simulation Results on Situation A

Based on figure 5.121, before swell, percentage of bus voltage was at 86.5 %kV. When the swell was occurred (from 0.5 s – 1.5 s), it was going up to 91.9 % kV and then it had been going down to 88.3 %kV in 1 second. After swell, percentage of bus voltage was dropped to 83.1 % kV and it was getting stable at 86.5 %kV 4.8th second.

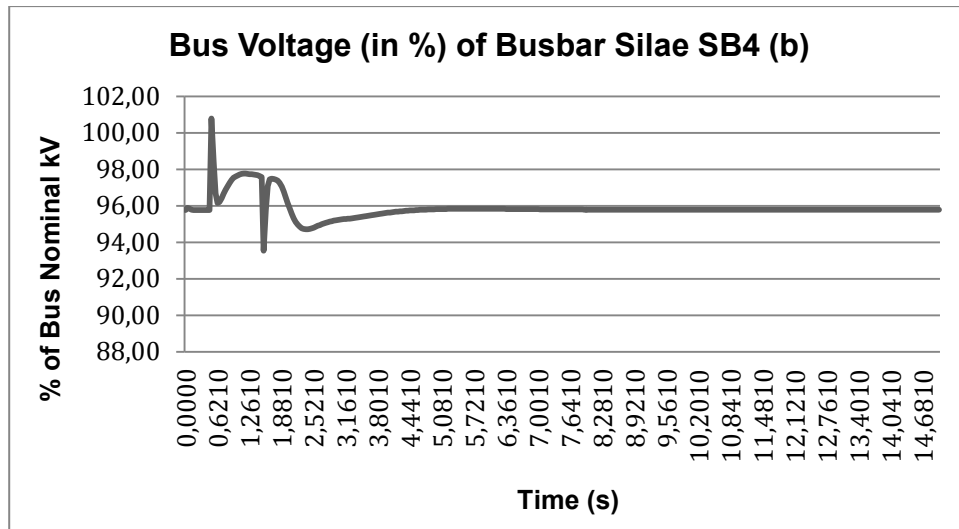


Figure 5-122: Silae SB4 Bus Voltage Swell Simulation Results on Situation B

Based on figure 5-122, before swell, percentage of bus voltage was at 96 %kV. When the swell was occurred (from 0.5 s – 1.5 s), it was going up to 101 %kV and then it had been going down to 96.3 %kV in 0.1 seconds. It had been going up to 97.8 %kV in 0.3 seconds and then it had been going down to 97 %kV in 0.6 seconds. After swell, percentage of bus voltage dropped to 93.5 %kV and then it had been going down again to 94.8 %kV in 0.8 seconds and it had been staying there for 0.2 seconds. It was going up to 96 %kV and getting stable there at 9.5th second.

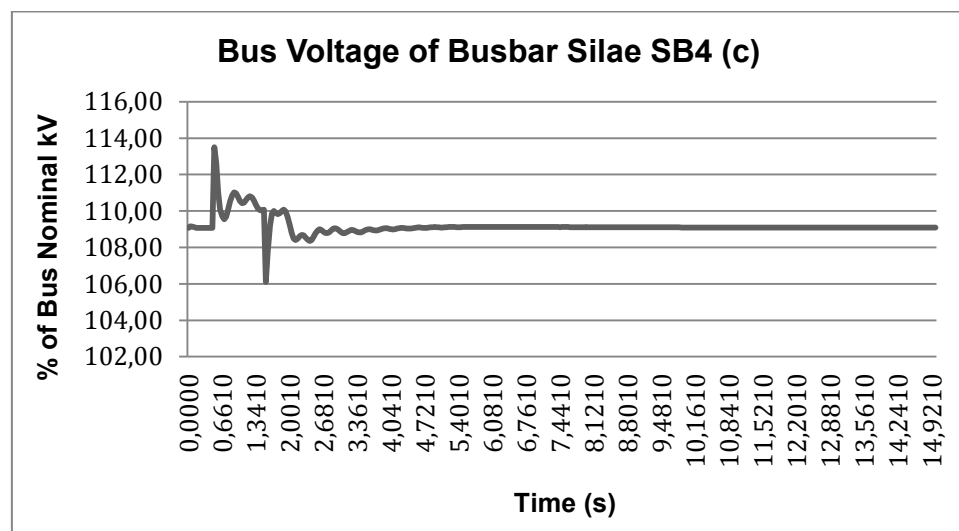


Figure 5-123: Silae SB4 Bus Voltage Swell Simulation Results on Situation C

Based on figure 5-123, before swell, percentage of bus voltage was at 109 %kV. When the swell was occurred (from 0.5 s – 1.5 s), it was at going up to 113.5 %kV and then it had been going down to 109.5 %kV in 0.2 seconds. It had been going up to 111 %kV in 0.3 second and then it had been going down again to 110 %kV in 0.5 seconds. After swell, percentage of bus voltage dropped to 106.4 %kV and then it had been going up again to 109.8 %kV in 0.2 seconds. It was getting stable at 109 %kV at 6.7th second.

Bus voltage of swell simulation results of bus bar Talise SB1 before RE integration, after RE integration and after RE integration using homer results can be seen below.

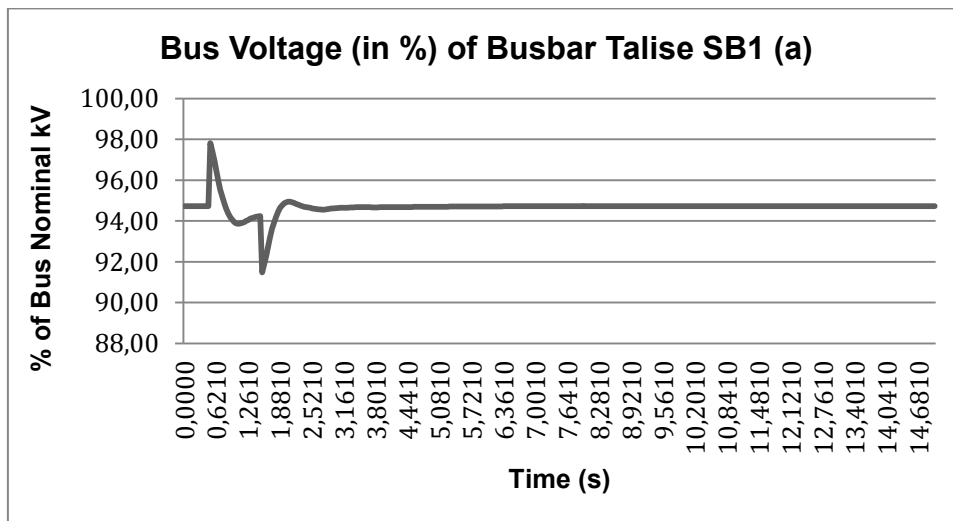


Figure 5-124: Talise SB1 Bus Voltage Swell Simulation Results on Situation A

Based on figure 5-124, before swell, percentage of bus voltage was at 94.8 %kV. When the swell was occurred (from 0.5 s – 1.5 s), it was going up to 97.8 % kV and then it had been going down to 95.6 %kV in 1 second. After swell, percentage of bus voltage dropped to 91.4 % kV and it was getting stable at 95.8 %kV 6th second.

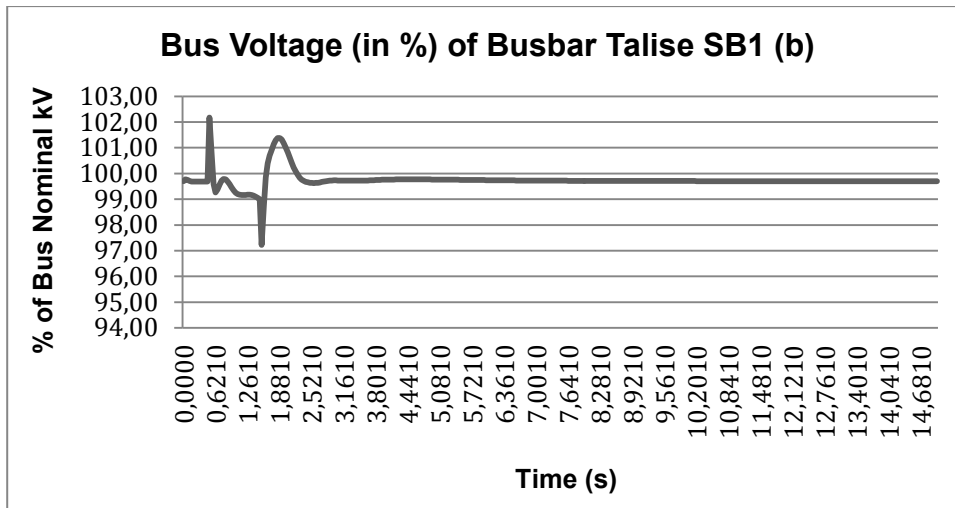


Figure 5-125: Talise SB1 Bus Voltage Swell Simulation Results on Situation B

Based on figure 5-125, before swell, percentage of bus voltage was at 99.8 %kV. When swell was occurred (from 0.5 s – 1.5 s), it was going up to 102.7 %kV and then it had been going down to 99.5 %kV in 0.1 seconds. It had been going up to 99.8 %kV in 0.3 seconds and then it had been going down to 98.7 %kV in 0.6 seconds. After swell, percentage of bus voltage dropped to 97.3 %kV and then it had been going up again to 98.8 %kV in 0.2 seconds. It had been going up to 101.5 %kV in 0.6 seconds and then it was getting stable at 99.8 %kV at 7.7th second.

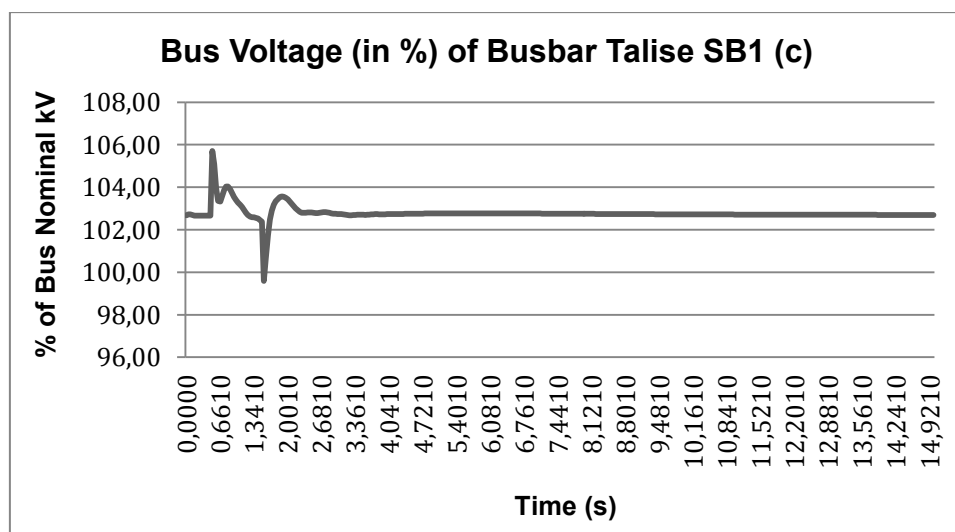


Figure 5-126: Talise SB1 Bus Voltage Swell Simulation Results on Situation C

Based on figure 5-126, before swell, percentage of bus voltage was at 102.8 %kV. When swell was occurred (from 0.5 s – 1.5 s), it was at going up to 105.6 %kV and then it had been going down to 103.6 %kV in 0.2 seconds. It had been going up to 104 %kV in 0.3 second and then it had been going down again to 103.4 %kV in 0.5 seconds. After swell, percentage of bus voltage dropped to 99.5 %kV and then it had been going up again to 103.5 %kV in 0.2 seconds. It was getting stable at 102.8 %kV at 12.1st second.

Bus voltage of swell simulation results of bus bar Talise SB2 before RE integration, after RE integration and after RE integration using homer results can be seen below.

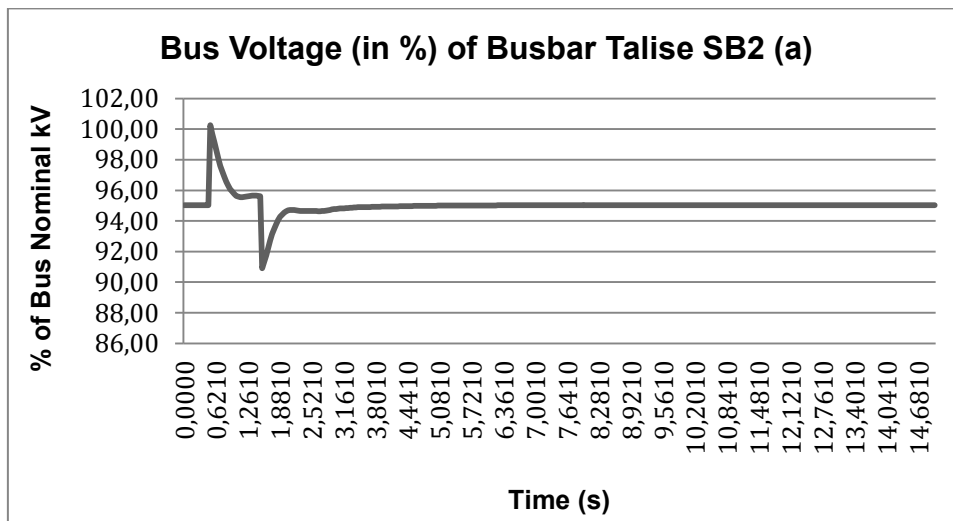


Figure 5-127: Talise SB2 Bus Voltage Swell Simulation Results on Situation A

Based on figure 5-127, before swell, percentage of bus voltage was at 95 %kV. When the swell was occurred (from 0.5 s – 1.5 s), it was going up to 100.3 % kV and then it had been going down to 97 %kV in 1 second. After swell, percentage of bus voltage dropped to 90.8 % kV and it was getting stable at 95 %kV 5.6th second.

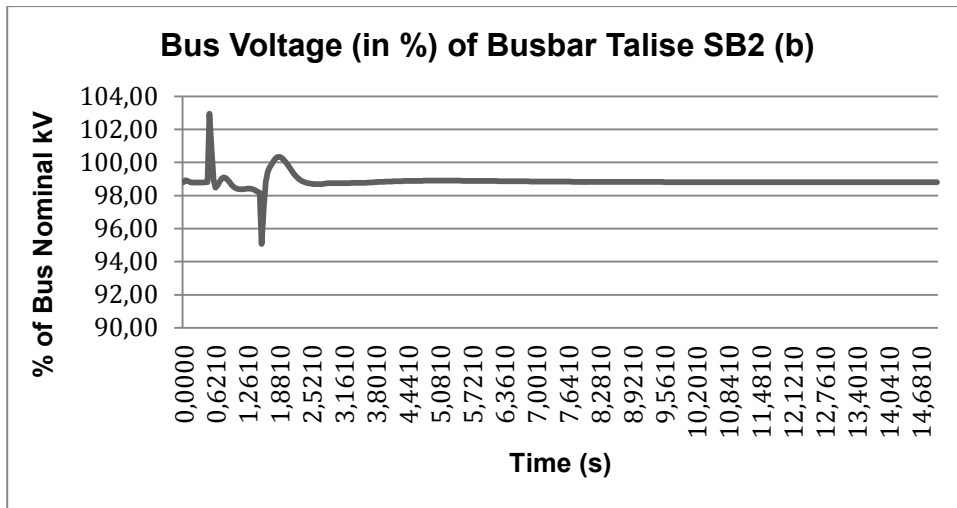


Figure 5-128: Talise SB2 Bus Voltage Swell Simulation Results on Situation B

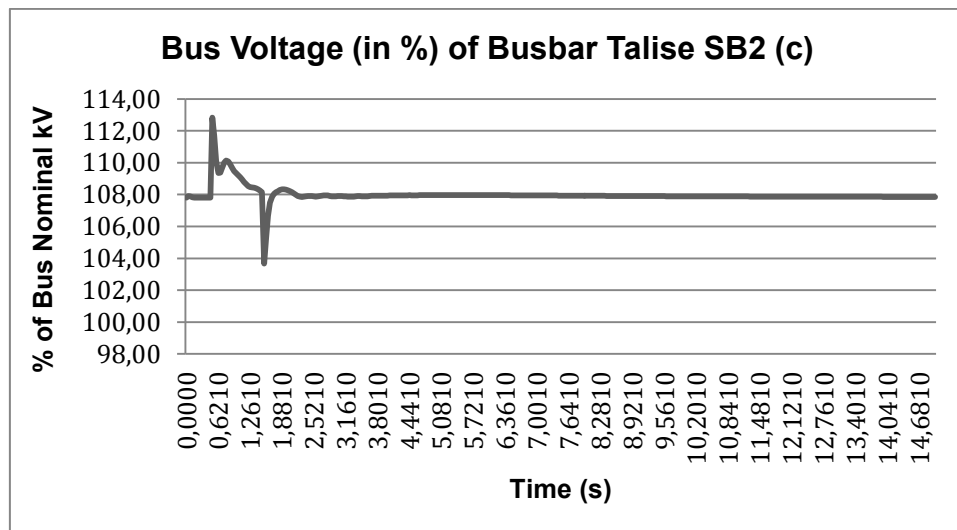


Figure 5-129: Talise SB2 Bus Voltage Swell Simulation Results on Situation C

Based on figure 5-129, before swell, percentage of bus voltage was at 108.1 %kV. When the swell was occurred (from 0.5 s – 1.5 s), it was at going up to 113 %kV and then it had been going down to 109.5 %kV in 0.2 seconds. It had been going up to 110.3 %kV in 0.3 second and then it had been going down again to 109.5 %kV in 0.5 seconds. After swell, percentage of bus voltage dropped to 103.7 %kV and then it had been going up again to 108.4 %kV in 0.2 seconds. It was getting stable at 108.1 %kV at 11.5th second.

Bus voltage of swell simulation results of bus bar Talise SB3 before RE integration, after RE integration and after RE integration using homer results is equal to bus voltage of swell simulation results of Talise SB2 bus bar on all situations.

Bus voltage of swell simulation results of bus bar Talise DB1 before RE integration, after RE integration and after RE integration using homer results can be seen below.

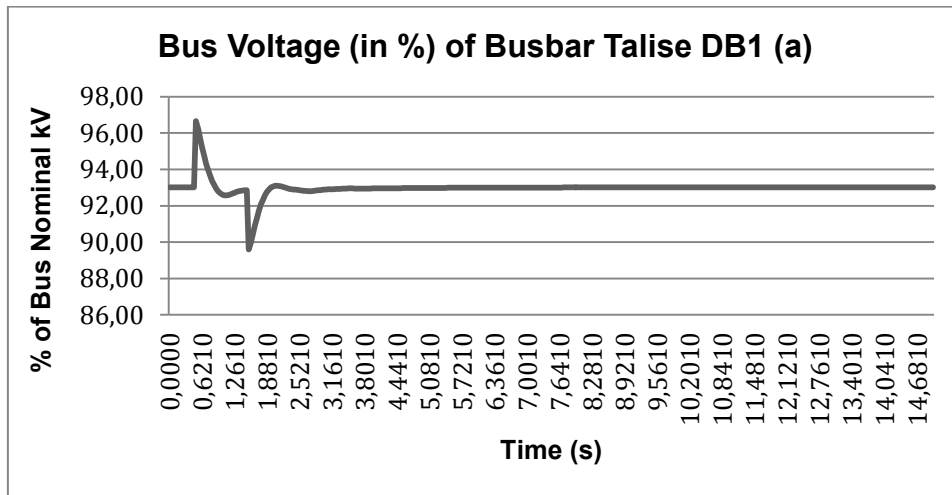


Figure 5-130: Talise DB1 Bus Voltage Swell Simulation Results on Situation A

Based on figure 5-130, before swell, percentage of bus voltage was at 93 %kV. When the swell was occurred (from 0.5 s – 1.5 s), it was going up to 96.8 % kV and then it had been going down to 92.8 %kV in 1 second. After swell, percentage of bus voltage dropped to 89.7 % kV and it was getting stable at 93 %kV 4.5th second.

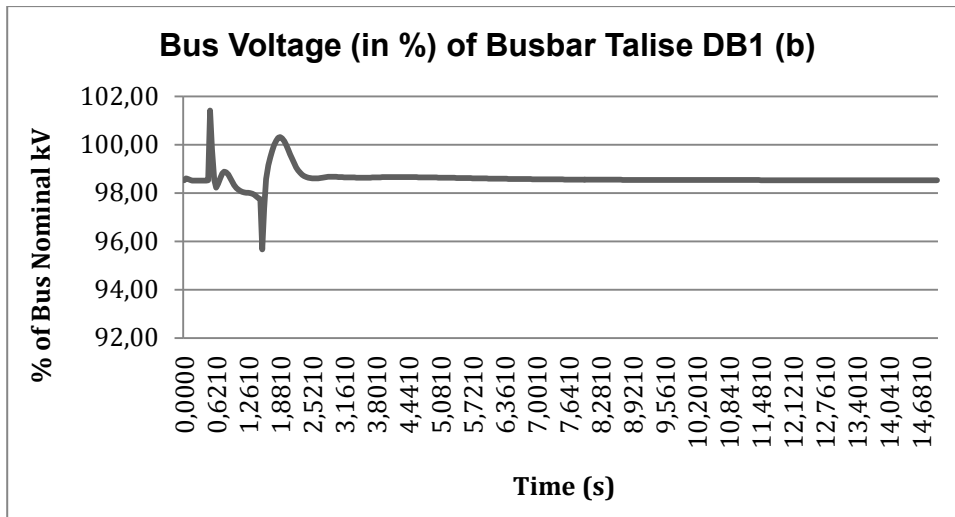


Figure 5-131: Talise DB1 Bus Voltage Swell Simulation Results on Situation B

Based on figure 5-131, before swell, bus voltage was at 98.7 %kV. When the swell was occurred (from 0.5 s – 1.5 s), it was going up to 101.5 %kV and then it had been going down to 98.2 %kV in 0.1 seconds. It had been going up to 98.8 %kV in 0.3 seconds and then it had been going down to 98 %kV in 0.6 seconds. After swell, percentage of bus voltage dropped to 95.5 %kV and then it had been going up again to 97.2 %kV in 0.2 seconds. It had been going up to 100.3 %kV in 0.6 seconds and then it was getting stable at 98.7 %kV at 10.7th second.

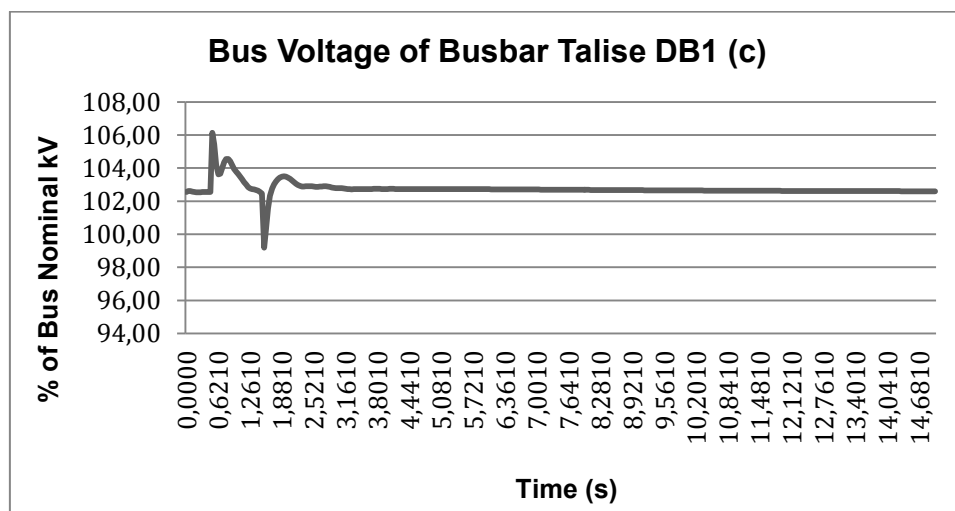


Figure 5-132: Talise DB1 Bus Voltage Swell Simulation Results on Situation C

Based on figure 5-132, before swell, percentage of bus voltage was at 102.7 %kV. When the swell was occurred (from 0.5 s – 1.5 s), it was at going up to 106.2 %kV and then it had been going down to 103.6 %kV in 0.2 seconds. It had been going up to 104.7 %kV in 0.3 second and then it had been going down again to 103.7 %kV in 0.5 seconds. After swell, percentage of bus voltage dropped to 99 %kV and then it had been going up again to 102.9 %kV in 0.2 seconds. It was getting stable at 102.7 %kV at 10.2nd second.

Bus voltage of swell simulation results of Talise DB11 bus bar before RE integration, after RE integration and after RE integration using homer results is equal to bus voltage of swell simulation results of Talise DB1 bus bar on all situations.

Bus frequency of swell simulation results of bus bar DB1 PJPP before RE integration, after RE integration and after RE integration using homer results can be seen below.

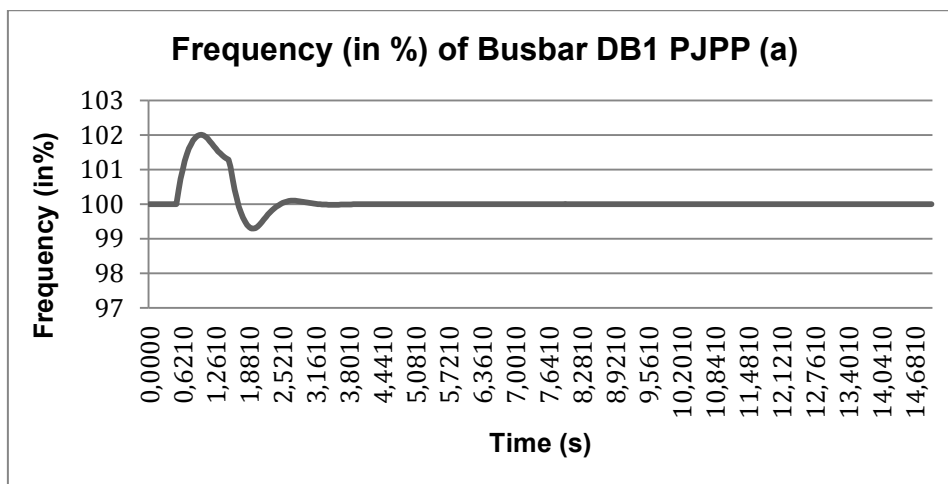


Figure 5-133: DB1 PJPP Bus Frequency Swell Simulation Results on Situation A

Based on figure 5-133, before swell, percentage of bus frequency was at 100 %. When the swell was occurred (from 0.5 s – 1.5 s), it had been going up to 102 % in 0.5 seconds and then it had been going down to 101.4 % in 0.5 seconds. After swell, percentage of bus frequency had been going down to 99.3 % in 0.5 seconds and it has been going up again to 100.03 % in 0.8 second. It was getting stable at 100 % at 4.5th seconds.

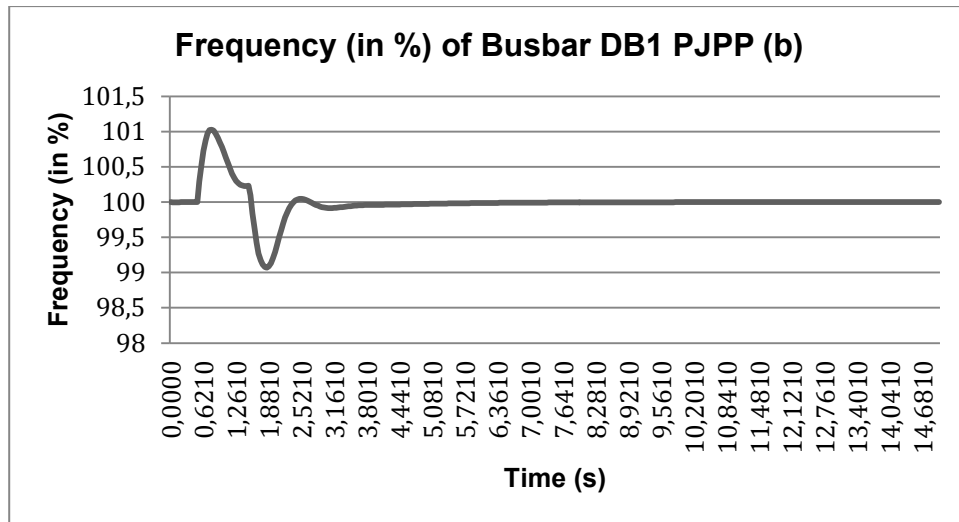


Figure 5-134: DB1 PJPP Bus Frequency Swell Simulation Results on Situation B

Based on figure 5-134, before swell, percentage of bus frequency was at 100 %. When the swell was occurred (from 0.5 s – 1.5 s), it had been going up to 101.4 % in 0.3 seconds and then it had been going down to 100.3 % in 0.4 seconds and it had been staying there for 0.3 seconds. After swell, percentage of bus frequency had been going down to 99.2 % in 0.5 seconds and then it had been going up again to 100.1 % in 0.8 seconds. It was getting stable at 100 % at 8.9th seconds.

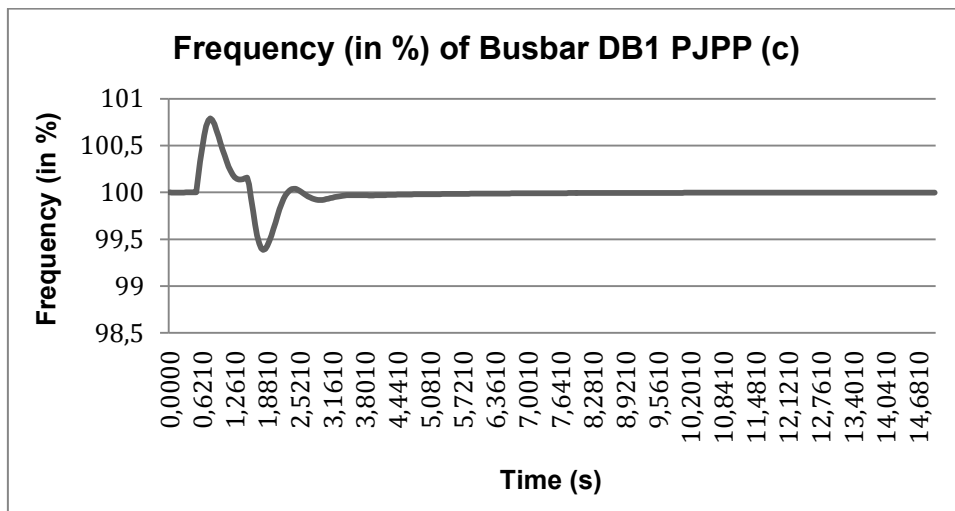


Figure 5-135: DB1 PJPP Bus Frequency Swell Simulation Results on Situation C

Based on figure 5-135, before swell, percentage of bus frequency was at 100 %. When the swell was occurred (from 0.5 s – 1.5 s), it had been going up to 100.7 % in

0.3 seconds and then it had been going down to 100.2 % for 0.5 seconds and it had been staying there for 0.2 seconds. After swell, percentage of bus frequency had been going down to 99.4 % in 0.3 seconds and then it was going up again to 100 % and it was getting stable at 6.5th seconds.

Bus frequency of swell simulation results of DB11 PJPP bus bar before RE integration, after RE integration and after RE integration using homer results is equal to bus frequency of swell simulation results of DB1 PJPP bus bar on all situations.

Bus frequency of swell simulation results of bus bar Donggala SB1 before RE integration, after RE integration and after RE integration using homer results can be seen below.

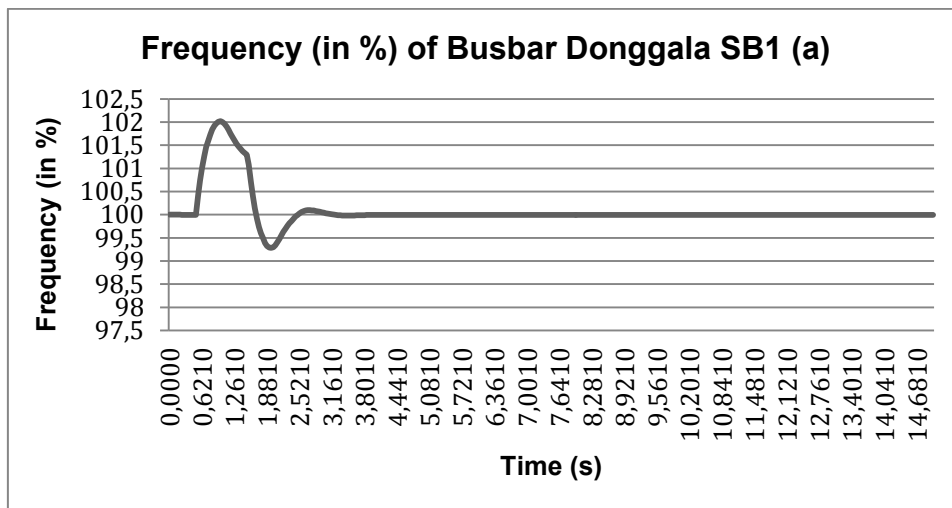


Figure 5-136: Donggala SB1 Bus Frequency Swell Simulation Results on Situation A

Based on figure 5-136, before swell, percentage of bus frequency was at 100 %. When the swell was occurred (from 0.5 s – 1.5 s), it had been going up to 102 % in 0.5 seconds and then it had been going down to 101.3 % in 0.5 seconds. After swell, bus frequency had been going down to 99.3 % in 0.5 seconds and it had been going up again to 100.03 % in 0.8 seconds. It was getting stable at 100 % at 3.5th second.

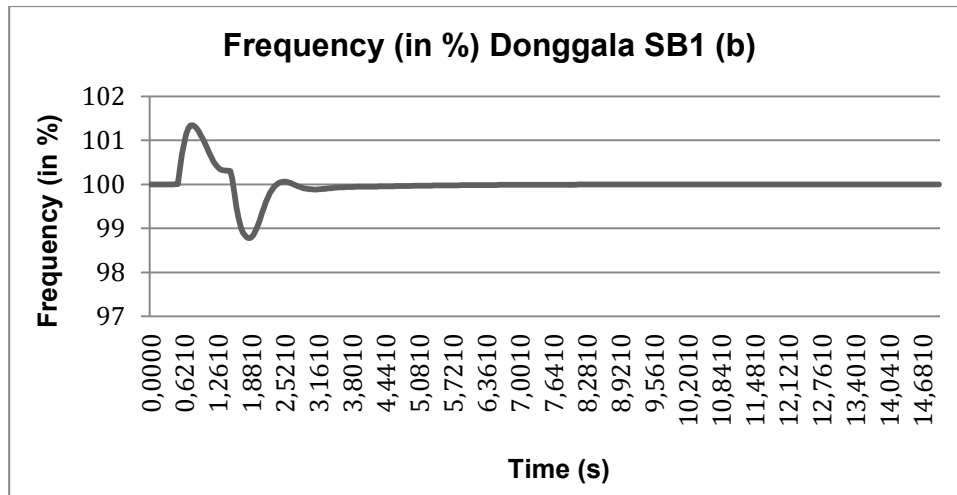


Figure 5-137: Donggala SB1 Bus Frequency Swell Simulation Results on Situation B

Based on figure 5-137, before swell, percentage of bus frequency was at 100 %. When the swell was occurred (from 0.5 s – 1.5 s), it had been going up to 101.4 % in 0.3 seconds and then it had been going down to 100.3 % in 4 seconds and it had been staying there for 0.3 seconds. After swell, percentage of bus frequency had been going down to 98.8 % in 0.4 seconds and then it had been going up again to 100 % in 0.8 seconds. It was getting stable at 100 % at 9.3rd second.

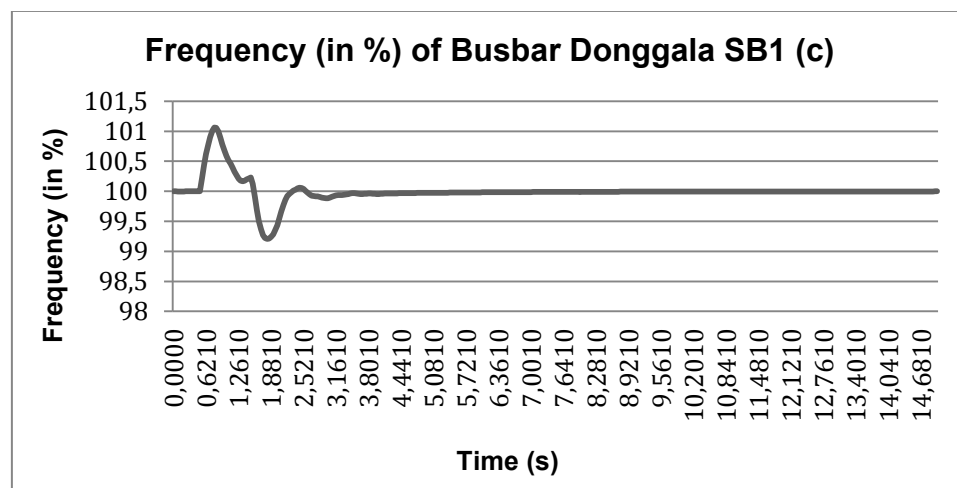


Figure 5-138: Donggala SB1 Bus Frequency Swell Simulation Results on Situation C

Based on figure 5-138, before swell, percentage of bus frequency was at 100 %. When the swell was occurred (from 0.5 s – 1.5 s), it had been at 101.1 % in 0.3 seconds and then it had been going down to 100.3 % for 0.5 seconds and it had

been staying there for 0.2 seconds. After swell, percentage of bus frequency had been going down to 99.2 % in 0.4 seconds and then it had been going up again to 100 % in 0.8 seconds and it was getting stable at 100 % at 9.3rd second.

Bus frequency of swell simulation results of bus bar Maesa SB1 before RE integration, after RE integration and after RE integration using homer results can be seen below.

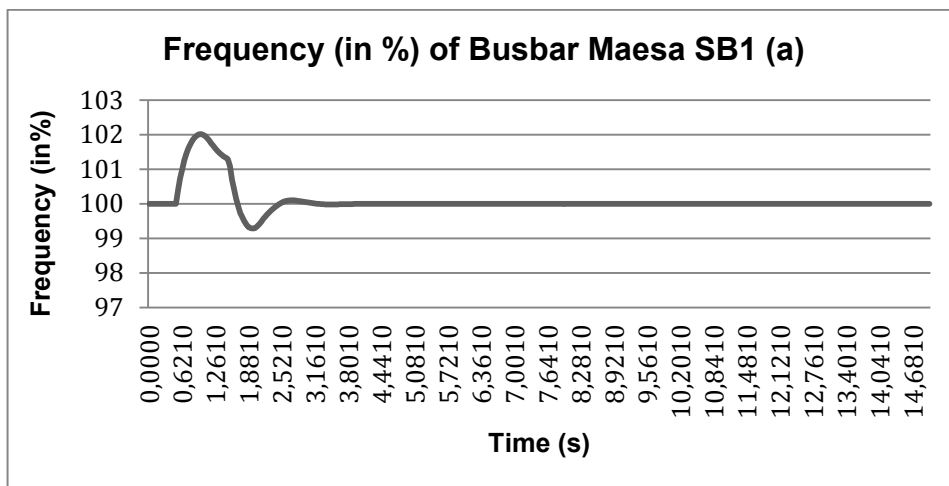


Figure 5-139: Maesa SB1 Bus Frequency Swell Simulation Results on Situation A

Based on figure 5-139, before swell, percentage of bus frequency was at 100 %. When the swell was occurred (from 0.5 s – 1.5 s), it had been going up to 102 % in 0.5 seconds and then it had been going down to 101.3 % in 0.5 seconds. After swell, percentage of bus frequency had been going down to 99.2 % in 0.5 seconds and it had been going up again to 100.03 % in 0.8 seconds. It was getting stable at 100 % at 3.8th second.

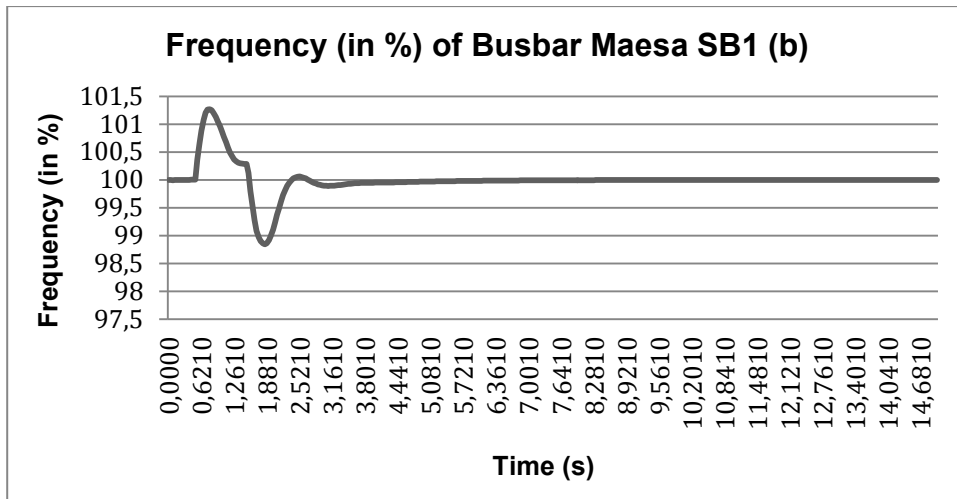


Figure 5-140: Maesa SB1 Bus Frequency Swell Simulation Results on Situation B

Based on figure 5-140, before swell, percentage of bus frequency was at 100 %. When the swell was occurred (from 0.5 s – 1.5 s), it had been going up to 101.3 % in 0.3 seconds and then it had been going down to 100.8 % in 4 seconds and it had been staying there for 0.3 seconds. After swell, it had been going down to 98.7 % in 0.5 seconds and then it had been going up again to 100 % in 0.8 seconds. It was getting stable at 100 % at 6.2nd second.

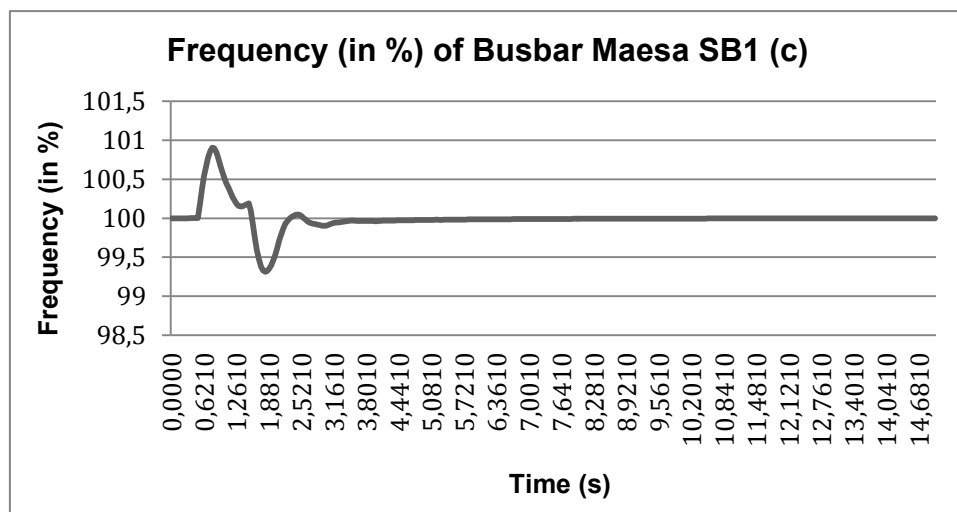


Figure 5-141: Maesa SB1 Bus Frequency Swell Simulation Results on Situation C

Based on figure 5-141, before swell, percentage of bus frequency was at 100 %. When the swell was occurred (from 0.5 s – 1.5 s), it had been going up to 100.8 % in 0.4 and then it had been going down to 100.2 % in 0.3 seconds and it had been staying there for 0.3 seconds. After swell, percentage of bus frequency had been going down to 99.8 % in 0.3 seconds and then it had been going up again to 100 % in 0.6 seconds and it was getting stable at 100 % at 9.4th second.

Bus frequency of swell simulation results of bus bar Maesa SB2 before RE integration, after RE integration and after RE integration using homer results is equal to bus frequency of swell simulation results of Maesa SB1 bus bar on all situations.

Bus frequency of swell simulation results of bus bar Parigi DB1 before RE integration, after RE integration and after RE integration using homer results can be seen below.

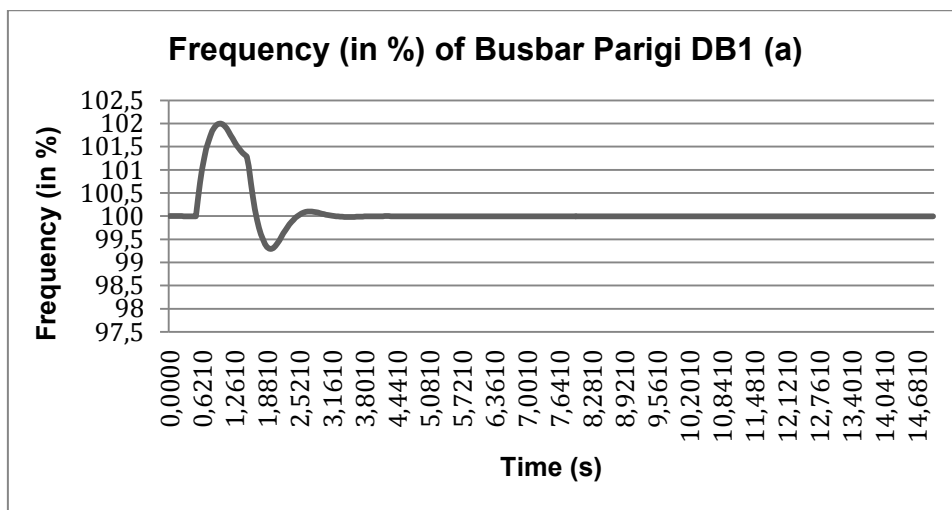


Figure 5-142: Parigi DB1 Bus Frequency Swell Simulation Results on Situation A

Based on figure 5-142, before swell, percentage of bus frequency was at 100 %. When the swell was occurred (from 0.5 s – 1.5 s), it had been going up to 102 % in 0.5 seconds and then it had been going down to 101.4 % in 0.5 seconds. After swell, percentage of bus frequency had been going down to 99.3 % in 0.4 seconds and it had been going up again to 100.2 % in 0.8 seconds. It was getting stable at 100 % at 3.8th second.

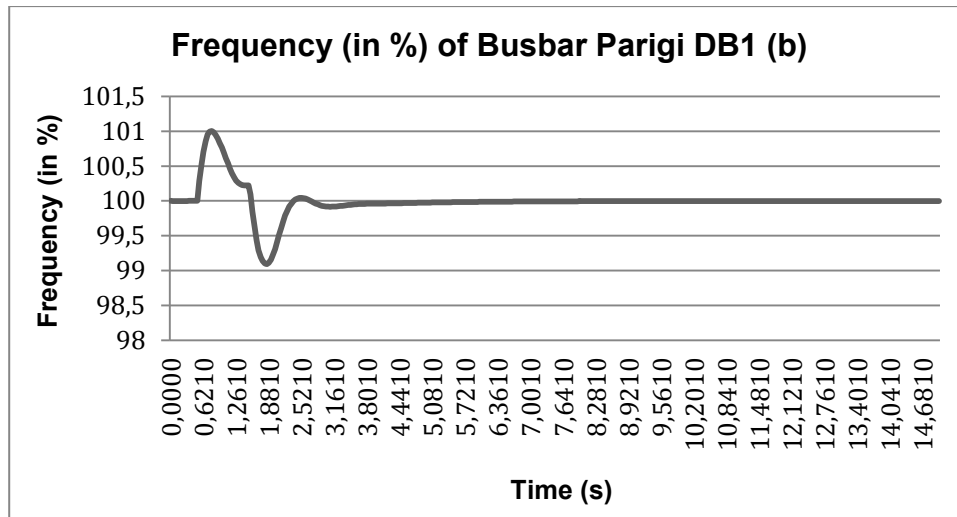


Figure 5-143: Parigi DB1 Bus Frequency Swell Simulation Results on Situation B

Based on figure 5-143, before swell, percentage of bus frequency was at 100 %. When the swell was occurred (from 0.5 s – 1.5 s), it had been going up to 101.3 % in 0.3 seconds and then it had been going down to 100.4 % in 4 seconds and it had been going up again to 100.5 % in 0.3 seconds. After swell, percentage of bus frequency had been going down to 99.1 % in 0.5 seconds and then it had been going up again to 100 % in 0.7 seconds. It was getting stable at 100 % at 8.7th second.

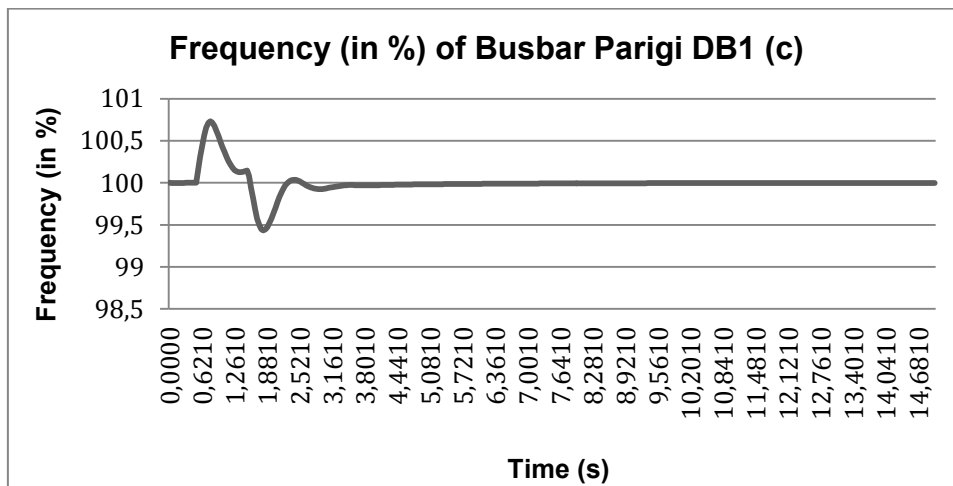


Figure 5-144: Parigi DB1 Bus Frequency Swell Simulation Results on Situation C

Based on figure 5-144, before swell, percentage of bus frequency was at 100 %. When the swell was occurred (from 0.5 s – 1.5 s), it had been going up to 100.7 % in 0.3 and then it had been going down to 100.3 % in 0.3 seconds and it had been

staying there for 0.3 seconds. After swell, percentage of bus frequency had been going down to 99.4 % in 0.3 seconds and then it had been going up again to 100 % in 0.6 seconds and it was getting stable at 100 % at 6.5th second.

Bus frequency of swell simulation results of Parigi DB1 (2) bus bar before RE integration, after RE integration and after RE integration using homer results is equal to bus frequency of swell simulation results of Parigi DB1 bus bar on all situations.

Bus frequency of swell simulation results of bus bar Parigi SB1 before RE integration, after RE integration and after RE integration using homer results can be seen below.

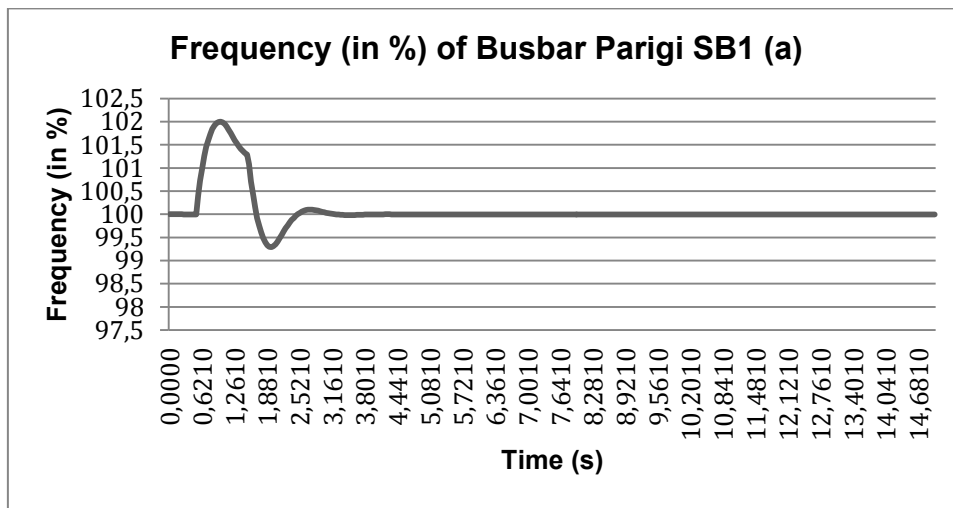


Figure 5-145: Parigi SB1 Bus Frequency Swell Simulation Results on Situation A

Based on figure 5-145, before swell, percentage of bus frequency was at 100 %. When the swell was occurred (from 0.5 s – 1.5 s), it had been going up to 102 % in 0.5 seconds and then it had been going down to 101.4 % in 0.5 seconds. After swell, percentage of bus frequency had been going down to 99.2 % in 0.5 seconds and it had been going up again to 100.1 % in 0.8 seconds. It was getting stable at 100 % at 3.8th second.

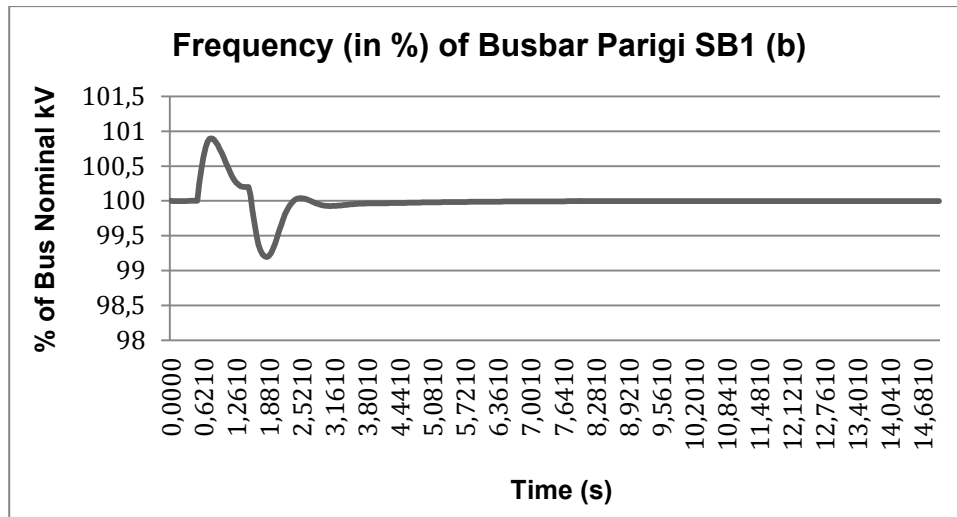


Figure 5-146: Parigi SB1 Bus Frequency Swell Simulation Results on Situation B

Based on figure 5-146, before swell, percentage of bus frequency was at 100 %. When the swell was occurred (from 0.5 s – 1.5 s), it had been going up to 100.9 % in 0.3 seconds and then it had been going down to 100.4 % in 4 seconds and it had been staying there for 0.3 seconds. After swell, percentage of bus frequency had been going down to 99.1 % in 0.5 seconds and then it had been going up again to 100 % in 0.7 seconds. It was getting stable at 100 % at 8.3rd second.

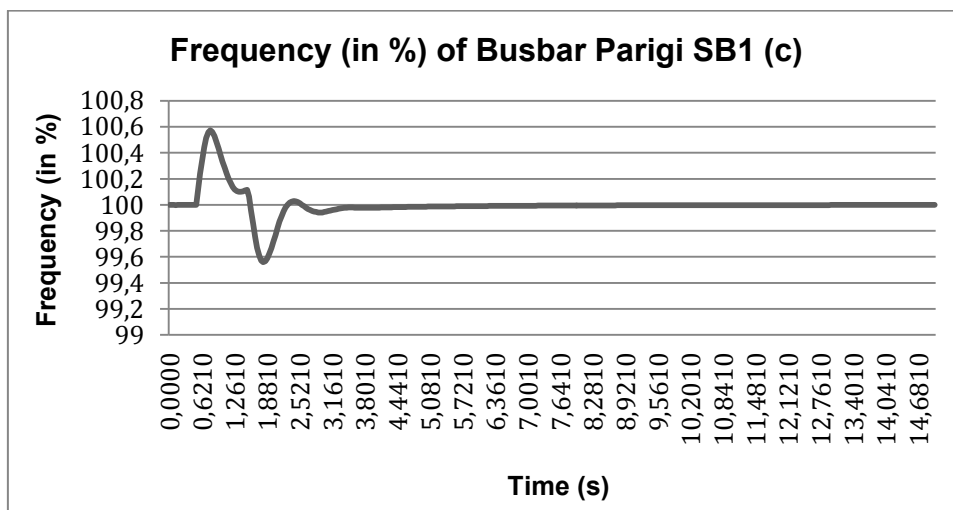


Figure 5-147: Parigi SB1 Bus Frequency Swell Simulation Results on Situation C

Based on figure 5-147, before swell, percentage of bus frequency was at 100 %. When the swell was occurred (from 0.5 s – 1.5 s), it had been going up to 100.6 % in

0.3 and then it had been going down to 100.1 % in 0.4 seconds and it had been staying there for 0.3 seconds. After swell, percentage of bus frequency had been going down to 99.5 % in 0.3 seconds and then it had been going up again to 100 % in 0.6 seconds. It was getting stable at 100 % at 7.7th second.

Bus frequency of swell simulation results of bus bar Parigi SB2 before RE integration, after RE integration and after RE integration using homer results can be seen below.

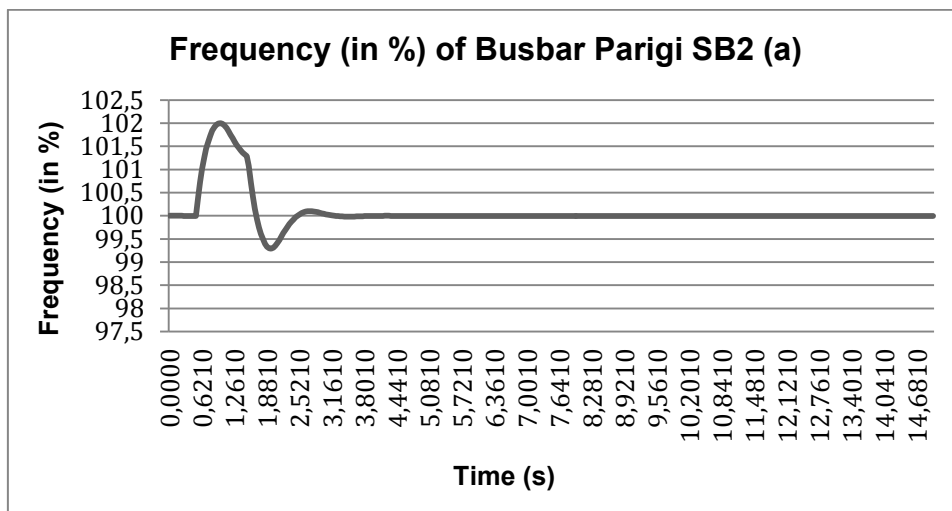


Figure 5-148: Parigi SB2 Bus Frequency Swell Simulation Results on Situation A

Based on figure 5-148, before swell, percentage of bus frequency was at 100 %. When the swell was occurred (from 0.5 s – 1.5 s), it had been going up to 102 % in 0.5 seconds and then it had been going down to 101.4 % in 0.5 seconds. After swell, percentage of bus frequency had been going down to 99.3 % in 0.5 seconds and it had been going up again to 100.3 % in 0.8 seconds. It was getting stable at 100 % at 3.4th second.

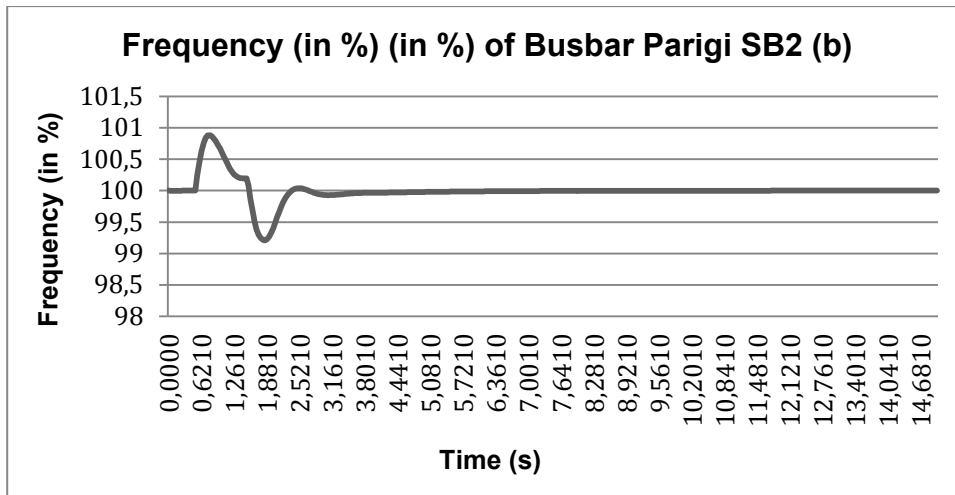


Figure 5-149: Parigi SB2 Bus Frequency Swell Simulation Results on Situation B

Based on figure 5-149, before swell, percentage of bus frequency was at 100 %. When the swell was occurred (from 0.5 s – 1.5 s), it had been going up to 100.9 % in 0.3 seconds and then it had been going down to 100.3 % in 4 seconds and staying there for 0.3 seconds. After swell, percentage of bus frequency had been going down to 99.2 % in 0.5 seconds and then going up again to 100 % in 0.7 seconds. It was getting stable at 100 % at 6th second.

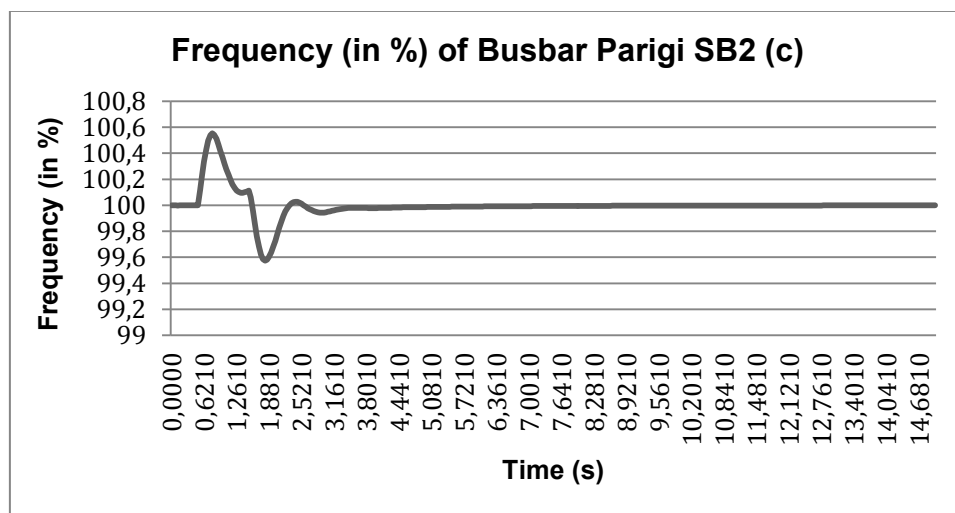


Figure 5-150: Parigi SB2 Bus Frequency Swell Simulation Results on Situation C

Based on figure 5-150, before swell, percentage of bus frequency was at 100 %. When the swell was occurred (from 0.5 s – 1.5 s), it had been going up to 100.5 % in 0.3 and then it had been going down to 100.1 % in 0.4 seconds and it had been

staying there for 0.3 seconds. After swell, percentage of bus frequency had been going down to 99.5 % in 0.3 seconds and then it had been going up again to 100 % in 0.6 seconds. It was getting stable getting stable at 100 % at 7.5th second.

Bus frequency of swell simulation results of bus bar PJPP SB1 before RE integration, after RE integration and after RE integration using homer results can be seen below.

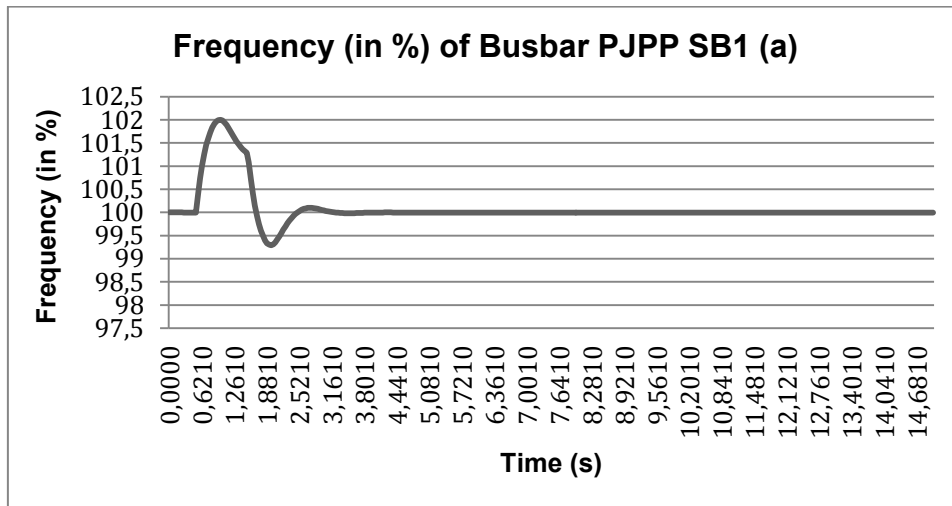


Figure 5-151: PJPP SB1 Bus Frequency Swell Simulation Results on Situation A

Based on figure 5-151, before swell, percentage of bus frequency was at 100 %. When the swell was occurred (from 0.5 s – 1.5 s), it had been going up to 102 % in 0.5 seconds and then it had been going down to 101.4 % in 0.5 seconds. After swell, percentage of bus frequency had been going down to 99.3 % in 0.5 seconds and it had been going up again to 100.2 % in 0.8 seconds. It was getting stable at 100 % at 4th second.

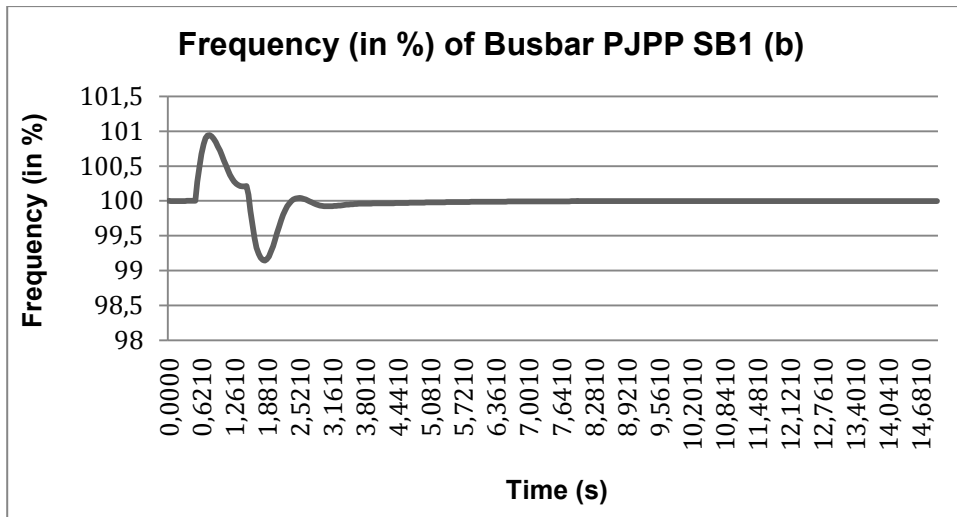


Figure 5-152: PJPP SB1 Bus Frequency Swell Simulation Results on Situation B

Based on figure 5-152, before swell, percentage of bus frequency was at 100 %. When the swell was occurred (from 0.5 s – 1.5 s), it had been going up to 100.9 % in 0.3 seconds and then it had been going down to 100.2 % in 4 seconds and it had been staying there for 0.3 seconds. After swell, it had been going down to 99.1 % in 0.5 seconds and then it had been going up again to 100 % in 0.7 seconds. It was getting stable at 100 % at 8.3rd second.

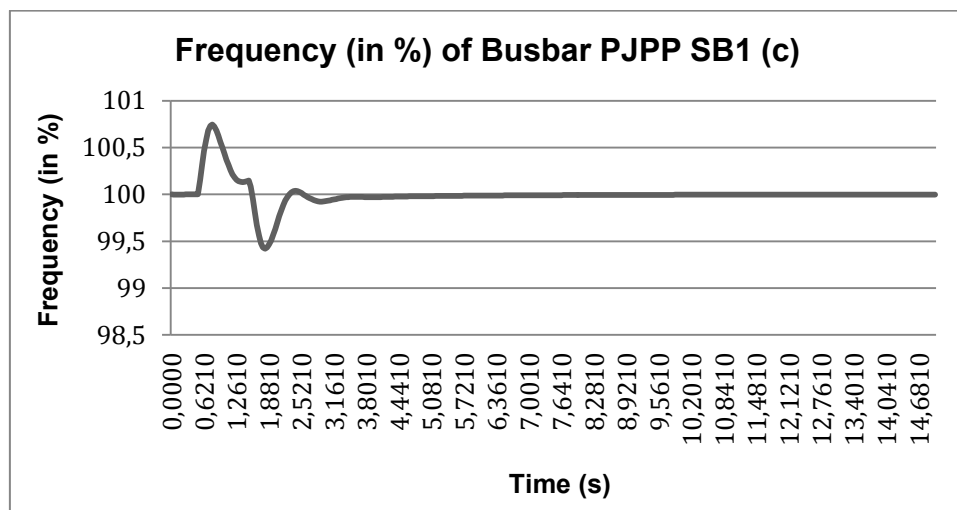


Figure 5-153: PJPP SB1 Bus Voltage Swell Simulation Results on Situation C

Based on figure 5-153, before swell, percentage of bus frequency was at 100 %. When the swell was occurred (from 0.5 s – 1.5 s), it had been going up to 100.7 % in

0.3 and then it had been going down to 100.2 % in 0.4 seconds and it had been staying there for 0.3 seconds. After swell, percentage of bus frequency had been going down to 99.4 % in 0.3 seconds and then it had been going up again to 100 % in 0.6 seconds. It was getting stable at 100 % at 6.3rd second.

Bus frequency of swell simulation results of bus bar Silae SB1 before RE integration, after RE integration and after RE integration using homer results can be seen below.

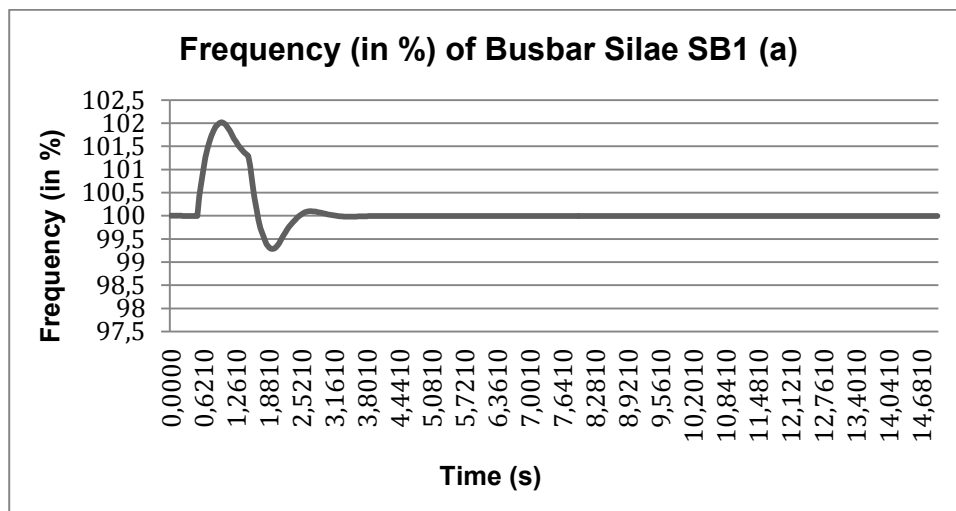


Figure 5-154: Silae SB1 Bus Frequency Swell Simulation Results on Situation A

Based on figure 5-154, before swell, percentage of bus frequency was at 100 %. When the swell was occurred (from 0.5 s – 1.5 s), it had been going up to 102 % in 0.5 seconds and then it had been going down to 101.4 % in 0.5 seconds. After swell, percentage of bus frequency had been going down to 99.3 % in 0.5 seconds and it had been going up again to 100.3 % in 0.8 seconds. It was getting stable at 100 % at 3.9th second.

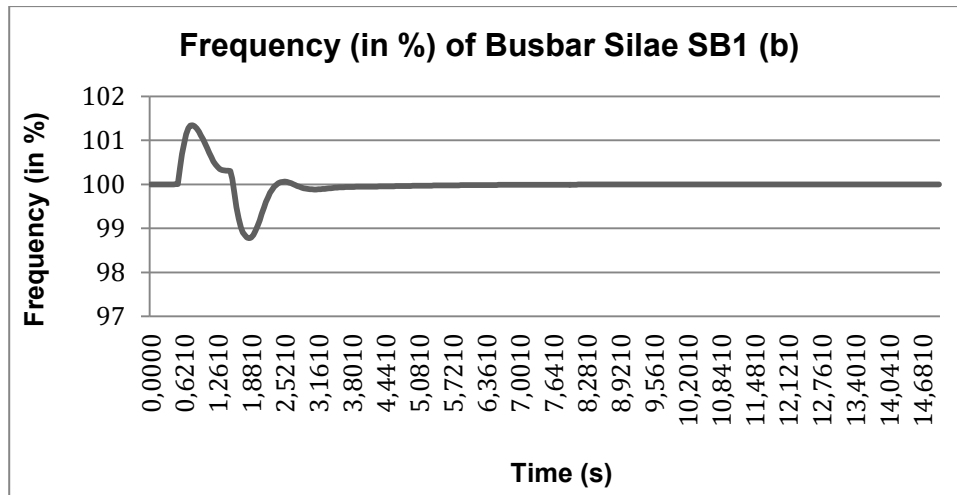


Figure 5-155: Silae SB1 Bus Frequency Swell Simulation Results on Situation B

Based on figure 5-155, before swell, percentage of bus frequency was at 100 %. When the swell was occurred (from 0.5 s – 1.5 s), it had been going up to 101.4 % in 0.3 seconds and then it had been going down to 100.3 % in 4 seconds and it had been staying there for 0.3 seconds. After swell, percentage of bus frequency had been going down to 98.7 % in 0.5 seconds and then it had been going up again to 100 % in 0.7 seconds. It was getting stable at 100 % at 9.2nd second.

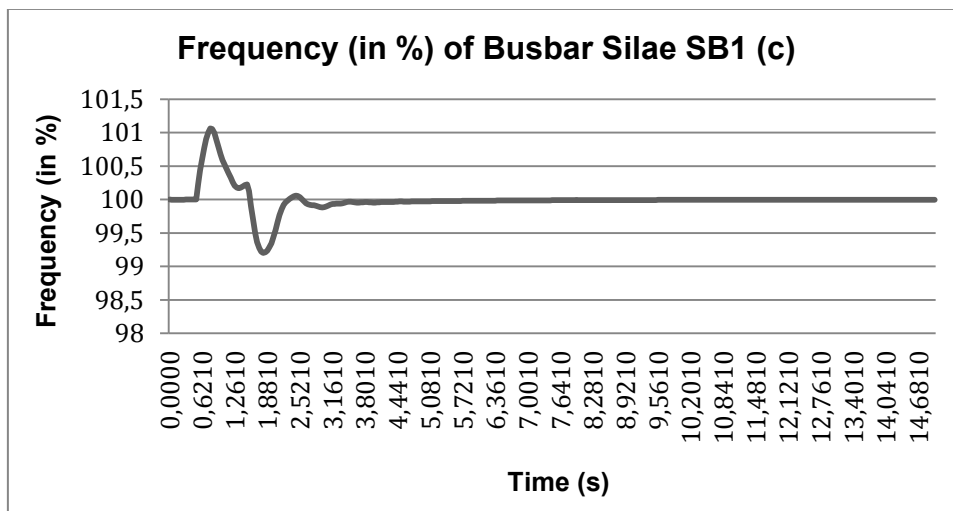


Figure 5-156: Silae SB1 Bus Frequency Swell Simulation Results on Situation C

Based on figure 5-156, before swell, percentage of bus frequency was at 100 %. When the swell was occurred (from 0.5 s – 1.5 s), it had been going up to 101.1 % in 0.3 and then it had been going down to 100.2 % in 0.4 seconds and it had been

staying there for 0.3 seconds. After swell, percentage of bus frequency had been going down to 99.2 % in 0.3 seconds and then it had been going up again to 100 % in 0.6 seconds. It was getting stable at 100 % at 6.3rd second.

Bus frequency of swell simulation results of Silae SB2 and Silae SB3 bus bar before RE integration, after RE integration and after RE integration using homer results is equal to bus frequency of swell simulation results of Silae SB1 bus bar on all situations.

Bus frequency of swell simulation results of bus bar Silae SB4 before RE integration, after RE integration and after RE integration using homer results can be seen below.

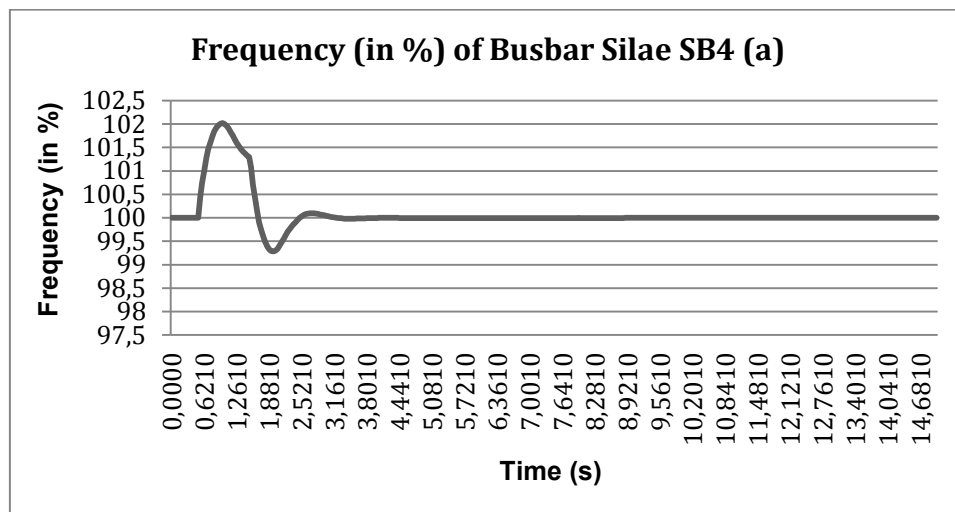


Figure 5-157: Silae SB4 Bus Frequency Swell Simulation Results on Situation A

Based on figure 5-157, before swell, percentage of bus frequency was at 100 %. When the swell is occurred (from 0.5 s – 1.5 s), it had been going up to 102 % in 0.5 seconds and then it had been going down to 101.4 % in 0.5 seconds. After swell, percentage of bus frequency had been going down to 99.3 % in 0.5 seconds and it had been going up again to 100.2 % in 0.8 seconds. It was getting stable at 100 % at 4.3.9th second.

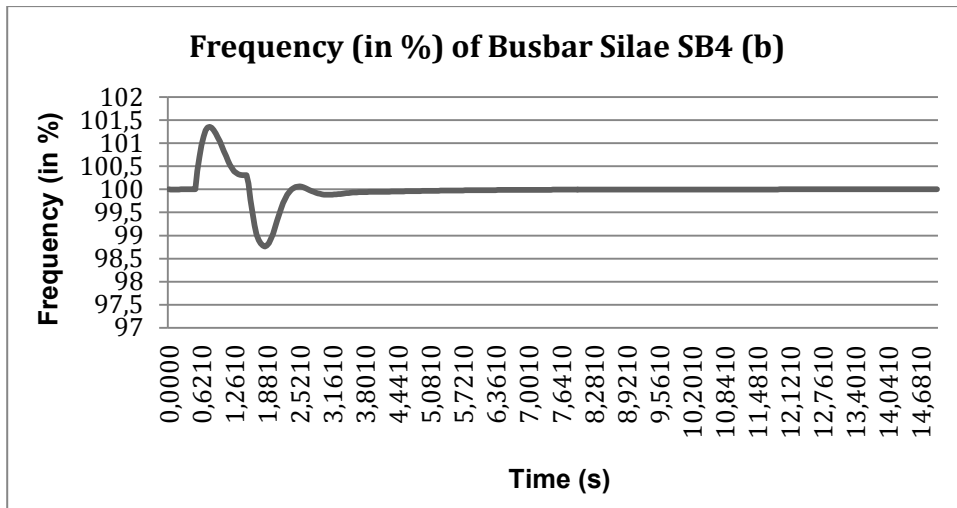


Figure 5-158: Silae SB4 Bus Frequency Swell Simulation Results on Situation B

Based on figure 5-158, before swell, percentage of bus frequency was at 100 %. When the swell was occurred (from 0.5 s – 1.5 s), it had been going up to 101.3 % in 0.3 seconds and then it had been going down to 100.4 % in 4 seconds and it had been staying there for 0.3 seconds. After swell, percentage of bus frequency had been going down to 98.7 % in 0.5 seconds and then it had been going up again to 100 % in 0.7 seconds. It was getting stable at 100 % at 9.5th second.

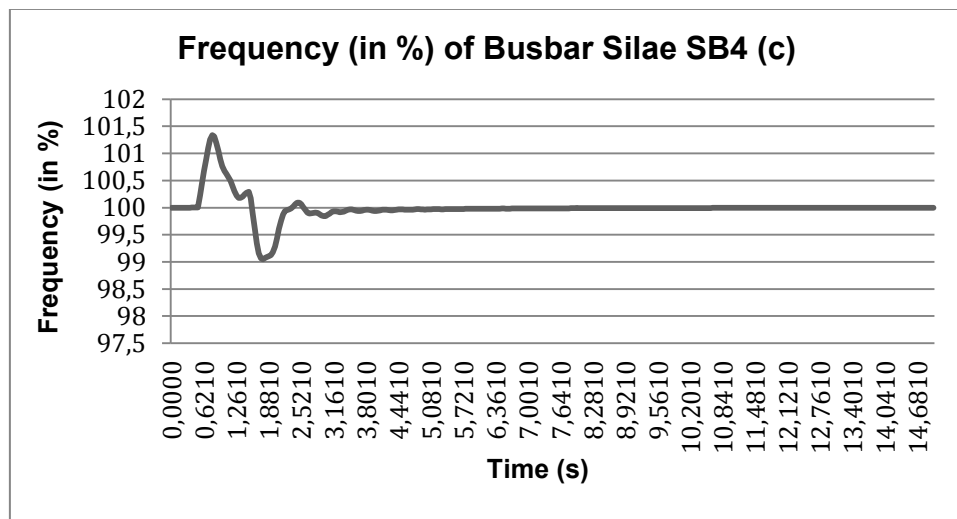


Figure 5-159: Silae SB4 Bus Frequency Swell Simulation Results on Situation C

Based on figure 5-159, before swell, percentage of bus frequency was at 100 %. When the swell was occurred (from 0.5 s – 1.5 s), it had been going up to 101.4 % in

0.3 and then it had been going down to 100.2 % in 0.4 seconds and it had been staying there for 0.3 seconds. After swell, percentage of bus frequency had been going down to 99 % in 0.3 seconds and then it had been going up again to 100 % in 0.6 seconds. It was getting stable at 100 % at 7.4th second.

Bus frequency of swell simulation results of bus bar Talise SB1 before RE integration, after RE integration and after RE integration using homer results can be seen below.

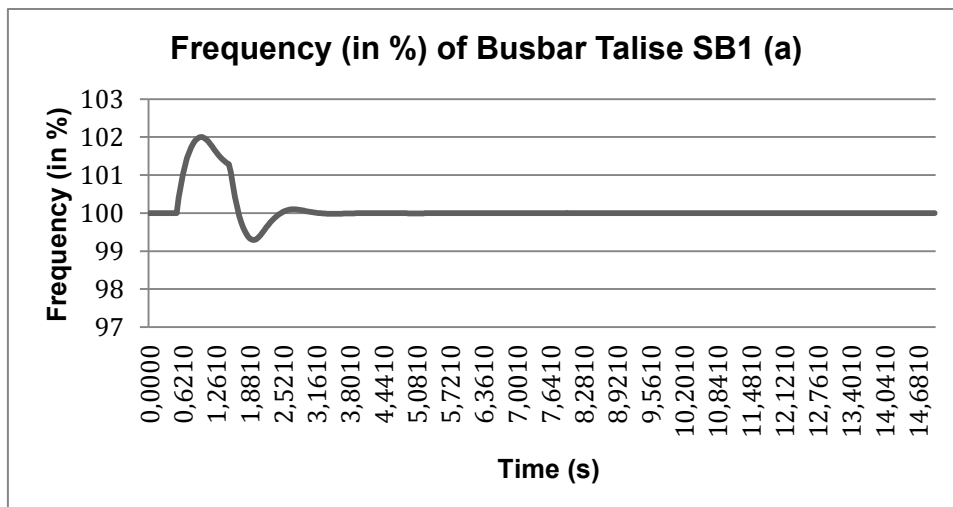


Figure 5-160: Talise SB1 Bus Frequency Swell Simulation Results on Situation A

Based on figure 5-160, before swell, percentage of bus frequency was at 100 %. When the swell was occurred (from 0.5 s – 1.5 s), it had been going up to 102 % in 0.5 seconds and then it had been going down to 101.4 % in 0.5 seconds. After swell, percentage of bus frequency had been going down to 99.3 % in 0.5 seconds and it had been going up again to 100.3 % in 0.8 seconds. It was getting stable at 100 % at 4.5th second.

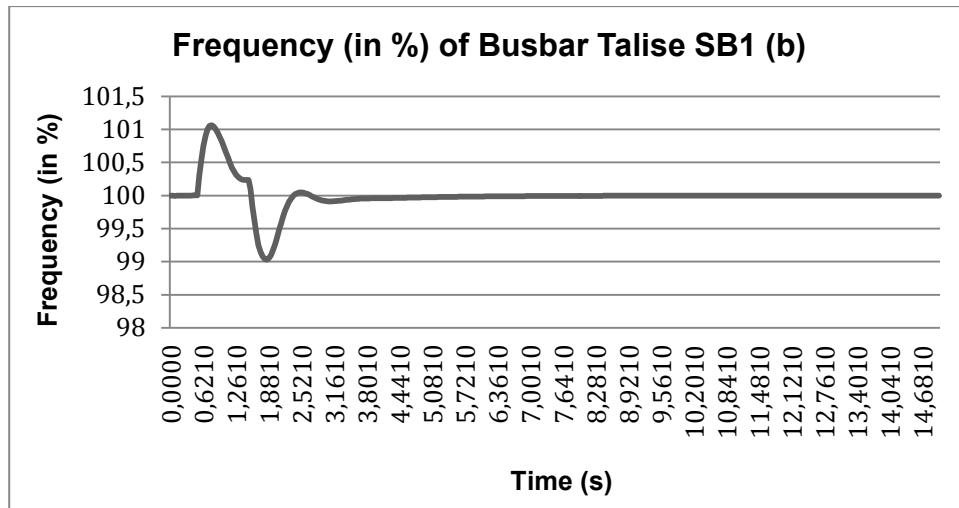


Figure 5-161: Talise SB1 Bus Frequency Swell Simulations on Situation B

Based on figure 5-161, before swell, percentage of bus frequency was at 100 %. When the swell was occurred (from 0.5 s – 1.5 s), it had been going up to 101.4 % in 0.3 seconds and then it had been going down to 100.5 % in 4 seconds and it had been staying there for 0.3 seconds. After swell, percentage of bus frequency had been going down to 99 % in 0.5 seconds and then it had been going up again to 100 % in 0.7 seconds. It was getting stable at 100 % at 8.6th second.

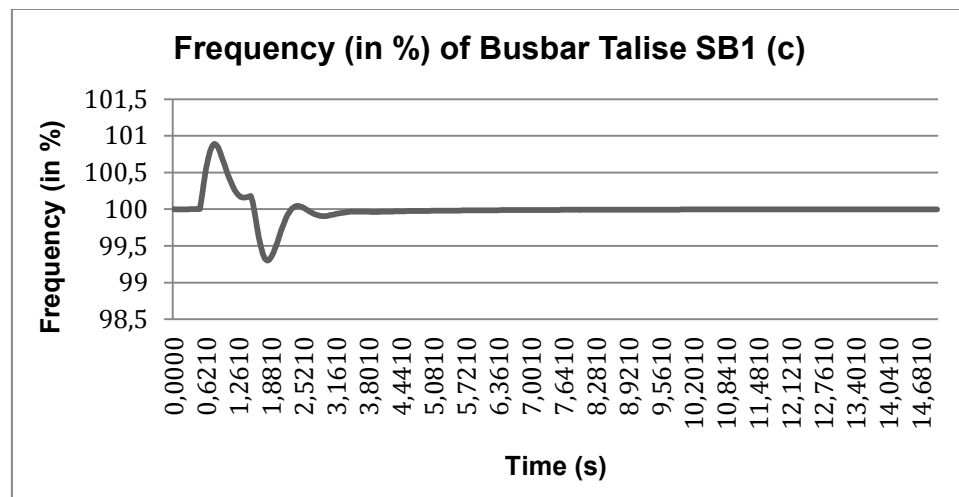


Figure 5-162: Talise SB1 Bus Frequency Swell Simulation Results on Situation C

Based on figure 5-162, before swell, percentage of bus frequency was at 100 %. When the swell was occurred (from 0.5 s – 1.5 s), it had been going up to 100.8 % in 0.3 and then it had been going down to 100.2 % in 0.4 seconds and it had been

staying there for 0.3 seconds. After swell, percentage of bus frequency had been going down to 99.8 % in 0.3 seconds and then it had been going up again to 100 % in 0.6 seconds and it was getting stable at 100 % at 9.4th second.

Bus frequency of swell simulation results of bus bar Talise SB2 before RE integration, after RE integration and after RE integration using homer results can be seen below.

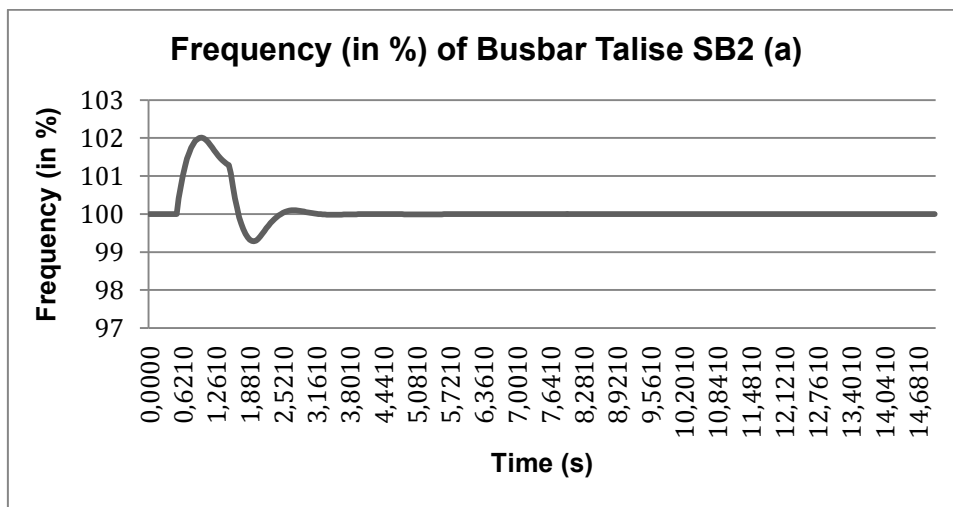


Figure 5-163: Talise SB2 Bus Frequency Swell Simulation Results on Situation A

Based on figure 5-163, before swell, percentage of bus frequency was at 100 %. When the swell was occurred (from 0.5 s – 1.5 s), it had been going up to 102 % in 0.5 seconds and then it had been going down to 101.4 % in 0.5 seconds. After swell, percentage of bus frequency had been going down to 99.3 % in 0.5 seconds and it had been going up again to 100.2 % in 0.8 seconds. It was getting stable at 100 % at 3.9th second.

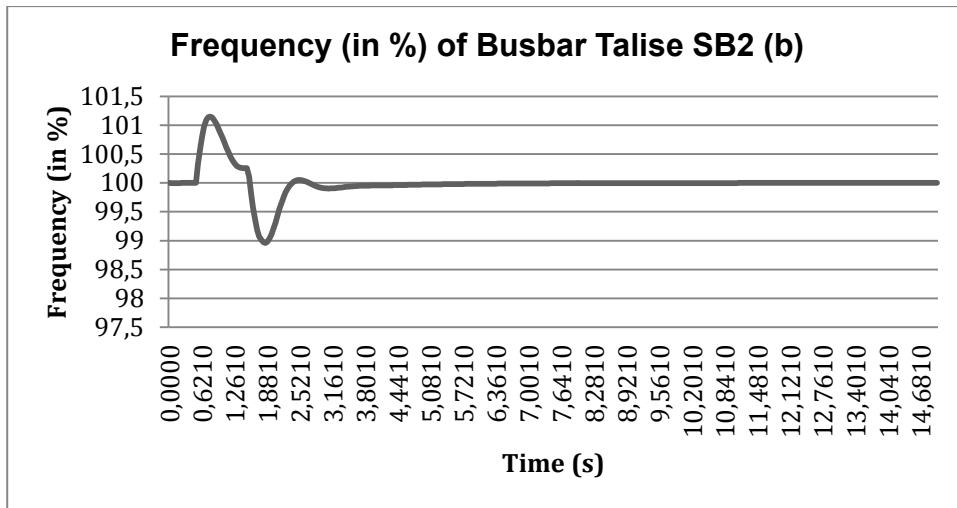


Figure 5-164: Talise SB2 Bus Frequency Swell Simulation Results on Situation B

Based on figure 5-164, before swell, When the swell was occurred (from 0.5 s – 1.5 s), it had been going up to 101.5 % in 0.3 seconds and then it had been going down to 100.3 % in 4 seconds and it had been staying there for 0.3 seconds. After swell, percentage of bus frequency had been going down to 98.7 % in 0.5 seconds and then it had been going up again to 100 % in 0.7 seconds. It was getting stable at 100 % at 10.2nd second.

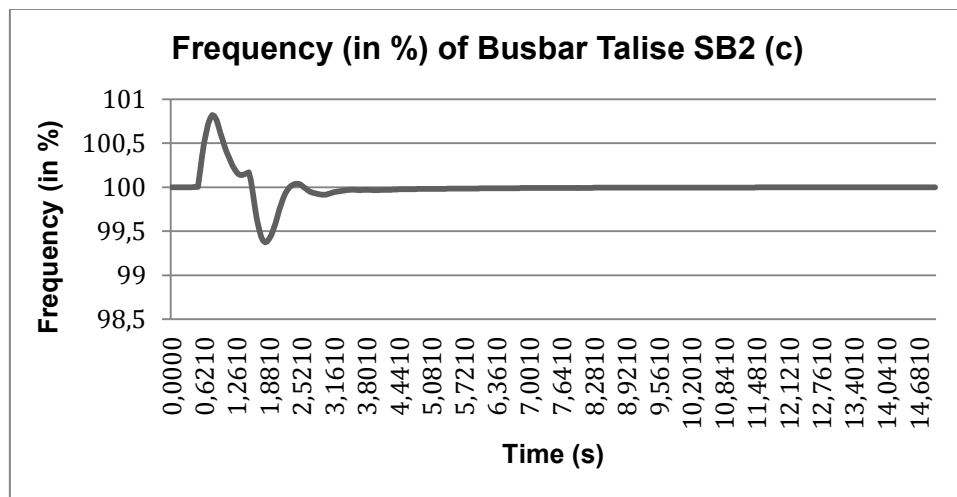


Figure 5-165: Talise SB2 Bus Frequency Swell Simulation Results on Situation C

Based on figure 5-165, before swell, percentage of bus frequency was at 100 %. When the swell was occurred (from 0.5 s – 1.5 s), it had been going up to 100.4 % in 0.3 and then it had been going down to 100.2 % in 0.4 seconds and it had been

staying there for 0.3 seconds. After swell, percentage of bus frequency had been going down to 99.4 % in 0.3 seconds and then it had been going up again to 100 % in 0.6 seconds and it was getting stable at 100 % at 14.0th second.

Bus frequency of swell simulation results of bus bar Talise SB3 before RE integration, after RE integration and after RE integration using homer results is equal to bus frequency of swell simulation results of Talise SB2 bus bar on all situations.

Bus frequency of swell simulation results of bus bar Talise DB1 before RE integration, after RE integration and after RE integration using homer results can be seen below.

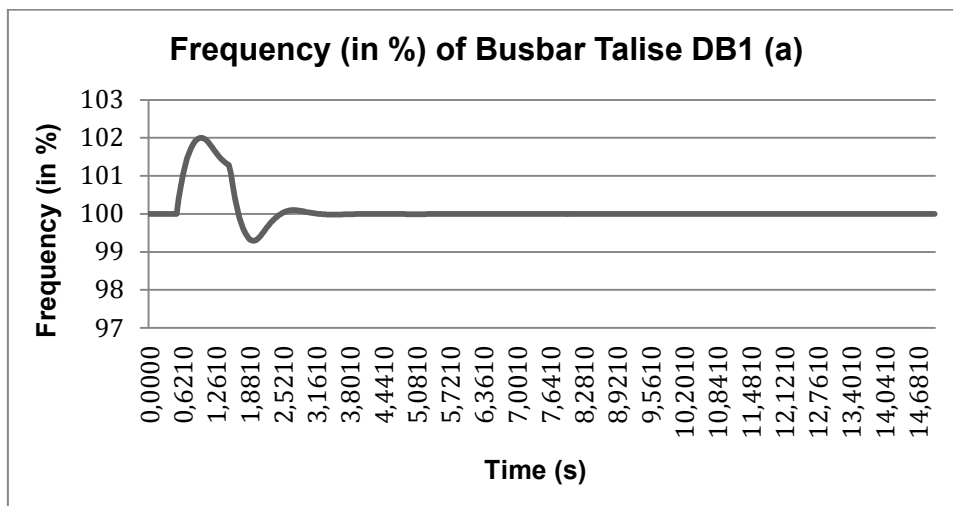


Figure 5-166: Talise DB1 Bus Frequency Swell Simulation Results on Situation A

Based on figure 5-166, before swell, percentage of bus frequency is at 100 %. When the swell was occurred (from 0.5 s – 1.5 s), it had been going up to 102 % in 0.5 seconds and then it had been going down to 101.4 % in 0.5 seconds. After swell, percentage of bus frequency had been going down to 99.3 % in 0.5 seconds and it had been going up again to 100.2 % in 0.8 seconds. It was getting stable at 100 % at 3.9th second.

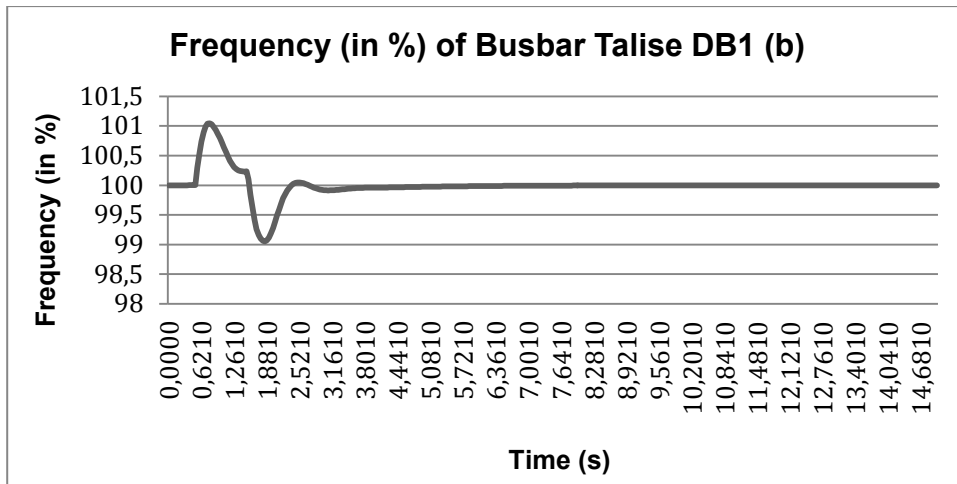


Figure 5-167: Talise DB1 Bus Frequency Swell Simulation Results on Situation B

Based on figure 5-167, before swell, percentage of bus frequency was at 100 %. When the swell was occurred (from 0.5 s – 1.5 s), it had been going up to 101.1 % in 0.3 seconds and then it had been going down to 100.3 % in 4 seconds and then it had been staying there for 0.3 seconds. After swell, percentage of bus frequency had been going down to 99 % in 0.5 seconds and then it had been going up again to 100 % in 0.7 seconds. It was getting stable at 100 % at 8.5th second.

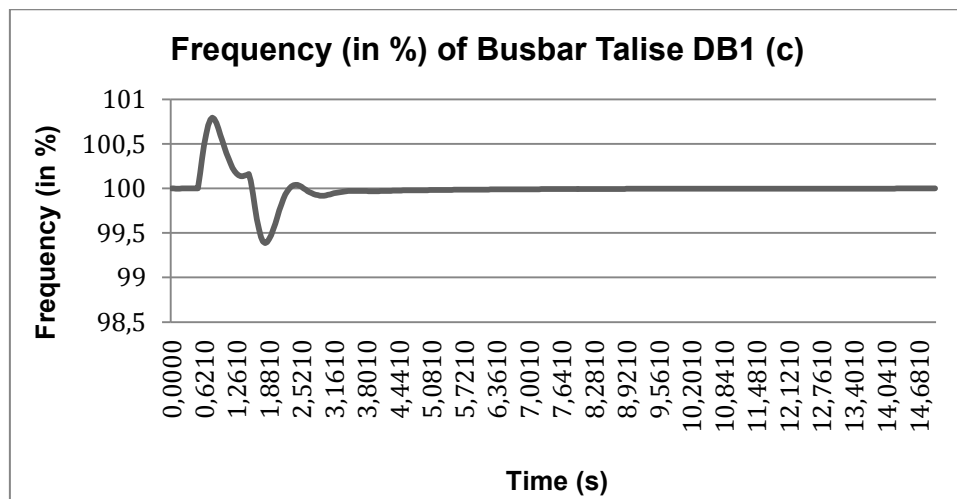


Figure 5-168: Talise DB1 Bus Frequency Swell Simulation Results on Situation C

Based on figure 5-168, before swell, bus frequency was at 100 %. When the swell was occurred (from 0.5 s – 1.5 s), percentage of bus frequency had been going up to 100.8 % in 0.3 and then it had been going down to 100.2 % in 0.4 seconds and it had

been staying there for 0.3 seconds. After swell, percentage of bus frequency had been going down to 99.4 % in 0.3 seconds and then it had been going up again to 100 % in 0.6 seconds and it was getting stable at 100 % at 13.5th second.

Bus frequency of swell simulation results of Talise DB11 bus bar before RE integration, after RE integration and after RE integration using homer results is equal to bus frequency of swell simulation results of Talise DB1 bus bar on all situations.

5.4.3 Interruption Simulation Results

Bus voltage of interruption simulation results of bus bar DB1 PJPP before RE integration, after RE integration and after RE integration using homer results can be seen below.

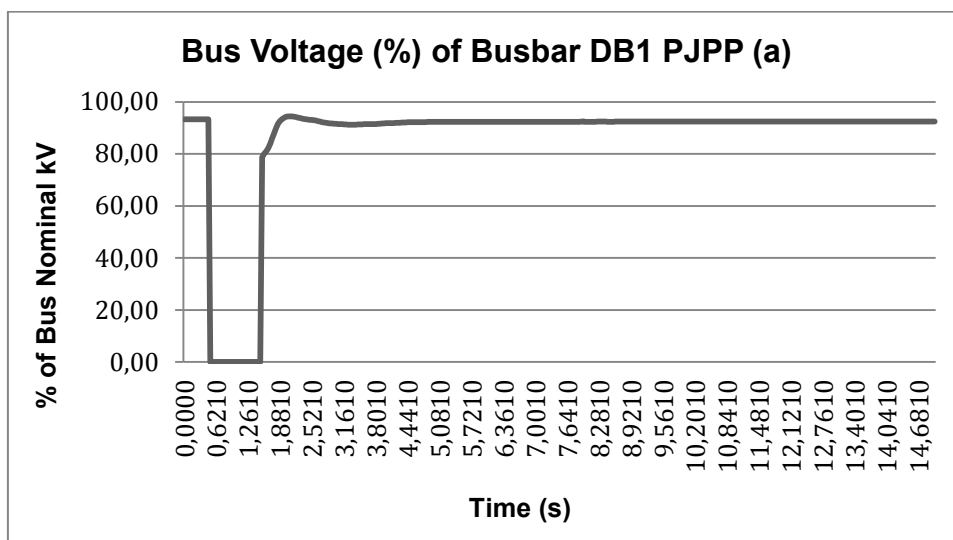


Figure 5-169: DB1 PJPP Bus Voltage Interruption Simulation Results on Situation A

Based on figure 5-169, before interruption, percentage of bus voltage was at 94 %kV. When the interruption was occurred, it dropped to zero during interruption. After interruption, percentage of bus voltage was going up until 79 %kV immediately after interruption and it had been going up to 96 %kV for 0.5 seconds and then it was slowly getting stable at 92 %kV at 4.7th second.

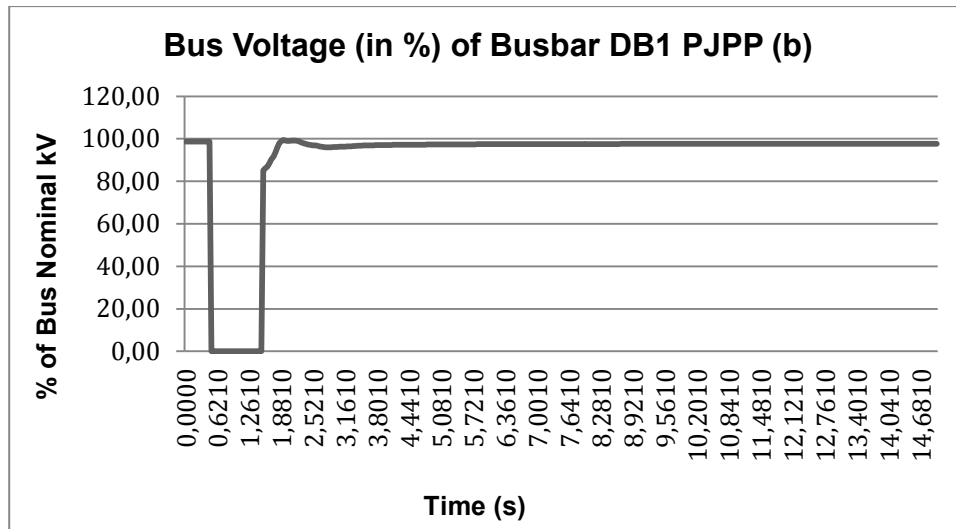


Figure 5-170: DB1 PJPP Bus Voltage Interruption Simulation Results on Situation B

Based on figure 5-170, before interruption, percentage of bus voltage was at 98 %kV. When the interruption was occurred, it dropped to zero during interruption. After interruption, percentage of bus voltage was going up until 82 %kV immediately after interruption and then it had been going up to 99 %kV in 0.5 seconds. It was getting stable at 95 %kV at 7.5th second.

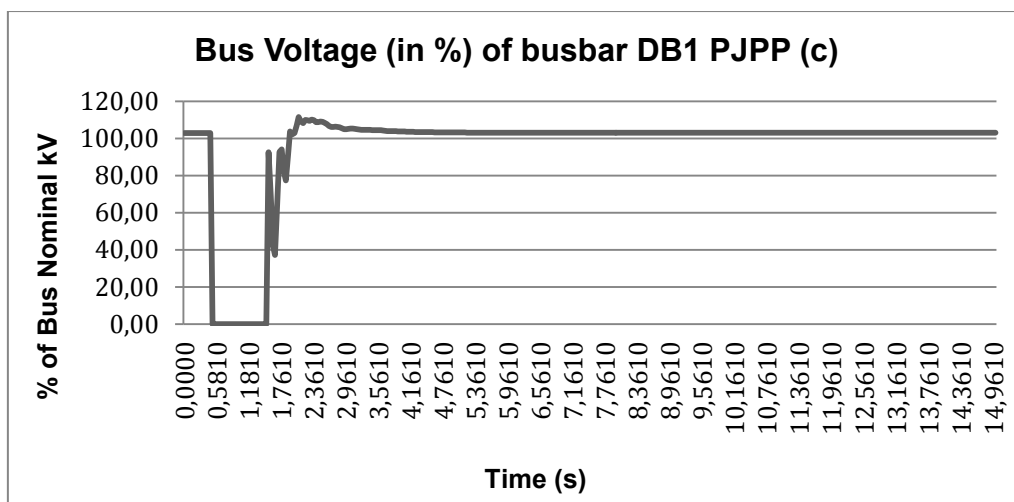


Figure 5-171: DB1 PJPP Bus Voltage Swell Simulation Results on Situation C

Based on figure 5-171, before interruption, percentage of bus voltage was at 102 %kV. When the interruption was occurred, it dropped to zero during interruption. After interruption, percentage of bus voltage was going up until 92 %kV and then it had

been fluctuating between 92 %kV and 38 %kV in 0.5 seconds. It was going up to 110 %kV and then it was getting stable at 102 %kV at 5.4th second.

Bus voltage of interruption simulation results of DB11 PJPP bus bar before RE integration, after RE integration and after RE integration using homer results is equal to bus voltage of interruption simulation results of DB1 PJPP bus bar on all situations.

Bus voltage of interruption simulation results of bus bar Donggala SB1 before RE integration, after RE integration and after RE integration using homer results can be seen below.

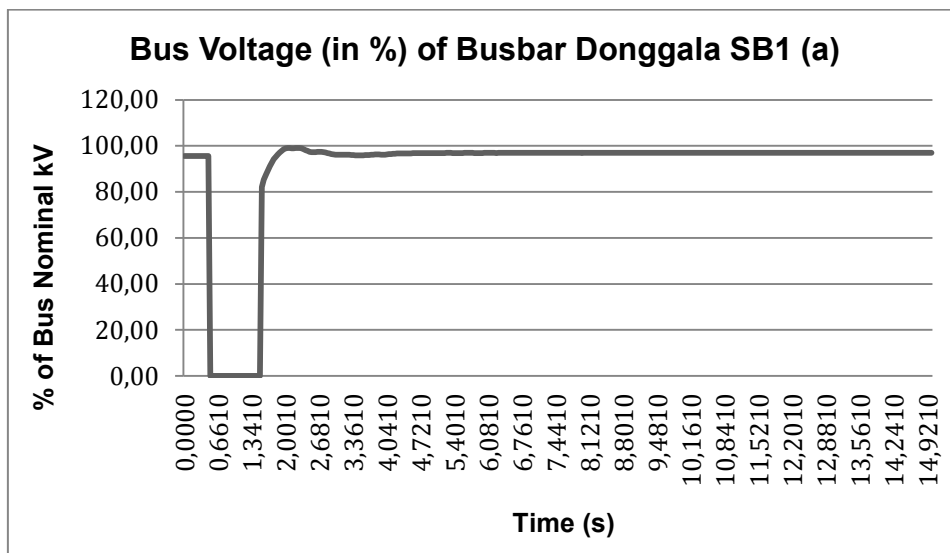


Figure 5-172: Donggala SB1 Bus Voltage Interruption Simulation Results on Situation A

Based on figure 5-172, before interruption, percentage of bus voltage was at 96 %kV. When the interruption was occurred, it dropped to zero during interruption. After interruption, percentage of bus voltage was going up until 82 %kV and then it had been going up to 96 %kV in 0.5 seconds. It was getting stable at 96 %kV at 7.7th second.

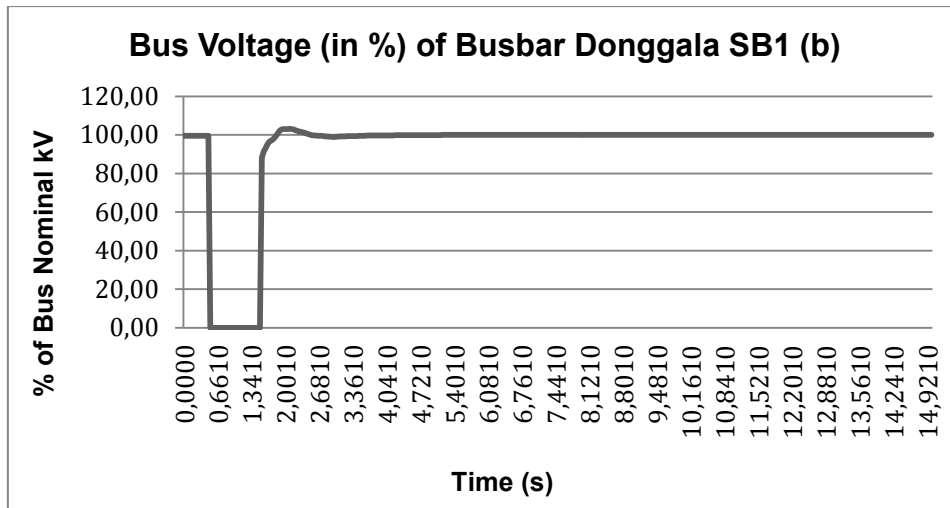


Figure 5-173: Donggala SB1 Bus Voltage Interruption Simulation Results on Situation B

Based on figure 5-173, before interruption, percentage of bus voltage was at 99 %kV. When the interruption was occurred, it dropped to zero during interruption. After interruption, percentage of bus voltage was going up until 83 %kV and then it had been going up to 101 % kV in 0.5 seconds. It was slowly getting stable at 99 %kV at 4th second.

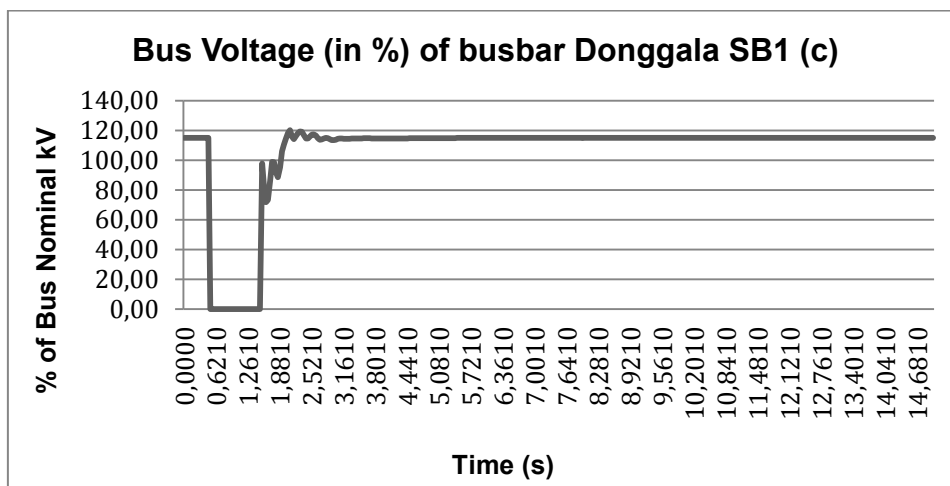


Figure 5-174: Donggala SB1 Bus Voltage Interruption Simulation Results on Situation C

Based on figure 5-174, before interruption, percentage of bus voltage was at 115 %kV. When the interruption was occurred, it dropped to zero during interruption. After interruption, percentage of bus nominal kV was going up until 99 %kV and then it had

been fluctuating between 99 %kV and 70 %kV for 0.5 seconds. It was going up to 119 %kV and then it was getting stable at 115 %kV at 3.9th second.

Bus voltage of interruption simulation results of bus bar Maesa SB1 before RE integration, after RE integration and after RE integration using homer results can be seen below.

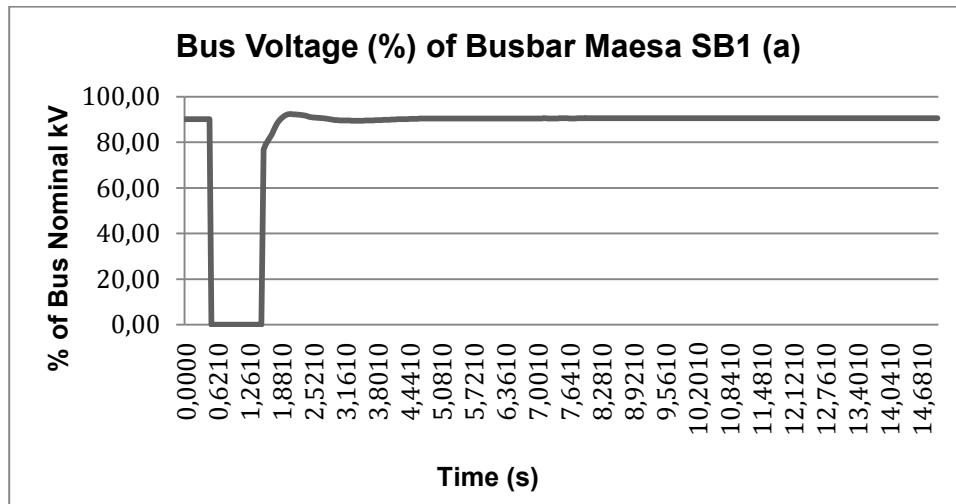


Figure 5-175: Maesa SB1 Bus Voltage Interruption Simulation Results on Situation A

Based on figure 5-175, before interruption, percentage of bus voltage was at 90 %kV. When the interruption was occurred, it dropped to zero during interruption. After interruption, percentage of bus voltage was going up until 77 %kV and then it had been going up to 92 %kV in 0.5 seconds. It was slowly getting stable at 90 %kV at 5.2nd second.

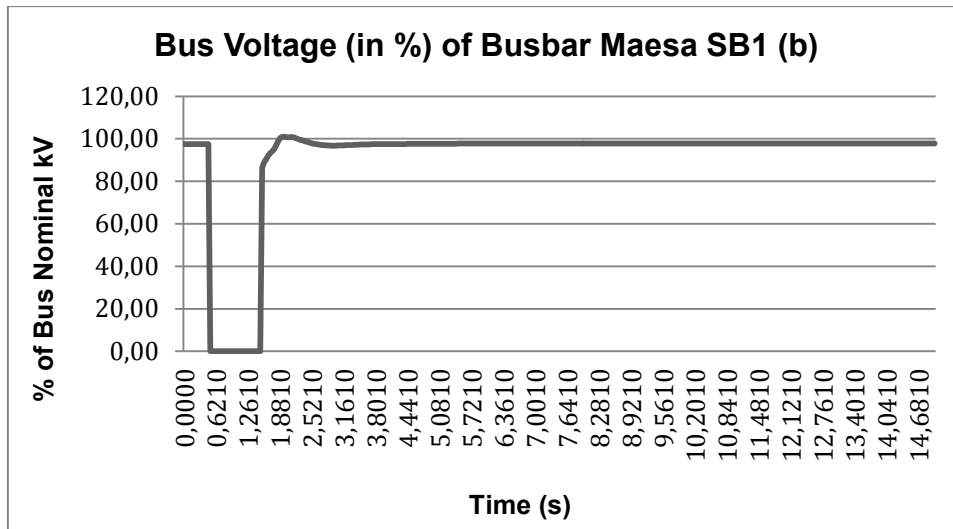


Figure 5-176: Maesa SB1 Bus Voltage Interruption Simulation Results on Situation B

Based on figure 5-176, before interruption, percentage of bus voltage was at 97 %kV. When the interruption was occurred, it dropped to zero during interruption. After interruption, percentage of bus voltage was going up until 83 %kV and then it had been going up to 101 %kV in 0.5 seconds. It was slowly getting stable at 97 %kV at 4.4th second.

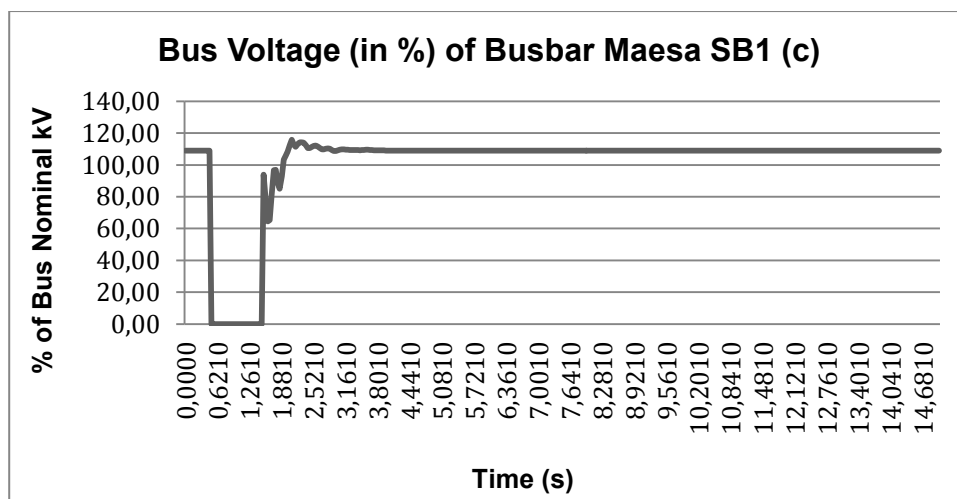


Figure 5-177: Maesa SB1 Bus Voltage Interruption Simulation Results on Situation C

Based on figure 5-177, before interruption, percentage of bus voltage was at 108 %kV. When the interruption was occurred, it dropped to zero during interruption. After interruption, percentage of bus voltage was going up until 97 %kV and then it had

been fluctuating between 97 %kV and 62 %kV in 0.5 seconds. It was going up to 118 %kV and then getting stable at 108 %kV at 4th second.

Bus voltage of interruption simulation results of Maesa SB1 (2) bus bar before RE integration, after RE integration and after RE integration using homer results is equal to bus voltage of interruption simulation results of Maesa SB1 bus bar on all situations.

Bus voltage of interruption simulation results of bus bar Parigi DB1 before RE integration, after RE integration and after RE integration using homer results can be seen below.

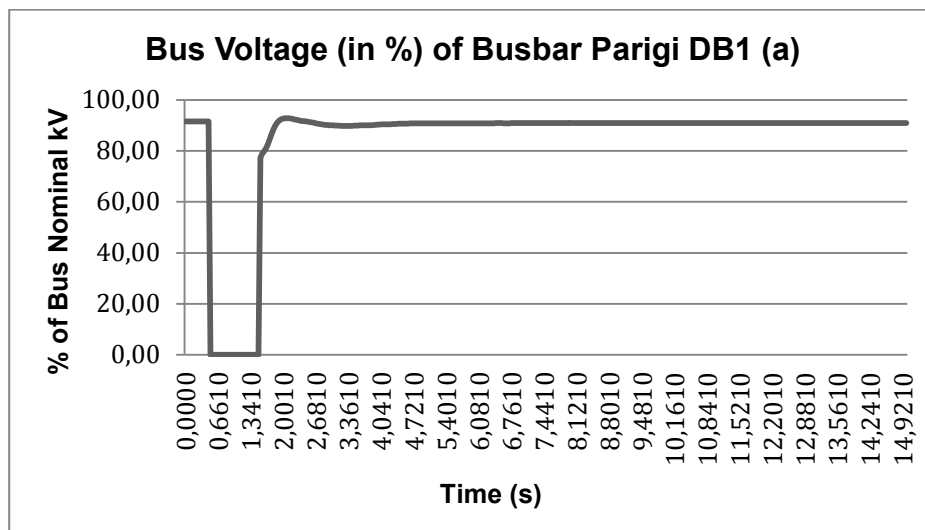


Figure 5-178: Parigi DB1 Bus Voltage Interruption Simulation Results on Situation A

Based on figure 5-178, before interruption, percentage of bus voltage was at 92 %kV. When the interruption was occurred, it dropped to zero during interruption. After interruption, percentage of bus voltage was going up until 77 %kV and then it had been going up to 92 %kV in 0.5 seconds. It was slowly getting stable at 90 %kV at 4.8th second.

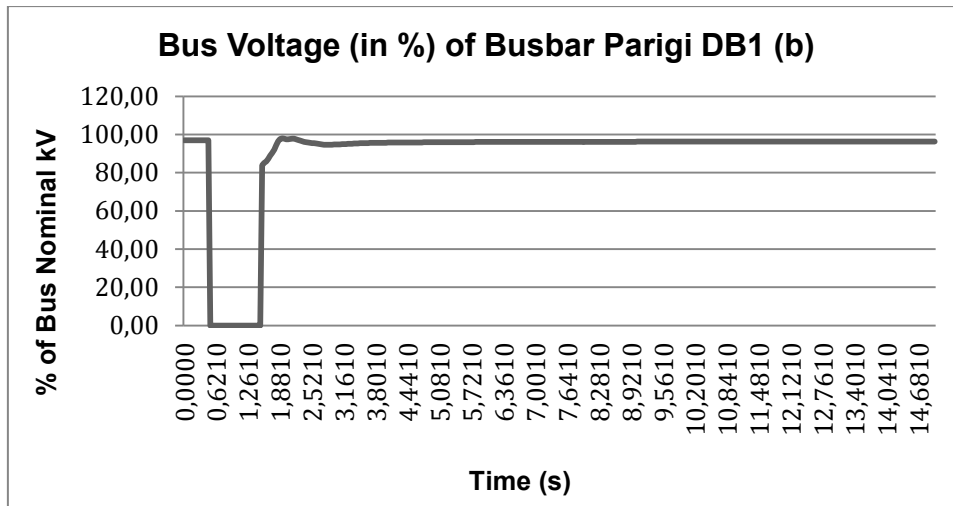


Figure 5-179: Parigi DB1 Bus Voltage Interruption Simulation Results on Situation B

Based on figure 5-179, before interruption, percentage of bus voltage was at 97 %kV. When the interruption was occurred, it dropped to zero during interruption. After interruption, percentage of bus voltage was going up until 83 %kV and then it had been going up to 99 %kV in 0.5 seconds. It was slowly getting stable at 96 %kV at 7.6th second.

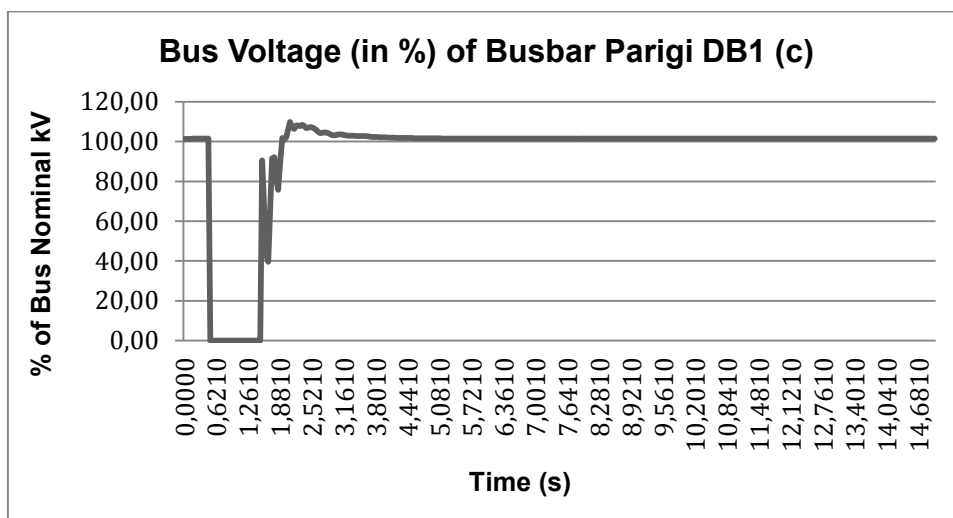


Figure 5-180: Parigi DB1 Bus Voltage Interruption Simulation Results on Situation C

Based on figure 5-180, before interruption, percentage of bus voltage was at 102 %kV. When the interruption was occurred, it dropped to zero during interruption. After interruption, percentage of bus voltage was going up until 92 %kV and then it had

been fluctuating between 92 %kV and 40 %kV in 0.5 seconds. It was going up to 110 and then it was getting stable at 102 %kV at 4.2nd second.

Bus voltage of interruption simulation results of Parigi DB1 (2) bus bar before RE integration, after RE integration and after RE integration using homer results is equal to bus voltage of interruption simulation results of Parigi DB1 bus bar on all situations.

Bus voltage of interruption simulation results of bus bar Parigi SB1 before RE integration, after RE integration and after RE integration using homer results can be seen below.

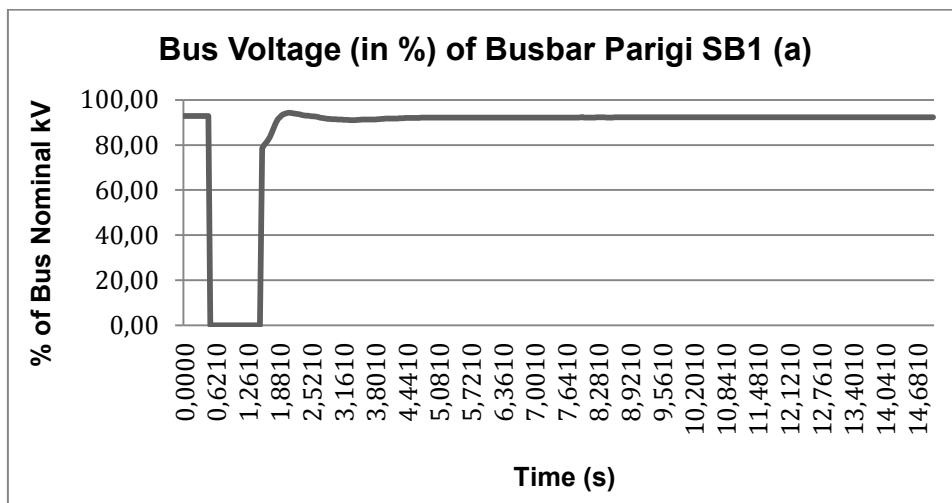


Figure 5-181: Parigi SB1 Bus Voltage Interruption Simulation Results on Situation A

Based on figure 5-181, before interruption, percentage of bus voltage was at 93 %kV. When the interruption was occurred, it dropped to zero during interruption. After interruption, percentage of bus voltage was immediately going up to 78 %kV and then it had been going up to 94 %kV in 0.5 seconds. It was slowly getting stable at 93 %kV at 4.7th second.

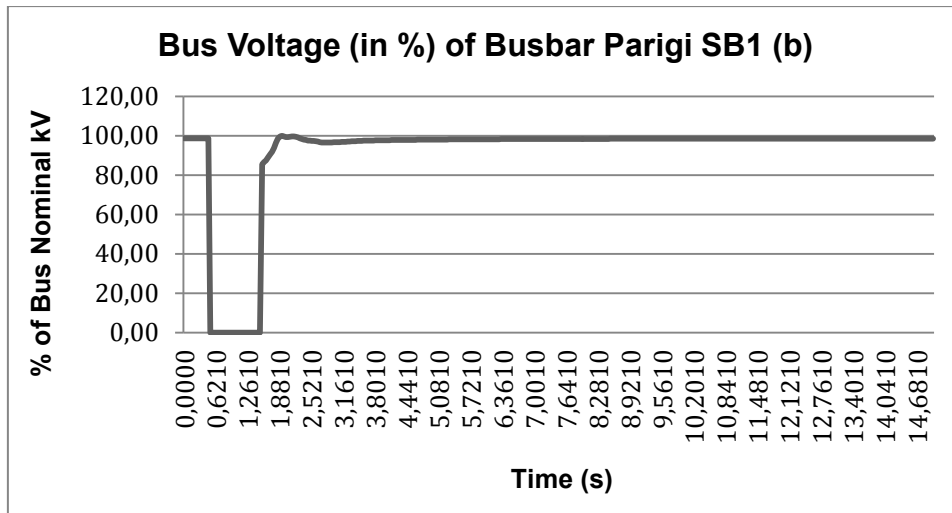


Figure 5-182: Parigi SB1 Bus Voltage Interruption Simulation Results on Situation B

Based on figure 5-182, before interruption, percentage of bus voltage was at 99 %kV. When the interruption was occurred, it dropped to zero during interruption. After interruption, percentage of bus voltage was immediately going up until 88 %kV and then it had been going up to 100 %kV in 0.5 seconds. It was slowly getting stable at 98 %kV at 7.4th second.

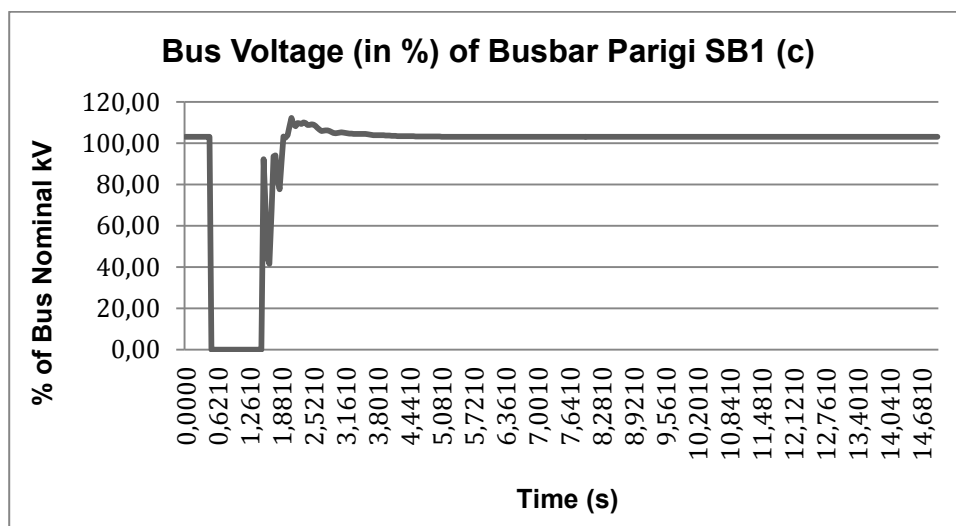


Figure 5-183: Parigi SB1 Bus Voltage Interruption Simulation Results on Situation C

Based on figure 5-183, before interruption, percentage of bus voltage was at 102 %kV. When the interruption was occurred, it dropped to zero during interruption. After interruption, percentage of bus voltage was going up until 100 %kV and then it had

been fluctuating between 92 %kV and 41 %kV. It was going up to 112 % and then it was getting stable at 102 %kV at 5.3rd second.

Bus voltage of interruption simulation results of bus bar Parigi SB2 before RE integration, after RE integration and after RE integration using homer results can be seen below.

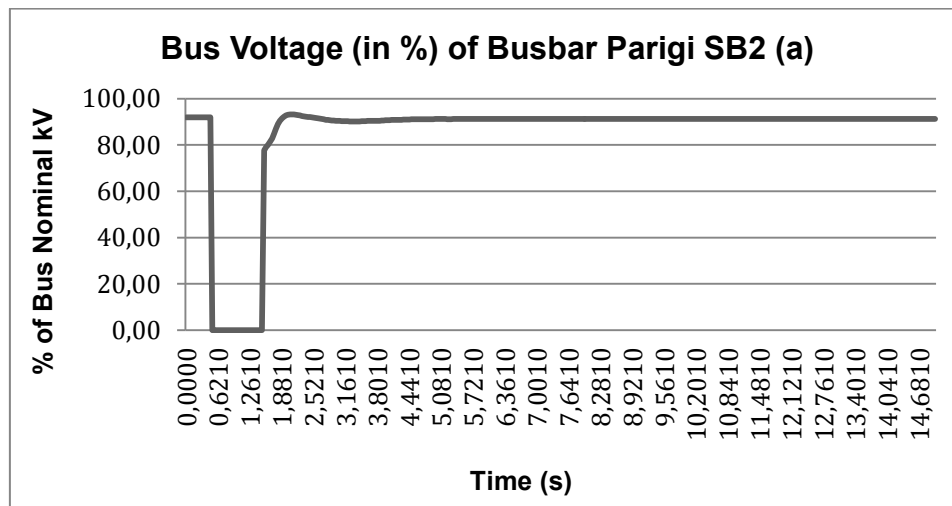


Figure 5-184: Parigi SB2 Bus Voltage Interruption Simulation Results on Situation A

Based on figure 5-184, before interruption, percentage of bus voltage was at 92 %kV. When the interruption was occurred, it dropped to zero during interruption. After interruption, percentage of bus voltage was immediately going up until 78 %kV and then it had been going up to 93 %kV in 0.5 seconds. It was slowly getting stable at 91 %kV at 4.7th second.

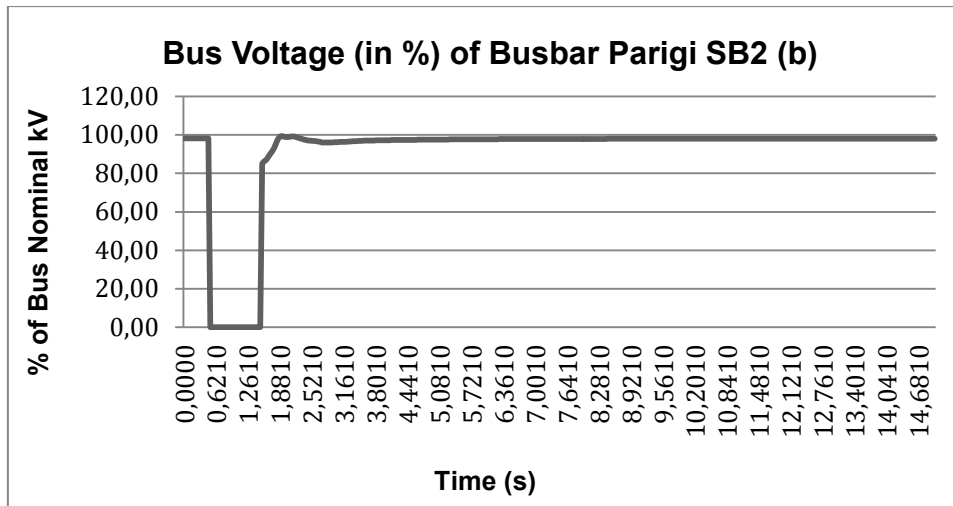


Figure 5-185: Parigi SB2 Bus Voltage Interruption Simulation Results on Situation B

Based on figure 5-185, before interruption, percentage of bus voltage was at 98 %kV. When the interruption was occurred, it dropped to zero during interruption. After interruption, percentage of bus voltage was immediately going up until 83 %kV and then it was going up to 99 %kV. It was slowly getting stable at 97 %kV at 8.9th second.

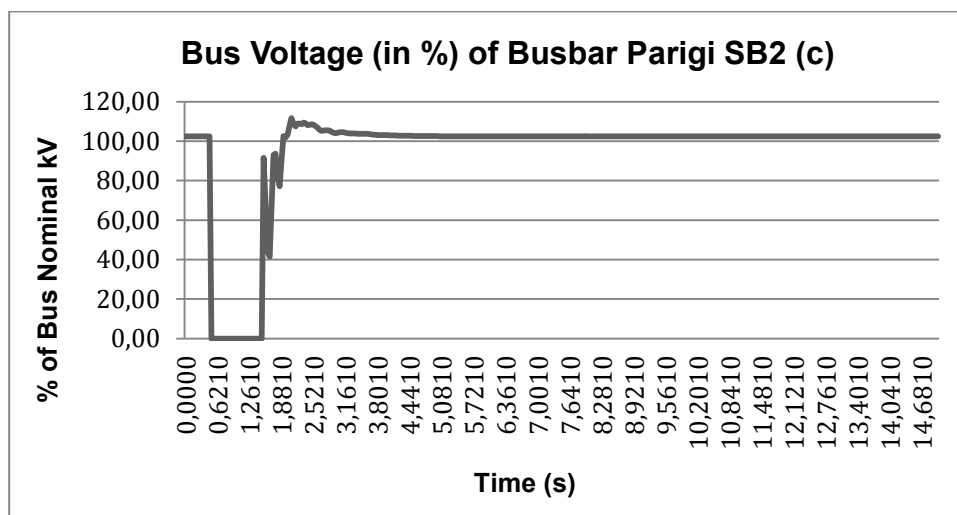


Figure 5-186: Parigi SB2 Bus Voltage Interruption Simulation Results on Situation C

Based on figure 5-186, before interruption, percentage of bus voltage was at 102 %kV. When the interruption was occurred, it dropped to zero during interruption. After interruption, percentage of bus voltage was going up until 92 %kV and then it had

been fluctuating between 92 %kV and 41 %kV for 0.5 seconds. It was going up to 110 %kV and it was slowly getting stable at 102 %kV at 4.6th second.

Bus voltage of interruption simulation results of bus bar PJPP SB1 before RE integration, after RE integration and after RE integration using homer results can be seen below.

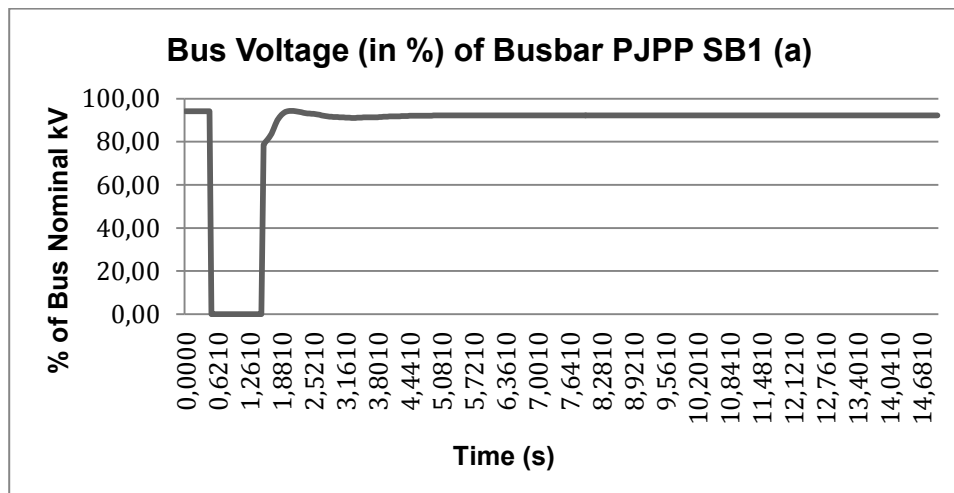


Figure 5-187: PJPP SB1 Bus Voltage Interruption Simulation Results on Situation A

Based on figure 5-187, before interruption, percentage of bus voltage was at 94 %kV. When the interruption was occurred, it dropped to zero during interruption. After interruption, percentage of bus voltage was immediately going up until 78 %kV and then it was going up to 95 %kV. It was slowly getting stable at 92 %kV at 7.5th second.

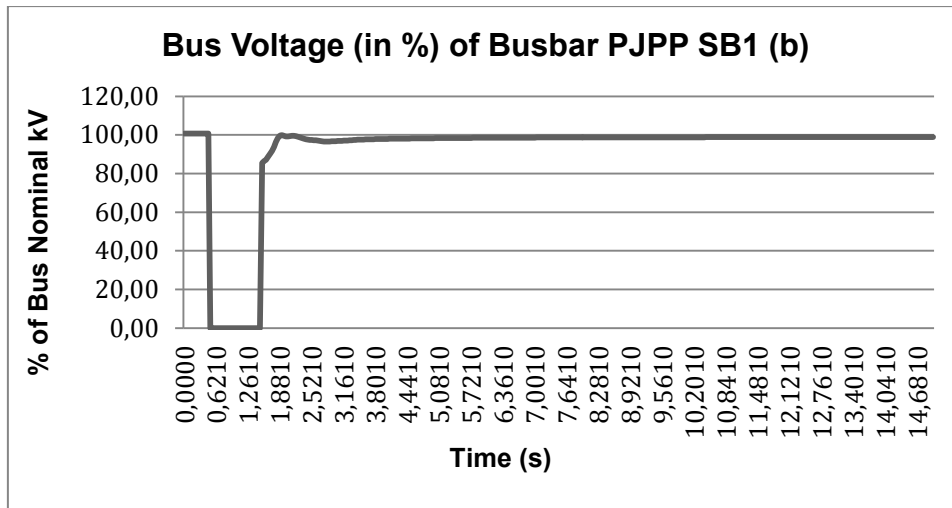


Figure 5-188: PJPP SB1 Bus Voltage Interruption Simulation Results on Situation B

Based on figure 5-188, before interruption, percentage of bus voltage was at 101 %kV. When the interruption was occurred, it dropped to zero during interruption. After interruption, percentage of bus voltage was going up until 88 %kV and then it had been going up to 100 %kV in 0.5 seconds. It was slowly getting stable at 100 %kV at 8.9th second.

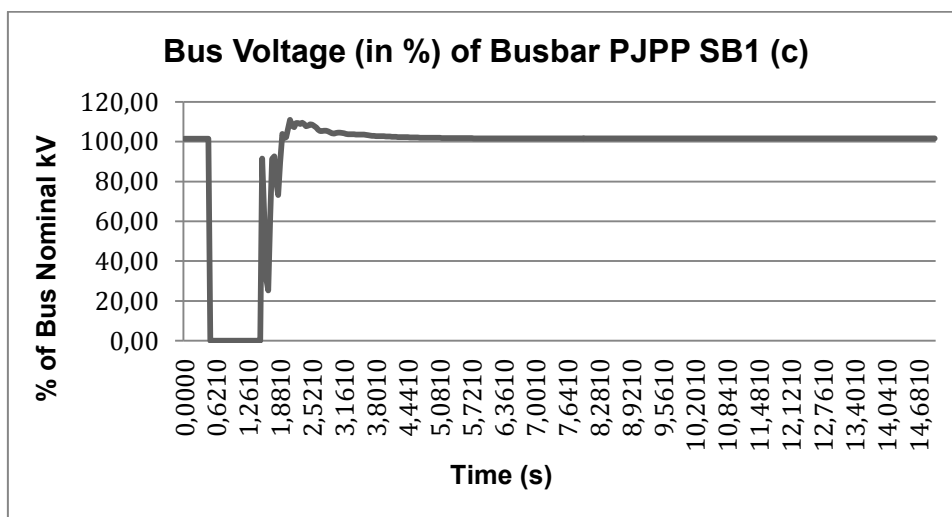


Figure 5-189: PJPP SB1 Bus Voltage Interruption Simulation Results on Situation C

Based on figure 5-189, before interruption, percentage of bus voltage was at 101.5 %kV. When the interruption was occurred, it dropped to zero during interruption. After interruption, percentage of bus voltage was going up until 92 %kV and then it had

been fluctuating between 92 %kV and 24 %kV for 0.5 seconds. It was going up to 110 %kV and getting stable at 101.5 %kV at 5.7th second.

Bus voltage of interruption simulation results of bus bar Silae SB1 before RE integration, after RE integration and after RE integration using homer results can be seen below.

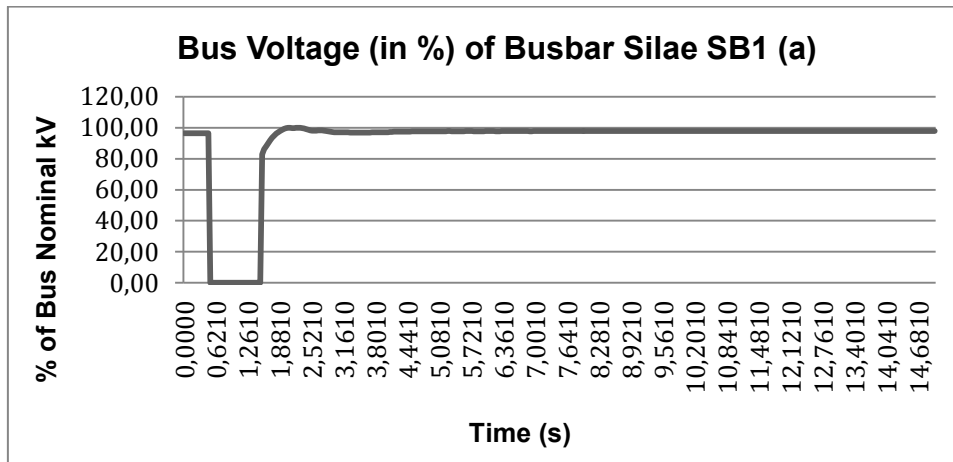


Figure 5-190: Silae SB1 Bus Voltage Interruption Simulation Results on Situation A

Based on figure 5-190, before interruption, percentage of bus voltage was at 97 %kV. When the interruption was occurred, it dropped to zero during interruption. After interruption, percentage of bus voltage was immediately going up until 83 %kV and then it had been going up to 100 %kV in 0.5 seconds. It was slowly getting stable at 98 %kV at 5.2nd second.

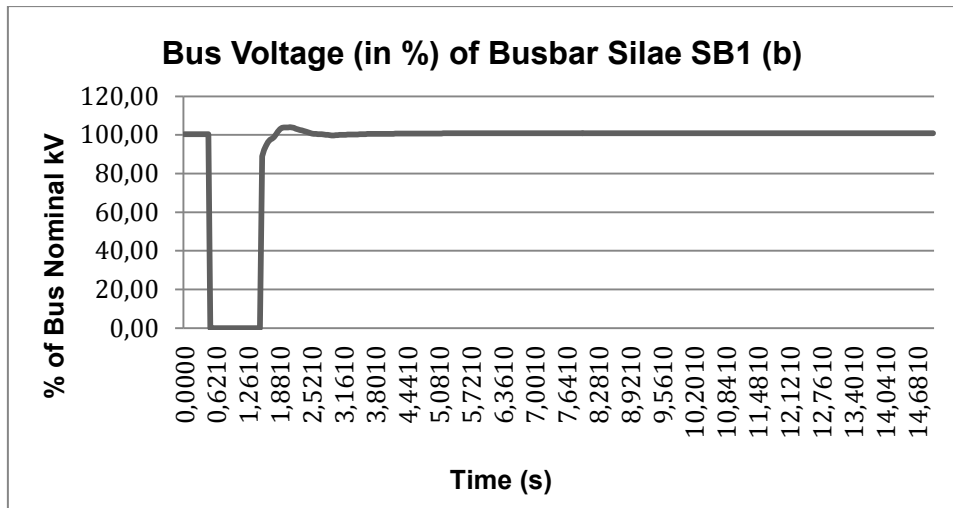


Figure 5-191: Silae SB1 Bus Voltage Interruption Simulation Results on Situation B

Based on figure 5-191, before interruption, percentage of bus voltage was at 100 %kV. When the interruption was occurred, it dropped to zero during interruption. After interruption, percentage of bus voltage was going up until 88 %kV and then it had been going up to 102 %kV in 0.5 seconds. It was slowly getting stable at 100 %kV at 7.4th second.

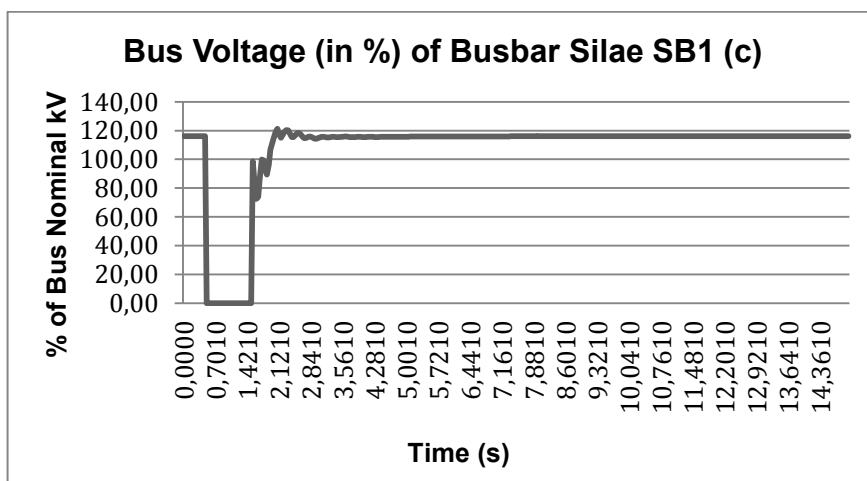


Figure 5-192: Silae SB1 Bus Voltage Interruption Simulation Results on Situation C

Based on figure 5-192, before interruption, percentage of voltage was at 116 %kV. When the interruption was occurred, it dropped to zero during interruption. After interruption, percentage of bus voltage was immediately going up until 99 %kV and

then it had been fluctuating between 99 %kV and 72 %kV for 0.5 seconds. It was going up to 121 %kV and it was getting stable at 116 %kV at 5.5th second.

Bus voltage of interruption simulation results of Silae SB2 and Silae SB3 bus bar before RE integration, after RE integration and after RE integration using homer results are equal to voltage simulation results of Silae SB1 bus bar on all situations.

Bus voltage of interruption simulation results of bus bar Silae SB4 before RE integration, after RE integration and after RE integration using homer results can be seen below.

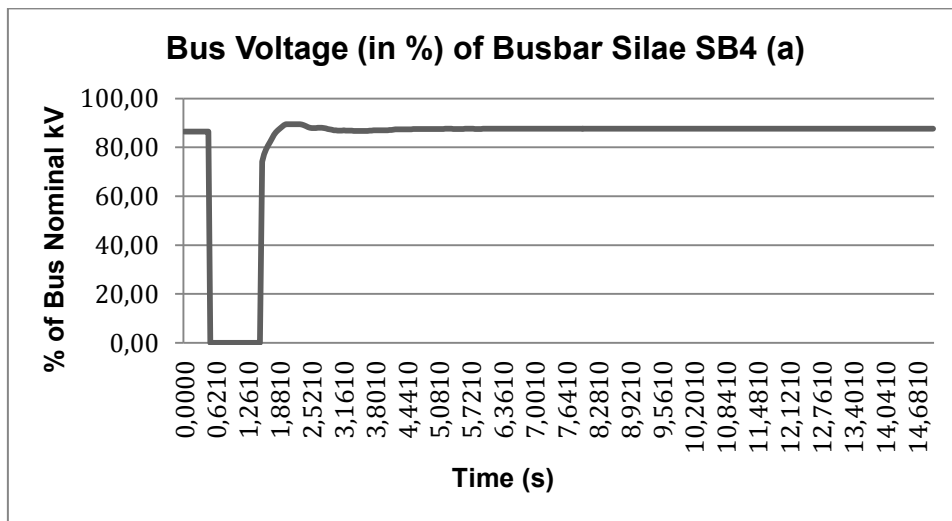


Figure 5-193: Silae SB4 Bus Voltage Interruption Simulation Results on Situation A

Based on figure 5-193, before interruption, percentage of bus voltage was at 96 %kV. When the interruption was occurred, it dropped to zero during interruption. After interruption, percentage of bus voltage was going up until 73 %kV and then it had been going up to 89 %kV in 0.5 seconds. It was slowly getting stable at 96 %kV at 4.7th second.

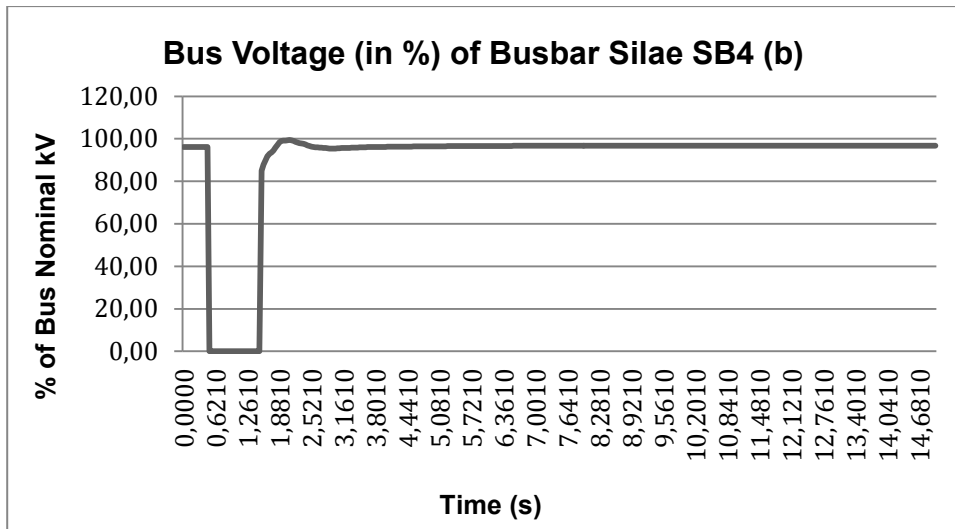


Figure 5-194: Silae SB4 Bus Voltage Interruption Simulation Results on Situation B

Based on figure 5-194, before interruption, percentage of bus voltage was at 96 %kV. When the interruption was occurred, it dropped to zero during interruption. After interruption, percentage of bus voltage was going up until 84 %kV and it had been going up to 99 %kV in 0.5 seconds. It was slowly getting stable at 99 %kV at 5.9th second.

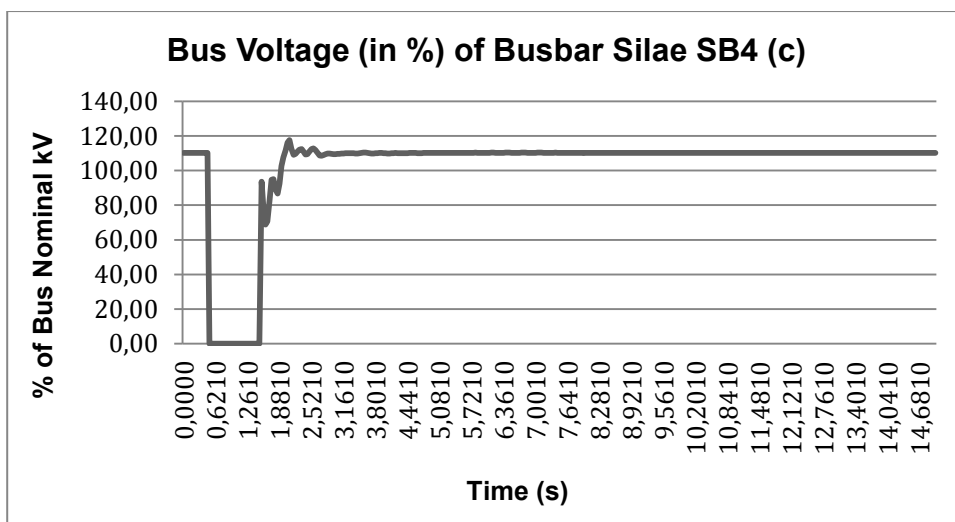


Figure 5-195: Silae SB4 Bus Voltage Interruption Simulation Results on Situation C

Based on figure 5-195, before interruption, percentage of bus voltage was at 109 %kV. When the interruption was occurred, it dropped to zero during interruption. After interruption, percentage of bus voltage was going up to 93 %kV and then it had been

fluctuating between 93 %kV and 68 %kV. It was going up to 118 %kV and then it was getting stable at 110 %kV at 5.4th second.

Bus voltage of interruption simulation results of bus bar Talise SB1 before RE integration, after RE integration and after RE integration using homer results can be seen below.

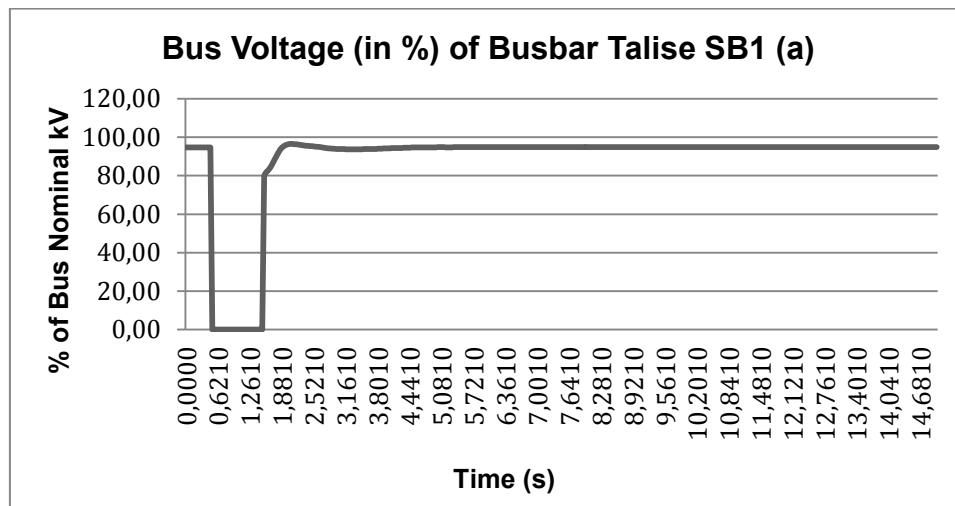


Figure 5-196: Talise SB1 Bus Voltage Interruption Simulation Results on Situation A

Based on figure 5-196, before interruption, percentage of bus voltage was at 95 %kV. When the interruption was occurred, it dropped to zero during interruption. After interruption, percentage of bus voltage was going up until 84 %kV and then it had been going up to 97 %kV in 0.5 seconds. It was slowly getting stable at 96 %kV at 4.6th second.

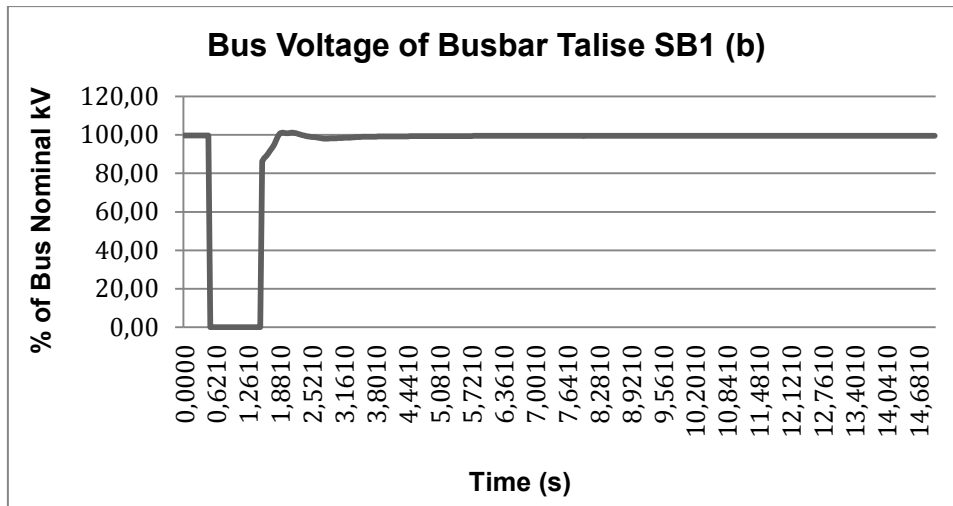


Figure 5-197: Talise SB1 Bus Voltage Interruption Simulation Results on Situation B

Based on figure 5-197, before interruption, percentage of bus voltage was at 99 %kV. When the interruption was occurred, bus voltage dropped to zero during interruption. After interruption, percentage of bus voltage was going up until 86 %kV and then it had been going up to 100 %kV in 0.5 seconds. It was slowly getting stable at 99 %kV at 5.7th second.

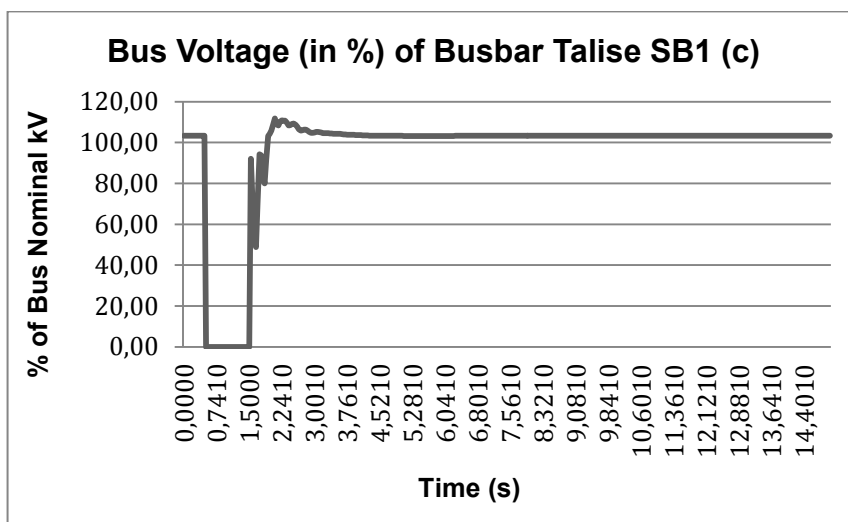


Figure 5-198: Talise SB1 Bus Voltage Interruption Simulation Results on Situation C

Based on figure 5-198, before interruption, percentage of bus voltage was at 103 %kV. When the interruption was occurred, it dropped to zero during interruption. After interruption, percentage of bus voltage was going up to 95 %kV and then it had been

fluctuating between 95 %kV and 49 %kV for 0.5 seconds. It was going up to 110 %kV and then it was getting stable at 102 %kV at 6.8th second.

Bus voltage of interruption simulation results of bus bar Talise SB2 before RE integration, after RE integration and after RE integration using homer results can be seen below.

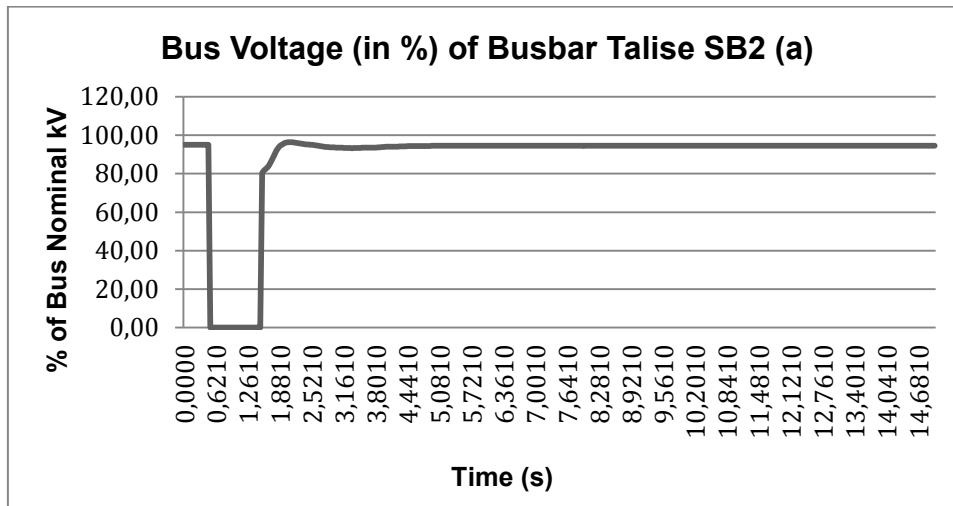


Figure 5-199: Talise SB2 Bus Voltage Interruption Simulation Results on situation A

Based on figure 5-199, before interruption, percentage of bus voltage was at 95 %kV. When the interruption was occurred, bus voltage dropped to zero during interruption. After interruption, percentage of bus voltage was going up to 80 %kV and then it had been going up to 96 %kV in 0.5 seconds. It was slowly getting stable at 94 %kV at 5.6th second.

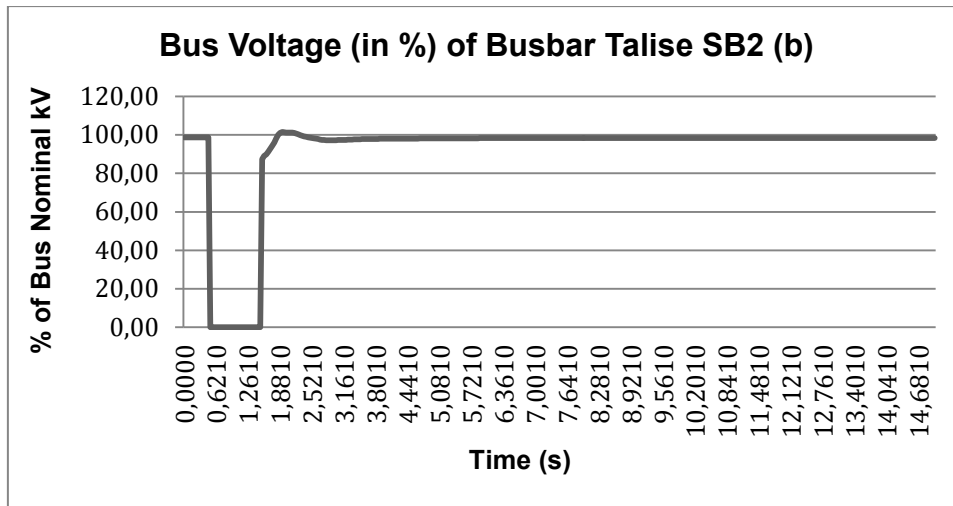


Figure 5-200: Talise SB2 Bus Voltage Interruption Simulation Results on Situation B

Based on figure 5-200, before interruption, percentage of bus voltage was at 98.5 %kV. When the interruption was occurred, it dropped to zero during interruption. After interruption, percentage of bus voltage was going up to 88 %kV and then it had been going up to 101 in 0.5 seconds. It was slowly getting stable at 99.5 %kV at 8th second.

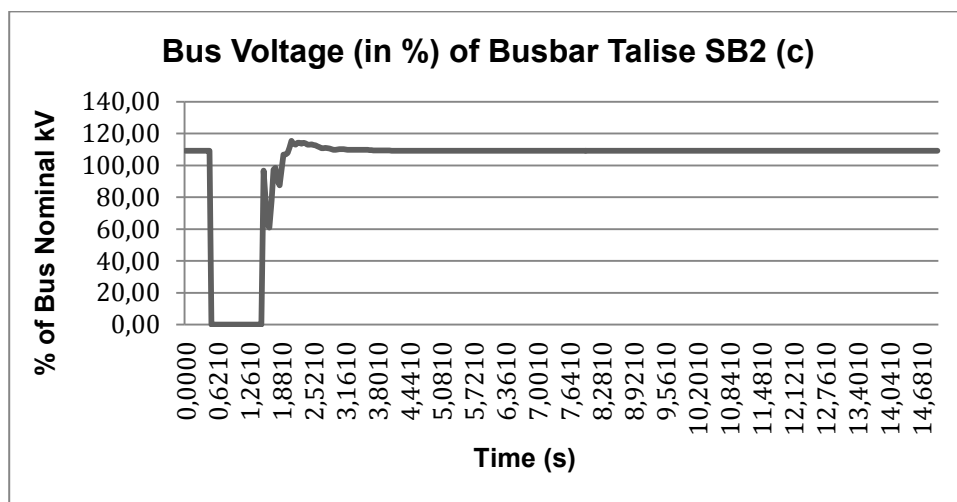


Figure 5-201: Talise SB2 Bus Voltage Interruption Simulation Results on Situation C

Based on figure 5-201, before interruption, percentage of bus voltage was at 109.5 %kV. When the interruption was occurred, it dropped to zero during interruption. After interruption, percentage of bus voltage was going up to 97 %kV and then it had been

fluctuating between 97 %kV and 61 %kV for 0.5 seconds. It was going up to 112 %kV and then it was getting stable at 109.5 %kV at 4.5th second.

Bus voltage of interruption simulation results of Talise SB3 bus bar before RE integration, after RE integration and after RE integration using homer results is equal to bus voltage of interruption simulation results of Talise SB3 bus bar on all situations.

Bus voltage of interruption simulation results of bus bar Talise DB1 before RE integration, after RE integration and after RE integration using homer results can be seen below.

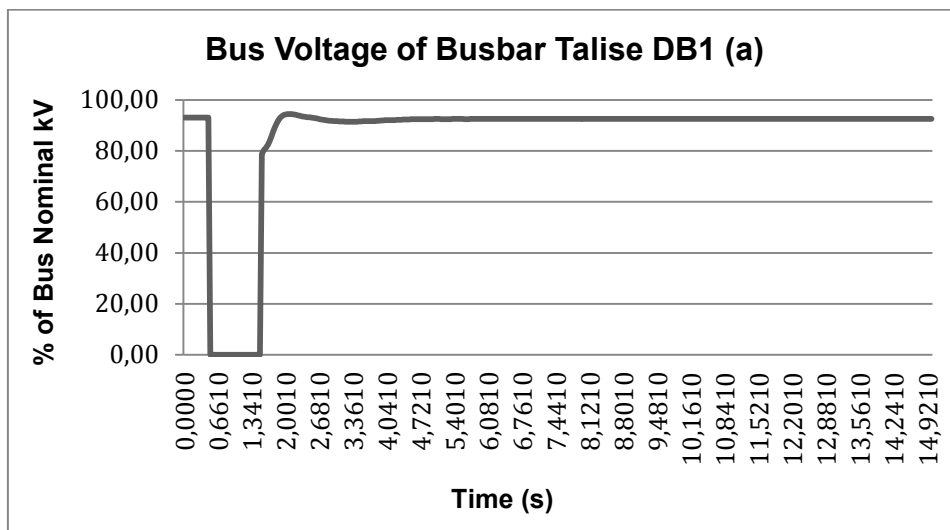


Figure 5-202: Talise DB1 Bus Voltage Interruption Simulation Results on Situation A

Based on figure 5-202, before interruption, percentage of bus voltage was at 94 %kV. When the interruption was occurred, it dropped to zero during interruption. After interruption, percentage of bus voltage was going up to 78 %kV and then it had been going up to 96 %kV in 0.5 seconds. It was slowly getting stable at 93 %kV at 4.8thsecond.

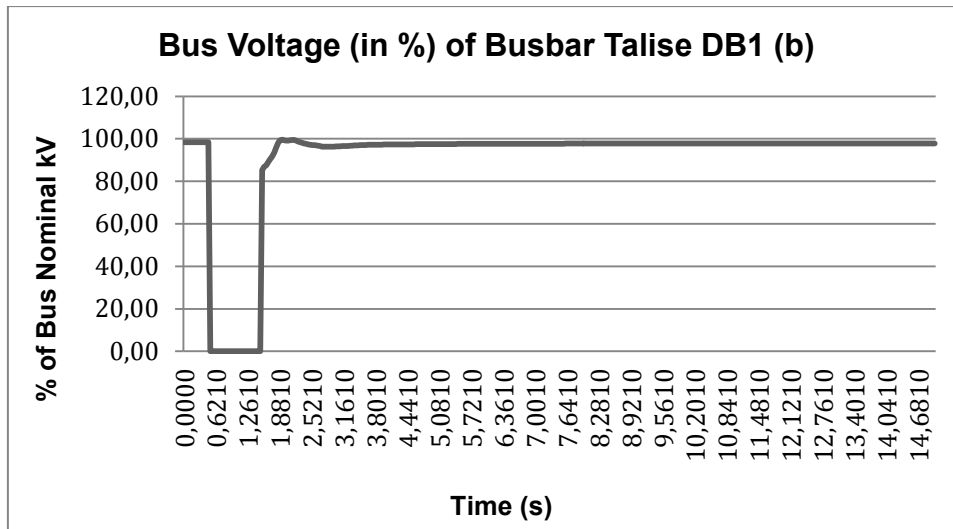


Figure 5-203: Talise DB1 Bus Voltage Interruption Simulation Results on Situation B

Based on figure 5-203, before interruption, percentage of bus voltage was at 99 %kV. When the interruption was occurred, it dropped to zero during interruption. After interruption, percentage of bus voltage was going up to 84 %kV and then it had been going up to 99 %kV in 0.5 seconds. It was slowly getting stable at 98 %kV at 4.9th second.

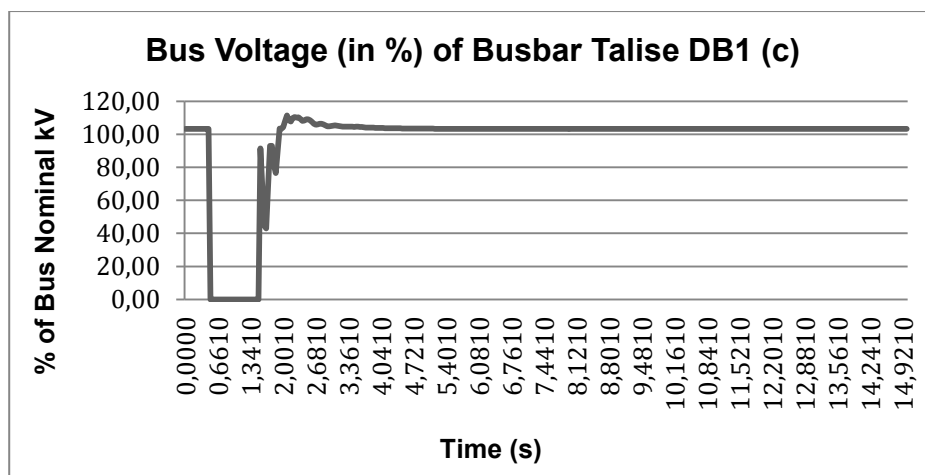


Figure 5-204: Talise DB1 Bus Voltage Interruption Simulation Results on Situation C

Based on figure 5-204, before interruption, percentage of bus voltage was at 102 %kV. When the interruption was occurred, it dropped to zero during interruption. After interruption, percentage of bus voltage was going up to 92 %kV and then it had been

fluctuating between 92 %kV and 41 %kV for 0.5 seconds. It was going up to 111 %kV and then getting stable at 102 %kV at 6th second.

Bus voltage of interruption simulation results of Talise DB11 bus bar before RE integration, after RE integration and after RE integration using homer results is equal to bus voltage of interruption simulation results of Talise DB1 bus bar on all situations.

Bus frequency of interruption simulation results of bus bar DB1 PJPP before RE integration, after RE integration and after RE integration using homer results can be seen below.

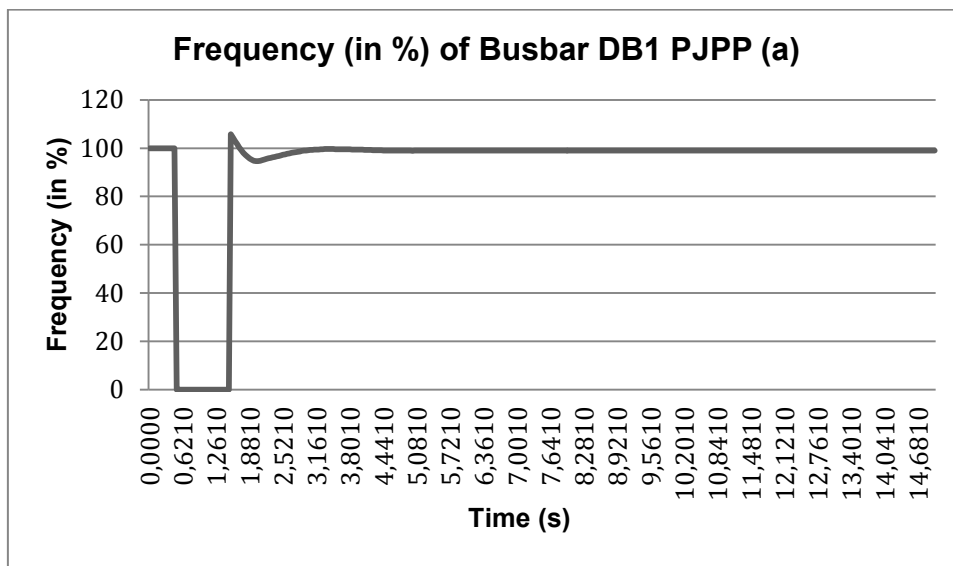


Figure 5-205: DB1 PJPP Bus Frequency Interruption Simulation Results on Situation A

Based on figure 5-205, before interruption, percentage of bus frequency was at 100 %. When the interruption was occurred, it dropped to zero during interruption. After interruption, bus frequency was starting going up until 107 % and then it had been going down until 94 % in 0.5 seconds. It got stable at 4.5th second at 100 %.

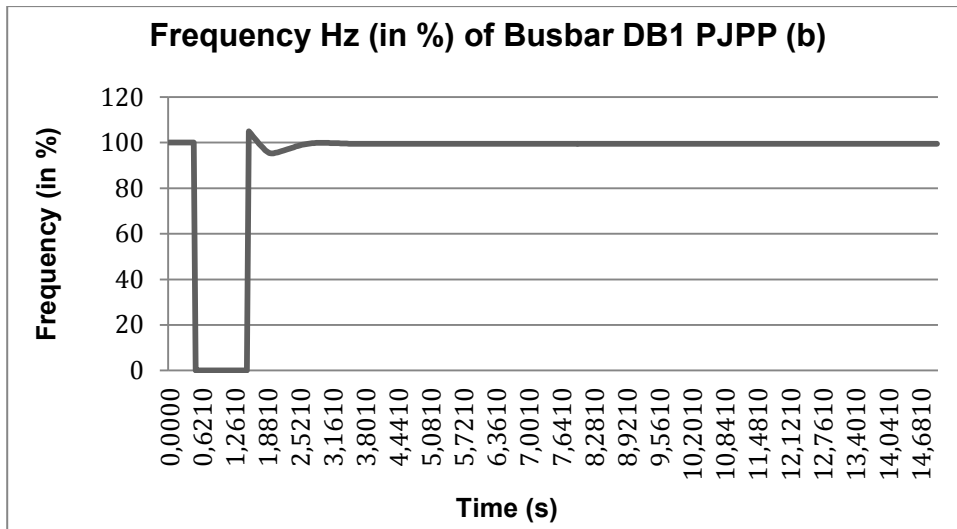


Figure 5-206: DB1 PJPP Bus Frequency Interruption Simulation Results on Situation B

Based on figure 5-206, before interruption, percentage of bus frequency was at 100 %. When the interruption was occurred, it dropped to zero during interruption. After interruption, percentage of bus frequency was starting going up until 105 % and then it had been going down until 95 % in 0.5 seconds. It gets stable at 3.3th second at 100 %.

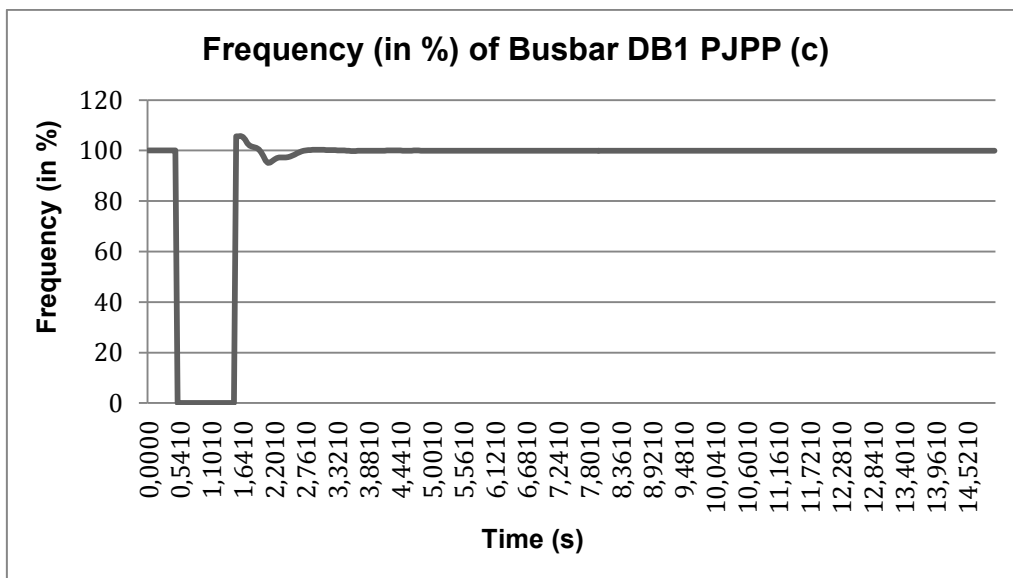


Figure 5-207: DB1 PJPP Bus Frequency Interruption Simulation Results on Situation C

Based on figure 5-207, before interruption, bus frequency was at 100 %. When the interruption was occurred, it dropped to zero during interruption. After interruption, bus frequency was starting going up until 106 % % and then it had been going down until 96 % with a small fluctuation in 0.5 seconds. It got stable at 3.3th second at 100 %.

Bus frequency of interruption simulation results of DB11 PJPP bus bar before RE integration, after RE integration and after RE integration using homer results is equal to bus frequency of interruption simulation results of DB1 PJPP bus bar on all situations.

Bus frequency of interruption simulation results of bus bar Donggala SB1 before RE integration, after RE integration and after RE integration using homer results can be seen below.

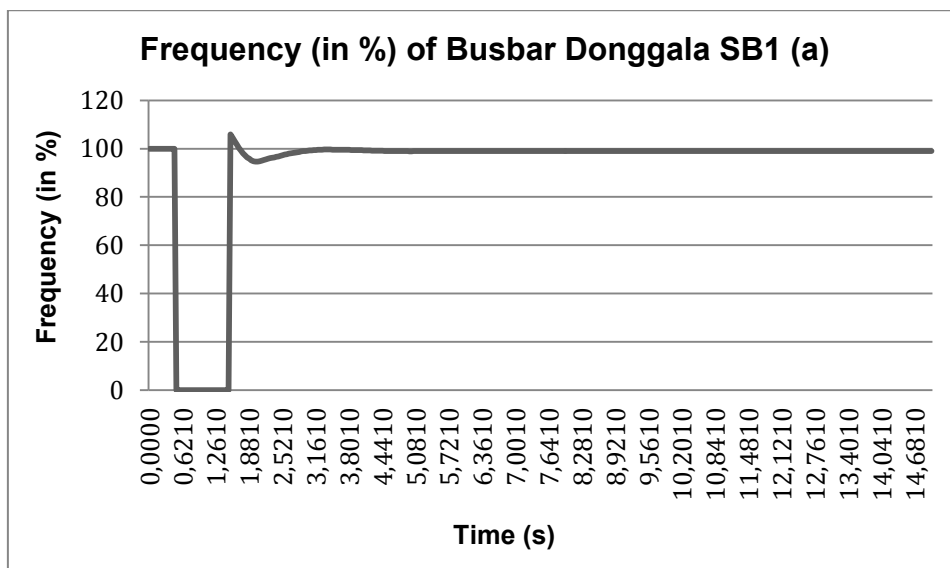


Figure 5-208: Donggala SB1 Bus Frequency Interruption Simulation Results on Situation A

Based on figure 5-208, before interruption, percentage of bus frequency was at 100 %. When the interruption was occurred, it dropped to zero during interruption. After interruption, percentage of bus frequency was starting going up until 106 % and then it had been going down until 92 % in 0.5 seconds. It reached stable at 13.7th second at 100 %.

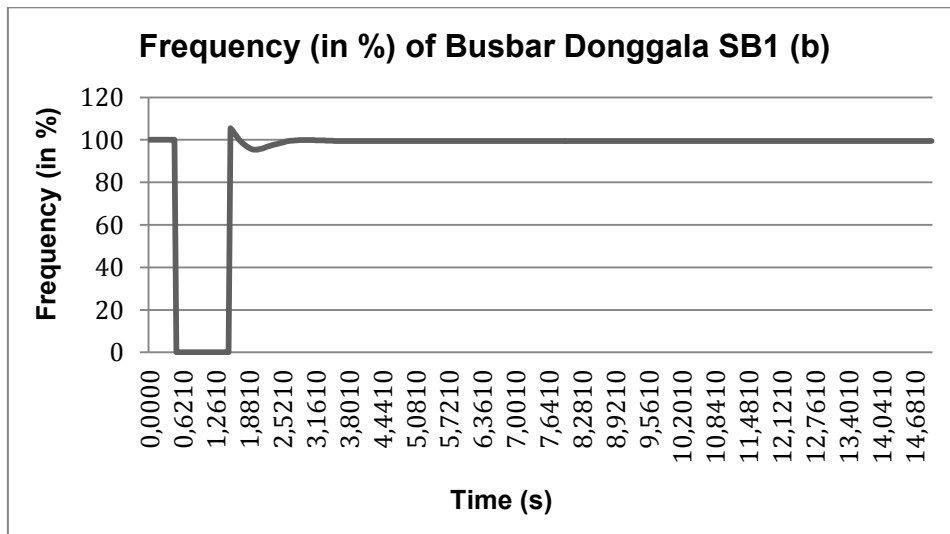


Figure 5-209: Donggala SB1 Bus Frequency Interruption Simulation Results on Situation B

Based on figure 5-209, before interruption, percentage of bus frequency was at 100 %. When the interruption was occurred, it dropped to zero during interruption. After interruption, bus frequency was starting going up until 106 % and then it had been going down until 96 % in 0.7 seconds. It reached stable at 3.4th second at 100 %.

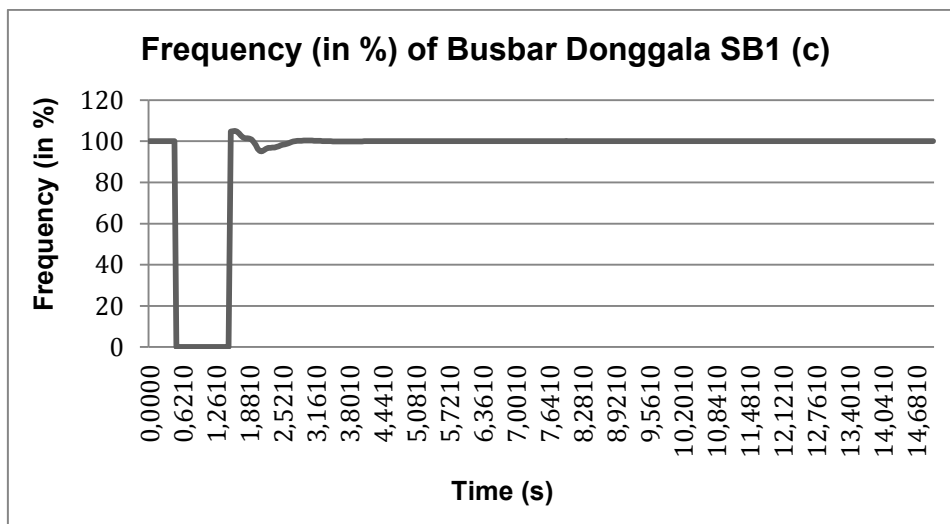


Figure 5-210: Donggala SB1 Bus Frequency Interruption Simulation Results on Situation C

Based on figure 5-210, before interruption, percentage of bus frequency was at 100 %. When the interruption was occurred, it dropped to zero during interruption. After

interruption, bus frequency was starting going up until 105 % and then it had been going down until 96 % in 0.7 seconds with a small fluctuation. It was getting stable at 3.1th second at 100 %.

Bus frequency of interruption simulation results of bus bar Maesa SB1 before RE integration, after RE integration and after RE integration using homer results can be seen below.

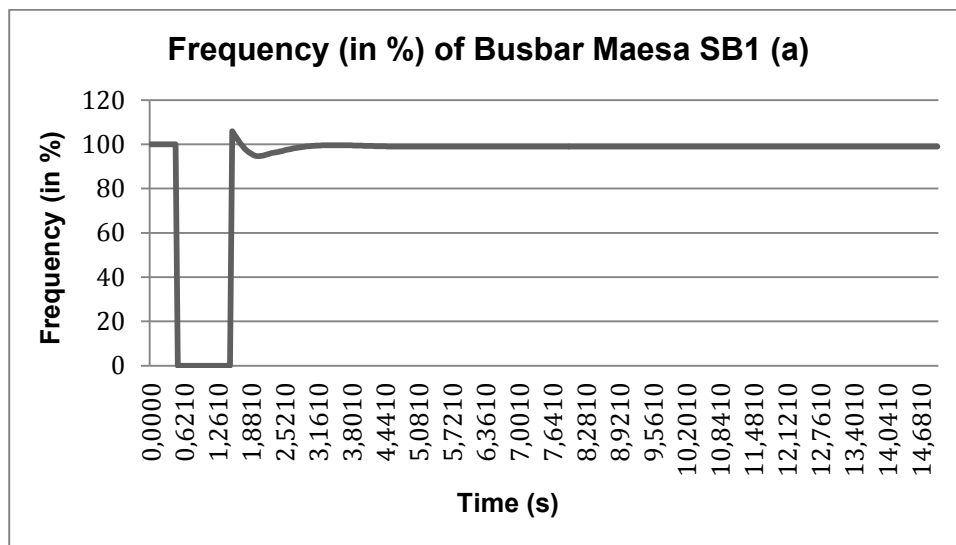


Figure 5-211: Maesa SB1 Bus Frequency Interruption Simulation Results on Situation A

Based on figure 5-211, before interruption, percentage of bus frequency was at 100 %. When the interruption was occurred, percentage bus frequency dropped to zero during interruption. After interruption, it was starting going up until 107 % and then it had been going down until 92 % in 0.5 seconds. It reached stable at 4.4th second at 100 %.

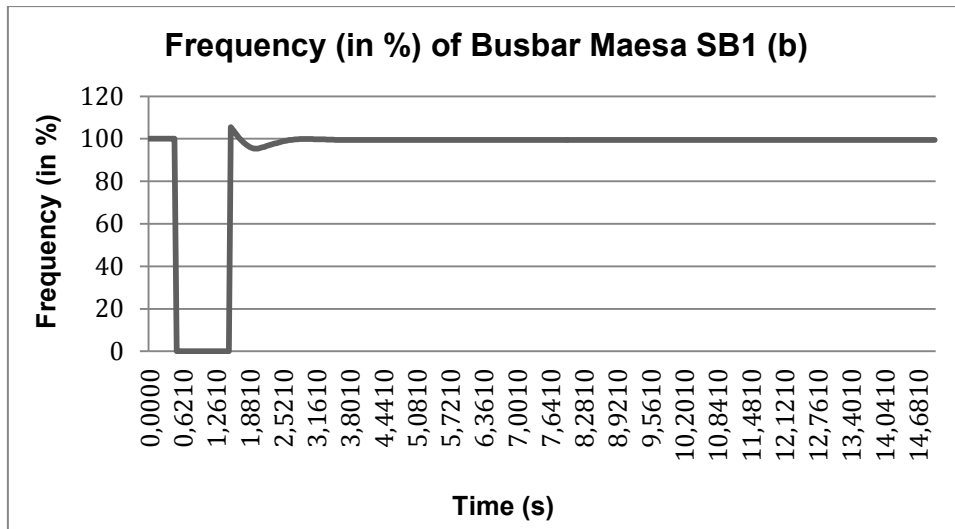


Figure 5-212: Maesa SB1 Bus Frequency Interruption Simulation Results on Situation B

Based on figure 5-212, before interruption, percentage of bus frequency was at 100 %. When the interruption is occurred, it dropped to zero during interruption. After interruption, it was starting going up until 106 % and then it had been going down until 96 % in 0.7 seconds. It reached stable at 3.5th second at 100 %.

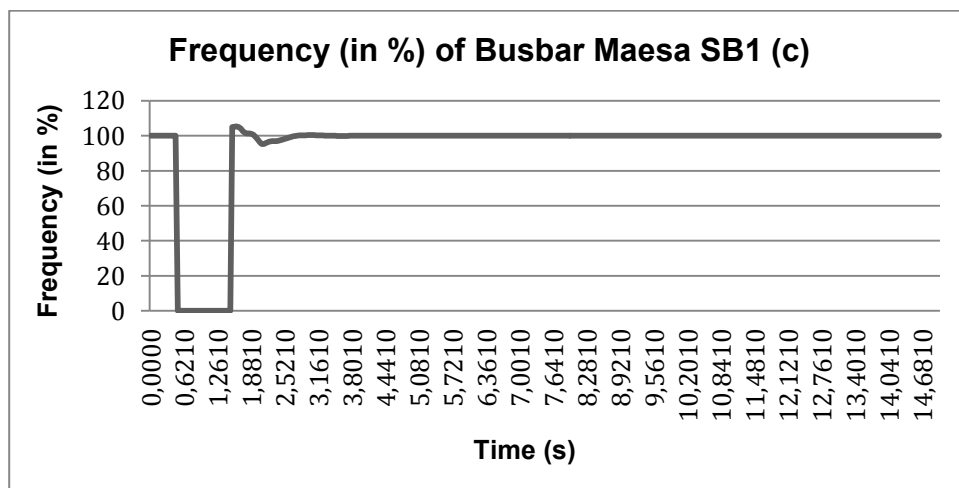


Figure 5-213: Maesa SB1 Bus Frequency Interruption Simulation Results on Situation C

Based on figure 5-213, before interruption, percentage of bus frequency was at 100 %. When the interruption was occurred, it dropped to zero during interruption. After interruption, percentage bus frequency was starting going up until 105 % % and then

it had been going down until 96 % in 0.7 seconds with a small fluctuation. It reached stable at 3.5th second at 100 %.

Bus frequency of interruption simulation results of Maesa SB1 (2) bus bar before RE integration, after RE integration and after RE integration using homer results is equal to bus frequency of interruption simulation results of Maesa SB1 bus bar on all situations.

Bus frequency of interruption simulation results of bus bar Parigi DB1 before RE integration, after RE integration and after RE integration using homer results can be seen below.

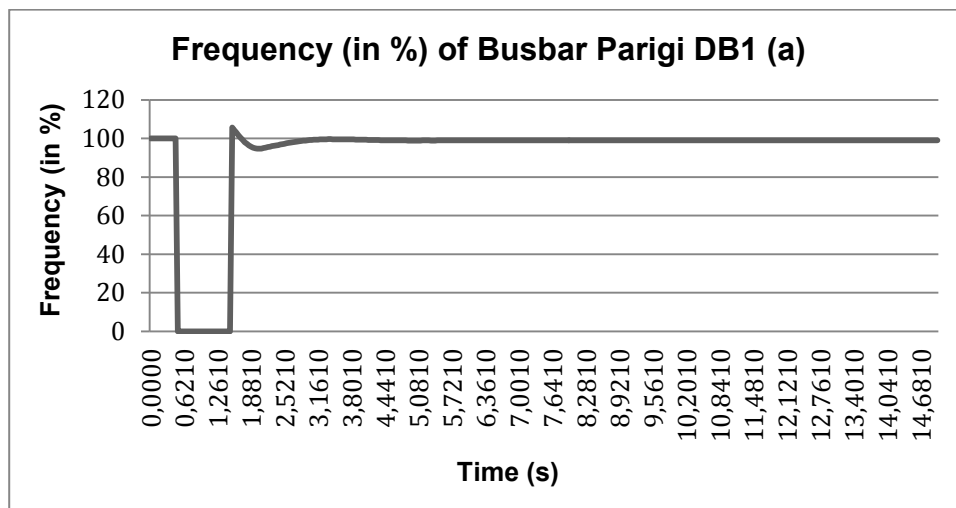


Figure 5-214: Parigi DB1 Bus Frequency Interruption Simulation Results on Situation A

Based on figure 5-214, before interruption, percentage of bus frequency was at 100 %. When the interruption was occurred, it dropped to zero during interruption. After interruption, percentage of bus frequency was starting going up until 105 % and then it had been going down until 92 % in 0.5 seconds. It reached stable at 11.5th second at 100 %.

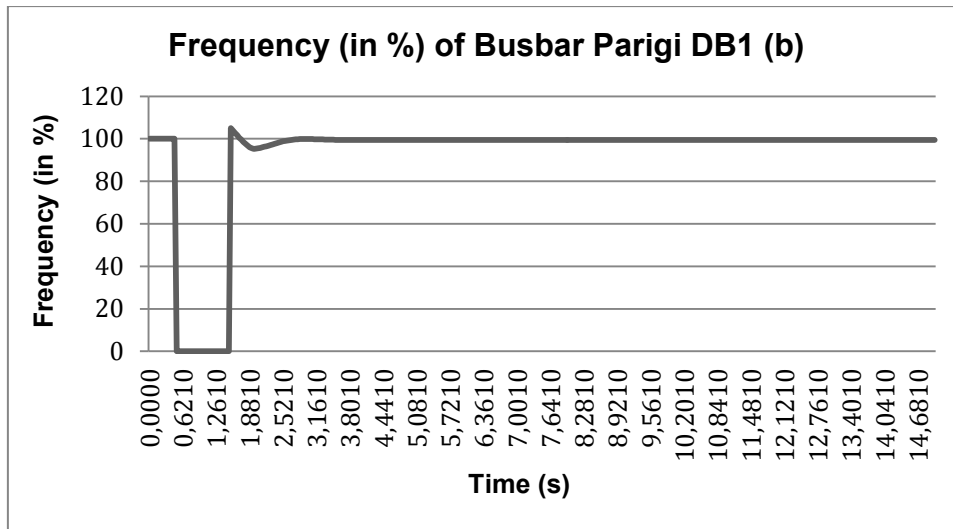


Figure 5-215: Parigi DB1 Bus Frequency Interruption Simulation Results on Situation B

Based on figure 5-215, before interruption, percentage of bus frequency was at 100 %. When the interruption was occurred, it dropped to zero during interruption. After interruption, percentage bus frequency was starting going up until 106 % and then it had been going down until 96 % in 0.7 seconds. It reached stable at 3.6th second at 100 %.

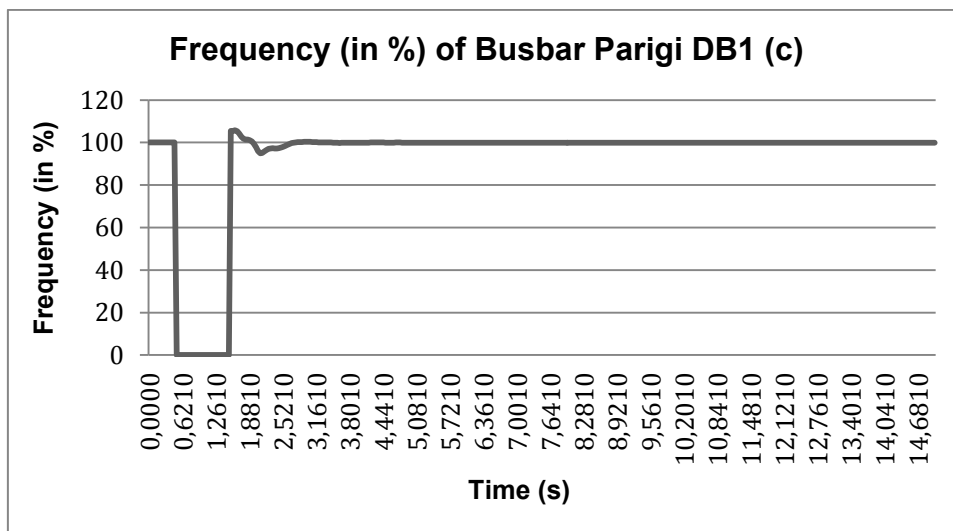


Figure 5-216: Parigi DB1 Bus Frequency Interruption Simulation Results on Situation C

Based on figure 5-216, before interruption, percentage of bus frequency was at 100 %. When the interruption was occurred, it dropped to zero during interruption. After

interruption, percentage of bus frequency was starting going up until 106 % and then it had been going down until 96 % in 0.7 seconds with a small fluctuation. It reached stable at 3.5th second at 100 %.

Bus frequency of interruption simulation results of Parigi DB1 (2) bus bar before RE integration, after RE integration and after RE integration using homer results is equal to bus frequency of interruption simulation results of Parigi DB1 bus bar on all situations.

Bus frequency of interruption simulation results of bus bar Parigi SB1 before RE integration, after RE integration and after RE integration using homer results can be seen below.

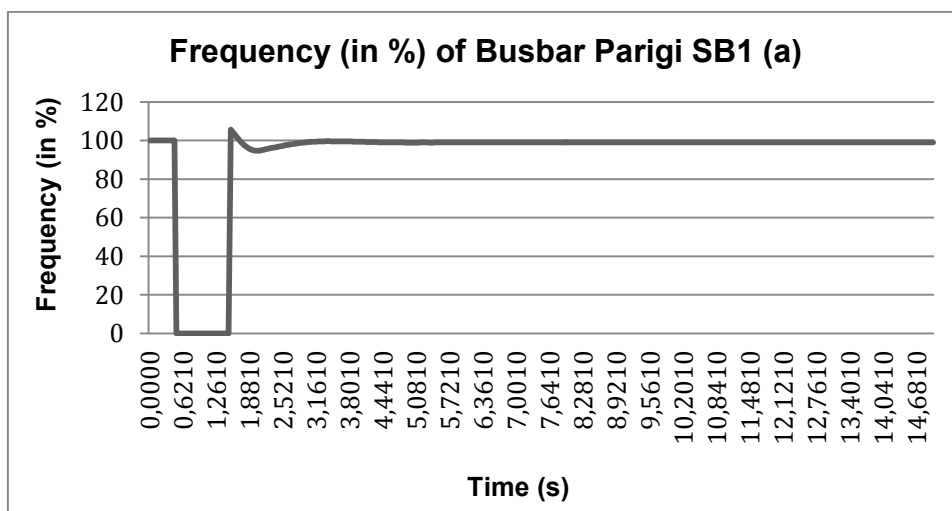


Figure 5-217: Parigi SB1 Bus Frequency Interruption Simulation Results on Situation A

Based on figure 5-217, before interruption, percentage of bus frequency was at 100 %. When the interruption was occurred, it dropped to zero during interruption. After interruption, percentage of bus frequency was starting going up until 106 % and then it had been going down until 92 % in 0.5 seconds. It reached stable at 4.5th second at 100 %.

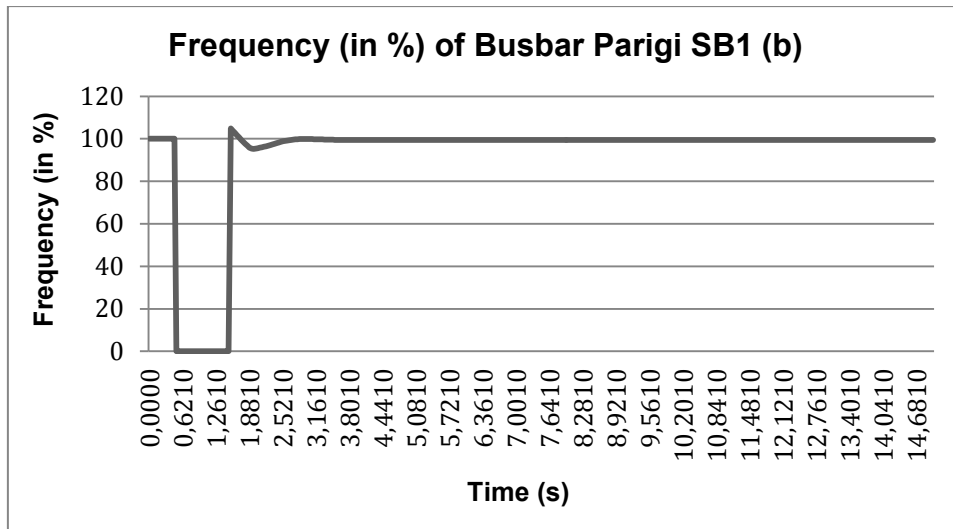


Figure 5-218: Parigi SB1 Bus Frequency Interruption Simulation Results on Situation B

Based on figure 5-218, before interruption, percentage of bus frequency was at 100 %. When the interruption was occurred, it dropped to zero during interruption. After interruption, percentage of bus frequency was starting going up until 106 % and then it had been going down until 96 % in 0.7 seconds. It reached stable at 3.4th second at 100 %.

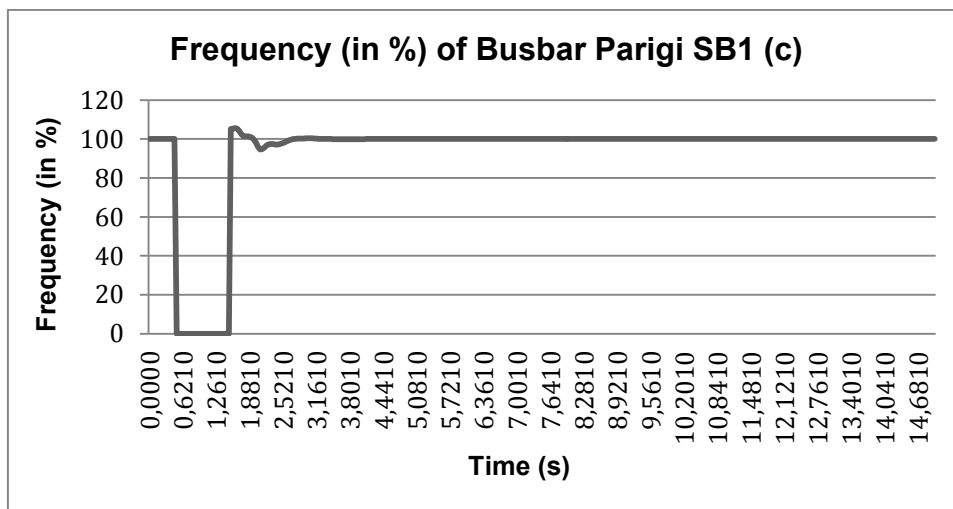


Figure 5-219: Parigi SB1 Bus Frequency Interruption Simulation Results on Situation C

Based on figure 5-219, before interruption, percentage of bus frequency was at 100 %. When the interruption was occurred, bus it dropped to zero during interruption.

After interruption, percentage bus frequency was starting going up until 106 % % and then it had been going down until 96 % in 0.7 seconds with a small fluctuation. It reached stable at 3.5th second at 100 %.

Bus frequency of interruption simulation results of bus bar Parigi SB2 before RE integration, after RE integration and after RE integration using homer results can be seen below.

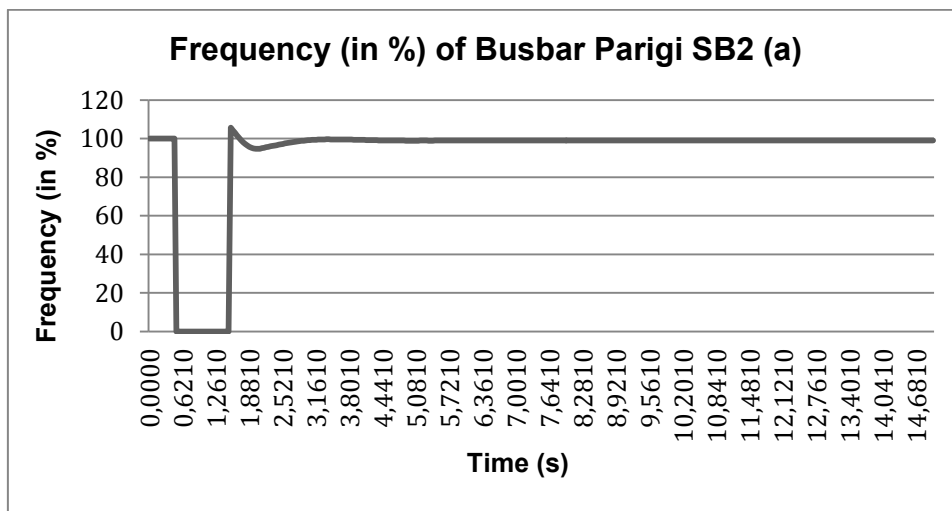


Figure 5-220: Parigi SB2 Bus Frequency Interruption Simulation Results on Situation A

Based on figure 5-220, before interruption, percentage of bus frequency was at 100 %. When the interruption was occurred, percentage of bus frequency dropped to zero during interruption. After interruption, it was starting going up until 106 % and then it had been going down until 92 % in 0.5 seconds. It was getting stable at 11.4th second at 100 %.

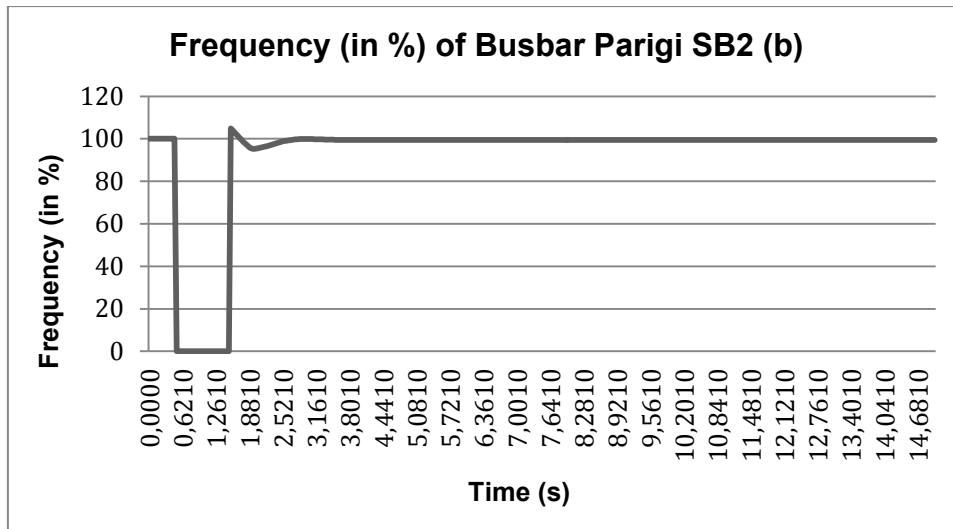


Figure 5-221: Parigi SB2 Bus Frequency Interruption Simulation Results on Situation B

Based on figure 5-221, before interruption, percentage of bus frequency was at 100 %. When the interruption was occurred, it dropped to zero during interruption. After interruption, percentage of bus frequency was starting going up until 106 % and then it had been going down until 96 % in 0.5 seconds. It reached stable at 3.4th second at 100 %.

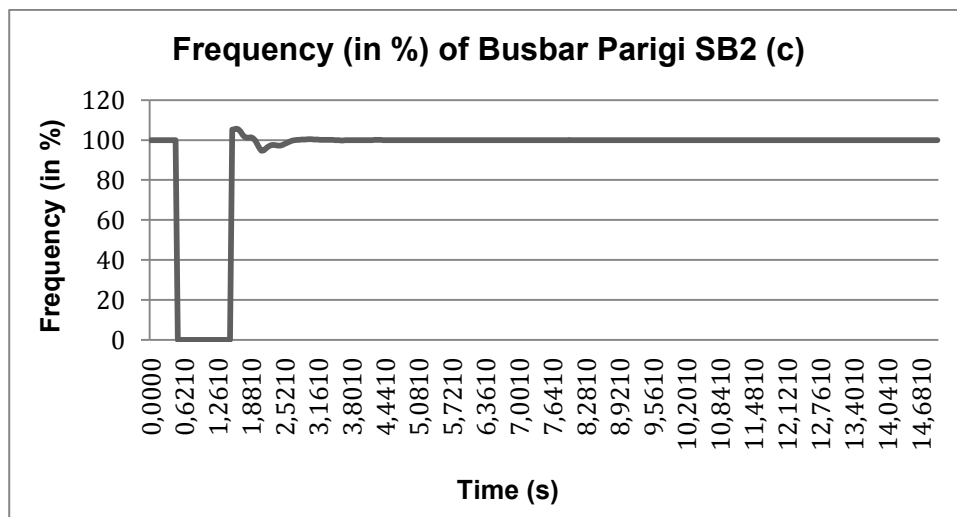


Figure 5-222: Parigi SB2 Bus Frequency Interruption Simulation Results on Situation C

Based on figure 5-222, before interruption, percentage of bus frequency was at 100 %. When the interruption was occurred, it dropped to zero during interruption. After

interruption, percentage of bus frequency was starting going up until 106 % and then it had been going down until 96 % in 0.7 seconds with a small fluctuation. It reached stable at 3.1st second at 100 %.

Bus frequency of interruption simulation results of bus bar Parigi SB1 (2) before RE integration, after RE integration and after RE integration using homer results can be seen below.

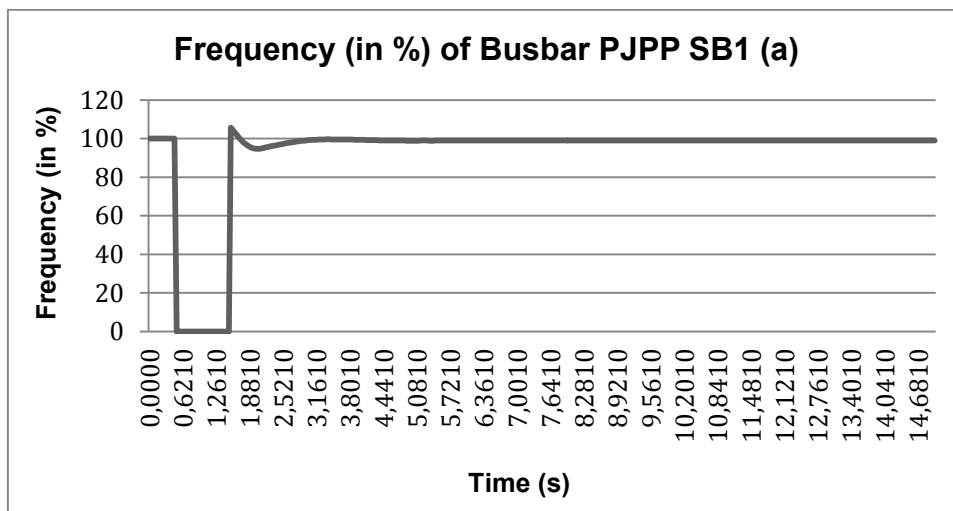


Figure 5-223: PJPP SB1 Bus Frequency Interruption Simulation Results on Situation A

Based on figure 5-223, before interruption, percentage of bus frequency was at 100 %. When the interruption was occurred, it dropped to zero during interruption. After interruption, percentage of bus frequency was starting going up until 106 % and then it had been going down until 93 % in 0.5 seconds. It reached stable at 4.5th second at 100 %.

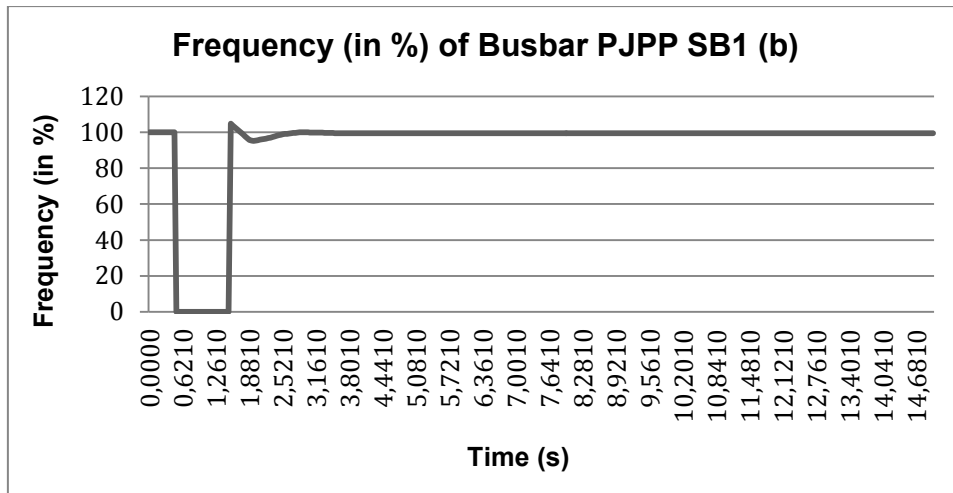


Figure 5-224: PJPP SB1 Bus Frequency Interruption Simulation Results on Situation B

Based on figure 5-224, before interruption, percentage of bus frequency was at 100 %. When the interruption was occurred, percentage of bus frequency dropped to zero during interruption. After interruption, it was starting going up until 106 % and then it had been going down until 96 % in 0.5 seconds. It reached stable at 3.6th second at 100 %.

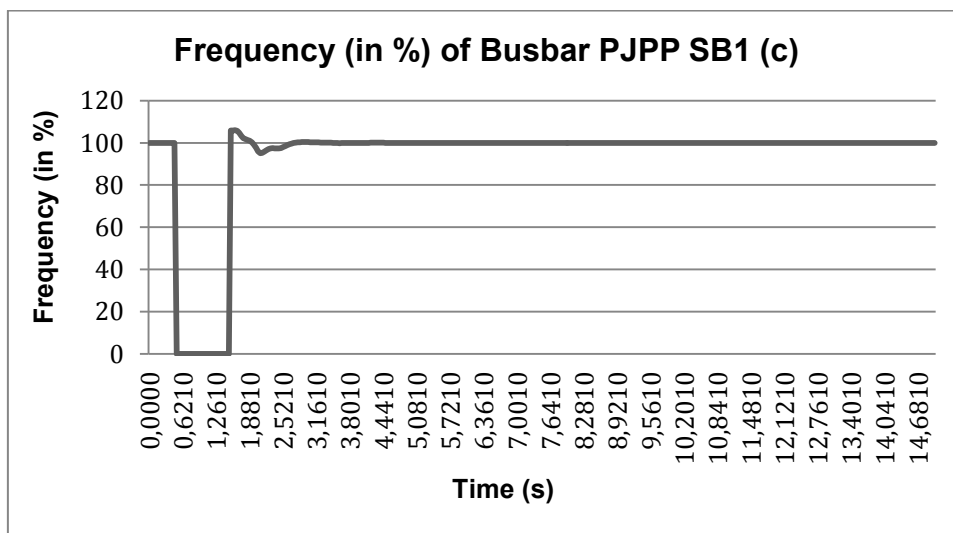


Figure 5-225: PJPP SB1 Bus Frequency Interruption Simulation Results on Situation C

Based on figure 5-225, before interruption, percentage of bus frequency was at 100 %. When the interruption was occurred, it dropped to zero during interruption. After

interruption, percentage of bus frequency was starting going up until 106 % and then it had been going down until 96 % in 0.7 seconds with a small fluctuation. It reached stable at 3th second at 100 %.

Bus frequency of interruption simulation results of bus bar Silae SB1 before RE integration, after RE integration and after RE integration using homer results can be seen below.

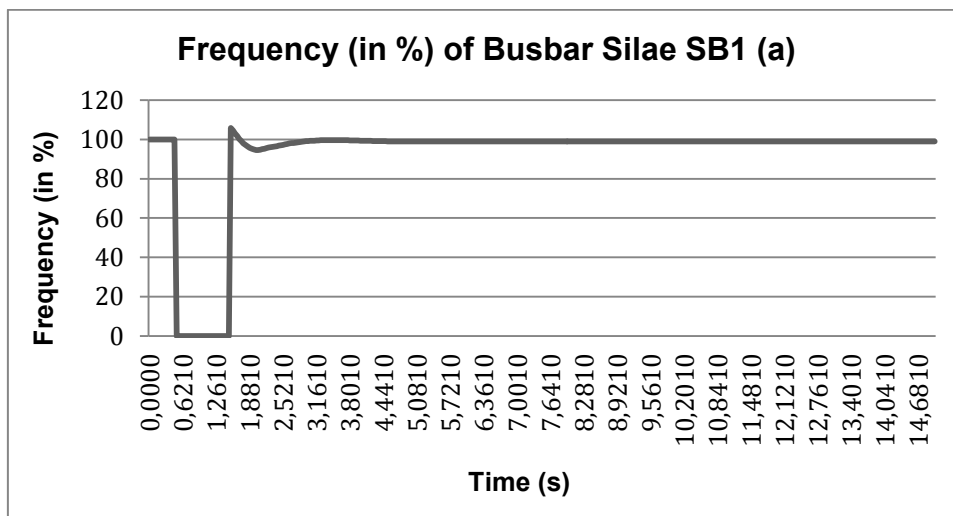


Figure 5-226: Silae SB1 Bus Frequency Interruption Simulation Results on Situation A

Based on figure 5-226, before interruption, percentage of bus frequency was at 100 %. When the interruption was occurred, it dropped to zero during interruption. After interruption, percentage of bus frequency was starting going up until 108 % and then it had been going down until 93 % in 0.5 seconds. It reached stable at 4.3rd second at 100 %.

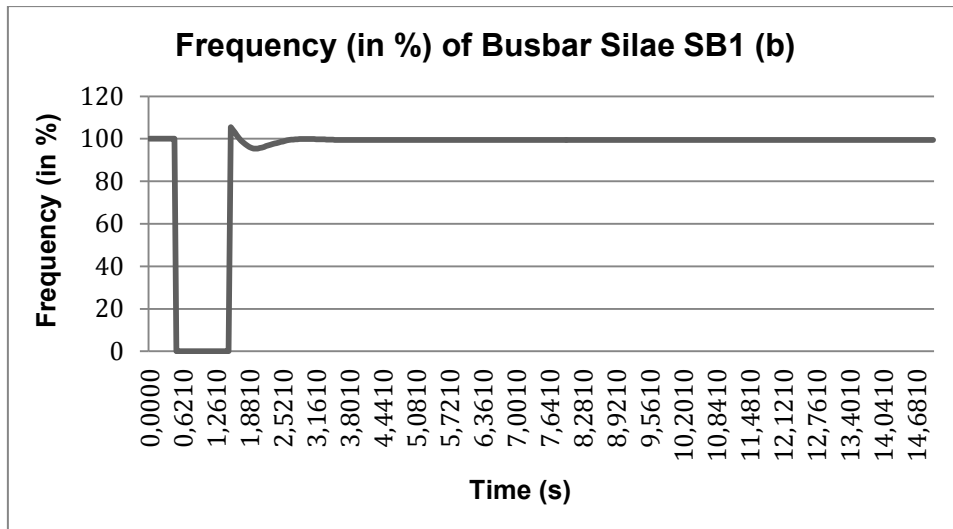


Figure 5-227: Silae SB1 Bus Frequency Interruption Simulation Results on Situation B

Based on figure 5-227, before interruption, percentage of bus frequency was at 100 %. When the interruption was occurred, it dropped to zero during interruption. After interruption, percentage of bus frequency was starting going up until 106 % and then it had been going down until 98 % in 0.5 seconds. It reached stable at 3.8th second at 100 %.

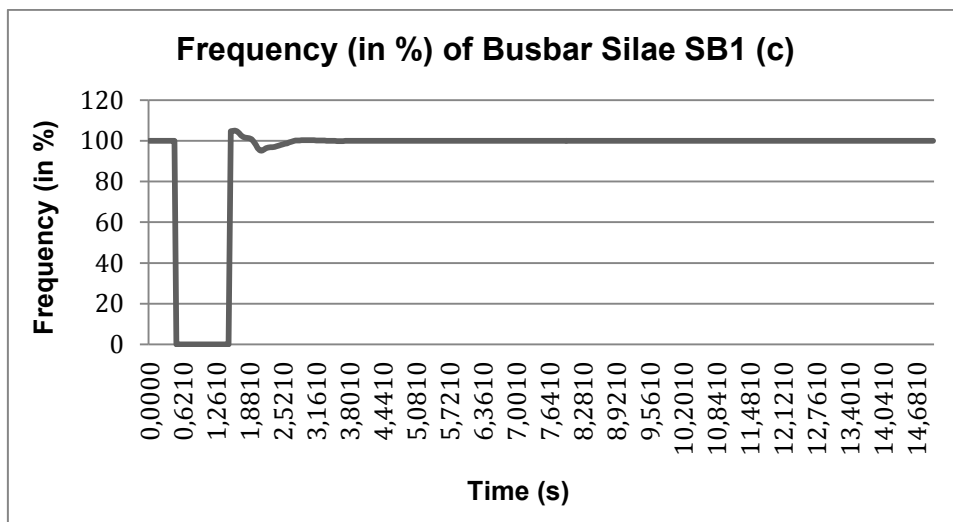


Figure 5-228: Silae SB1 Bus Frequency Interruption Simulation Results on Situation C

Based on figure 5-228, before interruption, percentage of bus frequency was at 100 %. When the interruption was occurred, it dropped to zero during interruption. After

interruption, percentage of bus frequency was starting going up until 106 % and then it had been going down until 98 % in 0.7 seconds with a small fluctuation. It was reaching stable at 3.4th second at 100 %.

Bus frequency of interruption simulation results of Silae SB2 and Silae SB3 bus bar before RE integration, after RE integration and after RE integration using homer results are equal to bus frequency of interruption simulation results of Silae SB1 bus bar on all situations.

Bus frequency of interruption simulation results of bus bar Silae SB4 before RE integration, after RE integration and after RE integration using homer results can be seen below.

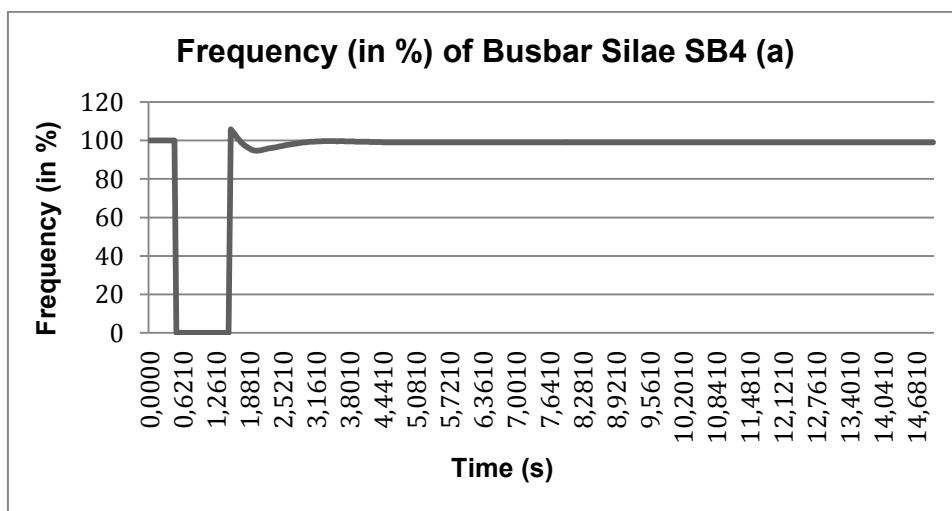


Figure 5-229: Silae SB4 Bus Frequency Interruption Simulation Results on Situation A

Based on figure 5-229, before interruption, percentage of bus frequency was at 100 %. When the interruption was occurred, it dropped to zero during interruption. After interruption, percentage of bus frequency was starting going up until 106 % and then it had been going down until 94 % in 0.5 seconds. It reached stable at 4.5th second at 100 %.

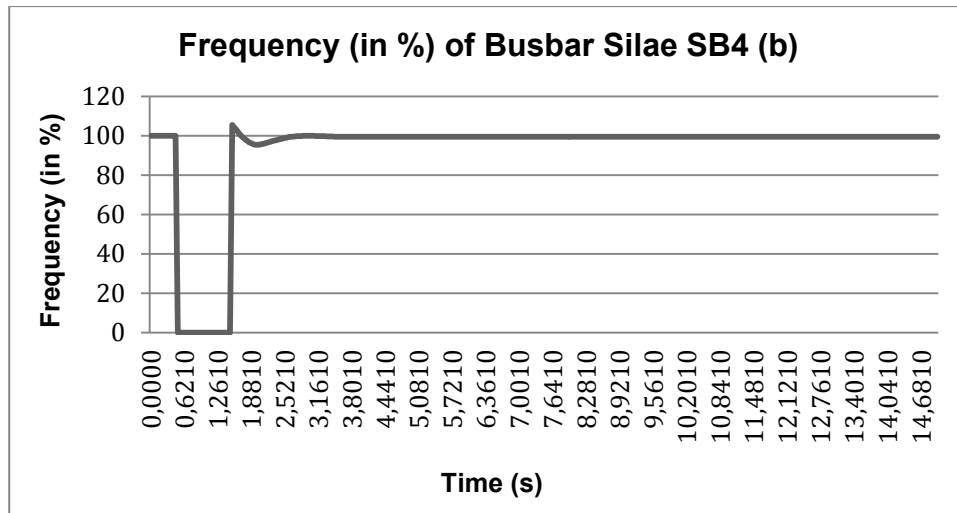


Figure 5-230: Silae SB4 Bus Frequency Interruption Simulation Results on Situation B

Based on figure 5-230, before interruption, percentage of bus frequency was at 100 %. When the interruption was occurred, it dropped to zero during interruption. After interruption, percentage of bus frequency was starting going up until 106 % and then it had been going down until 96 % in 0.6 seconds. It reached stable at 3.5th second at 100 %.

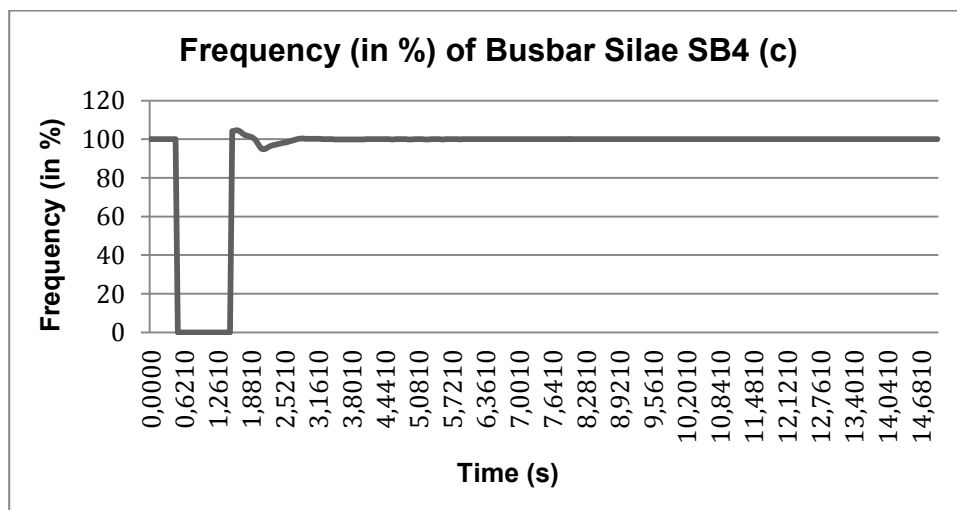


Figure 5-231: Silae SB4 Bus Frequency Interruption Simulation Results on Situation C

Based on figure 5-231, before interruption, percentage of bus frequency was at 100 %. When the interruption was occurred, it dropped to zero during interruption. After

interruption, percentage of bus frequency was starting going up until 105 % and then it had been going down until 96 % in 0.7 seconds with a small fluctuation. It reached stable at 3.4th second at 100 %.

Bus frequency of interruption simulation results of bus bar Talise SB1 before RE integration, after RE integration and after RE integration using homer results can be seen below.

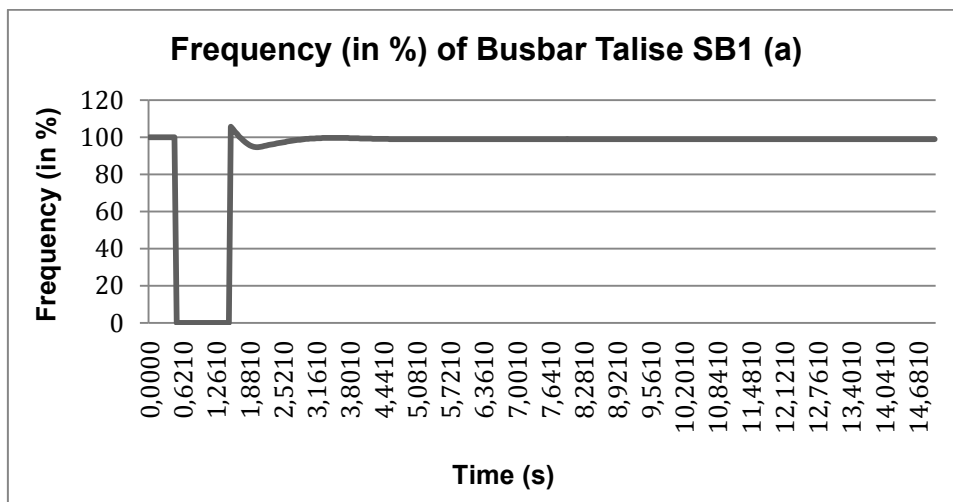


Figure 5-232: Talise SB1 Bus Frequency Interruption Simulation Results on Situation A

Based on figure 5-232, before interruption, percentage of bus frequency was at 100 %. When the interruption was occurred, it dropped to zero during interruption. After interruption, percentage of bus frequency was starting going up until 107 % and then it had been going down until 92 % in 0.5 seconds. It reached stable at 4.5th second at 100 %.

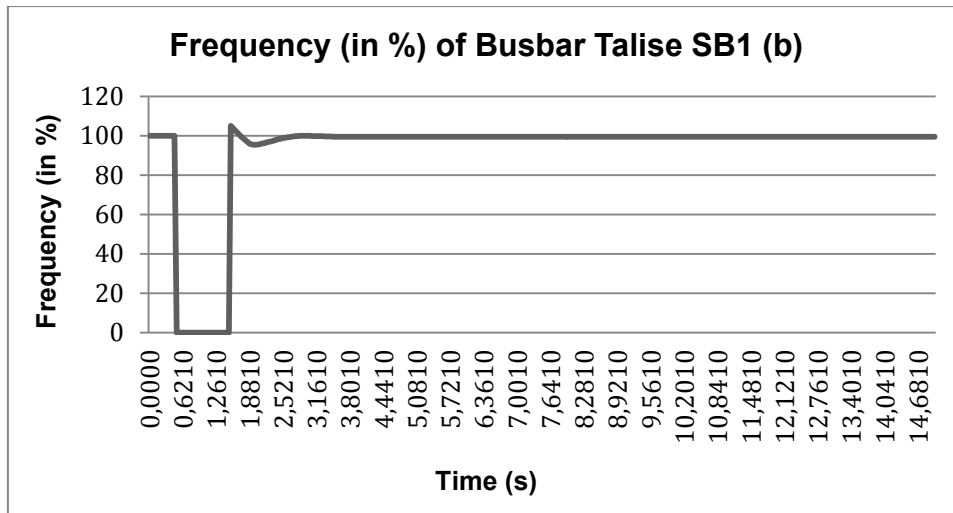


Figure 5-233: Talise SB1 Bus Frequency Interruption Simulation Results on Situation B

Based on figure 5-233, before interruption, percentage of bus frequency was at 100 %. When the interruption was occurred, it dropped to zero during interruption. After interruption, percentage of bus frequency was starting going up until 106 % and then it had been going down until 96 % in 0.6 seconds. It got stable at 3.5th second at 100 %.

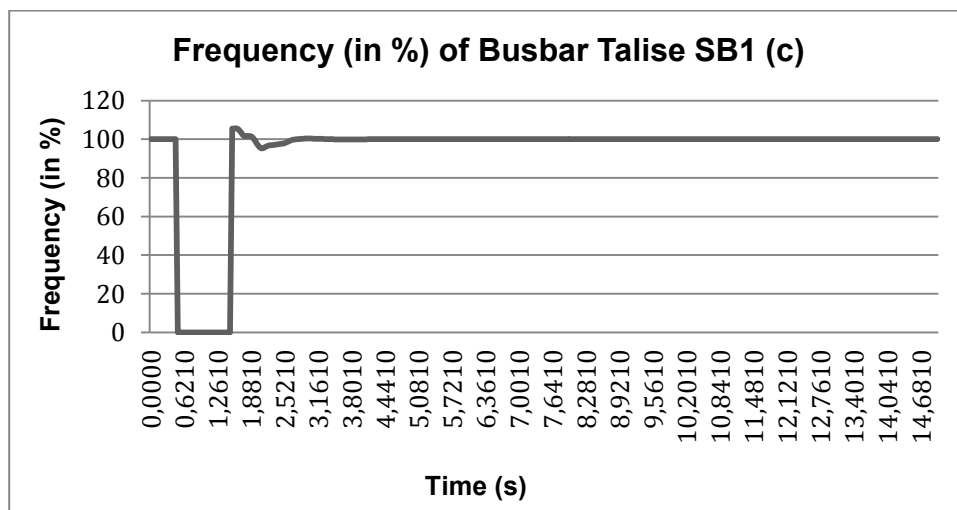


Figure 5-234: Talise SB1 Bus Frequency Interruption Simulation Results on Situation C

Based on figure 5-234, before interruption, percentage of bus frequency was at 100 %. When the interruption was occurred, it dropped to zero during interruption. After

interruption, percentage of bus frequency was starting going up until 106 % and then it had been going down until 96 % in 0.7 seconds with a small fluctuation. It reached stable at 3.3rd second at 100 %.

Bus frequency of interruption simulation results of bus bar Talise SB2 before RE integration, after RE integration and after RE integration using homer results can be seen below.

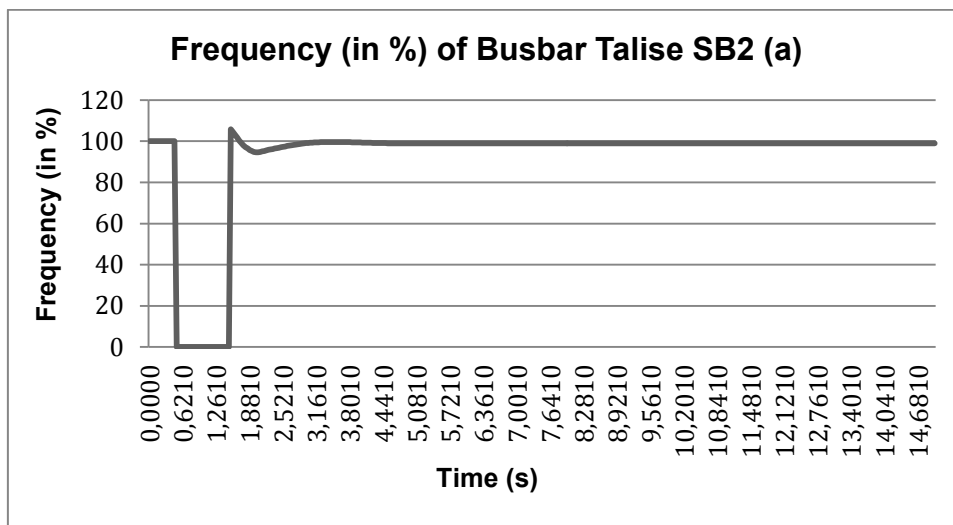


Figure 5-235: Talise SB2 Bus Frequency Interruption Simulation Results on Situation A

Based on figure 5-235, before interruption, percentage of bus frequency was at 100 %. When the interruption was occurred, it dropped to zero during interruption. After interruption, percentage of bus frequency was starting going up until 106 % and then it had going down until 92 % in 0.5 seconds. It reached stable at 4.5th second at 100 %.

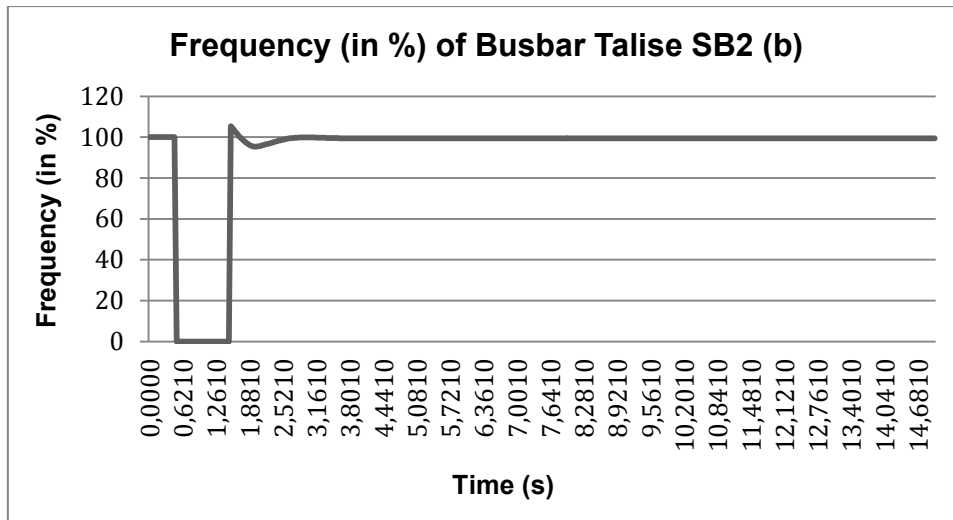


Figure 5-236: Talise SB2 Bus Frequency Interruption Simulation Results on Situation B

Based on figure 5-236, before interruption, percentage of bus frequency was at 100 %. When the interruption was occurred, it dropped to zero during interruption. After interruption, percentage of bus frequency was starting going up until 106 % and then it had been going down until 96 % in 0.6 seconds. It reached stable at 3.4th second at 100 %.

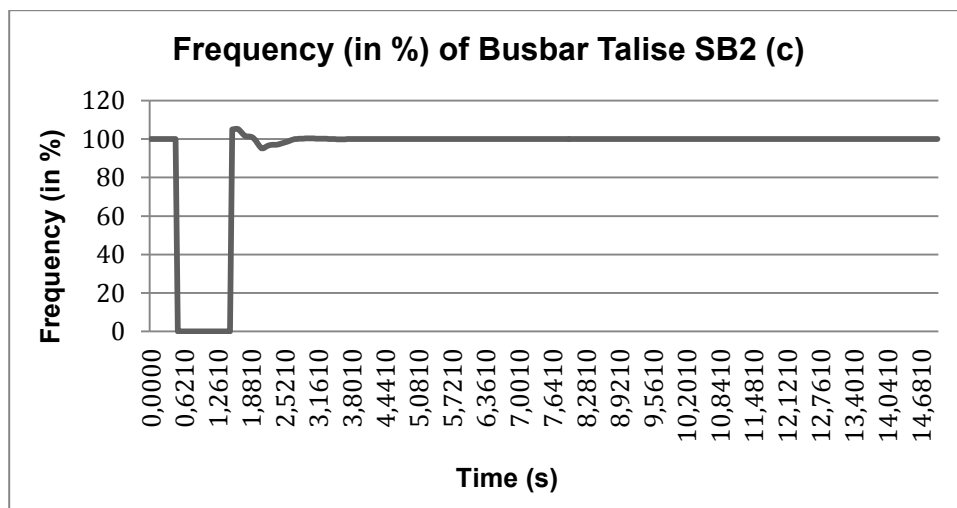


Figure 5-237: Talise SB2 Bus Frequency Interruption Simulation Results on Situation C

Based on figure 5-237, before interruption, percentage of bus frequency was at 100 %. When the interruption was occurred, it dropped to zero during interruption. After

interruption, percentage of bus frequency was starting going up until 106 % and then it had been going down until 96 % in 0.7 seconds with a small fluctuation. It reached stable at 3.3rd second at 100 %.

Bus frequency of interruption simulation results of Talise SB3 bus bar before RE integration, after RE integration and after RE integration using homer results is equal to bus frequency of interruption simulation results of Talise SB2 bus bar on all situations.

Bus frequency of interruption simulation results of bus bar Talise DB1 before RE integration, after RE integration and after RE integration using homer results can be seen below.

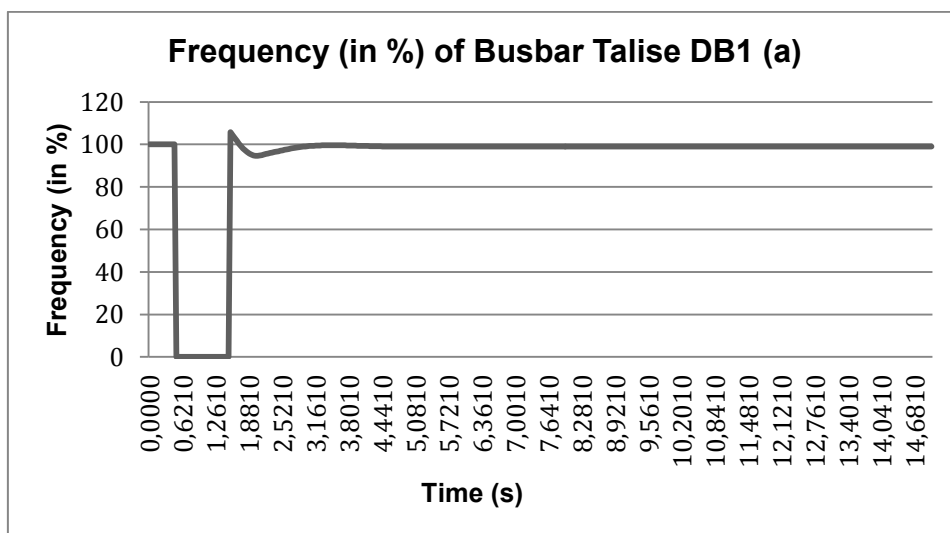


Figure 5-238: Talise DB1 Bus Frequency Interruption Simulation Results on Situation A

Based on figure 5-238, before interruption, percentage of bus frequency was at 100 %. When the interruption was occurred, it dropped to zero during interruption. After interruption, percentage of bus frequency was starting going up until 106 % and then it had been going down until 92 % in 0.5 seconds. It reached stable at 4.5th second at 100 %.

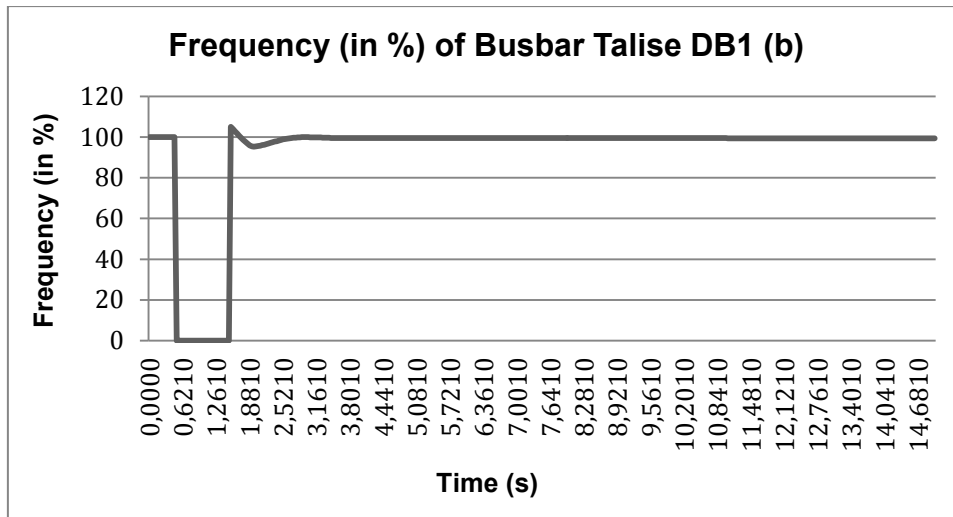


Figure 5-239: Talise DB1 Bus Frequency Interruption Simulation Results on Situation B

Based on figure 5-239, before interruption, percentage of bus frequency was at 100 %. When the interruption was occurred, it dropped to zero during interruption. After interruption, percentage of bus frequency was starting going up until 106 % and then it had been going down until 96 % in 0.6 seconds. It reached stable at 3.4th second at 100 %.

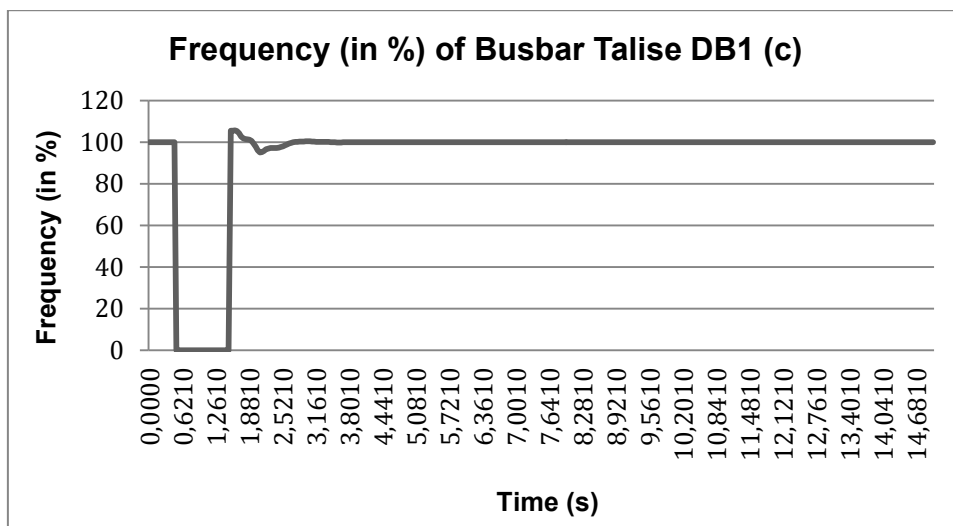


Figure 5-240: Talise DB1 Bus Frequency Interruption Simulation Results on Situation C

Based on figure 5-240, before interruption, percentage of bus frequency was at 100 %. When the interruption was occurred, it dropped to zero during interruption. After

interruption, percentage of bus frequency was starting going up until 106 % and then it had been going down until 96 % in 0.7 seconds with a small fluctuation. It reached stable at 3.3rd second at 100 %.

Bus frequency of interruption simulation results of Talise DB11 bus bar before RE integration, after RE integration and after RE integration using homer results is equal to bus frequency of interruption simulation results of Talise DB1 bus bar on all situations.

5.4.4 Harmonic Simulation Results

To make it easy to understand, situation A is the simulation before integrating RE into the grid, situation B is the simulation after integrating RE into the grid and situation C is the simulation after integrating RE into the grid based on homer results.

Harmonic simulation results of DB1 PJPP Bus bar on situation A, B and C can be seen below.

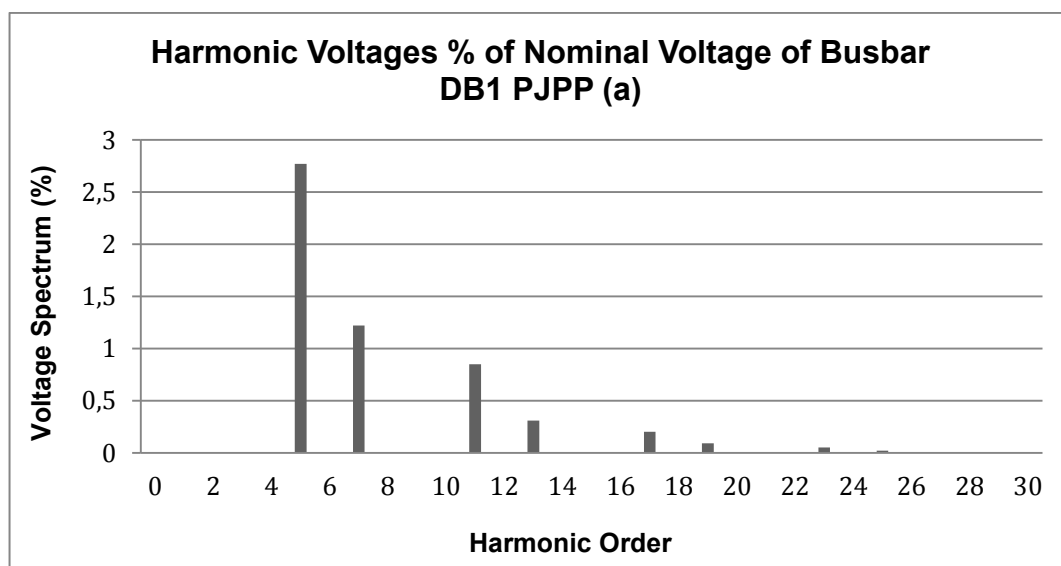


Figure 5-241: Harmonic Voltages (in %) of DB1 PJPP Bus bar on Situation A

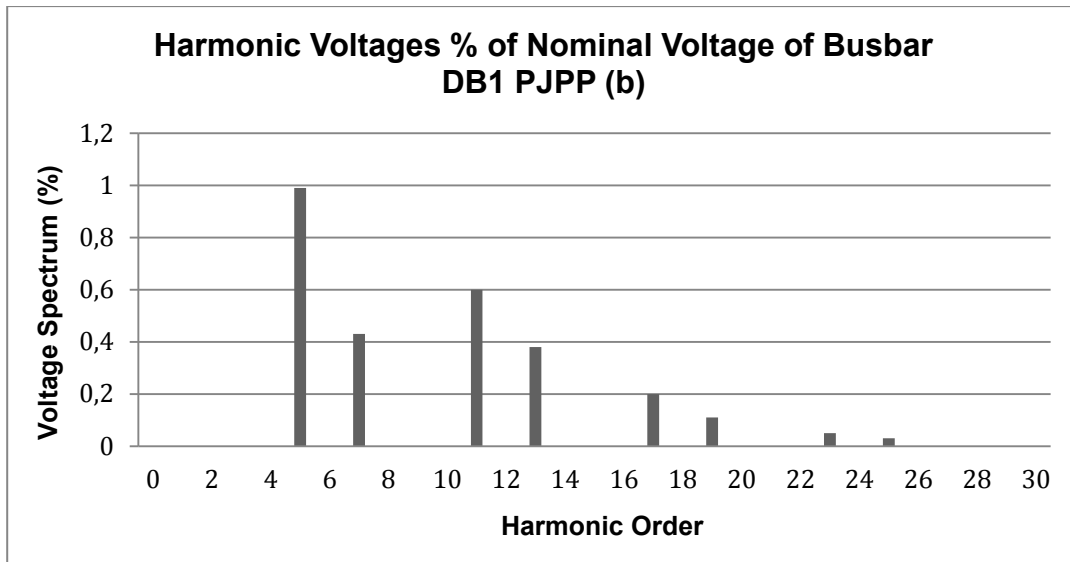


Figure 5-242: Harmonic Voltages of DB1 PJPP Bus bar on Situation B

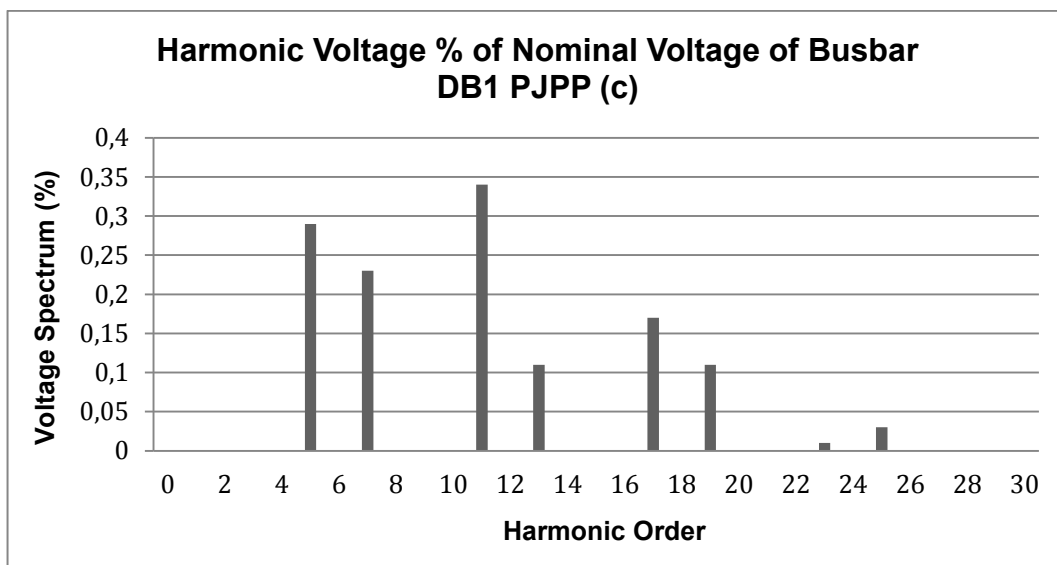


Figure 5-243: Harmonic Voltages of DB1 PJPP Bus bar on Situation C

Based on figure 5-242, figure 5-243, and figure 5-244, on situation A when harmonic order at 5th, the voltage spectrum is 2.75 %. On situation B when harmonic order at 5th the voltage spectrum is 0.99 %. On situation C, when harmonic order at 5th the voltage spectrum is 0.29 %. Therefore the difference among situation A, situation B and situation C is that there is a significant reduction of voltage spectrum from 2.75 % to 0.99 % and from 0.99 % to 0.29 %. On situation A, when harmonic order is at 7th the voltage spectrum is 1.3 %. On situation B, when harmonic order is at 7th the voltage spectrum is 0.44 %. On situation C, when harmonic order is at 7th the voltage

spectrum is 0.22 %. Therefore the difference among situation A, situation B and situation C is that there is a significant reduction of voltage spectrum from 1.3 % to 0.44 % and from 0.44 % to 0.22 %.

On situation A, when the harmonic order is at 11st the voltage spectrum is 0.6 %. On situation B, when harmonic order is at 11st the voltage spectrum is 0.34 %. On situation C, when harmonic order is at 11st the voltage spectrum is 0.34 %. Therefore the difference among situation A, situation B and situation C is that there is a significant reduction of voltage spectrum from 0.6 % to 0.34 %. On situation A, when the harmonic order is at 13rd the voltage spectrum is 0.35 %. On situation B, when harmonic order is at 13rd the voltage spectrum is 0.38 %. On situation C, when harmonic order is at 13rd the voltage spectrum is 0.11 %. The increase voltage spectrum from situation A to situation B but it is not significant as well as the decrease of voltage spectrum from situation B to situation C.

On situation A, when the harmonic order is at 17th the voltage spectrum is 0.2 %. On situation B, when harmonic order is at 17th the voltage spectrum is 0.2 %. On situation C, when harmonic order is at 17th the voltage spectrum is 0.17 %. Therefore the difference among situation A, situation B and situation C is that there is no reduction of voltage spectrum from situation A to situation B. Reduction from situation B to situation C is not significant. On situation A, when the harmonic order is at 19 the voltage spectrum is 0.1 %. On situation B, when harmonic order is at 19 the voltage spectrum is 0.11 %. On situation C, when harmonic order is at 19 the voltage spectrum is 0.1 %.

On situation A, when the harmonic order is at 23rd the voltage spectrum is 0.07 %. On situation B, when harmonic order is at 23rd the voltage spectrum is 0.04 %. On situation C, when harmonic order is at 23rd the voltage spectrum is 0.01 %. Therefore is not significant reduction among them. On situation A, when the harmonic order is at 25th the voltage spectrum is 0.035 %. On situation B, when harmonic order is at 25th the voltage spectrum is 0.03 %. On situation C, when harmonic order is at 25th the voltage spectrum is 0.02 %. There is no significant difference among them.

Table 5-1: Voltage Spectrum of DB1 PJPP Bus bar on Situation A, B and C

Bus DB1 PJPP Harmonic Order	Voltage Spectrum [%]		
	Situation A	Situation B	Situation C
5 th	2.75	0.99	0.29
7 th	1.3	0.44	0.22
11 st	0.6	0.34	0.34
13 rd	0.35	0.38	0.11
17 th	0.2	0.2	0.17
19 th	0.1	0.11	0.11
23 rd	0.07	0.04	0.01
25 th	0.035	0.03	0.02

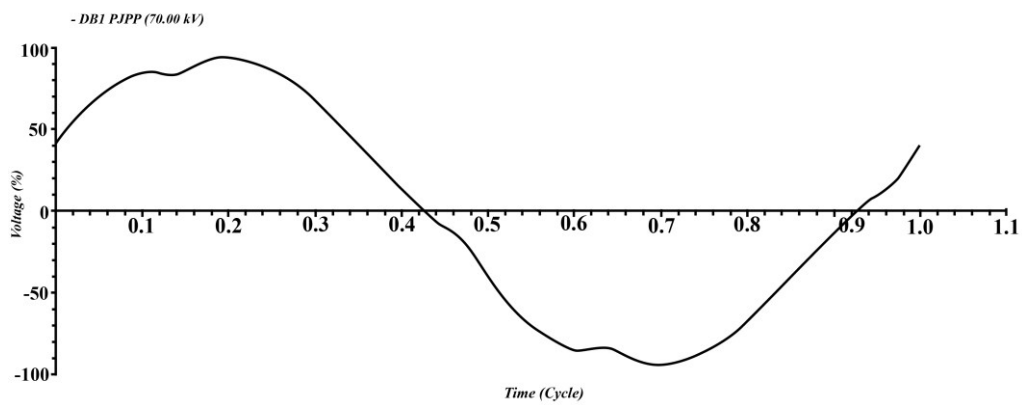


Figure 5-244: Voltage Waveform of DB1 PJPP Bus bar on Situation A

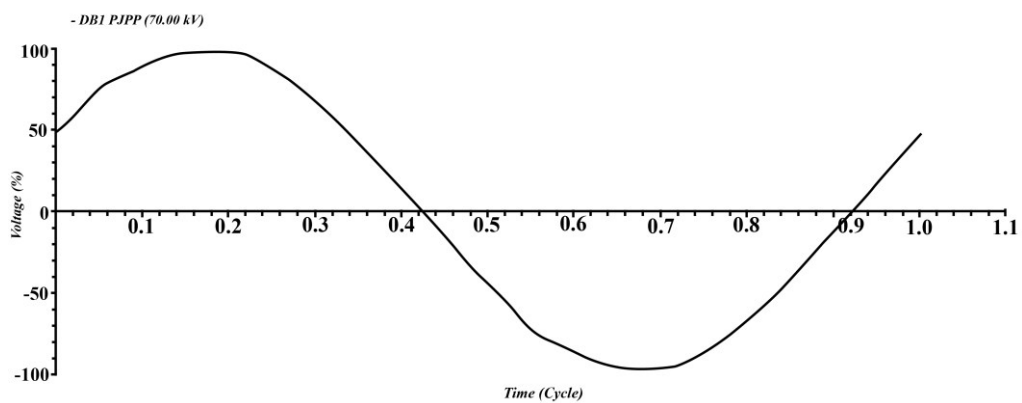


Figure 5-245: Voltage Waveform of DB1 PJPP Bus bar on Situation B

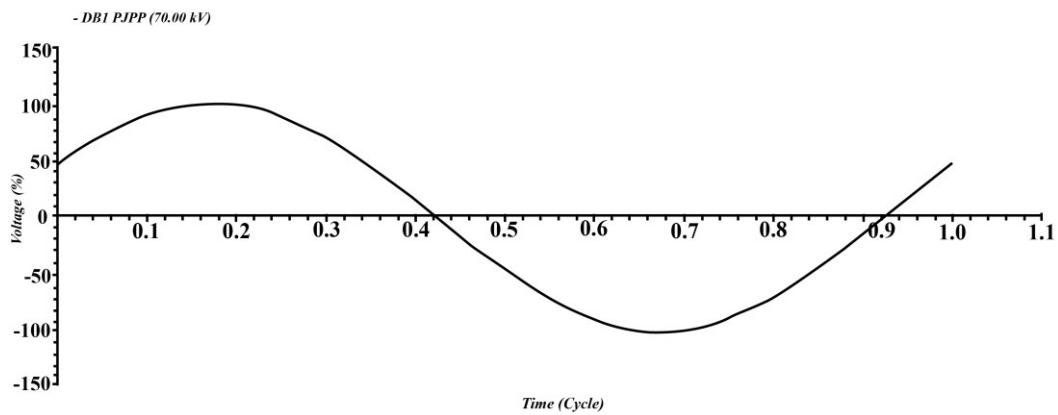


Figure 5-246: Voltage Waveform of DB1 PJPP Bus bar on Situation C

Based on figure 5-244, figure 5-245, figure 5-246, on situation A, there are some reductions of voltage sinusoidal waveform between 0.1 cycles and 0.2 cycles, between 0.4 cycles and 0.5 cycles, between 0.6 cycles and 0.7 cycles and between 0.9 cycles and 1.0 cycles.

On situation B, there are only two locations of reduction, between 0.06 cycles and 0.12 cycles and between 0.56 cycles to 0.65 cycles. The reductions of sinusoidal waveform in those locations are less than the reduction occurred in situation A. On situation C, the reduction of sinusoidal waveform is only between 0.45 cycles to 0.6 cycles, which is much less compared with the situation B. On this situation, the voltage sinusoidal waveform is almost perfect.

Table 5-2: The Reduction of Sinusoidal Waveform of DB1 PJPP Bus bar on Situation A, B and C

Sinusoidal Waveform Result of Bus DB1 PJPP			
	Situation A	Situation B	Situation C
1	0.1 cycle – 0.20 cycle	0.06 cycle – 0.12 cycle	0.45 cycle – 0.6 cycle
2	0.4 cycle – 0.5 cycle	0.56 cycle – 0.65 cycle	
3	0.6 cycle – 0.7 cycle		
4	0.9 cycle – 1.0 cycle		

Harmonic simulation results of bus bar DB11 PJPP of situation A, B and C are equal to harmonic simulation results of DB1 PJPP.

Harmonic simulation results of Donggala SB1 Bus bar of situation A, B and C can be seen below.

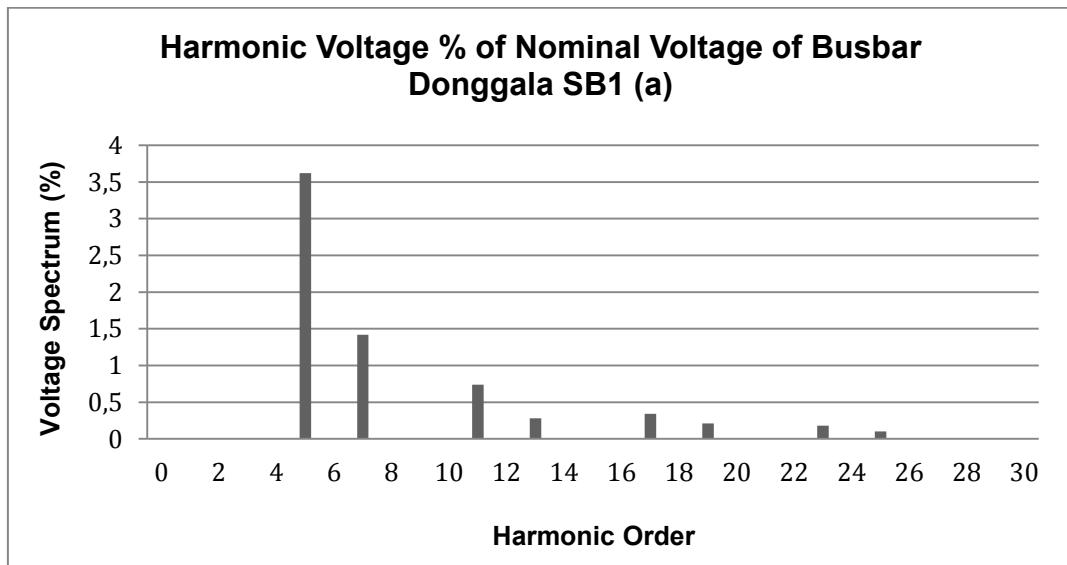


Figure 5-247: Harmonic Voltage of Donggala SB1 Bus bar on Situation A

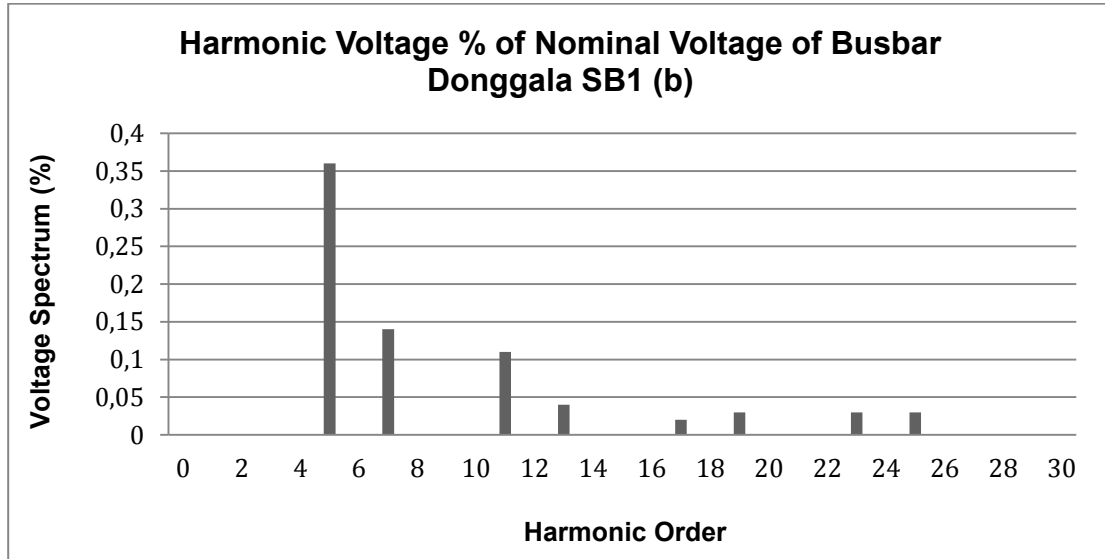


Figure 5-248: Harmonic Voltage of Donggala SB1 Bus bar on Situation B

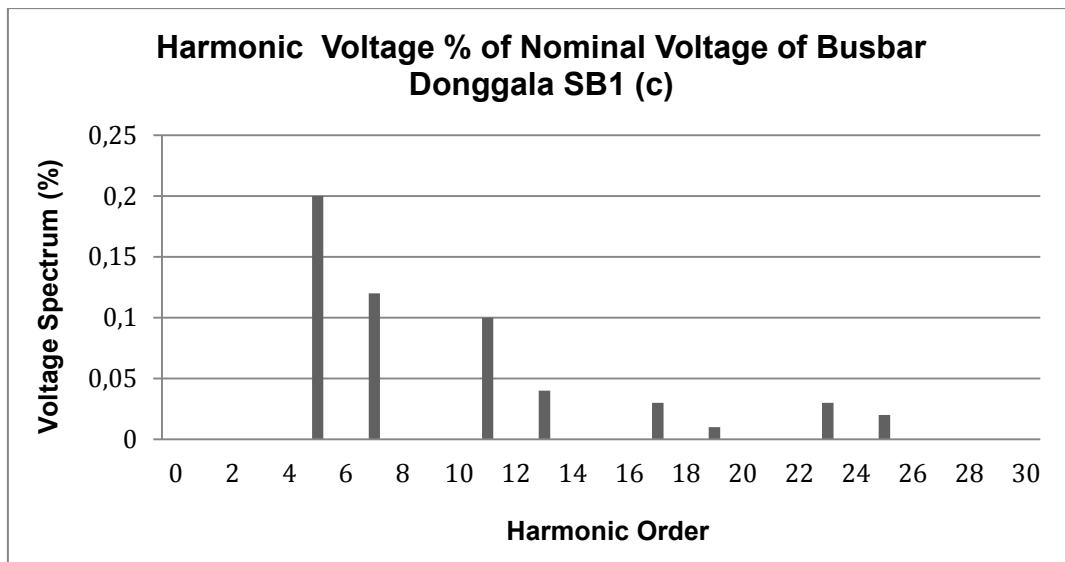


Figure 5-249: Harmonic Voltage of Donggala SB1 Bus bar on Situation C

Based on figure 5-247, figure 5-248, figure 5-249, When harmonic order is at 5th, voltage spectrum on situation A is 3.63 %, voltage spectrum on situation B is 0.36 % and voltage spectrum on situation C is 0.20. The reduction of voltage spectrum from situation A to situation B is 3.27 %. The reduction of voltage spectrum from situation B to situation C is 0.16 %. When harmonic order is at 7th, voltage spectrum on situation A is 1.10 %, voltage spectrum on situation B is 0.14 % and voltage spectrum on situation C is 0.12. The reduction of voltage spectrum from situation A to situation B is 0.96 %. The reduction of voltage spectrum from situation B to situation C is 0.02%.

When harmonic order is at 11st, voltage spectrum on situation A is 0.75 %, voltage spectrum on situation B is 0.11 % and voltage spectrum on situation C is 0.10 %. The reduction of voltage spectrum from situation A to situation B is 0.64 %. The decrease of voltage spectrum from situation B to situation C is 0.01 %. When harmonic order is at 13rd, voltage spectrum on situation A is 0.25 %, voltage spectrum on situation B is 0.04 % and voltage spectrum on situation C is 0.04 %. The reduction of voltage spectrum from situation A to situation B is 0.21 %.

When harmonic order is at 17th, voltage spectrum on situation A is 0.33 %, voltage spectrum on situation B is 0.02 % and voltage spectrum on situation C is 0.03 %. The reduction of voltage spectrum from situation A to situation B is 0.31 %. The increase

of voltage spectrum from situation B to situation C is 0.01 %. The decrease of voltage spectrum from situation A to situation B is 0.31 % while the increase of voltage spectrum from situation B and situation C is only 0.01 %. When harmonic order is at 19th, voltage spectrum on situation A is 0.17 %, voltage spectrum on situation B is 0.03 % and voltage spectrum on situation C is 0.01 %. The reduction of voltage spectrum from situation A to situation B is 0.14 %. The reduction of voltage spectrum from situation B to situation C is 0.02 %.

When harmonic order is at 23rd, voltage spectrum on situation A is 0.13 %, voltage spectrum on situation B is 0.03 % and voltage spectrum on situation C is 0.03 %. The reduction of voltage spectrum from situation A to situation B is 0.1 %. There is no any reduction from situation B to situation C. When harmonic order is at 25th, voltage spectrum on situation A is 0.08 %, voltage spectrum on situation B is 0.03 % and voltage spectrum on situation C is 0.02 %. The reduction of voltage spectrum from situation A to situation B is 0.05 %. The reduction of voltage spectrum from situation B to situation C is 0.01 %.

Table 5-3: Voltage Spectrum of Donggala SB1 Bus bar on Situation A, B and C

Bus Donggala SB1	Voltage Spectrum [%]		
Harmonic Order	Situation A	Situation B	Situation C
5 th	3.63	0.36	0.20
7 th	1.10	0.14	0.12
11 st	0.75	0.11	0.10
13 rd	0.25	0.04	0.04
17 th	0.33	0.02	0.03
19 th	0.17	0.03	0.01
23 rd	0.13	0.03	0.03
25 th	0.08	0.03	0.02

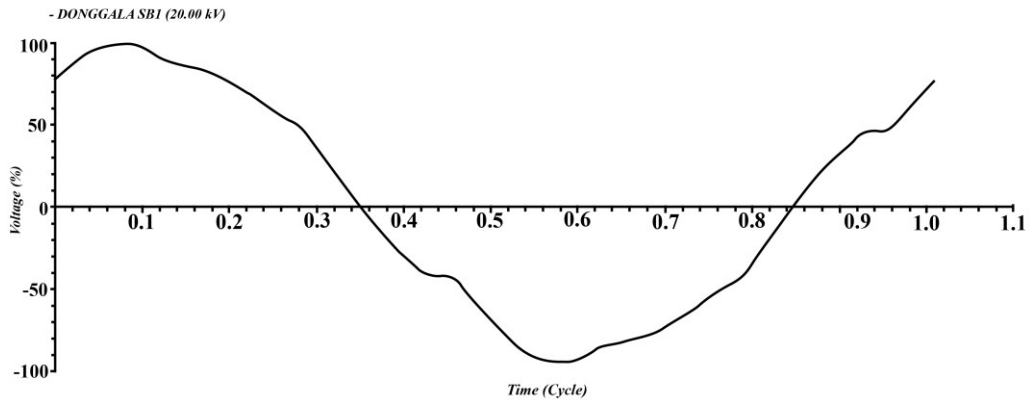


Figure 5-250: Voltage Waveform of Donggala SB1 Bus bar on Situation A

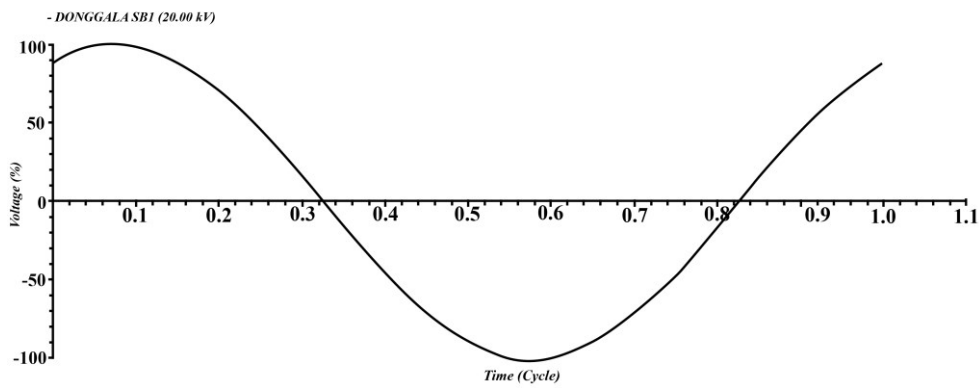


Figure 5-251: Voltage Waveform of Donggala SB1 Bus bar on Situation B

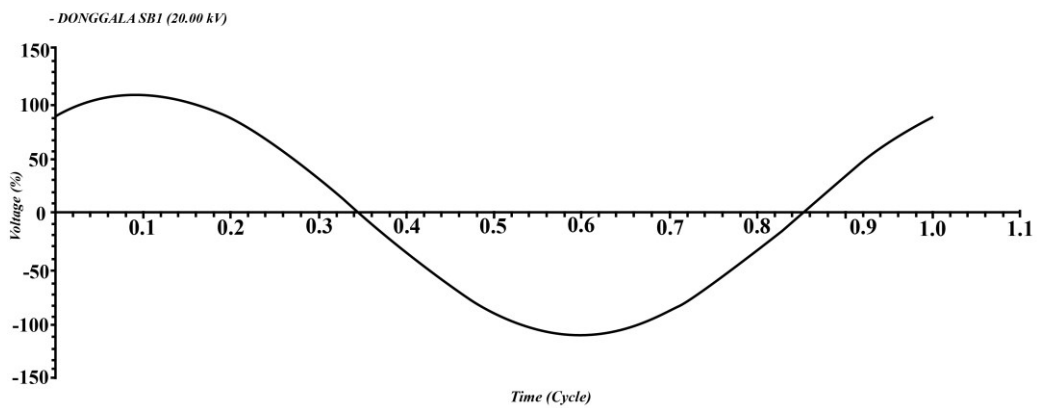


Figure 5-252: Voltage Waveform of Donggala SB1 Bus bar on Situation C

The voltage sinusoidal wave against time in cycle of these three situations is the following; on situation A, there are some reductions of voltage sinusoidal waveform between 0.1 cycles and 0.28 cycles, between 0.42 cycles and 0.48 cycles, between 0.59 cycles and 0.78 cycles and between 0.92 cycles and 1.0 cycles. On situation B and situation C there is no any reduction at all.

Table 5-4: The Reduction of Sinusoidal Waveform of Donggala SB1 Bus bar on Situation A, B and C

Sinusoidal Waveform Result			
	Situation A	Situation B	Situation C
1	0.1 cycle - 0.28 cycle	No reduction	No reduction
2	0.42 cycle - 0.48 cycle		
3	0.59 cycle - 0.78 cycle		
4	0.92 cycle - 1.0 cycle		

Harmonic simulation results of Maesa SB1 bus bar on situation A, B and C.

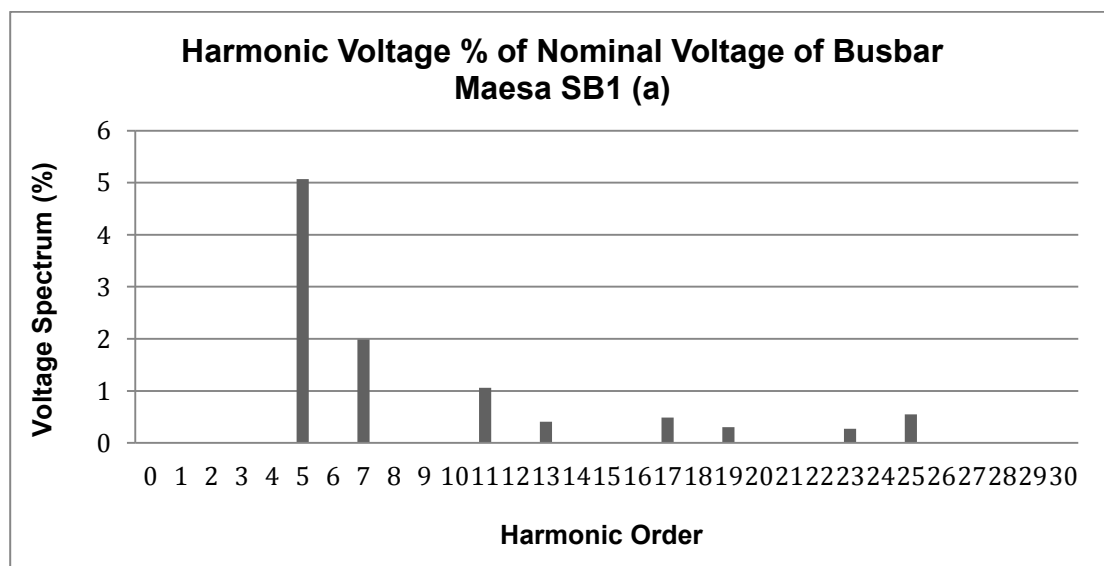


Figure 5-253: Harmonic Voltage of Maesa SB1 Bus bar on Situation A

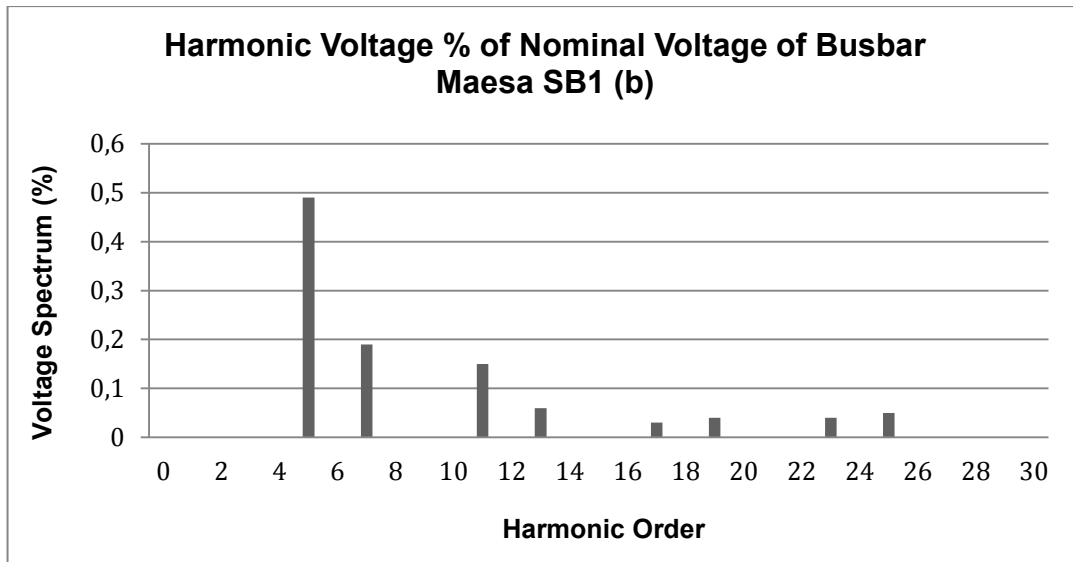


Figure 5-254: Harmonic Voltage of Maesa SB1 Bus bar on Situation B

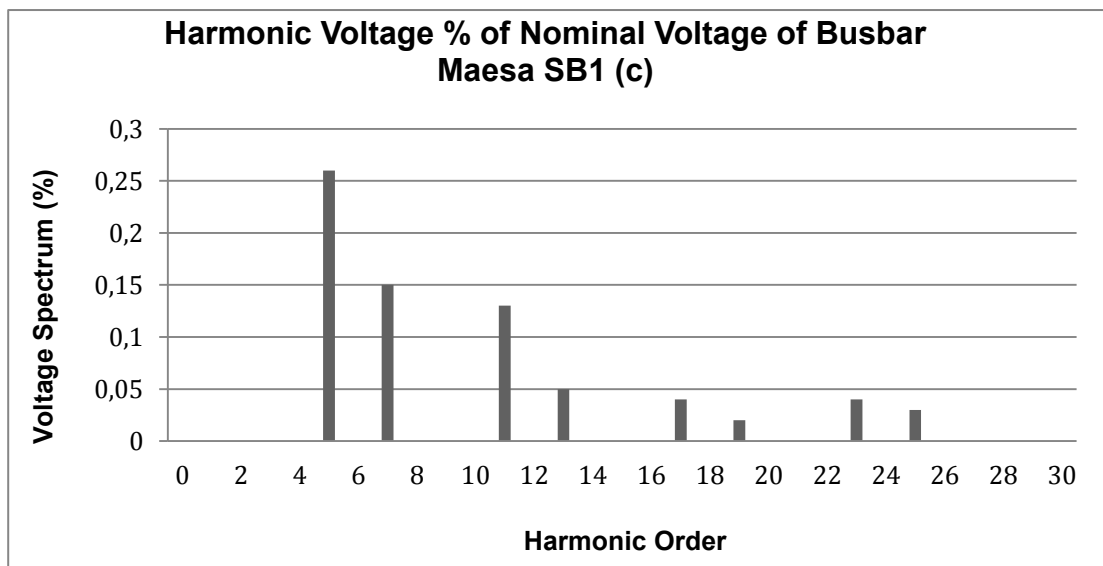


Figure 5-255: Harmonic Voltage of Maesa SB1 Bus bar on Situation C

Based on figure 5-253, figure 5-254 and figure 5-255, When harmonic order is at 5th, voltage spectrum on situation A is 5 %, voltage spectrum on situation B is 0.49 % and voltage spectrum on situation C is 0.26 %. The reduction of voltage spectrum from situation A to situation B is 7.52 %. The reduction of voltage spectrum from situation B to situation C is 0.19%. When harmonic order is at 7th, voltage spectrum on situation A is 2 %, voltage spectrum on situation B is 0.19 % and voltage spectrum on situation C is 0.15. The reduction of voltage spectrum from situation A to

situation B is 1.81 %. The decrease of voltage spectrum from situation B to situation C is 0.04 %.

When harmonic order is at 11st, voltage spectrum on situation A is 1 %, voltage spectrum on situation B is 0.15 % and voltage spectrum on situation C is 0.13 %. The reduction of voltage spectrum from situation A to situation B is 1.55 %. The decrease of voltage spectrum from situation B to situation C is 0.02 %. When harmonic order is at 13rd, voltage spectrum on situation A is 0.33 %, voltage spectrum on situation B is 0.05 % and voltage spectrum on situation C is 0.05 %. The reduction of voltage spectrum from situation A to situation B is 0.28 %. There is no any reduction from situation B to situation C.

When harmonic order is at 17th, voltage spectrum on situation A is 0.5 %, voltage spectrum on situation B is 0.03 % and voltage spectrum on situation C is 0.04 %. The reduction of voltage spectrum from situation A to situation B is 0.47 %. The increase of voltage spectrum from situation B to situation C is 0.01 %. When harmonic order is at 19th, voltage spectrum on situation A is 0.25 %, voltage spectrum on situation B is 0.05 % and voltage spectrum on situation C is 0.02 %. The reduction of voltage spectrum from situation A to situation B is 0.2 %. The reduction of voltage spectrum from situation B to situation C is 0.03 %.

When harmonic order is at 23rd, voltage spectrum on situation A is 0.25 %, voltage spectrum on situation B is 0.03 % and voltage spectrum on situation C is 0.04 %. The reduction of voltage spectrum from situation A to situation B is 0.22 %. The reduction of voltage spectrum from situation B to situation C is 0.01 %. When harmonic order is at 25th, voltage spectrum on situation A is 0.5 %, voltage spectrum on situation B is 0.05 % and voltage spectrum on situation C is 0.02 %. The reduction of voltage spectrum from situation A to situation B is 0.45 %. The reduction of voltage spectrum from situation B to situation C is 0.03 %.

Table 5-5: Voltage Spectrum of Maesa SB1 Bus bar on Situation A, B and C

Bus Maesa SB1 Harmonic Order	Voltage Spectrum [%]		
	Situation A	Situation B	Situation C
5 th	5	0.49	0.26
7 th	2	0.19	0.15
11 st	1	0.15	0.13
13 rd	0.33	0.05	0.05
17 th	0.5	0.03	0.04
19 th	0.25	0.05	0.02
23 rd	0.25	0.03	0.04
25 th	0.5	0.05	0.02

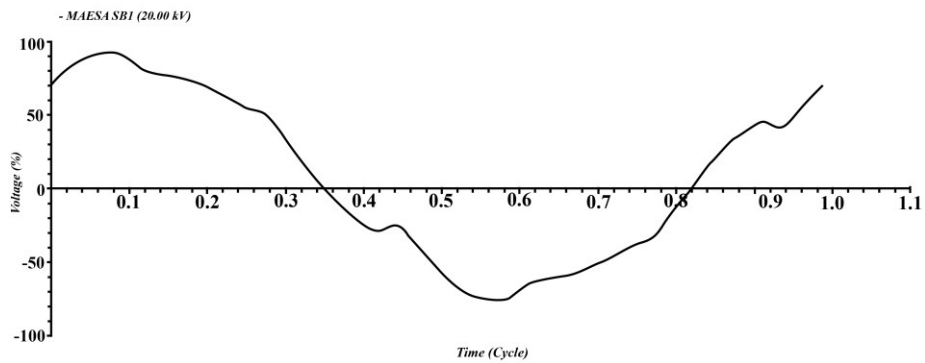


Figure 5-256: Voltage Waveform of Maesa SB1 Bus bar on Situation A

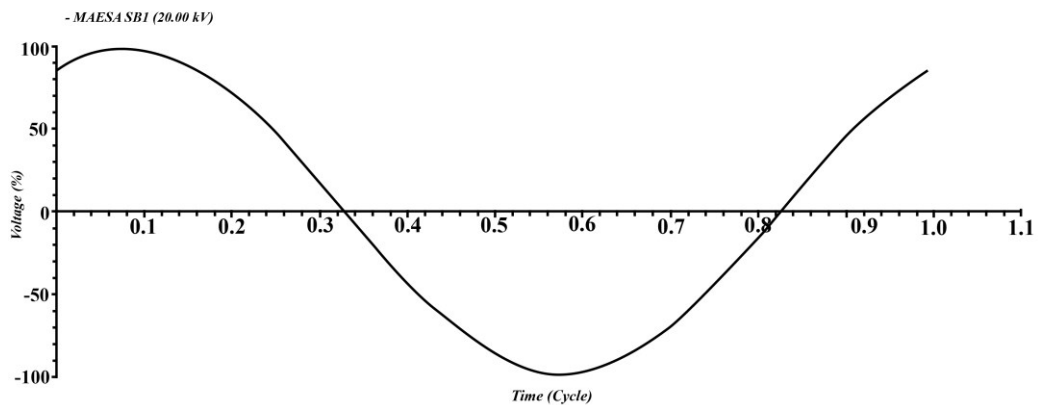


Figure 5-257: Voltage Waveform of Maesa SB1 Bus bar on Situation B

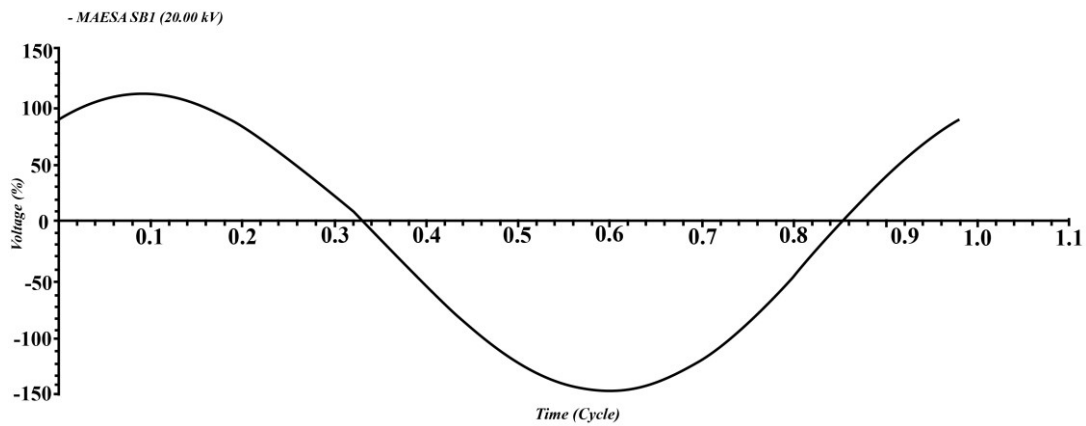


Figure 5-258: Voltage Waveform of Maesa SB1 Bus bar on Situation C

The voltage sinusoidal waveform of Maesa SB1 bus bar on three situations is equal to voltage sinusoidal waveform of Donggala SB1 bus bar.

Harmonic simulation results of Maesa SB1 (2) bus bar on situation A, B and C is equal to Maesa SB1 bus bar.

Harmonic simulation results of Parigi DB1 Bus bar on Situation A, B and C can be seen on the explanation below.

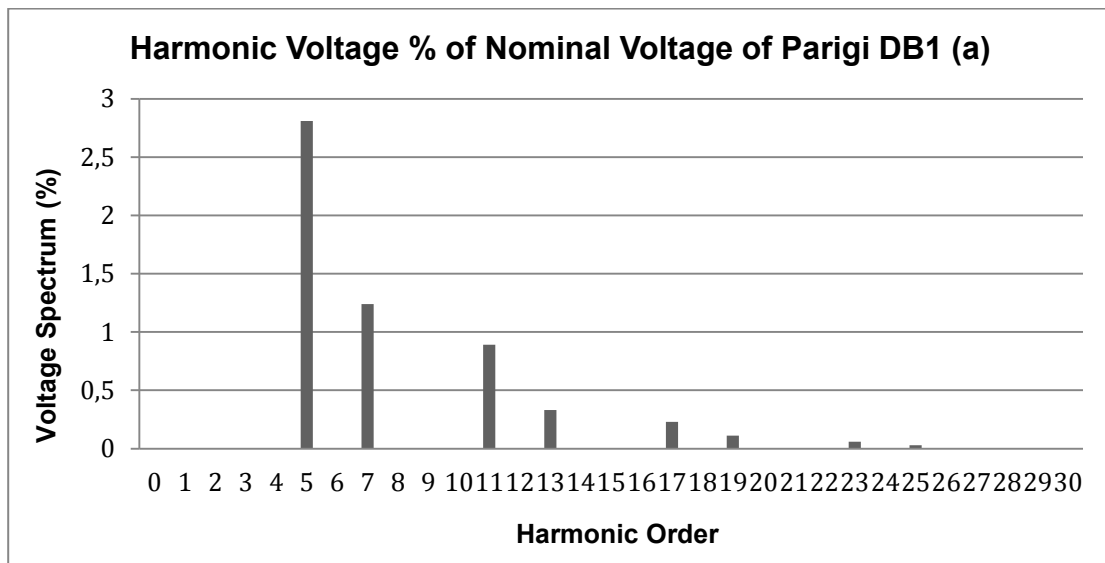


Figure 5-259: Harmonic Voltage of Parigi DB1 Bus bar on Situation A

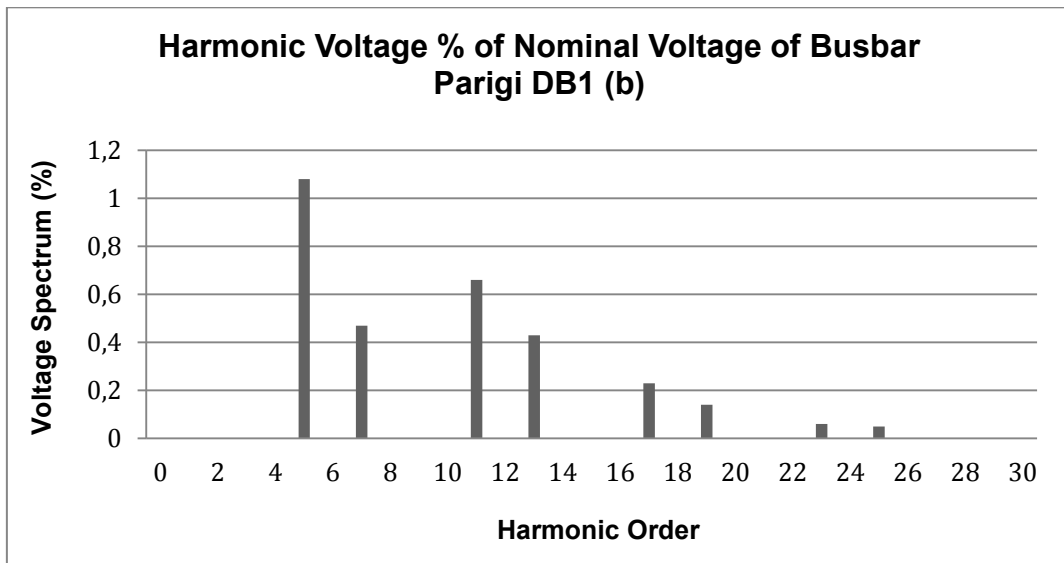


Figure 5-260: Harmonic Voltage of Parigi DB1 Bus bar on Situation B

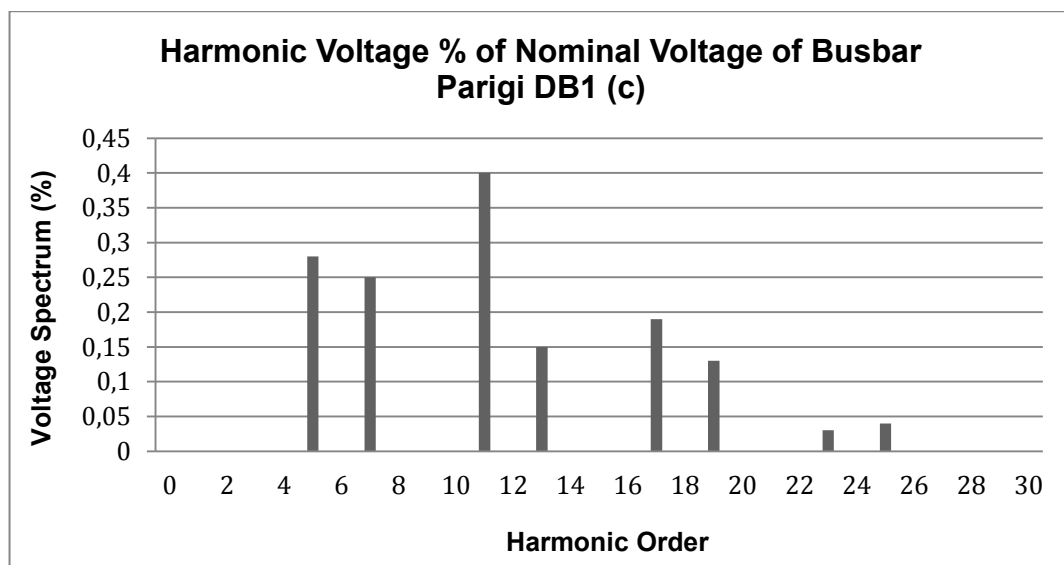


Figure 5-261: Harmonic Voltage of Parigi DB1 Bus bar on Situation C

Based on figure 5-259, figure 5-260 and figure 5-261, When harmonic order is at 5th, voltage spectrum on situation A is 2.83 %, voltage spectrum on situation B is 1.1 % and voltage spectrum on situation C is 0.28. The reduction of voltage spectrum from situation A to situation B is 1.73 %. The reduction of voltage spectrum from situation B to situation C is 0.82 %. When harmonic order is at 7th, voltage spectrum on

situation A is 1.15 %, voltage spectrum on situation B is 0.5 % and voltage spectrum on situation C is 0.25. The reduction of voltage spectrum from situation A to situation B is 0.75 %. The reduction of voltage spectrum from situation B to situation C is 0.25 %.

When harmonic order is at 11st, voltage spectrum on situation A is 0.88 %, voltage spectrum on situation B is 0.67 % and voltage spectrum on situation C is 0.4 %. The reduction of voltage spectrum from situation A to situation B is 0.21 %. The reduction of voltage spectrum from situation B to situation C is 0.27 %. When harmonic order is at 13rd, voltage spectrum on situation A is 0.33 %, voltage spectrum on situation B is 0.43 % and voltage spectrum on situation C is 0.15 %. The increase of voltage spectrum from situation A to situation B is 0.1 %. The reduction of voltage spectrum from situation B to situation C is 0.28 %.

When harmonic order is at 17th, voltage spectrum on situation A is 0.25 %, voltage spectrum on situation B is 0.23 % and voltage spectrum on situation C is 0.16 %. The reduction of voltage spectrum from situation A to situation B is 0.02 %. The reduction of voltage spectrum from situation B to situation C is 0.07 %. When harmonic order is at 19th, voltage spectrum on situation A is 0.08 %, voltage spectrum on situation B is 0.13 % and voltage spectrum on situation C is 0.13 %. The increase of voltage spectrum from situation A to situation B is 0.05 %. There is no anz reduction from situation B to situation C.

When harmonic order is at 23rd, voltage spectrum on situation A is 0.06 %, voltage spectrum on situation B is 0.07 % and voltage spectrum on situation C is 0.025 %. The increase of voltage spectrum from situation A to situation B is 0.01 %. The reduction of voltage spectrum from situation B to situation C is 0.045 %. When harmonic order is at 25th, voltage spectrum on situation A is 0.04 %, voltage spectrum on situation B is 0.04 % and voltage spectrum on situation C is 0.04 %. There is no reduction of voltage spectrum from situation A to situation B and from Situation B to situation C.

Table 5-6: Voltage Spectrum of Parigi DB1 Bus bar on Situation A, B and C

Bus Parigi DB1	Voltage Spectrum [%]		
Harmonic Order	Situation A	Situation B	Situation C
5 th	2.83	1.1	0.28
7 th	1.25	0.5	0.25
11 st	0.88	0.67	0.4
13 rd	0.33	0.43	0.15
17 th	0.25	0.23	0.16
19 th	0.08	0.13	0.13
23 rd	0.06	0.07	0.025
25 th	0.04	0.04	0.04

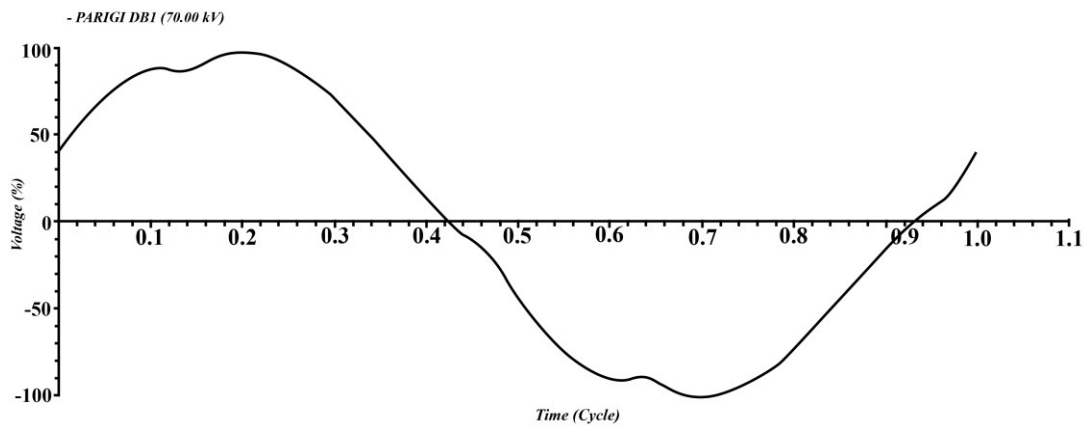


Figure 5-262: Voltage Waveform of Parigi DB1 Bus bar on Situation A

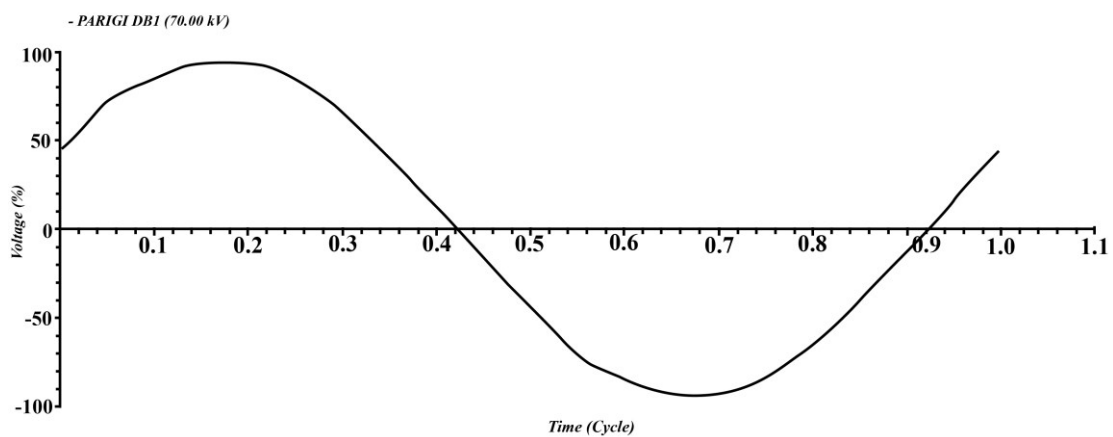


Figure 5-263: Voltage Waveform of Parigi DB1 Bus bar on Situation B

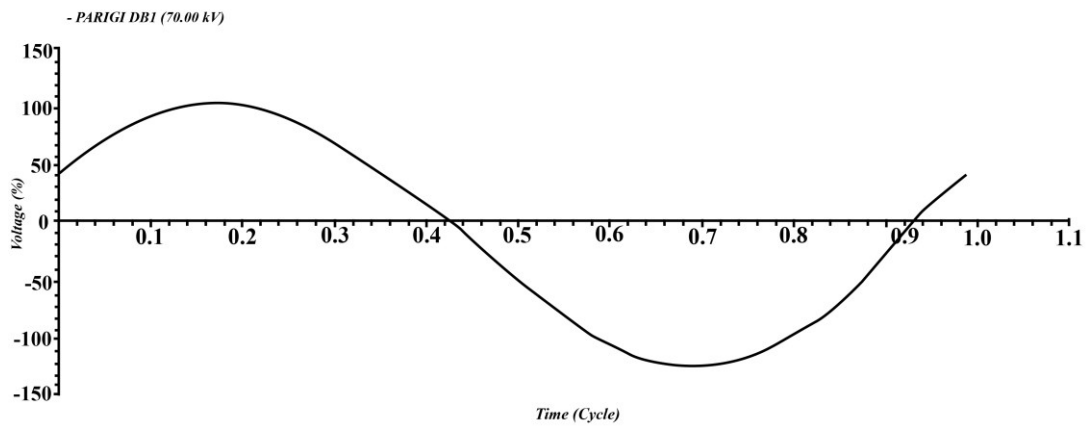


Figure 5-264: Voltage Waveform of Parigi DB1 Bus bar on Situation C

Based on figure 5-262, figure-263 and figure 5-264, The voltage sinusoidal wave against time in cycle of these three situations is the following; on situation A, there are some reductions of waveform sinusoidal voltage between 0.125 cycles and 0.2 cycles, between 0.45 cycles and 0.485 cycles, between 0.6 cycles and 0.685 cycles and between 0.94 cycles and 1.0 cycles. On situation B, there are some reductions of waveform sinusoidal voltage between 0.06 cycles and 0.12 cycles, between 0.16 cycles and 0.225 cycles and between 0.545 cycles and 0.72 cycles. There is no any reduction of sinusoidal waveform on situation C.

Table 5-7: The Reduction of Sinusoidal Waveform of Parigi DB1 Bus bar on Situation A, B and C

Sinusoidal Waveform Result of Bus Parigi DB1			
	Situation A	Situation B	Situation C
1	0.125 cycle – 0.2 cycle	0.06 cycle – 0.12 cycle	No Reduction
2	0.45 cycle – 0.485 cycle	0.16 cycle – 0.225 cycle	
3	0.6 cycle – 0.685 cycle	0.545 cycle – 0.72	
4	0.94 cycle – 1.0 cycle		

Harmonic Simulation results of Parigi DB1 (2) bus bar are equal to harmonic simulation results of Parigi DB1.

Harmonic Simulation results of Parigi SB1 bus bar on situation A, B and C can be seen on the explanation below.

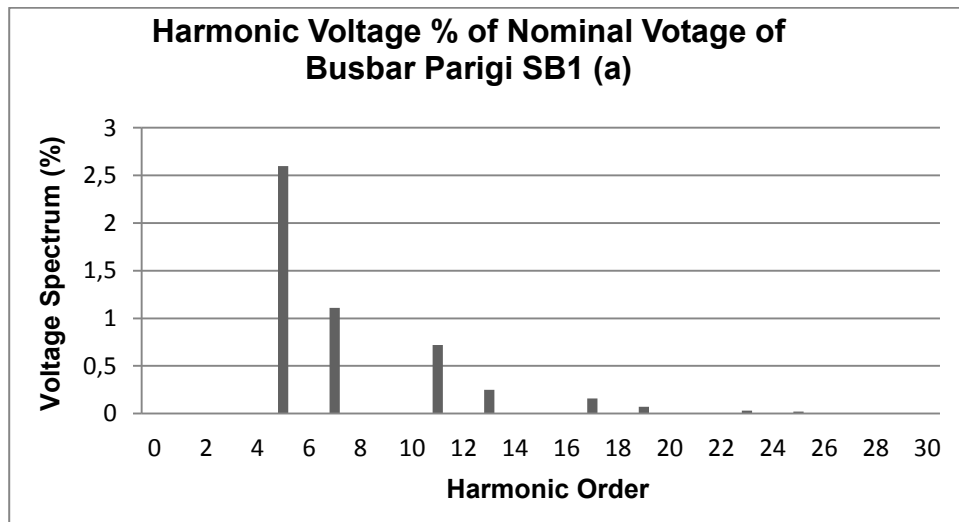


Figure 5-265: Harmonic Voltage of Parigi SB1 Bus bar on Situation A

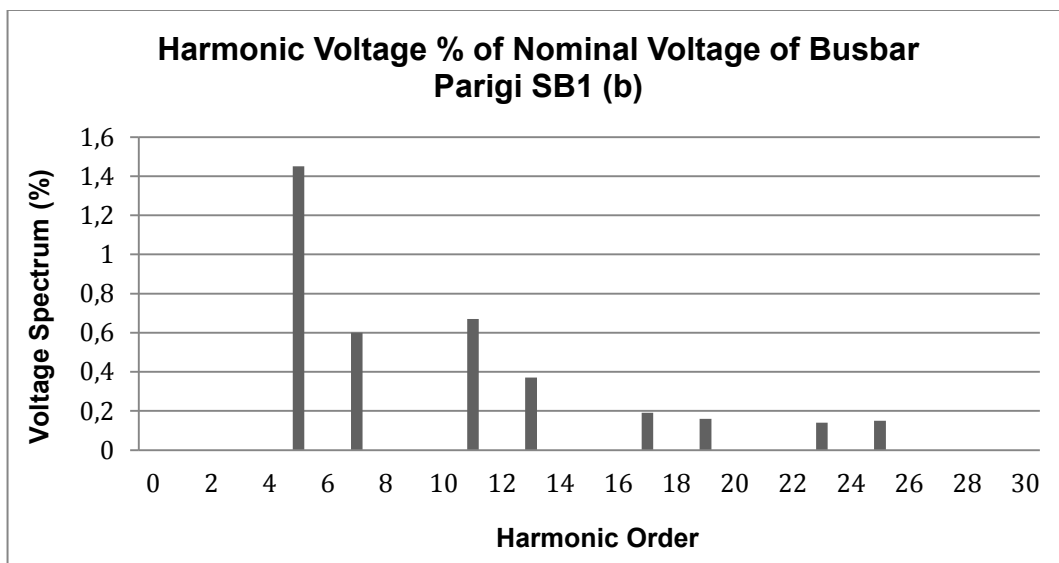


Figure 5-266: Harmonic Voltage of Parigi SB1 Bus bar on Situation B

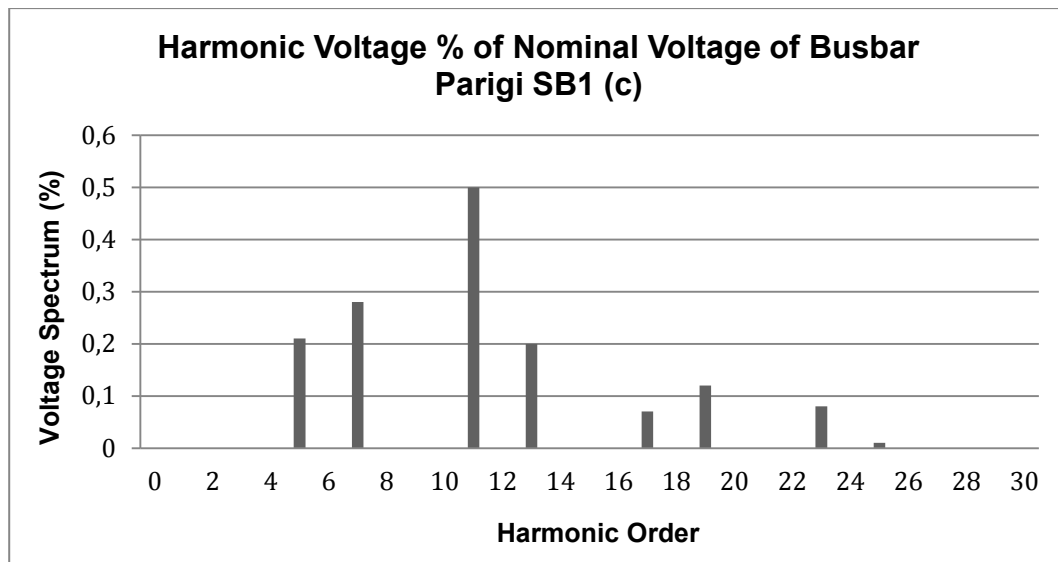


Figure 5-267: Harmonic Voltage of Parigi SB1 Bus bar on Situation C

Based on figure 5-265, figure 5-266 and figure 5-267, When harmonic order is at 5th, voltage spectrum on situation A is 2.6 %, voltage spectrum on situation B is 1.45 % and voltage spectrum on situation C is 0.21. The reduction of voltage spectrum from situation A to situation B is 1.15 %. The reduction of voltage spectrum from situation B to situation C is 1.24 %. When harmonic order is at 7th, voltage spectrum on situation A is 1.11 %, voltage spectrum on situation B is 0.6 % and voltage spectrum on situation C is 0.28. The reduction of voltage spectrum from situation A to situation B is 0.15 %. The reduction of voltage spectrum from situation B to situation C is 0.32 %.

When harmonic order is at 11st, voltage spectrum on situation A is 0.72 %, voltage spectrum on situation B is 0.67 % and voltage spectrum on situation C is 0.5 %. The reduction of voltage spectrum from situation A to situation B is 0.05 %. The reduction of voltage spectrum from situation B to situation C is 0.17 %. When harmonic order is at 13rd, voltage spectrum on situation A is 0.25 %, voltage spectrum on situation B is 0.37 % and voltage spectrum on situation C is 0.2 %. The increase of voltage spectrum from situation A to situation B is 0.12 %. The reduction of voltage spectrum from situation B to situation C is 0.17 %.

When harmonic order is at 17th, voltage spectrum on situation A is 0.16 %, voltage spectrum on situation B is 0.19 % and voltage spectrum on situation C is 0.07 %. The

increase of voltage spectrum from situation A to situation B is 0.03 %. The reduction of voltage spectrum from situation B to situation C is 0.12 %. When harmonic order is at 19th, voltage spectrum on situation A is 0.07 %, voltage spectrum on situation B is 0.16 % and voltage spectrum on situation C is 0.12 %. The increase of voltage spectrum from situation A to situation B is 0.09 %. The reduction of voltage spectrum from situation B to situation C is 0.04 %.

When harmonic order is at 23rd, voltage spectrum on situation A is 0.03 %, voltage spectrum on situation B is 0.14 % and voltage spectrum on situation C is 0.08 %. The increase of voltage spectrum from situation A to situation B is 0.11 %. The reduction of voltage spectrum from situation B to situation C is 0.06 %. When harmonic order is at 25th, voltage spectrum on situation A is 0.02 %, voltage spectrum on situation B is 0.15 % and voltage spectrum on situation C is 0.01 %. The increase of voltage spectrum from situation A to situation B is 0.13 %. The reduction of voltage spectrum from situation B to situation C is 0.14 %.

Table 5-8: Voltage Spectrum of Parigi SB1 Bus bar on Situation A, B and C

Bus Parigi SB1	Voltage Spectrum [%]		
Harmonic Order	Situation A	Situation B	Situation C
5th	2.6	1.45	0.21
7th	1.11	0.60	0.28
11st	0.72	0.67	0.50
13rd	0.25	0.37	0.20
17th	0.16	0.19	0.07
19th	0.07	0.16	0.12
23rd	0.03	0.14	0.08
25th	0.02	0.15	0.01

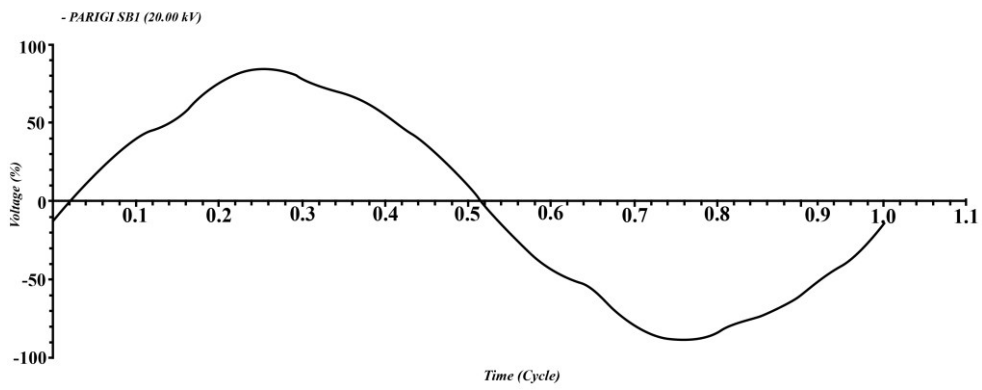


Figure 5-268: Voltage Waveform of Parigi SB1 Bus bar on Situation A

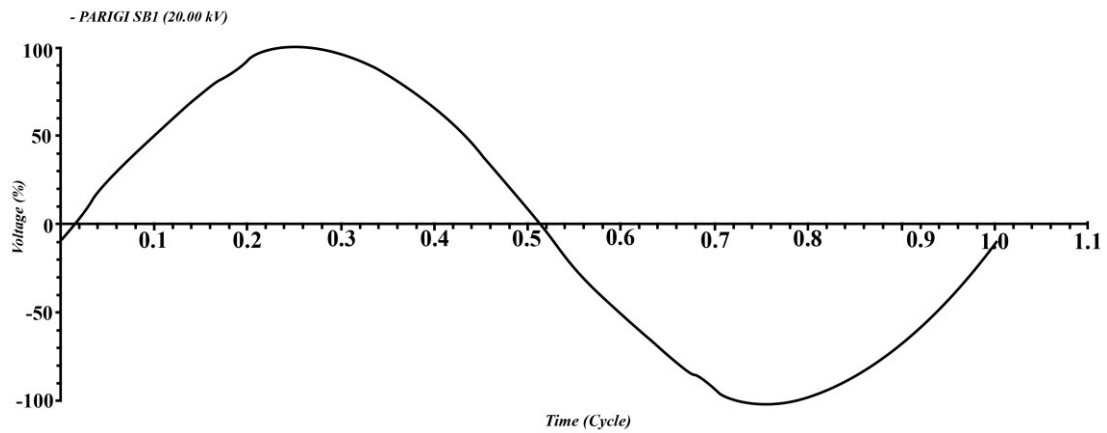


Figure 5-269: Voltage Waveform of Parigi SB1 Bus bar on Situation B

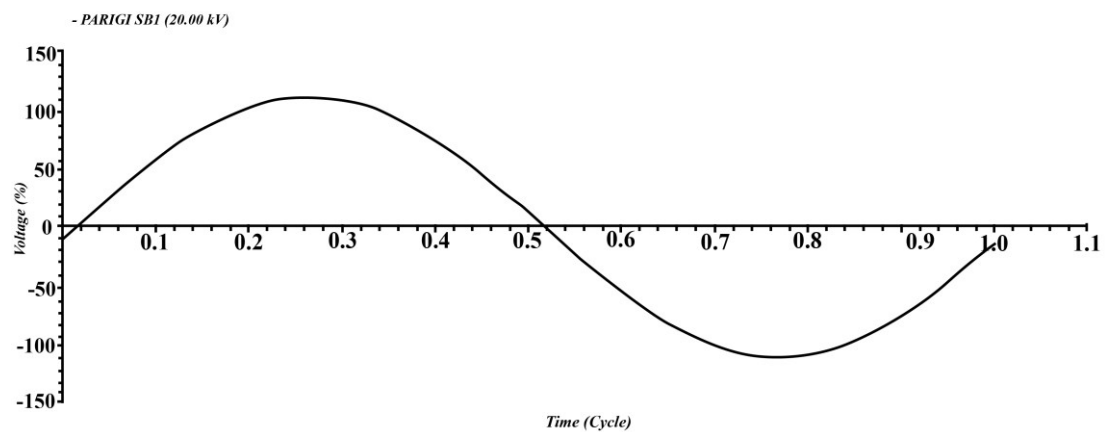


Figure 5-270: Voltage Waveform of Parigi SB1 Bus bar on Situation C

Based on figure 5-268, figure 5-269 and figure 5-270, The voltage sinusoidal wave against time in cycle of these three situations is the following; on situation A, there are some reductions of waveform sinusoidal voltage between 0.107 cycles and 0.18 cycles, between 0.3 cycles and 0.37 cycles, between 0.39 cycles and 0.47 cycles, between 0.61 cycles and 0.67 cycles, between 0.79 and 0.86 and between 0.87 and 0.96.

On situation B, there are some reductions of waveform sinusoidal voltage between 0.02 cycles and 0.2 cycles and between 0.54 cycles and 0.7 cycles. There is no any reduction of sinusoidal waveform on situation C.

Table 5-9: The Reduction of Sinusoidal Waveform of Parigi SB1 Bus bar on Situation C

Sinusoidal Waveform Result of Bus Parigi SB1			
	Situation A	Situation B	Situation C
1	0.107 cycle – 0.18 cycle	0.02 cycle – 0.2 cycle	No reduction
2	0.3 cycle – 0.37 cycle		
3	0.39 cycle – 0.47 cycle	0.54 cycle – 0.7 cycle	
4	0.61 ccycle – 0.67 cycle		

Harmonic simulation results of Parigi SB2 bus bar on situation A, B and C can be seen on the explanation below.

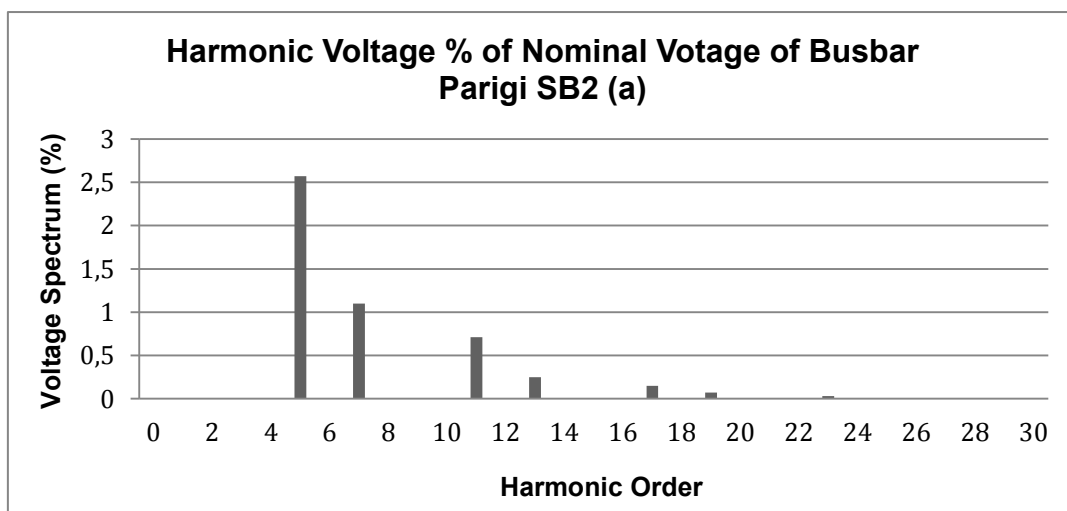


Figure 5-271: Harmonic Voltage of Parigi SB2 Bus bar on Situation A

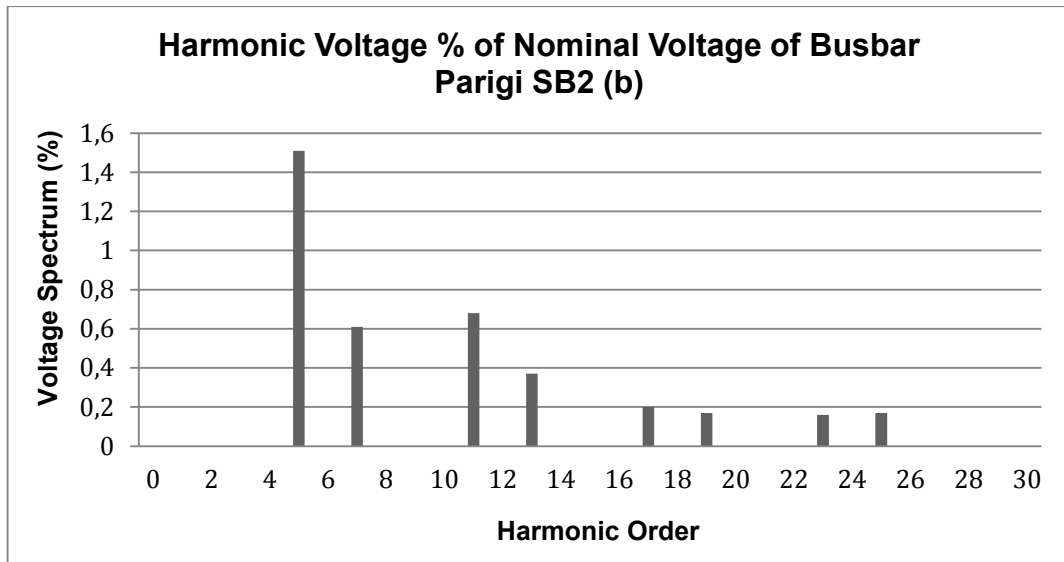


Figure 5-272: Harmonic Voltage of Parigi SB2 Bus bar on Situation B

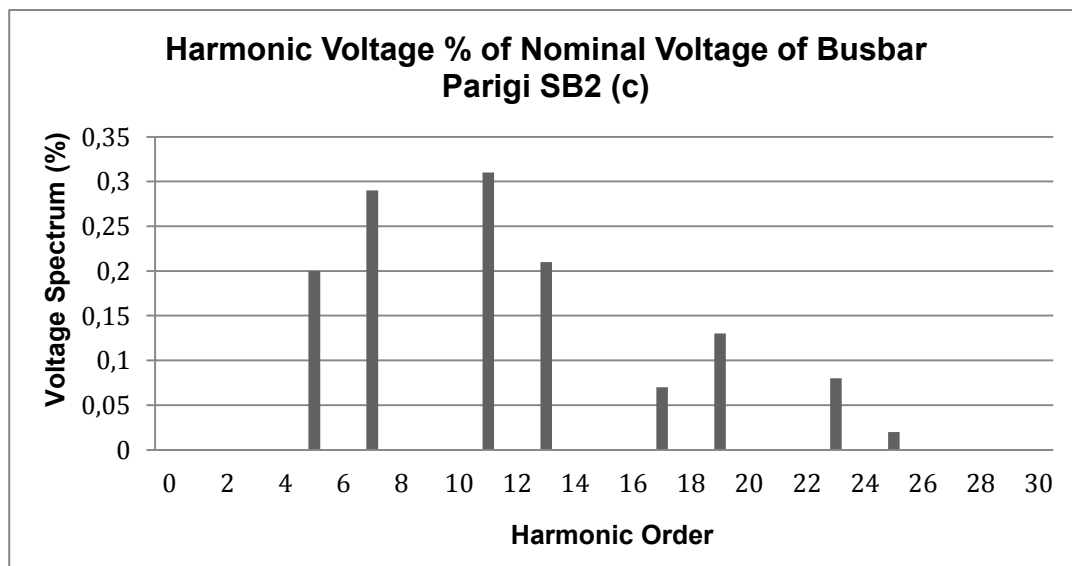


Figure 5-273: Harmonic Voltage of Parigi SB2 Bus bar on Situation C

Based on figure 5-271, figure 5-272 and figure 5-273, When harmonic order is at 5th, voltage spectrum on situation A is 2.57 %, voltage spectrum on situation B is 1.51 % and voltage spectrum on situation C is 0.2 %. The reduction of voltage spectrum from situation A to situation B is 1.06 %. The reduction of voltage spectrum from situation B to situation C is 1.31 %. When harmonic order is at 7th, voltage spectrum on situation A is 1.10 %, voltage spectrum on situation B is 0.61 % and voltage spectrum on situation C is 0.29. The reduction of voltage spectrum from situation A to

situation B is 0.49 %. The reduction of voltage spectrum from situation B to situation C is 0.32 %.

When harmonic order is at 11st, voltage spectrum on situation A is 0.71 %, voltage spectrum on situation B is 0.68 % and voltage spectrum on situation C is 0.31 %. The reduction of voltage spectrum from situation A to situation B is 0.03 %. The reduction of voltage spectrum from situation B to situation C is 0.37 %. When harmonic order is at 13rd, voltage spectrum on situation A is 0.25 %, voltage spectrum on situation B is 0.37 % and voltage spectrum on situation C is 0.21 %. The increase of voltage spectrum from situation A to situation B is 0.12 %. The decrease of voltage spectrum from situation B to situation C is 0.16 %.

When harmonic order is at 17th, voltage spectrum on situation A is 0.15 %, voltage spectrum on situation B is 0.2 % and voltage spectrum on situation C is 0.07 %. The increase of voltage spectrum from situation A to situation B is 0.05 %. The decrease of voltage spectrum from situation B to situation C is 0.13 %. When harmonic order is at 19th, voltage spectrum on situation A is 0.07 %, voltage spectrum on situation B is 0.17 % and voltage spectrum on situation C is 0.13 %. The increase of voltage spectrum from situation A to situation B is 0.1 %. The reduction of voltage spectrum from situation B to situation C is 0.04 %.

When harmonic order is at 23rd, voltage spectrum on situation A is 0.03 %, voltage spectrum on situation B is 0.16 % and voltage spectrum on situation C is 0.08 %. The increase of voltage spectrum from situation A to situation B is 0.13 %. The reduction of voltage spectrum from situation B to situation C is 0.08 %. When harmonic order is at 25th, voltage spectrum on situation A is 0.01 %, voltage spectrum on situation B is 0.17 % and voltage spectrum on situation C is 0.02 %. The increase of voltage spectrum from situation A to situation B is 0.16 %. The reduction of voltage spectrum from situation B to situation C is 0.15 %.

Table 5-10: Voltage Spectrum of Parigi SB2 Bus bar on Situation A, B and C

Bus Parigi SB2	Voltage Spectrum [%]		
Harmonic Order	Situation A	Situation B	Situation C
5 th	2.57	1.51	0.20
7 th	1.10	0.61	0.29
11 st	0.71	0.68	0.31
13 rd	0.25	0.37	0.21
17 th	0.15	0.20	0.07
19 th	0.07	0.17	0.13
23 rd	0.03	0.16	0.08
25 th	0.01	0.17	0.02

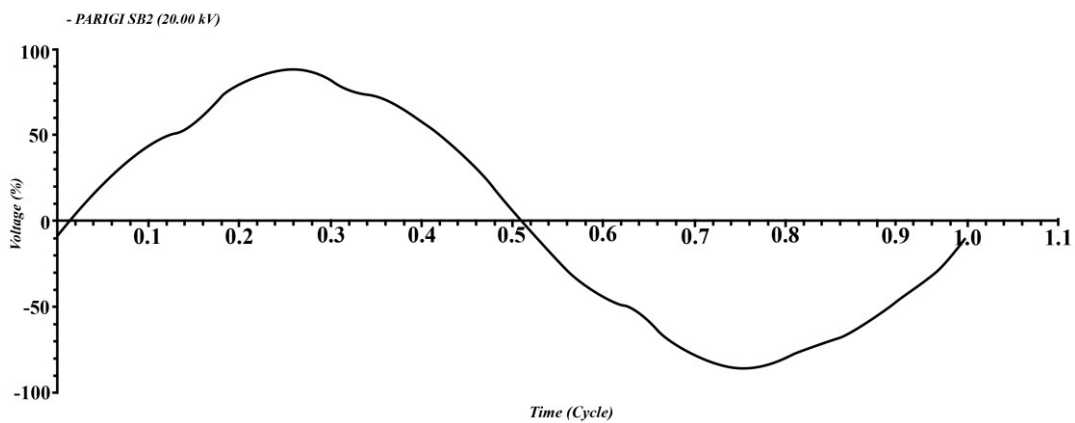


Figure 5-274: Voltage Waveform of Parigi SB2 Bus bar on Situation A

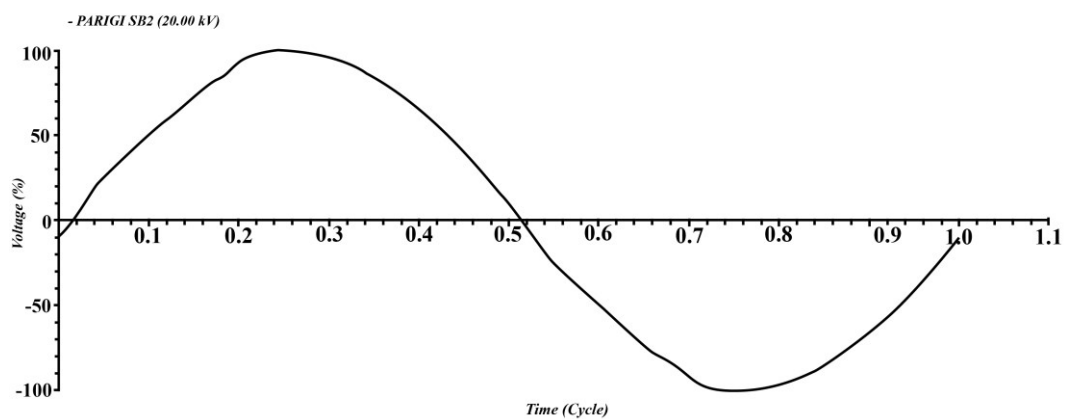


Figure 5-275: Voltage Waveform of Parigi SB2 Bus bar on Situation B

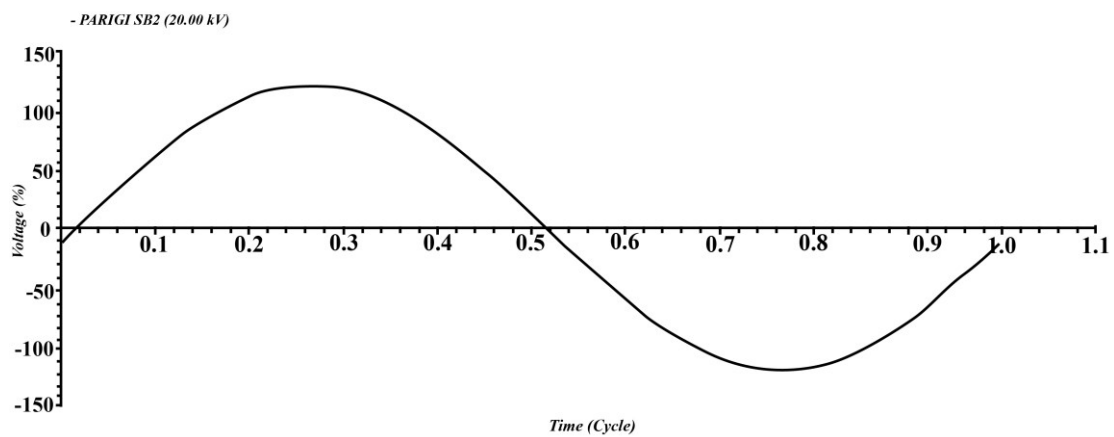


Figure 5-276: Voltage Waveform of Parigi SB2 on Situation C

Based on figure 5.274, figure 5-275 and figure 5-276, The voltage sinusoidal wave against time in cycle of these three situations is the following; on situation A, there are some reductions of waveform sinusoidal voltage between 0.12 cycles and 0.18 cycles, between 0.29 cycles and 0.36 cycles, between 0.48 cycles and 0.61 cycles, between 0.61 cycles and 0.68 cycles, between 0.78 and 0.87 and between 0.87 and 0.97.

On situation B, there are some reductions of waveform sinusoidal voltage between 0.04 cycles and 0.18 cycles and between 0.54 cycles and 0.7 cycles. There is no any reduction of sinusoidal waveform on situation C.

Table 5-11: : The Reduction of Sinusoidal Waveform of Parigi SB1 (2) Bus bar on Situation A, B and C

Sinusoidal Waveform Result of Bus Parigi SB2			
	Situation A	Situation B	Situation C
1	0.12 cycle – 0.18 cycle	0.04 cycle – 0.18 cycle	No reduction
2	0.29 cycle – 0.36 cycle		
3	0.48 cycle – 0.61 cycle		
4	0.61 cycle – 0.68 cycle	0.54 cycle – 0.7 cycle	
5	0.78 cycle – 0.87 cycle		
6	0.87 cycle – 0.97 cycle		

Harmonic Simulation results of PJPP SB1 bus bar on situation A, B and C can be seen on the explanation below.

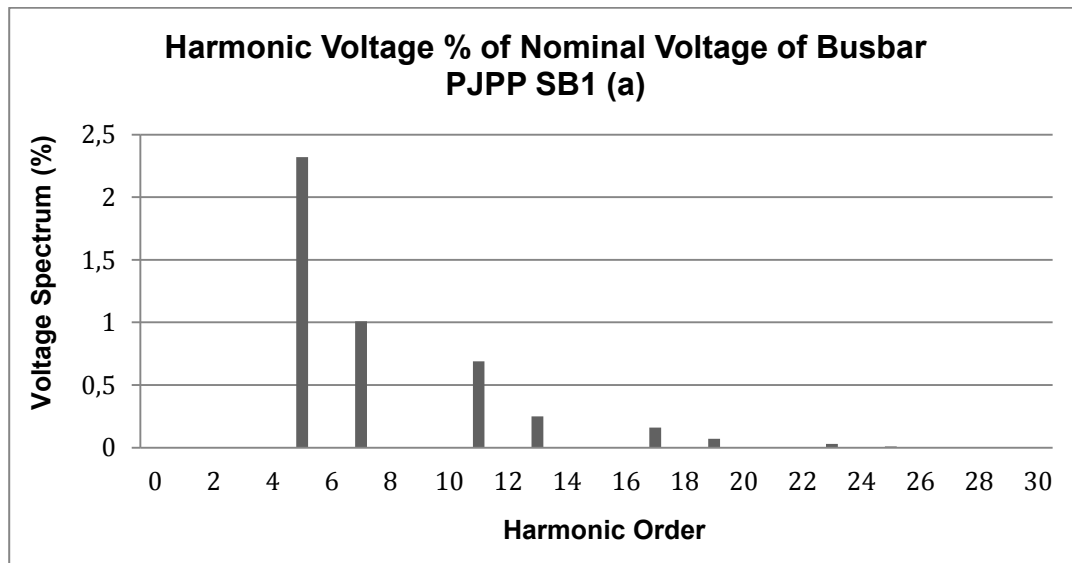


Figure 5-277: Harmonic Voltage of PJPP SB1 Bus bar on Situation A

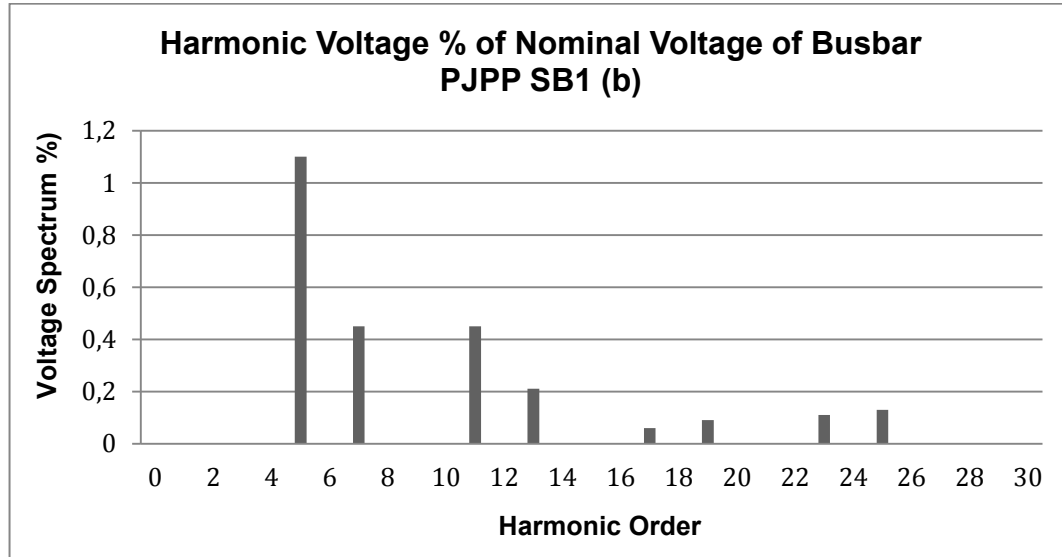


Figure 5-278: Harmonic Voltage of PJPP SB1 Bus bar on Situation B

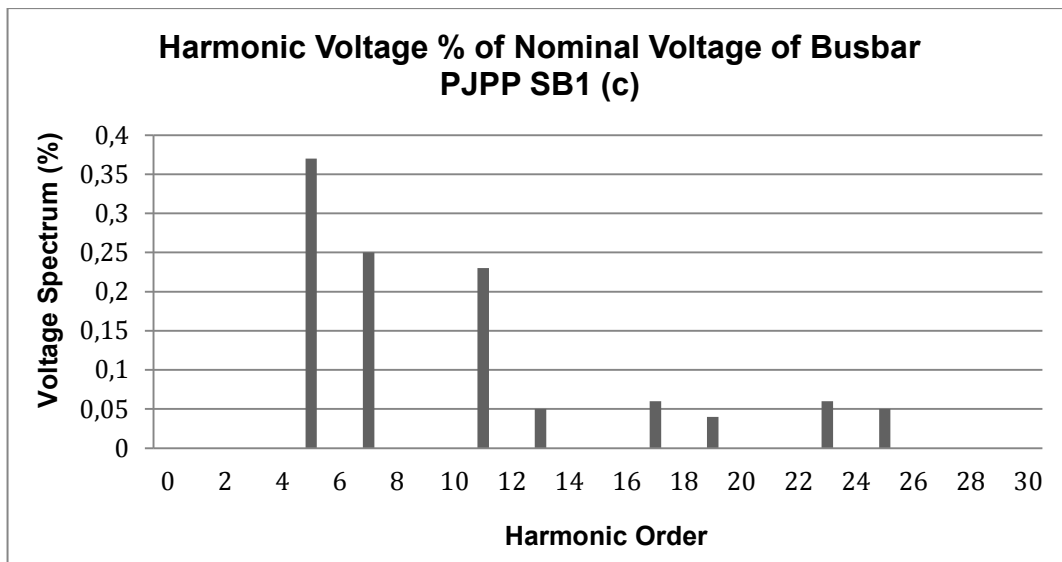


Figure 5-279: Harmonic Voltage of PJPP SB1 Bus bar on Situation C

Based on figure 5-277, figure 5-278 and figure 5-279, When harmonic order is at 5th, voltage spectrum on situation A is 2.32 %, voltage spectrum on situation B is 1.10 % and voltage spectrum on situation C is 0.37 %. The reduction of voltage spectrum from situation A to situation B is 1.22 %. The reduction of voltage spectrum from situation B to situation C is 0.73 %. When harmonic order is at 7th, voltage spectrum on situation A is 1.01 %, voltage spectrum on situation B is 0.45 % and voltage spectrum on situation C is 0.25. The reduction of voltage spectrum from situation A to situation B is 0.56 %. The reduction of voltage spectrum from situation B to situation C is 0.20 %.

When harmonic order is at 11st, voltage spectrum on situation A is 0.69 %, voltage spectrum on situation B is 0.45 % and voltage spectrum on situation C is 0.23 %. The reduction of voltage spectrum from situation A to situation B is 0.24 %. The reduction of voltage spectrum from situation B to situation C is 0.22 %. When harmonic order is at 13rd, voltage spectrum on situation A is 0.25 %, voltage spectrum on situation B is 0.21 % and voltage spectrum on situation C is 0.05 %. The decrease of voltage spectrum from situation A to situation B is 0.04 %. The decrease of voltage spectrum from situation B to situation C is 0.16 %.

When harmonic order is at 17th, voltage spectrum on situation A is 0.16 %, voltage spectrum on situation B is 0.06 % and voltage spectrum on situation C is 0.06 %. The

decrease of voltage spectrum from situation A to situation B is 0.10 %. There is no reduction from situation B to situation C. When harmonic order is at 19th, voltage spectrum on situation A is 0.07 %, voltage spectrum on situation B is 0.09 % and voltage spectrum on situation C is 0.04 %. The increase of voltage spectrum from situation A to situation B is 0.02 %. The reduction of voltage spectrum from situation B to situation C is 0.05 %.

When harmonic order is at 23rd, voltage spectrum on situation A is 0.03 %, voltage spectrum on situation B is 0.11 % and voltage spectrum on situation C is 0.06 %. The increase of voltage spectrum from situation A to situation B is 0.08 %. The decrease of voltage spectrum from situation B to situation C is 0.05. When harmonic order is at 25th, voltage spectrum on situation A is 0.01 %, voltage spectrum on situation B is 0.13 % and voltage spectrum on situation C is 0.05 %. The increase of voltage spectrum from situation A to situation B is 0.12 %. The reduction of voltage spectrum from situation B to situation C is 0.08 %.

Table 5-12: Voltage Spectrum of PJPP SB1 Bus bar on Situation A, B and C

Bus PJPP SB1	Voltage Spectrum [%]		
Harmonic Order	Situation A	Situation B	Situation C
5th	2.32	1.10	0.37
7th	1.01	0.45	0.25
11st	0.69	0.45	0.23
13rd	0.25	0.21	0.05
17th	0.16	0.06	0.06
19th	0.07	0.09	0.04
23rd	0.03	0.11	0.06
25th	0.01	0.13	0.05

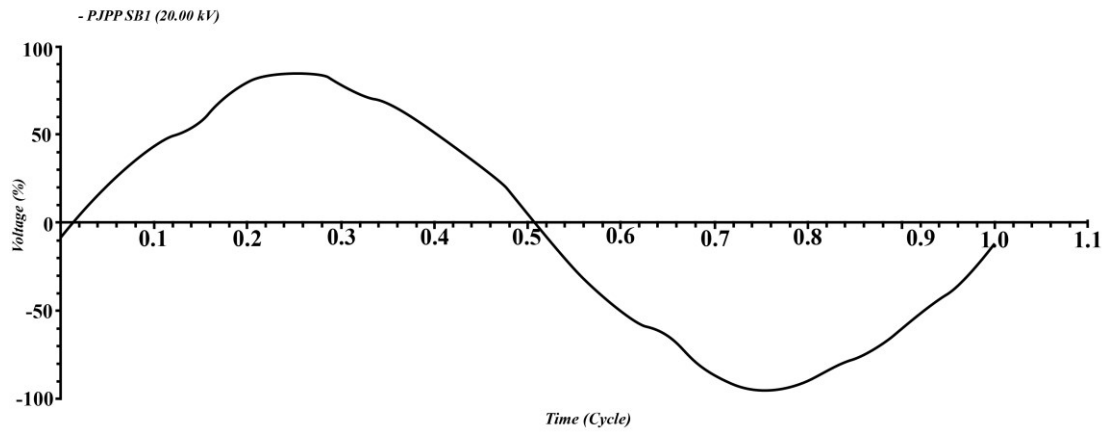


Figure 5-280: Voltage Waveform of PJPP SB1 Bus bar on Situation A

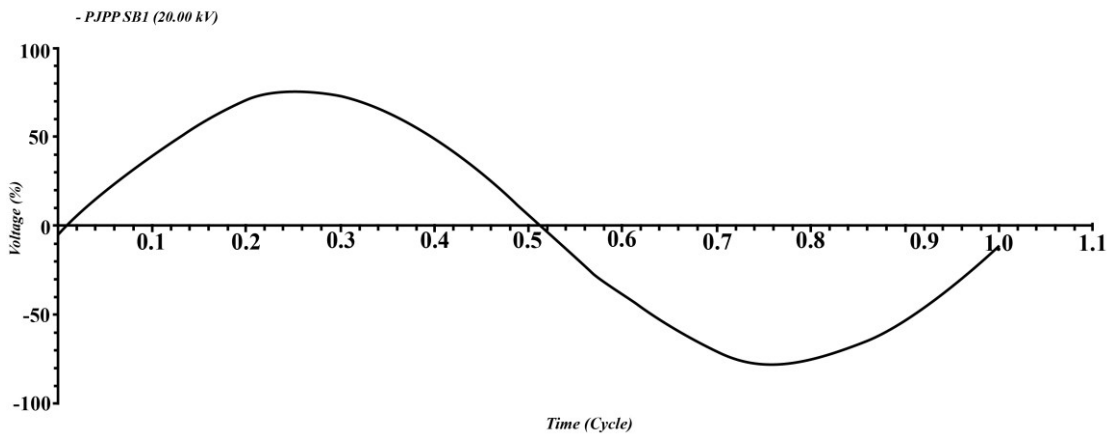


Figure 5-281: Voltage Waveform of PJPP SB1 Bus bar on Situation B

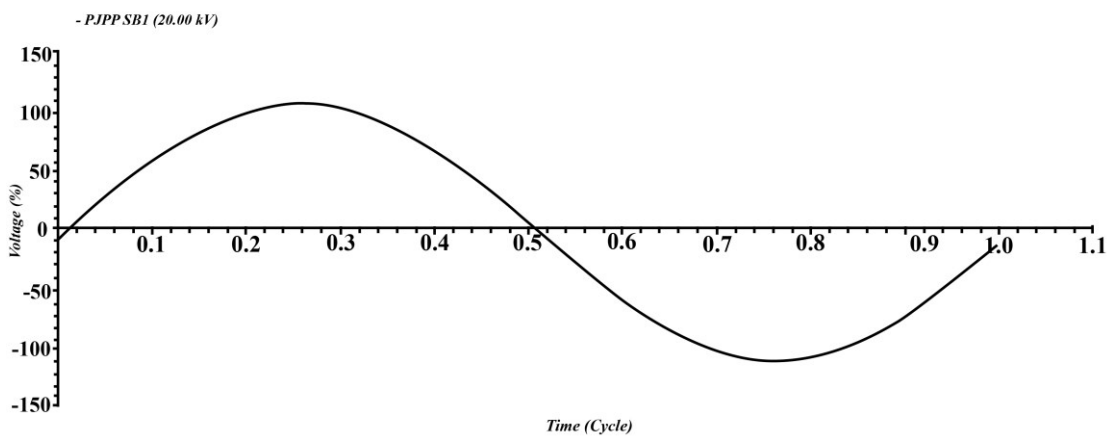


Figure 5-282: Voltage Waveform of PJPP SB1 Bus bar on Situation C

Based on figure 5-280, figure 5-281 and figur 5-282, The voltage sinusoidal wave against time in cycle of these three situations is the following; on situation A, there are some reductions of waveform sinusoidal voltage between 0.11 cycles and 0.18 cycles, between 0.28 cycles and 0.36 cycles, between 0.38 cycles and 0.48 cycles, between 0.6 cycles and 0.66 cycles and between 0.8 and 0.94. There is no reduction of sinusoidal waveform on situation B and situation C.

Table 5-13: The Reduction of Sinusoidal Waveform of PJPP SB1 Bus bar on Situation A, B and C

Sinusoidal Waveform Result of Bus PJPP SB1			
	Situation A	Situation B	Situation C
1	0.11 cycle – 0.18 cycle	No reduction	No reduction
2	0.28 cycle – 0.36 cycle		
3	0.38 cycle – 0.48 cycle		
4	0.6 cycle – 0.66 cycle		
5	0.8 cycle – 0.94 cycle		

Harmonic simulation results of Silae SB1 busbar on Situation A, B and C can be seen on the explanation below.

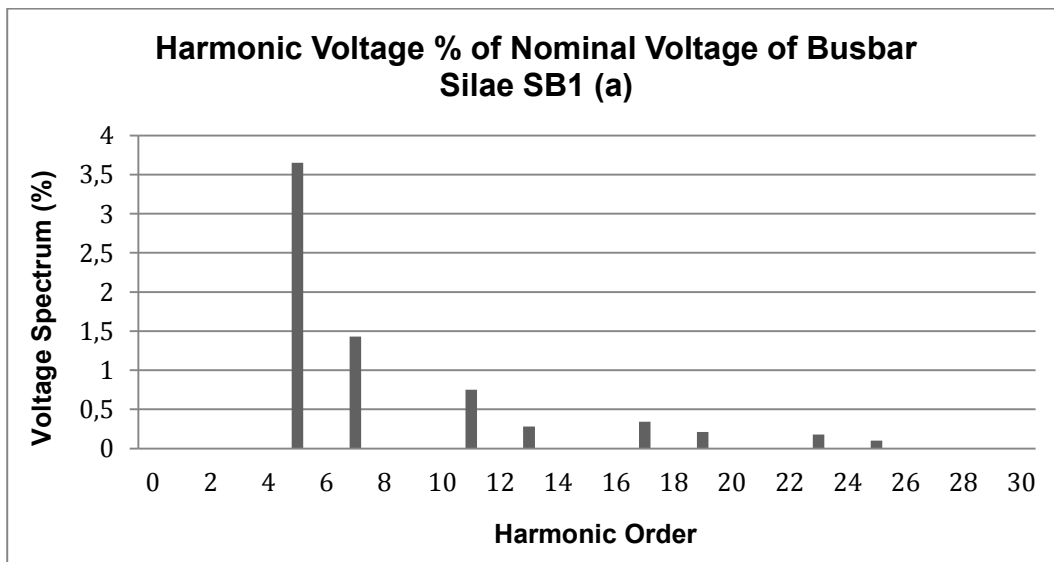


Figure 5-283: Harmonic Voltage of Silae SB1 Bus bar on Situation A

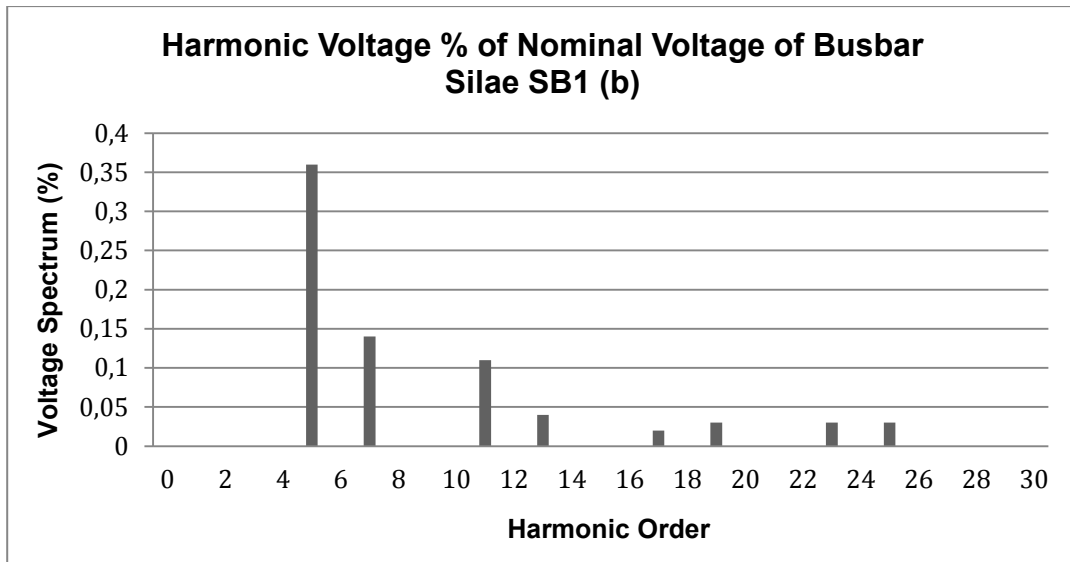


Figure 5-284: Harmonic Voltage of Silae SB1 Bus bar on Situation B

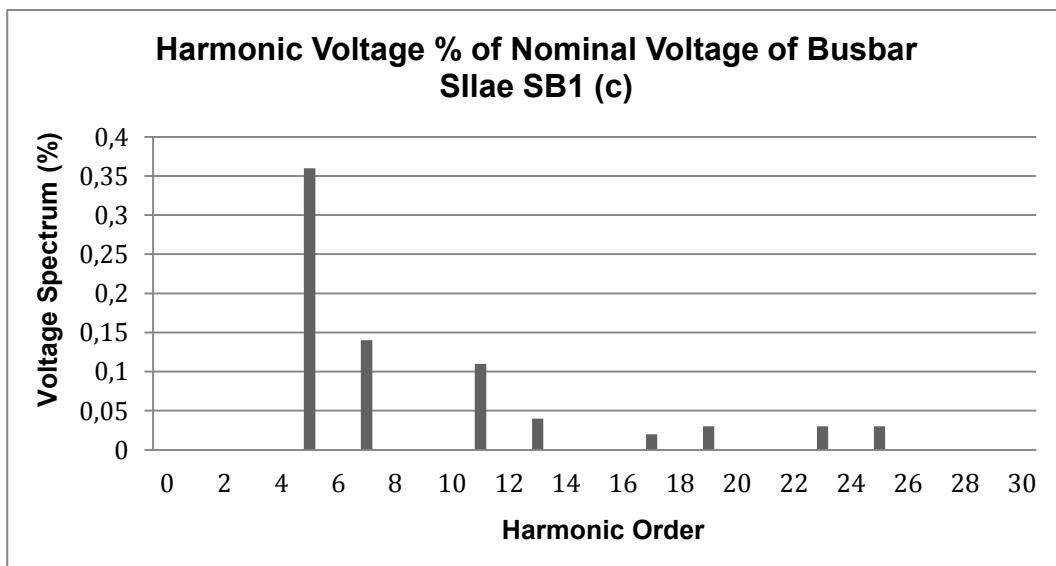


Figure 5-285: Harmonic Voltage of Silae SB1 Bus bar on Situation C

Based on figure 5-283, figure 5-284 and figure 5-285, When harmonic order is at 5th, voltage spectrum on situation A is 3.65 %, voltage spectrum on situation B is 0.36 % and voltage spectrum on situation C is 0.36 %. The reduction of voltage spectrum from situation A to situation B is 3.29 %. There is no reduction from situation B to situation C.

When harmonic order is at 7th, voltage spectrum on situation A is 1.43 %, voltage spectrum on situation B is 0.14 % and voltage spectrum on situation C is 0.14. The reduction of voltage spectrum from situation A to situation B is 1.29 %. There is no any reduction from situation B to situation C.

When harmonic order is at 11st, voltage spectrum on situation A is 0.75 %, voltage spectrum on situation B is 0.11 % and voltage spectrum on situation C is 0.11 %. The reduction of voltage spectrum from situation A to situation B is 0.64 %. There is no reduction from situation B to situation C.

When harmonic order is at 13rd, voltage spectrum on situation A is 0.28 %, voltage spectrum on situation B is 0.04 % and voltage spectrum on situation C is 0.04 %. The decrease of voltage spectrum from situation A to situation B is 0.24 %. There is no any reduction from situation B to situation C. When harmonic order is at 17th, voltage spectrum on situation A is 0.34 %, voltage spectrum on situation B is 0.02 % and voltage spectrum on situation C is 0.02 %. The decrease of voltage spectrum from situation A to situation B is 0.32 %. There is no any reduction from situation B to situation C.

When harmonic order is at 19th, voltage spectrum on situation A is 0.21 %, voltage spectrum on situation B is 0.03 % and voltage spectrum on situation C is 0.03 %. The reduction of voltage spectrum from situation A to situation B is 0.18 %. There is no any reduction from situation B to situation C.

When harmonic order is at 23rd, voltage spectrum on situation A is 0.18 %, voltage spectrum on situation B is 0.03 % and voltage spectrum on situation C is 0.03 %. The reduction of voltage spectrum from situation A to situation B is 0.15 %. There is no any reduction from situation B to situation C.

When harmonic order is at 25th, voltage spectrum on situation A is 0.1 %, voltage spectrum on situation B is 0.03 % and voltage spectrum on situation C is 0.03 %. The reduction of voltage spectrum from situation A to situation B is 0.07 %. There is no any reduction from situation B to situation C.

Table 5-14: Voltage Spectrum of Silae SB1 Bus bar on Situation A, B and C

Bus Silae SB1	Voltage Spectrum [%]		
Harmonic Order	Situation A	Situation B	Situation C
5 th	3.65	0.36	0.36
7 th	1.43	0.14	0.14
11 st	0.75	0.11	0.11
13 rd	0.28	0.04	0.04
17 th	0.34	0.02	0.02
19 th	0.21	0.03	0.03
23 rd	0.18	0.03	0.03
25 th	0.1	0.03	0.03

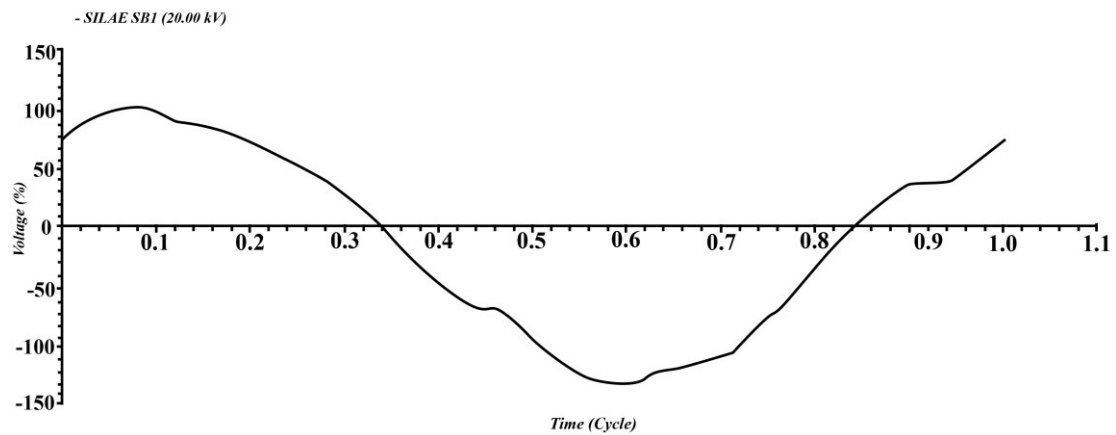


Figure 5-286: Voltage Waveform of Silae SB1 Bus bar on Situation A

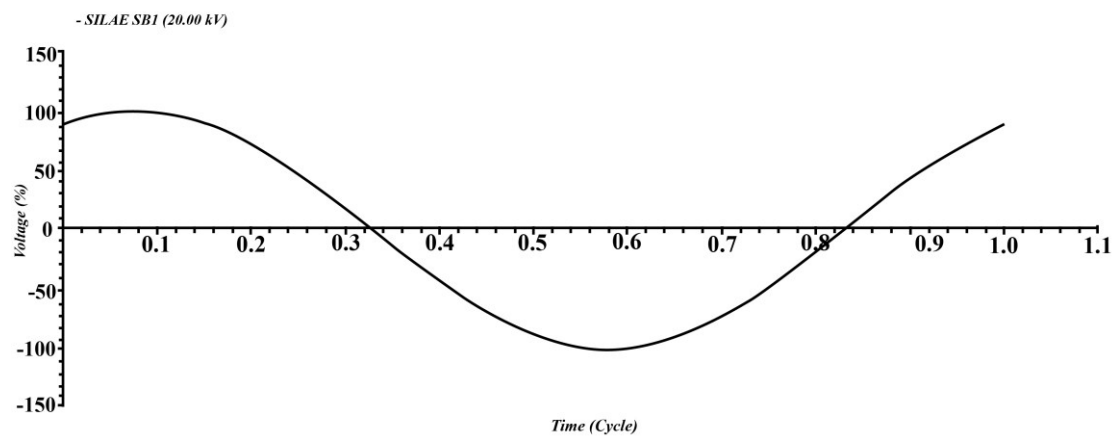


Figure 5-287: Voltage Waveform of Silae SB1 Bus bar on Situation B

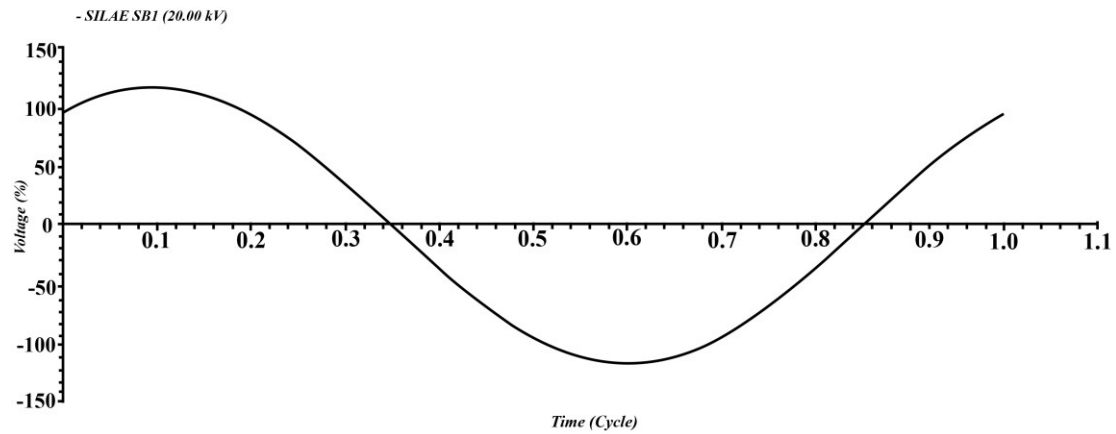


Figure 5-288: Voltage Waveform of Silae SB1 Bus bar on Situation C

Based on figure 5-286, figure 5-287 and figure 5-288, The sinusoidal wave voltage against time in cycle of these three situations is the following; on situation A, there are some reductions of waveform sinusoidal voltage between 0.1 cycles and 0.16 cycles, between 0.25 cycles and 0.29 cycles, between 0.42 cycles and 0.48 cycles, between 0.58 cycles and 0.68 cycles, between 0.74 and 0.8 and between 0.92 and 0.98. There is no reduction of sinusoidal waveform on situation B and situation C.

Table 5-15: The Reduction of Sinusoidal Waveform of Silae SB1 Bus bar on Situation A, B and C

Sinusoidal Waveform Result oSilae SB1 Bus bar			
	Situation A	Situation B	Situation C
1	0.1 cycle – 0.16 cycle	No reduction	No reduction
2	0.25 cycle – 0.29 cycle		
3	0.42 cycle – 0.48 cycle		
4	0.58 cycle – 0.68 cycle		
5	0.74 cycle – 0.8 cycle		
6	0.92 cycle – 0.98 cycle		

Harmonic simulation result of Silae SB2 and Silae SB3 bus bar on situation A, B and C is equal to Silae SB1 bus bar.

Harmonic simulation results of Silae SB4 bus bar on situation A, B and C can be seen on the explanation below.

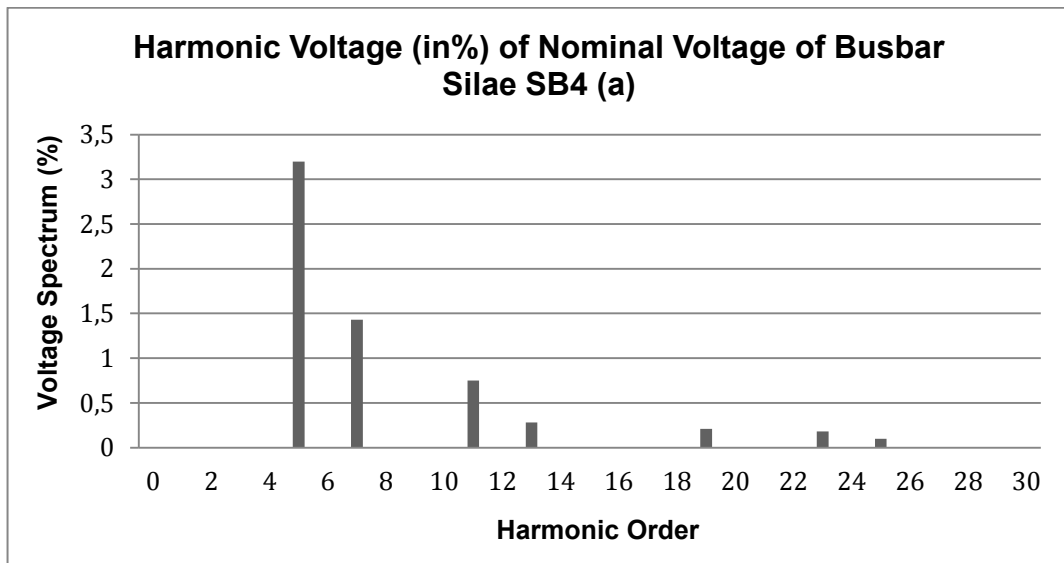


Figure 5-289: Harmonic Voltage of Silae SB4 Bus bar on Situation A

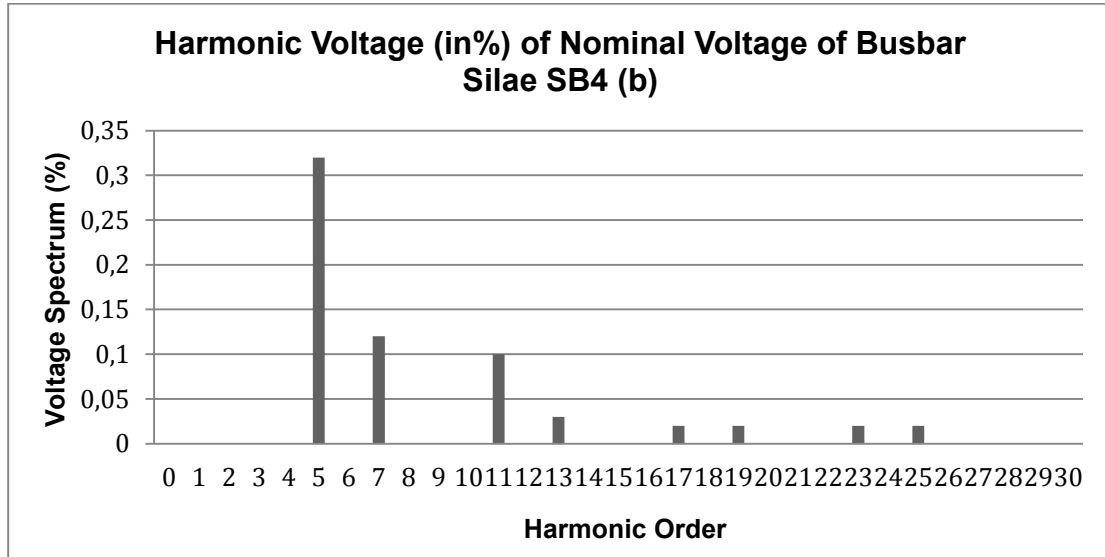


Figure 5-290: Harmonic Voltage of Silae SB4 Bus bar on Situation B

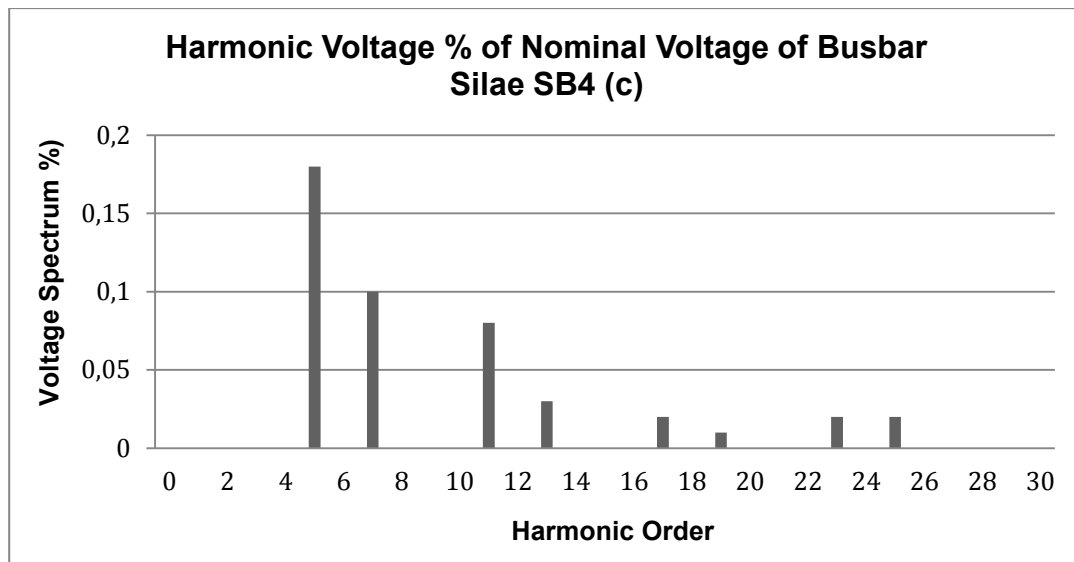


Figure 5-291: Harmonic Voltage of Silae SB4 Bus bar on Situation C

Based on figure 5-289, figure 5-290 and figure 5-291, When harmonic order is at 5th, voltage spectrum on situation A is 3.2 %, voltage spectrum on situation B is 0.32 % and voltage spectrum on situation C is 0.18 %. The reduction of voltage spectrum from situation A to situation B is 2.88 %. The reduction of voltage spectrum from situation B to situation C is 0.14 %. When harmonic order is at 7th, voltage spectrum on situation A is 1.43 %, voltage spectrum on situation B is 0.12 % and voltage spectrum on situation C is 0.10. The reduction of voltage spectrum from situation A to situation B is 1.31 %. The reduction of voltage spectrum from situation B to situation C is 0.02 %.

When harmonic order is at 11st, voltage spectrum on situation A is 0.75 %, voltage spectrum on situation B is 0.1 % and voltage spectrum on situation C is 0.08 %. The reduction of voltage spectrum from situation A to situation B is 0.65 %. The decrease of voltage spectrum from situation B to situation C is 0.02 %. When harmonic order is at 13rd, voltage spectrum on situation A is 0.28 %, voltage spectrum on situation B is 0.03 % and voltage spectrum on situation C is 0.03 %. The decrease of voltage spectrum from situation A to situation B is 0.25 %. There is no any reduction from situation B to situation C.

When harmonic order is at 17th, voltage spectrum on situation A is 0.34 %, voltage spectrum on situation B is 0.02 % and voltage spectrum on situation C is 0.02 %. The decrease of voltage spectrum from situation A to situation B is 0.32 %. There is no any reduction from situation B to situation C. When harmonic order is at 19th, voltage spectrum on situation A is 0.21 %, voltage spectrum on situation B is 0.02 % and voltage spectrum on situation C is 0.01 %. The reduction of voltage spectrum from situation A to situation B is 0.19 %. The reduction of voltage spectrum from situation B to situation C is 0.01 %.

When harmonic order is at 23rd, voltage spectrum on situation A is 0.18 %, voltage spectrum on situation B is 0.02 % and voltage spectrum on situation C is 0.02 %. The decrease of voltage spectrum from situation A to situation B is 0.16 %. There is no any reduction from situation B to situation C. When harmonic order is at 25th, voltage spectrum on situation A is 0.1 %, voltage spectrum on situation B is 0.02 % and voltage spectrum on situation C is 0.02 %. The reduction of voltage spectrum from situation A to situation B is 0.08 %. There is no any reduction from situation B to situation C.

Table 5-16: Voltage Spectrum of Silae SB4 Bus bar on Situation A, B and C

Bus Silae SB4	Voltage Spectrum [%]		
	Situation A	Situation B	Situation C
5 th	3.2	0.32	0.18
7 th	1.43	0.12	0.10
11 st	0.75	0.10	0.08
13 rd	0.28	0.03	0.03
17 th	0.34	0.02	0.02
19 th	0.21	0.02	0.01
23 rd	0.18	0.02	0.02
25 th	0.10	0.02	0.02

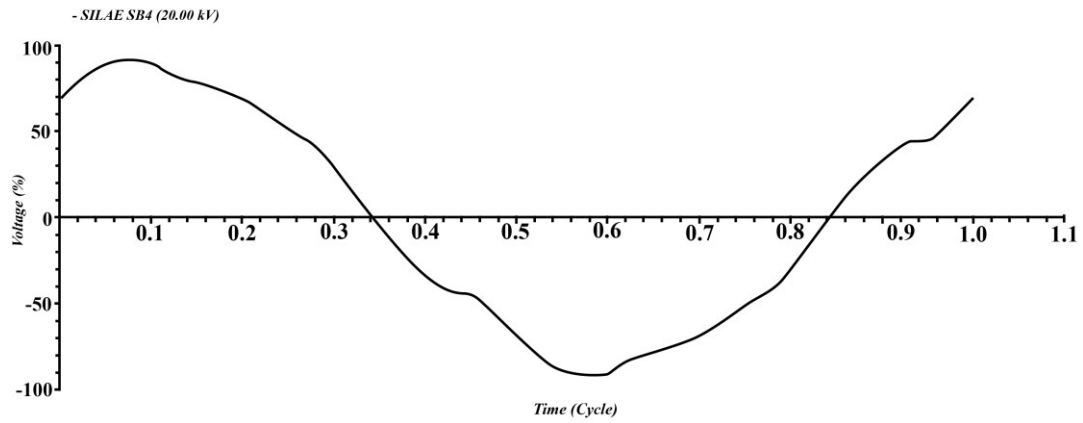


Figure 5-292: Voltage Waveform of Silae SB4 Bus bar on Situation A

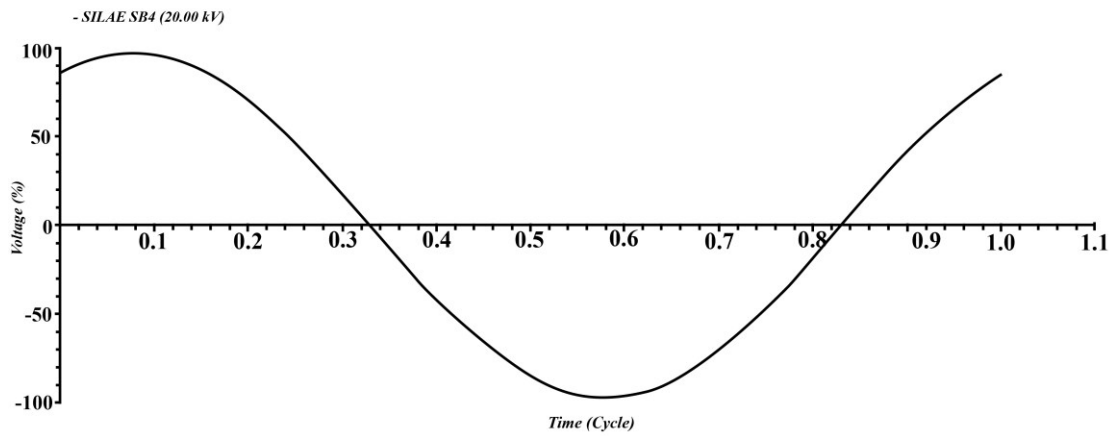


Figure 5-293: Voltage Waveform of silae SB4 Bus bar on Situation B

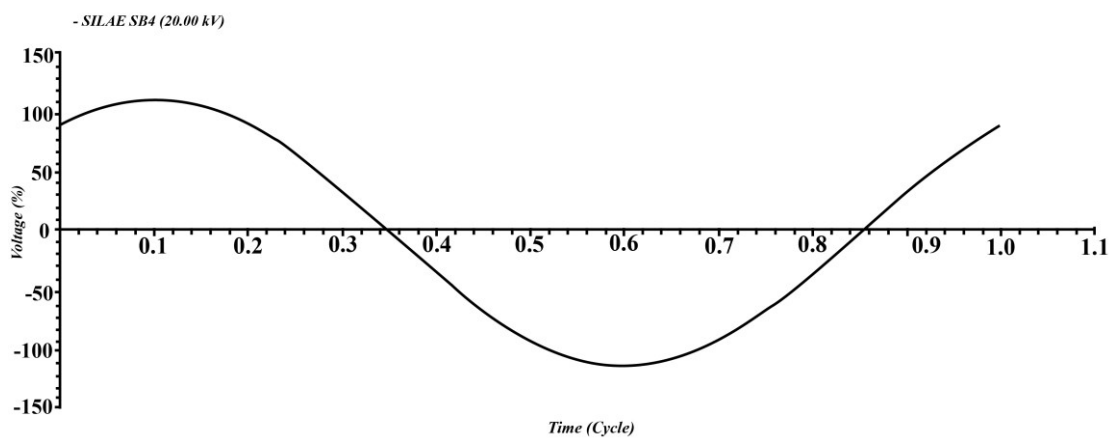


Figure 5-294: Voltage Waveform of Silae Sb4 Bus bar on Situation C

Based on figure 5-292, figure 5-293 and figure 5-294, the sinusoidal wave voltage against time in cycle of these three situations is similar to sinusoidal waveform voltage of Donggala SB1 and Maesa SB1 bus bar.

Harmonic simulation results of Talise SB1 bus bar on situation A, B and C can be seen on the explanation below.

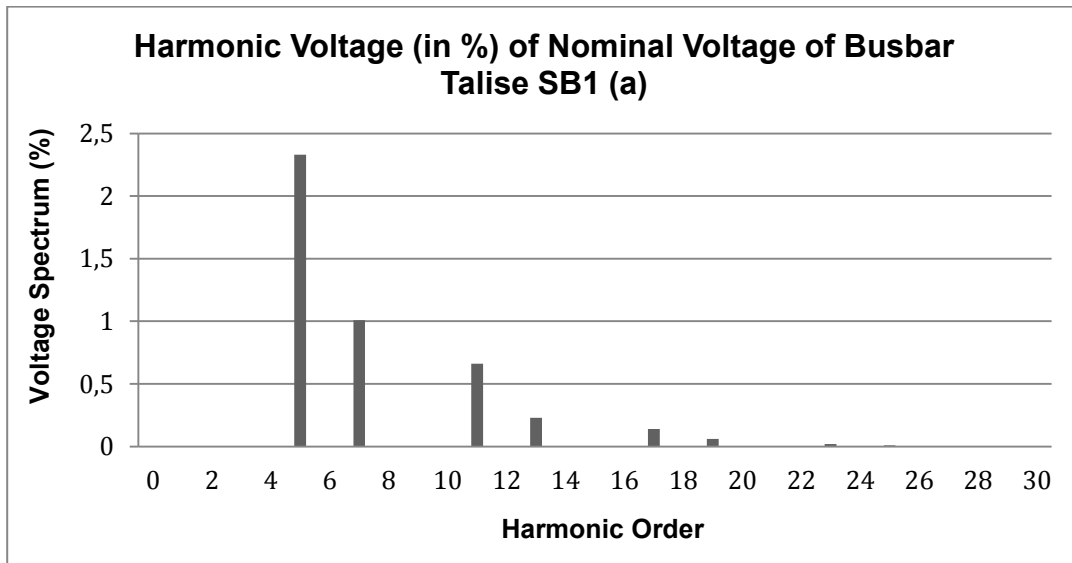


Figure 5-295: Harmonic Voltage of Talise SB1 Bus bar on Situation A

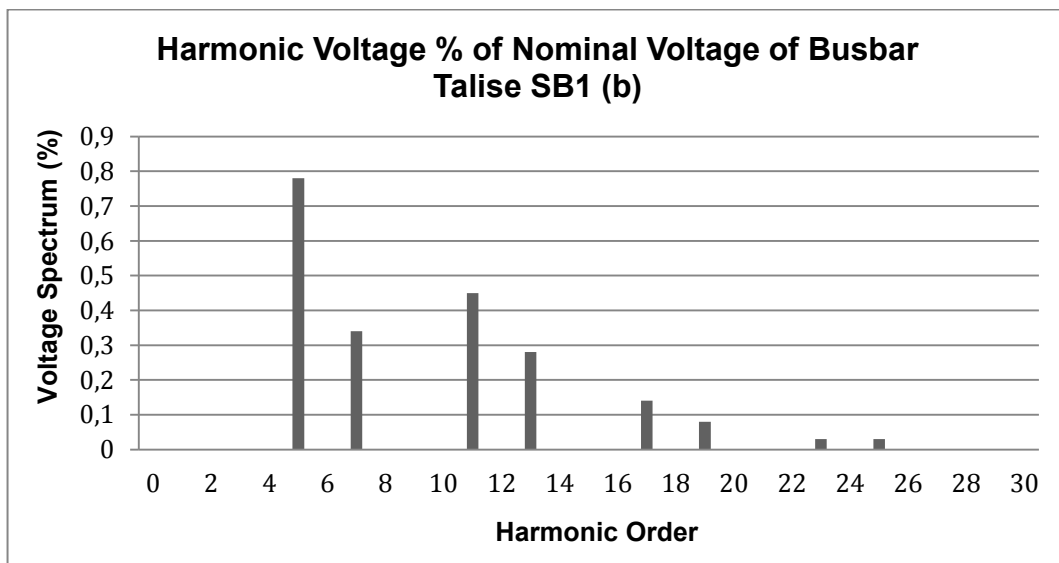


Figure 5-296: Harmonic Voltage of Talise SB1 Bus bar on Situation B

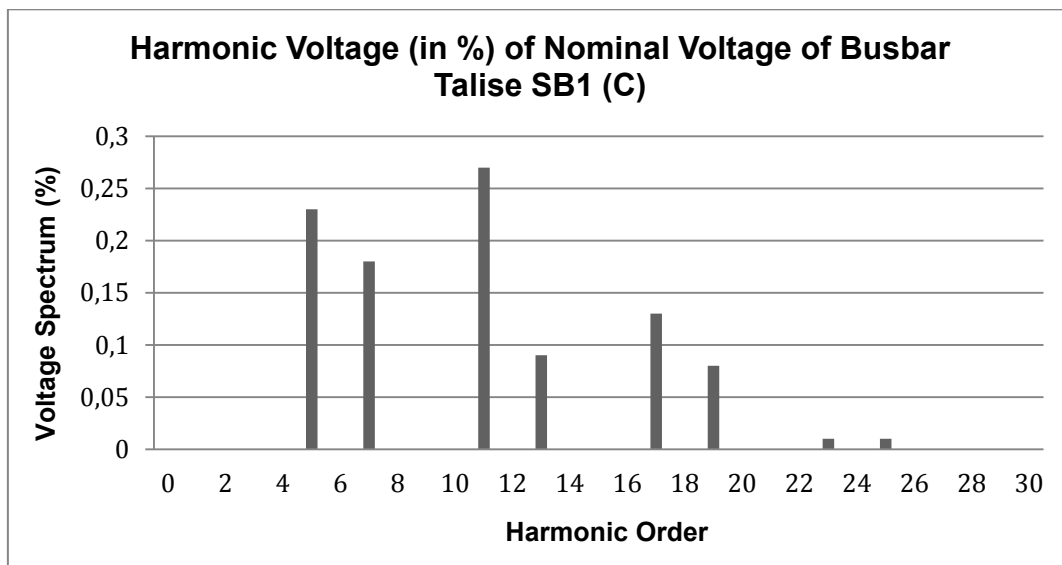


Figure 5-297: Harmonic Voltage of Talise SB1 Bus bar on Situation C

Based on figure 5-443, figure 5-444 and figure 5-445, When harmonic order is at 5th, voltage spectrum on situation A is 2.33 %, voltage spectrum on situation B is 0.78 % and voltage spectrum on situation C is 0.23 %. The reduction of voltage spectrum from situation A to situation B is 1.55 %. The reduction of voltage spectrum from situation B to situation C is 0.55 %. When harmonic order is at 7th, voltage spectrum on situation A is 1.01 %, voltage spectrum on situation B is 0.34 % and voltage spectrum on situation C is 0.18. The reduction of voltage spectrum from situation A to situation B is 0.67 %. The reduction of voltage spectrum from situation B to situation C is 0.16 %.

When harmonic order is at 11st, voltage spectrum on situation A is 0.66 %, voltage spectrum on situation B is 0.45 % and voltage spectrum on situation C is 0.27 %. The reduction of voltage spectrum from situation A to situation B is 0.21 %. The reduction of voltage spectrum from situation B to situation C is 0.18 %. When harmonic order is at 13rd, voltage spectrum on situation A is 0.23 %, voltage spectrum on situation B is 0.28 % and voltage spectrum on situation C is 0.09 %. The increase of voltage spectrum from situation A to situation B is 0.05 %. The reduction of voltage spectrum from situation B to situation C is 0.19 %.

When harmonic order is at 17th, voltage spectrum on situation A is 0.14 %, voltage spectrum on situation B is 0.14 % and voltage spectrum on situation C is 0.13 %. There is no any reduction from situation A to situation B.. The reduction of voltage spectrum from situation B to situation C is 0.01 %. When harmonic order is at 19th, voltage spectrum on situation A is 0.06 %, voltage spectrum on situation B is 0.08 % and voltage spectrum on situation C is 0.08 %. The increase of voltage spectrum from situation A to situation B is 0.02 %. There is no any reduction from situation B to situation C

When harmonic order is at 23rd, voltage spectrum on situation A is 0.02 %, voltage spectrum on situation B is 0.03 % and voltage spectrum on situation C is 0.01 %. The increase of voltage spectrum from situation A to situation B is 0.01 %. The decrease of voltage spectrum from situation B to situation C is 0.02 %. When harmonic order is at 25th, voltage spectrum on situation A is 0.01 %, voltage spectrum on situation B is 0.03 % and voltage spectrum on situation C is 0.02 %. The increase of voltage spectrum from situation A to situation B is 0.02 %. The reduction of voltage spectrum from situation B to situation C is 0.02 %.

Table 5-17: Voltage Spectrum of Talise SB1 Bus bar on Situation A, B and C

Bus Talise SB1	Voltage Spectrum [%]		
Harmonic Order	Situation A	Situation B	Situation C
5th	2.33	0.78	0.23
7th	1.01	0.34	0.18
11st	0.66	0.45	0.27
13rd	0.23	0.28	0.09
17th	0.14	0.14	0.13
19th	0.06	0.08	0.08
23rd	0.02	0.03	0.01
25th	0.01	0.03	0.01

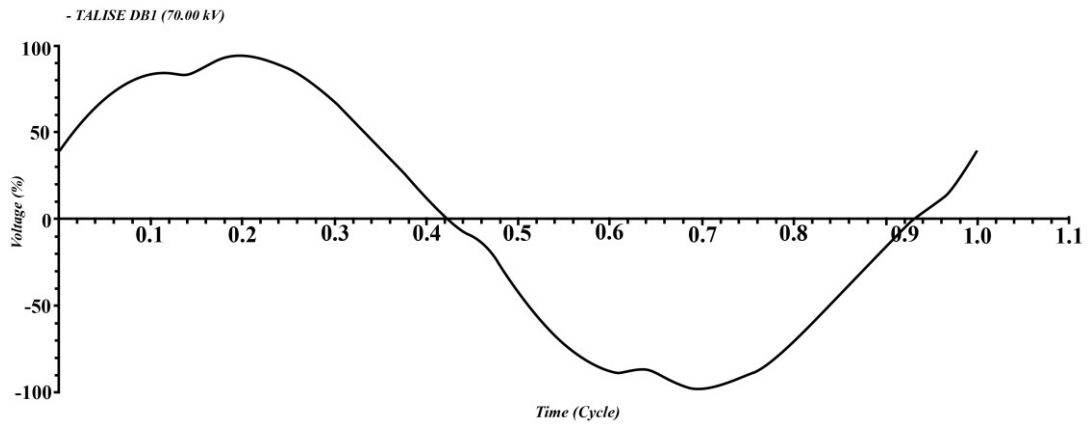


Figure 5-298: Voltage Waveform of Talise SB1 Bus bar on Situation A

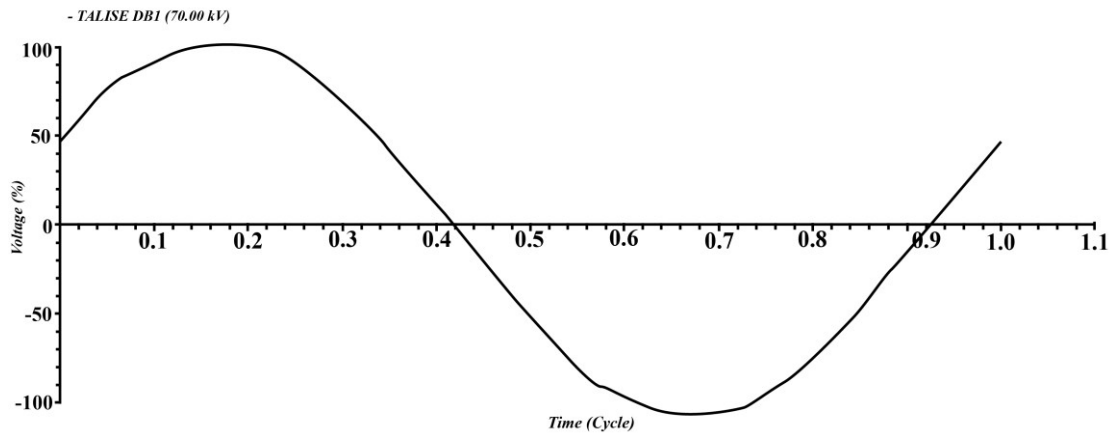


Figure 5-299: Voltage Waveform of Talise SB1 Bus bar on Situation B

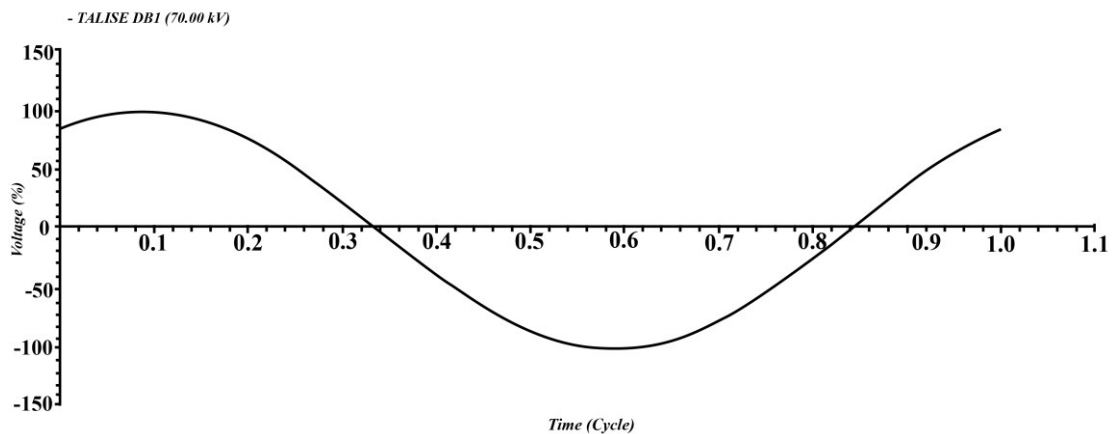


Figure 5-300: Voltage Waveform of Talise SB1 Bus bar on Situation C

Based on figure 5-298, figure 5-299 and figure 5-300, The sinusoidal wave voltage against time in cycle of these three situations is the following; on situation A, there are some reductions of waveform sinusoidal voltage between 0.1 cycles and 0.18 cycles, between 0.423 cycles and 0.5 cycles, between 0.59 cycles and 0.68 cycles and between 0.94 cycles and 1.0 cycles. On situation B, there are some reductions of waveform sinusoidal voltage between 0.06 cycles and 0.12 cycles and between 0.55 cycles and 0.64 cycles. There is no any reduction of sinusoidal waveform on situation C.

Table 5-18: The Reduction of Sinusoidal Waveform of Talise SB1 Bus bar on Situation A, B and C

Sinusoidal Waveform Result of Bus Talise SB1			
	Situation A	Situation B	Situation C
1	0.1 cycle – 0.18 cycle	0.06 cycle – 0.12 cycle	No reduction
2	0.423 cycle – 0.5 cycle		
3	0.59 cycle – 0.68 cycle	0.55 cycle – 0.64 cycle	
4	0.94 cycle – 1.0 cycle		

Harmonic simulation results of Talise Sb2 bus bar on situation A, B and C can be seen on the explanation below.

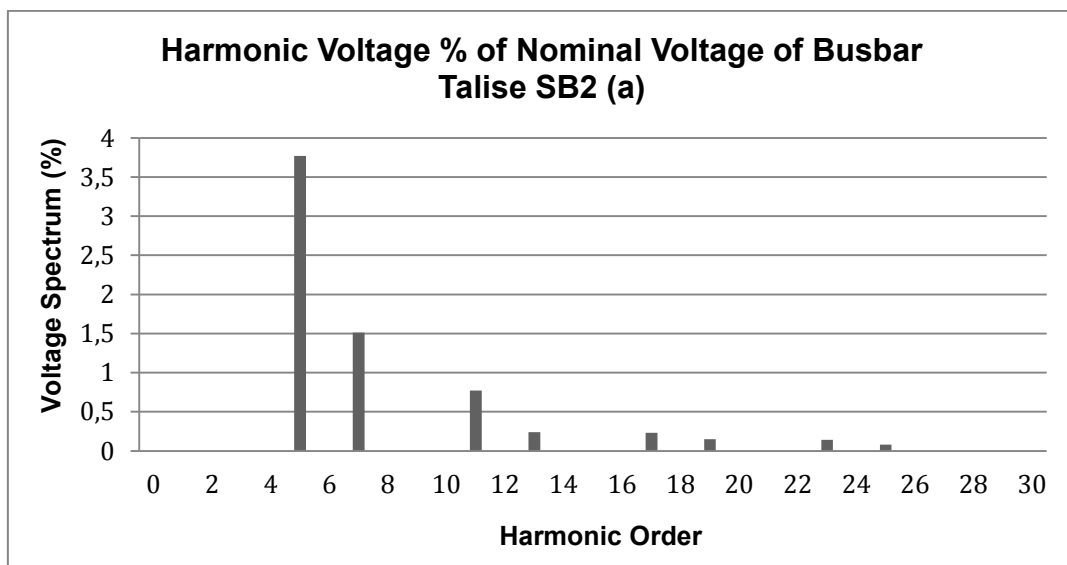


Figure 5-301: Harmonic Voltage of Talise SB2 Bus bar on Situation A

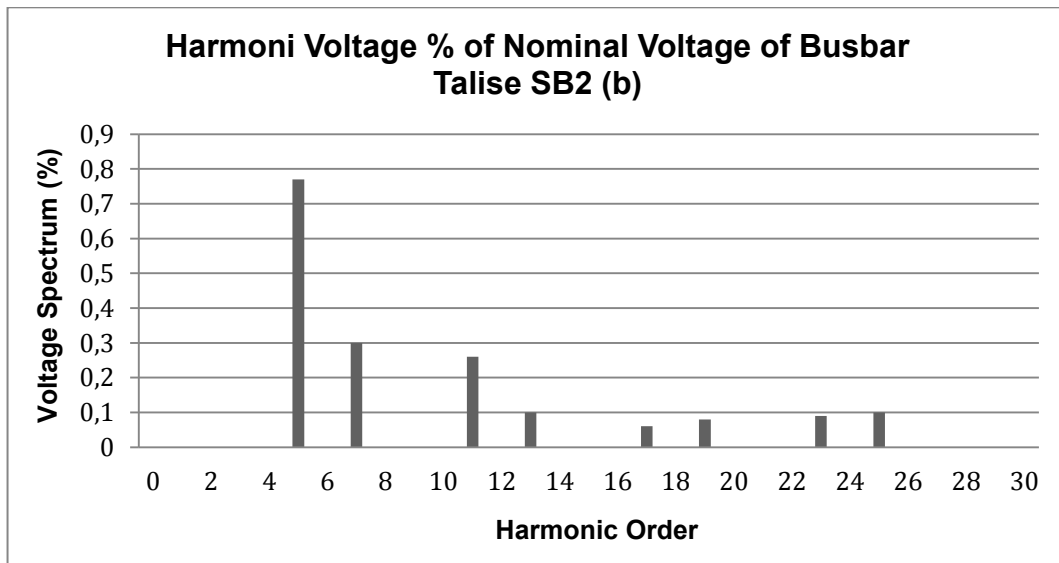


Figure 5-302: Harmonic Voltage of Talise SB2 Bus bar on Situation B

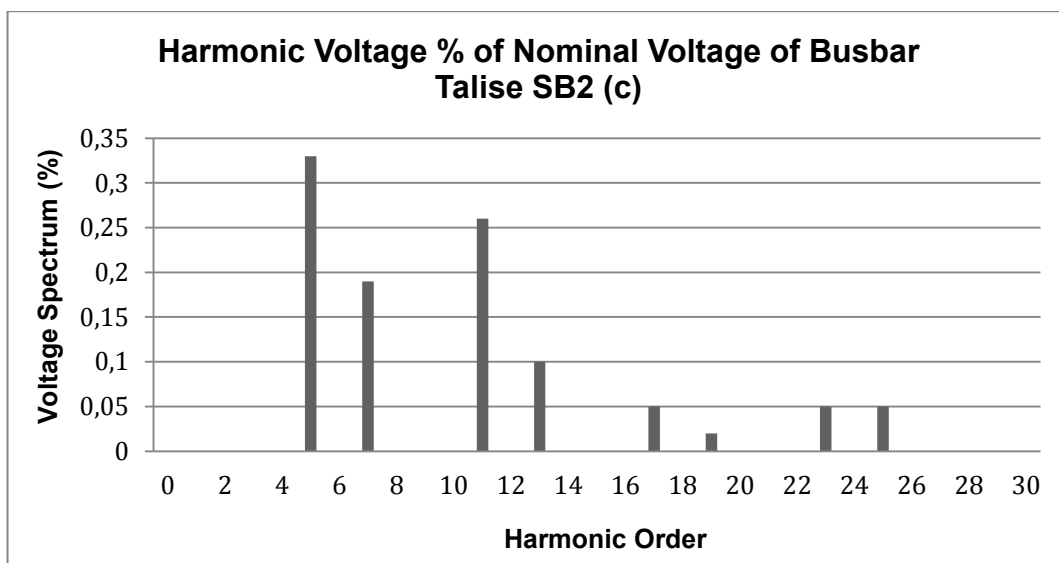


Figure 5-303: Harmonic Voltage of Talise SB2 Bus bar on Situation C

Based on figure 5-301, figure 5-302 and figure 5-303, When harmonic order is at 5th, voltage spectrum on situation A is 3.77 %, voltage spectrum on situation B is 0.77 % and voltage spectrum on situation C is 0.33 %. The reduction of voltage spectrum from situation A to situation B is 3 %. The reduction of voltage spectrum from situation B to situation C is 0.44 %. When harmonic order is at 7th, voltage spectrum

on situation A is 1.51 %, voltage spectrum on situation B is 0.3 % and voltage spectrum on situation C is 0.19. The reduction of voltage spectrum from situation A to situation B is 1.21 %. The reduction of voltage spectrum from situation B to situation C is 0.11 %.

When harmonic order is at 11st, voltage spectrum on situation A is 0.77 %, voltage spectrum on situation B is 0.26 % and voltage spectrum on situation C is 0.26 %. The decrease of voltage spectrum from situation A to situation B is 0.51 %. There is no any reduction from situation B to situation C. When harmonic order is at 13rd, voltage spectrum on situation A is 0.24 %, voltage spectrum on situation B is 0.1 % and voltage spectrum on situation C is 0.1 %. The reduction of voltage spectrum from situation A to situation B is 0.14 %. There is no any reduction from situation B to situation C.

When harmonic order is at 17th, voltage spectrum on situation A is 0.23 %, voltage spectrum on situation B is 0.06 % and voltage spectrum on situation C is 0.05 %. The reduction of voltage spectrum from situation A to situation B is 0.17 %. The reduction of voltage spectrum from situation B to situation C is 0.01 %. When harmonic order is at 19th, voltage spectrum on situation A is 0.15 %, voltage spectrum on situation B is 0.08 % and voltage spectrum on situation C is 0.02 %. The reduction of voltage spectrum from situation A to situation B is 0.07 %. The reduction of voltage spectrum from situation B to situation C is 0.06 %.

When harmonic order is at 23rd, voltage spectrum on situation A is 0.14 %, voltage spectrum on situation B is 0.09 % and voltage spectrum on situation C is 0.05 %. The increase of voltage spectrum from situation A to situation B is 0.05 %. The reduction of voltage spectrum from situation B to situation C is 0.04 %. When harmonic order is at 25th, voltage spectrum on situation A is 0.08 %, voltage spectrum on situation B is 0.1 % and voltage spectrum on situation C is 0.05 %. The increase of voltage spectrum from situation A to situation B is 0.2 %. The decrease of voltage spectrum from situation B to situation C is 0.05 %.

Table 5-19: Voltage Spectrum of Talise SB2 Bus bar on Situation A, B and C

Bus Talise SB2	Voltage Spectrum [%]		
Harmonic Order	Situation A	Situation B	Situation C
5 th	3.77	0.77	0.33
7 th	1.51	0.30	0.19
11 st	0.77	0.26	0.26
13 rd	0.24	0.10	0.10
17 th	0.23	0.06	0.05
19 th	0.15	0.08	0.02
23 rd	0.14	0.09	0.05
25 th	0.08	0.10	0.05

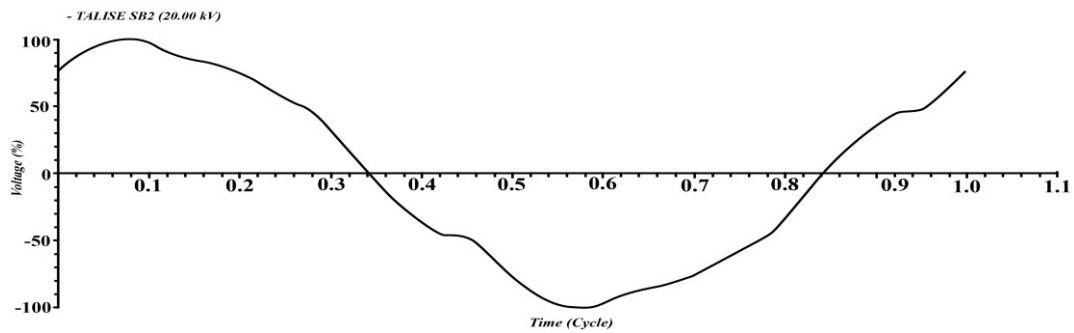


Figure 5-304: Voltage Waveform of Talise SB2 Bus bar on Situation A

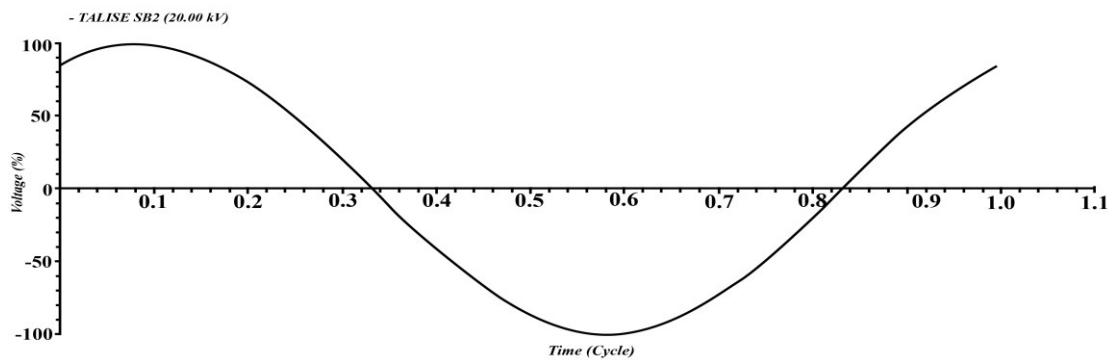


Figure 5-305: Voltage Waveform of Talise SB2 Bus bar on Situation B

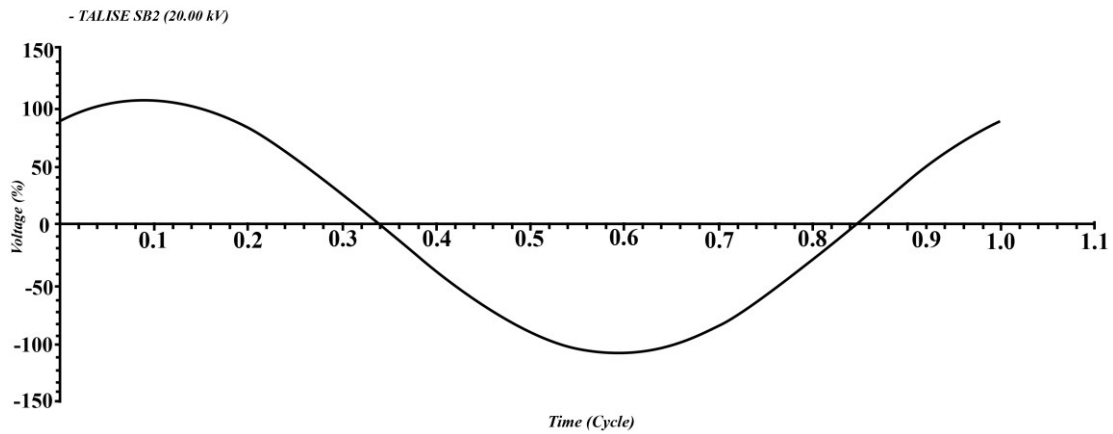


Figure 5-306: Voltage Waveform of Talise SB2 Bus bar on Situation C

The sinusoidal waveform voltage on all situations of Talise SB2 bus bar is similar to sinusoidal waveform voltage of Donggala SB1 bus bar.

Harmonic voltage simulation results of Talise SB3 bus bar on situation A, B and C is equal to harmonic simulation results of Talise SB2 bus bar.

Harmonic simulation results of Talise DB1 bus bar on situation A, B and C can be seen on the explanation below.

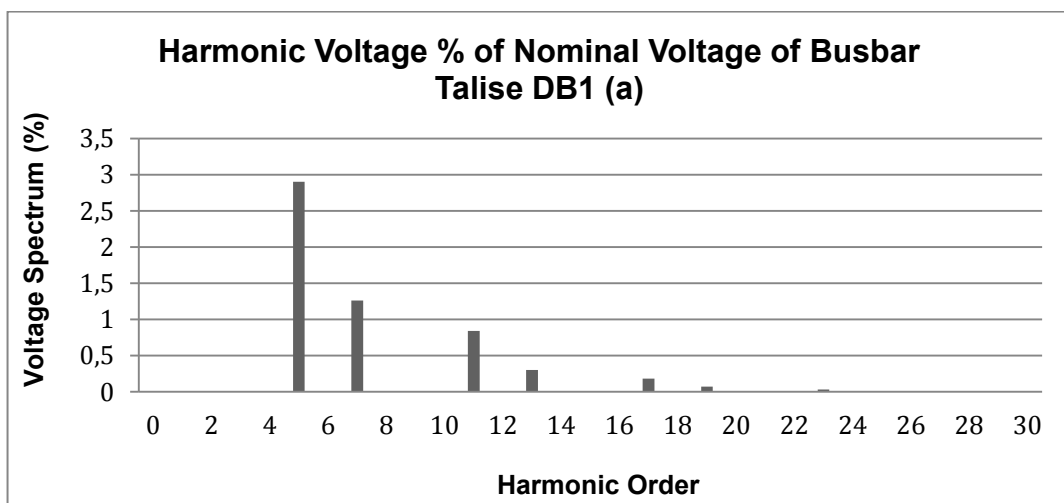


Figure 5-307: Harmonic Voltage of Talise DB1 Bus bar on Situation A

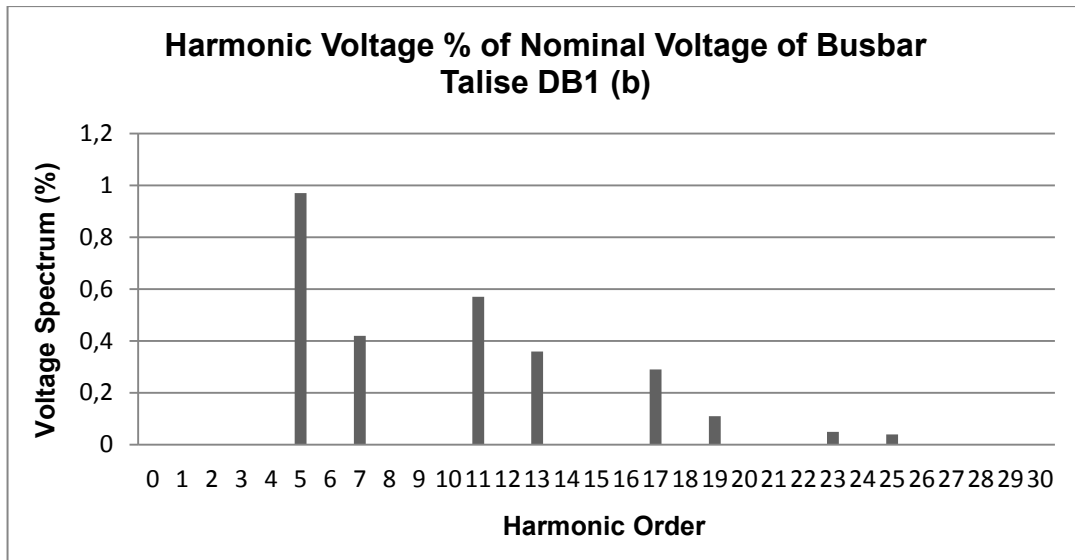


Figure 5-308: Harmonic Voltage of Talise DB1 Bus bar on Situation B

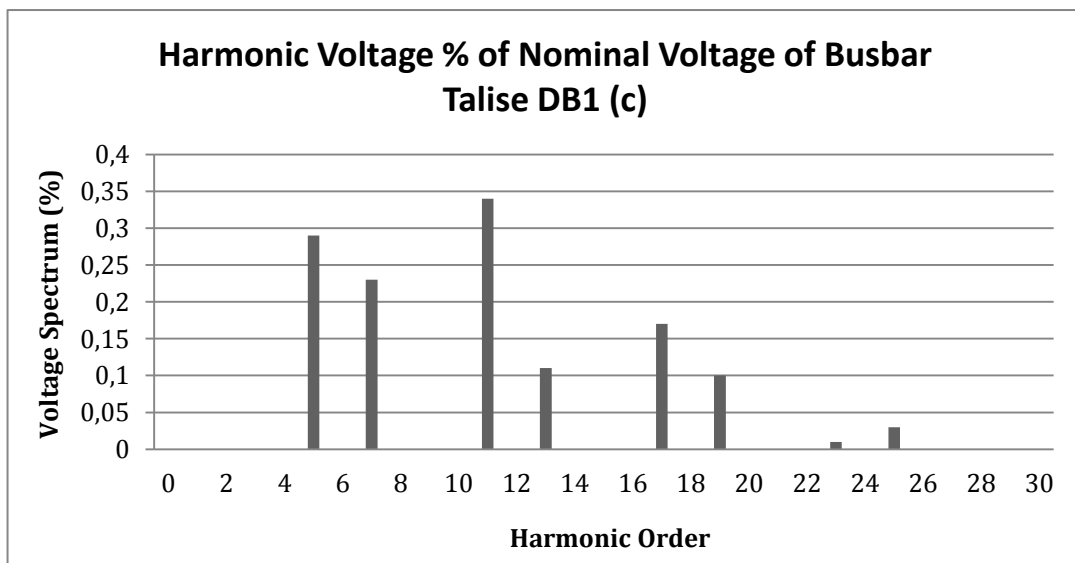


Figure 5-309: Harmonic Voltage of Talise DB1 Bus bar on Situation C

Based on figure 5-307, figure 5-308 and figure 5-309, When harmonic order is at 5th, voltage spectrum on situation A is 2.9 %, voltage spectrum on situation B is 0.97 % and voltage spectrum on situation C is 0.29 %. The reduction of voltage spectrum from situation A to situation B is 1.93 %. The reduction of voltage spectrum from situation B to situation C is 0.68 %. When harmonic order is at 7th, voltage spectrum on situation A is 1.26 %, voltage spectrum on situation B is 0.42 % and voltage

spectrum on situation C is 0.23 %. The reduction of voltage spectrum from situation A to situation B is 0.84 %. The reduction of voltage spectrum from situation B to situation C is 0.19 %.

When harmonic order is at 11st, voltage spectrum on situation A is 0.84 %, voltage spectrum on situation B is 0.57 % and voltage spectrum on situation C is 0.34 %. The reduction of voltage spectrum from situation A to situation B is 0.27 %. The reduction of voltage spectrum from situation B to situation C is 0.23 %. When harmonic order is at 13rd, voltage spectrum on situation A is 0.3 %, voltage spectrum on situation B is 0.36 % and voltage spectrum on situation C is 0.11 %. The increase of voltage spectrum from situation A to situation B is 0.06 %. The reduction of voltage spectrum from situation B to situation C is 0.25 %.

When harmonic order is at 17th, voltage spectrum on situation A is 0.18 %, voltage spectrum on situation B is 0.29 % and voltage spectrum on situation C is 0.17 %. The increase of voltage spectrum from situation A to situation B is 0.11 %. The reduction of voltage spectrum from situation B to situation C is 0.12 %.

When harmonic order is at 23rd, voltage spectrum on situation A is 0.03 %, voltage spectrum on situation B is 0.04 % and voltage spectrum on situation C is 0.01 %. The increase of voltage spectrum from situation A to situation B is 0.02 %. The decrease of voltage spectrum from situation B to situation C is 0.01 %.

When harmonic order is at 25th, voltage spectrum on situation A is 0.01 %, voltage spectrum on situation B is 0.04 % and voltage spectrum on situation C is 0.03 %. The increase of voltage spectrum from situation A to situation B is 0.03 %. The reduction of voltage spectrum from situation B to situation C is 0.01 %.

Table 5-20: Voltage Spectrum of Talise DB1 Bus bar on Situation A, B and C

Bus Talise DB1	Voltage Spectrum [%]		
Harmonic Order	Situation A	Situation B	Situation C
5 th	2.9	0.97	0.29
7 th	1.26	0.42	0.23
11 st	0.84	0.57	0.34
13 rd	0.30	0.36	0.11
17 th	0.18	0.29	0.17
19 th	0.07	0.11	0.10
23 rd	0.03	0.05	0.01
25 th	0.01	0.04	0.03

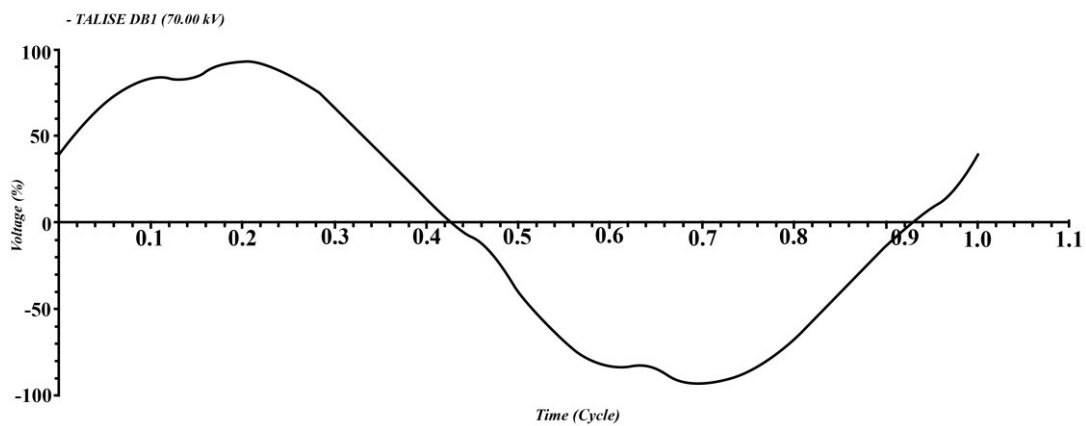


Figure 5-310: Voltage Waveform of Talise DB1 Bus bar on Situation A

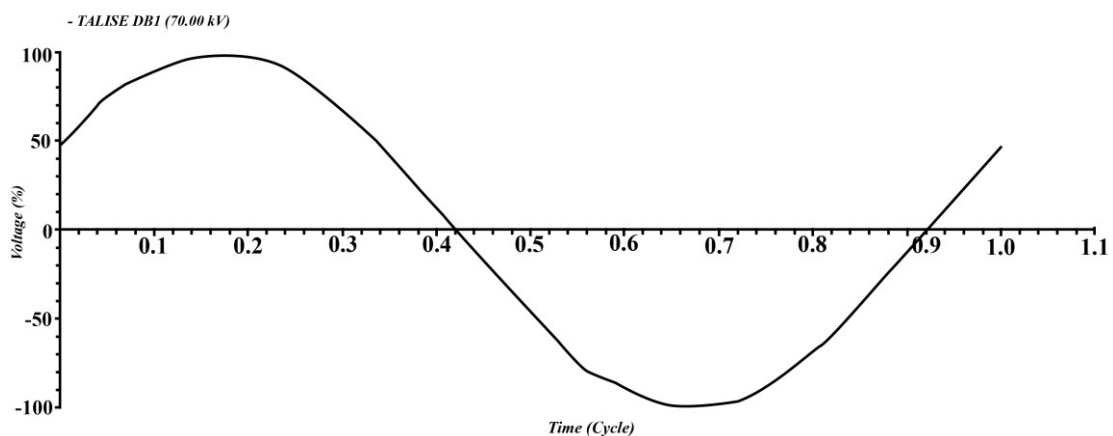


Figure 5-311: Voltage Waveform of Talise DB1 Bus bar on Situation B

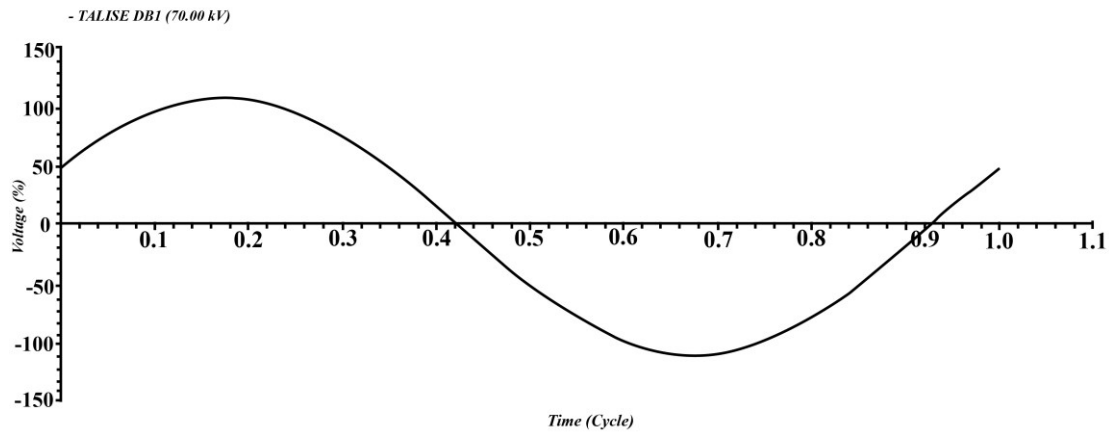


Figure 5-312: Voltage Waveform of Talise DB1 Bus bar on Situation C

Based on figure 5-310, figure 5-311 and figure 5-312, The sinusoidal wave voltage against time in cycle of these three situations is the following; on situation A, there are some reductions of waveform sinusoidal voltage between 0.105 cycles and 0.2 cycles, between 0.44 cycles and 0.5 cycles, between 0.6 cycles and 0.69 cycles and between 0.93 cycles and 1.0 cycles. On situation B, there are some reductions of waveform sinusoidal voltage between 0.05 cycles and 0.1 cycles and between 0.56 cycles and 0.64 cycles. There is no any reduction of sinusoidal waveform on situation C.

Table 5-21: The Reduction of Sinusoidal Waveform of Talise DB1 Bus bar on Situation A, B and C

Sinusoidal Waveform Result of Talise DB1			
	Situation A	Situation B	Situation C
1	0.105 cycle – 0.2 cycle	0.05 cycle – 0.1 cycle	No Reduction
2	0.44 cycle – 0.5 cycle		
3	0.6 cycle – 0.69 cycle	0.56 cycle – 0.64 cycle	
4	0.93 cycle – 1.0 cycle		

Harmonic simulation results of Talise DB11 bus bar on situation A, B and C is equal to simulation results of Talise DB1 bus bar.

6 References

Since many years ago world has been concerning about using green energy to preserve environment. Many researches have been conducted to discuss about this matter. Paper 1 (Hart, 2012) is discussing about a method to predict renewable energy resources potential in relation with their intermittent behavior to supply load combined with non-renewable energy sources. Paper 2 (Zhang H. , 2016) is talking about a control strategy based on DC-DC converter for integrating renewable energy into HVDC grid under normal condition and any fault conditions. Paper 3 (Young Joo, 2016) is analyzing about demand response in relation to huge customer (industrial customer), in this case is manufacturing plant in a frame of smart grid with high penetration of renewable energy (solar energy). The aim of this paper is to analyze the impact of manufacturing plant's demand response to smart grid.

Paper 4 (Hashim, 2015) is discussing about renewable energy potential in this case biomass in Sabah Malaysia. Policy approach regarding feed-in tariff and grid integration feasibility are also discussed with focusing on omitting high obstacles to make it real. Paper 5 (Nanewortor, 2015) is talking about analyzing the solution of intermittent behavior of renewable energy (PV and solar) in supplying some different load profiles. The idea of this paper is that by incorporating storage system into the grid can solve the problem. Paper 6 (Toma, 2014) is speaking about the impact of integrating renewable energy (wind) into the grid toward voltage stability of bus bar. Different level of wind penetration is also analyzed into the same bus bar. Paper 7 (Chaitusaney, 2014) is discussing about the key issues of integrating renewable energy into the grid and discussing about general solution for those issues. Paper 8 (Mukhopadhyay, 2012) is speaking about the strategy to increase the use of renewable energy in India. The policy and grid condition are also discussed in this paper.

Paper 9 (KOH, 2012) is talking about the effort of Singaporean government to reduce emission gas from conventional plant and natural gas by increasing the use of renewable energy sources. The effort is focused on modifying some policies. Paper 10 (Mariethoz, 2012) is discussing about control technic of prosumers to increase integrating renewable energy into the grid by shifting load but taking account its

constraints. Paper 11 (Delgado, 2011) is speaking about the possibility of using renewable energy in island (in Portugal) where conventional primary energy is expensive by considering the intermittent behavior of renewable energy sources (PV and wind). This paper is also talking about the possibility to integrate renewable energy into the grid by considering grid losses. Paper 12 (Kumar, 2015) is discussing about creating power quality events equipped by their parametric equation model. Paper 13 (Hamoud, 2017) is talking about control technic to increase power factor regarding integration renewable energy into the grid. The control technic used on this research is adaptive fuzzy logic control based D-STATCOM.

Paper 14 (Kumwenda, 2017) is speaking about integration renewable energy (solar) into the grid in Zambia by considering ramp rate constraints. This paper is analyzing the maximum PV that can be integrated into the grid combined with diesel generators with considering the ramp rate constraints of diesel generators. Paper 15 (Marilyn Winifred, 2017) is analyzing about grid in relation to integrate renewable energy into it. It is also discuss about how to strengthen the grid to minimize losses on the grid after integrating renewable energy into it. Paper 16 (Mathe, 2017) is analyzing about comparing SCIG (Squirrel Cage Induction Generator), DFIG (Doubly-Fed Induction Generator) and DDSG (Direct-Drive Synchronous Generator) of wind power generator regarding the impact of integrating into the grid. The voltage stability is the main focus on this research.

Paper 17 (Hossain, 2017) is speaking about the impact of incorporating solar and PV into the grid. This paper focuses on the impact on the distribution grid under three conditions; without voltage control capability, with voltage control capability and with power factor control mode. Paper 18 (Yan, 2017) is discussing about the impact of PV fluctuation to the grid stability caused by weather condition (clouds). Impact to the grid is focused on the difference of power flow and voltage drop in normal weather condition (without clouds) and with clouds. Paper 19 (Abdullah, 2011) is speaking about the quantification of reduced gas emission in relation to integration renewable energy into the grid. This paper is focused on calculation emission gas reduced before and after integrating renewable energy in distribution network. Paper 20 (Waqfi, 2017) is discussing about the impact of integrating PV and wind into the grid. This paper is focused on calculation fault current and frequency transient stability of

distribution network using etap software. Paper 21 (Al Haj Hassan, 2015) is talking about the use of renewable energy into cellular base station collaborating with smart grid equipped with energy storage. New architecture of smart grid is introduced on this paper. Paper 22 (Thakurta, 2015) is speaking about increasing reliability of grid in order to integrate more renewable energy (wind) into the grid by introducing to install controllable device to maintain power flow among TSOs in central Western Europe. However coordinating among TSOs is properly required here.

Paper 23 (Chen H. , 2016) is discussing about multi-time frame robust of scheduling to dispatch different type of renewable energy into the grid. This method consists of day-ahead scheduling, intraday dispatch and real time dispatch. Paper 24 (Sun, 2016) is speaking about balancing power between supply and demand in relation to integrate renewable energy into the grid. The grid on this research is combined with one diesel generator and multiple renewable energies with flexible load and storage system. Paper 25 (Javadi, 2017) is discussing about improving power quality at residential households by using multilevel-THSeAF. Paper 26 (Singh O. , 2016) is talking about integration hybrid system of renewable energy into micro-grid in rural area study case India. The aim of this integration is to reduce dependency of micro-grid from main grid supply. This paper was prepared based on review of some paper related to it economically and technically.

Paper 27 (Xu, 2011) is discussing about enhancing the use of renewable energy resources by incorporating electric vehicles. The use of electric vehicle on smart grid is to improve the use and supporting of renewable energy. Therefore in this case electrical vehicles serve as storage system. Paper 28 (Mangaraj, 2016) is discussing about power quality improvement on distribution network regarding integration renewable energy into the grid. Power quality enhancement is focused on reducing harmonic, current distortion, power factor correction and compensating reactive power on the grid by using 3-phase 4-leg super capacitor based on DSTATCOM. Paper 29 (Simon, 2016) is speaking about the impact of wind energy penetration into the grid based on doubly feed induction generator of wind turbine. The effect of short circuit current into the grid after the fault is focused on three different condition; fault at load bus, fault at generator bus and fault at the transmission line. Paper 30 (Sreedevi, 2016) is talking about the maximum wind penetration that can be

integrated into the grid without effecting grid stability and emerging the grid. Paper 31 (Ansari, 2016) is discussing about evaluation of reliability of micro grid that incorporating renewable energy by using hybrid analytical simulation method. This paper is also analyzing the impact of collapse islanding in relation to fault on the grid.

Paper 32 (Gheorghe, 2016) is discussing about monitoring power quality on distribution system operator and transmission system operator in Romania by using SCADA. Paper 33 (Ben Youssef, 2016) is speaking about incorporating content-centric networking to support integration renewable energy into the grid. The communication system is built to predict the delay supply from renewable energy sources regarding their intermittent behavior. Paper 34 (Chen X. , 2011) is discussing about the feasibility to integrate large-scale wind power into the grid by using multi-terminal direct current (MTDC) transmission system. Paper 35 (Singh A. , 2010) is speaking about the effect of integration renewable energy (PV and wind) into the grid toward power quality. By using DC link interface BESS study case India. Paper 36 (Concepcion, 2011) is talking about dynamic impact of high penetration of PV into the grid by using eigenvalue system configuration.

Paper 37 (Strasser, 2016) is discussing about the use of advance control system for integrating renewable energy sources into smart grid. Paper 38 (Sriboong, 2016) is discussing about integration of PV, wind and energy storage into the grid to supply electric vehicle charging station by using merit simulation. Economical aspect is also analyzed in this paper case study Bangkok. Paper 39 (Lin, 2016) is discussing about analyzing economical and technical part of integrating large scale of renewable energy into the grid. Analyzing the strategy how to optimize the system and calculating grid loss. Paper 40 (Ssekulima, 2016) is discussing about forecasting solar irradiance and wind speed. Different types of forecasting technics are applied to obtain accurate result. Paper 41 (Jeni, 2016) is speaking about the impact of PV penetration into the grid to distribution line voltage stability, which depends on power demand and produced power. Paper 42 (Sbordone, 2015) is discussing about aggregating between Transmission System Operator (TSO) and Distribution System Operator (DSO) by using information and communication technology to enhance dispatching distributed generation. Paper 43 (Gado, 2015) is discussing about the impact of PV penetration on distribution system study case Egypt. Installing rooftop

solar PV in some public building will contribute some voltage stability, transformer overloading, phase imbalance etc. This paper is using storage system to overcome his problem.

Paper 44 (Zhang Y. , 2015) is speaking about the influence of integrating renewable energy into the grid. Using certain method called sequential production method based on random units simulated daily power system operation. Paper 45 (Petinrin, 2015) is talking about the application of voltage control system so called A hybrid Particle Swarm Optimization-Gravitational Search Algorithm (PSOGSA) to reduce voltage deviation and grid loss. Paper 46 (Shafiullah, 2015) is analyzing the impact of penetration large scale of PV and wind into distribution network toward voltage, frequency and power quality. The result of this research states that the use of a static synchronous compensator (STATCOM) can reduce harmonics on distribution network.

Paper 47 (Khan, 2015) is discussing about the possibility of using renewable energy sources to replace fossil energy sources to supply electricity in Pakistan. Integrating hydro, PV and wind into public grid through DC transmission line bus bar by using step up DC-DC converter connected to DC distribution line. On DC distribution line, battery and other storage system technic are installed. DC distribution line is connected to AC distribution line through DC-AC inverter. Old public grid and load are connected to AC distribution line. Paper 48 (Dahal, 2015) is discussing about the framework of some policies related to renewable energy target to analyze the possibilities to increase the use of renewable energy sources to supply electricity.

Paper 49 (Jamal, 2015) is analyzing about the possibility of using solar power to supply electricity in Pakistan until the year of 2050 combined with conventional power sources and any other renewable energy sources. The simulation was conducted by using CPRESS (100 percent renewable based electric system simulation. Paper 50 (Ramdhin, 2015) is discussing about determining standard of grid integration of renewable energy sources by using South African, Eskom, and adapting generic planning guidelines. Paper 51 (Martinez, 2015) is speaking about restriction of wind power dispatching to maintain power system stability along certain time modest smoothness reactions.

Paper 52 (Mohammadi, 2014) is discussing about the effect of integrating some different type of distributed generation (DG) into utility grid by using Matlab Simulink. This research is focusing on its effect on voltage profile and fault current contribution on distribution network. Paper 53 (Pouresmaeil, 2015) is introducing control technic based on Direct Lyapunov Control Method (DLCM) for renewable energy penetration on utility grid. The control technic is focusing to compensate reactive power and reducing current harmonic.

Paper 54 (Zanabria, 2015) is discussing about the application of IEC 61850/61499 to support distributed generation (DG) as automation platform to support master and Phd research regarding integrating renewable energy into utility grid. Paper 55 (Sennou, 2015) is analyzing the application of PowerGAMA for integrating renewable energy into the grid, Moroccan study case. This method was used to analyze the reliability and optimize the grid for example possibly some diesel generator needs to be renew or adding some more lines. Paper 56 (Gupta, 2014) is speaking about the application of optimization method to determine the capacity size and sitting of renewable energy. This method will increase the performance of the grid to provide continuous supply for electricity demand.

Paper 57 (El Kanj, 2015) is reviewing the existing smart grid in relation with integration renewable energy sources. Some components for example inverter and any other power electronics components need to be reviewed to reach optimal and more reliable system performance. Paper 58 (Yuli, 2015) is introducing new configuration of hybrid grid system. This configuration focuses on control system coherency to enhance the reliability of hybrid grid system. Paper 59 (El Aimagi, 2014) is analyzing the impact of integrating 1.5 MW wind power (double feed induction generator) into the grid by using Matlab Simulink. The research focuses on the impact this integration on electric power if there is reversed power flow, impact on RMS voltage and flicker.

Paper 60 (Arrinda, 2014) is discussing about controlling current from renewable energy source (PV) to reach stable generation. By installing storage system on distributed generation system will increase the reliability of the system to support continuous electricity supply. Paper 61 (Junxia, 2014) is analyzing power losses as

the impact of distributed generation penetration on distribution system. This research is also analyzing reactive power from one node to other nodes in relation to optimize the system. Paper 62 (Hakimi, 2014) is planning about smart grid by controlling heat and cooling to reach optimal smart grid with high penetration renewable energy resources by using an active controller. Controlling heat and cooling will lower budget, capacity of renewable energy sources and dependent energy from the grid.

Paper 63 (Petintin, 2014) is controlling voltage of smart grid in relation to renewable energy source (PV) penetration. To do so, coordinating load tap changer of transformer and switched capacitor in order to maintain the voltage of grid. Paper 64 (Chattopadhyay, 2014) is discussing about the application High Voltage SiC Devices to lower losses devices in relation to integrate low voltage PV into medium voltage grid. Paper 65 (Forushani, 2014) is analyzing the impact of fluctuating load in relation to wind power penetration into the grid. Controlling demand response in smart grid by using Demand Response Programs (DRPs) will face intermittent and uncertainty of renewable energy sources.

Paper 66 (Calabria, 2014) is the optimization reliability by following load energy for distributed generation. Modeling the system, which include the grid and inverter by using high level cluster algorithm and taking into account forecasting weather. Paper 67 (De Almaide, 2014) is discussing about some requirements for grid integration of renewable energy sources (PV and wind) into the grid. The requirements is based on the existing grid code in relation to all power electronics device those will support additional devices. Before integrating renewable energy sources, the grid need to be flexible enough to withstand in relation to addition additional converters. Paper 68 (Xiaobo, 2014) is discussing about application large scale charging device regarding integration renewable energy into the grid as a storage system. The aim of using it is to increase grid stability and power quality. The simulation was done using homer software. Paper 69 (De Melo, 2013) is introducing the use of rectifier mode based on LEDs of distribution generation for street lightning. Paper 70 (Alvin, 2013) is discussing about the impact of integration renewable energy (distributed generation) into the grid to fault current. Using Matlab Simulink to model and simulate the system and the result is giving that current fault is low due to reversed power flow. Paper 71 (Ghorbanian, 2013) is discussing about the impact of integration large scale of wind

power into the grid to power quality of the grid. This research focuses on reactive power compensation, voltage regulation and total harmonic distortion, which is based on study literature.

Paper 72 (Beshr, 2013) is analyzing PV and wind penetration into the grid by using Matlab Simulink. This study focuses on comparing both PV and wind in supplying certain load at certain time period. The result of simulation is that PV can supply load more than wind by applying same simulation. Paper 73 (Rao, 2013) is discussing about wind integration into the grid in India based on study literatures. This research analysis about some considerations in planning wind integration into the grid for example current carrying capacity of conductors, types of conductors, diversity factor of wind farm, power factor to be maintain at wind farm, dynamic line rating, voltage profile and reactive power management. Paper 74 (Grünbaum, 2013) is discussing about different types FACTS (Flexible AC Transmission System) for example SVC (Static Voltage Compensator), STATCOM (Static Compensator) and series capacitors. This paper is discussing about the advantages of all FACTS devices, grid requirements for installing renewable energy sources, their characteristics etc.

Paper 75 (Haque, 2013) is discussing about forecasting power generation from PV by using Hybrid Intelligent Approach. This method is used to forecast short-term power generation from PV. The result showed this method is ideal for it. Paper 76 (Henneaux, 2013) is analyzing the impact of renewable energy sources into the grid especially thermal effect that can lead to blackout problem. Some different configuration systems were proposed in this simulation to find out the impact of different generated capacity to this effect. Paper 77 (Zhang H.-T. , 2013) is analyzing the difference between integrating large-scale wind power into the grid and distributed generation. Economically, the more capacity wind power installed, the investment cost becomes cheaper therefore installing large-scale wind power is cheaper than distributed generation. Technically, integration distributed generation is contributing more reliability of the system than installing large-scale wind power into the grid. Paper 78 (Shi, 2013) is analyzing about the influence of wind power (Double Feed Induction Generator) to the small signal stability of the grid. The results showed that reversed power flow caused by wind power influences small signal stability of the grid. Paper 79 (Krishna, 2013) is analyzing losses approximation and reducing radial

distribution system connected with distributed generation by using a Novel algorithm. By determining the location and the size of distributed generation it will contribute reducing grid losses. The result of this research showed that by installing distributed generation; it will reduce losses and improve bus voltage.

Paper 80 (Rana, 2013) is discussing about the impact of integrating wind farm into the grid to market price by using genetic algorithm. The result is showing that the more wind power installed the lower the market price will be. This situation will bring advantage to the customer as well as electricity supplier. Paper 81 (Schellong, 2013) is discussing about integration Combined Heat and Power into smart grid for system optimization. Actual system reliability was analysed by adopting linier algorithm method based on actual and forecasting data. The result of this research is that decentralized produced energy is used to supply electricity at the vicinity it produced while the actual plant is for supplying electricity when there is no production from wind and PV.

Paper 82 (de Groot, 2012) is discussing about the application of Distribution Automation System (DAS) on smart grid. This research is based on study literature that focuses on network configuration, diverting power flows, faults isolation and preventing network components overloading. The application of Distribution Automation System (DAS) can reduce Consumer Minute Lost (CML), improve system reliability and allow incessant penetration distributed generation into distribution network. Paper 83 (Brenna, 2012) is discussing about the possibility for integrating electric vehicle into the grid. The result of this research state that electric vehicle charging needs to be controlled and need advanced measurement in order to allow more integration of electric vehicle charging. Grid and electric vehicle charging will have mutual dependent by charging and discharging. Paper 84 (Kuwahata, 2012) is speaking about the advantage of micro grid on contributing to supply electricity in rural area and also other benefits for grid operator of utility grid. The availability of micro grid will briefly offer change for interconnection with utility grid and integrating renewable energy into it. It will synergize each other in supplying electricity to costumers. Paper 85 (Narayana, 2012) is talking about the application of statistical models and neural network techniques to forecast intermittent behavior of wind speed study case in Sri Lanka. This research is also analyzing the possibility to

integrate wind power into the grid. The result of this research states that adaptive prediction is contributing more accuracy by using one-hour ahead prediction than time series data learning method.

Paper 86 (Tan, 2012) is discussing about penetrating micro grid by optimizing distribution system by using Vaccine-AIS. By using such method integration micro grid into distribution network is more efficient and effective. Paper 87 (Fuchs, 2012) is discussing about research laboratory of penetration of distributed generation into the grid. All the design about grid and distributed generator including all parameters were presented in laboratory. Sag and voltage dip were created to measured power quality of the system. The result of this research showed that laboratory research is more efficient and low cost to conduct this research.

Paper 88 (Baker, 2012) is discussing about the application of Distributed Multi-Step Optimization to reach optimal integration renewable energy into the grid. This research also focuses on regulating between storage systems with renewable energy Sources (PV and wind) in multiple control area. By using this method, Problems can be easily identified and solved and by using storage system equipped by control system, more renewable energy source can be integrated, cheaper cost and low emissions. Paper 89 (Elombo A. E., 2010) is talking about economy analysis of integration renewable energy sources into the grid equipped with storage system by using a novel model predictive control (MPC)-based operation strategy. This method can reduce electricity purchase from distribution network by regulating supply electricity from both renewable energy sources and storage system. The result of this research showed that this method would increase the reliability of the system and lowers the cost. Paper 90 (Bhadane, 2012) is investigating the cause of decreased power quality on integrating renewable energy sources into the grid (wind). The result shows that application power electronics device for example inverter with high frequency switching will contribute to poor power quality. Paper 91 (Elombo A. I., 2010) is discussing about the impact of complementary of integrating renewable energy sources (PV and wind) into the grid. Renewable energy penetration will lead to voltage instability. Wind source is more fluctuating compared with PV source therefore this situation will lead to mismatching of reactive power. Wind integration will lead to decreasing voltage but PV integration will lead to increasing reactive

voltage. Therefore integration mixed renewable energies is more preferable than integration single renewable energy source. Integration renewable energy sources and off-grid will lead to negative impact. This negative impact is more obvious on off-grid.

Paper 92 (Wang P. , 2012) is discussing about impact of integrating renewable energy sources (Large PV) into the grid for example rising voltage. This paper is offering a solution to incorporating energy storage system to reduce rising voltage. Paper 93 (Ipinnimo, 2012) is discussing about the solution to reduce voltage dip on less strong grid by integration renewable energy resources (Wind and Hydro) into the grid by using distributed generation. Using power factory software with short time duration of fault at any different locations on the grid. Paper 94 (Wirasanti, 2012) is discussing about integrating group of distributed generation into the grid. Group Cluster Controller based on multilevel control strategy of conventional system was used to control group of distributed generation system. The result of this research states that the control system can solely manage energy dispatching, power exchanging and controlling frequency.

Paper 95 (Wang K. , 2012) is talking about integrating renewable energy into the grid by using stochastic power network calculus to deal with intermittent behavior of renewable energy sources. The system is also incorporated by storage system. The result of this research is contributing formula to determine the size of PV and wind combined with storage system and diesel generator to reach reliable system. Paper 96 (Singh R. , 2012) is discussing about stability analysis of wind power integration into the grid by using STATCOM (Static Synchronous Compensator). The result of this research states that reactive power demand during the fault will be fulfilled by STATCOM that can enhance transient stability and reliability of the system. Paper 97 (Modi, 2012) is discussing about re-visiting small signal stability of the Queensland network by taking into account wind power penetration. This paper focuses on the effect of wind power penetration on the electromagnetics mode damping on the grid in Queensland. The result of this research states that when synchronous generator is displaced by wind power, negative impact will occurred on the grid but by integrating wind power into the grid replacing synchronous generator, positive impact occurred on the grid.

Paper 98 (Muttaqi, 2011) is talking about optimal placement and size of mix renewable energy sources into the grid to reduce maximum emissions. Using time sequential optimization method, which result from maximum emission reduction. Paper 99 (Such, 2011) is discussing about storage system (battery) as an important role to stabilize the grid from integrating renewable energy source (wind). Some control system methods are discussed on this paper. The result of this research is that by incorporating battery storage system, it will control the intermittent behavior of wind power generation by providing different level of control system. This will enhance the reliability of smart grid.

Paper 100 (Guner, 2011) is discussing about transformation from convention power supply to modern power supply based on smart grid in Turkey. This research focuses on deregulation some policy to allow renewable energy sources penetration through smart grid. There are three steps of evolution from conventional power system to smart grid. First step is estimated will last from 3-4 years called first stage of smart grid evolution consisting of extension of distributed generation and renewable energy sources, monitoring and remote control infrastructure and bilateral contracting. Second step is estimated will last 7-8 years called intermediate stage of smart grid evolution consisting of management of penetration of distributed generation and renewable energy sources, deployment of smart metering equipment, constituting the storage facilities. Third step is estimated will last for 9-10 years called final stage of smart grid evolution consisting of full active power management, real-time communication, electrical vehicles, and cyber security. Paper 101 (Dewi, 2014) is discussing about PV and wind potential technically and economically to supply electricity in Palu (Indonesia).

This research is a completed combined technically and economically analysis for renewable energy integration (hydro, PV and wind) into public grid for developing countries especially for south east Asian countries in general where the use of renewable energy especially grid-connected are still very rare and for Indonesia (Palu) in particular. Economically, all costs (net present cost, levelized cost of energy, capital cost, operating cost, replacement cost, fuel cost and salvage) of all components (each of diesel generators, PV, wind etc) are briefly calculated including

sensitivity analysis. This research is also calculating and analyzing different configuration system before and after integrating renewable energy into the grid, off-grid and on-grid, and also with and without incorporating storage system with their own costs. Monthly energy purchased from the grid and energy sold to the grid are also calculated including their energy and demand charged in US\$.

Technically, determining the appropriate configuration system for example the size of PV panel, the number of wind turbine and the number of diesel generator with their own capacity is also done on this research. Homer also can optimize the number of diesel generator that will lead to simplify grid configuration. Emission gases consisting of Carbon Dioxide, Carbon Monoxide, Unburned Hydrocarbons, Particulate Matter, Sulfur Dioxide, and Nitrogen Oxides were also calculated on this research. Analysing and conducting simulation of three different wind turbines from three different manufacturers from three continents were also done by using homer software to find the best wind turbine economically and technically for the site.

This simulation part was not found from any papers mentioned above. Finally chosen wind turbine with its configuration system was brought to other simulation using Etap software for calculating power quality (sag, swell, interruption and harmonics). The simulation by using Etap was consisting three parts. First part, the simulation was done based on the configuration before integrating hydro, PV and wind into the grid. The second part, the simulation is based on configuration after integrating hydro, PV and wind into the grid. Third part, the simulation is based on configuration after integrating hydro, PV and wind based on Homer results. These three simulation parts were conducted to compare power quality result of three different configuration systems. This part of simulation was not found at any paper mentioned above.

7 Conclusions

This chapter contains overall conclusions based on calculations and simulation results done by using Etap and Homer and it will be ended by recommendations.

7.1 Conclusion

To solve shortage problem in Palu city (Indonesia) and surrounding area and based on some renewable energies potential those available in that area, it was proposed to install hydro PV and wind with certain capacity. To obtain the best configuration including the number and the size of all components of configuration systems, some simulations by using HOMER software were conducted including simulation before incorporating renewable energy sources (Diesel generators only). Simulation results showed that before integrating hydro, PV and wind with new configuration of diesel generators based on HOMER version shows that excess electricity, unmet electric load and capacity shortage are zero. This configuration consists of 5 (five) diesel generators with total capacity of 130.5 MW including coal plant. Diesel generator 1 is 30 MW, diesel generator 2 is 20 MW, diesel generator 3 is 10 MW, diesel generator 4 is 15 MW and diesel generator 5 is 55.5 MW.

This configuration system (before RE integration) needs to purchase electricity by 144 MWh per year from the grid but there is no electricity sale to the grid. Total NPC and operating cost of this configuration system are US\$ 938.28 million and US\$ 67.53 million respectively while LCOE is US\$ 0.145 per kWh. Sensitivity analysis of all costs against uncertainty of fuel price (from US\$ 0.4 to US\$ 1.6 per litre) is varied. LCOE is varied from 0.1445 US\$ per kWh to 0.455 US\$ per kWh. NPC is varied from US\$ 938 million to US\$ 2.95 billion. Operational cost is varied from US\$ 67.5 million to US\$ 223 million.

To choose configuration system after integrating hydro, PV and wind into the grid (on-grid) (combined with diesel generator), three simulations by using HOMER software were conducted. Each of simulation was using different wind turbine from three different manufacturers from three different continents. The chosen wind turbine is from United State manufacturer which technically and economically the

most reliable one. The chosen configuration system consists of five diesel generators with total capacity of 130.5 MW. The capacity of each diesel generator is same with configuration system with diesel generators only connected to the grid (before integrating hydro, PV and wind into the grid). This configuration system also consists of 3.3 MW of hydropower, 3 MW of PV and 12 MW of wind.

Electricity purchased by using this configuration system (after RE Integration) is 97 MWh per year but electricity sold to the grid is 172 MWh per year. The total cost of this entire configuration system for 25 years is US\$ 871.71 million and the operating cost of this configuration system is US\$ 59 million. Levelized cost of energy of this configuration system is US\$ 0.1334 per kWh. Sensitivity analysis of all costs against fluctuation of fuel price (from US\$ 0.4 to US\$ 1.6 per litre) is varied. LCOE is varied from US\$ 0.133 per kWh to US\$ 0.403 per kWh. NPC is varied from US\$ 871 million to US\$ 2.63 billion. Operating cost is varied from US\$ 59 million to US\$ 195 million.

Power quality (sag, swell, interruption and harmonic) results of doubled and coupled bus bar are same. In general, power quality results after RE integration is better than before RE integration and HOMER simulation results is the best results.

Power quality (sag) results are showing that before integrating RE into the grid (situation A) percentage of buses voltages are below 100 kV%, they are around 86 kV% - 99 kV%. Silae 4 Bus bar is the lowest one (86 kV%) and DB1 PJPP bus bar is the highest one (99 kV%). During the fault, percentage of buses voltages are around 0 kV% - 53 kV%. After the fault percentage of buses voltages are fluctuating below 100 kV% and then reach stable voltage at the same voltage before the fault occurred. Time duration after the fault to get stable voltage is around 3.8th second – 6.5th second. PJPP SB1 bus bar is the shortest one and Silae SB3 bus bar is the longest one. Percentage of buses frequencies on situation A is on 100 % before the fault (before sag occurred). During the fault buses frequencies are around 97 % - 99 %. After the fault percentage buses frequencies get stable at 100 % around 5th second – 9.8th second. Parigi SB2 bus bar is the longest one to get stable frequency and most of bus bars take 5th second to get stable frequency.

Power quality (sag) results are showing that after integrating renewable energy into the grid (situation B) percentage of buses voltage are around 96 kV% - 100.5 kV%. Silae SB4 bus bar is the lowest and PJPP SB1 bus bar is the highest one. During the fault, percentage of bus voltage is around 0 kV% - 61 kV%. Percentage of bus voltage of Maesa SB1 bus bar and Maesa SB1 (2) bus bar are in 0 kV% while others are below 62 kV%. After the fault, percentage of buses voltages are around 96 % - 105 kV% and taking around 4.5th second - 9.2th second to reach stable voltage. Parigi SB1 bus bar takes the shortest time to reach stable voltage. Buses frequencies before the fault occurred are 100 %. During the fault buses frequencies are around 99 % - 101 %. Percentage bus frequency of donggala SB1, Maesa SB1 bus bar, Maesa SB1 (2), Silae SB1 busbar, Silae SB2 bus bar, Silae SB3 bus bar, Silae SB4 bus bar are 101 % during the fault while others are 99 %. After the fault all buses frequencies are 100 % and take this stable position at 5th – 11.4th second. Silae SB2 bus bar takes the shortest one and donggala SB1 takes the longest one.

Power quality (sag) results are showing that after integrating RE into the grid based on HOMER results (situation C) before the fault all percentage of buses voltages are above 100 kV%. They are around 101 kV% - 116 kV%. Silae SB2 bus bar is the highest one. Parigi DB1 bus bar, parigi SB1 (2) bus bar and PJPP SB1 bus bar are the lowest ones. During the fault percentage of buses voltages are around 0 kV% - 38 kV%, which means some percentage of buses voltage are dropped to zero during the fault and some of them are not. Percentage of bus bar voltage of Maesa SB1 bus bar and Maesa SB1 (2) are dropped to zero during the fault. After the fault, all percentage of buses voltages get stable at the same position as before the fault occurred which is from 101 kV% - 116 kV%. All buses get stable voltage at around 4.5th – 6.6th second. Maesa SB1 bus bar takes the shortest one. DB1 PJPP bus bar and silae SB4 bus bar take the longest ones. Percentage of buses frequencies before the fault occurred on situation B is 100 %. During the fault, in general all buses are above 100 %. They are around 101 % - 102 %. Donggala SB1 bus bar, Maesa SB1 bus bar, maesa SB1 (2) bus bar, Silae SB4 bus bar are around 98 % - 99 % during fault but only at the beginning when the fault occurred, around 1 – 3 seconds. After 4th second percentage of buses frequencies are above 100 %. After the fault, all percentage of buses frequencies are getting stable at the same position as before the fault occurred which is 100 %. They get stable at around 4.6th – 9.8th

second. Bus frequency of parigi DB1 (2) bus bar, parigi SB1 bus bar and talise SB1 are the shortest ones. Donggala SB1 is the longest one.

Power quality (swell) results are showing that before integrating RE into the grid (situation A) percentage of buses voltages are below 100 kV%, they are around 86.5 kV% - 96.5 kV%. Silae SB4 is the lowest one. Silae SB1 bus bar, silae SB2 bus bar and silae SB3 bus bar are the highest ones. During the swell, percentage of buses voltages are fluctuating around 91 kV% - 102.5 kV%. After swell buses voltages are fluctuating around 83 kV% - 101 kV%. All buses are reaching the same stable voltage as before swell occurred at around 3.4th second to 9.2nd second. PJPP SB1 bus bar takes the shortest one and parigi DB1 bus bar takes the longest one. Power quality (swell) results are showing that before integrating RE into the grid (situation A) percentage of buses frequencies are 100 %. During swell, all percentage of buses frequencies are fluctuating around 100.2 % - 102 %. After swell, all percentage of buses frequencies is around 99 % - 102 %. All buses frequencies are getting the same stable frequency as before swell occurred at around 3.2nd second - 4.5th second. Maesa SB1 (2) takes the shortest one and DB1 PJPP bus bar takes the longest one.

Power quality (swell) results are showing that after integrating RE into the grid (situation B) percentage of buses voltages are around 96 kV% - 101 kV%. Silae SB4 bus bar is the lowest one and parigi SB1 is the highest one. During swell percentage of buses voltages are fluctuating around 94 kV% - 112 kV%. After swell, percentage of buses voltages are around 89 kV% - 102 kV%. All buses voltages are getting stable with the same voltage as before swell occurred at around from 4th second to 12.5th second. Maesa SB1 (2) takes the shortest one and parigi SB1 (2) takes the longest one. Power quality (swell) results are showing that after integrating RE into the grid (situation B) all percentage of buses frequencies are 100 %. During swell buses frequencies are fluctuating around 100.2 % - 102 %. After swell buses frequencies are fluctuating around 98 % - 100 %. All buses frequencies are getting stable at the same frequency as before swell occurred at around 5.9th second to 10.2nd second. Parigi DB1 takes the shortest one. Maesa SB1 (2) bus bar, talise SB2 bus bar and talise SB3 take the longest ones.

Power quality (swell) results are showing that after integrating RE into the grid based on HOMER results (situation C) percentage of buses voltages are around 100 kV% - 114 kV%. Talise DB11 bus bar is the lowest one. Donggala SB1 bus bar and silae SB1 bus bar are the highest ones. During swell percentage of buses voltages are fluctuating around 100 kV% - 120 kV%. After swell percentage of buses voltage are fluctuating around 98 kV% - 115 kV% before getting stable voltage. Buses voltages are getting stable with the same voltage before swell occurred at around 4.2rd second to 14th second. Maesa SB1 takes the shortest one and parigi SB1 (2) takes the longest one. Power quality (swell) results are showing that after integrating RE into the grid based on homer results (situation C) all percentage of buses frequencies are 100 %. During swell percentage of buses frequencies are fluctuating around 100 % - 101.4 %. After swell, percentage of buses frequencies are going down below 100 % around 98.8 % - 99.9 %. All percentage of buses frequencies is getting stable frequency as the same frequency before swell occurred. They are getting stable frequency at around 6.3rd second to 14th second. Maesa SB1 (2) bus bar, PJPP SB1 bus bar and silae SB1 bus bar take the shortest ones. Talise SB2 bus bar and talise SB3 take the longest ones.

Power quality (interruption) results are showing that before integrating RE into the grid (situation A) percentage of buses voltages before interruption are around 90 %kV – 97 %kV. Donggala SB1 bus bar and Maesa SB1 bus bar are the lowest ones. Silae SB1 bus bar, silae SB2 bus bar and silae SB3 are the highest ones. During interruption all percentage of buses voltages are dropped to zero. After interruption percentage of buses voltages are going up to from around 73 %kV – 89 %kV to around 92 %kV – 100 %kV in 0.5 seconds. After interruption only two percentages of buses voltages are getting stable at the same voltage as before interruption occurred. They are maesa SB1 (2) bus bar and parigi SB1. Ten buses are getting stable with lower voltage than the voltage before interruption occurred but the decrease percentage voltage is only 1 %kV or 2 %kV. They are DB1 PJPP bus bar, DB11 PJPP bus bar, maesa SB1 bus bar, parigi DB1 bus bar, parigi DB1 (2) bus bar, PJPP SB1 bus bar, talise SB2 bus bar, talise SB3 bus bar, talise DB1 bus bar and talise DB11 bus bar. Seven buses are getting stable with higher percentage voltage than the percentage voltage before interruption occurred but the increase is only 1 %kV or 2 %kV. They are donggala SB1 bus bar, silae SB1 bus bar, silae SB2 bus

bar, silae SB3 bus bar, silae SB4 bus bar and talise SB1 bus bar. Buses voltage are getting stable at around 4.5th second – 7.7th second. Talise DB11 bus bar is the shortest one and donggala SB1 is the longest one. Power quality (interruption) results are showing that before integrating RE into the grid (situation A) percentage of buses frequencies are 100 %. During interruption, percentage of buses frequencies are going up to around 105 % – 108 % and going down in 0.5 seconds to around 92 % – 95 %. After interruption percentage of buses frequencies are getting stable at the same percentage frequency as before interruption occurred. Buses frequencies are getting stable time around 4.3rd second – 4.6th second. Silae SB1 bus bar and talise SB3 are the shortest ones. DB11 PJPP is the longest one.

Power quality (interruption) results are showing that after integrating RE into the grid (situation B) percentage of buses voltages before interruption are around 97 %kV – 101 %kV. Maesa SB1 bus bar, parigi DB1 bus bar and silae SB4 bus bar are the lowest ones. PJPP SB1 bus bar is the highest one. During interruption percentage of buses voltages are dropped to zero. After interruption percentage of buses voltages are going up to around 82 %kV – 88 %kV and then going up again to around 99 %kV – 102 %kV in 0.5 seconds. Donggala SB1 bus bar, maesa SB1 bus bar, parigi SB1 bus bar, silae SB1 bus bar, silae SB2 bus bar, silae SB3 bus bar and talise SB1 bus bar are getting stable with the same percentage voltage as before interruption occurred. DB1 PJPP bus bar, DB11 PJPP bus bar, parigi DB1 bus bar, parigi DB1 (2) bus bar, parigi SB1 (2) bus bar, PJPP SB1 bus bar, talise DB1 bus bar and talise DB11 bus bar are getting stable with lower voltage than before interruption occurred but the difference percentage voltage is only around 1 %kV – 3 %kV. Maesa SB1 (2) bus bar, silae SB4 bus bar and talise SB2 bus bar are getting stable with higher percentage voltage than before interruption occurred but the difference percentage voltage is around 1 %kV – 2 %kV. Buses voltages are getting stable at around 4th second – 8.9th second. Donggala SB1 bus bar is the shortest one and parigi SB1 (2) is the longest one. Power quality (interruption) results are showing that after integrating RE into the grid (situation B) percentage of buses frequencies before interruption occurred are 100 %. During interruption percentage of buses frequencies are dropped to zero. After interruption percentage of buses frequencies immediately going up to around 105 % - 107 % and then going down to around 95 % - 98 % in 0.5 seconds. Buses frequencies are getting stable at the same frequency as before

interruption occurred. Buses frequencies are getting stable at around 3.3rd second – 3.8th second. DB1 PJPP bus bar and talise SB3 are the shortest ones. Silae SB1 is the longest one.

Power quality (interruption) results are showing that after integrating RE into the grid based on HOMER results (situation C) percentage of buses voltages before interruption are around 101.5 %kV – 116 %kV. Parigi DB1 bus bar and PJPP SB1 bus bar are the lowest ones. Silae SB1 bus bar and silae SB2 are the highest ones. During interruption percentage of buses voltages are dropped to zero. After interruption percentage of buses voltages are going up to around 91 %kV – 99 %kV and then fluctuating around 99 %kV – 99 %kV and 24 %kV – 72 %kV for 0.5 seconds. Percentage of buses voltages are going up to around 110 %kV – 121 %kV and then getting stable at the same percentage voltage as before interruption occurred. Buses voltages are getting stable at around 3.9th second – 6.8th second. Donggala SB1 bus bar takes the shortest one and talise SB1 bus bar takes the longest one. Power quality (interruption) results are showing that after integrating RE into the grid based on homer results (situation C) percentage of buses frequencies before interruption are 100 %. During interruption percentage of buses frequencies are dropped to zero. After interruption percentage of buses frequencies are going up to around 105 % - 106 % and going down to around 95 % - 98 % in 0.5 seconds. Buses frequencies are getting stable at the same frequency as before interruption occurred. They take around 3.1st second – 3.5th second to get stable frequency. DB1 PJPP bus bar, donggala SB1 bus bar and parigi SB1 (2) take the shortest ones. Maesa SB1 takes the longest one.

Power quality (harmonics) results are showing that before integrating RE into the grid (situation A) buses voltage spectrum of harmonics order 5th are started from 2.32 % to 3.77 %. Parigi SB1 (2 bus bar) is the lowest one. Talise SB2 bus bar and talise SB3 bus bar are the highest ones. Buses voltage spectrum of harmonics 25th are started from 0.01 % to 0.5 %. Parigi SB1 (2) bus bar, PJPP SB1 bus bar, silae SB4 bus bar, talise SB1 bus bar, talise DB1 bus bar and talise DB11 bus bar are the lowest ones while the highest ones are maesa SB1 bus bar and Maesa SB1 (2) bus bar. Power quality (harmonics) results are showing that before integrating RE into the grid (situation A) buses sinusoidal waveform distortions are started from 0.1 cycles to

0.92 cycles. Parigi SB1 (2) bus bar, silae SB1 bus bar, silae SB2 bus bar and silae SB3 bus bar are the longest ones. Others are shortest.

Power-quality (harmonics) results are showing that after integrating RE into the grid (situation B) buses voltage spectrum of harmonics order 5th are started from 0.32 % to 1.51 %. Silae SB4 bus bar is lowest one and parigi SB1 (2) is the highest one. Buses voltage spectrum of harmonics order 25th are started from 0.05 % to 0.17 %. Maesa sb1 bus bar and maesa SB1 (2) bus bar are the lowest ones while the highest one is parigi SB1 (2). Power quality (harmonics) results are showing that before integrating RE into the grid (situation B) buses sinusoidal waveform distortions are started from zero distortion to 0.90 %. Donggala SB1 bus bar, maesa SB1 bus bar, maesa SB1 (2) bus bar, PJPP SB1 buabar, silae SB1 bus bar, silae SB2 bus bar, silae SB3 bus bar, silae SB4 bus bar, talise SB2 and talise SB3 bus bar have sinusoidal with no distortion. Others have distortion from 0.06 cycles to 0.65 cycles.

Power quality (harmonics) results after integrating RE into the grid based on HOMER results (situation C) are showing that buses voltage spectrum of harmonic order 5th are started from 0.18 % to 0.37 %. Silae SB4 is the lowest one while PJPP SB1 bus bar is the highest one. Buses voltage spectrum of harmonics order 25th are started from 0.01 % to 0.06 %. Parigi SB1 bus bar and talise SB1 are the lowest one while the highest one is maesa SB1 (2). Power quality (harmonics) results after integrating RE into the grid based on homer results (situation C) are showing that buses sinusoidal waveform distortions are started from zero to 0.6 cycles. DB1 PJPP bus bar and DB11 PJPP bus bar have distortion from 0.45 cycles to 0.6 cycles while others are zero.

7.2 Future Work

Power quality of grid is also determined by properly placing of diesel generators. It is necessary to use special program to properly locate diesel generator to increase grid power quality.

8 Bibliography

- Abdullah, M. A. (2011). Quantification of Emission Reduction from Electricity Network with the Integration of renewable Resources.
- Al Haj Hassan, H. (2015). Integrating Cellular Network, Smart Grid and Renewable Energy: Analysis, Architecture and Challenges. 3.
- Alvin, T. G. (2013). Changes in Fault Current Levels due to Renewable Embadded Generation in a Distribution Network. *2013 IEEE Conference on Clean Energy Technology (CEAT)*. IEEE.
- Ansari, O. A. (2016). Reliability Assessment of Microgrid with Renewable Generation and Prioritized Loads. *2016 IEEE Green Energy and System Conference*. IEEE.
- Arrinda, J. (2014). Analysis of Massive Integration of Renewable Power Plants under new Regulatory Frameworks. *Third International Conference on Renewable Energy Research and Applications*. Milwaukee: IEEE.
- Atlas of the World*. (2016, March 27). Retrieved from http://www.welt.de/map_of_sulawesi_6-616.
- Ayu. (2014, November 19). Civil Engineer. (S. Dewi, Interviewer) Palu, Central Sulawesi.
- Baker, K. (2012). Optimal Integration of Intermittent Energy Sources Using Distributed Mutli-Step >Optimization. IEEE.
- Ben Youssef, N. E. (2016). Supporting Renewable Energy Resources Integration Using Content-Centric Networking.
- Beshr, E. (2013). Comparative Study of Adding PV/Wind Energy Systems to Autonomus Micro Grid. *2013 Third International Conference on Electric Power on Energy Conversion System*. Yildoz: IEEE.
- Bhadane, K. V. (2012). "Investigation for Causes for Poor Power Quality in Grid Connected Wind Energy" -A Review. IEEE.
- Booklet, R. C. (2014). *Pakava River report*. Rivel Hall of General Work branch Palu, General Work Ministry, Palu.
- Boyle. (2003). *renewable Energy* (second Edition ed.). Oxford University.
- BPS. (n.d.). Retrieved 2016, from <http://sulteng.bps.go.id>
- Brenna, M. (2012). Synergy between Renewable Sources and Electric Vehicles for Energy Integration in Distribution System. IEEE.

- Calabria, M. (2014). Stability Optimization for Distributed Generation of Load-Following Energy. *ENERGYCON2014*. Dubrovnik: IEEE.
- Chaitusaney, S. (2014). Key Issues for Integration of Renewable Energy and Distributed Generation into Thailand Power Grid.
- Chattopadhyay, R. (2014). Low Voltage PV Power Integration into Medium Voltage Grid Using High Voltage SiC Devices. *The 2014 International Power Electronics Conference*. IEEE.
- Chen, H. (2016). Key Technologies for Integration for Multitype Renewable Energy Sources -Research on Multi-Time Frame Robust Scheduling/Dispatch. *IEEE Transactions on Smart Grid* , 7.
- Chen, X. (2011). Integrating Wind Farm to the Grid Using Hybrid Multiterminal HVDC Technology . *IEEE Transactions on Industry Applications*. 47. IEEE.
- Concepcion, R. (2011). On Extended-Term Dynamic Simulation with High Penetrations of Photovoltaic Generation.
- Dahal, S. (2015). Renewable Energy Development in Australia: Regulatory to Technical Challenges. *2015 IEEE PES Asia-Africa Power and Energy Engineering Conference (APPEEC)*. IEEE.
- De Almeida, P. M. (2014). Grid Connection Consideration for the Integration of PV and Wind Sources. IEEE.
- de Groot, R. J. (2012). Smart Integration of Distribution Automation Applications. *2012 Third IEEE PES Innovative Smart Grid Technologies Europe (ISGT Europe), Berlin*. IEEE.
- De Melo, M. F. (2013). Hybrid System of Distributed Power Generation and Street Lightening based on LEDS: Grid Connection. IEEE.
- Delgado, J. (2011). Solutions to Mitigate Power Quality Disturbances Resulting From Integrating Intermittent Renewable Energy in the Grid of Porto Santo.
- Dewi, S. (2014). Integration PV and Wind into the Grid to Supply Electricity in Palu (Indonesia). *ICSEBS 2014. 747 2015*. Bali: Applied Mechanics and Material .
- El Aimagi, S. (2014). Trends in Grid Integration of Renewables Case of Doubly Fed Induction Wind Generator. IEEE.
- El Kanj, H. (2015). Review of Smart Grid Systems Requirementsd Renewable Energy. *2015 Tenth International Conference on Ecological Vehicles Energies (EVER)*. IEEE.

- Elombo, A. E. (2010). Impacts of Grid Integration of Wind Energy in the Namibian Power Network. *2010 International Conference on Power System Technology*. IEEE.
- Elombo, A. I. (2010). Grid Integration of Wind Energy: A Case Study on a Typical Sub-Transmission Network in Namibia. *UPEC 2010*. IEEE.
- Forushani, E. H. (2014). >Investigating the Effects of Flexible Load in the Grid Integration of Wind Power. IEEE.
- Fuchs, F. W. (2012). Research Laboratory for Grid Integration of Distributed Renewable Resources -Design and Realization-. IEEE.
- Gado, A. A.-M. (2015). Impact the Expansion of the Production of Generation of Solar Power on the Low Voltage Network in Egypt. IEEE.
- Gheorghe, S. (2016). Results of Power Quality Monitoring in Romanian Transmission and Distribution System Operators.
- Ghorbanian, M. J. (2013). Overview of Grid Connected Doubly Fed Induction Generator Power Quality. *2013 IEEE International Conference on Clean Energy and Technology*. IEEE.
- Grünbaum, R. (2013). FACTS for Grid Integration of Wind Power. IEEE.
- Guner, S. (2011). Turkish Power System: From Conventional Past to smart Future. *2011 Second IEEE PES International Conference and Exhibition on Innovative*. IEEE.
- Gupta, P. (2014). A review on Optimal Sizing and Sitting on Distributed Generation System. IEEE.
- Hakimi, S. M. (2014). Optimal Planning of a Smart Microgrid Including Demand Reponse and Intermittent Renewable Energy Resources. *IEEE Transactions on Smartgrid*. 5. IEEE.
- Hamoud, F. (2017). Power Factor Improvement Using Adaptive Fuzzy Logic Control Based D-STATCOM. *2017 Twelfth International Conference on Ecological Vehicles and renewable Energies (EVER)*. IEEE.
- Haque, A. U. (2013). Solar PV Power Generation Forecasting Using a Hybrid Intelligent Approach. IEEE.
- Hart, E. K. (2012, February 2). The Potential of Intermittent Renewables To Meet Electric Power Demand: Current Methods and Emerging Analytical Techniques. 100.

- Hashim, A. H. (2015). Integration of Renewable Energy into Grid System-The Sabah Green Grid.
- Henneaux, P. (2013). Blackout Probabilistic Risk Assessment and Thermal Effects: Impacts of Changes in generation. *IEEE Transaction on Power System*. 28. IEEE.
- Hossain, M. J. (2017). Impacts of Wind and Solar Integrations on the Dynamic Operations of Distribution Systems.
- International, S. E. *Photovoltaic Design and Installation Manual*.
- Ipinnimo, O. (2012). Mitigation of Multiple Voltage Dips in a Weak Grid Using Wind and Hydro-Based on Distributed Generation. IEEE.
- Jamal, N. (2015). Solar Resources Potential in the Development of renewable based on Electric Power System by 2050: the Case of Pakistan.
- Javadi, A. (2017). Power Quality Enhancement of Smart Households Using A Multilevel THSeHF. *IEEE Transactions on Smart Grids* , 8.
- Jeni, A. (2016). Photovoltaic Energy Impact on Grid's Distribution Line Voltage for Different Load Levels. IEEE.
- Junxia, M. (2014). Study on Power Loss of Distribution Network with Distributed Generation and its Reactive Power Optimization Problem. *2014 International Conference on Power System Technology (POWERCON 2014)*. Chengdu: IEEE.
- Khan, M. U. (2015). A New Proposed Hierarchy for Renewable Energy Generation to Distribution Grid Integration . IEEE.
- KOH, L. H. (2012). Renewable Energy Integration Into smart Grids: Problems and Solutions-Singapore Experience.
- Krishna, T. M. (2013). A Novel Algorithm for the Loss Estimation and Minimization of Radial Distribution System with Distributed Generation. IEEE.
- Kumar, V. (2015). Power Quality Event Generation in Matlab/Simulink Environment. 4.
- Kumwenda, B. (2017). Integration of Solar Energy into the Zambia Power Grid Considering Ramp Rate Constraints. *2017 IEEE PES-IAS Power Africa*. IEEE.
- Kuwahata, R. (2012). The Role of Microgrid in Accelerating Energy Access. *2012 Third IEEE PES Innovative Smart Grid Technology Europe (ISGT Europe) Berlin*. Berlin: IEEE.

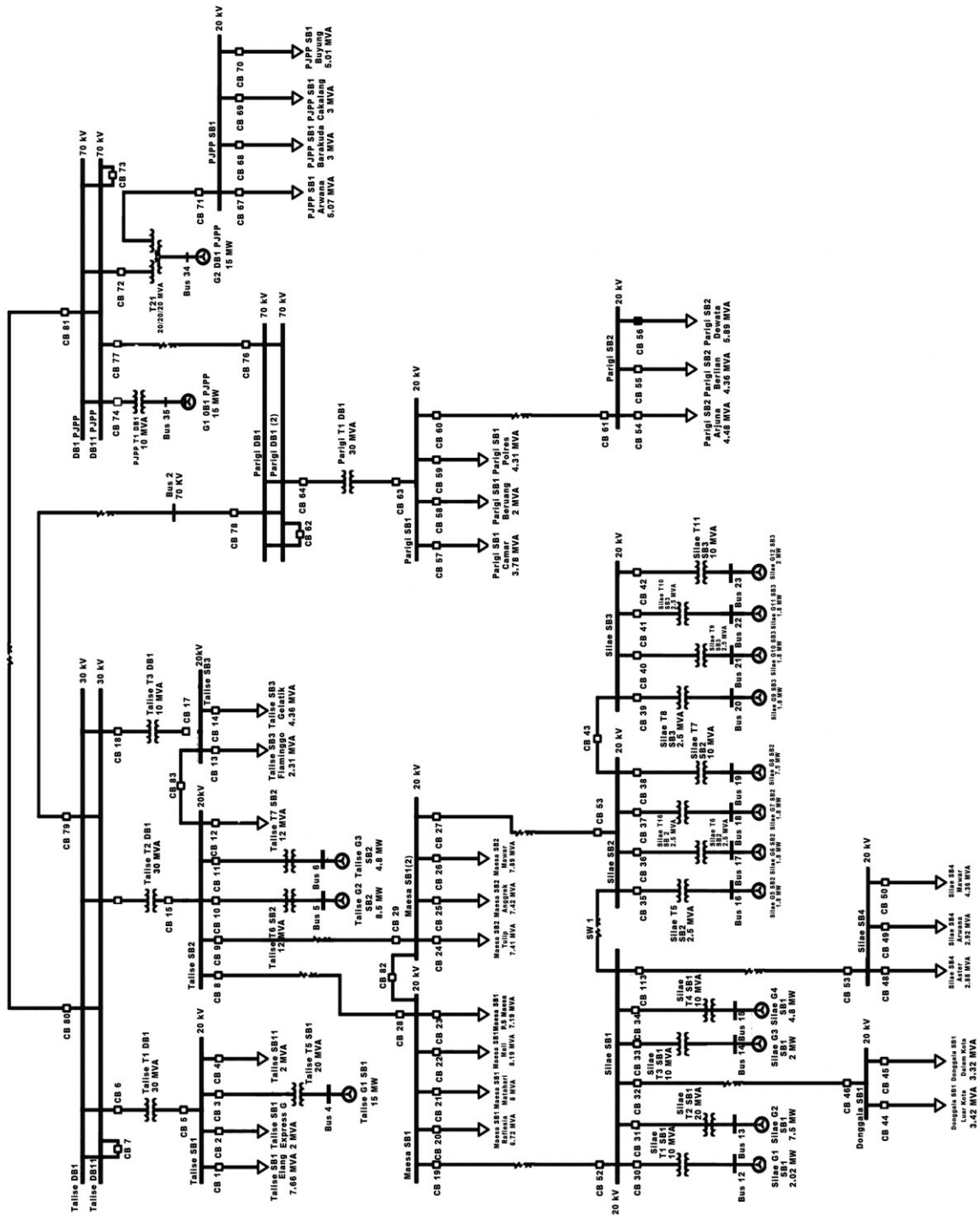
- Lendamanu, G. (2013, December 08). Electrical Engineer. (S. Dewi, Interviewer)
Palu, Central Sulawesi, Indonesia.
- Lin, Y. (2016). Integrating High-Penetration Renewable Energy into Power System-
Case Study. *2016 China International Conference On Electricity Distribution (CICED 2016)*. Xi'an: IEEE.
- Mangaraj, M. (2016, November 9). Power Quality Improvement ba a 3-phase 4-leg
SupercapacitorBased DSTATCOM. *2016 IEEE Uttar Pradesh Section International Conference on Electrical, Computer and Electronics Engineering* .
- Mariethoz, S. (2012, June 29). Modelling and Hierarchical Hybrid Optimal Control of
Prosumers for Improved Integration of Renewable energy Sources into the Grid.
- Marilyn Winifred, A. (2017). Strengthening the Ghanaian Transmission System to
Accomodate Variable renewable Energies. *2017 IEEE PES-IAS Power Africa*.
IEEE.
- Martinez, S. M. (2015). Wind Power Curtailment Analysis Under Generation
Flexibility requirements: the Spanish Case Study. IEEE.
- Mathe, R. (2017). The Impact of Large Scale Grid-Connected Wind Generators on
the Power System Network. *2017 IEEE PES-IAS Power Africa*. IEEE.
- Modi, N. (2012). Revisiting Damping Performance of the Queensland Network under
Wind Power Penetration. IEEE.
- Mohammadi, P. (2014). The Impact of Distributed Generation in Fault Detection and
Voltage Profile in Power Distribution Networks. IEEE.
- Mukhopadhyay, S. (2012). On the Progress of renewable Energy Integration into
Smart Grids in India.
- Muttaqi, K. M. (2011). Optimal Allocation of Renewable Energy Resources for
Minimising Emissions in Distribution Networks. *IET Conference on reliability of Transmission and Distribution Networks*. IEEE.
- Nanewortor, X. K. (2015). Analysis of renewable Energy Infeed Towards a Concept
of Storage Integration into Existing Grid.
- Narayana, M. (2012). Adaptive Prediction of Power Fluctuations from a Wind Turbine
at Kalpitiya Area in Sri Lanka. *ICIAfS 2012*. IEEE.
- Palu, P. B. (2011). *electricity System in Palu Area*. PLN, Palu.
- Petinrin, J. O. (2015). A Voltage Control Scheme in a Distribution Feeder with Wind
Energy Sources. IEEE.

- Petintin, J. (2014). Voltage Regulation in Smart Distribution System Incorporating Variable Renewable Generation. *2014 IEEE Innovative Smart Grid Technologies-Asia(ISGT ASIA)*. IEEE.
- Pouresmaeil, E. (2015). Integration of renewable Energy for Harmonic Current and reactive Power Compensation. *2015 IEEE Fifth International Conference on Power Engineering, Energy and Electrical Drives (POWERENG)*. IEEE.
- Ramdhin, A. (2015). A Network Planning Perspective for Grid Integration of Renewable Distributed Generation in South Africa. IEEE.
- Rana, V. (2013). Wind Farm Integration Effect on Electricity Market Price. IEEE.
- Rao, N. (2013). Wind Farm -Power Evacuation and Grid Integration. *IEEE ISGT ASIA 2013*. IEEE.
- Rumbayan, M. (2012, January 16). Mapping of Solar Energy Potential Using Artificial Neural Network and geographical Information system. *Renewable of Solar energy Potential in Indonesia using Artificial Neural Network and Geographical Information System* .
- Runa, T. (n.d.). *Hydro Power*. Retrieved March 2016, 2016, from Word Press: <https://taufikruna.wordpress.com>
- Sbordone, D. A. (2015). The Future Interaction between Virtual Aggregator-TSO-DSO to Increase DG Penetration. *2015 International Conference on Smart Grid and Clean Energy Technology*. IEEE.
- Schellong, W. (2013). Optimization of Distributed Cogeneration System. IEEE.
- Sennou, A. S. (2015). Renewable Energy Integration Using PowerGAMA: Moroccan Case Study. *First International Conference on Electrical and Information Technologies ICEIT2015*. IEEE.
- Shafiullah, G. M. (2015). Analysis of Harmonics with Renewable Energy Integration into the Distribution Network. IEEE.
- Shi, J. (2013). Impact of DFIG Wind Power on Power System Small Signal Stability. IEEE.
- Simon, L. (2016). Impact of DFIG based on Wind Energy Conversion System on Faults Study and Power Swings.
- Singh, A. (2010). Power Quality Issues related to Distributed Energy Source Integration to utility Grids. *2010 Annual IEEE India Conference*. IEEE.

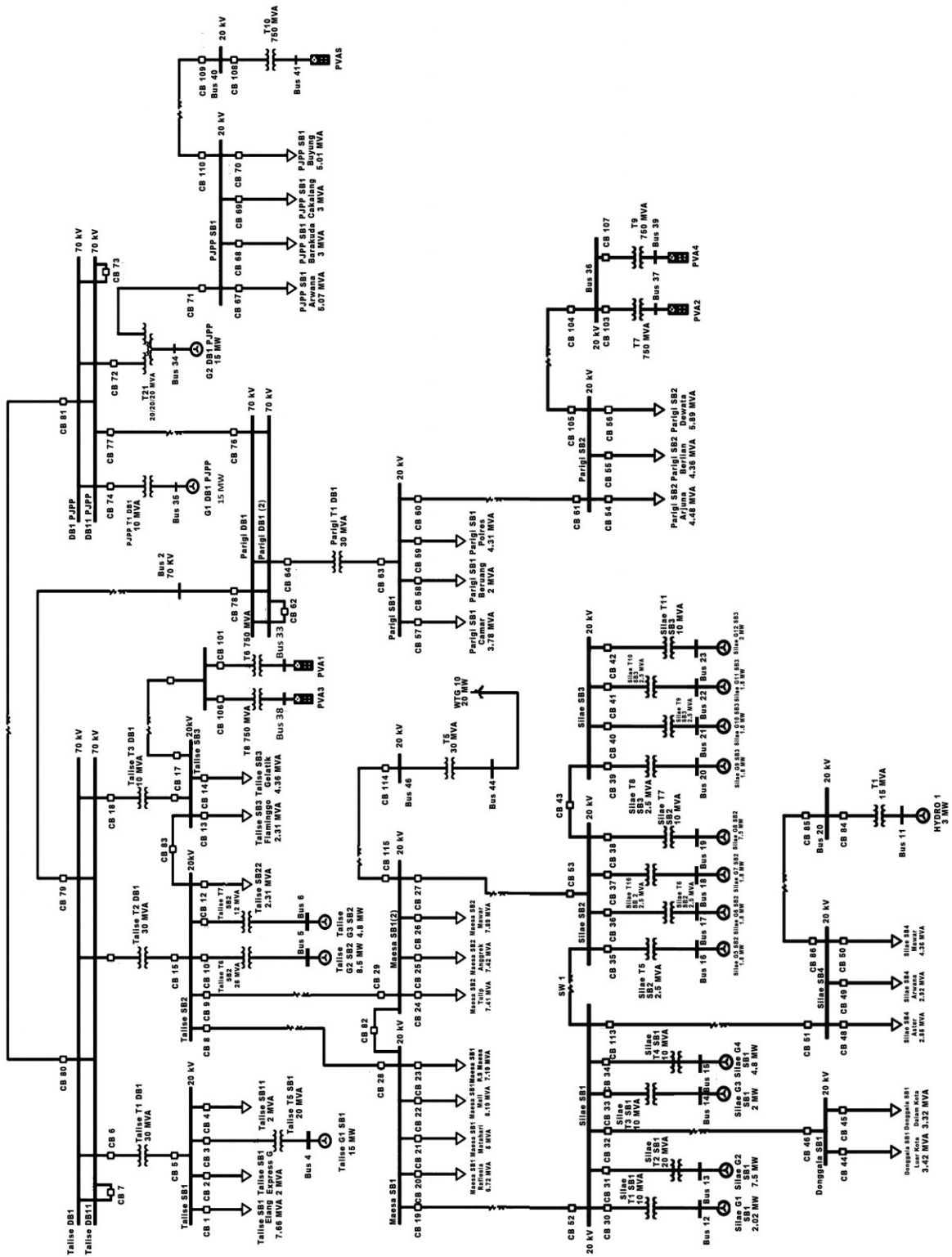
- Singh, O. (2016). Hybrid Renewable Energy System Integration in the micro-Grid: Indian Context. *2016 International Conference on Control, Computing, Communication and Material*. IEEE.
- Singh, R. (2012). An Improved Approach for Control of a Grid Connected Wind Farms and its STATCOM Based Stability Analysis. IEEE.
- Sreedevi, J. (2016). Grid Stability with Large Wind Power Generation-Case Study.
- Sriboong, T. (2016). Simulation and Analysis of Renewable Energy Resource Integration for Electric Vehicle Charging Station in Thailand. *2016 International Conference on Cogeneration, Small Power Plants and Distric Energy*. Bang Na: IEEE.
- Ssekulima, E. B. (2016). Wind Speed and Solar Irradiance Forecasting Techniques for Enhanced Renewable Energy Integration with the Grid:a review. *IET Journals* , 10.
- States, N. E. (n.d.). *Homer*. Retrieved from Homer Software:
<http://www.homerenergy.com>
- Strasser, T. (2016). Open and Interoperable ICT Solution for Integrating Distributed Energy Resources into Smart Grids.
- Such, M. C. (2011). Battery Energy Storage and Wind Energy Integrated into the Smart Grid. IEEE.
- Sun, S. (2016). Distributed Real-Time Power Balancing in Renewable-Integrated Power Grids with Storage and Flexible Loads. *IEEE Transactions on Smart Grid* , 7.
- Sutrisna, F. (n.d.). *Primary Energy, Renewable Energy, Indonesian Electricity*. Retrieved March 16, 2016
- Tan, S. (2012). Optimization of Distribution Network Incorporating Microgrid Using Vaccine -AIS. IEEE.
- Thakurta, P. G. (2015). Increasing Transmission Grid Flexibility by TSO Coordination to Integration more Wind Energy Source while Maintaining System Security . *IEEE Transaction on Sustainable Energy* , 6.
- Toma, R. (2014). The Impact on Voltage Stability of the Integration of renewable energy Sources into the Electric Grids.
- Wang, K. (2012). A Stochastic Power Network Calculus for Integrating Renewable Energy Sources into the Power Grid. *IEEE Journal on Selected Areas in Communications*. 30. IEEE.

- Wang, P. (2012). Customer LED Network Revolution-Integrating Renewable Energy into LV Networks Using Energy Storage. *CIREN Workshop*. Lisbon: IEEE.
- Waqfi, R. R. (2017). Impact of PV and Wind Penetration into a Distribution Network Using Etap.
- Wirasanti, P. (2012). Clustering Power System Strategy the Future of Distributed Generation. *2012 International Symposium of Power Electronics, Electrical Drives, and Motion*. IEEE.
- World Weather*. (n.d.). Retrieved March 26, 2016, from Weather Average of Central Sulawesi: <http://www.worldweatheronline.com>
- Xiaobo, Z. (2014). Utilization of Large-Scale Charging Devices Integration into Power Systems with Microgrids. IEEE.
- Xu, H. (2011). Towards Improving Renewable Resource Utilization with Plug-in Electric Vehicles.
- Yan, R. (2017). Impact of Photovoltaic Power Fluctuations by Moving Clouds on Network Voltage: A Case Study of an Urban Network.
- Young Joo, J. (2016, October). integration of Sustainable Manufacturing Systems into Smart Grids with High Penetration of Renewable Energy Resources.
- Yuli, W. (2015). Hierarchical Management Strategy of Hybrid Microgrid. IEEE.
- Zanabria, C. (2015). A Low Cost Open Source-based IEC 61850 /61499 Automation Platform for Distributed Energy Resources. IEEE.
- Zhang, H. (2016). Transmission Level MMC DC/DC Converter for Large Scale Integration of Renewable Energy into HVDC Grid.
- Zhang, H.-T. (2013). Reliability and Investment Assessment for Wind Energy Generation. IEEE.
- Zhang, Y. (2015). Study on Renewable Energy Integration Influence and Accommodation Capability in Regional Power Grid. *Fifth International Conference on Electric Utility Deregulation and Restructuring and Power Technology*. Changsha: IEEE.

Appendix A



Appendix B



Appendix C

